



HAL
open science

Dynamic covalent chemistry of C=N, C=C and quaternary ammonium constituents

Sirinan Kulchat

► **To cite this version:**

Sirinan Kulchat. Dynamic covalent chemistry of C=N, C=C and quaternary ammonium constituents. Other. Université de Strasbourg, 2015. English. NNT : 2015STRAF018 . tel-01255174

HAL Id: tel-01255174

<https://theses.hal.science/tel-01255174v1>

Submitted on 13 Jan 2016

HAL is a multi-disciplinary open access archive for the deposit and dissemination of scientific research documents, whether they are published or not. The documents may come from teaching and research institutions in France or abroad, or from public or private research centers.

L'archive ouverte pluridisciplinaire **HAL**, est destinée au dépôt et à la diffusion de documents scientifiques de niveau recherche, publiés ou non, émanant des établissements d'enseignement et de recherche français ou étrangers, des laboratoires publics ou privés.

ÉCOLE DOCTORALE DES SCIENCES CHIMIQUES
INSTITUT DE SCIENCE ET D'INGÉNIERIE
SUPRAMOLÉCULAIRES

THÈSE présentée par :

Sirinan KULCHAT

soutenue le : 16 Juillet 2015

pour obtenir le grade de : **Docteur de l'Université de Strasbourg**

Discipline/ Spécialité : CHIMIE

**DYNAMIC COVALENT CHEMISTRY OF
C=N, C=C AND QUATERNARY AMMONIUM
CONSTITUENTS**

THÈSE dirigée par :

M. LEHN, Jean-Marie

Professeur Emérite, Université de Strasbourg

RAPPORTEURS :

M. SEEBACH, Dieter

Professeur Emérite,
Eidgenössische Technische Hochschule, Zürich

M. LADAME, Sylvain

Dr., Imperial College, London

AUTRES MEMBRES DU JURY :

M. MORAN, Joseph

Maître de Conférences Associé,
Université de Strasbourg

Table of Contents

Table of Contents.....	3
Acknowledgements.....	7
Abstract.....	9
Abstract in Thai.....	13
Abbreviations.....	14
Résumé.....	17
Chapter 1 General Introduction.....	39
1.1 The concept of Dynamic Chemistry.....	41
1.2 Dynamic combinatorial chemistry using exchange reactions.....	44
1.2.1 Reversible exchange reactions based on covalent bonding.....	45
1.2.2 Reversible exchange reactions based on noncovalent bonding.....	48
1.3 The general characteristics of imine compounds.....	54
1.4 General aspects of <i>Knoevenagel</i> compound chemistry.....	59
1.5 General aspects of Organocatalysis.....	63
1.6 References.....	69
Chapter 2 Organocatalysis of Exchange Processes between Knoevenagel-and Imine-derivatives in Dynamic Covalent Chemistry.....	79
2.1 Introduction	81
2.2 Results and Discussion	82
2.2.1 Organocatalysis of imine/imine, C=N/C=N, exchange Processes.....	82
2.2.2 The C=N/C=N exchange using aniline as a nucleophilic Catalyst.....	93
2.2.3 Organocatalysis of benzylidene/imine, C=C/C=N, exchange Processes.....	94
2.2.4 Organocatalysis of Benzylidene/Benzylidene, C=C/C=C, Cross-exchange Processes.....	104
2.3 Conclusions	114
2.4 References.....	115

Chapter 3 Uncatalyzed C=C/C=N exchange Processes between Knoevenagel-and Imine-derivatives in Dynamic Covalent Chemistry	119
3.1 Introduction.....	121
3.2 Results and Discussion.....	122
3.2.1 Benzylidene-(dm)barbiturates/imine, C=C/C=N, exchange Processes.....	122
3.2.2 Theoretical Study of the Metathesis-like Mechanism of the Cross Exchange between a <i>Knoevenagel</i> -Type Substrate (C=C) and an Imine (C=N).....	129
3.2.3 Organogel selection based on the exchange reaction of C=C/C=N.....	133
3.3 Conclusions	137
3.4 References.....	138
Chapter 4 Dynamic Covalent Chemistry of Nucleophilic Substitution Component Exchange of Quaternary Ammonium Salts	141
4.1 Introduction	143
4.2 Results and Discussion.....	144
4.2.1 Study of exchange processes between quaternary allyl-ammonium salts and tertiary amines via S _N 2 or S _N 2' type nucleophilic substitution.....	144
4.2.2 Study of exchange processes between quaternary benzyl-ammonium salts and tertiary amines via S _N 2 type nucleophilic substitution.....	159
4.2.3 Study of exchange processes between <i>N</i> -allyl- and <i>N</i> -benzyl-pyridinium salts and pyridine components via S _N 2 and S _N 2' nucleophilic substitution processes.....	162
4.2.4 Generation of libraries of Dynamic Ionic Liquids (DILs).....	166
4.3 Conclusions.....	168
4.4 References.....	169

Chapter 5 Kinetic and Thermodynamic selectivity of Imine formation in Dynamic Covalent Chemistry	173
5.1 Introduction.....	175
5.2 Results and Discussion.....	176
5.2.1 The study of imines formation in aqueous solution of sodium 5-formyl-2-methoxybenzene sulfonate (1) and pyridoxal phosphate (2) toward different amino derivatives (A, B, C, D, and E).....	177
5.2.1.1 The study of imine formation from sulfonate aldehyde (1)	178
5.2.1.2 The study of imines formation from Pyridoxal phosphate (2).....	184
5.2.2 Imine formation from 2-pyridyl aldehyde (3) and salicylaldehyde (4) and various amino derivatives (B, F, G, and H) in organic solvents.....	187
5.2.2.1 Imine formation from 2-pyridyl aldehyde (3).....	187
5.2.2.2 Imine formation from salicylaldehyde (4).....	194
5.2.3 The kinetic/thermodynamic selectivity of imine formation on aminoglycoside.....	197
5.3 Conclusions.....	200
5.4 References.....	201
Chapter 6 Conclusions and Perspective	205
Chapter 7 Experimental Part	209
7.1 General Methods and Materials.....	211
7.1.1 Reagents.....	211
7.1.2 Instruments.....	212
7.2 Chapter 2 , Organocatalysis of exchange processes between <i>knoevenagel</i> and imine compounds in dynamic covalent chemistry.....	214
7.2.1 Synthesis procedure and characterization.....	214
7.2.2 Study of Imine/Imine (C=N/C=N) derivatives exchange.....	222
7.2.3 Study of <i>Knoevenagel</i> /Imine (C=C/C=N) derivatives exchange.....	250
7.2.4 Study of <i>Knoevenagel</i> / <i>Knoevenagel</i> (C=C/C=C) derivatives exchange.....	263

7.3 Chapter 3 , Uncatalyzed C=C/C=N Exchange Processes between <i>Knoevenagel</i> and Imine compounds in Dynamic Covalent Chemistry.....	272
7.3.1 Synthesis and Characterization.....	272
7.3.2 Study of <i>Knoevenagel</i> /Imine (C=C/C=N) derivatives exchange....	275
7.3.3 ¹ H-NMR spectra for <i>Knoevenagel</i> and imine (C=C/C=N) Exchange Processes.....	276
7.4 Chapter 4 , Dynamic Covalent Chemistry of Nucleophilic Substitution Component Exchange of Ammonium Salts.....	281
7.4.1 Synthesis and Characterization.....	281
7.4.2 Kinetic Study for Ammonium salt exchange with tertiary Amines.....	287
7.5 Chapter 5 , Thermodynamic and Kinetic Selection of imine formation in Dynamic Covalent chemistry.....	305
7.5.1 Synthesis and Characterization.....	305
7.5.2 General procedures for the study of kinetic and thermodynamic experiments.....	308
7.5.3 Results of kinetic experiments for the imine formation study.....	309
7.5.4 ¹ H-NMR spectra of dynamic covalent libraries in the mixture Of one aldehyde with various amines.....	315
7.6 References.....	319
Publications and Conferences.....	323

Acknowledgements

First and foremost I would like to thank my supervisor, Prof. Jean-Marie Lehn, for giving me the great opportunity to pursue my PhD at the University of Strasbourg and for his close and excellent guidance throughout the past four years of my research. His enthusiastic and understanding approach gave me enormous inspiration and he taught me so many things not only concerning chemistry but also about French culture.

I would also like to thank Prof. Jack Harrowfield, for many valuable discussions and for carefully checking my manuscripts, making sure both the English and the chemistry were up to scratch. I thank Dr. Jean-Louis Schmitt for his help in the laboratory, particularly with NMR spectroscopy, and also for checking the experimental sections of my manuscripts. I would particularly like to thank Dr. James Hutchison who supported me in many ways, including cheering me up during the difficult days of thesis writing.

I would like to express my gratitude to my parents (Mr. Wiriya Kulchat and Mrs. Nantawan Kulchat), my lovely brother (Mr. Siripong Kulchat), and my extended family for their encouragement, love, and support, without which I could never have begun my French adventure.

I would like to thank all my current and former colleagues in Prof. Lehn's group, particularly Dr. Nadine Wilhelms who taught me how to conduct lab work when I first arrived in Strasbourg in late September 2011, Dr. Petr Kovaříček who helped me with kinetics and NMR experimental analysis amongst many other discussions, and Dr. Lars Ratjen and Dr. Lutz Greb for their valuable assistance in completing projects. I must not forget to thank Qing-Yuan, Rafel, the warm grandfather, Anne, with her nice smile, Katerina and her nice teas, Annie for her kindness, Gaël for being a wonderful colleague and brother, and most of all, Ghislaine who stayed with me in lab 515 for three years, invited me to many social events, and translated endless French documents for me.

There are many more recent colleagues who I very much appreciate, Jan, who always makes me laugh, Karolina, a very kind colleague, Sebastien, Michel, Martin, Men, Mihail, Li-Yuan, Antonio for his Gaussian calculation experience, Annia for her help, and Sawsen for her kindness.

I must specially thank the people who proof-read my thesis, Dr. Ghislaine Vantomme for the French Résumé, Prof. Jack Harrowfield, Dr. James Hutchison, Dr. Nema Hafezi, and Dr. Kanchit Rongchai.

I am very grateful to Jacline for all her kindness and great help with visa and other documents throughout my stay in France.

I would like to say ‘Chok-dee’ to all of my Thai friends who live in Strasbourg and who supported me in so many ways, P’ Fair, P’ Nan, P’ Yimmy, P’ Sae, N’ Taddy, P’ Toon, P’ Paew, P’Pim, P’ Pekky. I will see you all at home soon!

Finally, I would like to acknowledge Khon Kaen University in Thailand, the Franco-Thai Scholarship program, and Prof. Jean Marie Lehn, for their financial support without which these studies would not have been possible. I acknowledge also, the Junior Science Talent Project (JSTP) in Thailand for guiding me on to a scientific pathway since I was 16 years old.

Thank you very much, everybody!

Sirinan (Tum) Kulchat

“If we knew what it was we were doing, it would not be called research, would it?”

Albert Einstein

Abstract

This thesis is divided into seven chapters describing the Dynamic Covalent/Combinatorial Chemistry (DCC) of imine/imine exchange ($C=N/C=N$), imine/*Knoevenagel* exchange ($C=N/C=C$), *Knoevenagel/Knoevenagel* exchange ($C=C/C=C$), and quaternary ammonium salts/amine exchange in the presence and absence of an appropriate catalyst. In addition, the kinetic and thermodynamic selectivity of imine formation is described in the last part of this thesis.

The first chapter provides a general overview of Constitutional Dynamic Chemistry (CDC) involving the concept of Dynamic Covalent/Combinatorial Chemistry (DCC). In particular, the reversibility of imine formation and the concept of imine exchange reactions are evaluated. The *Knoevenagel* condensation, a major focus of this thesis, is also analyzed in detail along with consideration of the nature of organocatalysis of these reaction types. Possible directions of further research in these areas are presented.

The second chapter describes organocatalysis of reversible exchange of components between imine/imine ($C=N/C=N$), *Knoevenagel*/imine ($C=C/C=N$), and *Knoevenagel/Knoevenagel* ($C=C/C=C$) exchanges in DCC. Several organocatalysts were investigated and the results showed that only L-proline proved to be a broadly useful catalyst allowing true equilibria to be attained. The crucial factors for fast imine/imine exchange were found to be the structure of the imines, the solvent, and the catalyst. Imines found to undergo exchange were those derived from nucleophilic aliphatic amines and electrophilic heteroaromatic aldehydes (2-pyridyl, 4-pyridyl, and 2-thiophene aldehydes) as from salicyl-aldehyde. The optimal catalytic amounts, solvent, and temperature, are 10 mol% L-proline, DMSO- d_6 /D₂O 99/1 and room temperature. In addition, 10 equiv of BIS-TRIS was added in order to avoid contributions from acid catalysis. With this knowledge in hand, a number of [2 × 2] imine libraries were explored. For each pair of imines, both the forward and reverse reactions were followed with and without added L-proline as a catalyst. The imine exchange processes were found to obey reversible first order reaction kinetics and, in most cases, reached a true equilibrium. With a 10 mol% catalyst loading, an acceleration of the $C=N/C=N$ exchange up to about 22-fold was achieved. In contrast, the $C=C/C=N$ interconversion of *Knoevenagel* substrates and imines could not be studied under similar conditions, as extensive hydrolysis was found to occur.

Conducting the reactions in pure DMSO- d_6 greatly reduced hydrolysis (less than 10 %) and C=C/C=N exchange took place, displaying marked acceleration by 10 mol% L-proline addition up to about 22-fold. Compounds bearing electron-donating substituents gave the least hydrolysis in the cross-exchange. Moreover, L-proline was able to accelerate the rate of cross-*Knoevenagel* C=C/C=C exchange up to about 89-fold with Michael-type adducts formed during the cross exchange process. The %-composition of products at equilibrium depended on the electron affinity of the starting substrates.

The third chapter describes DCC of benzylidene/imine (C=C/C=N) exchange processes involving *N,N'*-dimethyl barbituric acid. The exchange reactions were investigated in CDCl₃ due to the high solubility of all the substrates in that solvent. The results showed that the C=C/C=N exchange between imines and *Knoevenagel* derivatives of *N,N'*-dimethylbarbiturate is fast and reversible in CDCl₃ solution at room temperature in the absence of catalyst. This feature provides an efficient means for diversity generation via C=C/C=N exchange. It may also signify a change in mechanism to a metathesis-like process, perhaps via an azetidine intermediate. In addition, the formation of gels by this type of *Knoevenagel* compound was initially investigated by employing different solvent systems and some compounds were found to form a gel in EtOH or MeOH. A gel selection study was performed based on C=C/C=N exchange and it was found that the exchange reaction between the *Knoevenagel* and imine proceeded. The results described herein enable the creation of DCLs of higher chemical diversity, thus allowing for the generation by DCC of receptors, dynamic polymers, functional materials or biomaterials of increased complexity.

In the fourth chapter, the generation of DCLs based on nucleophilic substitution component exchange of quaternary ammonium salts is described. The exchange reactions are based on a quaternary allyl ammonium salt undergoing nucleophilic substitution reactions with the anion composing the ion pair to give a tertiary amine and allyl halide. The mechanism can be considered to proceed by either direct S_N2/S_N2' and indirect S_N2/S_N2' pathways. DCLs based on the nucleophilic substitution reaction between quaternary allyl ammonium salts and derivatives of tertiary amines were also generated. The capacity of various ammonium salts to participate in such exchange reaction processes in the presence of several tertiary amines (aliphatic or aromatic tertiary amines) was evaluated, both in the absence and in the presence of a nucleophilic catalyst. All of the exchange reactions between ammonium salts and aliphatic tertiary amines were

irreversible. However, the exchange reactions between ammonium salts and aromatic tertiary amines were reversible and under thermodynamic control. The acceleration in reaction rate by equimolar iodide ions addition was demonstrated to be ca. 2-fold. Moreover, the nucleophilic substitution exchange processes by the S_N2 mechanism were investigated between *N*-benzyl-*N,N*-dimethylanilinium salts and aromatic tertiary amines. The influence of counter-anions was also investigated for both a quaternary allyl ammonium salt and a quaternary benzyl ammonium salt by using PF_6^- or OTf as counter-anions. The exchange rate was found to be slower with constituents possessing these counter-anions rather than those ones with bromide counterions. To further expand DCLs generated by nucleophilic substitution processes (S_N2 and S_N2' types), the exchange reactions between pyridinium salts and derivatives of pyridine were studied by the use of microwave irradiation. All of the reactions are reversible and under thermodynamic control. Some of the pyridinium salts which constitute these dynamic libraries are known as ionic liquids, thus, we sought to generate ionic liquid dynamic libraries either in or in the absence of solvent. This approach has remarkably extended dynamic covalent chemistry, facilitating the formation of more dynamic libraries and allowing for new diversity generation.

In the fifth chapter is described studies of the kinetic and thermodynamic selectivity of imine formation in DCC. The degree of imine formation between different aldehydes and amines (primary amine, hydrazine, hydrazide and aminoxy compounds) was studied, both in aqueous solution and in an organic solvent. In addition, the competitive reactions amongst different amines to form different imines in a single system were studied in order to delineate the reactivity of amines and stability of imine constituents for DCL generation in both aqueous solutions and organic solvents. The imine formation was determined at various pD values (5.0, 8.5 and 11.4) in phosphate buffer (for sulfonate aldehyde and pyridoxal phosphate) and in organic solvent (for 2-pyridyl aldehyde and salicylaldehyde). The complete DCL of one aldehyde such as sulfonate aldehyde or pyridoxal phosphate with four different amines shows that the thermodynamically stable product is an oxime at low pD, and a hydrazone at high pD. The formation of the DCL from 2-pyridyl aldehyde with the different amines showed that the kinetic product was an imine derived from pentylamine while the thermodynamically preferred products were imines derived from *O*-benzylhydroxylamine, benzhydrazide, and phenylhydrazine. Furthermore, for the DCL derived from salicylaldehyde and different amines, the kinetic product was an imine

derived from pentylamine and the thermodynamic products were imines derived from *O*-benzylhydroxylamine, and phenylhydrazine. The insights gained from these experiments could be applied to other DCC systems and could provide a basis for the search for structural stability of imines under different conditions. It could also be applied for regioselective transformation of one molecule possessing different functional groups in order to select different products based on kinetic or thermodynamic selectivity.

Chapter six describes the general conclusions drawn from each chapter. Chapter seven provides the experimental section describing the synthesis and characterization of all compounds used in this thesis. Also, an analysis of the kinetic treatment of imine/imine and quaternary ammonium/tertiary amine exchange reactions is provided.

บทคัดย่อ

งานวิจัยนี้มีจุดมุ่งหมาย เพื่อที่จะศึกษาเกี่ยวกับการสร้างฐานข้อมูลของสารประกอบแบบไดนามิก แบบพันธะโควาเลนต์ ระหว่างสารประกอบ อิมมีนกับอิมมีน ($C=N/C=N$) คโนเวนาเกลกับอิมมีน ($C=C/C=N$) คโนเวนาเกลกับคโนเวนาเกล ($C=C/C=C$) โดยผ่านปฏิกิริยาผันกลับได้และมีการแลกเปลี่ยนหมู่ฟังก์ชันระหว่างสารประกอบ โดยใช้ กรดอะมิโนชนิด แอล-โพรลีน เป็นตัวเร่งปฏิกิริยาการแลกเปลี่ยน ทั้งนี้ปฏิกิริยาการแลกเปลี่ยนระหว่างสารประกอบคโนเวนาเกลกับอิมมีน โดยใช้สารประกอบคโนเวนาเกลที่สังเคราะห์จากกรดไคเมทิลบาบิทูริก พบว่าปฏิกิริยาการแลกเปลี่ยนสามารถเกิดได้ที่อุณหภูมิห้องโดยไม่ต้องใช้ตัวเร่งปฏิกิริยาใดๆทั้งสิ้น นอกจากนี้ยังได้ศึกษาเกี่ยวกับการสร้างฐานข้อมูลของสารประกอบแบบไดนามิก ของสารประกอบเกลือควอเตอร์นารีแอมโมเนียมแคทไอออน โดยผ่านปฏิกิริยาผันกลับได้ของการแทนที่แบบนิวคลีโอฟิลิก (S_N2' และ S_N2) ของเกลือควอเตอร์นารีแอมโมเนียม และเทอเชียรีเอมีน ในการทำปฏิกิริยาที่อุณหภูมิ 60 องศาเซลเซียส ซึ่งจะทำให้เกิดสารผสมที่ถูกควบคุมทางเทอร์โมไดนามิกและคิเนติกของสารประกอบควอเตอร์นารีแอมโมเนียมและเทอเชียรีเอมีน โดยใช้ไอโอดีนเป็นตัวเร่งปฏิกิริยาแบบนิวคลีโอฟิลิก และยังได้ใช้คลื่นไมโครเวฟเป็นตัวช่วยในการเร่งปฏิกิริยาการแลกเปลี่ยนระหว่างเกลือฟิรดินีแอมโมเนียมและอนุพันธ์ของฟิรดินี นอกจากนี้ได้มีการทดลองเกี่ยวกับการทำให้เกิดของเหลวไดนามิกไอออน ท้ายสุดเป็นการศึกษาการเกิดขึ้นของสารประกอบอิมมีน โดยผ่านวิธีการศึกษาแบบคิเนติกและเทอร์โมไดนามิก พบว่า สารประกอบอิมมีนแบบ ผลิตภัณฑ์คิเนติกและผลิตภัณฑ์เทอร์โมไดนามิกในระบบสารละลายเอเควีเอส คือสารประกอบออกซิมและไฮดราโซน ส่วนการเกิดขึ้นของสารประกอบ อิมมีนแบบผลิตภัณฑ์คิเนติก ในระบบที่ใช้ตัวทำละลายอินทรีย์คือ อิมมีนที่สังเคราะห์จากไพรมารีเอมีน และสารประกอบแบบผลิตภัณฑ์เทอร์โมไดนามิกคือ สารประกอบออกซิมและไฮดราโซน

Abbreviations

Å	Angström, 10^{-10} m
BIS-TRIS	2-Bis(2-hydroxyethyl)amino-2-(hydroxymethyl)-1,3-propanediol
B3LYP	Becke,3-parameter, Lee-Yang-Parr
C=C	<i>Knoevenagel</i> compound
C=N	Imine compound
CD ₂ Cl ₂	Deuterated dichloromethane
CD ₃ CN	Deuterated acetonitrile
CD ₃ OD	Deuterated methanol
CDC	Constitutional Dynamic Chemistry
CDCl ₃	Deuterated chloroform
CH ₂ Cl ₂	Dichloromethane
CH ₃ CN	Acetonitrile
CHCl ₃	Chloroform
COSY	Correlation spectroscopy
d	In NMR, doublet
D ₂ O	Deuterium oxide
DCC	Dynamic Covalent/Combinatorial Chemistry
DCL	Dynamic Covalent Library
dd	In NMR, doublet of doublet
DFT	Density Functional Theory
DMSO	Dimethyl sulfoxide
DMSO- <i>d</i> ₆	Deuterated dimethyl sulfoxide
EDG	Electron Donating Group
equiv	Equivalent
ESI	Electrospray Ionization
EtOAc	Ethyl acetate
EtOH	Ethanol
EWG	Electron withdrawing group
h	Hour
HRMS	High resolution mass spectroscopy

<i>k</i>	Rate constant
kcal	Kilocalories
K_{eq}	Equilibrium constant
LMWGs	Low molecular weight gelators
M	Molarity (mol L ⁻¹)
m	In NMR, multiplet
MeOH	Methanol
MgSO ₄	Magnesium sulfate
MHz	Megahertz (10 ⁶ Hertz)
min	Minute
mL	Milliliter, 10 ⁻³ litre
μL	Microliter, 10 ⁻⁶ litre
mM	Millimolar, 10 ⁻³ mol L ⁻¹
m.p.	Melting point
μm	Micrometre, 10 ⁻⁶ metre
MS	Mass spectrometry
MW	Microwave irradiation
nm	Nanometer, 10 ⁻⁹ metre
NMR	Nuclear Magnetic Resonance
NOESY	Nuclear Overhauser Effect Spectroscopy
OTf	Trifluoromethanesulfonate
PF ₆ ⁻	Hexafluorophosphate (V)
pH	Power of hydrogen
ppm	Part per million
q	In NMR, quartet
quint	In NMR, quintet
r.t.	Room temperature
s	In NMR, singlet
S _N 2	Bimolecular nucleophilic substitution
t	In NMR, triplet
<i>t</i> _{1/2}	Half-life
TBAF	Tetrabutyl ammonium fluoride

TBAI	Tetrabutyl ammonium iodide
TEAI	Tetraethyl ammonium iodide
TS	Transition state
UV-Vis	Ultra-violet-visible spectroscopy
W	Watt

Résumé

La Chimie Dynamique Constitutionnelle (CDC) implique la recombinaison dynamique de composants moléculaires liés par des interactions non covalentes ou des liaisons covalentes réversibles. Ces dernières années, la Chimie Covalente Dynamique (CCD) a émergé comme une approche puissante pour créer des bibliothèques dynamiques de composants afin d'analyser leur diversité structurelle. L'analyse de ces Bibliothèques Covalentes Dynamiques (BCDs) fournit de nouvelles perspectives dans l'élaboration de récepteurs, la découverte de médicaments, la résolution dynamique, l'auto-triage, la catalyse, la détection et pour des aspects variés de la science des matériaux. Des exemples représentatifs de réactions réversibles compatibles avec le concept de CCD comprennent les condensations amine/carbonyle, les transestérifications, les échanges de disulfures, les échanges de peptides, les échanges imine/*Knoevenagel*, les échanges *Knoevenagel/Knoevenagel*, la formation d'esters boroniques, la métathèse des oléfines et la condensation de Diels-Alder. Pour étendre davantage l'envergure de la CCD, un effort continu est réalisé pour découvrir de nouvelles BCDs réversibles ayant davantage de diversité structurelle, chimique, et de complexité. Le travail décrit ici est une contribution à ces développements.

Cette thèse est divisée en sept chapitres décrivant la CCD de systèmes imine/imine ($C=N/C=N$), imine/*Knoevenagel* ($C=N/C=C$), *Knoevenagel/Knoevenagel* ($C=C/C=C$), sels d'ammonium quaternaire/amine et leurs procédés d'échange de constituants en présence et en absence d'un catalyseur approprié. De plus, la sélectivité cinétique et thermodynamique de la formation d'imines est décrite dans le dernier chapitre de cette thèse.

Le chapitre un fournit une vue générale de la CDC impliquant le concept de Chimie Covalente Dynamique/ Combinatoire Dynamique (CCD). En particulier, la réversibilité de la formation d'imines et le concept de réactions d'échange d'imines sont évalués. La condensation de *Knoevenagel*, un point majeur de cette thèse, est aussi analysée en détails en considérant la nature de l'organocatalyseur de ce type de réaction. Les directions possibles pour d'autres recherches dans ce domaine sont aussi présentées.

Le chapitre deux décrit l'organocatalyse des échanges de $C=N/C=N$ et $C=C/C=N$, $C=C/C=C$ dans la CCD. L'organocatalyse par l'utilisation d'amines secondaires, via les intermédiaires amina et iminium, a été activement étudiée ces dernières années dans le but de faciliter les procédés de condensation de carbonyle, comme les réactions de *Knoevenagel* et les aldolisations. La réaction de *Knoevenagel* est la condensation d'un composant contenant un groupe méthylène actif comme un β -cétoester ou un malonate avec un aldéhyde ou une cétone en présence d'une amine secondaire, résultant en la formation d'une liaison $C=C$. Les catalyseurs amines secondaires les plus communément utilisés sont la piperidine, la sarcosine, la proline et leurs dérivés, cette dernière étant largement utilisée pour l'organocatalyse asymétrique. Récemment, la rapide réversibilité des procédés condensation/hydrolyse dans l'interconversion (amine+carbonyle)/imine a été largement développée pour des applications en CCD, et un des buts majeurs a été de réaliser des échanges de composants rapides, afin d'obtenir une réponse rapide à un stimulus appliqué. Considérant que les avantages des composants *Knoevenagel* ont déjà été appliqués en chimie médicinale et en science des matériaux, la mise en œuvre de l'organocatalyse dans les BCDs de *Knoevenagel* offre des possibilités pour étendre la portée des procédés d'échange et améliorer leur versatilité.

Les procédés de CCD décrits dans ce chapitre impliquent l'échange réversible de composants entre les constituants imines (échange imine/imine, $C=N/C=N$), les constituants *Knoevenagel* et imine (échange $C=C/C=N$) ainsi que les constituants benzylidènes (échange $C=C/C=C$) et contiennent une étude sur la capacité d'amines secondaires sélectionnées, comme la L-proline, à catalyser ces réactions. Une attention particulière a été portée aux échanges $C=C/C=N$ pour la diversité des systèmes dans lesquels ils peuvent être impliqués.

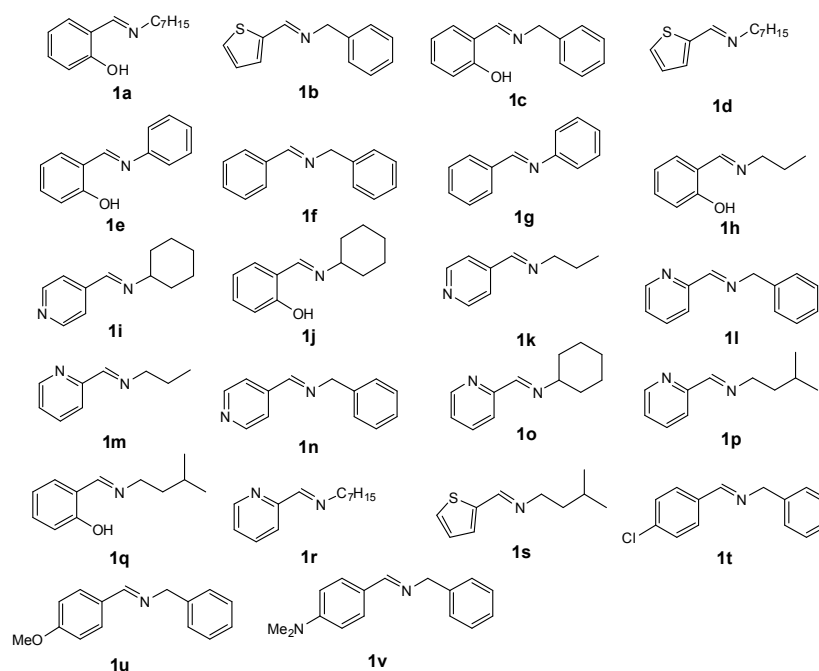


Figure 1 Structures des différentes imines utilisées dans les échanges imine/imine ($C=N/C=N$) et les échanges imine/Knoevenagel ($C=N/C=C$)

Dans cette étude, les réactions en présence de L-proline protégée en *N*-Boc, de L-proline *t*-butyle ester, de L-proline et d'acide benzoïque ont été comparées dans les mêmes conditions en présence et en absence de catalyseurs. Seule la L-proline a prouvé être un catalyseur largement utilisé permettant d'atteindre des équilibres. Les facteurs cruciaux pour l'échange rapide imine/imine ont été déterminés comme étant la structure des imines, le solvant et le catalyseur. Les imines qui s'échangent sont celles dérivées des amines aliphatiques nucléophiles et des aldéhydes hétéroaromatiques électrophiles (les 2-pyridyle, 4-pyridyle, et 2-thiophényle-carboxaldéhyde) ainsi que le salicylaldéhyde (Figure 1, **1a-d, h-s**). Les quantités optimales de catalyseur, de solvant et de température sont 10mol% de L-proline, dans le DMSO- d_6 /D₂O 99/1 et à température ambiante. De plus, 10 equiv. de BIS-TRIS ont été ajoutés pour éviter les contributions des catalyseurs acides.

Un certain nombre de bibliothèques d'imines [2x2] a été exploré (Table 1). Pour chaque paire d'imines, à la fois les réactions aller et retour ont été suivies avec et sans addition de L-proline comme catalyseur. Les procédés d'échange d'imines suivent une cinétique de réaction réversible de premier ordre et, dans la plupart des cas, atteignent un équilibre. Les études cinétiques conduisent à une vitesse calculée et aux constantes d'équilibre listées dans la Table 1. Avec un chargement en catalyseur de 10mol%, l'échange $C=N/C=N$ a été accéléré environ 22 fois (Table 1, Entrée 4).

Table 1 Réactions d'échange imine/imine dans des bibliothèques d'imines [2×2] avec l'organocatalyseur 10 mol% L-proline dans une solution de DMSO-*d*₆/D₂O 99/1, 10 equiv. BIS-TRIS à température ambiante (t.a.).

Entrée ER ^{a)}	A ^{a)}	B ^{a)}	C ^{a)}	D ^{a)}	b)	<i>k</i> _b ^{c)}	<i>k</i> _c ^{d)}	<i>K</i> _b ^{e)}	<i>K</i> _c ^{f)}	Acc ^{g)}
1	1h+1i ↕ 1j+1k	n-Propyle 	c-Hexyle 		f	0.0274	0.0761	1.18	1.18	2.8
					r	0.0233	0.0642			2.8
2	1h+1l ↕ 1c+1m	n-Propyle 	Benzyle 		f	0.0371	0.1239	0.46	0.52	3.3
					r	0.0811	0.2370			2.9
3	1i+1l ↕ 1n+1o	c-Hexyle 	Benzyle 		f	0.0080	0.0650	n.d. ^{j)}	2.70	8.1
					r	0.0008 ^{h,i)}	0.0241 0.0098 ⁱ⁾			12.3
4	1c+1d ↕ 1a+1b	n-Heptyle 	Benzyle 		f	0.0057	0.0759	n.d. ^{j)}	0.48	10.6
					r	0.0022 ^{h,i)}	0.1597 0.0472 ⁱ⁾			21.5
5	1p+1d ↕ 1r+1s	i-Pentyle 	n-Heptyle 		f	0.0387	0.3131	0.83	0.65	8.1
					r	0.0466	0.4854			10.4

^{a)} ER = réaction d'échange, A-D: substituents des imines étudiées. ^{b)} f = réaction aller; r = réaction retour. ^{c)} *k*_b = constante de vitesse de la réaction de contrôle [10⁻³ s⁻¹]. ^{d)} *k*_c = constante de vitesse de la réaction catalysée [10⁻³ s⁻¹]. ^{e)} *K*_b = constante d'équilibre de la réaction de contrôle = *k*_b (aller)/*k*_b (retour). ^{f)} *K*_c = constante d'équilibre de la réaction catalysée = *k*_c (aller)/*k*_c (retour). ^{g)} Acc. = Accélération = *k*_c/*k*_b; ^{h)} La réaction n'a pas atteint l'équilibre. ⁱ⁾ La constante de vitesse est calculée à partir des premiers 10% de la réaction. ^{j)} n.d. = non déterminé. Erreur sur l'intégration du signal ¹H-RMN, ~4-5%.

Les études sur les échanges imine/imine ont été étendues à des bibliothèques dynamiques [3x3] (Figure 2), catalysées par 10 mol% de L-proline dans DMSO-*d*₆/D₂O 99/1 et à température ambiante. Les résultats ont été comparés avec la bibliothèque de constituants [2x2]. Cette plus grande bibliothèque atteint l'équilibre à approximativement la même vitesse que la plus rapide des trois petites bibliothèques.

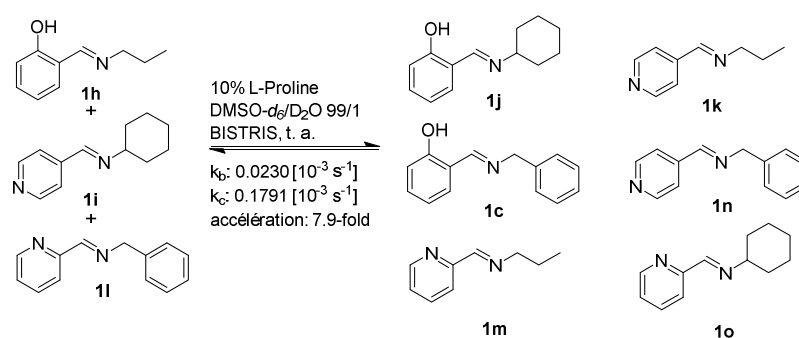


Figure 2 Echange d'imines sélectionnées dans une bibliothèque d'imines [3x3] - Application de l'organocatalyse à de plus grande bibliothèque pour augmenter la diversité.

Le mécanisme proposé de la réaction d'échange catalysée par la proline implique une attaque nucléophile de la L-proline sur l'imine pour former un aminal, lequel peut ensuite réaliser une élimination pour donner un intermédiaire zwitterionique hautement réactif (*Figure 3*). Cette espèce, bien plus réactive que le simple composé carbonyle qui peut être formé par hydrolyse, réalise une attaque rapide avec une amine libre pour donner un nouvel aminal qui ensuite élimine la L-proline pour former une nouvelle imine, complétant ainsi l'échange et la libération du catalyseur.

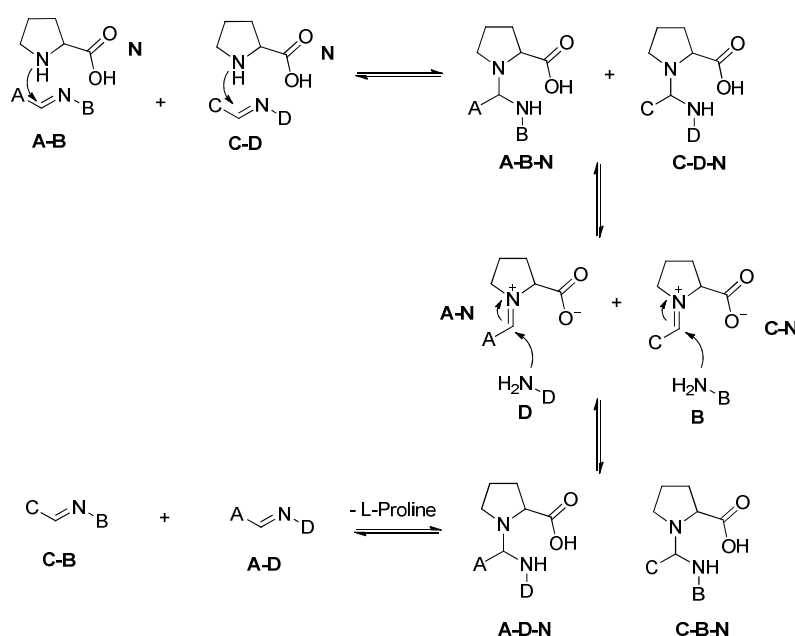
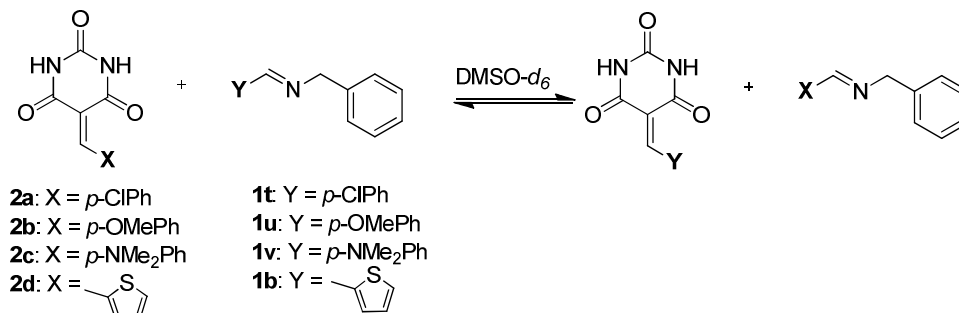


Figure 3 Le mécanisme proposé pour l'organocatalyse de l'échange C=N/C=N.

Forts de l'utilisation réussie de l'organocatalyse pour la génération de BCDs d'imines, son extension à d'autres réactions apparentées a été étudiée. En particulier, l'échange $C=C/C=N$, impliquant deux types différents de liaisons doubles, est considérablement prometteur pour former des bibliothèques dynamiques de grande diversité. La condensation donnant des dérivés de barbiturates de benzylidène a donc été étudiée dans le but de réaliser des procédés d'échanges réversibles. Les barbiturates de benzylidène **2a-2d** et les imines **1b, t-v**, comme montré dans la *Table 2*, ont été choisis comme substrats. Les réactions ont été réalisées en utilisant des quantités équimolaires de dérivées de benzylidène et de composants imines (19.35 mM chacun) dans un mélange de DMSO- d_6 /D $_2$ O 99/1 à 60°C avec 10 mol% de L-proline comme organocatalyseur. Comme pour l'étude sur les échanges $C=N/C=N$ mentionnés précédemment, les réactions ont été conduites avec l'addition de 1% de D $_2$ O, mais sans tampon de BIS-TRIS à cause de l'hydrolyse rapide des benzylidènes dans ces conditions. A la fois les réactions aller et retour ont été suivies par spectroscopie 1H -RMN. En comparaison avec l'échange $C=N/C=N$, une plus grande température fut nécessaire pour obtenir des vitesses de réaction comparables.

Tout d'abord, pour la réaction dans DMSO- d_6 /D $_2$ O 99/1 à 60°C, une grande quantité de produits d'hydrolyse (~20%) a été observée. Dans le but d'éviter, ou du moins de réduire la quantité d'hydrolyse, les réactions d'échange ont été ensuite réalisées en présence de moins d'eau. La réaction entre **2b** et **1v** a été réalisée avec 0.5% (DMSO- d_6 /D $_2$ O 99.5/0.5) ainsi qu'avec 0.2% (DMSO- d_6 /D $_2$ O 99.8/0.2) d'eau ajoutée. Les produits **2c** et **1u** ont été obtenus dans ces conditions (en moyenne 20% chacun), mais une hydrolyse significative était toujours observée. Dans le but de réduire davantage la quantité de produits d'hydrolyse, toutes les réactions d'échange furent réalisées dans le DMSO- d_6 pur à 60°C, avec les produits d'échange observés en présence de moins de 10% de produits d'hydrolyse. Les résultats sélectionnés sont décrits dans la *Table 2*. Pour chaque cas, les compositions des mélanges sont données à un temps de réaction pour lequel aucun changement dans la distribution des composants a été détecté par intégration des signaux des spectres RMN pour des temps plus longs.

Table 2 Les réactions d'échange sélectionnées catalysées par la L-proline entre un ensemble de produits Knoevenagel/imine. Les proportions (%) des différents composés dans les réactions d'échange C=C/C=N entre les barbiturates de benzylidène et les imines dans le DMSO-*d*₆ à 60°C. **h** = 4-méthoxybenzaldéhyde, **i** = 4-(diméthylamino)benzaldéhyde, **m** = 4-méthoxybenzaldéhyde hydraté, **n** = 4-(diméthylamino)benzaldéhyde hydraté.



Entrée a)	Temps réaction [h]	Distribution de composés [%]							
		Composés de départ 2b + 1v							
		2b	1v	2c	1u	h	i	m	n
1b	0	50	50	- ^{b)}	- ^{b)}	- ^{b)}	- ^{b)}	- ^{b)}	- ^{b)}
	2	50	50	<1 ^{c)}	<1 ^{c)}	<1 ^{c)}	<1 ^{c)}	<1 ^{c)}	- ^{b)}
	22	7	12	34	33	7	3	4	- ^{b)}
1c	0	50	50	- ^{b)}	- ^{b)}	- ^{b)}	- ^{b)}	- ^{b)}	- ^{b)}
	2	5	9	32	33	8	7	6	- ^{b)}
		Composés de départ 2c + 1u							
		2c	1u	2b	1v	h	i	m	n
2b	0	50	50	- ^{b)}	- ^{b)}	- ^{b)}	- ^{b)}	- ^{b)}	- ^{b)}
	2	49	49	1	1	<1 ^{c)}	<1 ^{c)}	<1 ^{c)}	- ^{b)}
	24	39	39	7	10	3	<1 ^{c)}	2	- ^{b)}
2c	0	50	50	- ^{b)}	- ^{b)}	- ^{b)}	- ^{b)}	- ^{b)}	- ^{b)}
	2	34	32	4	12	7	5	6	- ^{b)}

^{a)} b, réaction de contrôle, et c, réaction catalysée avec 10 mol% de L-proline comme catalyseur. ^{b)} Composé non observé. ^{c)} Seulement traces de produits détectés.

Le mécanisme proposé pour la réaction d'échange entre les substrats C=N et C=C en présence de L-proline implique des étapes séquentielles d'hydrolyse/condensation (Figure 4). La L-proline agit comme un nucléophile pour attaquer à la fois les centres imine et benzylidène, conduisant à la formation, via une élimination, d'un intermédiaire iminium hautement réactif une nouvelle fois. Les produits d'échange sont obtenus in fine par les condensations alternatives de l'anion barbiturique libéré et du benzylidène sur les aldéhydes libérés. Dans cette réaction, la formation d'hydrates des aldéhydes portant un groupe électro-attracteur supprime la formation du produit d'échange.

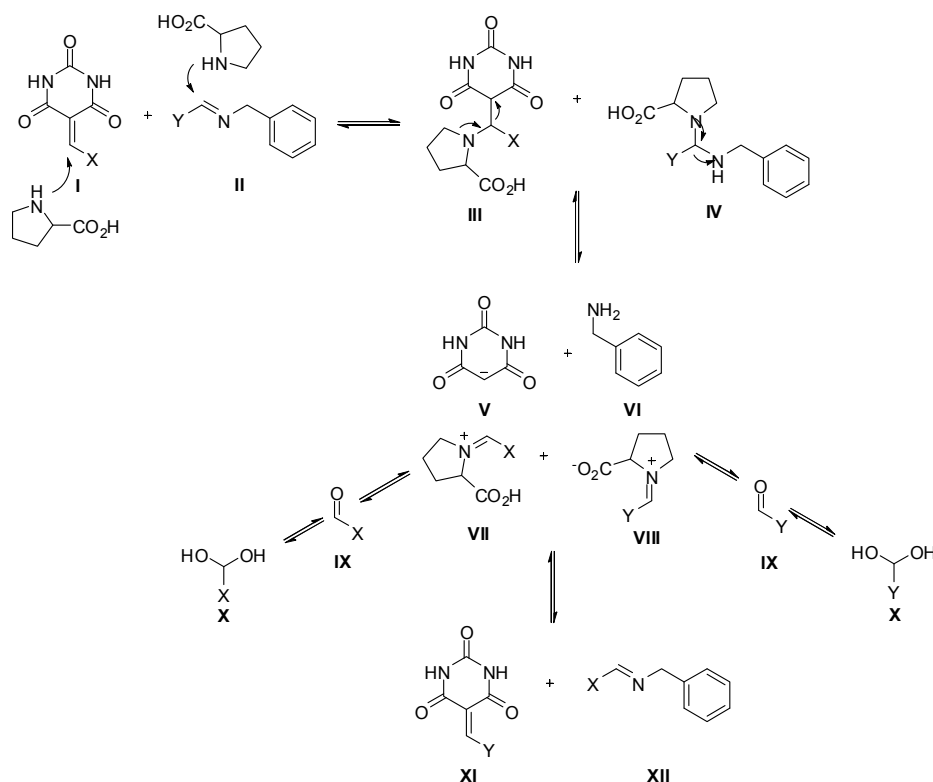
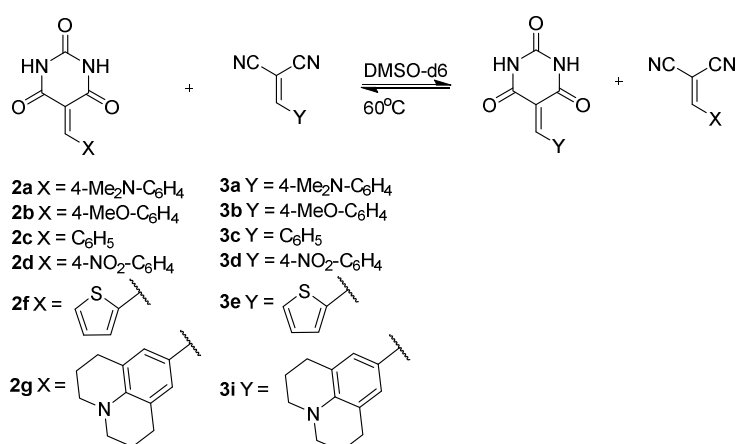


Figure 4 Le mécanisme possible de l'échange entre un substrat de type Knoevenagel ($C=C$) et une imine ($C=N$) suivant des étapes séquentielles d'addition/élimination.

Pour développer davantage les BCDs, les réactions d'échange benzylidène/benzylidène ($C=C/C=C$) entre barbiturates de benzylidène (**2a-d**, **2f-g**) et benzylidènes malononitriles (**3a-d**, **3i**) ont été étudiées. Les réactions ont été réalisées avec une quantité équimolaire de dérivés benzylidènes (12.8 mM chacun) dans le $DMSO-d_6$ pur, seul, ainsi qu'en présence de 10 mol% de L-proline. Les moments où la moitié des réactifs de départ est consommé (le premier temps de demi-vie, $t_{1/2}$) et les pourcentages des compositions des solutions obtenues sont listés dans la *Table 3*. Les paramètres d'équilibre n'ont pas été calculés, à cause de la quantité variable d'hydrolyse. Les résultats démontrent que la réaction d'échange entre les benzylidènes dépend du profil électronique des deux substrats. Des réactions secondaires, où l'adduit de type Michael se forme (voir *Figure 5*), ont été observées par spectroscopie de masse haute résolution. Dans cette étude, la L-proline utilisée comme organocatalyseur accélère efficacement l'échange, jusqu'à 89 fois (*Table 3*, *Entrée 4*).

Table 3 La sélection des transformations organocatalysées par la L-proline sur un ensemble de constituants Knoevenagel/Knoevenagel. Les paramètres cinétiques et thermodynamiques des réactions d'échange de Knoevenagel. Temps de demi-vie ($t_{1/2}$), (-) = réaction trop lente pour déterminer le paramètre, n.a. = non applicable. Proportions [%] des différents composés dans la réaction d'échange C=C/C=C entre barbiturate de benzylidène et benzylidène malononitrile dans le DMSO- d_6 à 60°C. **a** = 4-diméthylaminobenzaldéhyde, **d** = 4-méthoxybenzaldéhyde, **e** = 2-thiophène-carboxaldéhyde, **f** = 4-(diméthylamino)benzaldéhyde hydraté, **i** = 4-méthoxybenzal déhyde hydraté, **j** = thiophène-2-carboxaldéhyde hydraté, **B** = barbiturique, **M** = malononitrile, et **XI**, **XII** = adduits de type Michael.



Entrée a)	$t_{1/2}$ [h]	Temps réaction[h]]c)	Distribution de composés [%]											
			2a	3d	2d	3a	a	d	F	i	B	M	XI	XII
Composés de départ 2a + 3d														
1b	n.a.	23 ^{d)}	49	49	1	1	- ^{b)}	- ^{b)}	- ^{b)}	- ^{b)}	- ^{b)}	- ^{b)}	- ^{b)}	
	n.a.	488 ^{f)}	35	37	12	12	2	1	- ^{b)}	- ^{b)}	<1 ^{c)}	<1 ^{c)}	- ^{b)}	
1c	9	29	24	24	19	24	1	3	<1 ^{c)}	1	2	<1 ^{c)}	1	- ^{b)}
Composés de départ 2d + 3a														
2b	n.a.	95 ^{d)}	48	49	1	<1 ^{c)}	1	<1 ^{c)}	- ^{b)}	- ^{b)}	- ^{b)}	- ^{b)}	- ^{b)}	
	n.a.	533 ^{f)}	43	48	1	2	1	5	- ^{b)}	- ^{b)}	1	- ^{b)}	- ^{b)}	
2c	30	98	23	30	19	19	<1 ^{c)}	4	<1 ^{c)}	1	3	<1 ^{c)}	<1 ^{c)}	- ^{b)}
Composés de départ 2e + 3d														
3b	40	128	46	43	6	6	1	- ^{b)}	<1 ^{c)}	- ^{b)}	- ^{b)}	<1 ^{c)}	- ^{b)}	- ^{b)}
3c	2	6	43	40	6	7	2	- ^{b)}	<1 ^{c)}	- ^{b)}	1	1	1	- ^{b)}
Composés de départ 2d + 3e														
4b	180	532	8	8	42	40	2	- ^{b)}	- ^{b)}	- ^{b)}	1	<1 ^{c)}	- ^{b)}	- ^{b)}
4c	2	6	6	8	42	39	3	- ^{b)}	- ^{b)}	- ^{b)}	1	1	1	- ^{b)}

^{a)} b, réaction de contrôle, et c, réaction catalysée avec 10 mol% de L-proline comme catalyseur. ^{b)} Composé non observé. ^{c)} Seulement traces de produits détectés. ^{d)} La réaction au départ. ^{e)} Le temps de réaction indique le temps quand aucun changement supplémentaire n'est observé. ^{f)} La réaction n'a pas atteint l'équilibre. Toutes les mesures ont été répétées trois fois. La reproductibilité des valeurs obtenues est de $\pm 2\%$

Le mécanisme de la réaction d'échange proposé entre les composants C=C/C=C en présence de L-proline se déroule par un mécanisme similaire à celui proposé pour l'échange C=N/C=C (Figure 5). Ici, les composants benzylidène servent d'accepteur de Michael et réalisent une addition conjuguée par la L-proline pour remplacer les centres benzylidène, formant le même iminium réactif mentionné précédemment, qui facilite l'échange de composés. Ainsi les réactifs de départ ou les produits d'échanges dérivés de fonctions aldéhyde portant des groupes électro-attracteurs peuvent réagir avec le malononitrile anionique libéré pour donner des intermédiaires adduits de type Michael.

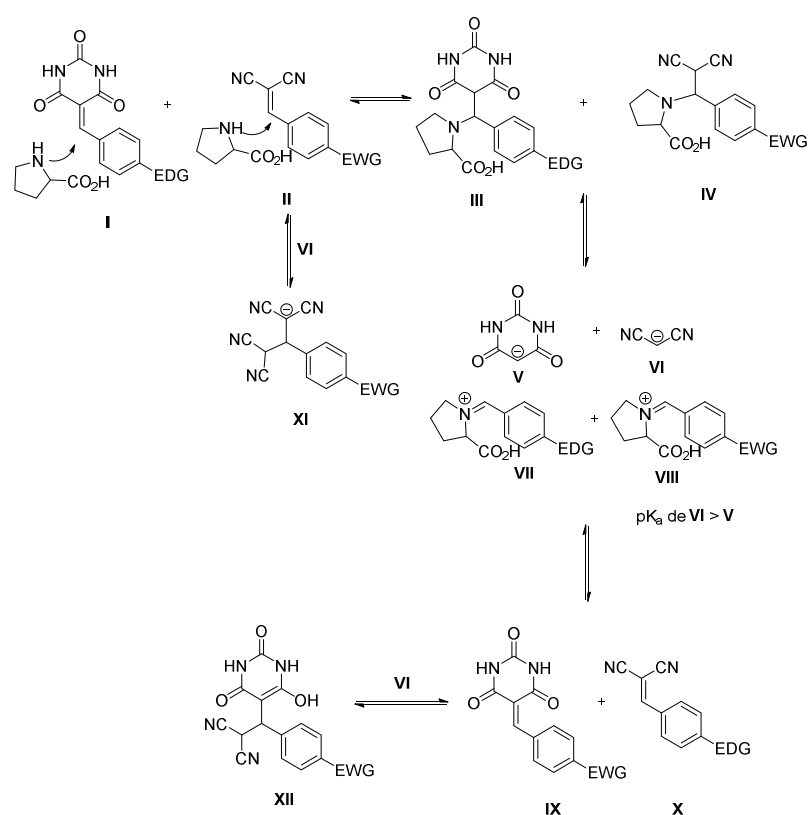


Figure 5 Mécanisme possible de la réaction d'échange entre les composés Knoevenagel suivant des étapes séquentielles d'hydrolyse/condensation.

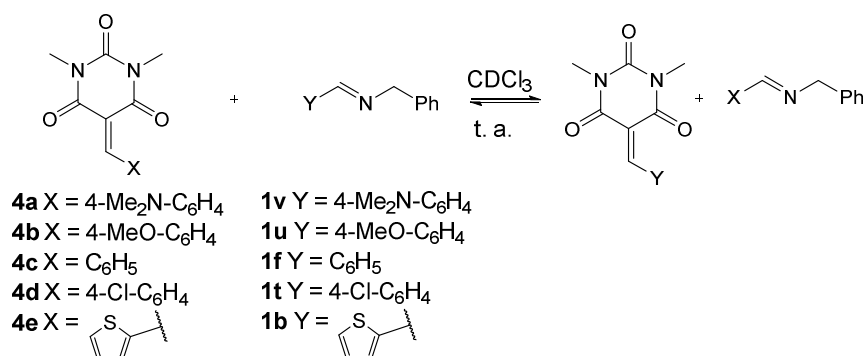
Les résultats décrits dans cette première section conduisent aux conclusions suivantes. (1) Une organocatalyse significative peut être réalisée par des procédés CCD. (2) L'amine secondaire, L-proline, est un organocatalyseur efficace capable d'accélérer les réactions d'échange d'imines jusqu'à environ 22 fois à température ambiante avec un chargement en catalyseur de 10 mol%. (3) Les imines dérivées d'amines aliphatiques/nucléophiles et d'aldéhydes très électrophiles sont apparues comme les

meilleurs composants de départ, donnant seulement de l'échange et pas de produits d'hydrolyse après la fin de la réaction. En revanche, les interconversions entre substrats *Knoevenagel* et imines $C=C/C=N$ n'ont pas pu être étudiées dans des conditions similaires, car beaucoup d'hydrolyse se forme. (4) La réalisation des réactions dans le DMSO- d_6 pur réduit grandement l'hydrolyse (moins de 10 %) et l'échange $C=C/C=N$ se déroule, exhibant une accélération marquée par la L-proline. (5) Les composants portant des substituants électro-donneurs donnent le moins d'hydrolyse dans les échanges. De plus, la L-proline est capable d'accélérer la vitesse de l'échange *Knoevenagel* $C=C/C=C$, et des adduits de type Michael sont formés durant le procédé d'échange. (6) La %-composition des produits à l'équilibre dépend de l'affinité électronique des substrats de départ.

Le chapitre trois décrit les échanges benzyldène/imine, $C=C/C=N$, impliquant l'acide *N,N'*-diméthylbarbiturique en CCD. Ici, des études précédentes ont été étendues pour l'échange $C=C/C=N$ entre les composants de *Knoevenagel* dérivés de l'acide 1,3-diméthylbarbiturique (**4a-4e**) et des mêmes composés imines (**1v**, **1u**, **1f**, **1t**, et **1b**) utilisés précédemment. La solubilité des composants de *Knoevenagel* a été analysée dans différents solvants et s'est avérée très élevée dans $CDCl_3$. Les réactions d'échange ont donc été réalisées dans $CDCl_3$ (filtré précédemment dans une colonne d'alumine basique pour retirer les traces fortuites de HCl qui peuvent causer de la catalyse acide) avec des quantités équimolaires de dérivés de diméthylbarbiturates de benzyldène et de composants imines (20 mM chacun). A la fois les réactions aller et retour ont été suivies par spectroscopie 1H -RMN. Au vue des vitesses rapides des réactions d'échange, les constantes de vitesse n'ont pas été obtenues, mais, les constantes d'équilibre ont été déterminées, et sont présentées dans la *Table 4*.

Les échanges $C=C/C=N$ entre les imines et les dérivées *Knoevenagel* du *N,N'*-diméthylbarbiturique sont rapides et réversibles dans une solution de $CDCl_3$ à température ambiante en absence de catalyseur, comme illustré en *Table 4*. Ce fait permet la formation efficace de diversité par échange $C=C/C=N$. Cela peut aussi signifier un changement dans le mécanisme pour un procédé plus proche de la métathèse, peut-être via un intermédiaire azétidine.

Table 4 La sélection de réactions d'échange Knoevenagel/imine. Les proportions [%] des différents composés dans les réactions d'échange C=C/C=N entre les diméthylbarbiturates de benzylidène et les imines dans CDCl₃ à température ambiante. **a** = 4-diméthylamino benzaldéhyde, **b** = benzaldéhyde, **c** = 4-nitrobenzaldéhyde, **d** = 4-méthoxybenzaldéhyde, et **e** = 2-thiophène-carboxaldéhyde.



Entrée	Composés de départ	de	Temps de réaction ^{c)} [min]	Distribution de composés [%]						K _{eq}	
				4a	1b	4e	1v	a	e		f
1	4a + 1b	f ^{a)}	68	22	21	28	29	<1 ^{c)}	- ^{d)}	- ^{d)}	2.5
	4e + 1v	r ^{b)}	69	18	17	33	32	<1 ^{c)}	- ^{d)}	- ^{d)}	
2	4b + 1f	f ^{a)}	2	13	14	37	36	<1 ^{c)}	<1 ^{c)}	- ^{d)}	7.3
	4c + 1u	r ^{b)}	2	13	14	37	36	<1 ^{c)}	<1 ^{c)}	- ^{d)}	
3	4b + 1b	f ^{a)}	60	6	4	44	45	- ^{d)}	- ^{d)}	- ^{d)}	92.1
	4e + 1u	r ^{b)}	13	5	4	46	45	<1 ^{c)}	- ^{d)}	- ^{d)}	
4	4b + 1v	f ^{a)}	11	9	7	43	42	<1 ^{c)}	- ^{d)}	- ^{d)}	30.4
	4a + 1u	r ^{b)}	3	7	8	45	41	<1 ^{c)}	- ^{d)}	- ^{d)}	

^{a)} f, Réaction aller. ^{b)} r, Réaction retour. ^{c)} Seulement traces de produits détectés. ^{d)} Composé non observé. ^{e)} Le temps de réaction indique le temps quand aucun changement supplémentaire n'est observé (<1-2%). Toutes les mesures ont été répétées 4-5 fois et moyennées. (Déviation standard <2%).

De plus, la formation de gels par ce type de composants *Knoevenagel* (**4f-4i**) a été initialement étudiée en utilisant différents systèmes de solvants (*Figure 6*). Les résultats montrent que **4f-4i** forment un gel dans l'éthanol, le méthanol, et l'acétonitrile, alors que **4i** et **4g** ne sont pas capables de former de gel dans l'acétonitrile et le méthanol, respectivement (en utilisant 1% w/v de gélificateur dans un solvant approprié).

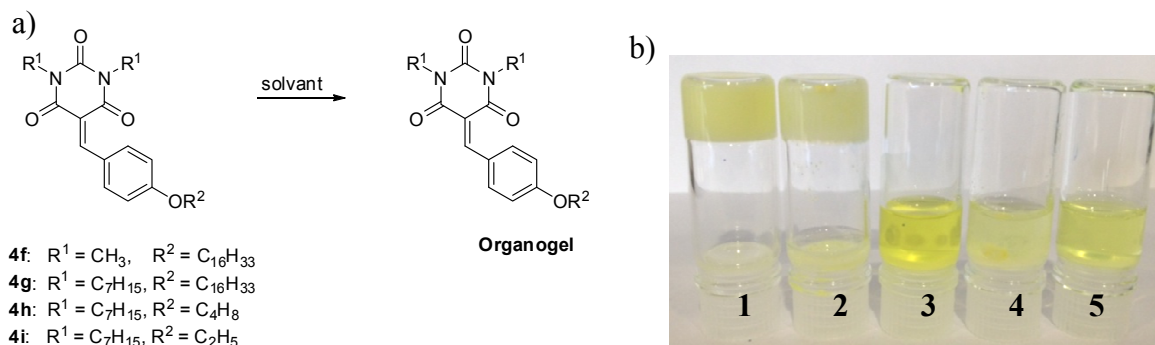


Figure 6 a) Représentation des composés barbiturates de benzylidène (**4f-4i**) utilisés dans l'étude de gel. b) La capacité de **4g** à former des gels ou non dans les solvants éthanol (1), acétonitrile (2), décanol (3), méthanol (4) et cyclohexane (5).

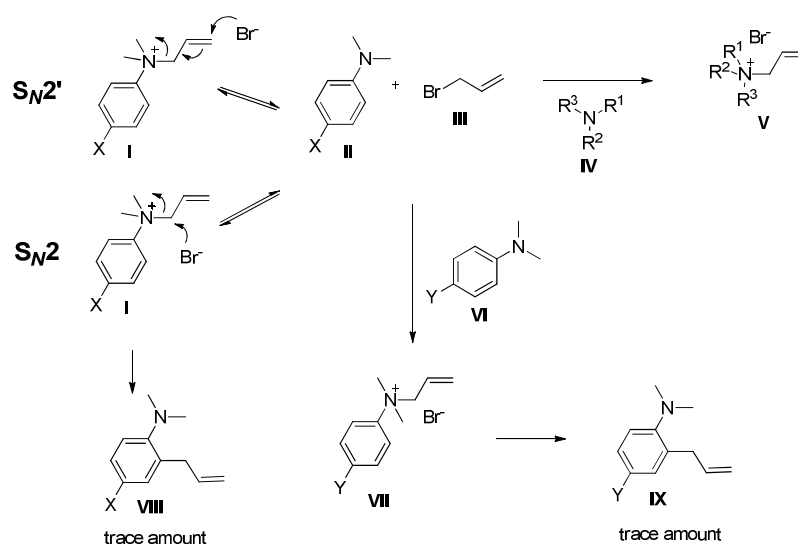
L'étude de la sélection de gel par l'échange C=C/C=N a été réalisée et il a été montré que la réaction d'échange entre **4b** et **1w** dans $\text{CD}_3\text{CN}/\text{EtOH}$ 9/1 à une concentration de 20 mM donne des produits d'échange dont **4f** pour former le gel, et pas de **1u** qui ne forme pas de gel. Les résultats décrits ici montrent la création de BCDs de grande diversité chimique, permettant ainsi la génération par CCD de récepteurs, de polymères dynamiques, de matériaux fonctionnels et de biomatériaux de plus en plus grande complexité.

Le chapitre quatre décrit l'échange de composants de sels d'ammonium quaternaires par substitution nucléophile bimoléculaire dans une CCD. Il y a plus d'un siècle, la première préparation d'un sel d'ammonium chiral $\text{Me}(\text{Et})\text{N}^+(\text{All})\text{PhI}^-\text{CHCl}_3$ a été réalisée par Wedekind, montrant une racémisation spontanée par une dissociation réversible en une amine rapidement inversée et un halogénure d'allyle. La vitesse de racémisation dépend du type d'anion: $\text{I} > \text{Br} > \text{Cl}$. De plus, Havinga décrit en 1954 une procédure pour réaliser la résolution de ce sel et pour confirmer ses propriétés chiroptiques. La structure du cristal est connue. Récemment, les sels d'ammonium chiraux ont été fréquemment utilisés comme catalyseurs dans la synthèse asymétrique, comme liquides ioniques, et dans l'ingénierie des cristaux. De plus, la réaction du sel de *N*-benzyl-*N,N*-diméthylanilinium avec un carbanion nucléophile, et la réversibilité de la réaction nucléophile entre le bromure de benzyle et la *N,N*-diméthylaniline ont été étudiées. La substitution nucléophile entre la pyridine et les dérivés du bromure de benzyle pour former le bromure de benzyle-pyridinium (réaction de Menshutkin) a été examinée en solution et dans un liquide ionique. Les sels de pyridinium peuvent être obtenus facilement, sont utilisés comme précurseurs versatiles dans la synthèse d'hétérocycles contenant de l'azote,

sont exploités de multiples façons dans la synthèse totale de produits naturels et sont utilisés dans l'addition asymétrique et régiosélective.

Dans ce chapitre, les principes de la CCD sont utilisés dans les échanges réversibles de composants de sels d'ammonium bimoléculaires pour générer des BCDs. Plus précisément, les réactions d'échange sont basées sur des sels d'allyle d'ammonium quaternaires permettant des réactions de substitutions nucléophiles avec les anions composant la paire d'ion pour donner une amine tertiaire et un halogénure d'allyle. Le mécanisme peut être décrit comme un passage direct S_N2/S_N2' ou indirect S_N2/S_N2' (Figure 7).

a) Indirect exchange pathway via allyl bromide



b) Direct exchange pathway

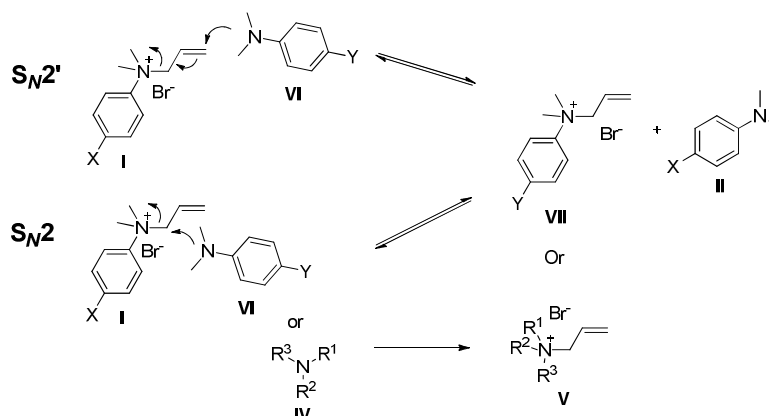


Figure 7 Les chemins possibles pour l'échange de groupe amine entre le bromure de *N*-allyl-*N,N*-diméthylanilinium et une amine tertiaire aliphatique ou aromatique via un mécanisme S_N2' .

Les BCDs basées sur les réactions de substitutions nucléophiles entre les sels d'allyle d'ammonium quaternaires et les dérivées d'amines tertiaires ont été générées. La capacité de multiple sels d'ammonium de participer à ces réactions d'échange en présence de plusieurs amines tertiaires (amines tertiaires aliphatiques ou aromatiques) a été évaluée, à la fois en absence et en présence de catalyseur nucléophile, comme montré en *Figure 8a*. Les constantes d'équilibre des substitutions nucléophiles d'échange des sels de pyridinium ont été calculées (*Table 5*).

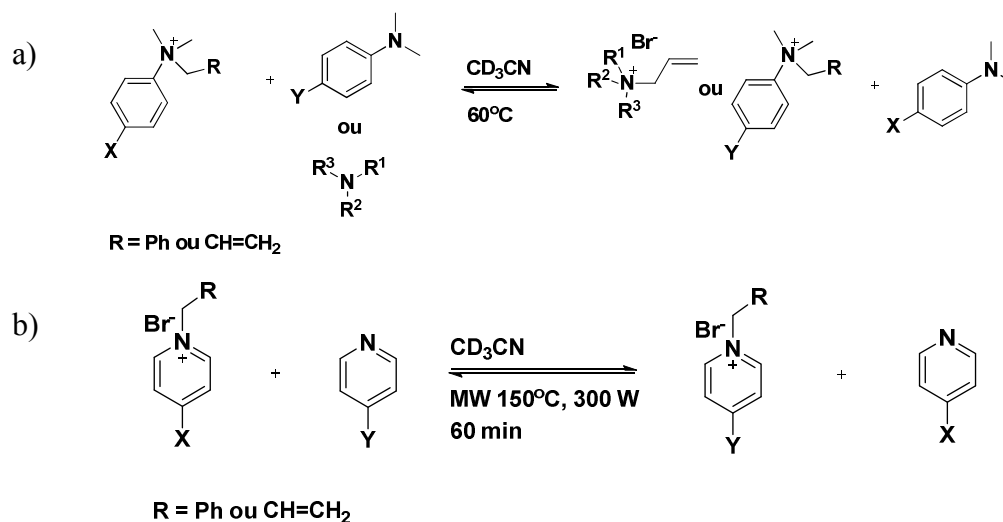


Figure 8 Représentation des réactions d'échange entre a) les sels d'allyle d'ammonium quaternaires et des dérivées d'amines tertiaires dans CD_3CN à 60°C . b) les sels de pyridinium et les dérivées de pyridine dans CD_3CN en utilisant l'irradiation du four à micro-ondes (MW) à 300 W à 150°C .

Pour toutes les réactions d'échange entre les sels d'ammonium et les amines aliphatiques tertiaires, les produits majoritaires dans l'équilibre ont été les produits d'échange, suggérant que la réaction est irréversible. Cependant, les réactions d'échange entre les sels d'ammonium et les amines aromatiques tertiaires ont été réversibles et sous contrôle thermodynamique. La réaction a été accélérée deux fois avec une quantité équimolaire d'ions iodure (*Table 5, Entrées 1 et 2*). De plus, les procédés d'échange de substitutions nucléophiles par le mécanisme $\text{S}_{\text{N}}2$ ont été étudiés entre les sels de *N*-benzyl-*N,N*-diméthylanilinium et les amines aromatiques tertiaires (*Table 5, Entrée 3*). L'influence du contre-ion a aussi été étudiée à la fois pour le sel d'allyle d'ammonium quaternaire et le sel de benzyle d'ammonium quaternaire en utilisant PF_6^- ou OTf^- . Les vitesses d'échange ont été déterminées comme plus lentes avec des constituants possédant ces contre-ions plutôt qu'avec les ions bromure.

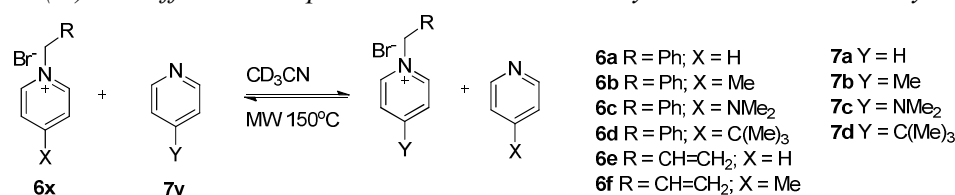
Table 5 Les paramètres cinétiques et thermodynamiques pour les réactions d'échange choisies entre les sels d'ammonium *N*-allyl-*N,N*-anilinium ou *N*-benzyl-*N,N*-diméthylanilinium **1a-1f** et les amines tertiaires aromatiques de type *N,N*-diméthylaniline **4a-4e** dans un ratio 1/1 à une concentration de 60 mM dans CD₃CN à 60°C. Temps de demi-vie $t_{1/2}$. Proportion (%) des différents composés. **a** = bromure d'allyle, **b** = iodure d'allyle, **c** et **d** = produits de réarrangement amino-Claisen, **e** = bromure de benzyle, **f** = iodure de benzyle. Dans cette table seul le cation organique est indiqué.

Entrée	Composé de départ	a)	Distribution de composés [%] ^{b)}							k [x10 ⁻³ M ⁻¹ s ⁻¹]	$t_{1/2}$ [h]	K_b ^{c)}	K_c ^{d)}	
			1a	4b	1b	4a	a	b	c					d
1	1a + 4b	f_b	13	19	28	29	4	n.a. ^{e)}	4	3	0.252	11	4.5	4.9
		f_c	13	18	29	33	3	1	2	1	0.516	6		
	1b + 4a	r_b	10	16	25	40	4	n.a. ^{e)}	2	3	0.177	9		
		r_c	11	15	25	40	3	1	1	3	0.283	4		
2	1a + 4c	f_b	9	13	36	35	3	n.a. ^{e)}	4	- ^{f)}	0.353	10	14.2	12.9
		f_c	10	14	36	35	2	<1	2	- ^{f)}	0.598	6		
	1c + 4a	r_b	8	10	39	39	3	n.a. ^{e)}	2	- ^{f)}	0.089	13		
		r_c	8	9	39	39	2	<1	2	- ^{f)}	0.097	8		
3	5a + 4b	f_b	6	32	23	30	9	n.a. ^{e)}	-	-	6.66	1.5	4.6	4.3
		f_c	6	34	23	29	6	2	-	-	12.3	0.9		
	5b + 4a	r_b	7	20	25	35	13	n.a. ^{e)}	-	-	2.72	1.8		
		r_c	7	20	21	39	10	3	-	-	5.83	1.2		

^{a)} f_b , Réaction aller en absence de catalyseur; f_c , Réaction retour en présence de TBAI (60 mM.) comme catalyseur; r_b , Réaction retour en absence de catalyseur; r_c , Réaction retour en présence de TBAI (60 mM) comme catalyseur. ^{b)} Erreur sur l'intégration des signaux ¹H-RMN: ±4%. ^{c)} K_b , Constantes d'équilibre de la réaction non catalysée. ^{d)} K_c , Constantes d'équilibre de la réaction catalysée. ^{e)} n.a., non applicable. ^{f)} Composé non observé.

Pour développer davantage les BCDs de substitutions nucléophiles (de types S_N2 et S_N2'), les réactions d'échange entre les sels de pyridinium et les dérivées de pyridine ont été étudiées par irradiation dans le four à micro-ondes à 150°C (300 W) dans CD₃CN, comme expliqué dans la *Figure 8b*. Toutes les réactions sont réversibles et sous contrôle thermodynamique. Les constantes d'équilibre des substitutions nucléophiles des sels de pyridinium ont été calculées (*Table 6*).

Table 6 Echanges de composés entre les sels de *N*-benzylpyridinium (**6a-f**) et les pyridines (**7a-d**) dans CD₃CN par irradiation dans le four à micro-ondes à 300 W à 150°C pour 60 min. Les proportions (%) des différents composés. **a** = bromure de benzyle et **b** = bromure d'allyle.



Entrée	Réaction	a)	Distribution de composés ^{c)}					K _{eq}
			6a	7b	6b	7a	a	
1	6a + 7b	f	14	16	35	33	2	5.16
	6b + 7a	r	14	16	35	33	2	
2	6e + 7b	f	16	22	30	29	3	3.99
	6f + 7a	r	11	16	34	35	4	

^{a)} f, Réaction aller; r, Réaction retour. ^{b)} Erreur sur l'intégration des signaux ¹H-RMN: ±4%. ^{c)} Composé non observé. ^{d)} n.d., non déterminé.

Certains de ces sels de pyridinium qui constituent ces bibliothèques dynamiques sont connus comme des liquides ioniques, ainsi, nous avons voulu générer des bibliothèques dynamiques de liquides ioniques avec ou en absence de solvant. Cette approche a remarquablement étendue la CCD, facilitant la formation de plus de bibliothèques dynamiques et permettant la génération de nouvelle diversité.

La chapitre cinq décrit la sélectivité cinétique et thermodynamique de la formation d'imines dans la CCD. Un pré-requis critique pour la génération de la CCD est l'opération d'un ou plusieurs procédés réversibles. En plus de ces transformations, la formation d'imines par condensation de groupes carbonyles avec des amines est d'intérêt considérable pour des applications chimiques et biologiques. En outre, la réactivité des amines utilisées (tels que les amines primaires, les composants oxyamine et les dérivées d'hydrazine) dans leur condensation avec un aldéhyde a été évaluée. Il est déjà connu que les composés possédant soit des groupes hydrazine soit des groupes oxyamine sont de meilleurs nucléophiles que les amines à cause de l'effet alpha et de leur faible basicité permettant de former des produits imines plus stables.

Ainsi, le degré de formation d'imines entre différents aldéhydes et amines (composants amine primaire, hydrazine, hydrazide et oxyamine) dans deux systèmes, en solution (*Figure 8*, aldéhydes **1-2**, amines **B-E**) ou en solvant organique (*Figure 8*, aldéhydes **3-4**, amines **B, F-H**) a été étudié. En outre, les réactions de compétition (pour générer une BCD) pour former différentes imines à partir de différentes amines dans un

unique système ont été explorées dans le but de définir la réactivité des amines et la stabilité des constituants imine dans les solutions aqueuses et dans les solvants organiques.

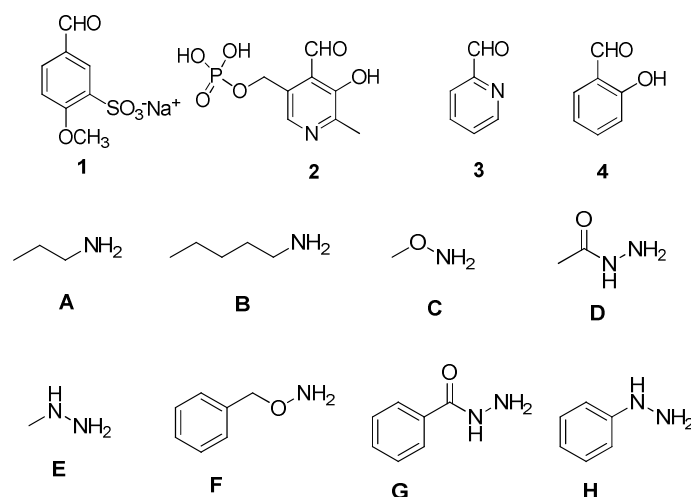


Figure 9 Représentation des structures des aldéhydes (**1-4**) et des différentes amines (**A-H**) utilisés dans la formation d'imines dans cette étude.

La formation d'imines individuelles en solution aqueuse à différentes valeurs de pD (5.0, 8.5 et 11.4) dans le tampon de phosphate de sodium avec le sulfonate d'aldéhyde **1** démontre que l'ordre de conversion en imine est le suivant **1C**>**1D**>**1E** (**1B** n'est pas capable de former d'imine) à pD 5.0, **1B**>**1E**>**1C** (**1D** n'est pas capable de former d'imine) à pD 8.5, et **1B**>**1E**>**1C**>**1D** à pD 11.4. Pour les vitesses de formation d'imines individuelles à partir du phosphate de pyridoxal **2** à différents pDs (5.0, 8.5, 11.4), l'évolution suivante a été observée, **2C**>**2E**>**2D**, et **2B** n'a pas été observé car la pentylamine n'est pas un bon compétiteur pour la formation d'hydrate avec le phosphate de pyridoxal. La BCD complète du sulfonate d'aldéhyde **1** avec les quatre amines différentes (**B**, **C**, **D**, **E**) a été réalisée dans trois mélanges tampon de phosphate différents (pD 5.0, 8.5, et 11.4), et a montré qu'à faible pD, le produit thermodynamiquement préféré est **1C**, alors que **1E** est majoritaire à un pD plus élevé (*Figure 10*). De la même manière, la BCD complète du phosphate de pyridoxal **2** avec les quatre amines différentes (*Figure 11*) dans les mêmes conditions qu'avec le sulfonate d'aldéhyde **1** a montré une évolution similaire où **2C** et **2E** sont les produits majoritaires. Ainsi, les produits préférés dans un milieu acide sont les oximes **1C** et **2C** alors qu'en solution basique les produits majoritaires sont les hydrazones **1E** et **2E**.

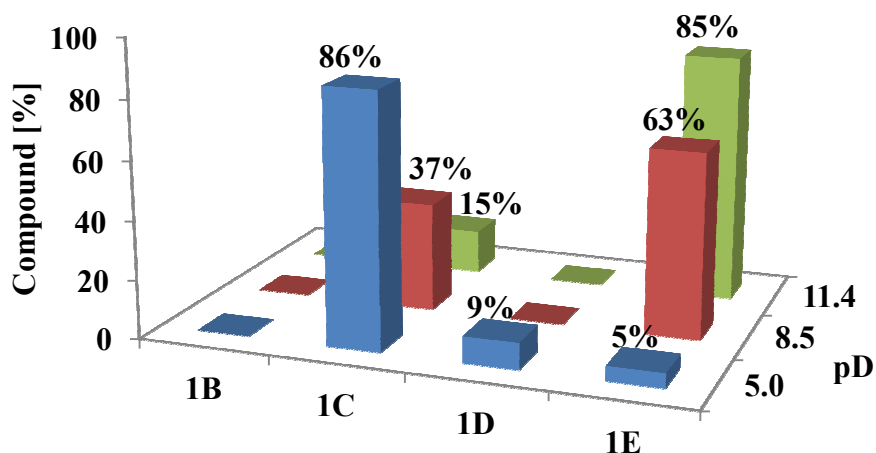


Figure 10 La distribution des différentes imines **1B-1E** dans la BCD générée à partir du mélange du sulfonate d'aldéhyde **1** et des différentes amines **B**, **C**, **D** et **E** (dans le tampon 160 mM $\text{NaH}_2\text{PO}_4/\text{Na}_2\text{HPO}_4$ pD 5.0, 8.5 et 11.4) en fonction du pD après que l'équilibre soit atteint. Les quantités de composés ont été calculées à partir de l'intégration des signaux ^1H -RMN des protons $-\text{CH}=\text{N}-$ face à une référence interne (1,4-dioxane).

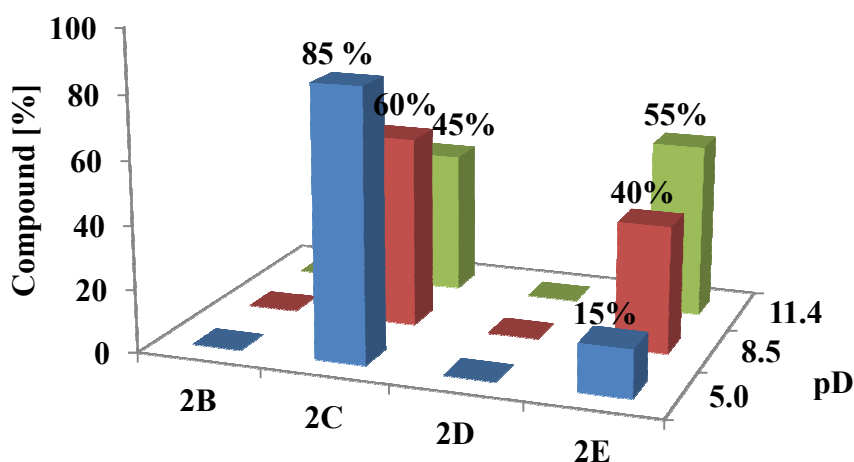


Figure 11 La distribution des différentes imines **2B-2E** dans la BCD générée à partir du mélange du phosphate de pyridoxal **2** et des différentes amines **B**, **C**, **D** et **E** (dans le tampon 160 mM $\text{NaH}_2\text{PO}_4/\text{Na}_2\text{HPO}_4$ pD 5.0, 8.5 et 11.4) en fonction du pD après que l'équilibre soit atteint. Les quantités de composés ont été calculées à partir de l'intégration des signaux ^1H -RMN des protons $-\text{CH}=\text{N}-$ face à une référence interne (1,4-dioxane).

Une étude indépendante sur la formation d'imines entre la 2-pyridylaldéhyde **3**, le salicylaldéhyde **4** et les différentes amines (**B**, **F**, **G**, et **H**) a indiqué que l'amine la plus réactive est la pentylamine **B** suivie par la phénylhydrazine **H**, la *O*-benzylhydroxylamine **F** et la benzhydrazide **G**. La formation du mélange de la BCD entre la 2-pyridylaldéhyde **3** et les différentes amines (**B**, **F**, **G**, et **H**) a montré que le produit cinétique est **3B** alors que les produits thermodynamiques sont **3F**, **3G** et **3H** (Figure 12 et Table 7, Entrée 1). Finalement, dans la BCD dérivée du salicylaldéhyde **4** et des différentes amines (**B**, **F**, **G**, et **H**), le produit cinétique est l'imine **4B** et les produits thermodynamiques sont **4F** et **4H**.

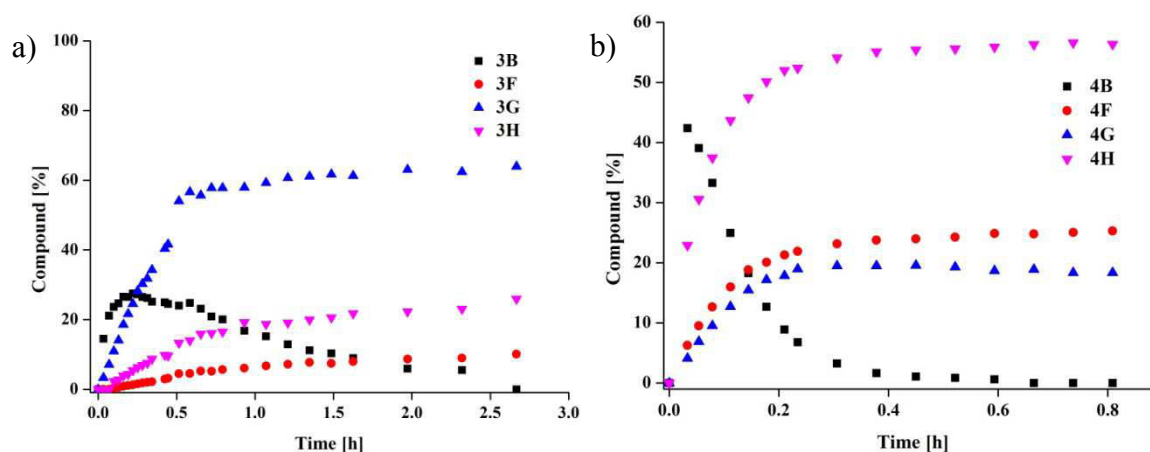


Figure 12 Les tracés de la cinétique de formation des imines dans CD_3OD dans le mélange réactionnel de a) **3** + **B** + **F** + **G** + **H**, b) **4** + **B** + **F** + **G** + **H**. La concentration finale est 20 mM. Chaque point a été obtenu par intégration des signaux des protons $-CH=N-$ contre une référence interne (1,4-dioxane). Les erreurs sur l'intégration 1H -RMN sont de $\pm 5\%$.

Table 7 La distribution des composés des BCDs des réactions de compétition de différents systèmes. La concentration finale est de 20 mM. Les quantités relatives ont été obtenues par intégration des signaux 1H -RMN des protons $-CH=N-$ contre une référence interne (1,4-dioxane).

Entrée	Réaction	Temps [h]	Distribution de composés [%] ^{a)}			
			3B	3F	3G	3H
1	3 + B + F + G + H	0.05	15	- ^{b)}	3	- ^{b)}
		0.48	28	5	54	13
		2.63	<1	10	64	26
		21.8	- ^{b)}	16	53	32
2	4 + B + F + G + H	0.03	42	6	4	23
		1.4	- ^{b)}	27	16	58
		3.5	- ^{b)}	29	9	63
		21	- ^{b)}	35	- ^{b)}	65

^{a)} Erreur sur l'intégration 1H -RMN: $\pm 5\%$. ^{b)} Composé non formé. ^{c)} n.d.; non déterminé.

La conception et l'étude de ces expériences pourraient être appliquées à d'autres systèmes CCD et pourraient fournir une base pour la recherche d'imines structurellement stables sous différentes conditions. Cela pourrait aussi être appliqué pour la transformation régiosélective de molécules possédant différents groupes fonctionnels dans le but de sélectionner différents produits sous sélection cinétique ou thermodynamique.

Le chapitre six décrit les conclusions générales présentées dans chaque chapitre.

Le chapitre sept fournit les données expérimentales où sont décrites les synthèses et les caractérisations des composants utilisés dans la thèse. De plus, une analyse des données sur la cinétique des réactions d'échange imine/imine et ammonium quaternaire/amine tertiaire est fournie.

Chapter 1

General Introduction

1.1 The concept of Dynamic Chemistry

Supramolecular chemistry has seen enormous development over the past half-century as chemistry moved beyond the molecule^[1,2] to investigate the use and control of non-covalent interactions such as van der Waals forces, π - π stacking, cation- π interactions, different types of dipole interactions, hydrogen bonding, ion-pairing, and coordinative metal complexation. It is a multidisciplinary field which has influenced diverse disciplines, for instance, the traditional areas of organic chemistry, inorganic chemistry and materials chemistry. Supramolecular chemistry is aimed at creating highly complex, self-organized systems by careful design of molecular precursors, thus paving the way towards chemistry as an information science. Information can be stored by appropriate manipulation at the molecular level and then transferred and processed at the supramolecular level through molecular recognition processes.

Supramolecular chemistry is intrinsically highly dynamic^[2] due to the lability of most non-covalent interactions. This allows self-organisation by design to evolve towards self-organisation by selection. For instance, in the presence of several different molecular precursors, the lowest energy self-organized system can emerge and come to dominate over the large number of other possible supramolecular systems by rapid exchange of molecular precursors.^[2] This is an example of *constitutional dynamics*, the reversible change in the constitution of a supramolecular entity by component exchange.

Chemistry involving the latter dynamics, so-called Constitutional Dynamic Chemistry (CDC) is the central focus of this thesis. CDC naturally occurs at the supramolecular level as described above. CDC at the molecular level is, however, less studied in organic system as non-labile bonding is normally employed in the quest for molecular stability (in particular, in the sense of kinetic inertness). Nevertheless CDC can indeed be implemented at the molecular level if reversible covalent bonding is employed (or a catalyst for the facile breaking and making of bonds is available, as happens in Nature, where enzymes can convert inherently very inert species into labile ones), allowing a continuous change in molecular constitution by reorganization and exchange (*Figure 1.1*). Whether at the molecular or supramolecular level, CDC can allow a system to react to external stimuli by component exchange, thus opening a path towards adaptive and evolutive chemistry.

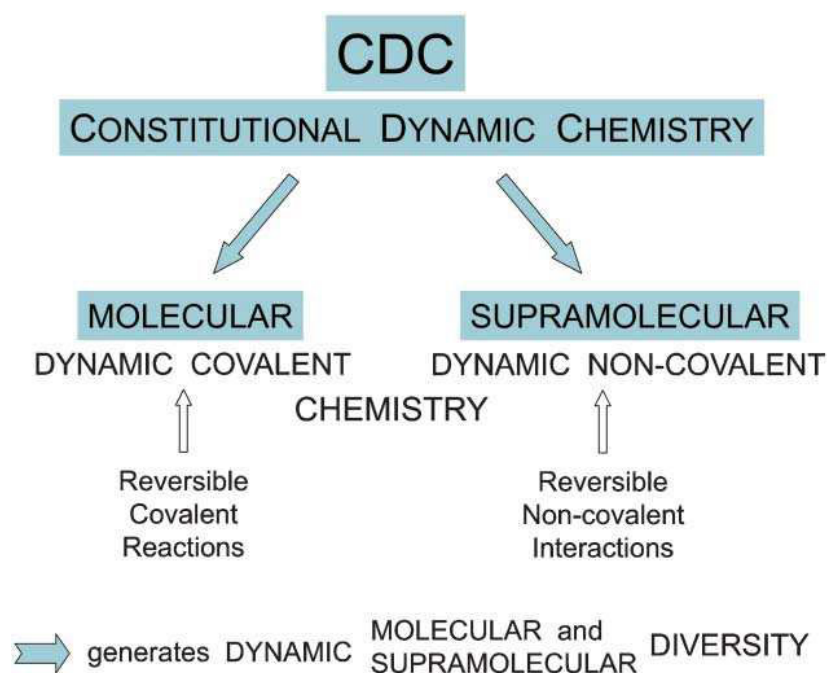


Figure 1.1 Constitutional dynamic chemistry (CDC) covers both dynamic molecular chemistry and supramolecular chemistry involving dynamic covalent and non-covalent bonds (Figure reproduced from reference [1])

Dynamic Combinatorial Chemistry (DCC)^[3-5] is a branch of CDC that focuses on the generation of diversity by constitutional exchange. The aim is to employ a small set of molecular or supramolecular components that can, by rapid and reversible reactions under thermodynamic control, form a much larger array of more complex species. This route to the generation of dynamic diversity, resulting in so-called dynamic combinatorial libraries (DCLs),^[6] is at the heart of DCC. A DCL can be characterized by three main features:

- **Conversion**, representing the total amount of constituents created with respect to free components;
- **Composition**, representing the distribution of relative amounts of the different constituents;
- **Expression of a given constituent**, which might be defined as the product of conversion and selectivity.

The conversion and composition of a DCL are determined by the relative thermodynamic stability of each component (relative Gibbs free energy of formation). Once a DCL has been established, one can employ external stimuli to alter the potential energy landscape, thus altering the DCL composition/conversion. That is to say, a DCL is not a fixed entity. For instance, non-covalent binding to an introduced template might amplify a particular component, an example of expression (*Figure 1.2*) and a demonstration of the adaptive capability of CDC.

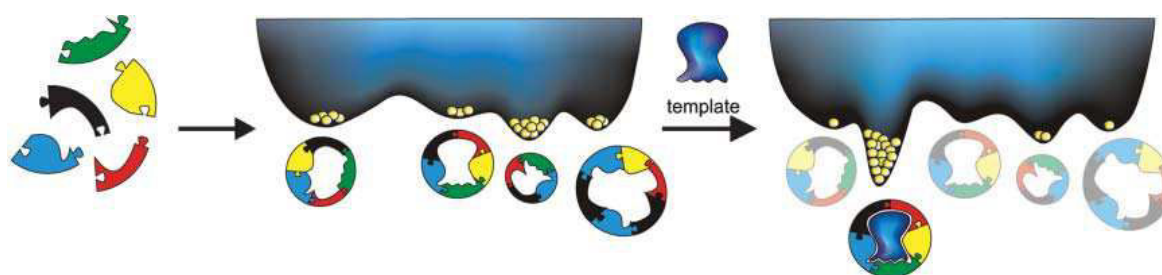


Figure 1.2 A DCL is generated from the reversible exchange of and between various components. The addition of a template to the library will change the component distribution, amplifying the component which forms the most stable complex with the template (*Figure reproduced from reference [7]*).

Figure 1.3 shows how DCC can be used to effectively search for a bioactive substance, where DCL components are represented as molecular ‘keys’ for a specific biological ‘lock’. The traditional approach^[1] to finding the right key would be to synthesize a particular key and test its activity for binding to the lock, and though laborious this could be done for many keys using high throughput screening. DCC provides an alternative and likely more efficient approach, in which the components for all possible keys are mixed together and allowed to exchange. The full range of possible keys from combinations of the keys’ fragments constitutes the ‘virtual’ DCL while the actual composition will depend on thermodynamic factors. Since many keys form by rapid exchange of fragments, finding a key, or key fragment, that fits the lock may be faster than in the traditional approach. The key or key fragment may enter the lock either under thermodynamic control (the best fit to the lock) or by kinetic selection (the fastest to bind).

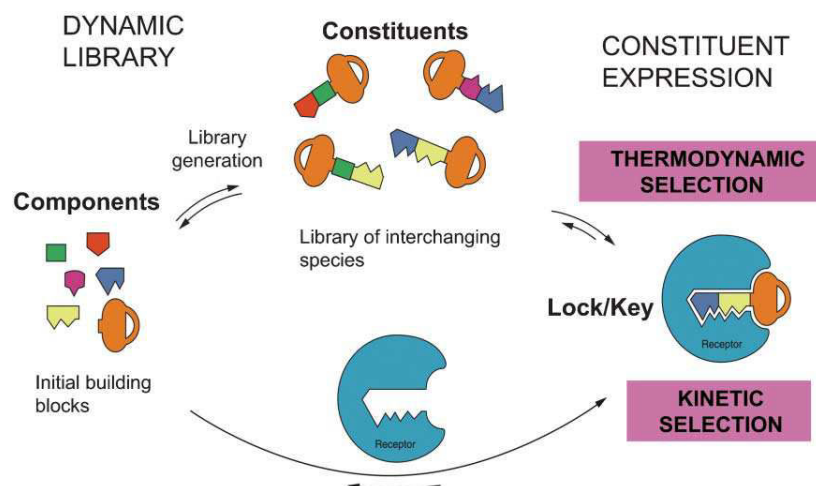


Figure 1.3 The representation scheme of the fundamental concept of dynamic combinatorial/covalent chemistry (DCC, Figure reproduced from reference [1]).

A decade ago, DCC was conceptualized and implemented in various chemical systems.^[8,9] Initial explorations focused on the principles and procedures required to generate dynamic libraries through reversible chemical transformations. These will be discussed in detail in the following section.

1.2 Dynamic combinatorial chemistry using exchange reactions

The main drivers of dynamic combinatorial chemistry (DCC) are the reversible reactions that exchange building blocks between the different components of the system. These reversible exchange reactions^[3] should have the following characteristics:

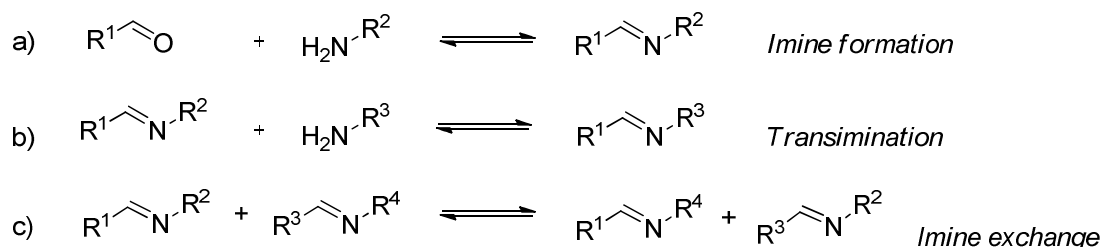
- The timescale of the exchange reaction should be short so that equilibration and selection occur essentially simultaneously.
- They need to operate under mild experimental conditions (e.g. temperature, pressure, concentration, solvent, pH, catalyst).
- The solubility of all building blocks and library components is required because if any insoluble material is present, it can act as a thermodynamic sink or slow the reaction rate (kinetic trap).

The reversible reactions are divided into three main types, depending on whether covalent, non-covalent, or coordinate bonds are involved. The non-covalent interactions typically reach equilibrium rapidly whereas the covalent reactions proceed more slowly and can require the presence of a catalyst to fulfill the requirement for lability listed above. Some examples of DCC using covalent exchange reactions are discussed next.

1.2.1 Reversible exchange reactions based on covalent bonding

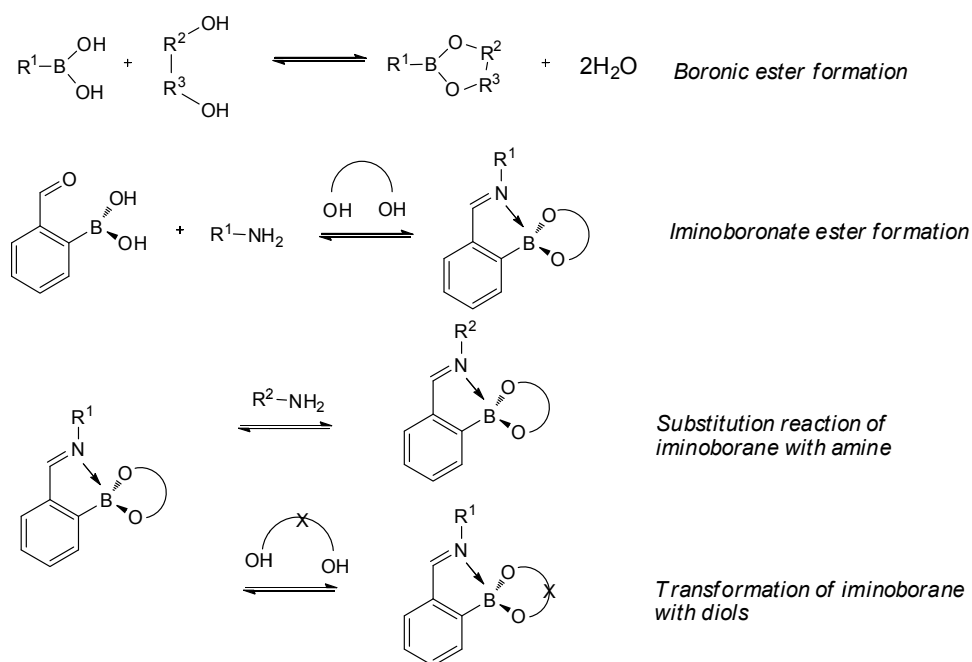
Recently, numerous covalent reversible exchange reactions have been used for DCC^[5,10–20] even though it is often difficult to establish true equilibrium. Some examples of the generation of dynamic covalent libraries (DCLs) involving labile covalent bonding are illustrated below.

● **Imine (C=N) formation and exchange** – The condensation product obtained by the reaction of a carbonyl compound and a primary amine is called an imine or, commonly, a Schiff base.^[21] Imine formation is reversible and the equilibrium can be forced towards the imine product by removing water.^[22,23] An imine can react with amine to undergo the reversible exchange process called transimination.^[10–15,17,24–27] Furthermore, an imine can exchange its amine component (and simultaneously its carbonyl compound component) for that of another imine, the so-called imine/imine exchange reaction (*Scheme 1.1*), via either nucleophilic catalysis,^[26] hydrolysis/re-combination being an obvious example of such a pathway,^[28] or by a direct metathesis involving a single, cyclic intermediate/transition state.^[29–40]



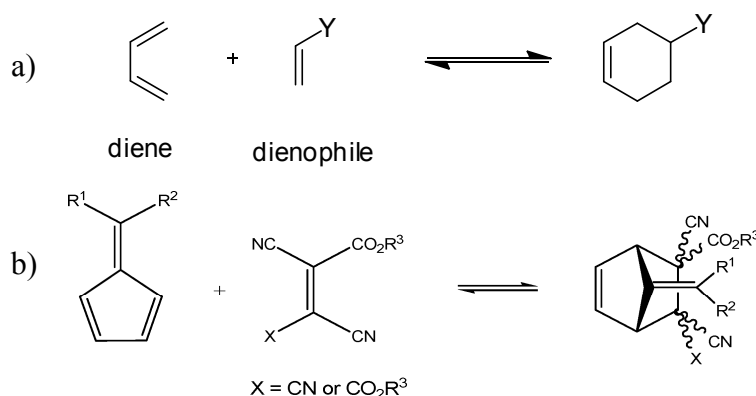
Scheme 1.1 Imine formation and exchange reactions.

● **Boronic ester formation and exchange** – Boronic esters are formed by the condensation between a boronic acid and alcohols and it usually requires a dehydration procedure to drive the reaction to completion. Recently, iminoborane compounds were used to perform self-assembly by reversible B-O and imine bond formation giving an iminoboronate ester.^[41,42] This suggests that the versatile exchange motif between imine and diol bonds could be useful in dynamic covalent systems (*Scheme 1.2*).



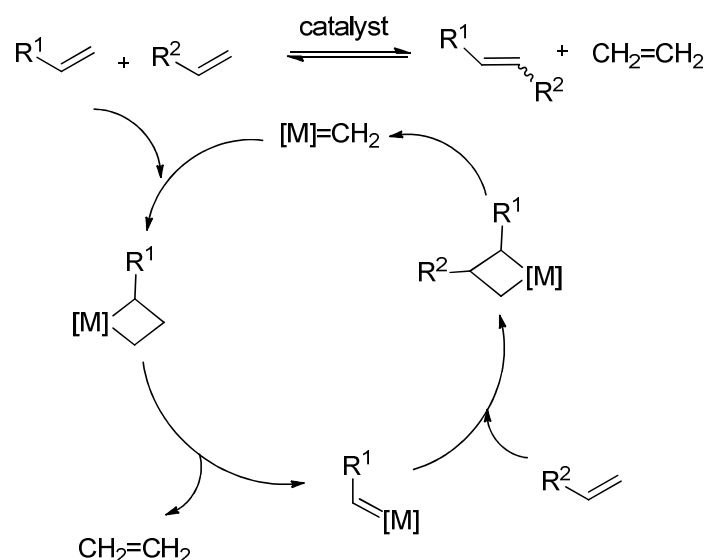
Scheme 1.2 Boronic ester and iminoboronate ester formation.

● **Diels-Alder Reaction** is the cyclization reaction between a diene and dienophile to form a substituted cyclohexene product. This reaction is reversible under certain conditions, where the reverse or retro-Diels-Alder reaction is efficient. These Dynamic Diels-Alder reactions have been shown to undergo reversible component exchange to form DCLs under mild conditions.^[43,44] Reversible Diels-Alder reactions have been used to generate dynamic polymers, “dynamers”, which undergo rapid exchange at room temperature.^[44] The use of such a system with a low equilibrium constant allowed the formation of materials with self-healing properties.



Scheme 1.3 a) The general equation for Diels-Alder (forward) and retro-Diels-Alder (reverse) reactions b) An example of a Diels-Alder reaction which is dynamic under mild conditions.^[45]

● **Olefin metathesis** is a versatile tool for organic^[46–48] and organometallic synthesis.^[49] This reaction occurs through an essentially reversible process via a series of [2+2] cycloaddition/cycloreversion steps using metallocatalysts,^[50] of which the family of Grubbs' catalysts^[51,52] is the most effective.



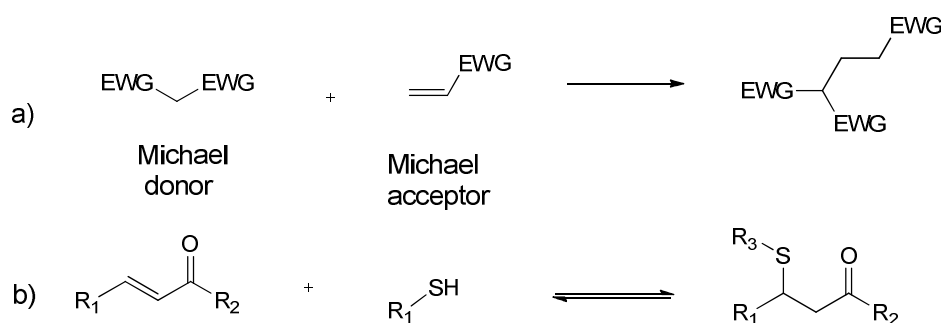
Scheme 1.4 The fundamental catalytic cycle for an olefin/alkene metathesis reaction.^[3] (Scheme reproduced from reference [3] and slightly modified)

● **Disulfide exchange** is an important reaction in biology, being, for instance, involved in the folding of proteins.^[53] It is one of the few reversible covalent reactions that are compatible with biomolecules.^[54–56] The mechanism of the exchange^[57] is the nucleophilic displacement of a thiolate anion from the disulfide through attack by another thiolate anion, thus, basic conditions are required.



Scheme 1.5 The general equation for a) disulfide formation (involves oxidation, with H_2 as the other formal product) and b) disulfide exchange (also involves oxidation state changes at sulfur).

● **Michael reaction** is the nucleophilic addition of a carbanion or another nucleophile to an α,β -unsaturated carbonyl compound or conjugate with an electron withdrawing group. It is one of the most useful methods to make C-C bonds. Cases, where the reverse (retro-Michael) reaction occurs readily, are known and studies of the thermodynamics and kinetics of Michael/retro-Michael reactions have been reported involving both sulfur and^[58] oxygen-derived nucleophiles.^[59] Thiol-based Michael donors can be used to generate DCLs based on the reversibility of this reaction.^[60]



Scheme 1.6 Equation for a) the Michael reaction in general and b) an example of a reversible Michael/retro-Michael reaction. EWG = electron-withdrawing group.

1.2.2 Reversible exchange reactions based on noncovalent bonding.

The kinetic lability of hydrogen bonds and many coordination bonds has been used to self-assemble diverse supramolecular architectures.^[61–66] Investigation of the generation of DCLs by reversible non-covalent assembly has been undertaken by several research groups.

● **Hydrogen Bonding** is an attractive interaction between a hydrogen-bond donor (HBD) XH and a hydrogen-bond acceptor (HBA).^[67] In general, the hydrogen bond reflects the ability of bound H to form additional weak interactions, usually to rather electronegative atoms with lone pairs. Many researchers have been inspired to investigate DCLs based on reversibly hydrogen-bonded assemblies.^[68–71] Often they have used a combination of H-donors and acceptors which build highly complex architectures with large numbers of hydrogen bonds (e.g. as many as 36).^[72] Hydrogen bonding has some limitations for the generation of DCLs as H-donors/acceptors can self-aggregate, or competitive binding by polar solvents or by the presence of traces of water can disrupt the assembly.

● **Metal-Ligand Coordination** – the use of metal-ligand coordination in DCLs requires at least some ligand substitution reactions within the coordination sphere to be fast. The rates of these reactions, however, depend on many factors relating to the nature of the ligand and metal and their complex but by careful control of these factors, complexes between metals (e.g. Co^{2+} , Cu^+ , Cu^{2+} , Fe^{2+} , Zn^{2+})^[73–78] and various ligands have been used to build-up DCLs via metal-ligand exchange. This type of DCL is compatible with biomolecules as either templates or building blocks (Figure 1.4).^[79,80]

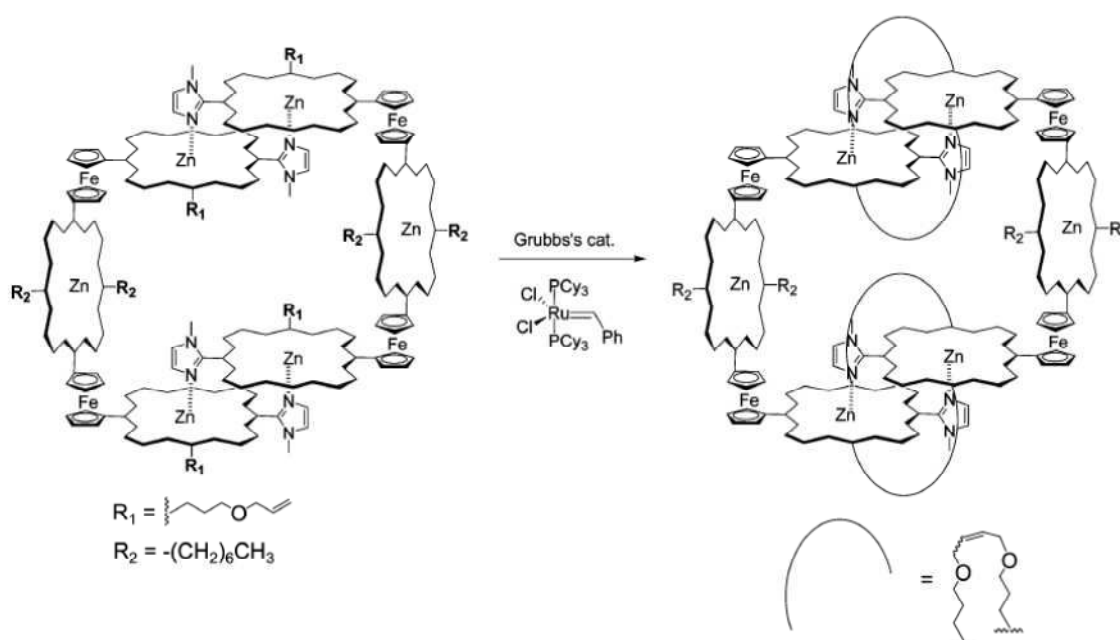


Figure 1.4 The composition of a DCL based on metal-ligand interactions using Zn^{2+} for self-selection through alkene metathesis.^[78] (Note: The ligand shown around the Zn^{2+} is porphyrin; this is a species where four sites (donor atoms from porphyrin) are inert and only the two axial sites are labile) The Fe in the ferrocene units is of course completely inert and the phosphine ligands on the Grubbs catalyst are also inert to substitution. (Figure reproduced from reference [3])

Example of selection in a DCL

The expression of a particular component of a DCL through its dynamic response to internal stimuli was shown by Lehn's group^[81] (Figure 1.5) working with DCLs of guanine quartet-based hydrogels. The guanosine hydrazide (**1**) was found to be a very powerful hydrogelator when linked by a metal ion into its quartet form. It is able to react with several aldehydes to form acylhydrazones which provide gels of different stability when a metal ion is added. Thus, by adding a metal ion to the DCL formed from **1**,

acetylserinehydrazide, **3**, and the aldehydes pyridoxal phosphate, **2**, and 2-formylbenzene sulfonate **4**, the reversibility of the hydrazone formation leads to the selective formation of the gel **B** containing the pyridoxal-derived hydrazone. This is an expression of triple constitutional dynamics, two at supramolecular levels (the metal complexation and the hydrogel formation of the guanosine hydrazone quartet) and a third (the acylhydrazone formation) at a dynamic covalent level.

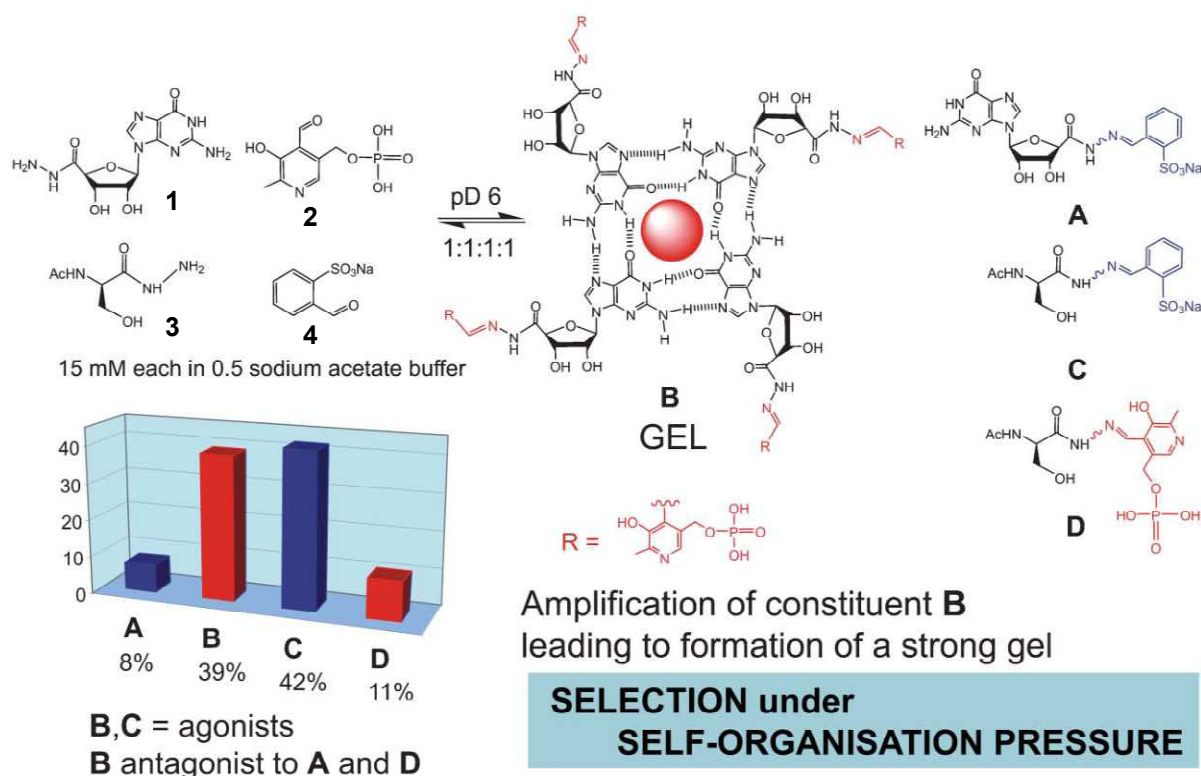


Figure 1.5 The constitutional dynamic selection driven by self-organisation in the formation of a G-quartet based gel (**B**).^[81] The red sphere indicates a metal ion. (Figure reproduced from reference [1])

Nitschke and Lehn also reported self-organization by selection with the generation of a tetranuclear [2x2] grid-type metallosupramolecular architecture (Figure 1.6).^[15] The grid formation involves two dynamic processes, which are reversible covalent bond connection (imine reversible bond) and reversible metal ion coordination. In the system, studied, aminophenols were mixed with carbonyl compounds in a solution to form a dynamic covalent library of imine. Then, Zn(II) was added to drive the system to that containing the most effective complexing agent (Figure 1.6). Again the expression of a single component of a virtual DCL was induced by the addition of a metal ion. The dominant DCL component was generated through both reversible covalent (imine)

exchange and reversible metal ion coordination. The two-level self-organization finally imposed selection or ‘self-design’ on otherwise dynamic diversity generated by the DCL building blocks.

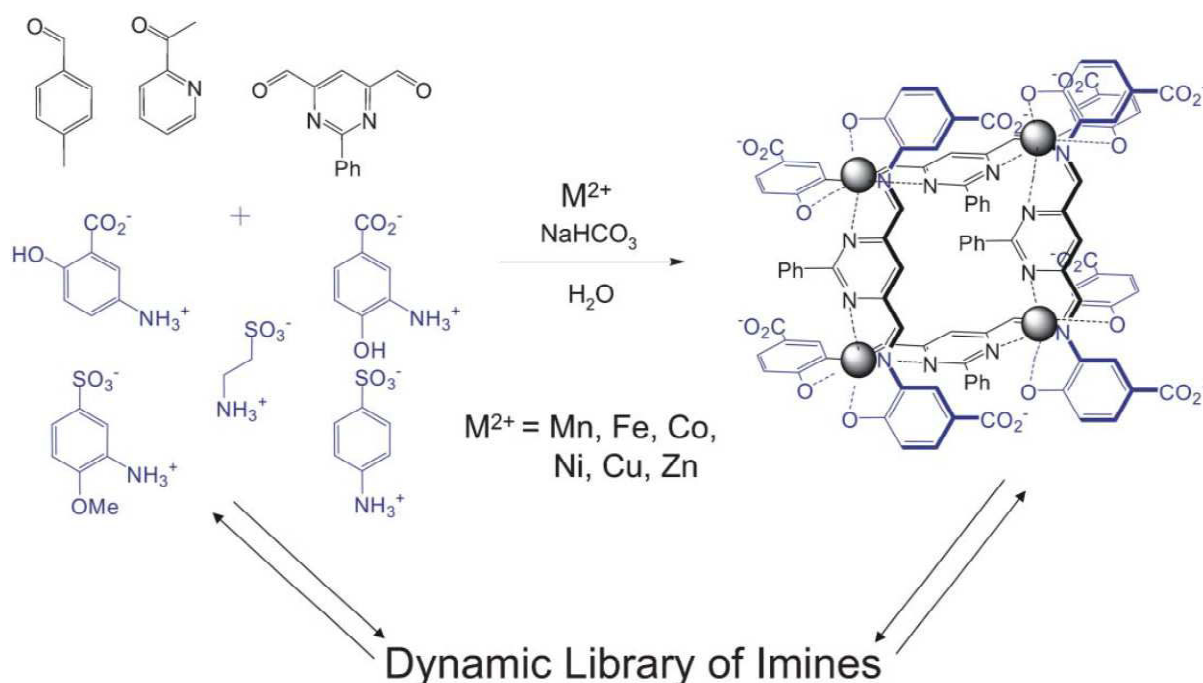


Figure 1.6 DCL formation with selection to generate a [2x2] grid complex from metal cations and organic building blocks using both reversible imine exchange and reversible metal-ligand interactions.^[1] (Figure reproduced from reference [1])

DCLs involving different types of dynamics

While constitutional dynamics only has been discussed so far, Lehn's group also reported other types of dynamics which can affect the composition/conversion of a DCL, for instance, motional dynamics, or configurational exchange, being the external and internal reorientations of a molecule.^[82–84] Particularly interesting again are the imines since they can be doubly dynamic, with both motional and constitutional functionality. They have been shown to have intrinsic properties of a molecular motor type, as they are able to undergo *cis-trans* isomerism and ring inversions which can be used to drive unidirectional rotation in the case of a chiral imine.^[82] Motional and constitutional exchange in imines typically occurs on very different timescales however. This fact has been used to control information storage for either the short or long term in doubly dynamic imine systems.^[83] In that work a hydrazone was shown to undergo photoinduced isomerization (with thermal back reaction), constitutional exchange with amines, and

finally metal ion binding, giving respectively short term, long term, and permanent (locked) information storage (*Figure 1.7a*).^[85] In other work, oligoamine chains were shown to undergo constitutional exchange with an aldehyde to form imine compounds (*Figure 1.7b*), which then underwent motional dynamics whereby the alkylidene residues were able to shift to a neighboring site.^[27] This work showed that oligoamines have the potential to provide a molecular “walking” track under the correct circumstances. Clearly imines behave as very simple but highly versatile systems for combining in beneficial ways both constitutional and motional dynamic processes.^[84,86]

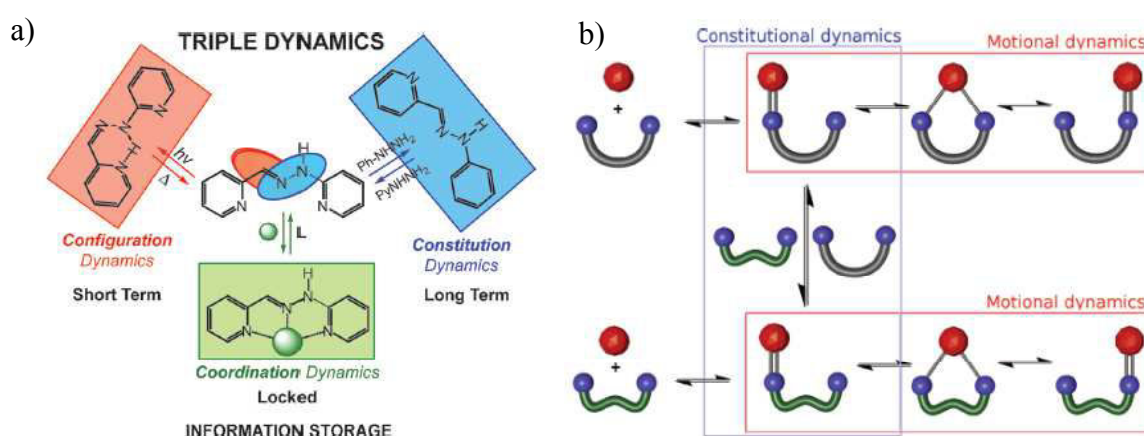


Figure 1.7 a) A bispyridyl-hydrazone molecule demonstrating three types of multiple dynamics: (1) configuration, photochemical, and thermal isomerization (short-term); (2) constitutional interconversion by component exchange (long-term); (3) lock-in by metal-ion (locked).^[84] b) The reversible formation of imines from a carbonyl entity (red sphere) and a terminal diamine (blue connected spheres), the exchange of diamines through transimination (blue frame), and the back and forth motion of the alkylidene moiety between the terminal amine sites (red frames) are indicated. (Figure reproduced from reference [84])

DCLs and multiple external stimuli

Recently, Lehn’s group reported a DCL of pyridylhydrazones and pyridylacylhydrazones which undergoes double adaptation in response to two orthogonal agents involving chemical effectors (metal cation) and a physical stimulus (light irradiation). These DCLs show a selection and adaptation in response to multiple external stimuli thus allowing component exchange and leading to adaptation of two orthogonal selection processes (*Figure 1.8*).^[71]

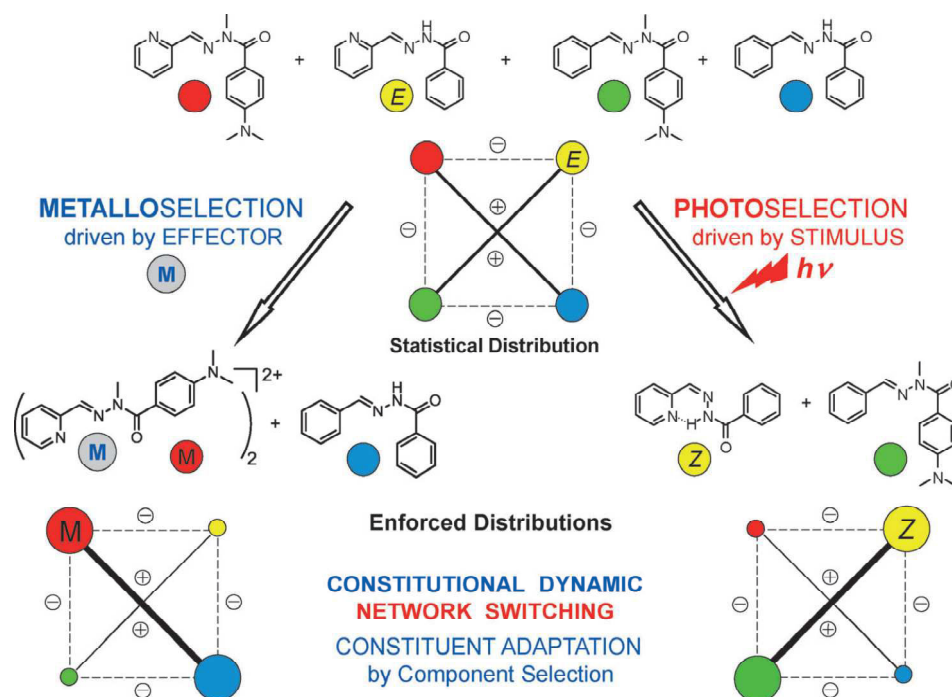


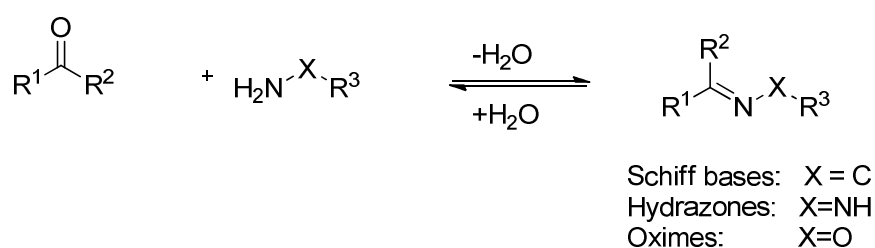
Figure 1.8 A DCL of four pyridylacylhydrazones (top) is influenced by external stimuli such as addition of a metal ion or light irradiation.^[87] (Figure reproduced from reference [84])

General direction of this thesis

Taking all the works mentioned above collectively, it is clear that CDC and the resulting DCLs give rapid access to a high level of self-organization and diversity. At the highest level of complexity, one may even begin to speak of constitutional dynamic networks (CDNs).^[1] Recently, CDC has been implemented to produce a diverse range of targets useful in, for instance, receptor design,^[88–105] biological studies,^[106–111] materials sciences,^[30,88,89,112–130] dynamic resolution,^[131] self-sorting,^[132] DNA-templated synthesis,^[133–135] catalysis,^[88,136–138] sensing,^[102,139–141] and the controlled release of bioactive compounds.^[117,140,142] Among the DCLs studied to date, the formation of imines by the reversible reaction of carbonyl compounds with amine derivatives is one of the most extensively investigated. This thesis expands on these studies and also investigates the dynamic covalent chemistry of *Knoevenagel* compounds, which have a variety of useful applications. Both imine and *Knoevenagel* CDC have been studied in the presence of organocatalysts. Thus, in the following, the chemistry of imines, *Knoevenagel* compounds, and organocatalysis, will be discussed in depth.

1.3 The general characteristics of imine compounds

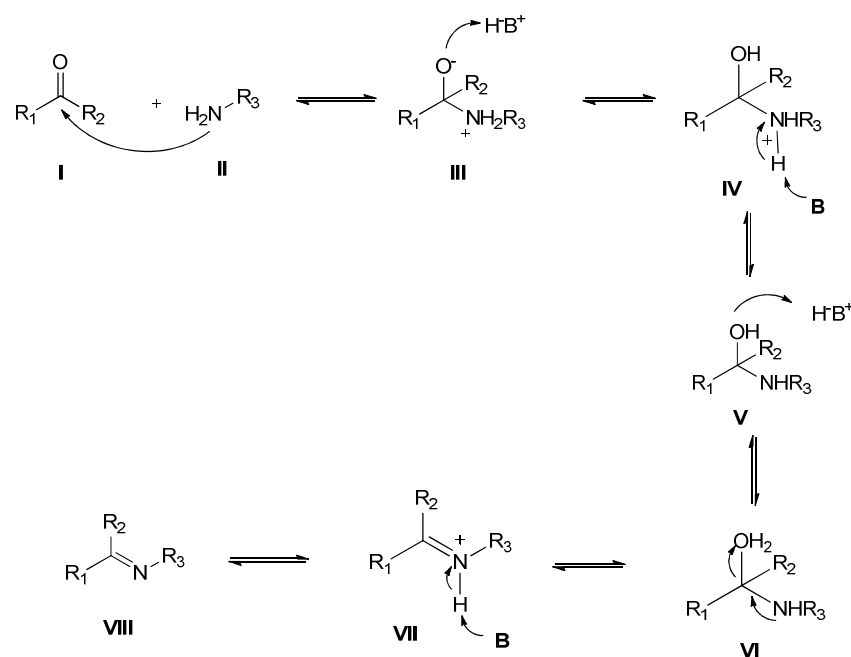
1.3.1 Imine formation – As noted earlier, imines (C=N) are compounds formed by the condensation between either an aldehyde or a ketone with a primary amine. They are called Schiff bases if just the C=N bond or the azomethine linkage is present (*Scheme 1.7*), the reaction being discovered in 1864 by Schiff.^[143] When the reaction is performed with an amino compound (H₂N-X) where X is an oxygen or a nitrogen atom, the resulting imine is called an oxime (-HC=NOR, i.e. X = OR), or a hydrazone (-HC=NNHR, X = NHR), respectively (*Scheme 1.7*). In addition, the condensation of an aldehyde or a ketone with a secondary amine results in an iminium ion which can convert to an enamine product.



Scheme 1.7 The reversible formation of imines, hydrazones, and oximes.^[142]

The reaction typically requires an acid catalyst and careful temperature control.^[17] The mechanism of imine formation (*Scheme 1.8*) is considered to be a nucleophilic addition-elimination reaction. In the first step of the formation of imines (**VIII**),^[144] the primary amine (**II**) attacks at the carbonyl carbon (**I**). Then, the alkoxide ion (**III**) abstracts a proton from an acid to form an ammonium species (**IV**). The loss of a proton from the ammonium ion (giving, overall, what is equivalent to an intramolecular proton transfer in **III**) then forms a neutral tetrahedral intermediate (**V**), called a carbinolamine or hemiaminal. The next step is protonation of the hydroxyl group and the elimination of water to generate a protonated imine (**VII**) and finally the loss of a proton to afford the imine (**VIII**). While the reaction proceeds, the removal of water is necessary in order to drive the equilibrium to the product side. The multiple proton transfers involved in this mechanism explain why the pH dependence of imine formation can be very complicated.^[145–147]

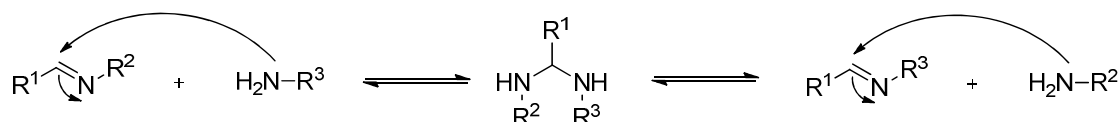
Thus, the pH at which imine formation is carried out must be carefully controlled. There must be sufficient acid present to protonate the tetrahedral intermediate, however if the medium is too acidic it will protonate the reactant amines. The resultant ammonium ion is not a nucleophile and will not react with the other reactant's carbonyl group. The intermediate (V), commonly termed a carbinolamine, is a labile species and generally cannot be isolated or detected. The stability of carbinolamines does depend on the nature of substituents, however, and this is not always the case.^[148–151]



Scheme 1.8 A proposed mechanism of imine formation (nucleophilic addition-elimination reaction) involving a primary amine (On the other hand, **III** can also undergo a direct intramolecular proton transfer to give **V**).^[144]

One of the most important characteristics of imine (C=N) compound formation is its reversibility. Imines occur naturally and are widely studied in biology,^[152–154] they are also of interest to organic chemists^[22,23,25,101,116,143,155–160] where their reversibility is exploited for applications. With regards to CDC and the generation of DCLs, the imine linkage has several practical advantages. The large variety of imines derived from the many substituents (R¹⁻³) possible, allows the formation of DCLs with a broad range of structural diversity. As just discussed, the rate of the imine formation is very sensitive to medium pH thus this can be one of the stimuli that control the composition/conversion of an equilibrated mixture of imines. Importantly, exchange reactions between imines and reactant amines, transimination, and exchange reactions between different product imines, imine metathesis, allow the system to attain even more diversity via a second generation of dynamic covalent chemistry. The mechanistic details of these exchanges will be described next.

1.3.2 Transimination - One mechanism of transimination is similar to imine formation, proceeding via reversible formation of an aminal which then releases fragments to afford a new imine and an amine (*Scheme 1.1b and 1.9*). The overall exchange process involves a proton transfer from the amine nitrogen atom to the imine nitrogen atom. The rates and equilibrium parameters depend on the relative basicity of amines. In fact, imines react with the nucleophiles N of amines more rapidly than the carbonyl compounds^[161,162] so that the alternative mechanism of hydrolysis followed by recondensation is not favored. During the transimination process, the rate-determining step is the addition step if the nucleophilicity of the amine is less than the basicity of the amine which is condensed as the imine. When the reaction is occurring in the opposite direction, the rate-determining step is the formation-decomposition of the aminal.^[163]

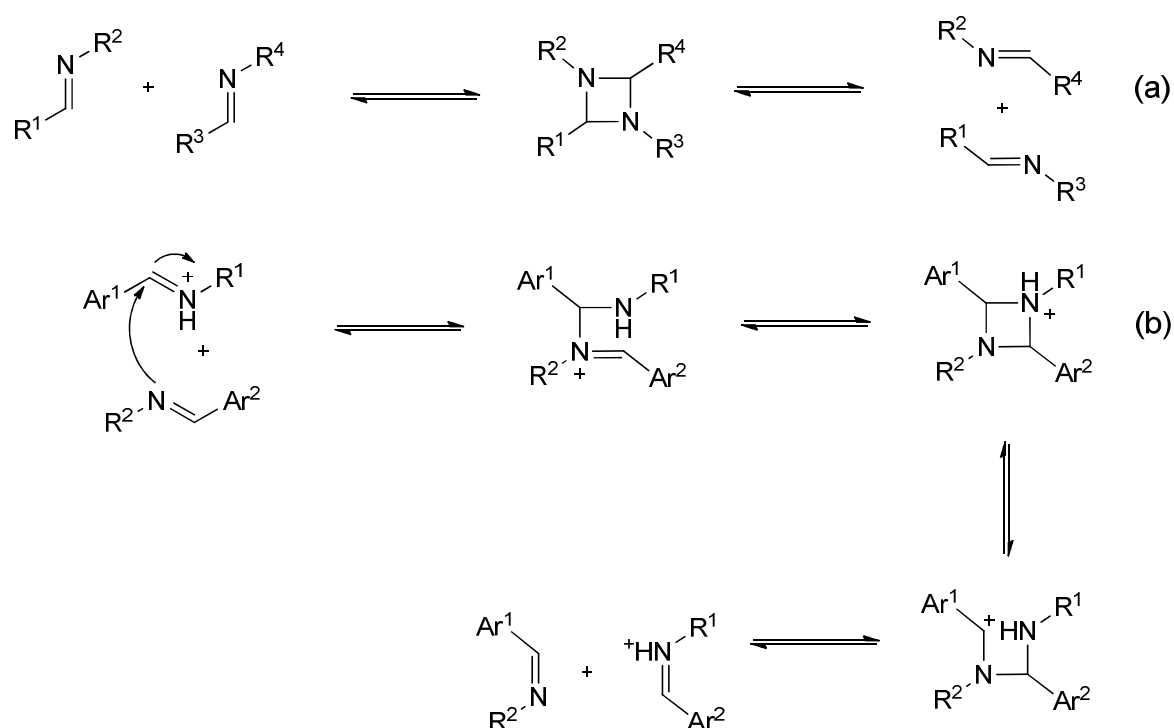


Scheme 1.9 The general mechanism of the transimination via aminal formation.^[164]

The influence of acids (Brønsted and Lewis acid) on the transimination reaction has been investigated^[17] and Sc(III) triflate, for example, has been shown to catalyze the rate of exchange between sterically hindered imines (derived from 9-anthracenecarboxaldehyde) and several amines by up to five-fold in CDCl_3 . A mechanism was proposed in which the metal ion polarises the imine, aiding the nucleophilic attachment of the free amine. In other work, the transition state of the transimination leading to the formation of aminal was proposed to be polar in the case of aliphatic amines and almost apolar in the case of aromatic amines.^[25]

1.3.3 Imine exchange - The imine exchange reaction, or imine metathesis, is the reaction between two imines to form two new imines (*Scheme 1.1c*). Nearly a century ago Ingold *et al.*^[165,166] suggested that the exchange proceeded by a concerted mechanism involving the formation and decomposition of a dimeric intermediate with a 1,3-diazetidene structure. However, the energy of the transition state for this symmetry forbidden $[2\pi + 2\pi]$ cycloaddition reaction has been calculated to be too high (*Scheme 1.10a*).^[29] About half a century ago, Messmer *et al.*^[167] suggested the imine exchange reaction could occur via a

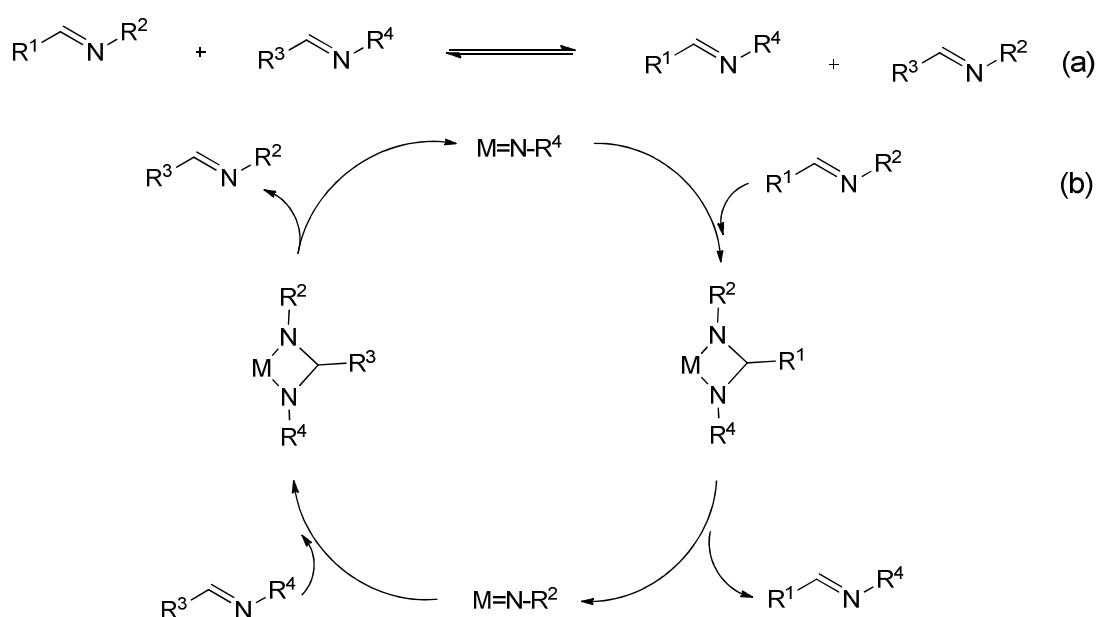
stepwise mechanism involving the formation of ionic intermediates (*Scheme 1.10b*). They showed that the rate constants of the exchange reaction in polar solvents were higher than in less polar solvents, consistent with formation of an ionic intermediate rather than the neutral intermediate of the concerted process. The exchange reaction did not occur in the absence of protons or in a high concentration of protons, consistent with an acid catalyzed nucleophilic attack. Attack of a neutral imine on a protonated imine could result in passage through three transient intermediates (*Scheme 1.10b*). The reaction does not take place in the absence of protons as one of the imines needs to be activated in the first step, while in excessively acidic conditions both imines would be also protonated preventing reaction.



Scheme 1.10 Possible mechanisms of the imine exchange reaction a) via concerted [2+2] mechanism b) for an aromatic Schiff base via the acid-catalyzed ionic intermediate pathway.^[167]

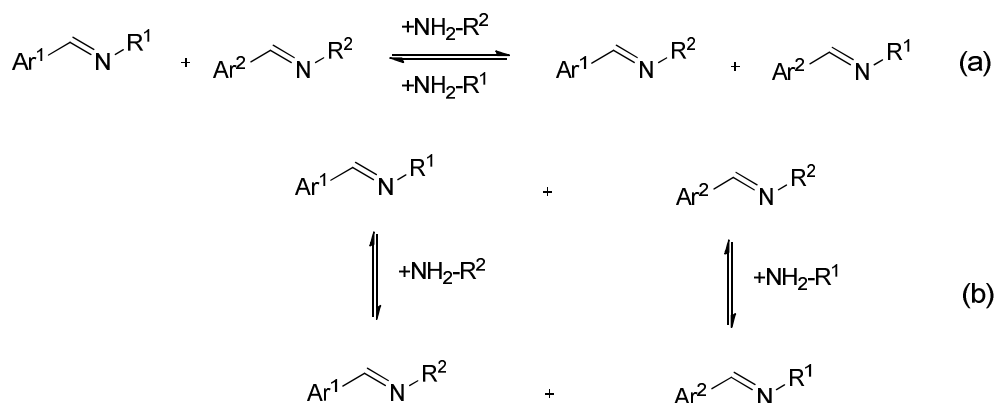
Olefin metathesis has generated great interest in organometallic chemistry leading to similar interest in analogous metal-catalyzed imine exchange metathesis.^[168–172] In the late 20th century, the imine cross-metathesis was investigated^[35,37–40,173–175] using CpM(=NR)Cl_2 as the catalyst (Cp = cyclopentadiene, M = Zr, Mo, Nb, Ti, Ta). The proposed mechanism for the metal-imido catalysis does not involve the direct reaction between imines. The reaction occurs via the imine reacting with a metal-imido compound

to form a diazametallacycle intermediate, its subsequent breakdown resulting in the imine exchange product and a new metal-imide (*Scheme 1.11*) following a Chauvin-type mechanism.^[176] Similarly, a second imine also reacts with metal-imido catalyst then gives a second imine exchange product. The metal complex can be thought to act as a Lewis acid activator of one imine toward nucleophilic attack of another imine reactant.^[36] The role of the trace amount of amines in the imine exchange via metal-imido ($\text{CpTa}(\text{dNBu}^1)\text{Cl}_2$) catalysis has also been investigated demonstrating that amines play a primary role in the reaction mechanism in the presence of excess imines.^[33]



Scheme 1.11 A possible mechanism of imine metathesis following a Chauvin-type catalytic cycle using a metal as the catalytic center.^[164] (Figure reproduced from reference [164] and slightly modified)

In other investigations, imine exchange via an amine-mediated mechanism has been suggested to occur via the coupled transiminations between imine reactants and trace amounts of amine. Recently, Di Stefano *et al.*^[25,26] have shown that transimination reactions are accelerated in organic solvents in the presence of trace amounts of amine (either aromatic or aliphatic). The amine initially undergoes transimination with one of the imines, the product amine then undergoing transimination with the other imine, and so on (see *Scheme 1.12b* for details).

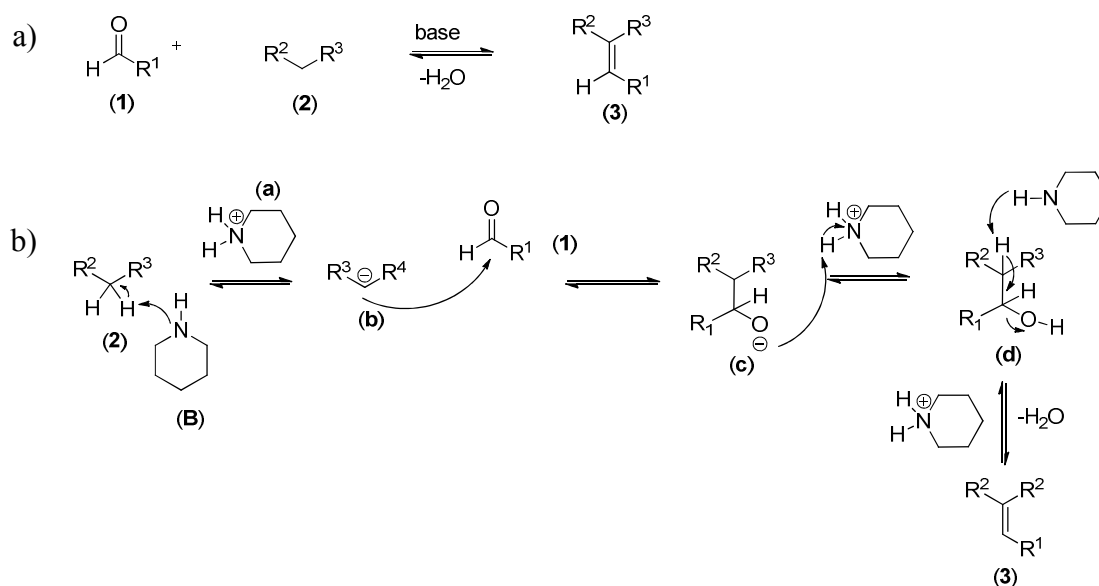


Scheme 1.12 The Imine metathesis catalyzed by the trace amount of primary amine. R^1 , R^2 = aliphatic or aromatic^[164] (Figure reproduced from reference [164] and slightly modified).

In summary the reversible formation, transimination and exchange reactions of imines under mild conditions, or in the presence of organocatalysts, have great potential for the generation of DCLs of imines which will be illustrated in *Chapters 2 and 5*.

1.4 General aspects of Knoevenagel compound chemistry

The *Knoevenagel* reaction is a facile and versatile method for the formation of carbon-carbon bonds named after Emil Knoevenagel, a German chemist (18 June 1865 – 11 August 1921).^[177,178] It is a nucleophilic addition between aldehydes or ketones and an active methylene compound, using ammonia or other weakly basic amines as catalysts in organic solvents, followed by elimination of water to afford a α,β -unsaturated compound (*Scheme 1.13a*). The methylene activity is induced by either R^3 or R^4 being a strong electron withdrawing group such as $-\text{CN}$, $-\text{COOR}$, or $-\text{NO}_2$, in order to facilitate deprotonation to give the enolate anion. If a strong base is used as a catalyst, the aldehyde or ketone may undergo self-condensation. The general mechanism for the *Knoevenagel* reaction shown in *Scheme 1.13b*, involves the deprotonation of an active methylene compound (**2**) by a weakly basic catalyst such as piperidine (**B**) to form a carbanion (**b**). This then reacts with an aldehyde (**1**) and the resulting aldol (**d**) undergoes subsequent base-induced elimination to form the *Knoevenagel* product (**3**).



Scheme 1.13 a) *Knoevenagel condensation of an aldehyde (1) with an active methylene compound (2) to form Knoevenagel product (3), b) The general mechanism of the Knoevenagel reaction in the presence of piperidine as a basic catalyst.*

This reaction is considered to be a modification of the aldol reaction; what distinguishes the *Knoevenagel* reaction is the more active methylene hydrogen when compared to an α -carbonyl hydrogen.^[179] The Henry reaction is a variant of the *Knoevenagel* condensation that uses compounds with an α -nitro active methylene.^[179] *Knoevenagel* compounds have been used to synthesize coumarins and their derivatives which are important intermediates in the cosmetic and pharmaceutical industries.^[180] A variety of *Knoevenagel* reaction products has also been used as efficient enzyme inhibitors, and anti-bacterial, anti-tumor, and anti-inflammatory agents.^[181–186] Next, some properties of *Knoevenagel* compounds are described.

Recent work using Knoevenagel compounds

In the group of Mayr, the electrophilicity of *Knoevenagel* compounds such as 5-benzylidene-1,3-dimethylbarbituric acid and thiobarbituric acid were studied (**1a-1e**, *Figure 1.9*).^[159] They were allowed to react with either neutral nucleophiles (e.g. enamines, amines, water, and hydroxide) in DMSO at 20°C. The electrophilicity parameter (E) of each compound was determined from kinetic studies and particularly the second-order rate constants for the reaction (using the Mayr-Patz equation^[189] ($\log(k) = s(N + E)$); where k is the second order reaction rate constant at 20°C, N is a nucleophilicity parameter, E is an

electrophilicity parameter, s is a nucleophile-dependent slope parameter. The constant s is defined as 1 with respect to 2-methyl-1-pentene as the nucleophile). They reported that the E parameters of the thiobarbituric acids were in the range of 10.4 – 13.9. These values are comparable with those of substituted benzylidene-malononitriles.^[188] These *Knoevenagel* compounds can also act as Michael acceptors and electronically neutral organic Lewis acids.^[190]

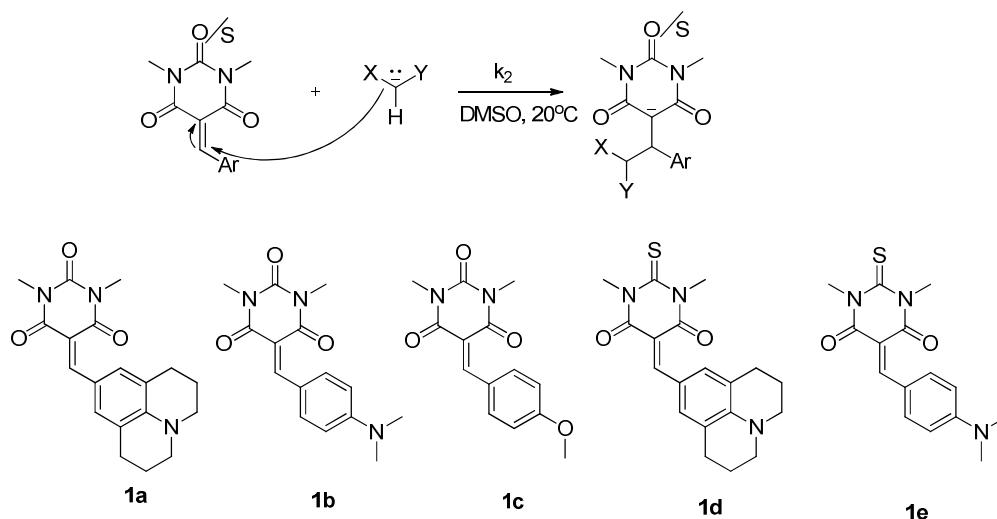


Figure 1.9 The reaction used in the investigation of the electrophilicity of *Knoevenagel* compounds **1a-e**.^[187]

The group of Wang reported that the *Knoevenagel* compounds derived from 5-benzylidene barbituric acid (*Figure 1.10*, **IIH** and **IIIM**) could be used as anion detectors by their colour changes in the visible spectrum.^[191] Both receptors showed a high sensitivity and a low detection limit for fluoride ion. The sensing mechanism for both **IIH** and **IIIM** occurs via the anion-induced retro-*Knoevenagel* reaction (anion-induced deprotonation at the methylene carbon) to liberate aldehyde and the corresponding barbituric acid, which then leads to a double addition product. The sensing behavior of **IIH** can also be driven by hydrogen bonding of, for instance, a fluoride ion with the receptor N-H proton, which shifts the charge transfer absorption band of **IIH**. This approach suggests new perspectives for anion sensing by barbituric acid derivatives.

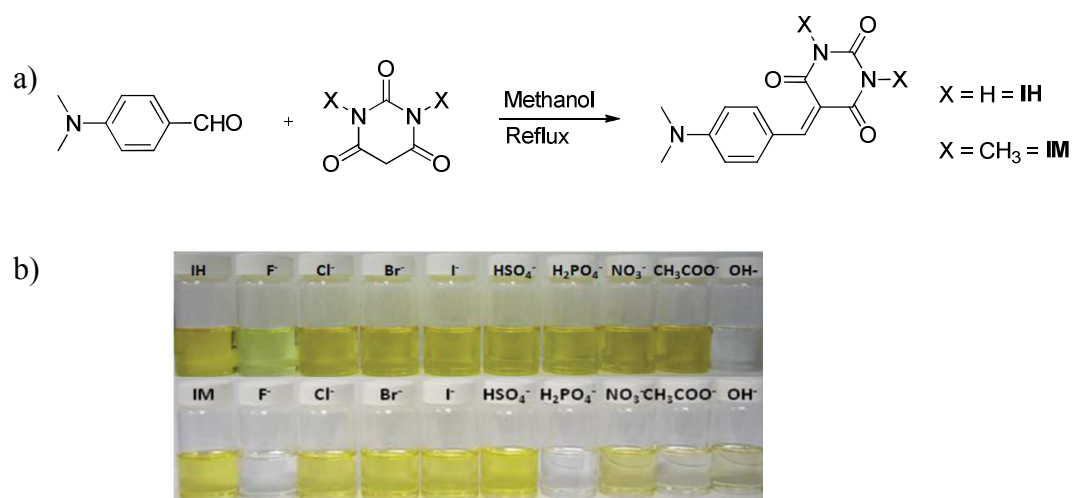


Figure 1.10 a) The Knoevenagel compounds **IH** and **IM** as anion receptors. b) Color changes observed after adding anions to solutions of **IH** and **IM**.^[191] (Figure reproduced from reference [191])

Spange *et al.* have shown that supramolecular self-assembly via hydrogen bonding interaction between a highly dipolar pyridinium-barbiturate-betaine (**3**) with 2,6-diacetamidopyridine (**DAC**) or 9-ethyladenine (**EtAd**), or 2,6-bis(trifluoroacetamino)pyridine (**BTF**) has a marked effect on the reactivity of the barbiturate with several nucleophiles (Figure 1.11a).^[192] They also demonstrated that barbituric-merocyanines (Figure 1.11b) could form a supramolecular complex via hydrogen bonding with **DAC** and have an electrophilic behavior enabling them to react with some nucleophiles.^[193]

In summary, with such a broad range of interesting properties and applications, the generation of DCLs based on dynamic covalent bonding of *Knoevenagel* compounds would be an important advance but this has never been attempted to date. The formation of *Knoevenagel* compounds (Scheme 1.13) is reversible and very sensitive to the strength of the base. Furthermore barbituric acid derivatives have been shown to bind efficiently to templates. All these features suggest that diverse DCLs with selective/adaptive capabilities could be formed by *Knoevenagel* compounds, as is described in detail in Chapters 2 and 3.

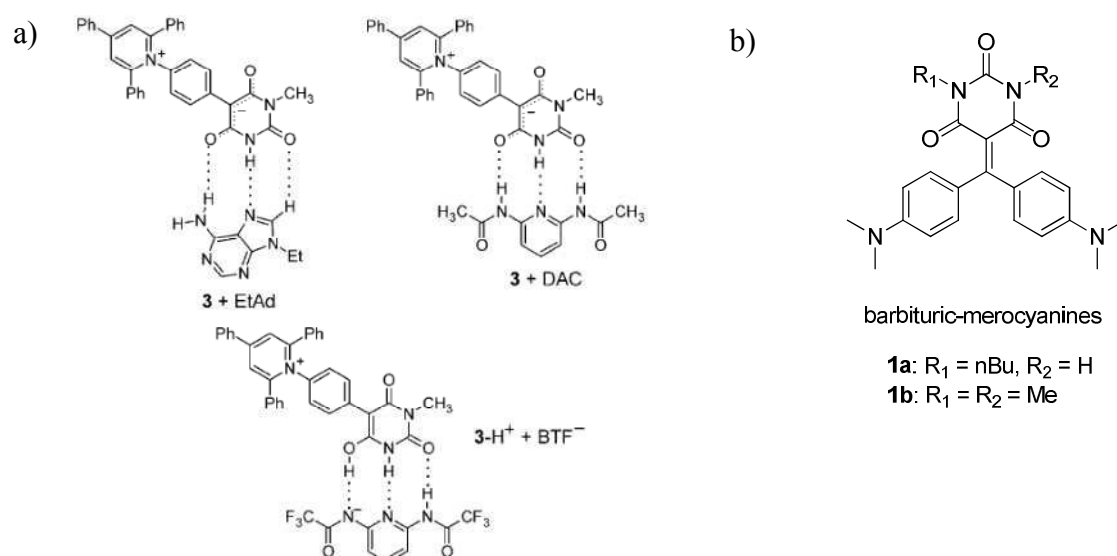
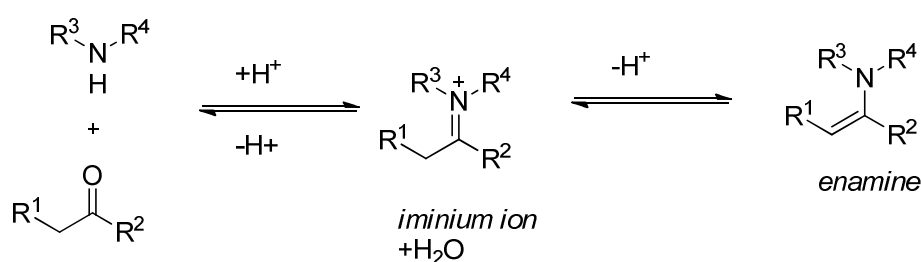


Figure 1.11 a) The supramolecular self-assembly via hydrogen-bonding of barbituric dye (**3**) with artificial receptors **DAC**, **EtAd**, or **BTF**,^[192] b) barbituric-merocyanines (**1a**, **1b**).^[193] (Figure reproduced from reference [192,193])

1.5 General aspects of Organocatalysis

Organocatalysis is the acceleration of chemical reactions with small amounts of an organic compound which does not contain a metal ion at the actual catalytic centre.^[194] In recent decades, the field of organocatalysis has expanded enormously as it has been shown that reaction pathways catalyzed by organocatalysts can have much lower transition state energies than the corresponding metal-catalyzed reactions, *i.e.* they can be more efficient, and also more environmentally/bio-friendly. Long known, transition-metal-mediated coupling reactions, such as Suzuki,^[195–197] Sonogashira,^[198] and Heck type reactions,^[199] can now be performed under metal-free conditions. The most common organocatalysts are bifunctional with both Bronsted acid and Lewis base centers which can activate the reagent and accelerate the reaction.^[200,201] Of course, organic molecules have been used since the beginnings of chemistry as catalysts, but new applications such as enantioselective catalysis continue to emerge or re-emerge.^[200,202–206] The majority of all organocatalytic reactions are amine-based reactions, so-called asymmetric aminocatalysed.^[207] Most of these processes pass through the formation of either iminium or through both iminium and enamine intermediates.

As noted earlier, the condensation reaction between aldehydes or ketones and a secondary amine can give an enamine product via an iminium ion intermediate (*Scheme 1.14*). Iminium salts are more electrophilic than aldehydes or ketones. Therefore, the reversible iminium salt/enamine formation can activate carbonyl compounds toward nucleophilic attack. These reactions include cycloadditions, nucleophilic additions (providing the formation and deprotonation of enamine components can occur), and also retro-aldol type reactions such as decarboxylation. An example of iminium activation is depicted in *Scheme 1.14*.^[208]



Scheme 1.14 The formation of imine or enamine via iminium ion.^[208]

The first established case of iminium catalysis was the *Knoevenagel* condensation catalyzed by primary or secondary amines.^[209] Knoevenagel himself suggested the possibility of an aldehyde-derived imine or aminal intermediate in this reaction.^[177] In 1952, Crowell and Peck^[210] obtained kinetic evidence for an imine/iminium intermediate in the *Knoevenagel* condensation between piperonal and nitromethane. Moreover, in 1962, Jencks and co-workers^[211] described an aniline catalyzed semicarbazone formation which occurred via transimination of the iminium ion. They confirmed the existence of the iminium intermediate by kinetic experiments.

Recently, secondary amines such as L-proline have found to be the most successful catalysts for the enamine-iminium catalytic pathway. *Figure 1.12* shows how L-proline can react with a ketone then transform to a nucleophilic iminium/enamine intermediate which is easy to trap with an introduced active electrophilic species (such as aldehyde ketone or an azocarboxylate), this leading to regeneration of an iminium ion which subsequently releases the product and L-proline to continue the cycle.

The *N*-atom of L-proline has a higher basicity and a greater nucleophilicity than those of other amino acids.^[194] It can react with carbonyl groups or Michael acceptors to form the iminium ion and/or enamine. The carboxylic group of L-proline can also act as a Bronsted acid, thus, it can be used as a bifunctional catalyst (*Figure 1.12*). Proline is not the only organic molecule which can activate iminium/enamine reactions, and not all iminium/enamine reactions can be catalyzed by L-proline. Nevertheless, L-proline and its derivatives (*Figure 1.13*) play a major role as organocatalysts.

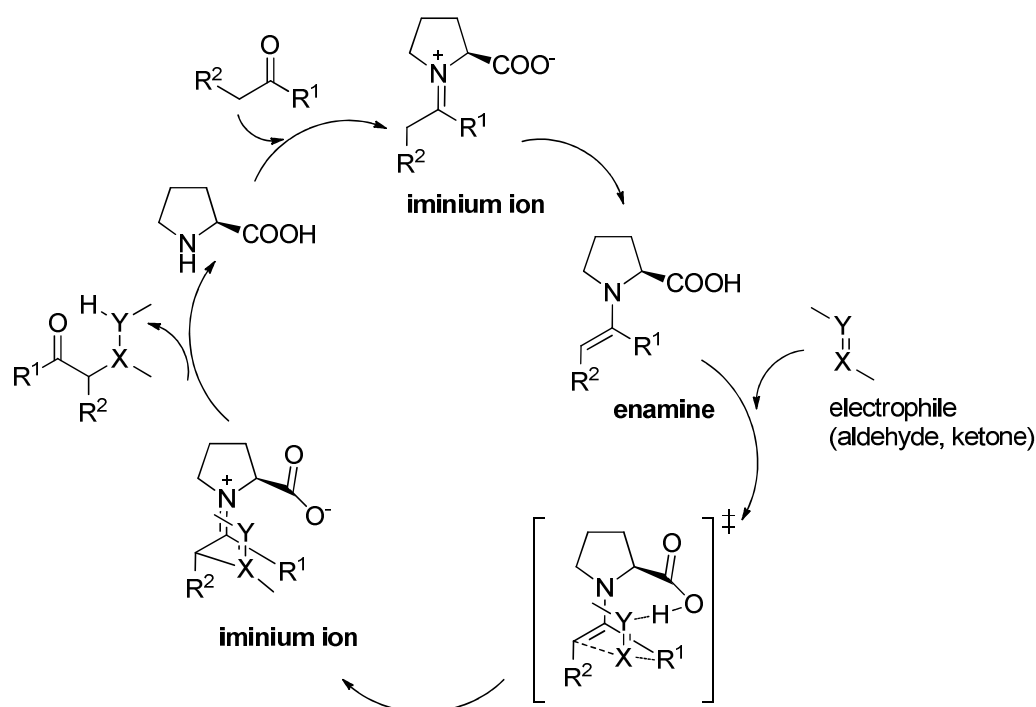


Figure 1.12 The enamine-iminium catalytic cycle in the presence of L-proline.^[194] (Figure reproduced from reference [194] with minor modification)

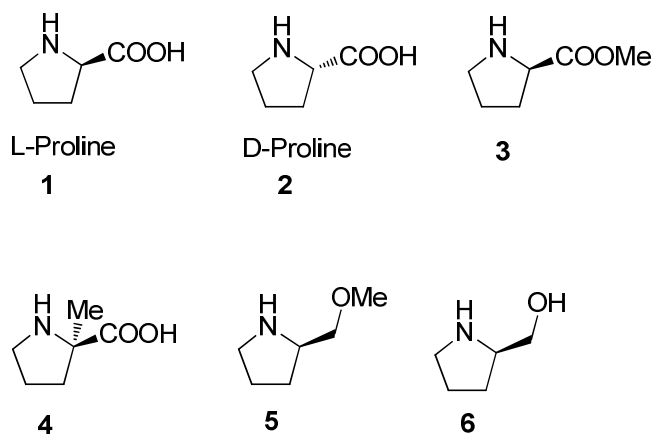


Figure 1.13 Examples of proline derivatives used as organocatalysts.^[194]

There are several amine-catalyzed reactions that cannot easily be classified into either enamine or iminium mechanism types, or it is possible that both mechanisms cooperate at the same time. Mostly the reactions proceed through enamines, but the possibility of iminium ions as active intermediates cannot be excluded.^[208] List *et al.* in 2004, reported the intramolecular Michael reaction (*Figure 1.14*), where a C-C bond is formed between the α -carbon of saturated aldehyde group and the carbon at the β -position of an enal or enone.^[212] They suggested that the reactions might proceed via either enamine catalysis or a dual enamine-iminium pathway.

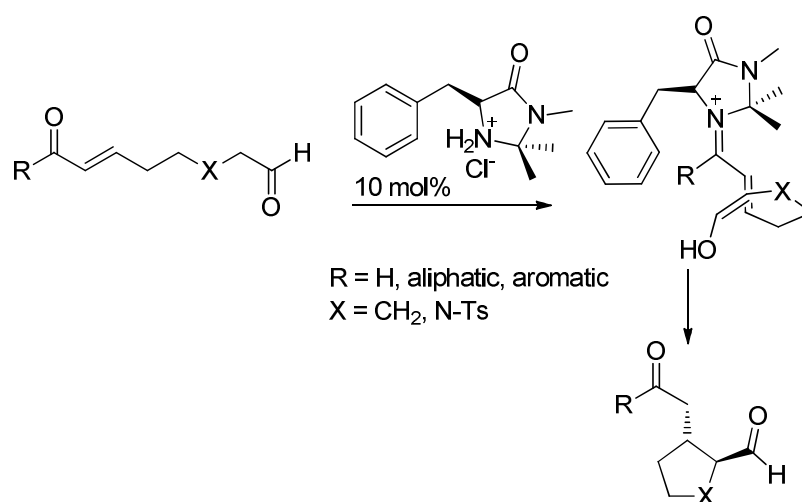


Figure 1.14 Intramolecular enantioselective Michael addition.^[208,212]

In 2000, MacMillan *et al.*^[213] described the first enantioselective organocatalyst for Diels-Alder cycloaddition reactions. Chiral amino derivative **7** was a suitable catalyst for the reaction between α,β -unsaturated aldehydes and various dienes through an iminium ion intermediate mechanism (*Figure 1.15*). The efficiency of the organocatalyst **7** depended on the diene structure.

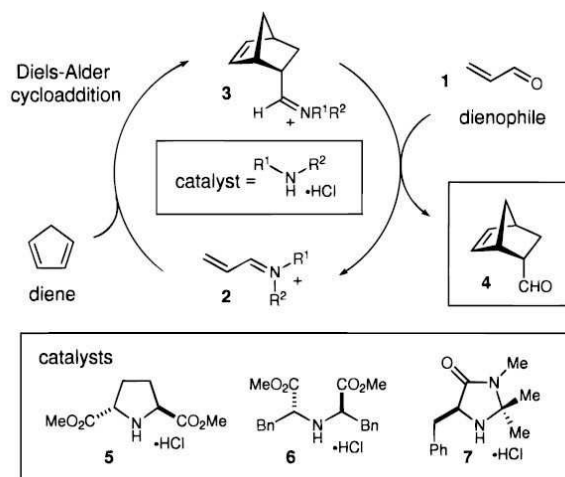
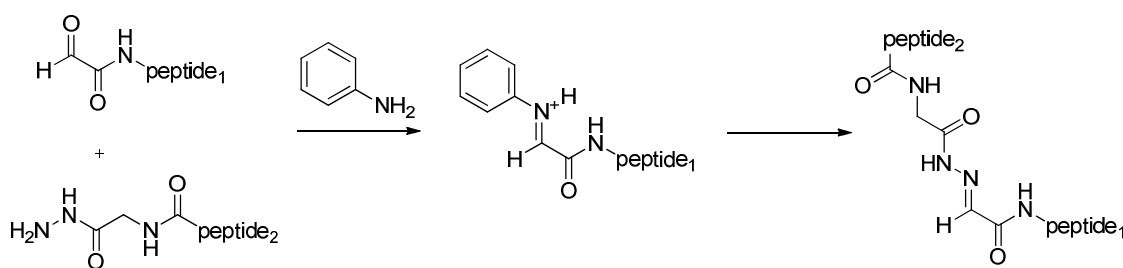


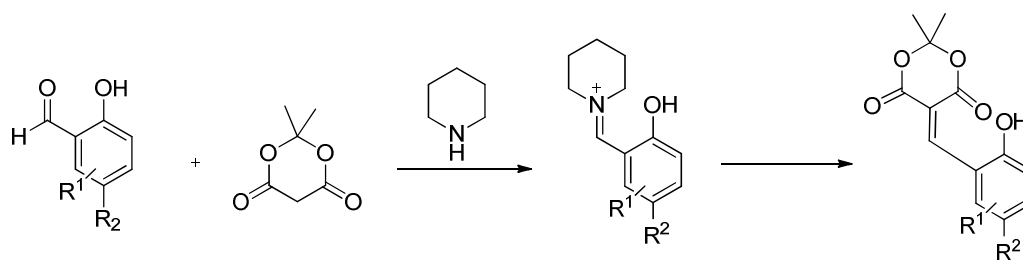
Figure 1.15 The first enantioselective organocatalyst for a Diels-Alder reaction via the formation of an iminium ion intermediate.^[213] (Figure reproduced from reference [213])

Dawson *et al.*^[214] examined the use of aniline as a nucleophilic catalyst in hydrazone formation between two unprotected peptides as well as the transimination reactions of these peptides with amines (*Scheme 1.16*). The reaction rates were compared in the presence and absence of aniline and showed a marked increase in the presence of the catalyst. They proposed that the formation and transimination reaction proceeded via an iminium intermediate as Jencks had suggested previously.^[211]



Scheme 1.16 Aniline-catalyzed hydrazone formation.^[208,214]

Lam *et al.*^[215] investigated the piperidinium-catalyzed condensation between 2-hydroxybenzaldehyde and Meldrum's acid in the synthesis of derivatives of coumarins (*Scheme 1.17*). The reactions proceeded in very high yields. Similarly, L-proline-catalyzed *Knoevenagel* condensation has been used^[216] in the synthesis of alkylidene and arylidene malonates.



Scheme 1.17 The condensation between aldehydes and Meldrum's acid via an iminium-catalyzed pathway.^[215]

Furthermore, proline has been used extensively in a nucleophilic catalytic cycle of aldol reactions based on cinchona alkaloids and oligopeptides. It has been used to catalyze an asymmetric intramolecular aldol reaction to obtain a bicyclic β -lactone cyclization product using O-acylated cinchona alkaloids.^[217] The synthesis of an analogue of a cinchona alkaloid has been achieved using a similar enantioselective reaction. Finally, oligopeptides with an *N*-terminal proline^[218] have been used instead of L-proline in asymmetric aldol reactions. The catalyst could be optimized for the substrate and reaction conditions.

In conclusion, an increasing number of organocatalysts is being developed especially for organic reactions involving iminium/enamine intermediates. These catalysts can allow otherwise slow reversible reactions to occur quickly under mild conditions, thus satisfying the criterion for fast exchange in the generation of DCLs. Therefore, the implementation of organocatalysis offers much potential for expanding the range of exchange processes that can be used in CDC as well as improving their reactional features. The organocatalytic pathway for the generation of a DCL is treated in detail in *Chapter 2*.

1.6 References

- [1] J.-M. Lehn, *Chem. Soc. Rev.* **2007**, *36*, 151–160.
- [2] J.-M. Lehn, *Supramolecular Chemistry Concepts and Perspectives*, Wiley-VCH, Weinheim, **1995**, p. 271.
- [3] P. T. Corbett, J. Leclaire, L. Vial, K. R. West, J.-L. Wietor, J. K. M. Sanders, S. Otto, *Chem. Rev.* **2006**, *106*, 3652–3711.
- [4] J.-M. Lehn, A. V. Eliseev, *Science* **2001**, *291*, 2331–2332.
- [5] S. J. Rowan, S. J. Cantrill, G. R. L. Cousins, J. K. M. Sanders, J. F. Stoddart, *Angew. Chem. Int. Ed.* **2002**, *41*, 898–952.
- [6] J.-M. Lehn, *Chem. – Eur. J.* **1999**, *5*, 2455–2463.
- [7] R. F. Ludlow, S. Otto, *Chem. Soc. Rev.* **2007**, *37*, 101–108.
- [8] A. Ganesan, *Angew. Chem. Int. Ed.* **1998**, *37*, 2828–2831.
- [9] G. R. Cousins, S.-A. Poulsen, J. K. Sanders, *Curr. Opin. Chem. Biol.* **2000**, *4*, 270–279.
- [10] J. T. Goodwin, D. G. Lynn, *J. Am. Chem. Soc.* **1992**, *114*, 9197–9198.
- [11] I. Huc, J.-M. Lehn, *Proc. Natl. Acad. Sci.* **1997**, *94*, 2106–2110.
- [12] B. Klekota, M. H. Hammond, B. L. Miller, *Tetrahedron Lett.* **1997**, *38*, 8639–8642.
- [13] M. Hochgürtel, R. Biesinger, H. Kroth, D. Piecha, M. W. Hofmann, S. Krause, O. Schaaf, C. Nicolau, A. V. Eliseev, *J. Med. Chem.* **2003**, *46*, 356–358.
- [14] S. J. Rowan, J. F. Stoddart, *Org. Lett.* **1999**, *1*, 1913–1916.
- [15] J. R. Nitschke, J.-M. Lehn, *Proc. Natl. Acad. Sci.* **2003**, *100*, 11970–11974.
- [16] C. Godoy-Alcántar, A. K. Yatsimirsky, J.-M. Lehn, *J. Phys. Org. Chem.* **2005**, *18*, 979–985.
- [17] N. Giuseppone, J.-M. Lehn, *Chem. – Eur. J.* **2006**, *12*, 1715–1722.
- [18] R. J. Lins, S. L. Flitsch, N. J. Turner, E. Irving, S. A. Brown, *Tetrahedron* **2004**, *60*, 771–780.
- [19] V. A. Polyakov, M. I. Nelen, N. Nazarpak-Kandlousy, A. D. Ryabov, A. V. Eliseev, *J. Phys. Org. Chem.* **1999**, *12*, 357–363.
- [20] N. Nazarpak-Kandlousy, M. I. Nelen, V. Goral, A. V. Eliseev, *J. Org. Chem.* **2002**, *67*, 59–65.
- [21] H. Schiff, *Justus Liebigs Ann. Chem.* **1864**, *131*, 118–119.
- [22] R. B. Moffett, W. M. Hoehn, *J. Am. Chem. Soc.* **1947**, *69*, 1792–1794.

- [23] M. Freifelder, *J. Org. Chem.* **1966**, *31*, 3875–3877.
- [24] M. C. Thompson, D. H. Busch, *J. Am. Chem. Soc.* **1962**, *84*, 1762–1763.
- [25] M. Ciaccia, R. Cacciapaglia, P. Mencarelli, L. Mandolini, S. D. Stefano, *Chem. Sci.* **2013**, *4*, 2253–2261.
- [26] M. Ciaccia, S. Pilati, R. Cacciapaglia, L. Mandolini, S. D. Stefano, *Org. Biomol. Chem.* **2014**, *12*, 3282–3287.
- [27] P. Kovaříček, J.-M. Lehn, *J. Am. Chem. Soc.* **2012**, *134*, 9446–9455.
- [28] N. Wilhelms, S. Kulchat, J.-M. Lehn, *Helv. Chim. Acta* **2012**, *95*, 2635–2651.
- [29] M. C. Burland, T. Y. Meyer, M.-H. Baik, *J. Org. Chem.* **2004**, *69*, 6173–6184.
- [30] D. Zhao, J. S. Moore, *J. Am. Chem. Soc.* **2002**, *124*, 9996–9997.
- [31] D. Zhao, J. S. Moore, *Macromolecules* **2003**, *36*, 2712–2720.
- [32] K. Oh, K.-S. Jeong, J. S. Moore, *Nature* **2001**, *414*, 889–893.
- [33] M. C. Burland, T. W. Pontz, T. Y. Meyer, *Organometallics* **2002**, *21*, 1933–1941.
- [34] M. C. Burland, T. Y. Meyer, *Inorg. Chem.* **2003**, *42*, 3438–3444.
- [35] G. K. Cantrell, T. Y. Meyer, *Organometallics* **1997**, *16*, 5381–5383.
- [36] G. K. Cantrell, T. Y. Meyer, *J. Am. Chem. Soc.* **1998**, *120*, 8035–8042.
- [37] K. E. Meyer, P. J. Walsh, R. G. Bergman, *J. Am. Chem. Soc.* **1994**, *116*, 2669–2670.
- [38] K. E. Meyer, P. J. Walsh, R. G. Bergman, *J. Am. Chem. Soc.* **1995**, *117*, 974–985.
- [39] S. W. Krska, R. L. Zuckerman, R. G. Bergman, *J. Am. Chem. Soc.* **1998**, *120*, 11828–11829.
- [40] R. L. Zuckerman, S. W. Krska, R. G. Bergman, *J. Am. Chem. Soc.* **2000**, *122*, 751–761.
- [41] M. Hutin, G. Bernardinelli, J. R. Nitschke, *Chem. – Eur. J.* **2008**, *14*, 4585–4593.
- [42] Y. Pérez-Fuertes, A. M. Kelly, A. L. Johnson, S. Arimori, S. D. Bull, T. D. James, *Org. Lett.* **2006**, *8*, 609–612.
- [43] N. Roy, J.-M. Lehn, *Chem. – Asian J.* **2011**, *6*, 2419–2425.
- [44] P. Reutenauer, E. Buhler, P. J. Boul, S. J. Candau, J.-M. Lehn, *Chem. – Eur. J.* **2009**, *15*, 1893–1900.
- [45] P. J. Boul, P. Reutenauer, J.-M. Lehn, *Org. Lett.* **2005**, *7*, 15–18.
- [46] R. H. Grubbs, S. Chang, *Tetrahedron* **1998**, *54*, 4413–4450.
- [47] P. C. M. van Gerven, J. A. A. W. Elemans, J. W. Gerritsen, S. Speller, R. J. M. Nolte, A. E. Rowan, *Chem. Commun.* **2005**, 3535–3537.

- [48] K. C. Nicolaou, R. Hughes, S. Y. Cho, N. Winssinger, C. Smethurst, H. Labischinski, R. Endermann, *Angew. Chem. Int. Ed.* **2000**, *39*, 3823–3828.
- [49] L. K. Johnson, S. C. Virgil, R. H. Grubbs, J. W. Ziller, *J. Am. Chem. Soc.* **1990**, *112*, 5384–5385.
- [50] A. Fürstner, K. Grela, *Angew. Chem. Int. Ed.* **2000**, *39*, 1234–1236.
- [51] F. D. Toste, A. K. Chatterjee, R. H. Grubbs, *Pure Appl. Chem.* **2002**, *74*, 7–10.
- [52] Y.-X. Lu, Z. Guan, *J. Am. Chem. Soc.* **2012**, *134*, 14226–14231.
- [53] H. F. Gilbert, *J. Biol. Chem.* **1997**, *272*, 29399–29402.
- [54] S. Sando, A. Narita, Y. Aoyama, *Bioorg. Med. Chem. Lett.* **2004**, *14*, 2835–2838.
- [55] Y. Krishnan-Ghosh, A. M. Whitney, S. Balasubramanian, *Chem. Commun.* **2005**, 3068–3070.
- [56] S.-F. Chong, R. Chandrawati, B. Städler, J. Park, J. Cho, Y. Wang, Z. Jia, V. Bulmus, T. P. Davis, A. N. Zelikin, et al., *Small* **2009**, *5*, 2601–2610.
- [57] A. Fava, A. Iliceto, E. Camera, *J. Am. Chem. Soc.* **1957**, *79*, 833–838.
- [58] V. van Axel Castelli, F. Bernardi, A. Dalla Cort, L. Mandolini, I. Rossi, L. Schiaffino, *J. Org. Chem.* **1999**, *64*, 8122–8126.
- [59] A. G. Myers, S. B. Herzon, *J. Am. Chem. Soc.* **2003**, *125*, 12080–12081.
- [60] B. Shi, M. F. Greaney, *Chem. Commun.* **2005**, 886–888.
- [61] M. M. Conn, J. Rebek, *Chem. Rev.* **1997**, *97*, 1647–1668.
- [62] B. Linton, A. D. Hamilton, *Chem. Rev.* **1997**, *97*, 1669–1680.
- [63] K. Pandurangan, J. A. Kitchen, T. McCabe, T. Gunnlaugsson, *CrystEngComm* **2013**, *15*, 1421–1431.
- [64] P. J. Woodward, D. Hermida Merino, B. W. Greenland, I. W. Hamley, Z. Light, A. T. Slark, W. Hayes, *Macromolecules* **2010**, *43*, 2512–2517.
- [65] G. B. W. L. Ligthart, H. Ohkawa, R. P. Sijbesma, E. W. Meijer, *J. Am. Chem. Soc.* **2005**, *127*, 810–811.
- [66] Y. Li, T. Park, J. K. Quansah, S. C. Zimmerman, *J. Am. Chem. Soc.* **2011**, *133*, 17118–17121.
- [67] C. Laurence, K. A. Brameld, J. Graton, J.-Y. Le Questel, E. Renault, *J. Med. Chem.* **2009**, *52*, 4073–4086.
- [68] M. C. Calama, P. Timmerman, D. N. Reinhoudt, M. C. Calama, R. Hulst, P. Timmerman, R. Fokkens, N. M. M. Nibbering, *Chem. Commun.* **1998**, 1021–1022.

- [69] A. Wu, A. Chakraborty, J. C. Fettinger, R. A. Flowers II, L. Isaacs, *Angew. Chem. Int. Ed.* **2002**, *41*, 4028–4031.
- [70] J. Lin, J. Wu, X. Jiang, Z. Li, *Chin. J. Chem.* **2009**, *27*, 117–122.
- [71] J.-B. Lin, X.-N. Xu, X.-K. Jiang, Z.-T. Li, *J. Org. Chem.* **2008**, *73*, 9403–9410.
- [72] P. Timmerman, R. H. Vreekamp, R. Hulst, W. Verboom, D. N. Reinhoudt, K. Rissanen, K. A. Udachin, J. Ripmeester, *Chem. – Eur. J.* **1997**, *3*, 1823–1832.
- [73] I. Huc, M. J. Krische, D. P. Funeriu, J.-M. Lehn, *Eur. J. Inorg. Chem.* **1999**, *1999*, 1415–1420.
- [74] V. Goral, M. I. Nelen, A. V. Eliseev, J.-M. Lehn, *Proc. Natl. Acad. Sci.* **2001**, *98*, 1347–1352.
- [75] E. Stulz, Y.-F. Ng, S. M. Scott, J. K. M. Sanders, *Chem. Commun.* **2002**, 524–525.
- [76] E. Stulz, S. M. Scott, A. D. Bond, S. J. Teat, J. K. M. Sanders, *Chem. – Eur. J.* **2003**, *9*, 6039–6048.
- [77] A. C. Try, M. M. Harding, A. C. Try, M. M. Harding, D. G. Hamilton, J. K. M. Sanders, *Chem. Commun.* **1998**, 723–724.
- [78] O. Shoji, S. Okada, A. Satake, Y. Kobuke, *J. Am. Chem. Soc.* **2005**, *127*, 2201–2210.
- [79] C. Karan, B. L. Miller, *J. Am. Chem. Soc.* **2001**, *123*, 7455–7456.
- [80] M. A. Case, G. L. McLendon, *J. Am. Chem. Soc.* **2000**, *122*, 8089–8090.
- [81] N. Sreenivasachary, J.-M. Lehn, *Proc. Natl. Acad. Sci.* **2005**, *102*, 5938–5943.
- [82] L. Greb, J.-M. Lehn, *J. Am. Chem. Soc.* **2014**, *136*, 13114–13117.
- [83] M. N. Chaur, D. Collado, J.-M. Lehn, *Chem. – Eur. J.* **2011**, *17*, 248–258.
- [84] J.-M. Lehn, *Angew. Chem. Int. Ed.* **2013**, *52*, 2836–2850.
- [85] J.-M. Lehn, *Chem. – Eur. J.* **2006**, *12*, 5910–5915.
- [86] D. Kühne, F. Klappenberger, W. Krenner, S. Klyatskaya, M. Ruben, J. V. Barth, *Proc. Natl. Acad. Sci.* **2010**, *107*, 21332–21336.
- [87] G. Vantomme, S. Jiang, J.-M. Lehn, *J. Am. Chem. Soc.* **2014**, *136*, 9509–9518.
- [88] J. Li, P. Nowak, S. Otto, *J. Am. Chem. Soc.* **2013**, *135*, 9222–9239.
- [89] Y. Liu, Z.-T. Li, *Aust. J. Chem.* **2013**, *66*, 9–22.
- [90] S. Otto, R. L. E. Furlan, J. K. M. Sanders, *Drug Discov. Today* **2002**, *7*, 117–125.
- [91] S. Otto, R. L. Furlan, J. K. Sanders, *Curr. Opin. Chem. Biol.* **2002**, *6*, 321–327.
- [92] C. Karan, B. L. Miller, *Drug Discov. Today* **2000**, *5*, 67–75.
- [93] B. Linton, A. D. Hamilton, *Curr. Opin. Chem. Biol.* **1999**, *3*, 307–312.

- [94] R. L. E. Furlan, S. Otto, J. K. M. Sanders, *Proc. Natl. Acad. Sci.* **2002**, *99*, 4801–4804.
- [95] C. Schmuck, P. Wich, *New J. Chem.* **2006**, *30*, 1377–1385.
- [96] M. J. MacLachlan, *Pure Appl. Chem.* **2006**, *78*, 873–888.
- [97] P. C. Haussmann, J. F. Stoddart, *Chem. Rec.* **2009**, *9*, 136–154.
- [98] M. Mastalerz, *Angew. Chem. Int. Ed.* **2010**, *49*, 5042–5053.
- [99] N. M. Rue, J. Sun, R. Warmuth, *Isr. J. Chem.* **2011**, *51*, 743–768.
- [100] B. de Bruin, P. Hauwert, J. N. H. Reek, *Angew. Chem. Int. Ed.* **2006**, *45*, 2660–2663.
- [101] C. D. Meyer, C. S. Joiner, J. F. Stoddart, *Chem. Soc. Rev.* **2007**, *36*, 1705–1723.
- [102] S. Otto, K. Severin, *Top. Curr. Chem.*, **2007**, *277*, 267–288.
- [103] J. W. Sadownik, R. V. Ulijn, *Curr. Opin. Biotechnol.* **2010**, *21*, 401–411.
- [104] S. Otto, *Acc. Chem. Res.* **2012**, *45*, 2200–2210.
- [105] B. Fuchs, *Isr. J. Chem.* **2013**, *53*, 45–52.
- [106] O. Ramström, J.-M. Lehn, *Nat. Rev. Drug Discov.* **2002**, *1*, 26–36.
- [107] O. Ramström, S. Lohmann, T. Bunyapaiboonsri, J.-M. Lehn, *Chem. – Eur. J.* **2004**, *10*, 1711–1715.
- [108] T. Hotchkiss, H. B. Kramer, K. J. Doores, D. P. Gamblin, N. J. Oldham, B. G. Davis, *Chem. Commun.* **2005**, 4264–4266.
- [109] G. Nasr, E. Petit, C. T. Supuran, J.-Y. Winum, M. Barboiu, *Bioorg. Med. Chem. Lett.* **2009**, *19*, 6014–6017.
- [110] D. E. Scott, G. J. Dawes, M. Ando, C. Abell, A. Ciulli, *ChemBioChem* **2009**, *10*, 2772–2779.
- [111] R. Caraballo, H. Dong, J. P. Ribeiro, J. Jiménez-Barbero, O. Ramström, *Angew. Chem. Int. Ed.* **2010**, *49*, 589–593.
- [112] J.-M. Lehn, *Prog. Polym. Sci.* **2005**, *30*, 814–831.
- [113] R. J. Williams, A. M. Smith, R. Collins, N. Hodson, A. K. Das, R. V. Ulijn, *Nat. Nanotechnol.* **2009**, *4*, 19–24.
- [114] S. Otto, *Nat. Nanotechnol.* **2009**, *4*, 13–14.
- [115] R. Nguyen, E. Buhler, N. Giuseppone, *Macromolecules* **2009**, *42*, 5913–5915.
- [116] N. Giuseppone, *Acc. Chem. Res.* **2012**, *45*, 2178–2188.
- [117] E. Moulin, G. Cormos, N. Giuseppone, *Chem. Soc. Rev.* **2012**, *41*, 1031–1049.
- [118] M. Barboiu, *Chem. Commun.* **2010**, *46*, 7466–7476.

- [119] Y. Xin, J. Yuan, *Polym. Chem.* **2012**, *3*, 3045–3055.
- [120] A. W. Jackson, D. A. Fulton, *Polym. Chem.* **2012**, *4*, 31–45.
- [121] C. J. Kloxin, C. N. Bowman, *Chem. Soc. Rev.* **2013**, *42*, 7161–7173.
- [122] T. Maeda, H. Otsuka, A. Takahara, *Prog. Polym. Sci.* **2009**, *34*, 581–604.
- [123] J.-M. Lehn, *Aust. J. Chem.* **2010**, *63*, 611–623.
- [124] A. Ciesielski, P. Samori, *Nanoscale* **2011**, *3*, 1397–1410.
- [125] A. L. Korich, P. M. Iovine, *Dalton Trans.* **2010**, *39*, 1423–1431.
- [126] D. Roy, J. N. Cambre, B. S. Sumerlin, *Prog. Polym. Sci.* **2010**, *35*, 278–301.
- [127] K. Severin, *Dalton Trans.* **2009**, 5254–5264.
- [128] A.-J. Avestro, M. E. Belowich, J. F. Stoddart, *Chem. Soc. Rev.* **2012**, *41*, 5881–5895.
- [129] C. Wang, Z. Wang, X. Zhang, *Acc. Chem. Res.* **2012**, *45*, 608–618.
- [130] H. Otsuka, *Polym. J.* **2013**, *45*, 879–891.
- [131] M. Sakulsombat, Y. Zhang, O. Ramström, *Top. Curr. Chem.*, **2012**, *322*, 55–86.
- [132] K. Osowska, O. Miljanić, *Synlett* **2011**, *2011*, 1643–1648.
- [133] R. Nguyen, I. Huc, *Angew. Chem. Int. Ed.* **2001**, *40*, 1774–1776.
- [134] Z. J. Gartner, *Pure Appl. Chem.* **2006**, *78*, 1–14.
- [135] M. M. Rozenman, B. R. McNaughton, D. R. Liu, *Curr. Opin. Chem. Biol.* **2007**, *11*, 259–268.
- [136] P. A. Brady, J. K. M. Sanders, *Chem. Soc. Rev.* **1997**, *26*, 327–336.
- [137] G. Gasparini, M. Dal Molin, L. J. Prins, *Eur. J. Org. Chem.* **2010**, *2010*, 2429–2440.
- [138] P. Dydio, P.-A. R. Breuil, J. N. H. Reek, *Isr. J. Chem.* **2013**, *53*, 61–74.
- [139] S. Ladame, *Org. Biomol. Chem.* **2008**, *6*, 219–226.
- [140] A. Herrmann, *Chem. – Eur. J.* **2012**, *18*, 8568–8577.
- [141] M. Vendrell, S. Feng, Y.-T. Chang, in *Chemosensors: Principles, Strategies, and Applications*, ed. B. Wang and E.V. Anslyn, John Wiley & Sons, Hoboken, **2011**, pp. 87–106.
- [142] A. Herrmann, *Org. Biomol. Chem.* **2009**, *7*, 3195–3204.
- [143] R. W. Layer, *Chem. Rev.* **1963**, *63*, 489–510.
- [144] P.Y. Bruice, *Organic Chemistry*, 4th, **2004**, p. 1228.
- [145] E. H. Cordes, W. P. Jencks, *J. Am. Chem. Soc.* **1962**, *84*, 832–837.
- [146] H. Fischer, F. X. DeCandis, S. D. Ogden, W. P. Jencks, *J. Am. Chem. Soc.* **1980**, *102*, 1340–1347.

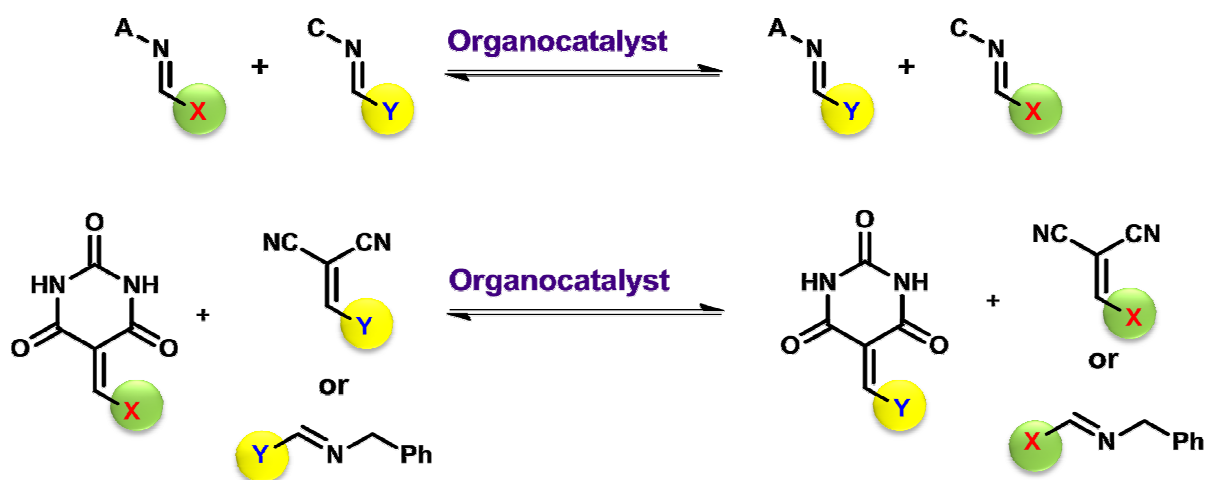
- [147] W. P. Jencks, *J. Am. Chem. Soc.* **1959**, *81*, 475–481.
- [148] D. A. Evans, G. Borg, K. A. Scheidt, *Angew. Chem. Int. Ed.* **2002**, *41*, 3188–3191.
- [149] R. J. Hooley, T. Iwasawa, J. Rebek, *J. Am. Chem. Soc.* **2007**, *129*, 15330–15339.
- [150] T. Kawamichi, T. Haneda, M. Kawano, M. Fujita, *Nature* **2009**, *461*, 633–635.
- [151] D. S. Yufit, J. A. K. Howard, *J. Mol. Struct.* **2010**, *984*, 182–185.
- [152] W.P. Jencks, *Catalysis in Chemistry and Enzymology*, McGraw-Hill, New York, **1969**, p. 644.
- [153] L. Stryer, *Biochemistry*, W. H. Freeman And Company, New York, 4th edn, **1995**.
- [154] M. Hochgurtel, J.-M. Lehn, in *Fragment-based Approaches in Drug Discovery*, ed. R. Mannhold, H. Kubinyi and G. Folkers, Wiley-VCH, Weinheim, **2006**, pp. 361–364.
- [155] S. Patai, *The Chemistry of the Carbon-Nitrogen Double Bond*, Interscience, London, **1970**.
- [156] F.A. Carey, R.J. Sundberg, *Advanced Organic Chemistry*, Springer, New York, 5th edn, **2007**.
- [157] M. E. Belowich, J. F. Stoddart, *Chem. Soc. Rev.* **2012**, *41*, 2003–2024.
- [158] A. J. Bissette, S. P. Fletcher, *Angew. Chem. Int. Ed.* **2013**, *52*, 12800–12826.
- [159] S. H. Yoo, B. J. Lee, H. Kim, J. Suh, *J. Am. Chem. Soc.* **2005**, *127*, 9593–9602.
- [160] S. Morales, F. G. Guijarro, J. L. García Ruano, M. B. Cid, *J. Am. Chem. Soc.* **2013**, *136*, 1082–1089.
- [161] D. L. Leussing, B. E. Leach, *J. Am. Chem. Soc.* **1971**, *93*, 3377–3384.
- [162] M. J. O'Donnell, R. L. Polt, *J. Org. Chem.* **1982**, *47*, 2663–2666.
- [163] L. do Amaral, W. A. Sandstrom, E. H. Cordes, *J. Am. Chem. Soc.* **1966**, *88*, 2225–2233.
- [164] M. Ciaccia, S. D. Stefano, *Org. Biomol. Chem.* **2014**, *13*, 646–654.
- [165] C.K. Ingold, H.A. Piggott, *J. Chem. Soc.*, **1922**, *121*, 2793–2804.
- [166] C.K. Ingold, H.A. Piggott, *J. Chem. Soc.*, **1923**, *123*, 2745–2752.
- [167] G. Tóth, I. Pintér, A. Messmer, *Tetrahedron Lett.* **1974**, *15*, 735–738.
- [168] R. H. Grubbs, W. Tumas, *Science* **1989**, *243*, 907–915.
- [169] R. R. Schrock, *Acc. Chem. Res.* **1990**, *23*, 158–165.
- [170] T. M. Trnka, R. H. Grubbs, *Acc. Chem. Res.* **2001**, *34*, 18–29.
- [171] S. Monfette, D. E. Fogg, *Chem. Rev.* **2009**, *109*, 3783–3816.
- [172] G. C. Vougioukalakis, R. H. Grubbs, *Chem. Rev.* **2010**, *110*, 1746–1787.

- [173] G. K. Cantrell, T. Y. Meyer, *Chem. Commun.* **1997**, 1551–1552.
- [174] W.-D. Wang, J. H. Espenson, *Organometallics* **1999**, *18*, 5170–5175.
- [175] J. W. Bruno, X. J. Li, *Organometallics* **2000**, *19*, 4672–4674.
- [176] P. Jean-Louis Hérisson, Y. Chauvin, *Makromol. Chem.* **1971**, *141*, 161–176.
- [177] E. Knoevenagel, *Berichte Dtsch. Chem. Ges.* **1898**, *31*, 2596–2619.
- [178] S. V. Ryabukhin, A. S. Plaskon, D. M. Volochnyuk, S. E. Pipko, A. N. Shivanyuk, A. A. Tolmachev, *J. Comb. Chem.* **2007**, *9*, 1073–1078.
- [179] R. Menegatti, in *Green Chem. - Environ. Benign Approaches*, InTech Europe, pp. 13–32.
- [180] Tietze, L.F., Beifuss, U., in *Compr. Org. Synth.*, Perkamon Press, Oxford, UK, pp. 341–394.
- [181] W. Lubisch, E. Beckenbach, S. Bopp, H.-P. Hofmann, A. Kartal, C. Kästel, T. Lindner, M. Metz-Garrecht, J. Reeb, F. Regner, et al., *J. Med. Chem.* **2003**, *46*, 2404–2412.
- [182] J. P. Petzer, S. Steyn, K. P. Castagnoli, J.-F. Chen, M. A. Schwarzschild, C. J. Van der Schyf, N. Castagnoli, *Bioorg. Med. Chem.* **2003**, *11*, 1299–1310.
- [183] N. Vlok, S. F. Malan, N. Castagnoli Jr., J. J. Bergh, J. P. Petzer, *Bioorg. Med. Chem.* **2006**, *14*, 3512–3521.
- [184] R. M. Lyall, A. Zilberstein, A. Gazit, C. Gilon, A. Levitzki, J. Schlessinger, *J. Biol. Chem.* **1989**, *264*, 14503–14509.
- [185] T. Shiraishi, M. K. Owada, M. Tatsuka, T. Yamashita, K. Watanabe, T. Kakunaga, *Cancer Res.* **1989**, *49*, 2374–2378.
- [186] K. Nakayama, Y. Ishida, M. Ohtsuka, H. Kawato, K. Yoshida, Y. Yokomizo, S. Hosono, T. Ohta, K. Hoshino, H. Ishida, et al., *Bioorg. Med. Chem. Lett.* **2003**, *13*, 4201–4204.
- [187] F. Seeliger, S. T. A. Berger, G. Y. Remennikov, K. Polborn, H. Mayr, *J. Org. Chem.* **2007**, *72*, 9170–9180.
- [188] T. Lemek, H. Mayr, *J. Org. Chem.* **2003**, *68*, 6880–6886.
- [189] H. Mayr, M. Patz, *Angew. Chem. Int. Ed. Engl.* **1994**, *33*, 938–957.
- [190] Kunz, F. J., Margaretha, P., Polansky, O. E., *Chimia*, 1970, 165–181.
- [191] C. Saravanan, S. Easwaramoorthi, L. Wang, *Dalton Trans.* **2014**, *43*, 5151–5157.
- [192] I. Bolz, D. Schaarschmidt, T. Ruffer, H. Lang, S. Spange, *Angew. Chem. Int. Ed.* **2009**, *48*, 7440–7443.

- [193] M. Bauer, S. Spange, *Angew. Chem. Int. Ed.* **2011**, *50*, 9727–9730.
- [194] P. I. Dalko, L. Moisan, *Angew. Chem. Int. Ed.* **2004**, *43*, 5138–5175.
- [195] N. E. Leadbeater, M. Marco, *Angew. Chem.* **2003**, *115*, 1445–1447.
- [196] N. E. Leadbeater, M. Marco, *Angew. Chem. Int. Ed.* **2003**, *42*, 1407–1409.
- [197] N. E. Leadbeater, M. Marco, *J. Org. Chem.* **2003**, *68*, 5660–5667.
- [198] N. E. Leadbeater, M. Marco, B. J. Tominack, *Org. Lett.* **2003**, *5*, 3919–3922.
- [199] R. Zhang, F. Zhao, M. Sato, Y. Ikushima, *Chem. Commun.* **2003**, 1548–1549.
- [200] J.-A. Ma, D. Cahard, *Angew. Chem. Int. Ed.* **2004**, *43*, 4566–4583.
- [201] J.-A. Ma, D. Cahard, *Angew. Chem.* **2004**, *116*, 4666–4683.
- [202] P. I. Dalko, L. Moisan, *Angew. Chem. Int. Ed.* **2001**, *40*, 3726–3748.
- [203] M. Benaglia, A. Puglisi, F. Cozzi, *Chem. Rev.* **2003**, *103*, 3401–3430.
- [204] H. Tye, P. J. Comina, *J. Chem. Soc. [Perkin 1]* **2001**, 1729–1747.
- [205] S. Bräse, F. Lauterwasser, R. E. Ziegert, *Adv. Synth. Catal.* **2003**, *345*, 869–929.
- [206] P. McMorn, G. J. Hutchings, *Chem. Soc. Rev.* **2004**, *33*, 108–122.
- [207] B. Westermann, *Angew. Chem. Int. Ed.* **2003**, *42*, 151–153.
- [208] A. Erkkilä, I. Majander, P. M. Pihko, *Chem. Rev.* **2007**, *107*, 5416–5470.
- [209] E. Knoevenagel, *Berichte Dtsch. Chem. Ges.* **1894**, *27*, 2345–2346.
- [210] T. I. Crowell, D. W. Peck, *J. Am. Chem. Soc.* **1953**, *75*, 1075–1077.
- [211] E. H. Cordes, W. P. Jencks, *J. Am. Chem. Soc.* **1962**, *84*, 826–831.
- [212] M. T. Hechavarria Fonseca, B. List, *Angew. Chem. Int. Ed.* **2004**, *43*, 3958–3960.
- [213] K. A. Ahrendt, C. J. Borths, D. W. C. MacMillan, *J. Am. Chem. Soc.* **2000**, *122*, 4243–4244.
- [214] A. Dirksen, S. Dirksen, T. M. Hackeng, P. E. Dawson, *J. Am. Chem. Soc.* **2006**, *128*, 15602–15603.
- [215] A. Song, X. Wang, K. S. Lam, *Tetrahedron Lett.* **2003**, *44*, 1755–1758.
- [216] G. Cardillo, S. Fabbroni, L. Gentilucci, M. Gianotti, A. Tolomelli, *Synth. Commun.* **2003**, *33*, 1587–1594.
- [217] G. S. Cortez, R. L. Tennyson, D. Romo, *J. Am. Chem. Soc.* **2001**, *123*, 7945–7946.
- [218] J. Kofoed, J. Nielsen, J.-L. Reymond, *Bioorg. Med. Chem. Lett.* **2003**, *13*, 2445–2447.

CHAPTER 2

Organocatalysis of Exchange Processes between Knoevenagel and Imine Compounds in Dynamic Covalent Chemistry



2.1 Introduction

Dynamic Covalent Chemistry (DCC),^[1-3] the covalent wing of Constitutional Dynamic Chemistry (CDC),^[4,5] rests on the implementation of reversible chemical reactions to generate dynamic covalent libraries (DCLs) based on interconverting molecular constituents. A major feature of DCLs is the production of high molecular-structural diversity for application in both biological^[1-13] and material sciences.^[1-5,14-19] Reversible reactions such as amine/carbonyl condensations, disulfide exchange, boronic ester formation, Diels-Alder condensations *etc.*, have been implemented in numerous studies in DCC.^[1,2,4-9,11-30] The C=N bond is of particular interest in the view of its range of structural variations, such as in imines, hydrazones and oximes, its reversibility, its easy synthesis, and its broad range of implementation.^[1-5,20,21,27-30]

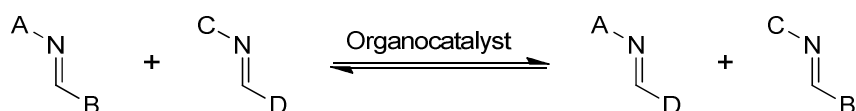
The rapidity of formation and breakdown (amine+carbonyl)/imine formation and breakdown reactions is highly suitable for DCC applications, and a major goal is to optimize fast component exchange. In recent years, organocatalysis has been developed as an efficient methodology for the acceleration of various chemical reactions.^[31-35] Among the different types of catalytic processes involving unsaturated reactants, that involving the enamine/iminium pathway is well established. In particular, L-proline, a naturally occurring chiral secondary amine, and its derivatives have been extensively used and studied as catalysts for numerous reactions, including asymmetric synthesis.^[36-39] The implementation of organocatalysis in dynamic covalent chemistry offers much potential for extending the range of exchange processes and improving their reactional features.

The work presented in this chapter was performed in collaboration with Dr. Nadine Wilhelms and Assist. Prof. Kamel Meguellati. It concerned DCC processes involving reversible exchange of components between imine constituents (imine/imine, C=N/C=N exchange) as well as between benzylidene and imine constituents (C=C/C=N exchange), and involved the investigation of the use of L-proline, its derivatives, and other organocatalysts such as aniline, to catalyze these reactions. The dynamic exchange between *Knoevenagel*-type C=C bonds and imines is of special interest for generating increased diversity. In the last part of this chapter, catalysis of the exchange of substituents around C=C bonds^[40-42] using secondary amine catalysis including L-proline is described. Such exchange has already been described for Michael reactions of benzylidene compounds.^[43]

2.2 Results and Discussion

2.2.1 Organocatalysis of imine/imine, C=N/C=N, exchange processes.

The C=N/C=N exchange of residues within pairs of imines, chosen among the imines **1a-1s** (Figure 2.1 – 2.2, 2.4 and Table 2.2), was examined under different reaction conditions. The process is represented in Scheme 2.1. It generates [2 x 2] DCLs of four constituents. The acid catalyzed version of the imine exchange reaction has been described in the literature.^[44,45] For the present study of organocatalysis, DMSO-*d*₆ was chosen as solvent, in view of its ability to dissolve most organic substances. 1% D₂O was added to ensure avoidance of variable exchange caused by hydrolysis due to indefinite trace amounts of water in different samples of the solvent.



Scheme 2.1 Representation of the [2x2] exchange reaction (C=N/C=N) implemented for the investigation of organocatalysis.

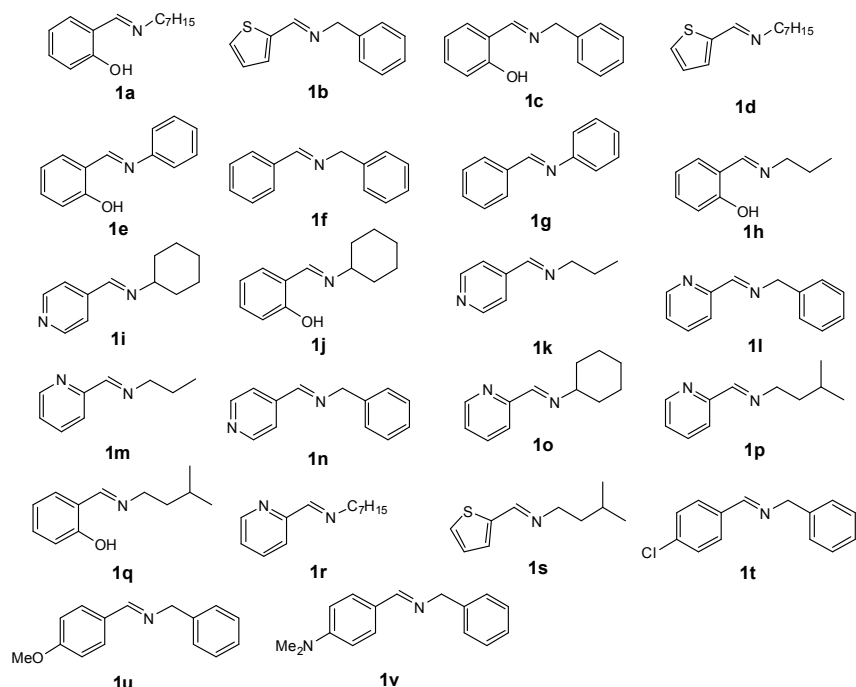


Figure 2.1 Structures of the different imines used in the present study (Imines derived from aliphatic aldehydes were not studied because they were too sensitive to hydrolysis).

Furthermore, in order to avoid acid-dependent reaction pathways, the reaction mixtures were made basic by the addition of a large excess of the hindered tertiary amine Bis(2-hydroxyethyl)amino-tris(hydroxymethyl)methane (BIS-TRIS). It is highly soluble in DMSO- d_6 and in addition to being a poor nucleophilic cannot undergo elimination, so that at most it can undergo addition only to a carbonyl center. In fact, no evidence was obtained that even just this occurred to an appreciable extent. All imines were prepared by a standard procedure.^[46] Figure 2.2 shows a control experiment, indicating that for the particular imines chosen the imine/imine exchange was not greatly influenced by the added D₂O and BIS-TRIS.

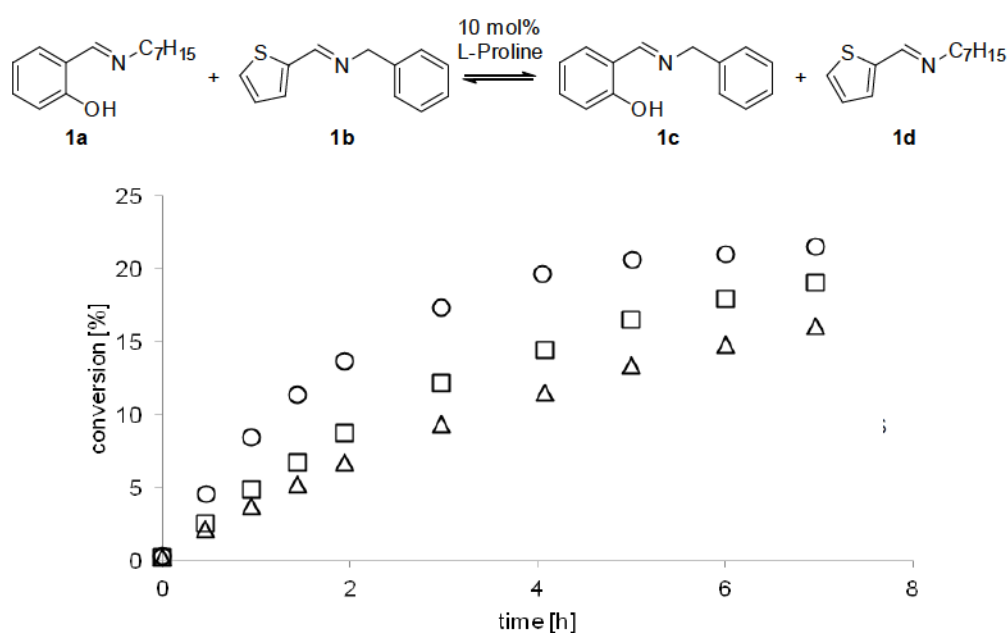
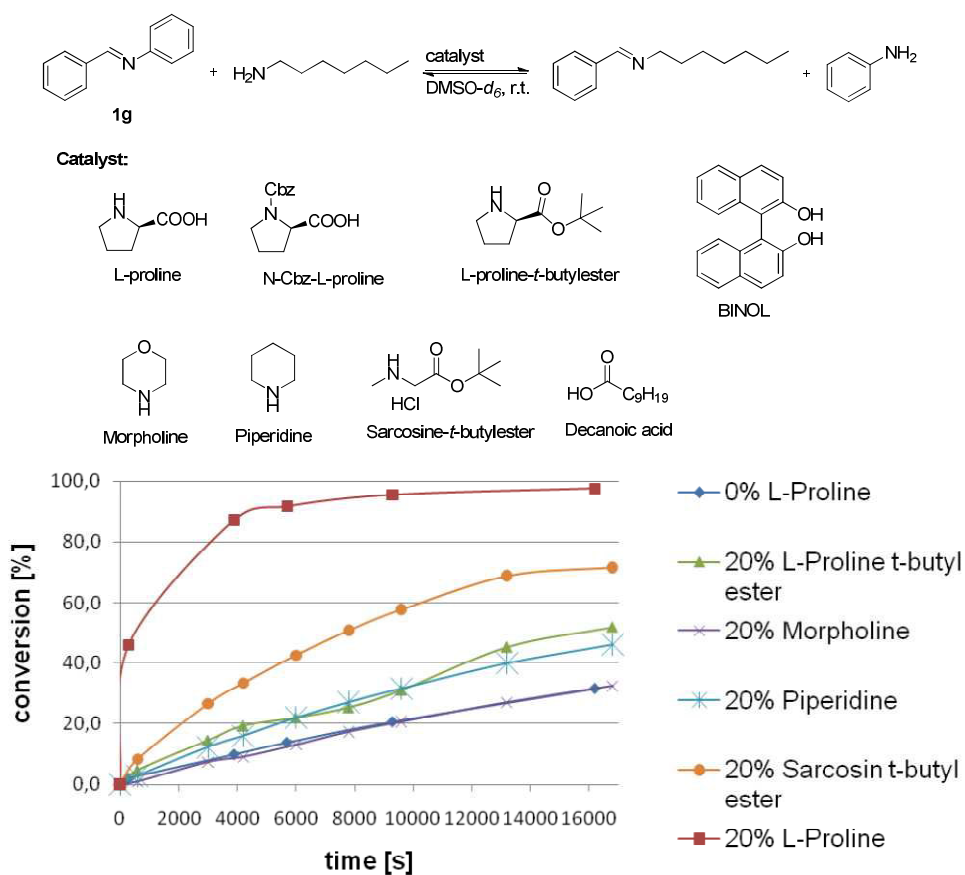


Figure 2.2 Influence of the addition of 1% D₂O and 10 equiv. BIS-TRIS in the presence of 10 mol% L-proline in DMSO- d_6 solution. o = DMSO- d_6 /D₂O 99/1 + 10 equiv. BIS-TRIS, □ = DMSO- d_6 /D₂O 99/1, Δ = DMSO- d_6 .

To investigate the potential of organocatalysis in imine/imine exchange, the exchange reactions were studied in the absence and presence of L-proline and of its derivatives. The results are presented in Figure 2.4 and 2.5, and in Table 2.2. A possible mechanism of the process is depicted in Scheme 2.2, following that proposed in the literature.^[31–35] The reactions in the presence of *N*-Boc protected L-proline, L-proline *tert*-butyl ester, L-proline and benzoic acid were compared with the blank reaction. Only in the case of L-proline did a marked increase in C=N/C=N exchange rate occur and the equilibrium state of the mixture was reached within a comparatively short time. These

results indicate the likely participation of L-proline carboxylic acid in the catalytic mechanism (The benzoic acid and L-proline *tert*-butyl ester are ineffective indicating that L-proline may act as a bifunctional catalyst).^[31]

Additionally, Dr. Nadine Wilhelms investigated the transimination between **1g** and heptylamine in the presence of the different organocatalysts (20 mol% each) L-proline, L-proline-*tert*-butyl ester, *N*-Cbz-L-proline, morpholine, piperidine, sarcosine-*tert*-butylester, decanoic acid, thiourea, and BINOL (2,2'-binaphthol) in pure DMSO- d_6 at room temperature (Figure 2.3). All of these catalysts were able to catalyze the transimination reactions. L-proline, *N*-Cbz-L-proline and decanoic acid were far more effective than other catalysts, indicating that the dominant catalytic pathway must involve substrate protonation due to the carboxylic groups. Since acid catalysis of transimination reactions has been previously characterized (see above), studies in pure (neutral) DMSO were discontinued.



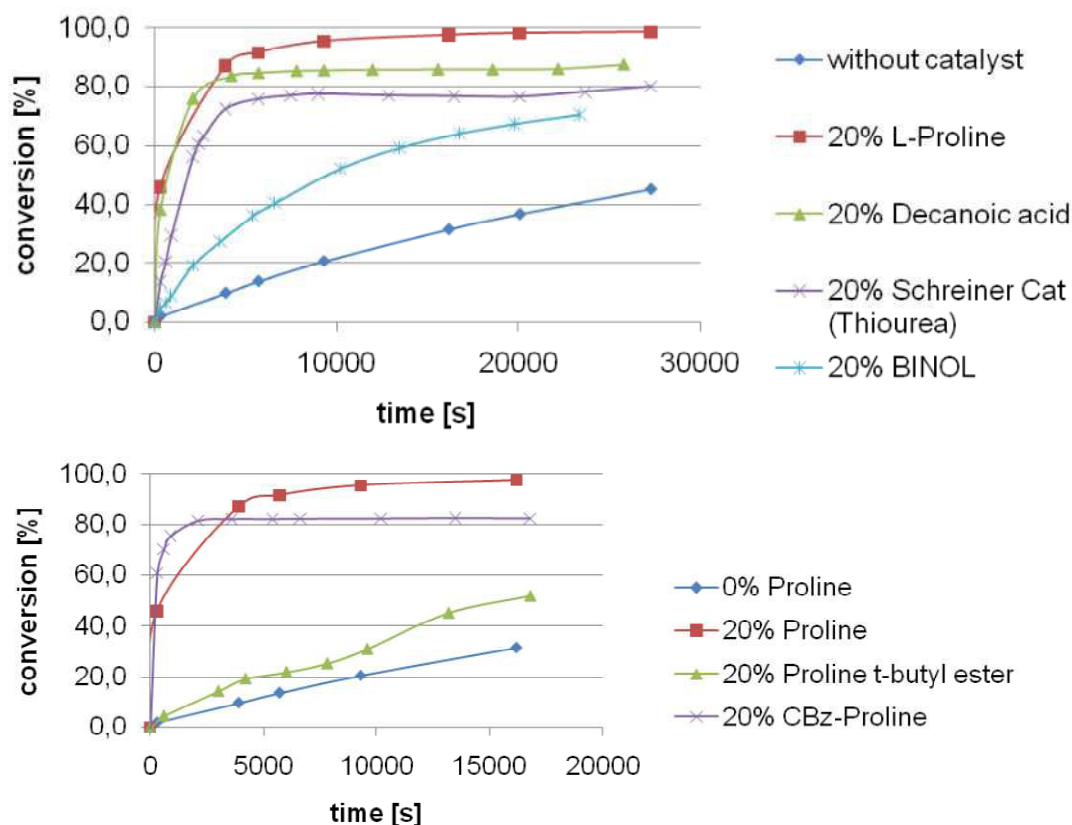


Figure 2.3 Transimination between *N*-benzylidene aniline (**1g**) and *n*-heptylamine conducted in the presence of the different catalysts *L*-proline, *L*-proline-*tert*-butyl ester, *N*-Cbz-*L*-proline, morpholine, piperidine, sarcosine-*tert*-butylester, decanoic acid, Scheiner catalyst (thiourea), and BINOL in $DMSO-d_6$ at room temperature.

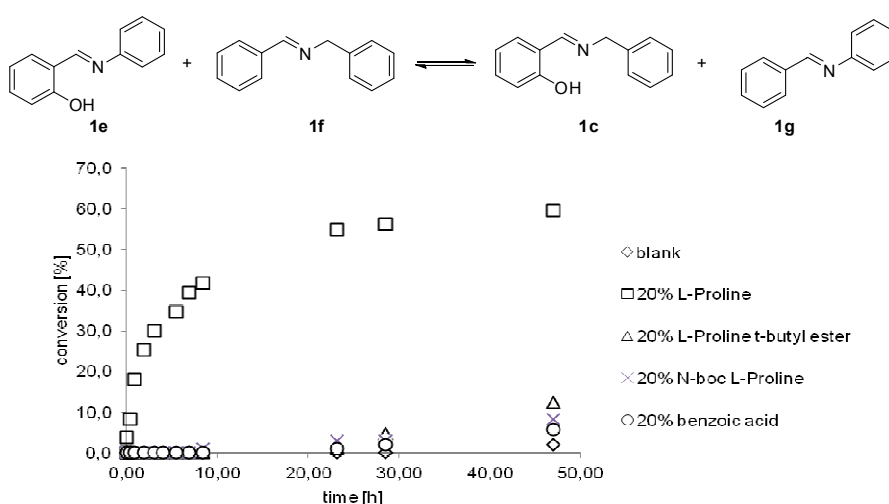
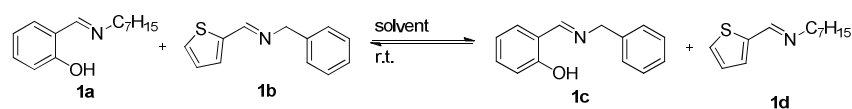


Figure 2.4 Screening for organocatalytic activity of *L*-proline, of its derivatives and benzoic acid on the imine exchange process shown above

These preliminary results established that crucial factors for fast imine/imine exchange were the structure of the studied imines, the solvent, and the catalyst. Initially, imines with only aromatic substituents were used in DMSO-*d*₆/D₂O 99/1 as a solvent system. In these reactions, the exchange could not be achieved either with or without a catalyst. The only reaction observed was that of hydrolysis, indicating that the aromatic amines were insufficiently nucleophilic to maintain imine formation under the given conditions. Next, an attempt to conduct the exchange reaction with imines derived from aliphatic amines and aliphatic aldehydes failed as well because again of the fast hydrolysis of both imines.

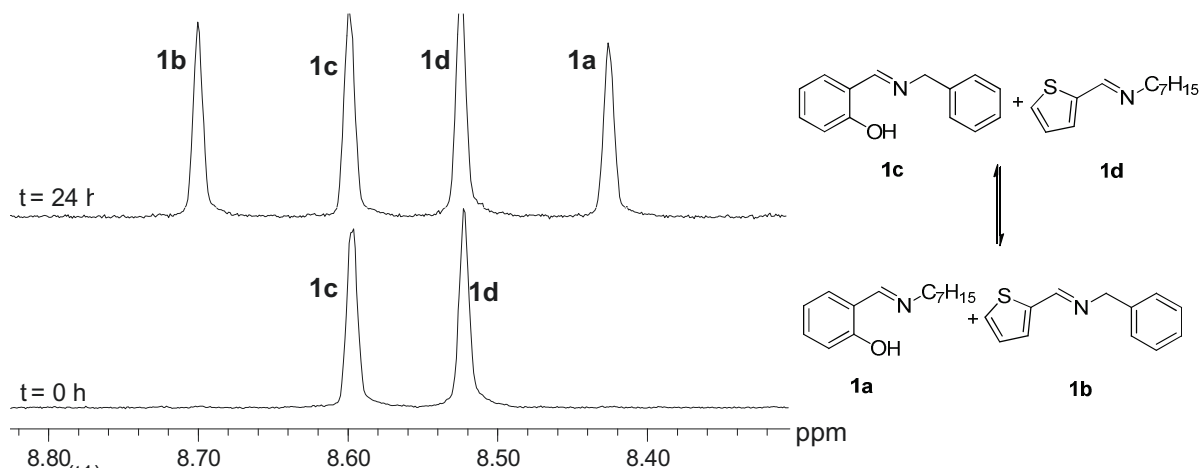
The influence of the solvent was investigated using the reaction of **1a** and **1b** to give **1c** and **1d** as the exchange products in the presence of the catalysts 10 mol% L-proline and 10 mol% decanoic acid. The five different solvent systems used are given in *Table 2.1*. The exchange reaction occurred without appreciable interference from hydrolysis in DMSO-*d*₆/D₂O mixtures, as well as in pure DMSO-*d*₆, and was most rapid when BIS-TRIS was added to the mixture. No reaction was apparent in either CD₃CN or CDCl₃, although it was only possible to examine decanoic acid as a catalyst in these solvents because the solubility of L-proline in both is very low. That decanoic acid in DMSO-*d*₆ showed its greatest efficiency in the presence of BIS-TRIS is interesting and may mean that protonated BIS-TRIS is a more effective acid catalyst than decanoic acid. The catalysis is nonetheless far less effective, by nearly two orders of magnitude, than that of L-proline under the same conditions, showing that a nucleophilic catalytic pathway must be dominant there.

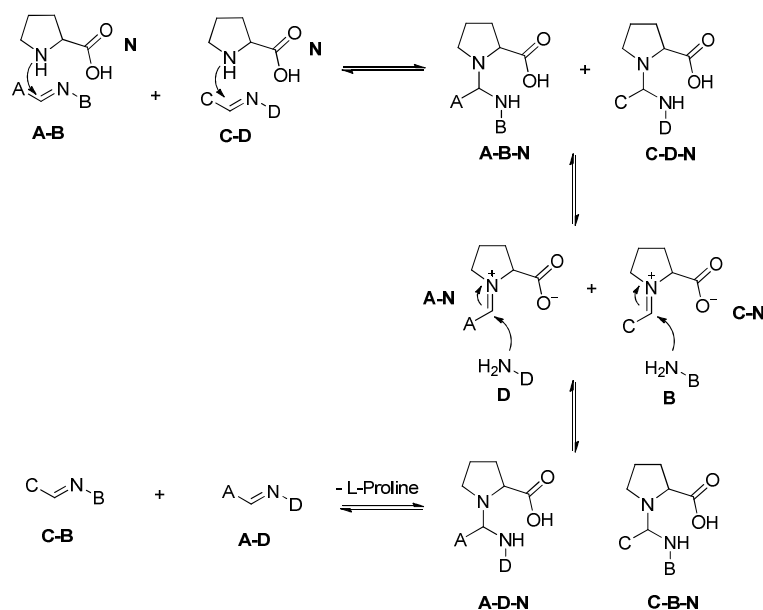
Finally, nucleophilic aliphatic amines were condensed with electrophilic heteroaromatic aldehydes (2-pyridyl, 4-pyridyl, and 2-thiophenyl-carboxaldehydes) as well as with salicyl aldehyde to give the imines **1a-d,h-s**. Using these substrates did lead to the desired C=N/C=N exchange, that could be followed conveniently by ¹H-NMR spectroscopy (*Figure 2.5*). No hydrolysis products could be detected up to the time that the exchange appeared to reach equilibrium. The exchanges were catalyzed by L-proline in basic (BIS-TRIS) solution and on the basis of literature precedents [see ref. 31-35], the proposed mechanism for these exchanges is one involving the action of L-proline as a nucleophile (*Scheme 2.2*) to react at both imines leading to iminium intermediates by addition-elimination, followed by the condensation of the released amines with the iminium intermediates to provide the exchange products.

Table 2.1 The imine/imine exchange reactions for the **1a**, **1b**/**1c**, **1d** system in the presence of 10 mol% L-proline and 10 mol% decanoic acid in different solvents at room temperature

Entry	Conditions	Compound distribution [%] ^{c)}				$t_{1/2}$ [h] ^{d)}	K_{eq} ^{e)}
		1b	1b	1c	1d		
1 ^{a)}	DMSO- <i>d</i> ₆ /D ₂ O 99/1 10eq BIS-TRIS	26	31	23	21	3	0.60
1 ^{b)}	DMSO- <i>d</i> ₆ /D ₂ O 99/1 10eq BIS-TRIS	25	30	23	22	7	0.67
2 ^{a)}	DMSO- <i>d</i> ₆ /D ₂ O 99/1	25	30	23	22	3	0.67
2 ^{b)}	DMSO- <i>d</i> ₆ /D ₂ O 99/1	27	31	21	20	10	0.50
3 ^{a)}	DMSO- <i>d</i> ₆	22	35	22	20	8	0.57
3 ^{b)}	DMSO- <i>d</i> ₆ ^{b)}	27	33	21	20	16	0.47
4 ^{a)}	CD ₃ CN	f)	f)	f)	f)	g)	g)
5 ^{a)}	CDCl ₃	f)	f)	f)	f)	g)	g)

^{a)} The reaction in the presence of 10mol% L-proline, ^{b)} The reaction in the presence of 10 mol% decanoic acid ^{c)} Compound distributions were followed until no further change in composition could be observed (<2%) and error on ¹H-NMR signal integration is ~4%. ^{d)} $t_{1/2}$, half-lives (the half-lives of the reactions were determined by integration of the decreasing ¹H-NMR signals of the starting material as a function of time and analyzing the curve obtained). ^{e)} $K_{eq} = [C][D]/[A][B]$. ^{f)} L-proline insufficiently soluble to be used. ^{g)} No reaction detectable.

**Figure 2.5** ¹H-NMR study of C=N/C=N exchange of **1c** and **1d** by observation of the signals of the imine protons –CH=N– before (bottom) and after (top) exchange

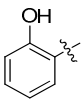
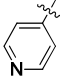
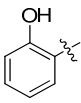
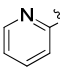
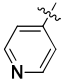
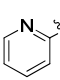
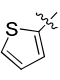
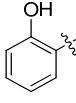
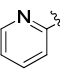
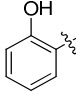
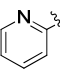
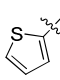
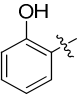
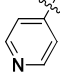
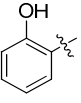
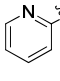


Scheme 2.2 Proposed mechanism for the organocatalysis of C=N/C=N exchange.^[31–35] Hydrolysis has not been represented in this mechanistic scheme.

In order to evaluate the scope of the organocatalysis of imine/imine exchange, a number of $[2 \times 2]$ imine libraries were explored (Table 2.2). For each pair of imines, both the forward and reverse reactions were followed without (blank) or with added L-proline. The imine exchanges processes were found to obey the kinetics of a reversible first order reaction. It might be expected that such reactions would obey the kinetics for reversible second order processes but attempts to fit the obtained data to this behavior were unsuccessful (the Rorabacher equation^[47] plot being far from linear). Actually, the data provided a good fit to a reversible first order reaction. This indicated that the imine exchange reaction obeyed a reversible first order behavior. (See more details in Experimental part of Chapter 7).

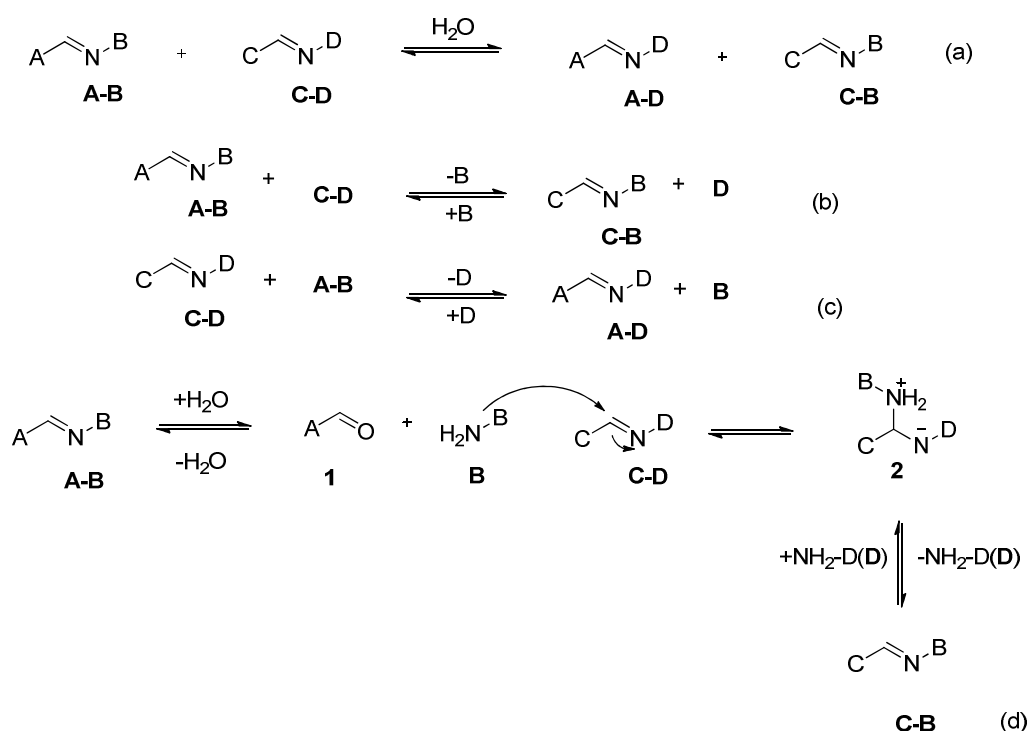
Thus, the corresponding rate constants, k_c and k_b , were calculated as indicated in the Experimental Part (Chapter 7) and are listed in Table 2.2.^[48] The reaction in the absence of catalyst for reverse reactions in Table 2.2, Entry 3 (**1n** + **1o**) and 4 (**1a** + **1b**) were very slow and the rate constants were calculated from the first 10% of the reaction^[49] using the irreversible first-order kinetic equation. Then, the rate constants for the reaction in the presence of catalyst for both reactions ((**1n** + **1o**) and (**1a** + **1b**)) were also calculated using the first 10% of the reaction in order to estimate the acceleration ratio. The equilibrium constants were calculated from the rate constants (see caption of Table 2.2).^[48] An acceleration of the C=N/C=N exchange by 10 mol% L-proline up to about 22-fold was achieved (Table 2.2, Entry 4). The accelerations of the forward and reverse reactions were similar. The equilibrium constants K_b and K_c obtained for the blank and catalyzed reactions in both the forward and backward directions were similar within the experimental uncertainty, indicating that the reactions were under thermodynamic control.

Table 2.2 Organocatalysis by 10 mol% L-proline of a set of imine/imine exchange reactions for [2×2] imine libraries in DMSO-d₆/D₂O 99/1, 10 equiv. BIS-TRIS solution at room temperature.

Entry	ER ^{a)}	A ^{a)}	B ^{a)}	C ^{a)}	D ^{a)}	b)	k _b ^{c)}	k _c ^{d)}	K _b ^{e)}	K _c ^{f)}	Acc ^{g)}
1	1h+1i ↕ 1j+1k	n-Propyl		c-Hexyl		f	0.0274	0.0761	1.18	1.18	2.8
						r	0.0233	0.0642			2.8
2	1h+1l ↕ 1c+1m	n-Propyl		Benzyl		f	0.0371	0.1239	0.46	0.52	3.3
						r	0.0811	0.2370			2.9
3	1i+1l ↕ 1n+1o	c-Hexyl		Benzyl		f	0.0080	0.0650	n.d. ^{j)}	2.70	8.1
						r	0.0008 ^{h,i)}	0.0241 0.0098 ⁱ⁾			12.3
4	1c+1d ↕ 1a+1b	n-Heptyl		Benzyl		f	0.0057	0.0759	n.d. ^{j)}	0.48	10.6
						r	0.0022 ^{h,i)}	0.1597 0.0472 ⁱ⁾			21.5
5	1p+1c ↕ 1l+1q	i-Pentyl		Benzyl		f	0.0949	0.2413	1.79	1.22	2.5
						r	0.0529	0.1980			3.7
6	1p+1d ↕ 1r+1s	i-Pentyl		n-Heptyl		f	0.0387	0.3131	0.83	0.65	8.1
						r	0.0466	0.4854			10.4
7	1h+1n ↕ 1e+1w	n-Propyl		Benzyl		f	0.0140	0.0658	1.07	1.34	4.7
						r	0.0131	0.0492			3.8
8	1h+1o ↕ 1j+1m	n-Propyl		c-Hexyl		f	0.0471	0.1315	0.66	1.08	2.8
						r	0.0714	0.1213			1.7

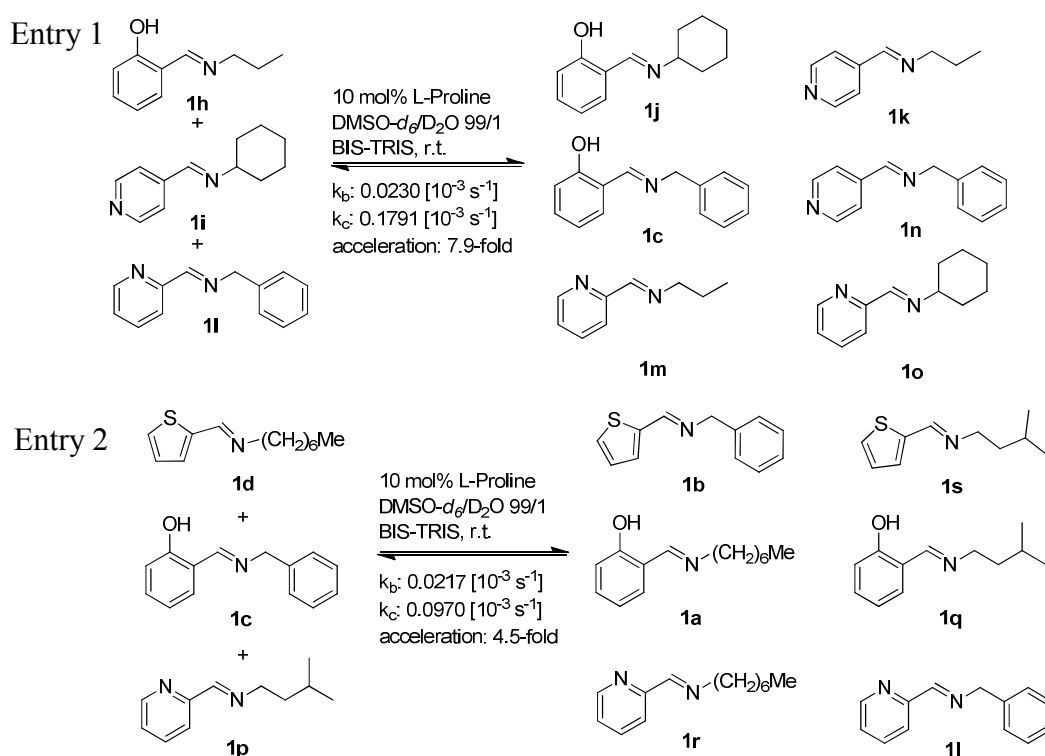
^{a)} ER = exchange reaction, A-D: substituents of the studied imines. ^{b)} f = forward reaction; r = reverse reaction. ^{c)} k_b = rate constant of the blank reaction [10⁻³ s⁻¹]. ^{d)} k_c = rate constant of the catalyzed reaction [10⁻³ s⁻¹]. ^{e)} K_b = equilibrium constant of the blank reaction = k_b (forward)/k_b (reverse). ^{f)} K_c = equilibrium constant of the catalyzed reaction = k_c (forward)/k_c (reverse). ^{g)} Acc. = Acceleration = k_c/k_b; ^{h)} The reaction did not reach equilibrium. ⁱ⁾ Rate constant is calculated from the first 10% of the reaction. ^{j)} n.d. = not determined. Error in ¹H-NMR signal integration, ~4-5%.

Continuing the investigation of imine exchanges, the reactions in the absence of catalyst were also monitored but the rates were very slow. In fact, any reaction seemed to be attributable to a hydrolysis mechanism involving catalysis by water. A plausible mechanism for such catalysis is shown in *Scheme 2.3*. While simple hydrolysis of both reactants would lead to a mixture of aldehydes and amines which could then combine in the alternate ways (as well as to regenerate the reactants), the fact that imines are known^[50] to be much more rapidly attacked by amines than are their parent carbonyl compounds leads to the proposal that attack of free amine on residual imine species to give aminal intermediates would provide a more efficient catalytic pathway for exchange. Thus, if a small amount of H₂O is present in a mixture of **A-B** and **C-D**, some **A-B** can be hydrolyzed to liberate amine (**B**) which can then react with imine **C-D** through an aminal-intermediate to provide the imine **C-B** as an exchange product. Similarly, if **C-D** is partly hydrolyzed to liberate amine **D**, it will then react with **A-B** to give **A-D** as the exchange product. The net result is that **A-D** and **C-B** gradually increase in the reaction mixture at the expense of **A-B** and **C-D**, respectively, until the two equilibria ((b) and (c)) are simultaneously established.



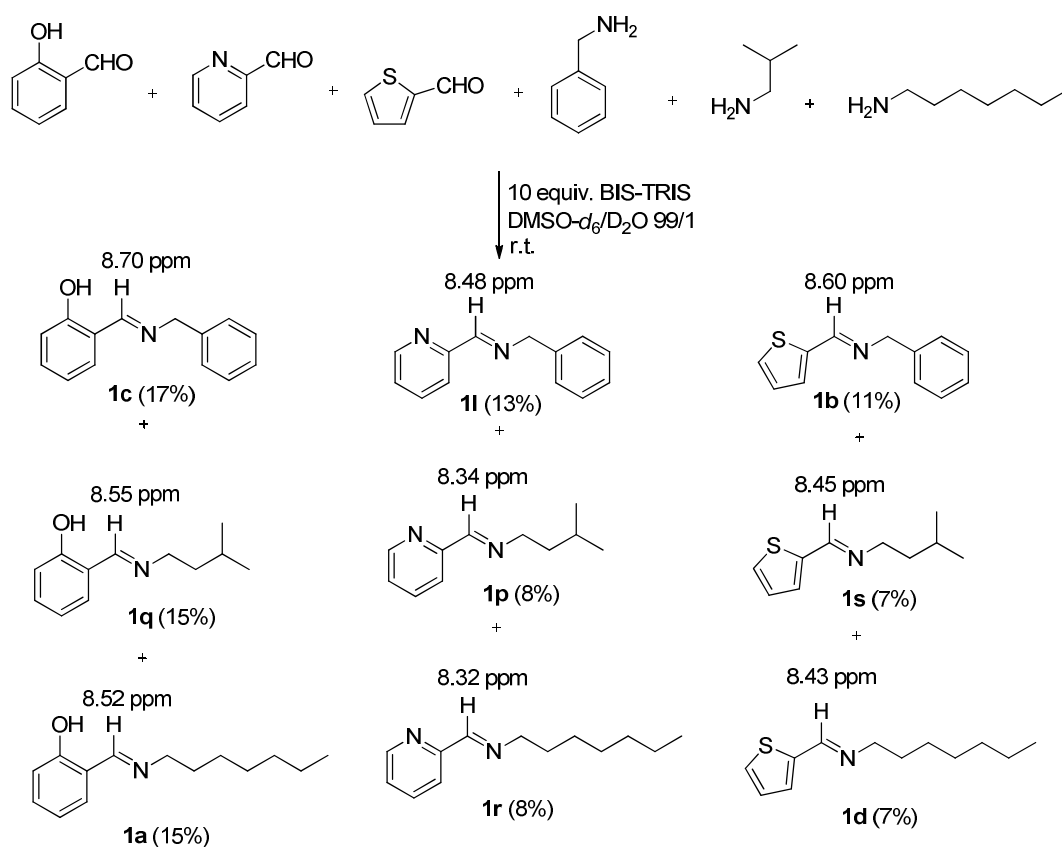
Scheme 2.3 The imine exchange mechanism in the absence of organocatalyst via hydrolysis and aminal formation reactions (the water acts as a nucleophilic catalyst).

To explore the broader applicability of the present organocatalysis procedure to biology and materials science, two [3x3] dynamic libraries of imines were generated (Scheme 2.4) in the presence of 10 mol% L-proline and in the absence of catalyst in DMSO-*d*₆/D₂O 99/1 with addition of 10 equiv BIS-TRIS at room temperature. Library 1 consisted of the previously studied imines **1h**, **1i** and **1l** (see Table 2.2, Entries 1-3). Thus, the three [2x2] libraries can be directly compared to the equivalent [3x3] library based on the same three aldehydes and three amines. Here, an acceleration of 7.9-fold was observed, which corresponds to the exchange of Entry 3. Thus, the larger library reaches equilibrium at approximately the same rate as the fastest of the three smaller libraries. The second DCL consisted of **1c**, **1d** and **1p** and refers to the [2x2] libraries shown in Entries 4-6 of Table 2.2. Precise values of the equilibrium constants were not obtained for the [3x3] libraries. While the reactions were followed until the spectra did reach a point where further changes were not detectable and thus it was assumed that equilibrium had been attained, this was not confirmed by studying the reverse process.



Scheme 2.4 Imine exchange in two [3 × 3] imine libraries - Applicability of organocatalysis to larger libraries for increasing diversity.

In addition, we studied the formation of the imines which were used in the exchange processes. Three different aldehydes (salicylaldehyde, 2-pyridyl aldehyde, and 2-thiophenol aldehyde) and three amines (benzylamine, isobutylamine, and heptylamine) were employed in a single reaction. The reaction was run in $DMSO-d_6/D_2O$ 99/1 using 10 equiv. BIS-TRIS in the absence of catalyst at room temperature (Scheme 2.5). All nine possible imines were detectable immediately after mixing, although the equilibration time for this reaction was about 60 minutes, indicating relatively facile imine formation under these conditions, leading to equilibrium %ratios of **1c** (17%), **1l** (13%), **1b** (11%), **1q** (15%), **1p** (8%), **1s** (7%), **1a** (15%), **1r** (8%), **1d** (7%), respectively.



Scheme 2.5 Study of the formation and equilibrium distribution of nine imines from three different aldehydes and amines using 10 equiv. BIS-TRIS in $DMSO-d_6/D_2O$ 99/1 at room temperature.

2.2.2 The C=N/C=N exchange using aniline as a nucleophilic catalyst.

Recently, nucleophilic catalysts have been shown to accelerate hydrazone and oxime formation as well as transimination and imine metathesis reactions. Aniline and its derivatives having been found to be effective,^[29,50,51] we turned to aniline as a possible catalyst of the presently studied imine exchange. A preliminary investigation was based on **1h** and **1o** as representative substrates for imine exchange in DMSO-*d*₆/D₂O 99/1 at room temperature.

Table 2.3 Thermodynamic and kinetic parameters for the imine exchange between **1h** and **1o** using aniline as a nucleophilic catalyst.

Entry	Condition	K_{eq} ^{a)}	k ($10^{-3} s^{-1}$) ^{b)}
1	Blank	1.13	0.0173
2	0.1 equiv. Aniline	1.23	0.0346
3	10.0 equiv. Aniline	1.13	0.1082

^{a)} $K_{eq} = [C][D]/[A][B]$, ^{b)} As in earlier work, the reaction was found experimentally to conform to first-order kinetics. Error in ¹H-NMR signal integration, ~4-5%.

Although the imine exchange of **1h** and **1o** to give **1j** and **1m** occurs, it is very slow (Table 2.3) in the absence of aniline and is only accelerated by a factor of ~2 in the presence of 0.1 equiv. aniline. Under this condition, a trace amount (~0.7%) of an intermediate (aminal) was observed. In the presence of 10 equiv. aniline, the reaction is about 11 times faster than in the absence of catalyst and a trace amount of aniline imine could be detected along with the same aminal intermediate being observed (~1.8%) as well. In comparison, the reaction in the presence of 0.1 equiv. aniline as the catalyst is ca. 3 times slower than the one in the presence of 0.1 equiv. of L-proline. L-proline can be considered a better catalyst than aniline both because it gives a faster reaction and because side products and intermediates do not attain appreciable levels. Moreover, L-proline is to be preferred for use as a catalyst because it has much lower toxicity.

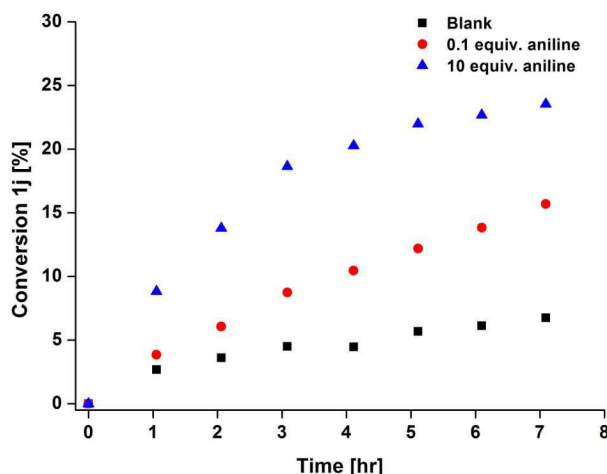


Figure 2.5 Influence of aniline as a nucleophilic catalyst in the imine exchange reaction between **1h** and **1o** in $DMSO-d_6/D_2O$ 99/1.

2.2.3 Organocatalysis of benzylidene/imine, $C=C/C=N$, exchange processes.

After the successful implementation of organocatalysis in the generation of DCLs of imines, we explored its extension to other related reactions. In particular, the $C=C/C=N$ exchange, involving two different types of double bonds, appears to have much potential for generating dynamic libraries of constituents of great diversity. Given the reversibility of imine formation, that of the condensations giving benzylidene barbiturate derivatives (and similar species) seemed to be a promising accompaniment for achieving such an exchange process.

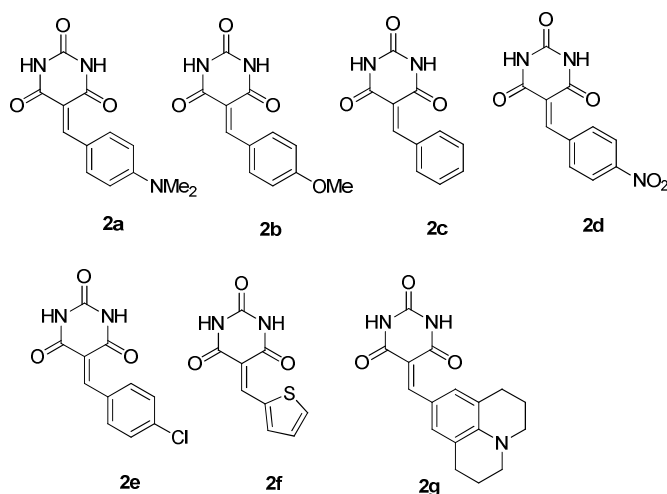


Figure 2.6 Structure of the benzylidene barbiturates (**2a-2g**) used in the present study.

Firstly, possible substrates for the C=C/C=N exchange were investigated under different conditions in the presence and absence of a catalyst. 4-Dibutylamino-benzylidenebarbiturate was reacted with aromatic imines (*Figure 2.7a*) in the presence of the catalysts such as L-proline, L-proline *t*-butyl ester, *N*-Cbz-L-proline, and benzoic acid in pure DMSO-*d*₆. No changes were apparent at room temperature in the ¹H-NMR spectra. Heating at 80°C still did not lead to exchange but instead to hydrolysis and some decomposition. Next, the same benzylidene-barbiturate was reacted with aliphatic imines (*Figure 2.7b*) using various catalysts. In the presence of 20 mol% L-proline, the new imine formed but the new benzylidene barbiturate was not present, with only the hydrate form of benzaldehyde being observable. In DMSO-*d*₆/D₂O 99/1 solvent (added 1% of D₂O to ensure a known %water in the solvent system), the 4-nitrobenzylidene-barbiturate was used to exchange with an aliphatic imine (*Figure 2.7c*) and although the new imine appeared, the benzylidene-barbiturate underwent rapid hydrolysis, making this also an unsuitable system for study of the simple equilibrium.

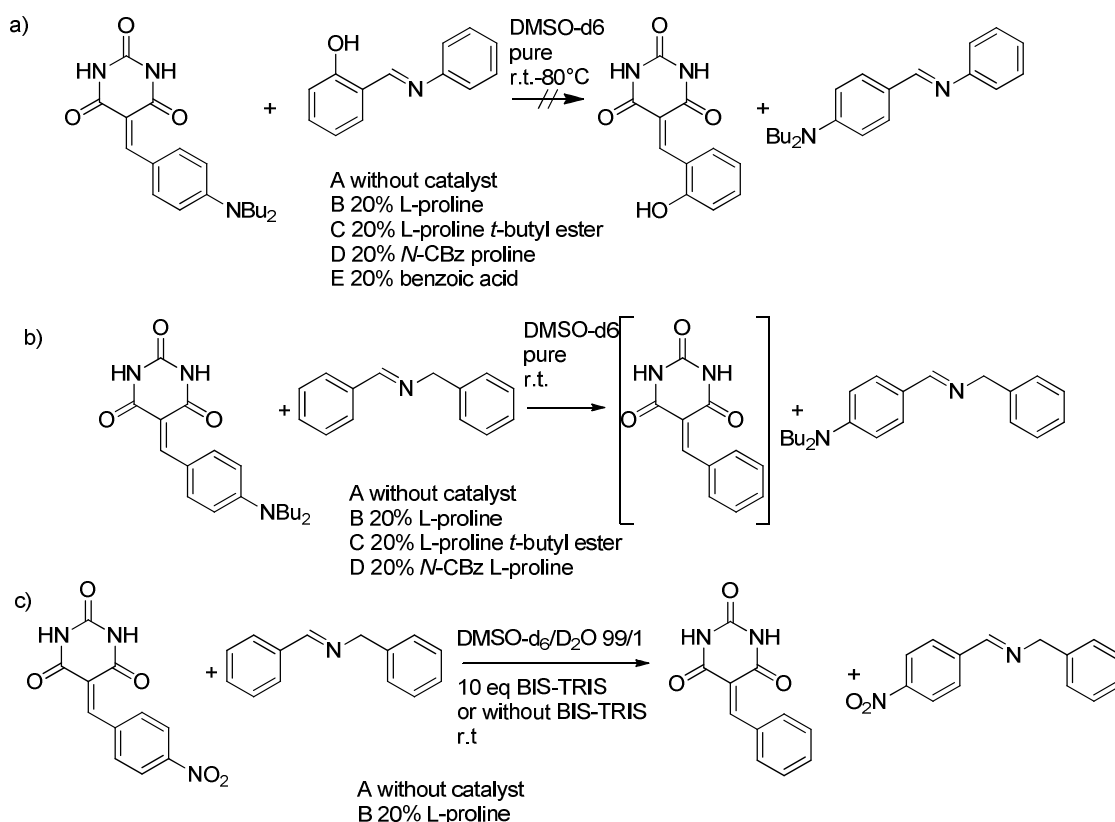


Figure 2.7 Screening reactions for C=C/C=N exchange using different starting materials and different conditions.

The next cross exchange reaction investigated was that of the $C=C$ substrate derived from benzylidene-barbiturate and the imine derived from 2-pyridyl aldehyde and benzylamine (Figure 2.8a). However, after 3 h, although the new imine could be detected, both benzaldehyde and its hydrate were present due to hydrolysis of the barbiturate.

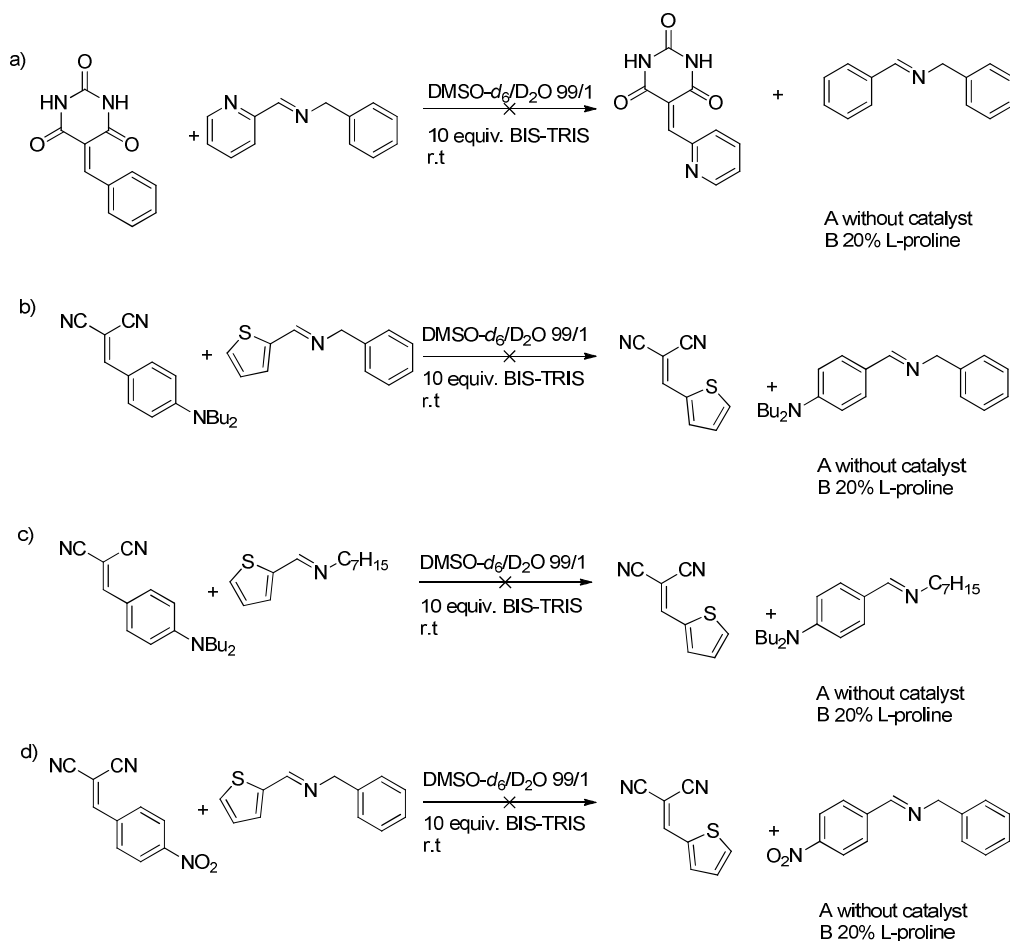


Figure 2.8 Screening for $C=C/C=N$ exchange with different starting materials and under different conditions.

The barbiturate was then substituted with benzylidene-malononitrile (Figure 2.8b). Here, in the reaction mixture with L-proline as catalyst, hydrolysis of benzylidene-malononitrile was observed and formation of the new imine was not detectable. The analogous reaction with a 2-thiophenol aldehyde imine (Figure 2.8c) did give a small amount of the new imine but again involved mostly hydrolysis of the benzylidene malononitrile. The reaction of 4-nitrobenzylidene-malononitrile with **1b** gave similar results (Figure 2.8d).

Overall, it was clear that benzylidene-barbiturates derived from salicylaldehyde and 2-pyridyl aldehyde were not suitable as cross-exchange substrates because of their fast hydrolysis. In fact even during the synthesis of these benzylidene-barbiturates, it was difficult to isolate the product.

These preliminary results showed that the C=C/C=N cross exchange reaction is very sensitive to the starting substrates and that the reaction conditions have to be compatible with the persistence of both *Knoevenagel* (C=C) and imine (C=N) compounds. Therefore, the C=C substrates should contain a moderately reactive aldehyde and the imine compound should be derived from a reactive amine (for instance, an aliphatic amine) in order to assure the formation of a new imine in the cross exchange reaction.

Thus, the benzylidene barbiturates **2a**, **2b**, **2e**, **2f** and imines **1b**, **t-v** were chosen to be the substrates for the exchange reaction with imines derived from aliphatic amines and aromatic aldehydes (*Scheme 2.6*). The reactions were carried out using equimolar amounts of benzylidene derivatives and imine compounds (19.35 mM each) in a mixture of DMSO-*d*₆/D₂O 99/1 at 60°C with 10 mol% L-proline as organocatalyst. As for the C=N/C=N exchange studies described in the previous section, BIS-TRIS did not have much influence on the reaction rate. In contrast, in DMSO-*d*₆/D₂O 99/1 solvent and in the presence of 10 equiv. BIS-TRIS, the hydrolysis of benzylidene-barbiturate (**2c**) occurred immediately (*Figure 2.9*). Therefore, for the cross exchange of C=C/C=N, BIS-TRIS could not be used in the medium.

Both forward and reverse reactions were followed by ¹H-NMR spectroscopy. Compared to C=N/C=N exchange, a higher temperature was required. The proportions of the different compounds were determined by integration of the imine CH=N as well as of the benzylidene CH=C proton ¹H-NMR signals. The hydrolysis accompanying the exchange rendered the reaction kinetics too complicated for a precise analysis. The results are illustrated in *Figure 2.10* and listed in *Table 2.4*. In all cases, the compositions of the mixtures are given for a reaction time at which no further change in compound percent was detectable.

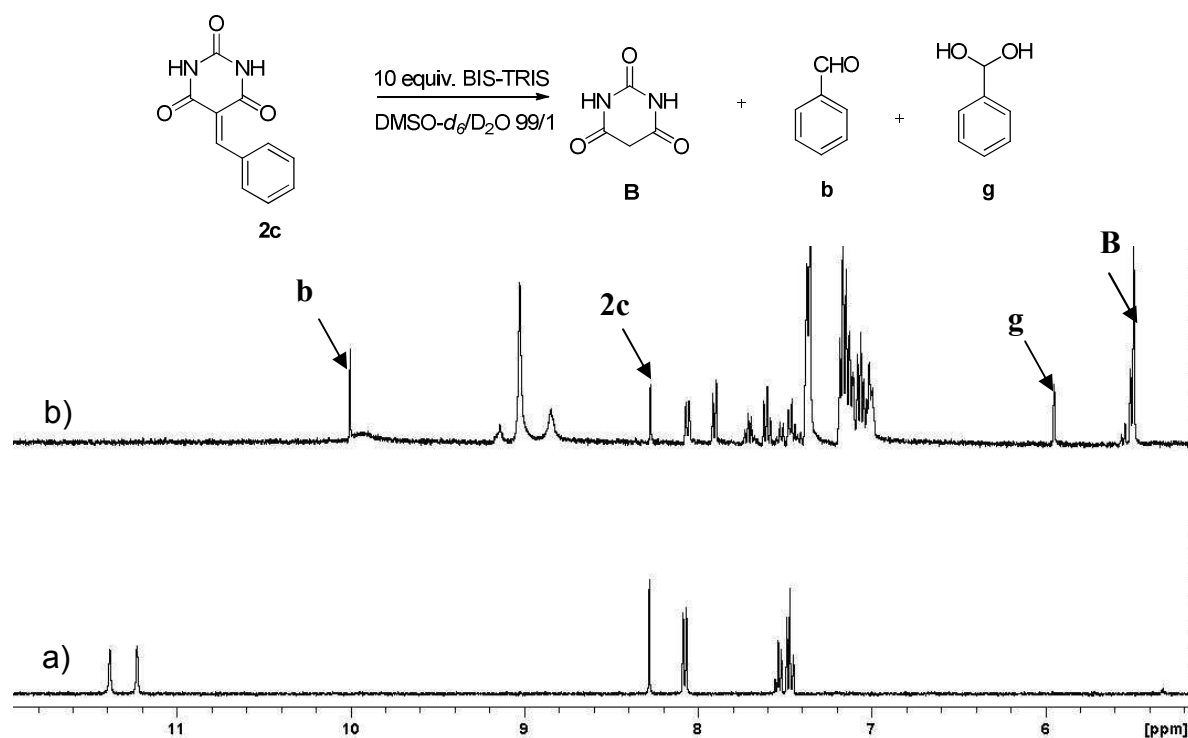
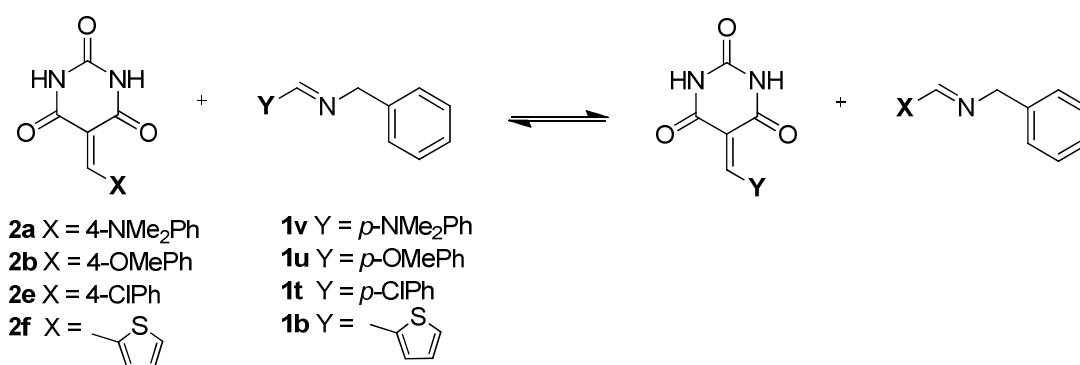


Figure 2.9 $^1\text{H-NMR}$ spectra of a) **2c** in $\text{DMSO-}d_6/\text{D}_2\text{O}$ 99/1 b) **2c** plus 10 equiv. BIS-TRIS in $\text{DMSO-}d_6/\text{D}_2\text{O}$ 99/1 showing the hydrolysis of **2c** after adding BIS-TRIS to a solution. **b** = benzaldehyde formyl proton, **g** = benzaldehyde hydrate methane proton, and **B** = barbituric acid methylene protons



Scheme 2.6 Representation of the cross-exchange $C=C/C=N$ reaction between the benzylidene-barbiturate derivatives and different imines.

These studies were extended to an evaluation of the influence of substitution within the vinylidene head-groups on the exchange reaction. Thus, the reaction between the benzylidene barbiturate **2a**, bearing an electron-donating group (EDG), and the imine **1t**, bearing an electron-withdrawing group (EWG), gave only the imine **1v**, but the expected new benzylidene barbiturate **2e** was lost, due to hydrolysis (Table 2.4, Entry 1). The ¹H-NMR spectrum of the equilibrated mixture (Figure 2.10) showed a signal at 5.9 ppm assigned to be the –CH(OH)₂- methane proton of 4-chlorobenzaldehyde hydrate. The formation of **2e** is apparently hindered by the tendency of 4-chlorobenzaldehyde to give a hydrate at equilibrium. Hence, it was surmised that decreasing the hydration tendency of the aldehyde of the imine by replacing the EWG by an EDG would favor its condensation with barbiturate to give the *Knoevenagel* product in this medium.

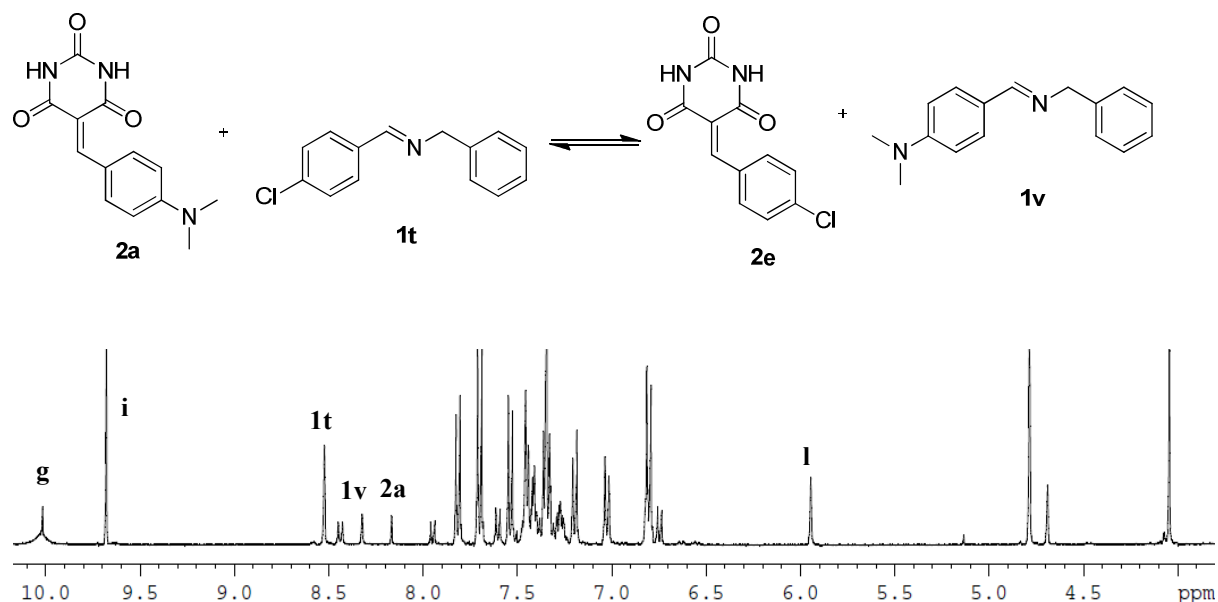


Figure 2.10 ¹H-NMR spectrum of the products of the exchange reaction between **2a** and **1t** at equilibrium. The characteristic –CH=N peaks are indicated for **2a**, **1t**, **1v**, 4-chlorobenzaldehyde (**g**), 4-dimethylamino benzaldehyde (**i**), 4-chlorobenzaldehyde hydrate (**l**) in 99/1 DMSO-*d*₆/D₂O.

The reverse reaction was performed by mixing compounds **2e** and **1v** in 1:1 ratio in the same solvent (Table 2.4, Entry 2). Here, both starting compounds hydrolyzed over a few hours (as followed by observation of the aldehydes formed) after mixing. Simultaneously, the new exchanged compounds, the benzylidene-barbiturate **2a** and the imine **1t**, were progressively formed, but at the end of the reaction the hydrolyzed

Table 2.4 Proportions (%) of the different compounds in the cross-exchange reactions C=C/C=N between benzylidene barbiturates and imines in 99/1 DMSO-*d*₆/D₂O at 60° C (Scheme 2.6). **g** = 4-chlorobenzaldehyde, **h** = 4-methoxybenzaldehyde, **i** = 4-dimethylamino benzaldehyde, **j** = 2-thiophenecarboxaldehyde, **l** = 4-chlorobenzaldehyde hydrate, **m** = 4-methoxybenzaldehyde hydrate, **n** = 4-dimethylamino benzaldehyde hydrate, **o** = 2-thiophenecarboxaldehyde hydrate

Entry ^{a)}	Reaction Time [h] ^{b)}	Compound Distribution [%] ^{c)}							
		Starting compounds 2a + 1t							
		2a	1t	2e	1v	g	i	l	n
1b	0	48	52	- ^{d)}	- ^{d)}	- ^{d)}	- ^{d)}	- ^{d)}	- ^{d)}
	5	35	36	<1 ^{e)}	10	1	13	5	- ^{d)}
	30	17	21	<1 ^{e)}	11	20	20	11	- ^{d)}
1c	0	48	52	- ^{d)}	- ^{d)}	- ^{d)}	- ^{d)}	- ^{b)}	- ^{d)}
	5	6	22	<1 ^{e)}	7	19	29	17	- ^{d)}
Starting compounds 2e + 1v									
		2e	1v	2a	1t	g	i	l	n
2b	0	28	48	- ^{d)}	- ^{d)}	15	<1 ^{e)}	9	- ^{d)}
	6	<1 ^{e)}	14	21	21	16	14	14	- ^{d)}
	20	<1 ^{e)}	9	16	22	22	18	13	- ^{d)}
2a	0	30	46	- ^{d)}	2	1	14	7	- ^{d)}
	6	<1 ^{e)}	5	8	21	18	30	18	- ^{d)}
Starting compounds 2a + 1b									
		2a	1b	2e	1v	i	j	n	o
3b	0	50	50	- ^{d)}	- ^{d)}	- ^{d)}	- ^{d)}	- ^{d)}	- ^{d)}
	4	43	43	7	7	1	<1 ^{e)}	- ^{d)}	1
	24	20	20	24	25	4	3	- ^{d)}	5
3c	0	45	55	- ^{d)}	- ^{d)}	- ^{d)}	- ^{d)}	- ^{d)}	- ^{d)}
	4	11	18	16	20	19	5	0	11
Starting compounds 2e + 1v									
		2e	1v	2a	1b	i	j	n	o
4b	0	50	50	- ^{d)}	- ^{d)}	- ^{d)}	- ^{d)}	- ^{d)}	- ^{d)}
	2	50	50	- ^{d)}	- ^{d)}	- ^{d)}	- ^{d)}	- ^{d)}	- ^{d)}
	27	21	21	15	18	12	7	- ^{d)}	6
4c	0	50	50	- ^{d)}	- ^{d)}	- ^{d)}	- ^{d)}	- ^{d)}	- ^{d)}
	3	13	14	7	17	25	12	- ^{d)}	12
Starting compounds 2b + 1v									
		2b	1v	2a	1u	h	i	m	n
5b	0	49	51	- ^{d)}	- ^{d)}	- ^{d)}	- ^{d)}	- ^{d)}	- ^{d)}
	1	42	47	2	1	4	<1 ^{e)}	4	- ^{d)}
	6	4	17	24	22	16	7	10	- ^{d)}
5c	0	50	50	- ^{d)}	- ^{d)}	- ^{d)}	- ^{d)}	- ^{d)}	- ^{d)}
	1	2	12	14	21	15	21	15	- ^{d)}
Starting compounds 2a + 1u									
		2a	1u	2b	1v	h	i	m	n
6b	0	52	48	- ^{d)}	- ^{d)}	- ^{d)}	- ^{d)}	- ^{d)}	- ^{d)}
	2	49	48	<1 ^{e)}	2	1	<1 ^{e)}	<1 ^{e)}	- ^{d)}
	22	26	23	1	16	16	8	10	- ^{d)}
6c	0	48	52	- ^{d)}	- ^{d)}	- ^{d)}	- ^{d)}	- ^{d)}	- ^{d)}
	2	23	23	1	14	16	12	11	- ^{d)}

^{a)} b, blank reactions, and c, catalyzed reactions with 10 mol% L-proline as a catalyst. ^{b)} Reaction time indicates the time when no further change in composition could be observed. ^{c)} Error on ¹H-NMR signal integration, ~4-5%. ^{d)} Compound not observed. ^{e)} Only traces of product detected.

compounds were predominant. The 4-chlorobenzaldehyde recombined partially with the benzylamine to form **1v**, while the 4-dimethylaminobenzaldehyde gave only a small amount of the condensation product with barbiturate, **2a**. The addition of 10% L-proline increased the speed of the reaction, leading to completion within 6 hours compared to 20 hours in the absence of L-proline.

Confirming the conclusion drawn above as to the influence of substituents on the reactant structures, the exchange between **2a** and **1b**, both bearing EDGs, was found to give rise to both products **2e** and **1v** (*Table 2.4, Entry 3*) although the hydrolysis products 4-dimethylaminobenzaldehyde and 2-thiophenecarboxaldehyde were still present in significant amounts. The reverse reaction with **2e** and **1v** (*Table 2.4, Entry 4*) gave the same final product distribution, showing that a true equilibrium was attained despite the concomitant hydrolysis.

In another case of both reactants having EDG substituents, the exchange reaction of **2b** and **1v** to give **2a** and **1u** (*Table 2.4, Entry 5*) was also successful but was associated with almost complete hydrolysis of **2b**, so that very little was detectable at equilibrium. Thus, in DMSO-*d*₆/D₂O 99/1, it appeared very difficult to avoid interference from hydrolysis and thus to obtain accurate values of the exchange equilibrium constants.

In order to avoid, or at least to reduce the amount of hydrolysis, exchange reactions were performed in the presence of lower amounts of water. The reaction between **2b** and **1v** (*Table 2.5, Entry 1*) was run with 0.5 vol% D₂O (DMSO-*d*₆/D₂O 99.5/0.5) as well as with only 0.2 vol% D₂O (*Table 2.5, Entry 2*) (DMSO-*d*₆/D₂O 99.8/0.2) added water. The products **2a** and **1u** were obtained in these conditions (averaging 20% each), but also large amounts of hydrolysis products (>10%) in the presence of L-proline.

Table 2.5 Proportions (%) of products of the cross exchange reaction between **2b** and **1v** in DMSO-*d*₆/D₂O 99.5/0.5 and DMSO-*d*₆/D₂O 99.8/0.2 at 60°C. **h** = 4-methoxybenzaldehyde, **i** = 4-dimethylaminobenzaldehyde, **m** = 4-methoxybenzaldehyde hydrate, and **n** = 4-dimethylaminobenzaldehyde hydrate.

Entry ^{a)}	Time [h] ^{b)}	Compound distribution [%] ^{c)}							
		Starting compound 2b + 1v ^{e)}							
		2b	1v	2a	1u	h	i	m	n
1b	0	50	50	- ^{d)}	- ^{d)}	- ^{d)}	- ^{d)}	- ^{d)}	- ^{d)}
	2	2	12	20	25	11	18	12	- ^{d)}
1c	0	50	50	- ^{e)}	- ^{e)}	- ^{e)}	- ^{e)}	- ^{e)}	- ^{d)}
	2	42	43	3	3	4	1	4	- ^{d)}
	11	4	13	30	28	12	6	7	- ^{d)}
		Starting compound 2b + 1v ^{f)}							
		2b	1v	2a	1u	h	i	m	n
2b	0	50	50	- ^{d)}	- ^{d)}	- ^{d)}	- ^{d)}	- ^{d)}	- ^{d)}
	3	1	18	19	28	7	16	11	- ^{d)}
2a	0	50	50	- ^{d)}	- ^{d)}	- ^{d)}	- ^{d)}	- ^{d)}	- ^{d)}
	3	40	42	4	5	4	1	4	- ^{d)}
	23	3	13	32	29	12	5	6	- ^{d)}

^{a)} b, Blank reactions, and c, catalyzed with 10 mol% L-proline as a catalyst. ^{b)} Reaction time indicates the time when no further change in composition could be observed. ^{c)} Error on ¹H-NMR signal integration, ~4-5%. ^{d)} -, compound not observed. ^{e)} in DMSO-*d*₆/D₂O 99.5/0.5. ^{f)} DMSO-*d*₆/D₂O 99.5/0.2.

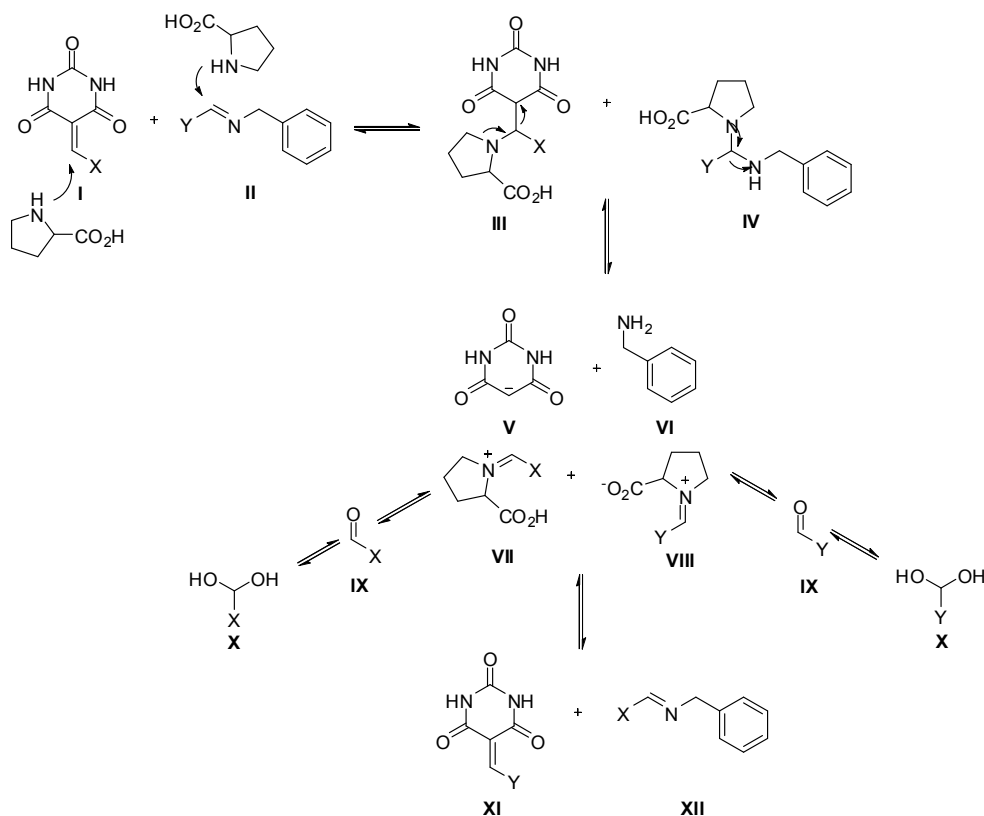
In a further attempt to decrease amount of hydrolysis products, the benzylidene/imine exchange was run in pure DMSO-*d*₆ (given as containing less than 0.02% of water) at 60°C. The reaction of benzylidene **2b** with imine **1v** (Table 2.6, Entry 1), both bearing an EDG, gave **2a** and **1u**. The equilibrium was reached after 2 hours in the presence of 10% L-proline as compared to 22 hours in its absence. Under these conditions, the hydrolysis products amounted now to less than 10%. The reverse process, starting with **2a** and **1u** formed **2b** and **1v** and gave the same final product distribution. Finally, the exchange reaction between **2f** and **1v** (Table 2.6, Entry 3) and its reverse reaction with **2a** and **1b** (Table 2.6, Entry 4) gave identical final distributions, consistent with a true equilibrium being attained. In these conditions, L-proline performed marked organocatalysis, as it accelerated the reaction from 6-fold (Table 2.6, Entry 4) up to 22-fold (Table 2.6, Entry 3) when one compares the blank reaction at the same reaction time to that of the completed catalyzed reaction.

Table 2.6 Proportions (%) of the different compounds in the cross exchange reactions C=C/C=N between benzylidene barbiturates and imines in DMSO-*d*₆ at 60°C. **h** = 4-methoxybenzaldehyde, **i** = 4-dimethylaminobenzaldehyde, **j** = 2-thiophenecarboxaldehyde, **m** = 4-methoxybenzaldehyde hydrate, **n** = 4-dimethylaminobenzaldehyde hydrate, **o** = 2-thiophenecarboxaldehyde hydrate.

Entry a)	Reaction Time [h] ^{b)}	Compound Distribution [%] ^{c)}							
Starting compounds 2b + 1v									
		2b	1v	2a	1u	h	i	m	n
1b	0	50	50	- ^{d)}	- ^{d)}	- ^{d)}	- ^{d)}	- ^{d)}	- ^{d)}
	2	50	50	<1 ^{e)}	<1 ^{e)}	<1 ^{e)}	<1 ^{e)}	<1 ^{e)}	- ^{d)}
	22	7	12	34	33	7	3	4	- ^{d)}
1c	0	50	50	- ^{d)}	- ^{d)}	- ^{d)}	- ^{d)}	- ^{d)}	- ^{d)}
	2	5	9	32	33	8	7	6	- ^{d)}
Starting compounds 2a + 1u									
		2a	1u	2b	1v	h	i	m	n
2b	0	50	50	- ^{d)}	- ^{d)}	- ^{d)}	- ^{d)}	- ^{d)}	- ^{d)}
	2	49	49	1	1	<1 ^{e)}	<1 ^{e)}	<1 ^{e)}	- ^{d)}
	24	39	39	7	10	3	<1 ^{e)}	2	- ^{d)}
2c	0	50	50	- ^{d)}	- ^{d)}	- ^{d)}	- ^{d)}	- ^{d)}	- ^{d)}
	2	34	32	4	12	7	5	6	- ^{d)}
Starting compounds 2f + 1v									
		2f	1v	2a	1b	i	j	n	o
3b	0	50	50	- ^{d)}	- ^{d)}	- ^{d)}	- ^{d)}	- ^{d)}	- ^{d)}
	3	50	50	<1 ^{e)}	<1 ^{e)}	<1 ^{e)}	<1 ^{e)}	- ^{d)}	<1 ^{e)}
	66	28	27	20	20	3	<1 ^{e)}	- ^{d)}	2
3c	0	50	50	- ^{d)}	- ^{d)}	- ^{d)}	- ^{d)}	- ^{d)}	- ^{d)}
	3	21	28	16	20	10	<1 ^{e)}	- ^{d)}	5
Starting compounds 2a + 1b									
		2a	1b	2e	1v	i	j	n	o
4b	0	50	50	- ^{d)}	- ^{d)}	- ^{d)}	- ^{d)}	- ^{d)}	- ^{d)}
	4	42	44	7	7	<1 ^{e)}	<1 ^{e)}	- ^{d)}	<1 ^{e)}
	25	22	24	26	26	<1 ^{e)}	1	- ^{d)}	1
4c	0	50	50	- ^{d)}	- ^{d)}	- ^{d)}	- ^{d)}	- ^{d)}	<1 ^{e)}
	4	16	24	23	29	4	<1 ^{e)}	- ^{d)}	4

^{a)} b, blank reactions, and c, catalyzed reactions with 10 mol% L-proline as a catalyst. ^{b)} Reaction time indicates the time when no further change in composition could be observed. ^{c)} Error on ¹H-NMR signal integration, ~4-5%. ^{d)} Compound not observed. ^{e)} Only traces of product detected.

A plausible mechanism for exchange between C=C and C=N in the presence of L-proline and water is shown in *Scheme 2.7*, following sequential hydrolysis/condensation steps (see also ref. [52]). It may be considered to involve addition of L-proline to the benzylidene and imine reactants leading to iminium intermediates by subsequent elimination, followed by condensation of the released anionic barbiturate and benzylamine with the aldehydes resulting from the cleavage. The formation of hydrates^[53] of the aldehydes bearing electron-withdrawing substituents opposes the formation of the exchanged products.



Scheme 2.7 Possible mechanism of the cross exchange between a Knoevenagel-type substrate ($C=C$) and an imine ($C=N$) following sequential hydrolysis/condensation steps.^[52]

2.2.4 Organocatalysis of Benzylidene/Benzylidene, $C=C/C=C$, Cross-exchange Processes.

In published work,^[54] we have already described some aspects of the generation of DCLs involving imine/imine ($C=N/C=N$) and benzylidene/imine ($C=C/C=N$) exchange processes and exploiting L-proline as an organocatalyst. To further extend the range of covalent dynamic libraries, we investigated the benzylidene/benzylidene ($C=C/C=C$) cross-exchange reaction between benzylidenebarbiturates (**2a-d**, **2f-g**) and differently substituted benzylidenemalononitriles (**3a-3e**, **3i**) as depicted in *Scheme 2.8*. The barbiturate-benzylidene compounds are easily hydrolyzed in DMSO- d_6 /D₂O 99/1 solution so that pure DMSO- d_6 (given as containing less than 0.02% of H₂O) was chosen as a solvent. Even then, some contribution of hydrolysis could not be avoided.

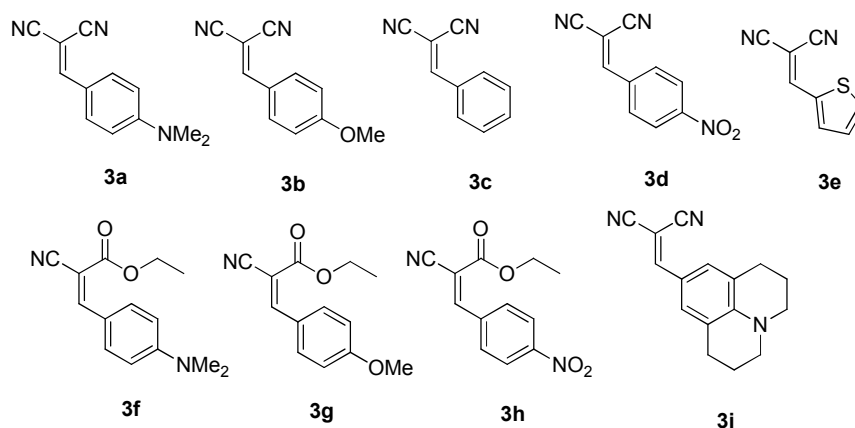
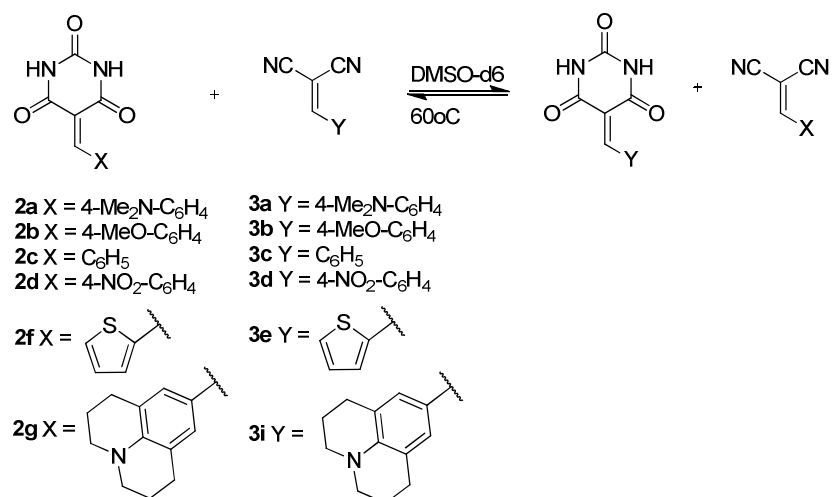


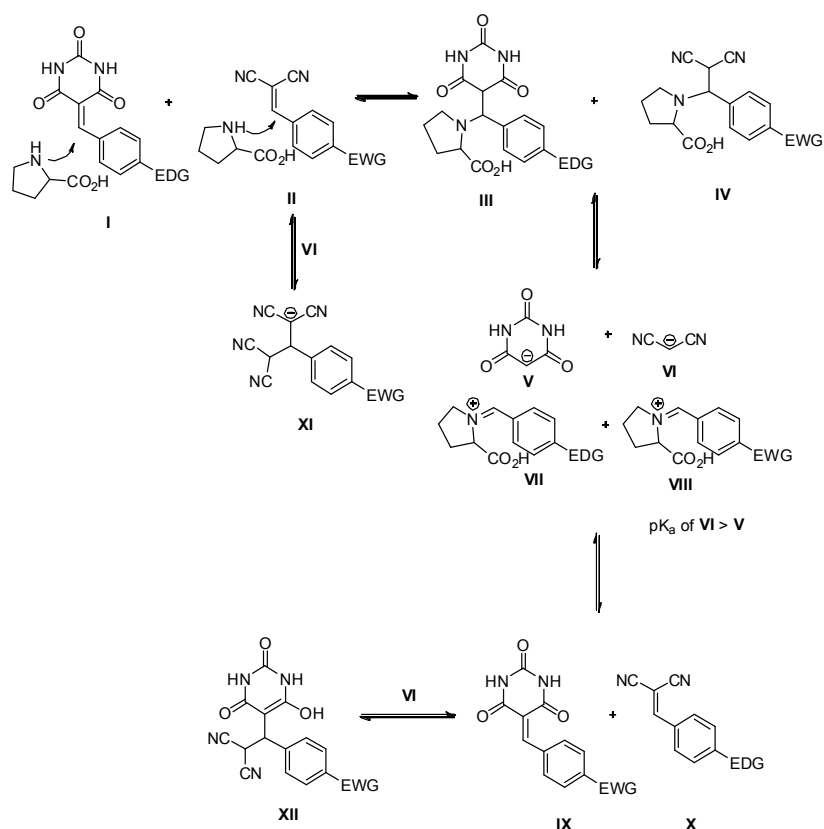
Figure 2.11 Structure of the benzylidene malononitrile derivatives (**3a-3i**) used in the present study

Benzylidenebarbiturates (**2a-d**, **2f-g**) and benzylidenemalononitriles (**3a-3e**, **3i**) were selected as substrates for this exchange study. The reactions were carried out with equimolar amounts of the benzylidene derivatives (12.8 mM each) in pure DMSO-*d*₆ as well as in the presence of 10 mol% L-proline. The corresponding kinetic parameter (half-lives *t*_{1/2}) (the half-lives of the reactions were determined by integration of the decreasing ¹H-NMR signals of the starting material as a function of time and analyzing the curve obtained) and %composition of the final solutions are listed in *Table 2.7*. Equilibrium constants were not calculated, due to the occurrence of variable amounts of hydrolysis and because some reactions did not reach equilibrium in a reasonable time.



Scheme 2.8 Representation of the C=C/C=C cross-exchange reaction between barbiturate-benzylidene (**2a-d**, **2f-g**) and differently substituted malononitrile-benzylidenes (**3a-e**, **3i**) in DMSO-*d*₆ at 60°C.

Here again, the efficiency of benzylidene exchange depended on the nature of the head group substituent in these Michael acceptors. Considering first the pair of compounds **2a**, bearing an electron-donating group (EDG), and **3d**, bearing an electron-withdrawing group (EWG), the cross-exchange reaction is expected to yield the products **2d** and **3a** (Table 2.7, Entry 1). The ¹H-NMR spectrum of the mixture after the exchange reaction started showed new signals at 4.73, 4.94, 5.32, 6.21, 7.26, 7.63, 7.76, 7.91, 9.50, and 12.2 ppm, which were assigned to the Michael-type adducts **XI** and **XII** shown in Scheme 2.9. In addition, the electrospray high resolution mass spectrum also supported the formation of adducts **XI** and **XII**, showing respectively peaks at *m/z* 338.343 ([M+H⁺+Na⁺]+CH₃OH+H₂O) and 360.324 ([M+H⁺]+CH₃OH). Neither adduct could be isolated. In the reaction mixture, the most reactive electrophiles^[55] are **2d** and **3d**, so they may react with the better nucleophile, the malononitrile anion formed from **3d** (p*K*_a of **VI** > **V**), affording adducts **XI** and **XII**. Thus, product **2c** is formed, but it is trapped as its Michael-type adduct **XII**. On the other hand, the reaction of malononitrile with **3d** precludes the formation of the product **3a**. A possible mechanism of this cross exchange reaction is shown in Scheme 2.9.



Scheme 2.9 Possible mechanism of the Cross-Exchange reaction between Knoevenagel compounds following sequential hydrolysis/condensation Steps.^[31,52]

The reversibility of this reaction was studied by combining **2d** and **3a** (Table 2.7, Entry 2). Both starting compounds were fully hydrolyzed, and the anticipated products **2a** and **3d** did not form even after 20 days, at which time decomposition of the compounds had occurred. This result indicates that hydrolysis precludes the recondensation to form **2a** and **3d** and thus the exchange reaction. For the same reason, no Michael-type adduct **XII** was observed.

Next, **2c** and **3d** were selected as starting compounds, both bearing EWGs (Table 2.7, Entry 3). These substrates were more suitable for the cross-exchange than the molecules exhibiting a large difference in their electrophilicity (**2a** and **3d**), and both products **2d** and **3c** were formed. The hydrolysis products were observed to be less than 10% at equilibrium. In addition, the Michael-type adducts **XI** and **XII** were also detected in the ¹H-NMR spectrum of the mixture which showed characteristic doublet peaks at 4.94, 5.32 ppm belonging to adduct **XI** (1%) and 4.72, 6.20 ppm belonging to adduct **XII** (9%), in agreement with reported values^[56] and with mass spectral data (see below). The reverse reaction was performed by mixing compound **2d** and **3c** (Table 2.7, Entry 4), and components **2c** and **3d** were obtained in comparable amounts as in the forward case, indicating that the reaction was reversible and that the equilibrium had more or less been reached. In the reverse case, only Michael-type adduct **XII** was detected, its ¹H-NMR spectrum showing an OH signal at 12.18 ppm and doublet peaks at 4.74 and 6.20 ppm of about 5% intensity under these conditions both in the presence and absence of L-proline. Formation of **XII** was also confirmed by the electrospray high resolution mass spectrum showing a peak at m/z 346.34 ([M+H₃O⁺]).

Next, compounds **2a** and **3b**, both bearing EDGs, were reacted (Table 2.7, Entry 5), giving **2b** (19%) and **3a** (24%) as products at equilibrium after about 29 h. The ¹H-NMR doublet signals at 4.48 and 6.09 ppm, observed during the exchange process in the presence of L-proline, are characteristic of the Michael-type adduct **XI** (1%), whose formation was confirmed by HR-MS data with a peak at m/z 287.21 ([M+2H₃O⁺]). The hydrolysis products in the presence of L-proline were less than 4%. Equilibrium was reached after 29 h in the presence of 10 mol% L-proline but in its absence the reaction was extremely slow, barely showing exchange after 23 h (1% each of the products **2b** and **3a**). After 20 days, **2b** and **3a** formed in 12% yield each, showing that the reaction in the absence of catalyst was extremely slow. The uncatalyzed reaction did not show any Michael-adduct formation and involved the formation of trace amounts (1%) of hydrolysis

products. The reverse reaction, starting with **2b** and **3a** (*Table 2.7, Entry 6*), gave **2a** and **3b** in similar amounts to those of the forward reaction and approached equilibrium after 98 h in the presence of 10 mol% L-proline. Again, in the absence of L-proline, the exchange reaction was significantly slower with exchange products formed only in trace amounts (about 1% each) after 4 days, with little change after 22 days where only **2a** (1%) and **3b** (2%) were observed. For both forward and back reactions (in the presence of L-proline), hydrolysis products were formed in yields of less than 4%.

The exchange reaction between **2f** and **3b** (*Table 2.7, Entry 7*) and its reverse reaction between **2b** and **3e** (*Table 2.7, Entry 8*), yielding essentially identical mixtures in the presence of 10 mol% L-proline and were faster than other L-proline catalyzed *Knoevenagel* cross-exchanges, approaching equilibrium after 6 h. The Michael-type adduct **XI** was observed in trace amounts (1%) for both forward and reverse reactions, showing the characteristic doublets peaks at 4.46 and 6.07 ppm. Electrospray high resolution mass spectroscopy was used to confirm the formation of the addition product showing a peak at m/z 287.2 ($[M+2H_3O^+]$). In the absence of L-proline, exchange products could only be observed after 23 h for both forward and reverse reactions. The equilibrium was approached after 128 h and 532 h for forward and backward directions, respectively. Interestingly, the reaction in the absence of L-proline did not result in the formation of any Michael-type adducts, instead only the hydrolysis products formed, although the hydrolysis products in both the presence and absence of L-proline were less than 2%.

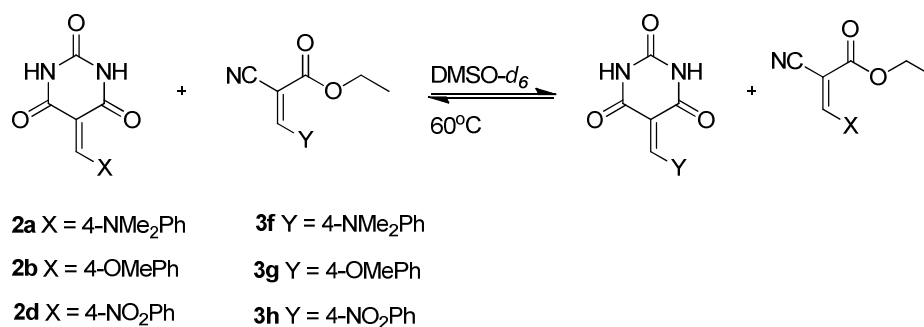
Finally, the exchange reaction between **2g** and **3e** (*Table 2.7, Entry 9*) both bearing electron donating groups, in the presence of 10 mol% L-proline was studied, giving the product distribution as following **2g** (30%), **3e** (22%), **2f** (23%), and **3i** (23%) after 23 h with half-life ($t_{1/2}$) of 5 h. The reaction in the absence of L-proline was very slow, giving the exchange products **2f** (10%) and **3i** (3%) after 168 h. Interestingly, the Michael-type adducts were not present in both conditions and the hydrolysis products were observed in less than 7% yield. Next, the reversibility of this reaction was examined by mixing **2f** and **3i** (*Table 2.7, Entry 10*) both in the presence and absence of the catalyst. The reverse reactions in both conditions were extremely slow, giving the exchange products **2g** (3%) and **3e** (7%) after 220 h. The addition of 10 mol% L-proline did not affect the rate of the reverse process. Under these conditions, L-proline demonstrated marked organocatalysis, as it accelerated the reaction from two-fold (*Table 2.7, Entry 3*) up to about 89-fold (*Table 2.7, Entry 8*), when one compares the blank reaction at the same reaction time as that of the completed catalyzed reaction.

Table 2.7 Kinetic and equilibrium parameters for Knoevenagel cross-exchange reactions (Scheme 2.8). Half-life ($t_{1/2}$), (-) = reaction too slow to determine the parameter, n.a. = not applicable. Proportions [%] of the different compounds in the cross-exchange reaction C=C/C=C between benzylidene-barbiturates and benzylidene-malononitriles in DMSO- d_6 at 60°C. **a** = 4-dimethylaminobenzaldehyde, **b** = benzaldehyde, **c** = 4-nitrobenzaldehyde, **d** = 4-methoxybenzaldehyde, **e** = 2-thiophene carboxaldehyde, **f** = 9-julolidenecarboxaldehyde, **g** = 4-(dimethylamino)benzaldehyde hydrate, **h** = benzaldehyde hydrate, **i** = 4-nitrobenzaldehyde hydrate, **j** = 4-methoxybenzaldehyde hydrate, **k** = 2-thiophene carboxaldehyde hydrate, **l** = 9-julolidene carboxaldehyde hydrate, **B** = barbiturate, **M** = malononitrile, and **XI**, **XII** = Michael-type adducts.

Entry a)	$t_{1/2}$ [h]	Reaction Time[h] ^c	Compound Distribution [%]											
Starting compound 2a + 3d														
			2a	3d	2d	3a	a	c	g	i	B	M	XI	XII
1b	50	164	35	30	5	11	1	6	- ^b	- ^b	3	3	- ^b	6
1c	45	144	33	26	5	13	2	4	- ^b	- ^b	4	3	2	7
Starting compound 2d + 3a														
			2d	3a	2a	3d	a	c	g	i	B	M	XI	XII
2b	n.a.	142	33	50	- ^b	- ^b	<1 ^c	12	<1 ^c	1	2	1	- ^b	- ^b
2c	n.a.	142	32	52	- ^b	- ^b	<1 ^c	9	<1 ^c	3	2	1	- ^b	- ^b
Starting compound 2c + 3d														
			2c	3d	2d	3c	b	c	h	i	B	M	XI	XII
3b	8	53	16	10	22	31	1	7	<1 ^c	1	3	3	<1 ^c	5
3c	3	24	12	9	20	26	8	3	<1 ^c	2	5	5	1	9
Starting compound 2d + 3c														
			2d	3c	2c	3d	b	c	h	i	B	M	XI	XII
4b	20	55	22	33	14	7	1	9	<1 ^c	2	3	3	- ^b	5
4c	14	32	23	36	13	7	1	6	<1 ^c	2	3	3	- ^b	5
Starting compound 2a + 3b														
			2a	3b	2b	3a	a	d	g	j	B	M	XI	XII
5b	n.a.	23 ^d	49	49	1	1	- ^b	- ^b	- ^b	- ^b	- ^b	- ^b	- ^b	- ^b
	n.a.	488 ^f	35	37	12	12	2	1	- ^b	- ^b	<1 ^c	<1 ^c	- ^b	- ^b
5c	9	29	24	24	19	24	1	3	<1 ^c	1	2	<1 ^c	1	- ^b
Starting compound 2b + 3a														
			2b	3a	2a	3b	a	d	g	j	B	M	XI	XII
6b	n.a.	95 ^d	48	49	1	<1 ^c	1	<1 ^c	- ^b	- ^b	- ^b	- ^b	- ^b	- ^b
	n.a.	533 ^f	43	48	1	2	1	5	- ^b	- ^b	1	- ^b	- ^b	- ^b
6c	30	98	23	30	19	19	<1 ^c	4	<1 ^c	1	3	<1 ^c	<1 ^c	- ^b
Starting compound 2f + 3b														
			2f	3b	2b	3e	d	e	j	k	B	M	XI	XII
7b	40	128	46	43	6	6	1	- ^b	<1 ^c	- ^b	- ^b	<1 ^c	- ^b	- ^b
7c	2	6	43	40	6	7	2	- ^b	<1 ^c	- ^b	1	1	1	- ^b
Starting compound 2b + 3e														
			2b	3e	2f	3b	d	e	j	k	B	M	XI	XII
8b	180	532	8	8	42	40	2	- ^b	- ^b	- ^b	1	<1 ^c	- ^b	- ^b
8c	2	6	6	8	42	39	3	- ^b	- ^b	- ^b	1	1	1	- ^b
Starting compound 2g + 3e														
			2g	3e	2f	3i	e	f	k	l	B	M	XI	XII
9b	n.a.	168 ^f	45	38	10	3	2	- ^b	- ^b	1	- ^b	<1 ^c	- ^b	- ^b
9c	5	23	30	22	23	23	1	- ^b	- ^b	1	- ^b	- ^b	- ^b	- ^b
Starting compound 2f + 3i														
			2f	3i	2g	3e	e	f	k	l	B	M	XI	XII
10b	n.a.	220 ^f	43	41	3	7	1	- ^b	- ^b	6	- ^b	- ^b	- ^b	- ^b
10c	n.a.	220 ^f	47	45	2	6	1	- ^b	- ^b	3	- ^b	- ^b	- ^b	- ^b

^{a)} b, blank reactions, and c, catalyzed reaction with 10 mol% L-proline as a catalyst. ^{b)} Compound not observed. ^{c)} Only traces of product detected. ^{d)} The reaction started. ^{e)} Reaction time indicates the time when no further change in composition could be observed. ^{f)} The reaction did not reach equilibrium. All measurements were repeated three times and averaged. The reproducibility of the values obtained was $\pm 2\%$

In principle, the electrophilic behavior of the benzylidene derivative is strongly dependent on the nature of the probe head (barbituric acid or malononitrile). The most reactive are the benzylidene derivatives whose probe-head is the strongest EWG and has the lowest pK_a . Therefore, diethylbenzylidenemalonate (pK_a (diethyl malonate) = 16.4) proved to be less reactive than the benzylidene-malononitrile (pK_a (malononitrile) = 11.1), and much less reactive than the barbituric acid (pK_a (barbituric) = 4.0).^[43] To further explore this hypothesis, we prepared the ethylbenzylidene malonates (**3f**, **3g**, and **3h**), and studied their exchange reactions with benzylidene barbituric acid (**2a-b**, **2d**) as depicted in *Scheme 2.10*.



Scheme 2.10 Representative of the metathesis C=C/C=C reaction between barbiturate-benzylidenes (**2a,b,d**) and differently substituted cyanoacetate-benzylidenes (**3f,g,h**) in DMSO-*d*₆ at 60°C.

Firstly, the exchange process between **2a** and **3h** (*Table 2.8, Entry 1*) was studied in pure DMSO-*d*₆ at 60°C with and without 10 mol% L-proline. After 7 h, trace amounts of exchange products, **2d** and **3f**, started appearing in the ¹H-NMR spectrum indicating that this reaction occurred very slowly. The %-composition of reaction was unchanged after 94 h, giving **2d** (3%) and **3f** (5%). In addition, the hydrolysis products, for instance, 4-nitrobenzaldehyde (5%), 4-dimethylaminobenzaldehyde (5%), and ethyl cyanoacetate (4%) were also detected. In the absence of L-proline, the exchange was detectable after 94 h, giving **2d** (2%) and a trace amount of **3f** (1%). New ¹H-NMR multiplet peaks near 6.05, 7.27, and 7.78 – 7.51 ppm were detected here as well and assigned to Michael-adducts. In the reverse process, compound **2d** and **3f** (*Table 2.8, Entry 2*) were mixed. The anticipated products **2a** and **3h** did not form; only hydrolysis products were detected indicating that equilibrium could not be achieved in this system.

Next, **2a** was combined with **3g** (*Table 2.8, Entry 3*) in pure DMSO-*d*₆ at 60°C in the presence of 10 mol% L-proline. As expected, products **2b** and **3f**, formed to the extent of 13% and 20% after 121 h. The reaction in the absence of L-proline occurred very slowly

and the %-composition was unchanged after 178 h. For the reverse process, **2b** and **3f** (Table 2.8, Entry 4) were also mixed, and **2a** and **3g** started forming after 33 h indicating that this reaction was reversible. In the absence of L-proline, the reverse reaction was not detectable. These results show that ethylbenzylidenemalonate compounds are significantly less reactive than benzylidene-malononitrile derivatives.

Table 2.8 Proportions (%) of the different compounds in the metathesis reaction C=C/C=C between benzylidene-barbiturates and benzylidene-ethylcyanoacetate in DMSO-*d*₆ at 60°C. **f** = 4-dimethyl aminobenzaldehyde, **h** = 4-nitrobenzaldehyde, **i** = 4-methoxybenzaldehyde, **j** = 4-nitrobenzaldehyde hydrate, **B** = barbiturate, **E** = ethylcyanoacetate.

Entry a)	Reaction Time [h]	Compound Distribution [%] ^{b)}							
Starting Compound 2a + 3h									
		2a	3h	2d	3f	f	h	B	E
1b	94 ^{e)}	48	47	2	1	1	1	<1 ^{d)}	1
1c	94	41	38	3	5	5	5	<1 ^{d)}	4
Starting Compound 2d + 3f									
		2d	3f	2a	3h	f	h	j	E
2b	74	34	51	- ^{e)}	- ^{e)}	2	8	4	<1 ^{d)}
2c	74	25	62	- ^{e)}	- ^{e)}	2	4	7	<1 ^{d)}
Starting Compound 2a + 3g									
		2a	3g	2b	3f	f	i	B	E
3b	178	37	37	7	16	1	<1 ^{d)}	1	<1 ^{d)}
3c	121	29	29	13	20	1	2	4	1
Starting Compound 2b + 3f									
		2b	3f	2a	3g	f	i	B	E
4b	151	46	46	- ^{e)}	- ^{e)}	<1 ^{d)}	8	<1 ^{d)}	<1 ^{d)}
4c	121	15	53	7	6	<1 ^{d)}	4	14	1

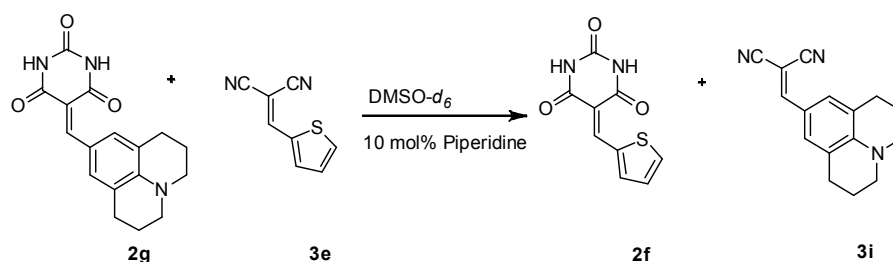
^{a)} b, blank reactions, and c, catalyzed reaction with 10 mol% L-proline as a catalyst. ^{b)} Error on ¹H-NMR signal integration, ~4-5%. ^{c)} The reaction started. ^{d)} Only traces of product detected. ^{e)} Compound not observed.

The electronic absorption spectra of benzylidene barbiturates (**2a-2f**, **2g**) and benzylidene malononitrile (**3a-3e**) were measured in DMSO at room temperature, Table 2.9 being a compilation of the absorption maxima wavelengths and molar absorptivities. This indicated that the benzylidene-barbiturates or benzylidene malononitriles which contained the probe-head with an EDG showed a red-shift of the principal absorption band compared to those with an EWG. This is potentially a measure of the effectiveness of the substituents in influencing the exchange equilibrium position.

Table 2.9 The absorption maxima and molar absorptivity values for **2a** - **2f** and **3a** - **3f** (1×10^{-5} M in DMSO)

Entry	Compound	λ_{\max} (nm)	ϵ (cm ⁻¹ mol ⁻¹ L)
1	2a	465	66496
2	2b	373	30118
3	2c	325	18981
4	2d	318	13601
5	2f	371	24566
6	2g	490	81132
7	3a	440	64687
8	3b	354	28850
9	3c	311	23429
10	3d	310	18402
11	3e	353	21891

In a search for other organocatalysts, piperidine, as a secondary amine like L-proline, was investigated for its effects on these C=C/C=C exchanges. Benzylidene-barbituric acid **2g** and benzylidene-malononitrile **3e**, both bearing electron-donating group were selected for examination using this catalyst as shown in *Scheme 2.11*.

**Scheme 2.11** Representative metathesis C=C/C=C reaction between **2g** and **3e** in 100% $\text{DMSO-}d_6$ at 60°C using piperidine as catalyst.

The $^1\text{H-NMR}$ spectrum of the exchange reaction mixture in the presence of piperidine showed a broad peak at 10.8 ppm belonging to the barbituric protons of **2g** (*Figure 2.12*) indicating that they could possibly exchange with the $-\text{NH}$ proton of piperidine. A control experiment was conducted by adding piperidine to **2g** alone in $\text{DMSO-}d_6$ and a broad peak at 10.8 ppm was again observed. The exchange products **2f** and **3i** were formed in significant yield (*Figure 2.13*), with **2g** (19%), **3e** (15%), **2f** (31%), and **3i** (31%) present after 25 h (equilibration time). The half-life ($t_{1/2}$) of this reaction was 6 h. The hydrolysis products and Michael-adduct were observed but were less than 3% each. In addition, this reaction was conducted in the presence of 10 mol% L-proline, giving the compound distribution **2g** (30%), **3e** (22%), **2f** (23%), and **3i** (23%) after 23 h with half-life ($t_{1/2}$) of 5 h.

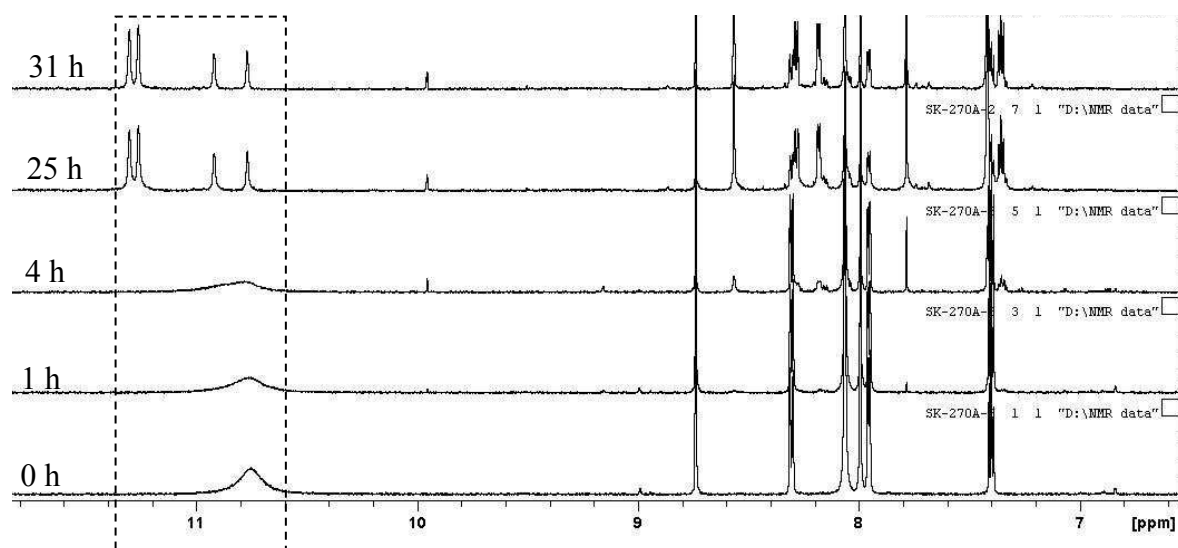


Figure 2.12 ^1H -NMR spectrum of the exchange reaction between compound **2g** and **3e** in $\text{DMSO-}d_6$ in the presence of 10mol% piperidine as a function of time.

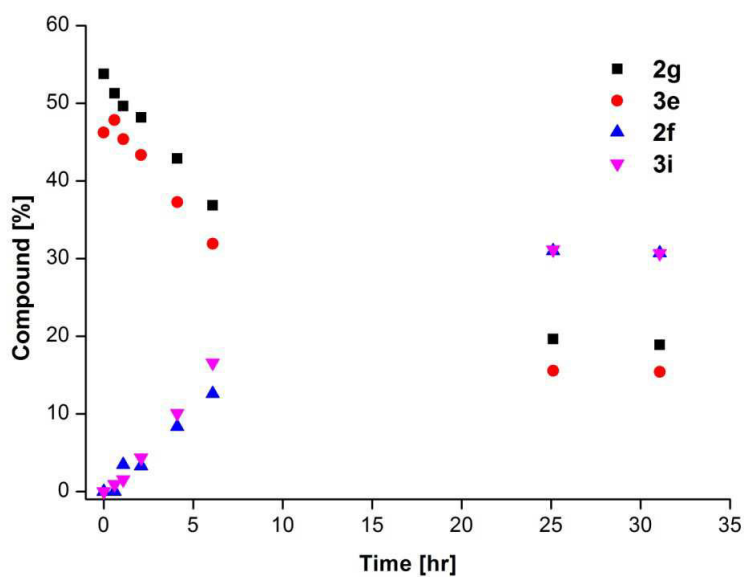


Figure 2.13 The exchange reaction profile between compound **2g** and **3e** in $\text{DMSO-}d_6$ in the presence of 10 mol% piperidine as a function of time.

2.3 Conclusions

The results described above lead to the following conclusions:

1) Significant organocatalysis can be achieved in Dynamic Covalent Chemistry processes.

2) The secondary amine L-proline is an efficient organocatalyst for $C=N/C=N$ imine exchange reactions at a catalyst loading of 10 mol%, providing accelerations up to 22-fold at ambient temperature. Imines derived from aliphatic/nucleophilic amines and highly electrophilic aldehydes were found to be the most suitable starting components, giving only the exchange and no hydrolysis products after completion of the reaction.

3) In contrast, the $C=C/C=N$ interconversion of *Knoevenagel* substrates and imines cannot be performed under similar conditions, as extensive hydrolysis occurs. Conducting the reactions in pure DMSO- d_6 at 60°C greatly reduced hydrolysis (less than 10 %) and $C=C/C=N$ exchange took place, displaying marked acceleration in the presence of 10 mol% L-proline of up to 22-fold. Compounds bearing electron-donating substituents gave the least hydrolysis in the cross-exchange.

4) Furthermore, 10 mol% L-proline is able to accelerate the rate of cross-*Knoevenagel* $C=C/C=C$ exchange up to about 89-fold at 60°C, although Michael-type adducts are also formed during the cross exchange process. The %-composition of products at equilibrium depends on the electron affinity of the starting substrates.

5) The results described herein stress the potential of organocatalysis for DCC, facilitating the formation of dynamic libraries and allowing for increased diversity generation.

2.4 References

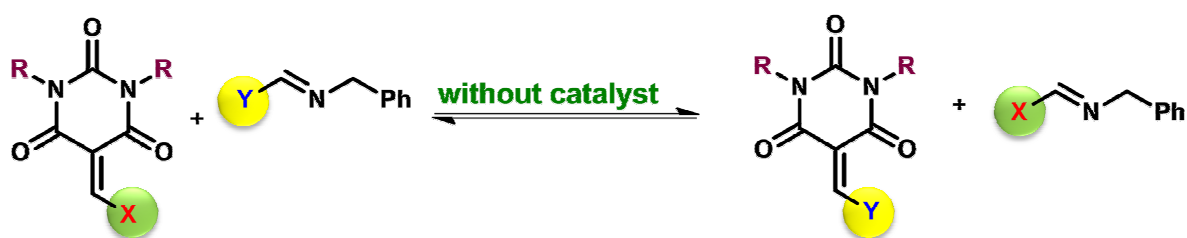
- [1] P. T. Corbett, J. Leclaire, L. Vial, K. R. West, J.-L. Wietor, J. K. M. Sanders, S. Otto, *Chem. Rev.* **2006**, *106*, 3652–3711.
- [2] S. Ladame, *Org. Biomol. Chem.* **2008**, *6*, 219–226.
- [3] J.-M. Lehn, *Chem. – Eur. J.* **1999**, *5*, 2455–2463.
- [4] J.-M. Lehn, *Chem. Soc. Rev.* **2007**, *36*, 151–160.
- [5] J.-M. Lehn, in *Top. Curr. Chem.*, Ed. M. Barboiu, Springer-Verlag, Berlin, Heidelberg, **2012**, pp. 1–32.
- [6] O. Ramström, J.-M. Lehn, *Nat. Rev. Drug Discov.* **2002**, *1*, 26–36.
- [7] O. Ramström, S. Lohmann, T. Bunyapaiboonsri, J.-M. Lehn, *Chem. – Eur. J.* **2004**, *10*, 1711–1715.
- [8] T. Hotchkiss, H. B. Kramer, K. J. Doores, D. P. Gamblin, N. J. Oldham, B. G. Davis, *Chem. Commun.* **2005**, 4264–4266.
- [9] M. Hochgürtel, J.-M. Lehn, in *Fragm.-Based Approaches Drug Discov.* (Eds.: W. Jahnke, D.A. Erlanson), Wiley-VCH Verlag GmbH & Co. KGaA, **2006**, pp. 341–364.
- [10] O. Ramström, J.-M. Lehn, in *Compr. Med. Chem. II* (Ed.: J.B.T.J. Triggler), Elsevier, Oxford, **2007**, pp. 959–976.
- [11] G. Nasr, E. Petit, C. T. Supuran, J.-Y. Winum, M. Barboiu, *Bioorg. Med. Chem. Lett.* **2009**, *19*, 6014–6017.
- [12] D. E. Scott, G. J. Dawes, M. Ando, C. Abell, A. Ciulli, *ChemBioChem* **2009**, *10*, 2772–2779.
- [13] R. Caraballo, H. Dong, J. P. Ribeiro, J. Jiménez-Barbero, O. Ramström, *Angew. Chem. Int. Ed.* **2010**, *49*, 589–593.
- [14] J.-M. Lehn, *Prog. Polym. Sci.* **2005**, *30*, 814–831.
- [15] J. Lehn, *Aust. J. Chem.* **2010**, *63*, 611–623.
- [16] D. Zhao, J. S. Moore, *J. Am. Chem. Soc.* **2002**, *124*, 9996–9997.
- [17] R. J. Williams, A. M. Smith, R. Collins, N. Hodson, A. K. Das, R. V. Ulijn, *Nat. Nanotechnol.* **2009**, *4*, 19–24.
- [18] S. Otto, *Nat. Nanotechnol.* **2009**, *4*, 13–14.
- [19] R. Nguyen, E. Buhler, N. Giuseppone, *Macromolecules* **2009**, *42*, 5913–5915.
- [20] B. L. Miller, *Dynamic Combinatorial Chemistry*, Wiley, Chichester, **2010**.

- [21] J.N.H. Reek, S. Otto, *Dynamic Combinatorial Chemistry*, Wiley-VCH, Weinheim, **2010**.
- [22] T. D. James, K. R. A. S. Sandanayake, S. Shinkai, *Angew. Chem. Int. Ed. Engl.* **1996**, *35*, 1910–1922.
- [23] L. M. Greig, A. M. Z. Slawin, M. H. Smith, D. Philp, *Tetrahedron* **2007**, *63*, 2391–2403.
- [24] B. Masci, S. Pasquale, P. Thuéry, *Org. Lett.* **2008**, *10*, 4835–4838.
- [25] P. Reutenauer, E. Buhler, P. J. Boul, S. J. Candau, J.-M. Lehn, *Chem. – Eur. J.* **2009**, *15*, 1893–1900.
- [26] N. Roy, J.-M. Lehn, *Chem. – Asian J.* **2011**, *6*, 2419–2425.
- [27] M. E. Belowich, J. F. Stoddart, *Chem. Soc. Rev.* **2012**, *41*, 2003–2024.
- [28] C. Godoy-Alcántar, A. K. Yatsimirsky, J.-M. Lehn, *J. Phys. Org. Chem.* **2005**, *18*, 979–985.
- [29] A. Dirksen, S. Dirksen, T. M. Hackeng, P. E. Dawson, *J. Am. Chem. Soc.* **2006**, *128*, 15602–15603.
- [30] V. A. Polyakov, M. I. Nelen, N. Nazarpak-Kandlousy, A. D. Ryabov, A. V. Eliseev, *J. Phys. Org. Chem.* **1999**, *12*, 357–363.
- [31] P. I. Dalko, L. Moisan, *Angew. Chem. Int. Ed.* **2004**, *43*, 5138–5175.
- [32] S. Mukherjee, J. W. Yang, S. Hoffmann, B. List, *Chem. Rev.* **2007**, *107*, 5471–5569.
- [33] A. Erkkilä, I. Majander, P. M. Pihko, *Chem. Rev.* **2007**, *107*, 5416–5470.
- [34] A. B. Northrup, I. K. Mangion, F. Hettche, D. W. C. MacMillan, *Angew. Chem. Int. Ed.* **2004**, *43*, 2152–2154.
- [35] A. B. Northrup, D. W. C. MacMillan, *J. Am. Chem. Soc.* **2002**, *124*, 6798–6799.
- [36] D. A. Bock, C. W. Lehmann, B. List, *Proc. Natl. Acad. Sci.* **2010**, *107*, 20636–20641.
- [37] C. F. Barbas, *Angew. Chem. Int. Ed.* **2008**, *47*, 42–47.
- [38] D. Seebach, A. K. Beck, D. M. Badine, M. Limbach, A. Eschenmoser, A. M. Treasurywala, R. Hobi, W. Prikoszovich, B. Linder, *Helv. Chim. Acta* **2007**, *90*, 425–471.
- [39] D. Seebach, U. Grošelj, W. B. Schweizer, S. Grimme, C. Mück-Lichtenfeld, *Helv. Chim. Acta* **2010**, *93*, 1–16.
- [40] E. Knoevenagel, *Berichte Dtsch. Chem. Ges.* **1896**, *29*, 172–174.
- [41] B. List, *Angew. Chem. Int. Ed.* **2010**, *49*, 1730–1734.

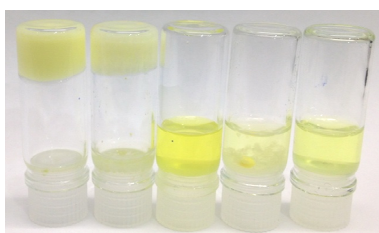
- [42] S. Kulchat, K. Meguellati, J.-M. Lehn, *Helv. Chim. Acta* **2014**, *97*, 1219–1236.
- [43] O. Kaumanns, R. Lucius, H. Mayr, *Chem. – Eur. J.* **2008**, *14*, 9675–9682.
- [44] H. Fischer, F. X. DeCandis, S. D. Ogden, W. P. Jencks, *J. Am. Chem. Soc.* **1980**, *102*, 1340–1347.
- [45] G. Tóth, I. Pintér, A. Messmer, *Tetrahedron Lett.* **1974**, *15*, 735–738.
- [46] L. Cuesta, I. Maluenda, T. Soler, R. Navarro, E. P. Urriolabeitia, *Inorg. Chem.* **2011**, *50*, 37–45.
- [47] N. E. Meagher, D. B. Rorabacher, *J. Phys. Chem.* **1994**, *98*, 12590–12593.
- [48] R.G. Mortimer, *Physical Chemistry*, Elsevier, 3rd, **2008**.
- [49] K. J. Hall, T. I. Quickenden, D. W. Watts, *J. Chem. Educ.* **1976**, *53*, 493.
- [50] M. Ciaccia, S. Pilati, R. Cacciapaglia, L. Mandolini, S. D. Stefano, *Org. Biomol. Chem.* **2014**, *12*, 3282–3287.
- [51] E. H. Cordes, W. P. Jencks, *J. Am. Chem. Soc.* **1962**, *84*, 826–831.
- [52] C. F. Bernasconi, G. D. Leonarduzzi, *J. Am. Chem. Soc.* **1980**, *102*, 1361–1366.
- [53] R. A. McClelland, M. Coe, *J. Am. Chem. Soc.* **1983**, *105*, 2718–2725.
- [54] N. Wilhelms, S. Kulchat, J.-M. Lehn, *Helv. Chim. Acta* **2012**, *95*, 2635–2651.
- [55] T. Lemek, H. Mayr, *J. Org. Chem.* **2003**, *68*, 6880–6886.
- [56] F. Seeliger, S. T. A. Berger, G. Y. Remennikov, K. Polborn, H. Mayr, *J. Org. Chem.* **2007**, *72*, 9170–9180.

CHAPTER 3

Uncatalyzed C=C/C=N exchange Processes between Knoevenagel and Imine Compounds in Dynamic Covalent Chemistry



**Supramolecular
Organogel**



3.1 Introduction

Dynamic Covalent Chemistry (DCC)^[1] is the branch of Constitutional Dynamic Chemistry (CDC),^[2] resting on the implementation of reversible covalent reactions for the generation of dynamic covalent/combinatorial libraries (DCLs) of constituents from the reversibly connecting components. The implementation of DCLs requires fast conversion of components into equilibrated systems under mild conditions under which the equilibrium can be perturbed later by external stimuli (chemical or physical) to reorganize the system. In this way, the system is able to undergo adaptation to build up more complicated system.^[1,3,4]

Recently, among the reversible covalent reactions, the condensation between a carbonyl and an amine to form the imine bond (C=N) has been of much interest for DCC and materials science.^[5-11] Imines are formed readily and reversibly and they can also react with an introduced amine via a transimination process to give an amine-exchange product,^[12-14] as well as with another imine to undergo exchange of both amine and carbonyl compound pairs, the imine-exchange reaction.^[15-17] Furthermore, the condensation between an aldehyde or ketone and an active methylene compound to form a *Knoevenagel* compound (C=C) has also received considerable attention, especially concerning the derivatives of benzylidene barbituric acid.^[18] The benzylidene barbituric acids are defined by their strongly polarized exocyclic double bond with a positive partial charge on the arylidene carbon.^[19,20] They have been classified as electrically neutral organic Lewis acids^[21] because they are able to react with Lewis bases, for instance, alkoxides,^[22] amines,^[22-24] thiols,^[25] water,^[26,27] hydrogen sulfide ion,^[28,29] and carbon nucleophiles.^[30-33] They can be used as building blocks for the synthesis of pyrimidine derivatives^[34] and have also been used to trap radicals and as the stabilizers in PVC.^[35] The electrophilicity of 5-benzylidene-1,3-dimethylbarbituric acid and thiobarbituric acids has been recently quantified by Mayr *et al.*^[36] To further extend the scope of DCC, reactions based on dimethylbenzylidene-barbituric acid and imine compounds were exploited in the work described in this chapter.

Thus, investigation have been made of the generation of DCC processes based on the interconversion of constituents between C=C/C=N species in the absence of a catalyst. In addition, a theoretical study of the mechanism has been undertaken to try to understand the metathesis-like mechanism of C=C/C=N exchange and to draw comparisons with imine/imine (C=N/C=N) exchange^[16]. Finally, the production of organogels produced by

the exchange process between C=C/C=N substrates is also reported. All of the processes investigated here were followed by $^1\text{H-NMR}$ spectroscopy and the fractions of the different compounds in the DCLs were determined by signal integration.

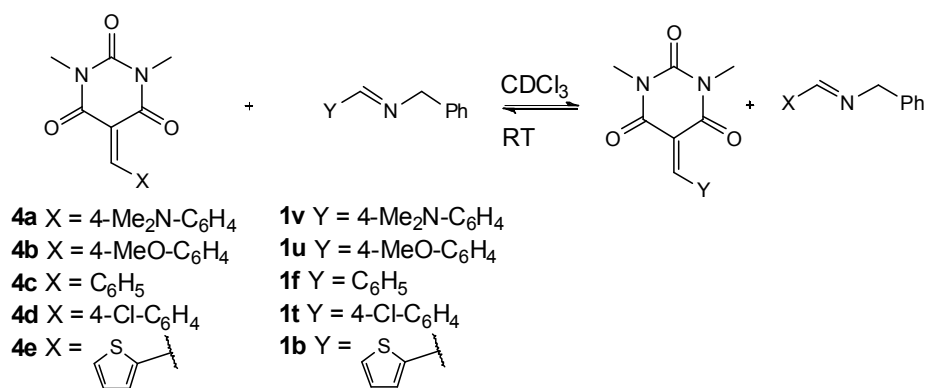
3.2 Results and Discussion

3.2.1 Benzylidene-(dm)barbiturates/imine, C=C/C=N, exchange processes.

In *Chapter 2*, the C=C/C=N interconversion implementing *Knoevenagel* compounds formed from barbituric acid (**2a-b**, **e-f**) to achieve the cross exchange in pure DMSO- d_6 using 10 mol% L-proline as an organocatalyst was described. Herein, these studies are extended to the manipulation of the C=C/C=N cross-exchange between *Knoevenagel* compounds derived from 1,3-dimethylbarbituric acid ((dm)barbituric acid) (**4a-4e**) and the same imines as in *Chapter 2*. The solubility of the *Knoevenagel* compounds was screened in different solvents and found in particular to be high in CDCl_3 . The cross-exchange reactions could therefore be carried out in CDCl_3 (filtered prior to use through a column of basic alumina to remove HCl and avoid acid-catalysis) with equimolar amounts of benzylidene-(dm)barbiturate derivatives and imine compounds (20 mM each). Both the forward and reverse reactions were followed by $^1\text{H-NMR}$ spectroscopy. In view of the fast rates of the exchange reactions, the rate constants could not be obtained by NMR but the equilibrium constants were determined instead, using the equation below, and are given in *Table 3.1*.

$$K_{\text{eq}} = [\mathbf{4x}][\mathbf{1y}]/[\mathbf{4y}][\mathbf{1x}] \quad (3.1)$$

In one of the initial C=C/C=N cross exchange experiments, **4a** and **1b** (*Table 3.1, Entry 1*), both bearing electron donating groups, were combined in CDCl_3 . After 68 min, no further change in the percentage of the exchange products **4e** and **1v** could be detected, indicating that equilibrium had been reached. When **4e** and **1v** were mixed under the same conditions, **4a** and **1b** were formed to give a mixture containing, after the same time, the same relative percentage of all four compounds, thus confirming that an effective thermodynamic equilibrium has been attained.



Scheme 3.1 Representation of the C=C/C=N cross-exchange reaction between benzylidene-(dm)barbiturate derivatives (**4a-e**) and various imines (**1b,f,t-v**) in CDCl₃ at room temperature.

Table 3.1 Proportions (%) of the different compounds in the C=C/C=N cross-exchange reactions between benzylidene-(dm)barbiturates and imines in CDCl₃ at room temperature. **a** = 4-dimethylaminobenzaldehyde, **b** = benzaldehyde, **c** = 4-nitrobenzaldehyde, **d** = 4-methoxybenzaldehyde, **e** = 2-thiophene carboxaldehyde.

Entry	Starting compounds	Reaction time ^{c)} [min]	Compound distribution [%]									K _{eq}	
			4a	1b	4e	1v	a	e	f	4b	1f		4c
1	4a + 1b	f ^{a)}	68	22	21	28	29	<1 ^{c)}	- ^{d)}	- ^{d)}	2.5		
	4e + 1v	r ^{b)}	69	18	17	33	32	<1 ^{c)}	- ^{d)}	- ^{d)}			
2	4b + 1f	f ^{a)}	2	13	14	37	36	<1 ^{c)}	<1 ^{c)}	- ^{d)}	7.3		
	4c + 1u	r ^{b)}	2	13	14	37	36	<1 ^{c)}	<1 ^{c)}	- ^{d)}			
3	4b + 1b	f ^{a)}	60	6	4	44	45	- ^{d)}	- ^{d)}	- ^{d)}	92.1		
	4e + 1u	r ^{b)}	13	5	4	46	45	<1 ^{c)}	- ^{d)}	- ^{d)}			
4	4b + 1v	f ^{a)}	11	9	7	43	42	<1 ^{c)}	- ^{d)}	- ^{d)}	30.4		
	4a + 1u	r ^{b)}	3	7	8	45	41	<1 ^{c)}	- ^{d)}	- ^{d)}			
5	4d + 1v	f ^{a)}	11	5	4	46	45	<1 ^{c)}	<1 ^{c)}	- ^{d)}	152.8		
	4a + 1t	r ^{b)}	3	3	3	47	47	- ^{d)}	- ^{d)}	- ^{d)}			
6	4d + 1u	f ^{a)}	3	14	14	37	35	<1 ^{c)}	<1 ^{c)}	- ^{d)}	7.3		
	4b + 1t	r ^{b)}	2	12	14	38	36	- ^{d)}	- ^{d)}	- ^{d)}			

^{a)} f, Forward reaction. ^{b)} r, Reverse reaction. ^{c)} Only traces of product detected. ^{d)} Compound not observed.
^{e)} Reaction time indicates the time when no further change (<1-2%) in composition could be observed.
 %-Compound distribution values measured 4-5 times and averaged (Standard deviation <2%).

The first set of experiments (*Entry 1, Table 3.1*) demonstrated that the interconversion of the *Knoevenagel* compound and an imine was facile and under thermodynamic control when the substrates both bore EDGs. We continued exploring the interconversion efficiency as a function of substrate electron affinity, choosing next compounds **4b**, bearing EDGs, and **1f**, bearing EWGs (*Table 3.1, Entry 2*). The interconversion products in CDCl₃, **4c** and **1u**, were formed immediately after mixing in a ratio that did not change after 2 min. In addition, the reverse reaction, determined by combining **4c** and **1u** under the same conditions, also furnished the products **4b** and **1f**. For this exchange, **4c** and **1u** were the more thermodynamically stable pair in these conditions. In this reaction, hydrolysis products were observed in trace amounts.

Next, we selected the substrates **4b** and **1b** for the forward reaction and combined **4e** and **1u** for the reverse one (*Table 3.1, Entry 3*). The electronic donating properties of the substituent on **4b** are expected to be weaker than those on **4a** (*Table 3.1, Entry 1*). The favored compounds at equilibrium were **4e** and **1u** as expected from the predicted electronic effects of the substituents. In this case, for both forward and reverse reactions, hydrolysis products formed in trace amounts.

The substrates for the next experiment were **4b** and **1v** for the forward and **4a** and **1u** for the reverse reaction (*Figure 3.1 and Table 3.1, Entry 4*). The forward and reverse reactions reached equilibrium after 11 min and 3 min, respectively. As compared to the reaction in *Entry 2*, **1v** has higher electron donating ability than **1f**; therefore the forward reaction in *Entry 4* was slightly slower than the one in *Entry 2*. Clearly the efficiency of *Knoevenagel*/imine exchange depends on the electronic affinity of both substrates.

In order to explore the exchange reaction between substrates of markedly different electron withdrawing ability, a mixture of **4d** and **1v**, bearing EWGs and EDGs respectively, was studied. Following mixing, the reaction again occurred immediately and reached equilibrium after 11 min, with only small amounts of the starting materials unreacted (about 3%). Conversely, the backward reaction was performed by combining **4a** and **1t**, giving **4d** and **1v** as the exchange products (3% each at equilibrium). Thus, the favored products at equilibrium were **4a** and **1t** for both the forward and backward reactions under these conditions.

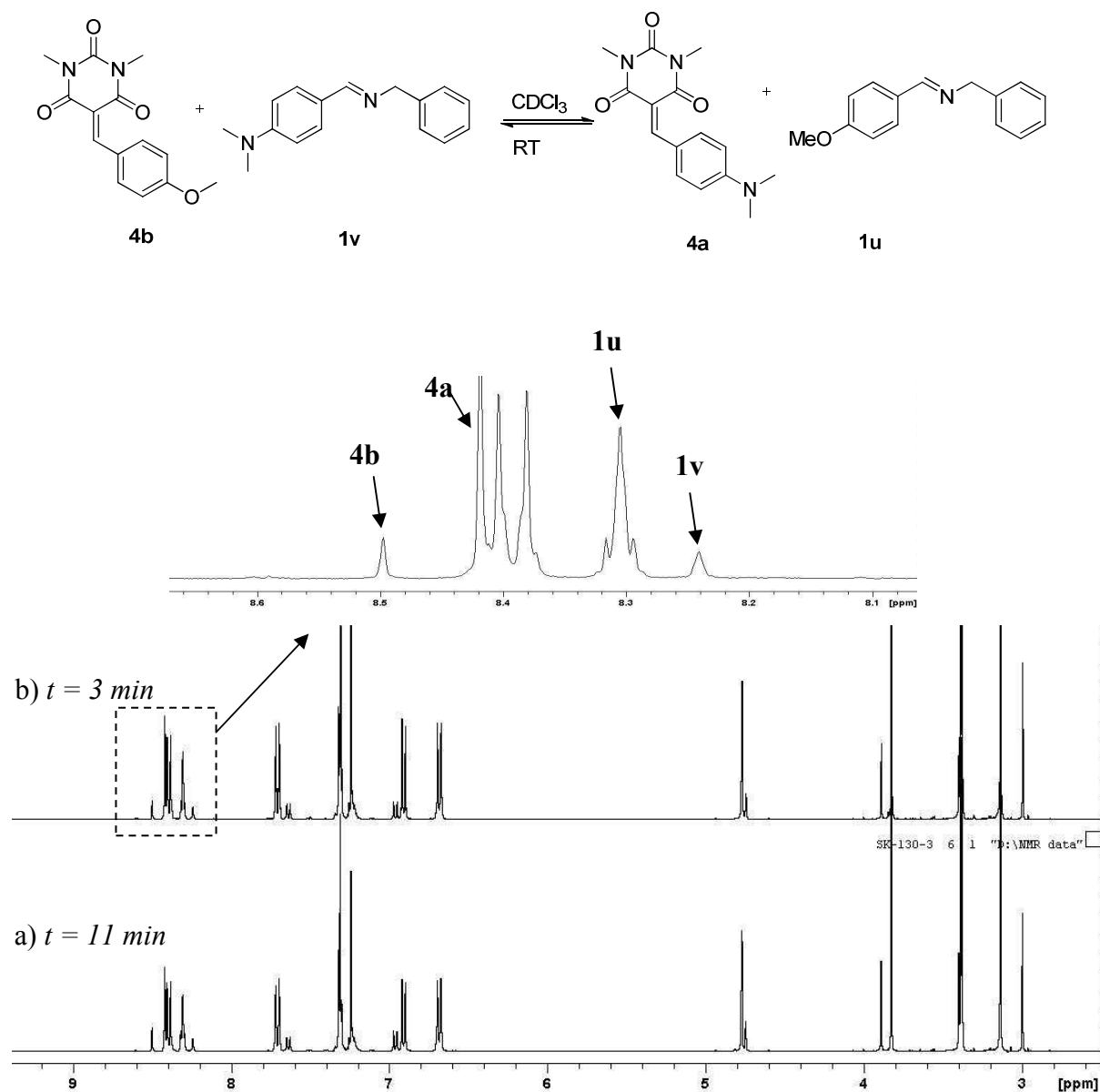


Figure 3.1 The $^1\text{H-NMR}$ spectrum of the exchange reaction at equilibrium between a) **4b** and **1v**, b) **4a** and **1u** CDCl_3 at room temperature.

Finally, the reaction of substrates **4d** and **1u** (Table 3.1, Entry 6) was examined, where **1u** has less electron donating ability than **1v** (Table 3.1, Entry 5). The formation of the products **4b** and **1t** was instantaneous. The reverse reaction was performed by mixing **4b** and **1t** which gave immediately **4d** and **1u**. Both the forward and reverse reactions gave the same mixture of the four constituents, indicating that thermodynamic equilibrium was reached immediately after mixing.

Another experiment was performed by using CD_2Cl_2 because this solvent contained less hydrochloric acid than CDCl_3 . The reaction between **4a** and **1b** was evaluated, giving **4e** and **1v** and reaching equilibrium after 30 minutes. In the reverse process, starting with **4e** and **1v**, compounds **4a** and **1b** were obtained, with equilibrium attained after 3 hours. To investigate the influence of the solvent, 1,2-dichlorobenzene- d_4 was selected for the same reaction as described above. The behavior of the **4a** and **1b** exchange reaction was similar to the one performed in CD_2Cl_2 .

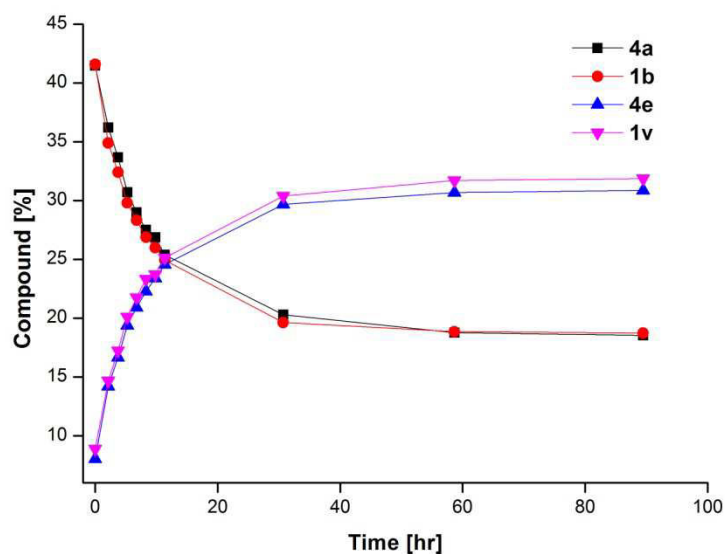
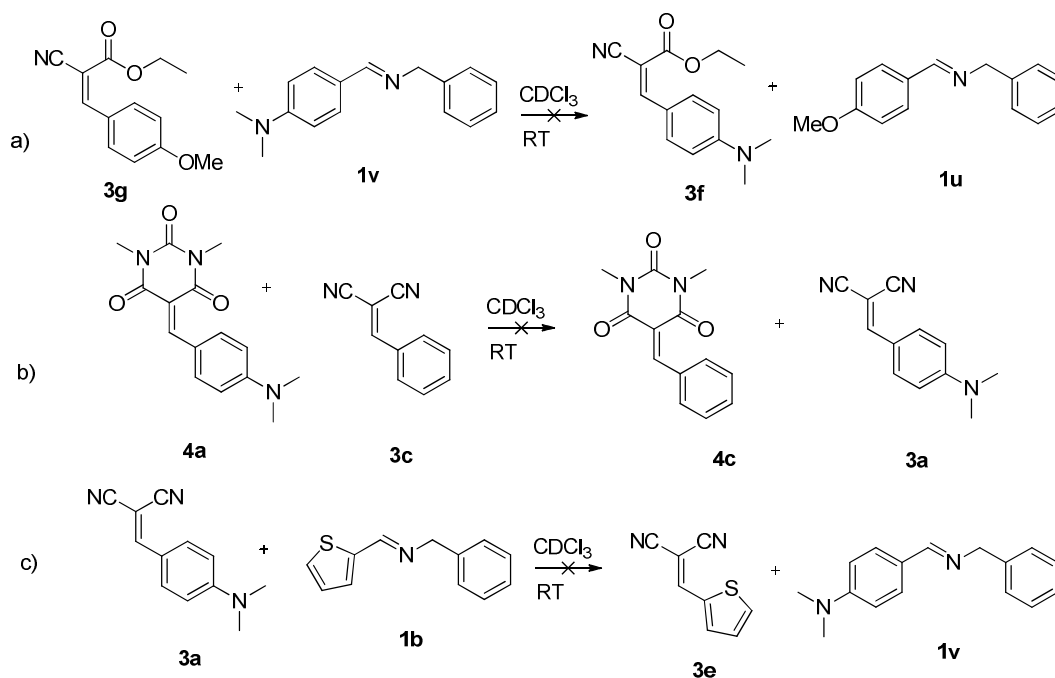


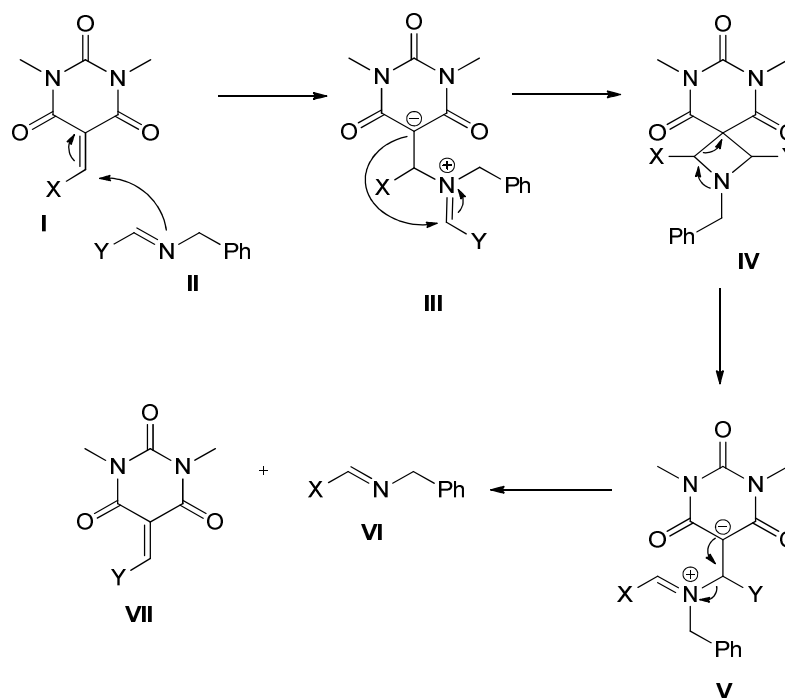
Figure 3.2 a) The exchange reaction between **4a** and **1b** giving the exchange product **4e** and **1v** in CD_2Cl_2 . Experiments were performed at room temperature.

Another benzylidene derivative was investigated by using benzylidene-ethyl cyanoacetate (**3g**) to exchange with **1v** in filtered CDCl_3 (Scheme 3.2a). The anticipated exchange products (**3f** and **1u**) were not formed. Next, the reaction between **4a** and **3c** was studied under the same conditions (Scheme 3.2b). The reaction did not afford the exchange products, even with piperidine added as a catalyst. However, when using a nucleophilic catalyst such as 10% n-propylamine, a trace amount (~2-3%) of exchange products was formed. Lastly, the exchange reaction between **3a** and **1b** was attempted (Scheme 3.2c), but again the exchange products could not be detected. All of the results mentioned above strongly suggest that 5-benzylidene-1,3-dimethylbarbituric acid (**4a-4e**) has a special characteristic (neutral Lewis acid) allowing it to undergo exchange reactions with some imine derivatives.



Scheme 3.2 The exchange reaction between a) **3g** and **1v** b) **4a** and **3b** c) **4a** and **3b** in CDCl_3 at room temperature. All of these reactions did not give the exchange products.

The cross-exchange reactions observed here may proceed in principle following two different mechanisms. A dissociation/recondensation process may well take place due to the presence of (unobservable) traces of water, similarly to the reaction scheme of the L-proline catalyzed reactions conducted in DMSO (*Scheme 2.9*). On the other hand, the very fast exchange observed in chloroform, where no aldehyde could be detected, would suggest a mechanism of metathesis type, whereby the benzylidene-(dm)barbiturate would function as a neutral organic Lewis acid while the imine would be able to act as neutral organic nucleophile. Such a metathesis-like mechanism of C=C/C=N interchange would involve the nucleophilic addition of the imine nitrogen at the CH end of (ring)C=CH-double bond of the benzylidene-(dm)barbiturate to form the benzylidene-(dm)barbiturate-iminium adduct **III**, followed by internal cyclization to a four-membered azetidine ring intermediate **IV**, which then could break up giving either the starting compounds back or the products **VII** and **VI**, resulting from the cross-exchange of the components as represented in *Scheme 3.3*. In a related fashion, the formation of a four-membered carbocyclic intermediate has been found to occur in organocatalysis of Michael addition reactions of aldehydes to nitro olefins,^[37, 38] and also in the interconversion of carbonyl compounds and iminium ion through 1,3-oxazetidinium ions.^[39]



Scheme 3.3 Possible metathesis-like mechanism of the cross-exchange between a Knoevenagel-type substrate (C=C) and an imine (C=N).

In summary, the interconversion between benzylidene-(dm)barbiturate and imine, depends on the attached aldehyde of both the benzylidene-(dm)barbiturate and the imine. The dimethyl barbituric acid acts as an electron withdrawing group, causing the benzylidene-(dm)barbiturate to be a push-pull molecule. The more favoured reactant compounds for the exchange reactions of C=C/C=N type are the benzylidene-(dm)barbiturates with an aldehyde containing an EDG moiety at the *para*-position and the imines with an aldehyde contained an EWG. Interestingly, this exchange reaction of C=C/C=N type between *Knoevenagel*-type compounds and imines in the absence of catalyst is not general and fails for other types of *Knoevenagel* compounds such as **3g** and **3a** with imines and also for C=C/C=C exchange with **4a** and **3c**. These results suggest that benzylidene-(dm)barbiturates have special characteristics in the presence of imines derived from benzylamine which leads to their efficient interconversion.

3.2.2 Theoretical Study of the Metathesis-like Mechanism of the Cross-Exchange between a Knoevenagel-Type Substrate (C=C) and an Imine (C=N).

In the previous section, the exchange reaction between benzylidene-(dm)barbiturates and imines involving fast exchange rate in the absence of catalyst was described. The proposed mechanism is shown in *Scheme 3.3* indicating that the exchange reaction between these two different substrates might occur via the metathesis-like mechanism to form an azetidine intermediate (**IV**), with the subsequent release of the exchange products is shown in *Scheme 3.3*. Herein, a computational study using the density-functional theory (DFT) method was carried out in order to assess the plausibility of the results obtained. The B3LYP functional in combination with the 6-31G* basis set were used throughout the calculations. In this investigation, starting materials (**4a** and **1b**) and the exchange products (**4e** + **1v**) were selected as an example model for the calculation. The result obtained from the calculation represents gas phase conditions.

In the work of Baik, the investigation of the acid catalysis of imine metathesis employing the DFT calculation method was carried out in analogy to that of olefin metathesis.^[16] The models for their calculation were imine metathesis of PhHC=NPr + PrN=CHPh (Pr = propyl) and the analogous reaction of *N*-aryl imine PhHC=NTol + TolHC=NPh (Tol = 4-methylphenyl). Their calculations revealed, in solution phase and in the absence of proton as a catalyst, activation free energies of 78.8 and 68.5 kcal/mol for the *N*-alkyl and *N*-aryl cases, respectively. This result indicated that replacing the =CR₂ functionality by =NR is not compatible with a [2+2] cyclization reaction in the solution phase due to the high activation energy. Importantly, protonation of one imine nitrogen lowered the transition state energy from ~70 kcal/mol to about ~25 kcal/mol. The relative energies of the four-membered ring intermediate of the [2+2] cyclization reaction, for both *N*-alkyl and *N*-aryl cases, were about 13 kcal/mol higher.

Accordingly, a similar approach to Baik's work was followed in terms of the C=C (*Knoevenagel* type compound) and CH=NR (imine compounds) functionality. Herein, the activation energy (transition state) of the reaction was not calculated. The geometry of the starting materials (**4a** and **1b**) and exchange products (**4e** and **1v**) were optimized by using DFT method with B3LYP/6-31G* (d, p) type wave functions. Also, the energy of the azetidine intermediate (**IV** from *Scheme 3.3*) was calculated by using the same method as for starting materials and products. The results are shown in *Table 3.2* and *Figure 3.3* and *3.4*.

Table 3.2 Optimization energy for the starting materials (**4a**, **1b**), exchange products (**4e**, **1v**), and intermediate **4a** + **1b** using the DFT (B3LYP/6-31G* (d, p)) method.

Entry	Compounds	Energy (a.u.)	Sum energy (a.u.) ^{a)}	Relative Energy (kcal/mol) ^{a,b)}
1	4a	-971.86202778		
2	1b	-916.84376413	-1888.70579 (S.M.)	$\Delta E_{I-S.M.} = +12.0$
3	4a + 1b (I)	-1888.68656230	-1888.68656230 (I)	$\Delta E_{P-I} = -10.8$
4	4e	-1158.63374140		
5	1v	-730.07016573	-1888.70391 (P)	$\Delta E_{P-S.M.} = -1.1$

^{a)} S.M.; Starting Material, I; Intermediate, P; Product. ^{b)} 1 a.u. = 627.5095388 kcal/mol

The optimized structures show a C=C bond length of 1.38 Å in **4a**, a C=N bond length of 1.28 Å in **1b**, a C=C bond length in **4e** of 1.38 Å, and a C=N bond length in **1v** of 1.28 Å. The structure for the four-membered intermediate, **IV**, shows an unsymmetrical four-membered ring with a C₁-C₂ bond length of 1.60 Å, a C₂-C₃ bond length of 1.61 Å, a C₃-N bond length of 1.48 Å and a N-C₁ bond length of 1.46 Å (*Figure 3.3*). Once the four-membered ring is formed, the C-C bond length elongates to 1.61 Å from 1.38 Å and one of the C-N bonds elongates to 1.48 Å from 1.38 Å. Furthermore, the four-membered ring shows an angle inside the ring between C₁-C₂-C₃ of 84.5°, C₂-C₃-N of 89.4°, C₃-N-C₁ of 94.6°, and N-C₁-C₂ of 88.3°, respectively.

The energy of adduct **IV** relative to the sum of the energies of the starting material is 12.0 kcal/mol, similar to the relative intermediate energy in the imine metathesis studied by Baik (~13 kcal/mol).^[16] Thus, the metathesis-like exchange mechanism between C=C/C=N is reasonable from an energetic perspective. Of course, that does not state anything about the kinetic feasibility. From this initial exploration, it is worth investigating the possible transition states (TS1 and TS2 in *Figure 3.3a*) of this metathesis-like exchange reaction in order to explain the mechanistic behavior.

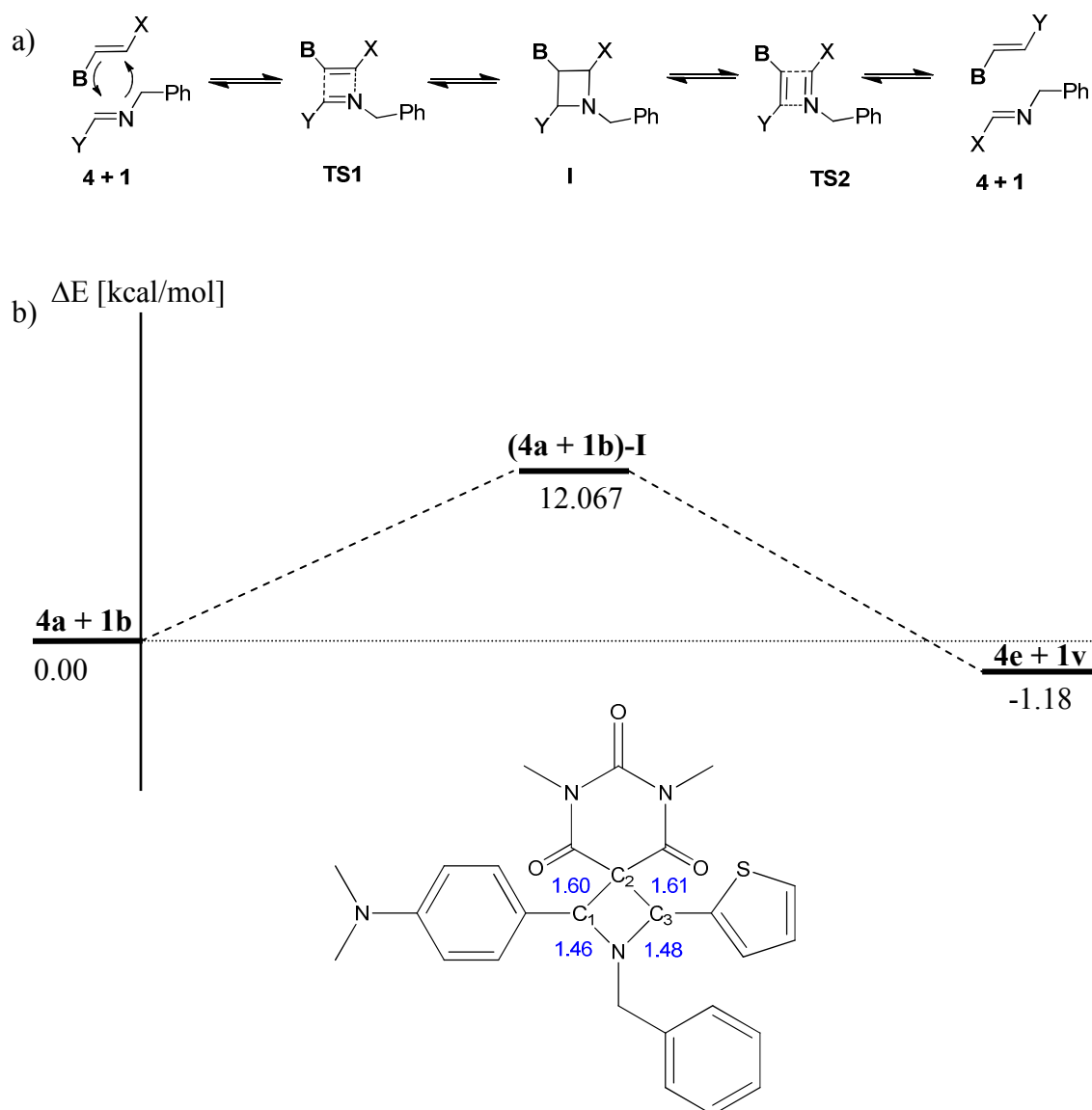


Figure 3.3 a) Representative of a possible intermediate in the exchange reaction of Knoevenagel-Type (C=C) and Imine (C=N) compounds, b) Relative energy of the starting materials ($4a + 1b$), products ($4e + 1v$) involved intermediate ($4a + 1b$)-I, obtained with the DFT (B3LYP/6-31G* (d,p)) method. The small numbers in blue next to bond are distances in Angstrom.

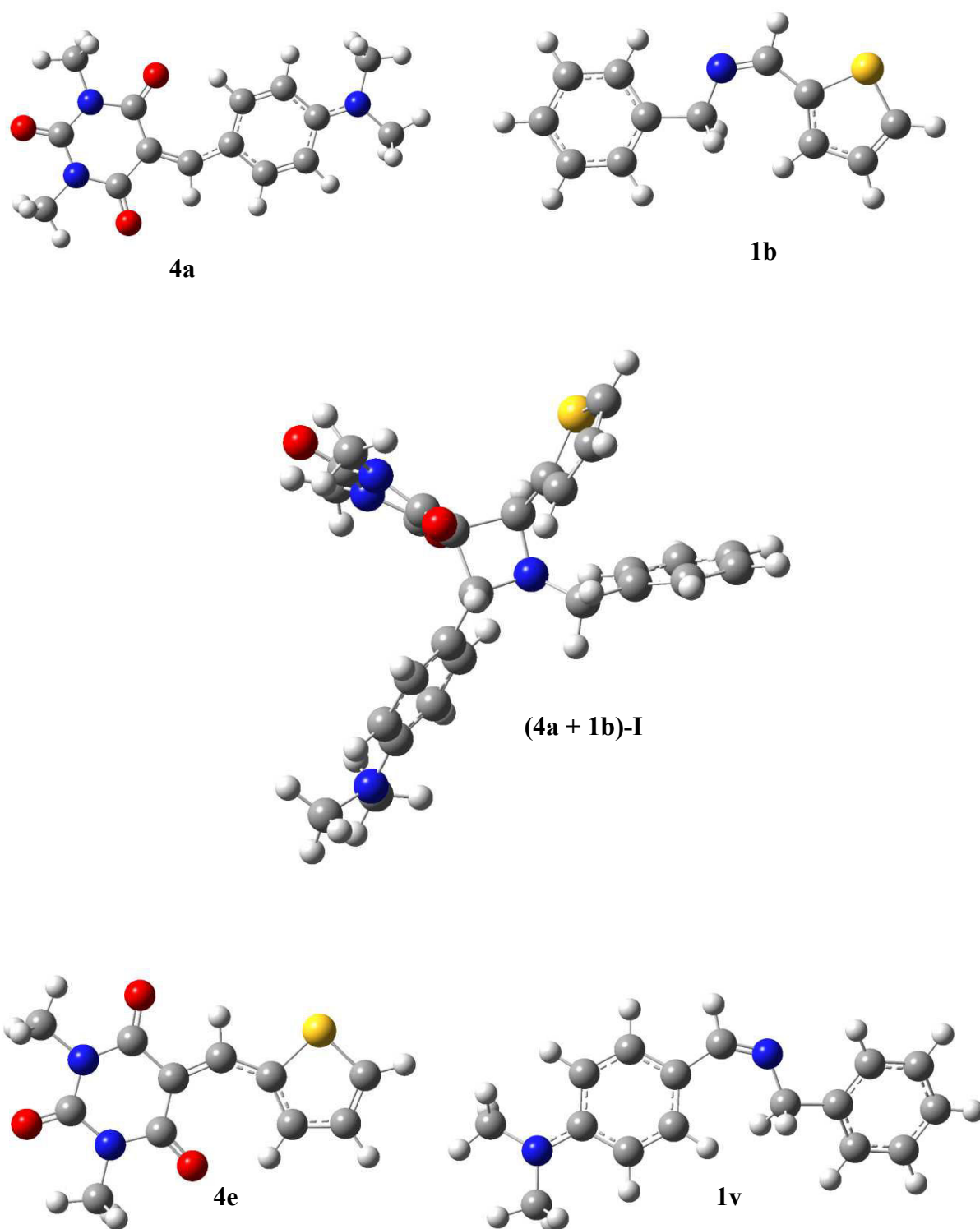


Figure 3.4 Optimized equilibrium geometry structures of the starting materials (**4a** and **1b**), products (**4e** and **1v**), and intermediates (**(4a + 1b)-I**), obtained with the DFT (B3LYP/6-31G* (d,p)) method.

3.2.3 Organogel selection based on the exchange reaction of C=C/C=N

Gels are soft materials and defined as substantially dilute cross-linked systems, which exhibit no flow in the steady state. This internal network structure may result from physical bonds (physical gel) or chemical bonds (chemical gel). A supramolecular gel is often composed of a low-molecular weight gelator (LMWGs) that can self-assemble in suitable conditions to form micro- or nano- scale networks, for instance, fibers, ribbons, sheets, or spheres. That structure then forms higher order three-dimensional networks.^[40] The self-assembly of LMWGs to form supramolecular gels is an important phenomenon that demonstrates the power of supramolecular chemistry in materials science,^[41–43] and also in drug delivery.^[44] However, gels have their own dynamic and reversible character due to the non-covalent interactions that define their structures, thus, they can respond sensitively to external stimuli (temperature, pH, solvent, light and redox reactions).^[40,45–48] Recently, organogels based on bismelamine-cyanurate/barbiturates were investigated using hydrogen-bonding interactions to form the gel in binary systems.^[49–51]

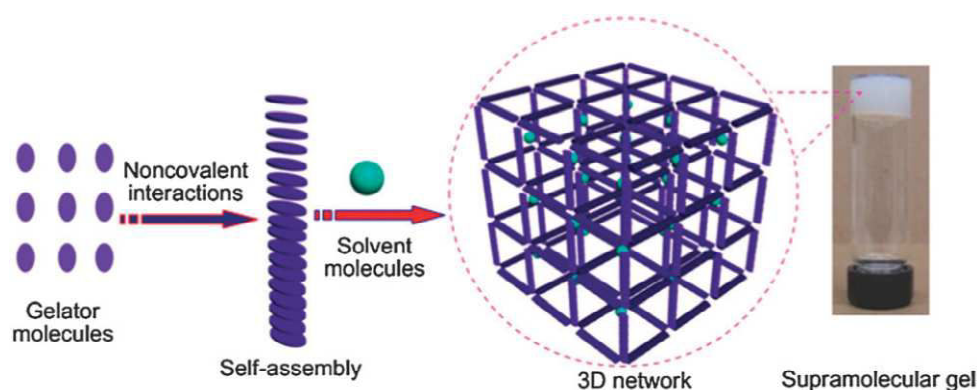
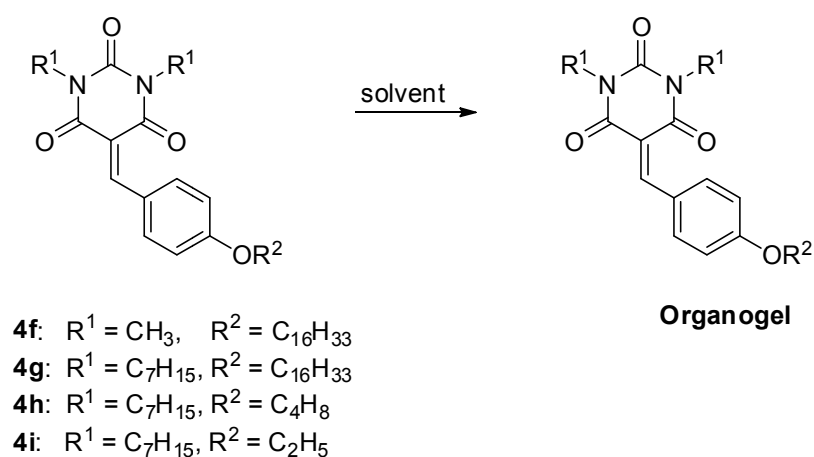


Figure 3.5 Representation of the formation of a supramolecular gel from a 3D network of self-assembled structures such as fibers, ribbons, sheets, and spheres.^[40] (Figure reproduced from reference [40])

Importantly, gel selection in a DCC system has been demonstrated using a hydrogel based on guanine-quartet formation to drive the selection of the components that form the constituent leading to the most stable gel in the system.^[52] Following DCC-based, gel selection, *Knoevenagel/imine* (C=C/C=N) exchange was examined in order to find appropriate components to select the most stable gel in the system.

Firstly, the benzylidene-barbiturates (**4f-4i**, Scheme 3.4) were synthesized by condensations between barbituric acid and aldehydes (see Chapter 7). Then, the gel formation ability of these compounds was evaluated in different solvents systems such as ethanol, methanol, cyclohexane, acetonitrile, and decanol. The result of the gel formation of **4g** (Table 3.3, Entry 2) is shown in Figure 3.6a, the gel of **4g** formed best in ethanol followed by acetonitrile (using 1% w/v of gelator in the solvent). In addition, the gel of **4g** was also observed under an optical microscope (Figure 3.6b) showing the cross-linking between gelator structures (fibers) in the system.



Scheme 3.4 Representation of the benzylidene barbiturate compounds (**4f-4i**) which were used in gel investigations.

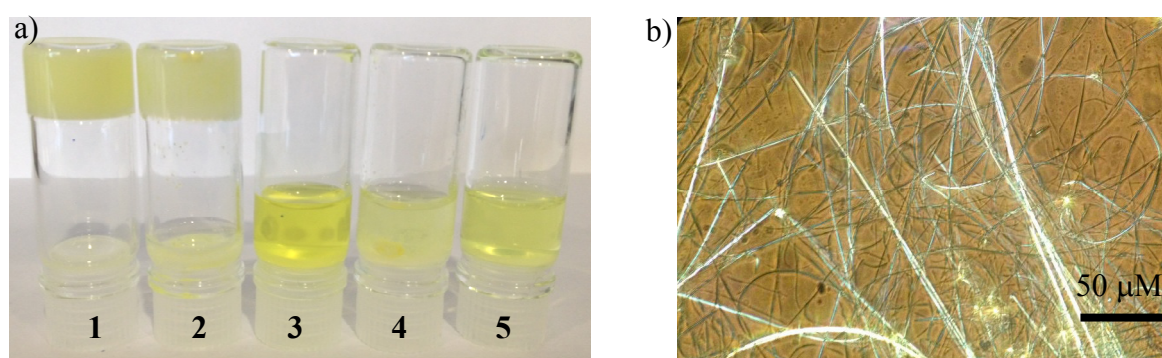


Figure 3.6 a) the gel formation ability of **4g** in different solvents, 1) EtOH, 2) CH_3CN , 3) Decanol, 4) MeOH, and 5) Cyclohexane. b) Observation of the gel formation of **4g** in EtOH by Optical Microscope.

Next, a gel formation study of **4h** was performed in the same range of solvents as used for **4g** (Figure 3.7, Table 3.3, Entry 3). The results showed that gel formation of **4h** occurs in ethanol and methanol but only partially in acetonitrile. A gel of **4h** could not be obtained in decanol and cyclohexane. Finally, the gel formation ability of **4i** was also studied in the same range of solvents (Table 3.3, Entry 4). A gel of **4i** formed fastest in MeOH followed by EtOH. In decanol, the gel also formed but at a very slow rate and in CH₃CN, a small amount of fiber formation was observed only. A gel of **4i** did not form in cyclohexane. Finally, a gel of **4f** was formed in EtOH, MeOH, and acetonitrile (Table 3.3, Entry 1).

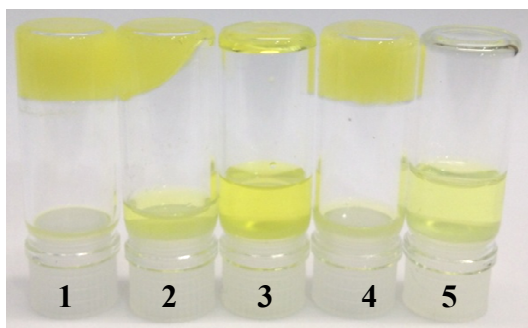


Figure 3.7 The gel formation ability of **4h** in different solvents in 1) EtOH, 2) CH₃CN, Decanol, MeOH, and Cyclohexane.

Thus, gel formation from *Knoevenagel* compounds such as **4h** and **4i** with a shorter carbon chain on the benzaldehyde moiety (-OR) occur quickly in MeOH. In contrast, with a longer carbon chain, gel formation formed fastest in ethanol. For all the derivatives investigated, no gel was formed in cyclohexane.

Table 3.3 Gelation properties of organogelators (**4f-4i**) at room temperature

Entry	Compounds ^{a)}	Solvents ^{b)}				
		EtOH	CH ₃ CN	Decanol	MeOH	Cyclohexane
1	4f	G	G	S	G	S
2	4g	G	G	S	P	S
3	4h	G	G	S	G	S
4	4i	G	F	G (slow)	G	S

^{a)} [Gelator] = 1 %w/v. ^{b)} G, gel; S, solution; P, precipitate; F, fiber.

Next, the exchange reaction in a benzylidene-barbiturate/imine (C=C/C=N) system was performed in CD₃CN/EtOH 9/1. The chosen starting substrates were **4b** and **1w** which could not form a gel in this solvent system although **1w** can form a crystalline precipitate. The reaction was left for 21 h at room temperature to ensure that the system reached equilibrium (Figure 3.8a). ¹H-NMR spectroscopy was used to characterize the gel selection from the exchange study (Figure 3.9). In the reaction mixture, the exchange reaction gave the compound distribution as **4b** (20%), **1w** (14%), **4f** (33%), and **1u** (33%) after 21 h. *T*_{gel} of the exchange reaction mixture was measured, and a value of 57°C was obtained.

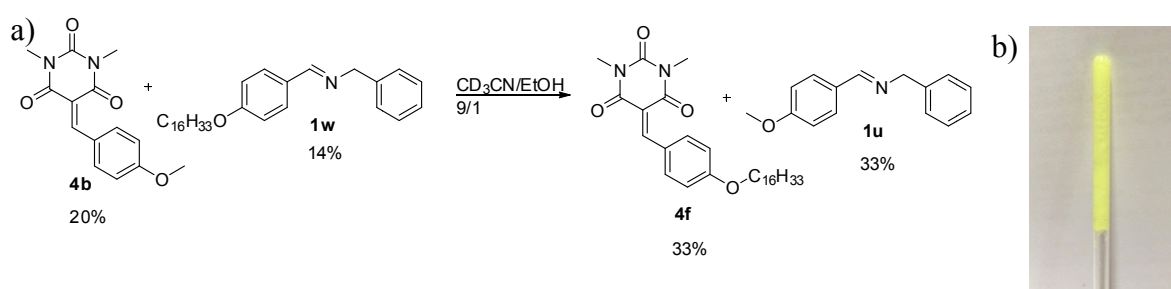


Figure 3.8 a) The exchange reaction C=C/C=N between **4b** and **1w** to give the exchange product **4f** and **1u** in CD₃CN/EtOH. b) The NMR tube of the mixture of exchange reaction between **4b** and **1w** after 21 h.

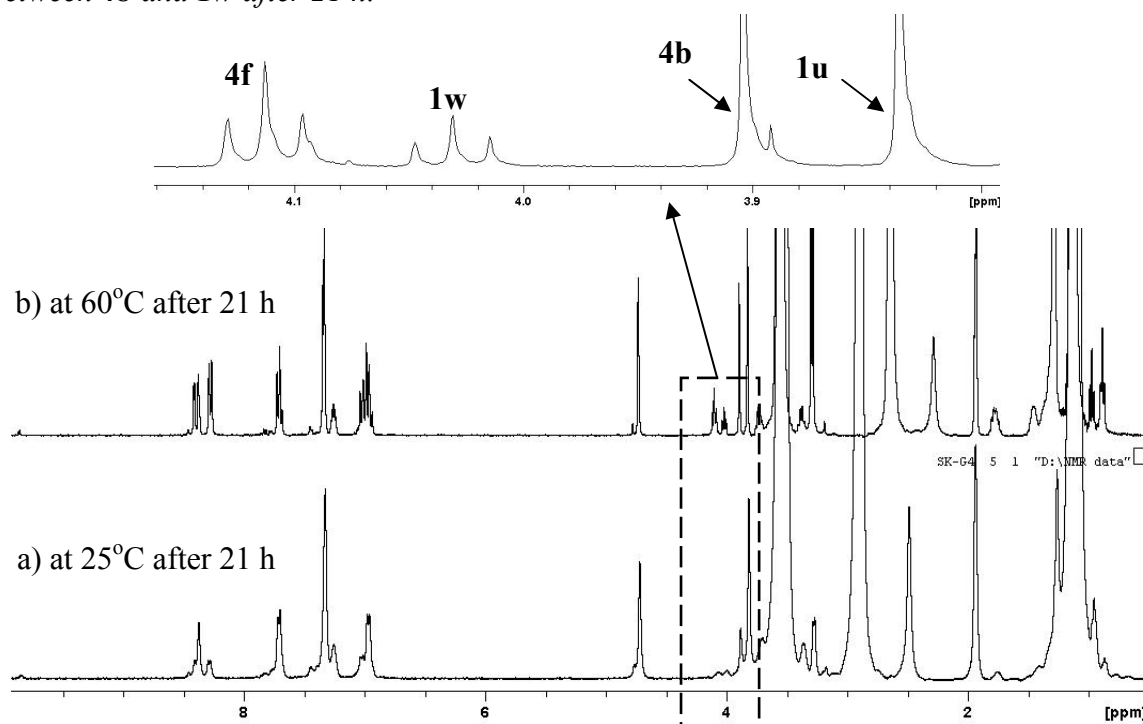


Figure 3.9 ¹H-NMR spectra of the exchange reaction a) measured at 25°C showing the broad peaks of **4f** and **1w**, b) measured at 60°C showing the sharp peaks of **4f** and **1w**.

Based on these preliminary results, more complex DCLs will be developed for gel selection from non-gel starting material. The discovery of new gels is important for materials science and drug delivery.

3.3 Conclusions

The results described above for the exchange reaction between C=C/C=N species lead to a number of conclusions:

1) The C=C/C=N exchange between imines and *Knoevenagel* derivatives of *N,N*-dimethylbarbiturate is fast and reversible in CDCl₃ solution at room temperature in the absence of catalyst. This feature provides access to efficient diversity generation via C=C/C=N exchange. It may also signify a change in mechanism to a metathesis-like process, via an azetidine intermediate.

2) The computational study suggested the metathesis-like mechanism of the exchange reaction between C=C/C=N component is reasonable at least on energetic grounds.

3) The gel formation investigation showed that the *Knoevenagel* compounds (**4f-4i**) were able to form a gel in an appropriate solvent. Moreover, the C=C/C=N exchange reaction could be applied to select for a gel.

The results described herein enable the creation of DCLs of higher chemical diversity, thus allowing for the generation by DCC of receptors, dynamic polymers or biomaterials of increased complexity.

3.4 References

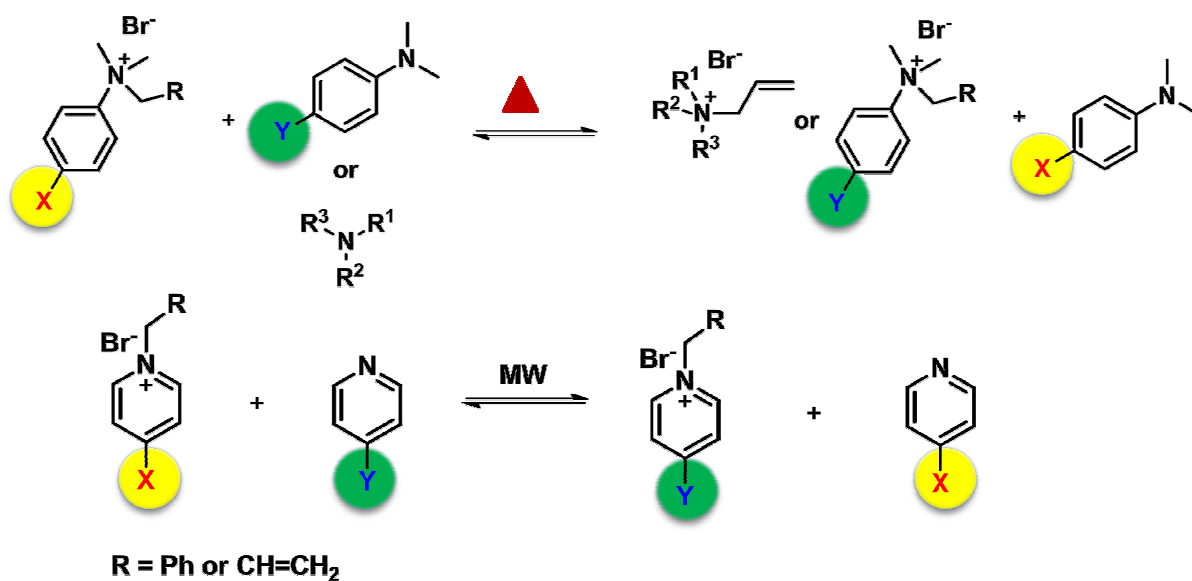
- [1] P. T. Corbett, J. Leclaire, L. Vial, K. R. West, J.-L. Wietor, J. K. M. Sanders, S. Otto, *Chem. Rev.* **2006**, *106*, 3652–3711.
- [2] J.-M. Lehn, *Chem. Soc. Rev.* **2007**, *36*, 151–160.
- [3] J.-M. Lehn, *Angew. Chem. Int. Ed.* **2013**, *52*, 2836–2850.
- [4] J.-M. Lehn, *Chem. – Eur. J.* **1999**, *5*, 2455–2463.
- [5] A. Ciesielski, M. El Garah, S. Haar, P. Kovaříček, J.-M. Lehn, P. Samorì, *Nat. Chem.* **2014**, *6*, 1017–1023.
- [6] D. Zhao, J. S. Moore, *J. Am. Chem. Soc.* **2002**, *124*, 9996–9997.
- [7] Z. Rodriguez-Docampo, S. Otto, *Chem. Commun.* **2008**, 5301–5303.
- [8] T. Aida, E. W. Meijer, S. I. Stupp, *Science* **2012**, *335*, 813–817.
- [9] J. B. Matson, S. I. Stupp, *Chem. Commun.* **2011**, *47*, 7962–7964.
- [10] E. Moulin, G. Cormos, N. Giuseppone, *Chem. Soc. Rev.* **2012**, *41*, 1031–1049.
- [11] Y. Jin, C. Yu, R. J. Denman, W. Zhang, *Chem. Soc. Rev.* **2013**, *42*, 6634–6654.
- [12] P. Kovaříček, J.-M. Lehn, *J. Am. Chem. Soc.* **2012**, *134*, 9446–9455.
- [13] M. Ciaccia, R. Cacciapaglia, P. Mencarelli, L. Mandolini, S. D. Stefano, *Chem. Sci.* **2013**, *4*, 2253–2261.
- [14] M. Ciaccia, S. Pilati, R. Cacciapaglia, L. Mandolini, S. D. Stefano, *Org. Biomol. Chem.* **2014**, *12*, 3282–3287.
- [15] N. Wilhelms, S. Kulchat, J.-M. Lehn, *Helv. Chim. Acta* **2012**, *95*, 2635–2651.
- [16] M. C. Burland, T. Y. Meyer, M.-H. Baik, *J. Org. Chem.* **2004**, *69*, 6173–6184.
- [17] M. Ciaccia, S. D. Stefano, *Org. Biomol. Chem.* **2014**, *13*, 646–654.
- [18] R. Menegatti, in *Green Chem. - Environ. Benign Approaches*, InTech Europe, **2012**, pp. 13 – 32.
- [19] Bednar, R., Polansky, O. E., Wolschann, P. Z., *Naturforsch., B: Chem. Sci.* **1975**, *30*, 582–586.
- [20] J. T. Bojarski, J. L. Mokrosz, H. J. Bartoń, M. H. Paluchowska, in *Adv. Heterocycl. Chem.* (Ed.: A.R. Katritzky), Academic Press, **1985**, *38*, 229–297.
- [21] Kunz, F. J., Margaretha, P., Polansky, O. E., *Chimia*, **1970**, *24*, 165–181.
- [22] Bednar, R., Haslinger, E., Herzig, U., Polansky, O. E., Wolschann, P., *Monatsh. Chem.*, **1976**, *107*, 1115–1125.
- [23] B. Schreiber, H. Martinek, P. Wolschann, P. Schuster, *J. Am. Chem. Soc.* **1979**, *101*, 4708–4713.

- [24] R. Cremlyn, J. P. Bassin, F. Ahmed, M. Hastings, I. Hunt, T. Mattu, *Phosphorus Sulfur Silicon Relat. Elem.* **1992**, *73*, 161–172.
- [25] A. R. Katritzky, I. Ghiviriga, D. C. Oniciu, F. Soti, *J. Heterocycl. Chem.* **1996**, *33*, 1927–1934.
- [26] Dyachkov, A. I., Ivin, B. A., Smorygo, N. A., Sochilin, E. G., *J. Org. Chem. USSR*, **1976**, *12*, 1124–1129.
- [27] Dyachkov, A. I., Ivin, B. A., Smorygo, N. A., Sochilin, E. G., *Zh. Org. Khim.* **1976**, *12*, 1115–1122.
- [28] Moskvina, A. V., Kulpina, G. V., Strelkova, L. F., Gindin, V. A., Ivin, B. A., *J. Org. Chem. USSR*, **1989**, *25*, 1995–2001.
- [29] Moskvina, A. V., Kulpina, G. V., Strelkova, L. F., Gindin, V. A., Ivin, B. A., *Zh. Org. Khim.*, **1989**, *25*, 2208–2216.
- [30] F. M. Soliman, K. M. Khalil, *Phosphorous Sulfur Relat. Elem.* **1987**, *29*, 165–167.
- [31] F. M. Soliman, M. M. Said, S. S. Maigali, *Heteroat. Chem.* **1997**, *8*, 157–164.
- [32] H. Allouchi, Y. Fellahi, C. Héabert, Y. Frangin, C. Courseille, *J. Heterocycl. Chem.* **2003**, *40*, 51–55.
- [33] Y. Frangin, C. Guimbal, F. Wissocq, H. Zamarlik, *Synthesis* **1986**, *1986*, 1046–1050.
- [34] H. S. Thokchom, A. D. Nongmeikapam, W. S. Laitonjam, *Can. J. Chem.* **2005**, *83*, 1056–1062.
- [35] M. W. Sabaa, N. A. Mohamed, K. D. Khalil, A. A. Yassin, *Polym. Degrad. Stab.* **2000**, *70*, 121–133.
- [36] F. Seeliger, S. T. A. Berger, G. Y. Remennikov, K. Polborn, H. Mayr, *J. Org. Chem.* **2007**, *72*, 9170–9180.
- [37] J. Burés, A. Armstrong, D. G. Blackmond, *J. Am. Chem. Soc.* **2012**, *134*, 6741–6750.
- [38] D. Seebach, X. Sun, C. Sparr, M.-O. Ebert, W. B. Schweizer, A. K. Beck, *Helv. Chim. Acta* **2012**, *95*, 1064–1078.
- [39] D. Seebach, T. Yoshinari, A. K. Beck, M.-O. Ebert, A. Castro-Alvarez, J. Vilarrasa, M. Reiher, *Helv. Chim. Acta* **2014**, *97*, 1177–1203.
- [40] G. Yu, X. Yan, C. Han, F. Huang, *Chem. Soc. Rev.* **2013**, *42*, 6697–6722.
- [41] P. Terech, R. G. Weiss, *Chem. Rev.* **1997**, *97*, 3133–3160.
- [42] D. J. Abdallah, R. G. Weiss, *Adv. Mater.* **2000**, *12*, 1237–1247.

- [43] J. H. van Esch, B. L. Feringa, *Angew. Chem. Int. Ed.* **2000**, *39*, 2263–2266.
- [44] A. Vintiloiu, J.-C. Leroux, *J. Controlled Release* **2008**, *125*, 179–192.
- [45] S. R. Haines, R. G. Harrison, *Chem. Commun.* **2002**, 2846–2847.
- [46] K. Tsuchiya, Y. Orihara, Y. Kondo, N. Yoshino, T. Ohkubo, H. Sakai, M. Abe, *J. Am. Chem. Soc.* **2004**, *126*, 12282–12283.
- [47] T. Ogoshi, Y. Takashima, H. Yamaguchi, A. Harada, *J. Am. Chem. Soc.* **2007**, *129*, 4878–4879.
- [48] A. R. Hirst, B. Escuder, J. F. Miravet, D. K. Smith, *Angew. Chem. Int. Ed.* **2008**, *47*, 8002–8018.
- [49] S. Yagai, M. Higashi, T. Karatsu, A. Kitamura, *Chem. Mater.* **2004**, *16*, 3582–3585.
- [50] S. Yagai, T. Karatsu, A. Kitamura, *Langmuir* **2005**, *21*, 11048–11052.
- [51] T. Seki, T. Karatsu, A. Kitamura, S. Yagai, *Polym. J.* **2012**, *44*, 600–606.
- [52] N. Sreenivasachary, J.-M. Lehn, *Proc. Natl. Acad. Sci.* **2005**, *102*, 5938–5943.

CHAPTER 4

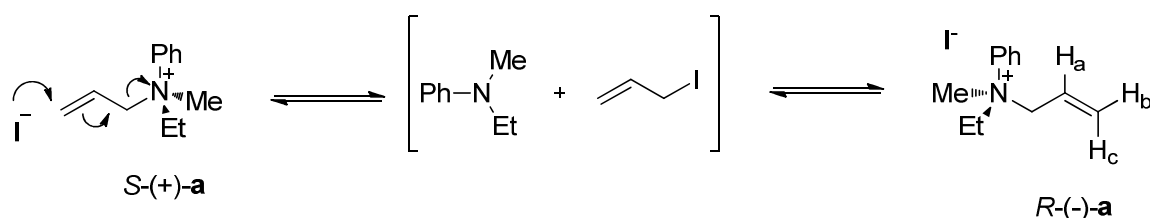
Dynamic Covalent Chemistry of Nucleophilic Substitution: Component Exchange of Quaternary Ammonium Salts



4.1 Introduction

Constitutional dynamic chemistry (CDC) and in particular on the molecular level, dynamic covalent chemistry (DCC) play an increasingly important role in diverse research fields.^[1-5] DCC is based on the implementation of rapid reversible covalent bond formation and breakage reactions to generate dynamic covalent libraries (DCLs) of molecular constituents interconverting through component exchange and that are in thermodynamic equilibrium.^[6,7] These libraries may contain the full set of constituents resulting from all possible combinations of the available components although they can remain virtual,^[6] depending on the reaction and the conditions. Representative examples of reversible reactions implemented in DCC by different research groups over the last decade comprise: amine/carbonyl condensation,^[8-11] disulfide exchange,^[12-14] olefin metathesis,^[15,16] imine exchange,^[17-19] *Knoevenagel*/imine exchange,^[17,20] *Knoevenagel*/*Knoevenagel* exchange,^[20] boronic ester formation,^[21,22] peptide exchange,^[23] and Diels-Alder condensation.^[24-27] CDC, both molecular and supramolecular, also provides new perspectives in areas such as materials science^[28-42] and drug design.^[43-50] To further extend the realm of DCC, there is a constant requirement for new reversible reactions to generate DCLs of increasing structural and chemical diversity and complexity.

More than a century ago, the first preparation and study of the chiral ammonium salt $[\text{Me}(\text{Et})\text{N}^+(\text{All})\text{Ph}]\text{I}\cdot\text{CHCl}_3$ (All = allyl, $\text{CH}_2\text{CH}=\text{CH}_2$) in 1903^[51] revealed the occurrence of racemisation by reversible dissociation into the amine and allyl halide. The rate of racemisation depended on the anion, decreasing in the sequence $\text{I} > \text{Br} > \text{Cl}$.^[51] Half a century later, in 1954 the spontaneous resolution of this salt was described and its chiroptical active properties were confirmed.^[52] Again about half a century later, solid state molecular structure of this salt was determined^[53] and its conglomerate formation features were investigated.^[54] Racemisation was proposed to occur via attack of the halide at the γ -position of the allyl group of the quaternary cation following what has been termed an $\text{S}_{\text{N}}2'$ mechanism (*Scheme 4.1*).^[53]



Scheme 4.1 Racemisation of the Wedekind-Fock-Havinga's salt (*S*-(+)-**a**) via an $\text{S}_{\text{N}}2'$ mechanism, as proposed by Kostyanovsky, where iodide attacks at the γ -carbon of the allyl group of the ammonium salt to give the inverting amine and allyliodide.^[53]

In recent times, chiral ammonium salts have been frequently used as catalysts in asymmetric synthesis,^[55–57] as ionic liquids,^[58–60] and in crystal engineering.^[61] Furthermore, the reaction of an ammonium cation such as *N*-benzyl-*N,N*-dimethylanilinium salt with nucleophilic carbanions^[62] and the reversibility of the nucleophilic reaction between benzyl bromide and *N,N*-dimethylaniline have been investigated.^[63] The long known reaction between tertiary amines or aza-aromatics (e.g. pyridine) and alkyl halides to give quaternary ammonium/pyridinium cations, the Menshutkin reaction,^[64–66] has been studied in detail in the case of reactions of pyridine with benzylic halides in a variety of molecular solvents and ionic liquids.^[67–69] In general, pyridinium salts are easily accessed and are versatile precursors to expanded nitrogen-containing heterocycles. They have been exploited for the total synthesis of natural products as well as in asymmetric or regioselective addition reactions.^[70–74]

In this chapter, the generation of dynamic covalent libraries based on nucleophilic substitution reactions is reported. More specifically, a study of new DCC processes involving the exchange of the tertiary amine component of quaternary ammonium salts based on S_N2' and S_N2 types of nucleophilic substitution reactions are presented (see *Scheme 4.3*). The ability of iodide to act as a nucleophile to catalyze the exchange between components is described. Iodide catalysis of such reactions has also been reported, for example, in the self-assembly of donor-acceptor[3]catenanes.^[75] Microwave heating irradiation was used to assist the exchange between pyridinium salts and pyridine derivatives. In addition, as some ammonium salts used in this study are ionic liquids,^[76] the generation of dynamic libraries in these ionic liquids as well as in their solutions in molecular solvents has been explored. All the processes investigated were followed by ¹H-NMR spectroscopy and the fractions of the different compounds in the DCLs were determined by signal integration.

4.2 Results and Discussion

4.2.1 Study of exchange processes between quaternary allyl-ammonium salts and tertiary amines via S_N2' type nucleophilic substitution.

Quaternary allyl ammonium salts are obtained by reaction of an allyl halide with a tertiary amine. Based on the work, mentioned above, on racemisation of optically active quaternary allyl-ammonium salts, the reversibility of the process is presumed to involve

the dissociation into tertiary amine and allyl halide via attack of the anion on the allyl double bond within the salt following an S_N2' mechanism (Scheme 4.1).^[53]

On the basis of this reversible reaction, we have generated dynamic covalent libraries based on quaternary allyl ammonium salts and tertiary amines. The capacity of various ammonium salts **1a-1e** or **3a-3e** (Figure 4.1) to undergo exchange with several aliphatic (**2a-e**) and *N,N*-dimethylaniline-type aromatic (**4a-e**) tertiary amines (Figure 4.2) was evaluated at 1/1 ratio in the absence or in the presence of iodide as nucleophilic catalyst in the form of tetraethyl- or tetrabutyl-ammonium iodide (TEAI or TBAI, respectively).

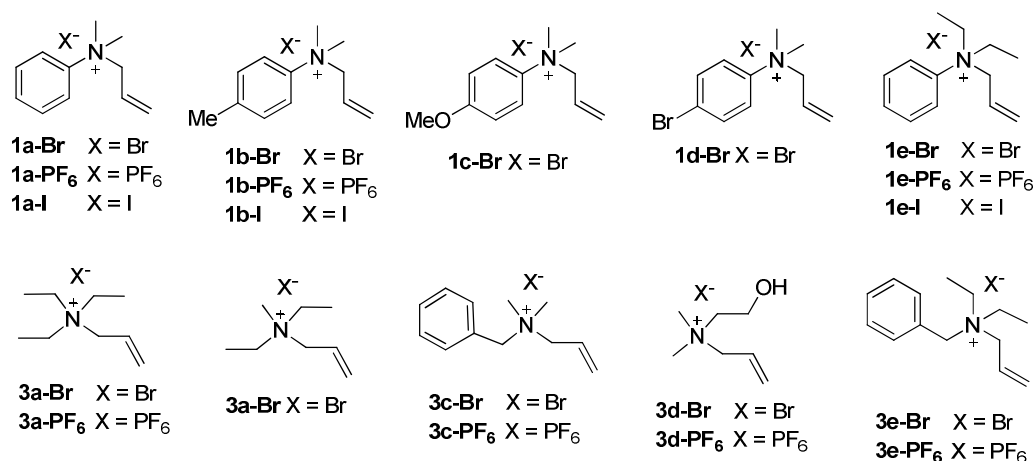


Figure 4.1 Structures of the quaternary allyl ammonium salts of aromatic (**1a-e**) and aliphatic (**3a-e**) types used in the present study.

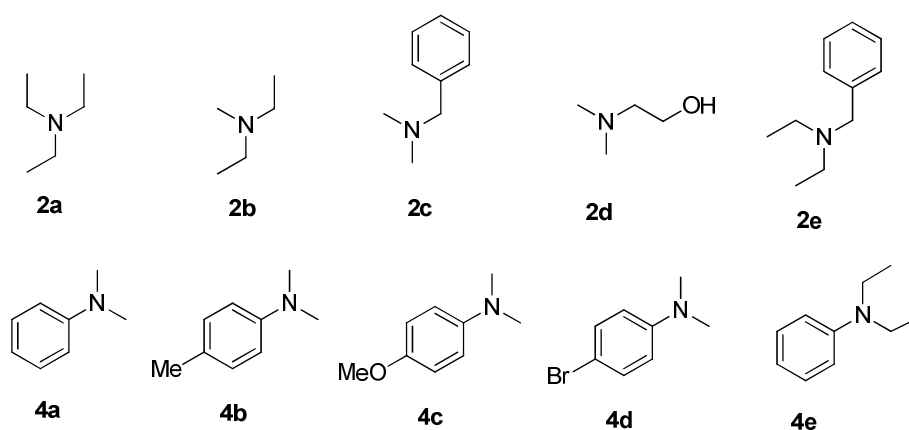


Figure 4.2 Structure of aliphatic (**2a-e**) and *N,N*-dimethylaniline-type aromatic (**4a-e**) tertiary amines used in the present study.

The exchange reaction between **1a-Br** and **2a** was used first to identify the best solvent out of CDCl_3 , $\text{DMSO-}d_6$, CD_3OD , CD_3CN , and $\text{CD}_3\text{CN}/\text{D}_2\text{O}$ 9/1 for reaction at 20 mM concentration. It was found to occur in all these solvents, as shown in *Table 4.1*. However, the best conditions were in CD_3CN at 60°C , for which the fastest rate of exchange to give **3a-Br** and **4a** was observed (*Table 4.1*, *Entries 5 and 6*).

This exchange is consistent with the reaction following either an $\text{S}_{\text{N}}2$ or an $\text{S}_{\text{N}}2'$ mechanism. The reaction also occurred in $\text{DMSO-}d_6$ but was slower than in CD_3CN , consistent with the fact that charge dispersal must occur in the transition state and thus is favoured in a solvent which is a poorer ion solvator. Also, the reactions which were performed in $\text{CD}_3\text{CN}/\text{D}_2\text{O}$ 9/1 containing 10% of polar protic solvent (D_2O ; the heavy water contains deuterons and not protons, but it would still be classified as a protic solvent), showed a slower rate of exchange than in CD_3CN . The reaction in a pure polar protic solvent (CD_3OD) was slow also. In addition to any influence it may have on transition state properties (see above), a protic solvent can strongly solvate nucleophiles through donor H-bonding, thus reducing their nucleophilicity.^[77] In the very weakly polar and poor H-bond donor solvent CDCl_3 , the reaction rate was the slowest observed.

In all reaction mixtures, a trace amount (~3%) of the amino-claisen product 2-allyl-*N,N*-dimethylaniline (**VIII**)^[78,79] was detected in the $^1\text{H-NMR}$ spectrum, which showed a characteristic peak at 3.93 ppm ($-\text{CH}_2\text{CH}=\text{CH}_2$), and was also apparent in the electrospray high resolution mass spectrum (peak at m/z 162.128 $[\text{M}+\text{H}]^+$).

The potential reverse reaction, that of **3a-Br** and **4a**, was investigated under various conditions (*Table 4.2*) but was not detectable even after 14 days. Thus, the reaction between **1a-Br** and **2a** appeared to be essentially irreversible. Another exchange was performed by mixing **1a-Br** and **2c** in CD_3CN at 60°C , yielding largely **3c** (43%) and **4a** (40%) (*Table 4.3*). The reaction between **1a-Br** and **2d** gave the exchange products **3d-Br** and **4a** after a few hours but this reaction also was irreversible.

Table 4.1 Optimization of conditions in the exchange reaction between **1a** and **2a**. In this table only the organic cation is indicated, all anions are bromide.

Entry	Cat./equiv	Solvent	T/°C	Time [days]	Compound Distribution [%] ^{a)}			
					1a	2a	3a	4a
1	-	CDCl ₃	rt	6	40	40	10	10
2	TEAI/1	CDCl ₃	rt	6	34	31	18	17
3	-	DMSO- <i>d</i> ₆	60	2	39	39	8	13
4	TEAI/1	DMSO- <i>d</i> ₆	60	2	32	32	14	21
5	-	CD ₃ CN	60	2	8	<1 ^{b)}	43	49
6	TEAI/1	CD ₃ CN	60	2	1	<1 ^{b)}	46	53
7	-	CD ₃ CN/D ₂ O (9/1)	60	11	41	37	11	11
8	TEAI/1	CD ₃ CN/D ₂ O (9/1)	60	11	17	17	34	33
9	-	MeOD	60	2	48	48	<1 ^{b)}	<1 ^{b)}
10	TEAI/1	MeOD	60	2	45	45	4	3

^{a)} Error on ¹H-NMR signal integration: ±4%. ^{b)} Only trace amount of compound was detected.

Table 4.2 Optimization of conditions in the exchange reaction between **3a** and **4a**. In this table only the organic cation is indicated, all anions are bromide.

Entry	Cat./equiv	Solvent	T/°C	Time [days]	Compound Distribution [%] ^{a)}			
					3a	4a	1a	2a
1	-	CDCl ₃	rt	8	50	50	- ^{b)}	- ^{b)}
2	TEAI/1	CDCl ₃	rt	8	50	50	- ^{b)}	- ^{b)}
3	-	CD ₃ CN	60	16	50	50	- ^{b)}	- ^{b)}
4	TEAI/1	CD ₃ CN	60	16	50	50	- ^{b)}	- ^{b)}
5	-	MeOD	rt	6	50	50	- ^{b)}	- ^{b)}
6	TEAI/1	MeOD	rt	6	50	50	- ^{b)}	- ^{b)}
7	TEAI/2	MeOD	rt	5	50	50	- ^{b)}	- ^{b)}
8	TEAI/4	MeOD	rt	5	50	50	- ^{b)}	- ^{b)}
9	-	DMSO- <i>d</i> ₆	60	10	50	50	- ^{b)}	- ^{b)}
10	TEAI/4	DMSO- <i>d</i> ₆	60	10	50	50	- ^{b)}	- ^{b)}

^{a)} Error on ¹H-NMR signal integration: ±4%. ^{b)} Compound not observed.

Table 4.3 Screening results of the S_N2' exchange reaction for various pairs under different conditions. In this table only the organic cation is indicated, all anions are bromide.

Entry	Reaction	Cat./equiv	Solvent	T/°C	Time [h]	Compound Distribution [%] ^{a)}			
						1a	2c	3c	4a
1	1a + 2c	-	CD ₃ CN	60	64	4	13	43	40
2	1a + 2c	TEAI/1	CD ₃ CN	60	64	1	16	43	41
3	3c + 4a	-	CD ₃ CN	60	72	3c	4a	1a	2c
4	3c + 4a	TEAI/1	CD ₃ CN	60	72	50	50	- ^{b)}	- ^{b)}
5	1a + 2d	-	CD ₃ CN	60	41	1a	2d	3d	4a
6	1a + 2d	TEAI/1	CD ₃ CN	60	41	8	21	37	34
7	3d + 4a	-	CD ₃ CN	60	41	6	12	42	40
8	3d + 4a	TEAI/1	CD ₃ CN	60	41	3d	4a	1a	2d
9	3d + 4a	-	CD ₃ CN	60	41	50	50	- ^{b)}	- ^{b)}
10	3d + 4a	TEAI/1	CD ₃ CN	60	41	50	50	- ^{b)}	- ^{b)}

^{a)} Error on ¹H-NMR signal integration: ±4%. ^{b)} Compound not observed.

In order to evaluate the scope of the exchange reactions of **1a-Br** and **1e-Br**, those with the aliphatic tertiary amines (**2a-2e**) were monitored by $^1\text{H-NMR}$ spectroscopy (Table 4.4). For each pair of the exchange reactions, only the reaction starting from **1a-Br** and **2a-2e** were followed, both without (in the absence of catalyst) or with added iodide (1 equiv.). Second-order rate constants for the forward reaction were estimated by treating the process as an irreversible second order reaction for the first 10% of conversion (see the experimental part, Chapter 7). The half-lives ($t_{1/2}$) of the reactions were determined by integration of the decreasing $^1\text{H-NMR}$ signals of the starting material as a function of time and analyzing by estimating the time at which starting material was reduced to 50%.

In all six cases, **1a-Br** and **1e-Br** underwent exchange with the aliphatic tertiary amines **2a-e** giving the products **3a-3e**, but the reverse reactions were not detectable, indicating that the reaction was completely in favour of the products, with the equilibrium being strongly shifted towards the formation of the aliphatic allyl ammonium product. The addition of iodide (1 equiv. TEAI) resulted in an acceleration of up to ca. 2-fold (Figure 4.3).

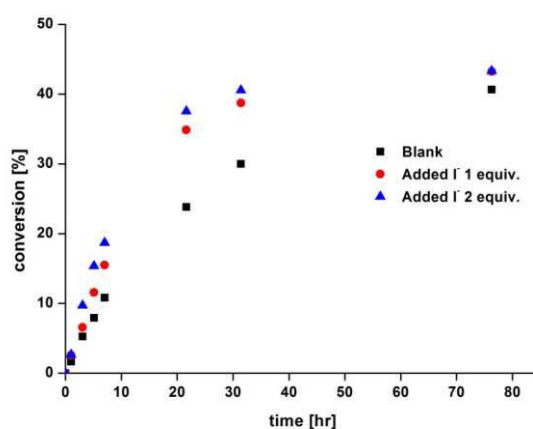


Figure 4.3. Effect of the addition of iodide anion on the nucleophilic substitution exchange reaction between **1a** and **2c** in CD_3CN at 60°C . Tetraethylammonium iodide (TEAI) was used as iodide source (1 equiv.)

Attempts to observe an exchange reaction between **3c-Br** and **2a** or its formal reverse as the reaction between **3a-Br** and **2c** were unsuccessful in that no reaction in either sense was detectable over 3 days in CD_3CN at 60°C . This indicated that any reaction between a quaternary aliphatic ammonium salt and a tertiary amine must be extremely slow.

Table 4.4 Kinetic and thermodynamic parameters for the exchange reaction between the *N*-allyl-*N,N*-dimethyl-anilinium salt **1a-Br** and **1e-Br** and the aliphatic tertiary amines **2a-2e** 1/1 each at 20 mM concentration in CD₃CN at 60°C. Half-life $t_{1/2}$. Proportion (%) of the different compounds. **a** = allyl bromide, **b** = allyl iodide, **c** = amino-Claisen rearrangement product. In this table only the organic cation is indicated, all anions are bromide.

Entry	Starting compound	a)	Compound distribution [%] ^{b)}							k [x10 ⁻³ M ⁻¹ s ⁻¹]	$t_{1/2}$ [h]
			1a	2a	3a	4a	a	b	c		
1	1a + 2a	f_b	<1	<1	44	44	3	n.a. ^{c)}	8	0.622	16
		f_c	<1	<1	47	48	1	<1	3	1.070	12
2	1a + 2b	f_b	2	<1	44	44	4	n.a. ^{c)}	4	0.530	18
		f_c	7	<1	44	44	2	<1	3	0.892	13
3	1a + 2c	f_b	5	<1	48	44	- ^{d)}	n.a. ^{c)}	3	0.779	14
		f_c	6	<1	47	44	- ^{d)}	- ^{d)}	2	1.353	8
4	1a + 2d	f_b	7	<1	47	46	- ^{d)}	n.a. ^{c)}	<1	0.672	16
		f_c	4	<1	49	47	- ^{d)}	- ^{d)}	<1	1.180	13
5	1a + 2e	f_b	12	12	30	35	8	n.a. ^{d)}	4	0.729	20
		f_c	9	5	37	39	5	<1	5	1.203	12
6	1e + 2e	f_b	5	16	28	43	8	n.a. ^{d)}	<1	0.056	24
		f_c	4	14	31	43	7	2	<1	0.084	18

^{a)} f_b , forward reaction in the absence of catalyst; f_c , forward reaction in the presence of TEAI (1 equiv.) as catalyst. ^{b)} Error on ¹H-NMR signal integration: ±4%. ^{c)} n.a., not applicable. ^{d)} Compound not observed.

As seen above, *N*-allyl-*N,N*-dimethylanilinium bromide (**1a-Br**) did exchange with aliphatic tertiary amines but these reactions were irreversible. Consequently, it appeared that in order to achieve reversibility, it would be necessary to perform the exchange reactions between aromatic partners. To this end, the reactions of *N*-allyl-*N,N*-dimethylanilinium bromide (**1a-Br**) with *N,N*-dimethylaniline-type aromatic tertiary amines (**4a-e**) were investigated in CD₃CN at 60°C at 1/1 ratio and 60 mM final concentration with TBAI (60 mM) as catalyst (in the earlier study the final concentration for exchange between **1a-Br** and aliphatic tertiary amines was 20 mM, but the exchange reactions of **1a-Br** with aromatic tertiary amines were performed at 60 mM to attain a more convenient rate of reaction). It was found that the exchange between **1a-Br** and the aromatic tertiary amines was now indeed reversible.

For all of the exchange processes of allyl-*N,N*-anilinium salts (**1a-1f**) and the *N,N*-dimethylaniline-type aromatic tertiary amines (**4a-4e**), the second-order rate constants for both forward and reverse reactions were estimated by treating the process as an irreversible second order reaction for the first 10% of conversion (*see experimental part, Chapter 7*). The half-lives ($t_{1/2}$) of the reactions were determined by integration of the decreasing $^1\text{H-NMR}$ signals of the starting material as a function of time and taken to be the time at which the starting material was reduced to 50% with respect to the equilibrium value. No special significance is given to the half-lives measured in this way; they are simply a convenient way to compare the rates of several reactions. In addition, the equilibrium constants for the exchange processes were calculated from the product distributions in the cases where equilibrium had been reached (*see experimental part*).

The results, compound distributions, rate constants of the exchange reactions, and equilibrium constants are listed in *Table 4.5*. The distributions were the same for both forward and reverse reactions, indicating that thermodynamic equilibrium had been reached. Furthermore, the reactions were accelerated by a factor of about 1.5-2 on addition of an equimolar amount of iodide (TBAI) as nucleophilic catalyst.

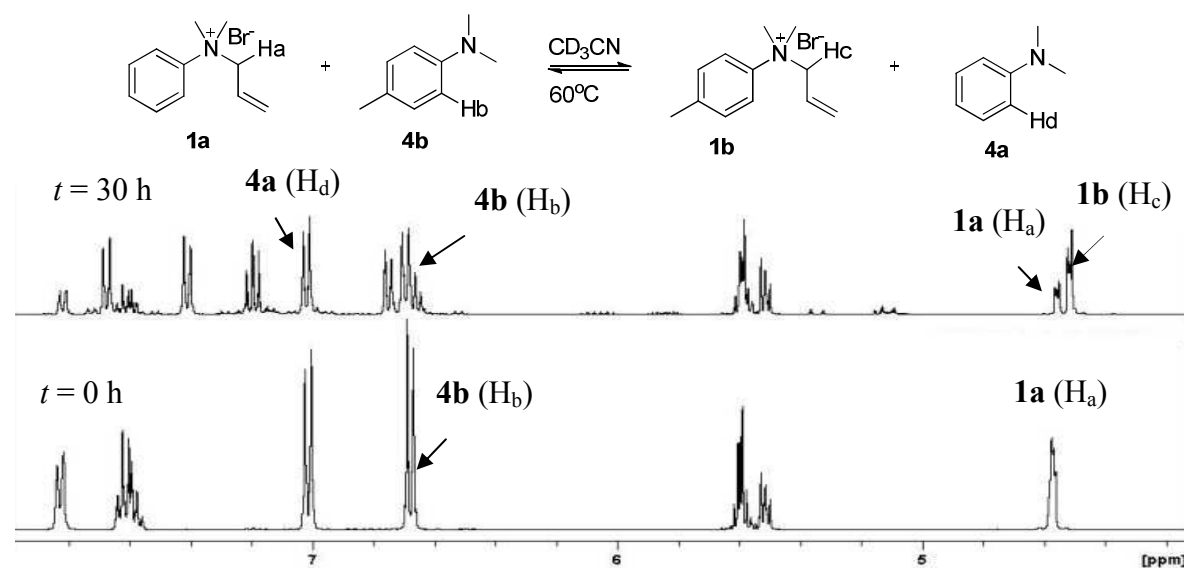


Figure 4.4 $^1\text{H-NMR}$ study of the nucleophilic substitution exchange of *N*-allyl-*N,N*-dimethylanilinium bromide (**1a-Br**) and 4-*N,N*-trimethylaniline (**4b**) by observation of the signals of the aromatic H_d and H_b proton (**4a** and **4b**) and the α - CH_2 -proton signal of the allyl group (**1a-Br** and **1b-Br**), before (bottom, $t = 0$ h) and after (top, $t = 30$ h) exchange at equilibrium.

Table 4.5 Kinetic and thermodynamic parameters for the exchange reaction between the *N*-allyl-*N,N*-anilinium salts **1a-1e** and the *N,N*-dimethylaniline-type aromatic tertiary amines **4a-4e** in 1/1 ratio at 60 mM concentration in CD₃CN at 60°C. Half-life $t_{1/2}$. Proportion (%) of the different compounds. **a** = allyl bromide, **b** = allyl iodide, **c** and **d** = amino-Claisen rearrangement products. In this table only the organic cation is indicated, all anions are bromide except entries 5 and 6 where the anions are iodides.

Entry	Starting compound	a)	Compound distribution [%] ^{b)}							k [$\times 10^{-3}$ M ⁻¹ s ⁻¹]	$t_{1/2}$ [h]	K_b ^{c)}	K_c ^{d)}	
			1a	4b	1b	4a	a	b	c					d
1	1a + 4b	f_b	13	19	28	29	4	n.a. ^{e)}	4	3	0.252	11	4.5	4.9
		f_c	13	18	29	33	3	1	2	1	0.516	6		
	1b + 4a	r_b	10	16	25	40	4	n.a. ^{e)}	2	3	0.177	9		
		r_c	11	15	25	40	3	1	1	3	0.283	4		
2	1a + 4c	f_b	9	13	36	35	3	n.a. ^{e)}	4	- ^{f)}	0.353	10	14.2	12.9
		f_c	10	14	36	35	2	<1	2	- ^{f)}	0.598	6		
	1c + 4a	r_b	8	10	39	39	3	n.a. ^{e)}	2	- ^{f)}	0.089	13		
		r_c	8	9	39	39	2	<1	2	- ^{f)}	0.097	8		
3	1e + 4a	f_b	6	27	19	34	10	n.a. ^{e)}	2	2	0.266	13	10.7	10.8
		f_c	5	22	22	37	9	2	1	2	0.522	10		
	1a + 4e	r_b	2	19	20	42	13	n.a. ^{e)}	- ^{e)}	4	0.372	6		
		r_c	3	18	22	42	10	<1	2	3	0.501	3		
4	1e + 4b	f_b	6	15	28	40	7	n.a. ^{e)}	3	1	0.217	14	22.3	26.1
		f_c	6	14	31	40	4	1	3	1	0.358	9		
	1b + 4e	r_b	2	12	28	46	8	n.a. ^{e)}	2	2	0.244	5		
		r_c	2	11	29	47	6	1	3	1	0.236	2		
5	Anion I ⁻		1e	4b	1b	4e	a	b	c	d				
	1e + 4b	f_b	4	9	34	45	n.a. ^{e)}	3	2	3	0.385	11	46.2	
	1b + 4e	r_b	4	7	31	46	n.a. ^{e)}	3	5	4	0.155	10		
6	Anion I ⁻		1a	4b	1b	4a	a	b	c	d				
	1a + 4b	f_b	13	21	33	29	n.a. ^{e)}	3	1	- ^{f)}	0.483	6	4.2	
	1b + 4a	r_b	14	15	30	36	n.a. ^{e)}	2	3	- ^{f)}	0.234	6		
7	1d + 4a	f_b	No Reaction											
		f_c	No Reaction											

^{a)} f_b , forward reaction in the absence of catalyst; f_c , forward reaction in the presence of TBAI (60 mM.) as catalyst; r_b , Reverse reaction in the absence of catalyst; r_c , Reverse reaction in the presence of TBAI (60 mM) as catalyst. ^{b)} Error in ¹H-NMR signal integration: $\pm 4\%$. ^{c)} K_b , Equilibrium constant of the uncatalyzed. ^{d)} K_c , Equilibrium constant of the catalyzed reaction. ^{e)} n.a., not applicable. ^{f)} Compound not observed.

When *N*-allyl-4-bromo-*N,N*-dimethylanilinium bromide (**1d-Br**) was combined with *N,N*-dimethylaniline (**4a**) or, in reverse, *N*-allyl-*N,N*-dimethylanilinium bromide (**1a-Br**) combined with 4-bromo-*N,N*-dimethylaniline (**4d**), no reaction was observed in either case other than a very slow decomposition to unidentifiable materials. Thus, neither bromide ion catalysis nor direct attack of the aromatic amines seemed to be effective in these cases.

Exchange was observed in the cases of **1e-Br**+**4a** and **1e-Br**+**4b**, and marked line broadening was observed for the aromatic $^1\text{H-NMR}$ signals of liberated diethyl aniline both in the presence and absence of iodide ion (Figures 4.5 and 4.6). It may be due to the formation of the radical cation of free diethyl aniline by oxidation in the conditions of the experiments. When the corresponding iodide **1e-I** was used in the exchange reaction with **4b** (Table 2, Entry 5), no such line broadening of liberated diethyl aniline was observed (Figure 4.7). This suggested that in addition to the faster reaction of iodide ion at the γ -position of the allyl group of **1e-I**, compared to bromide in **1e-Br**, if the radical species of diethyl aniline was generated, it might be reduced by iodide ion (the yellow colour of the solution was observed).

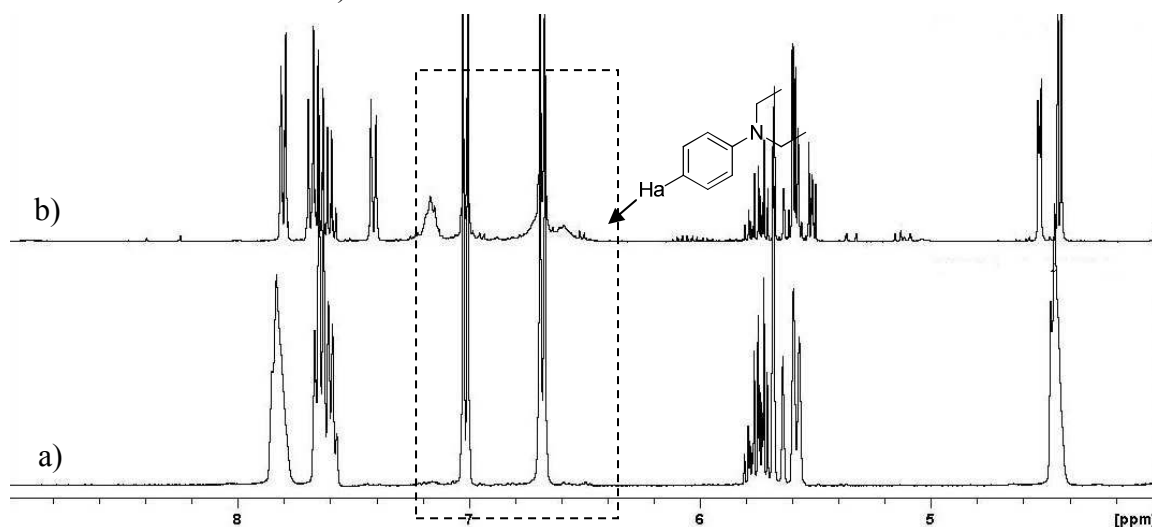


Figure 4.5. $^1\text{H-NMR}$ spectra for the exchange reaction between **1e-Br** and **4b** in CD_3CN at 60°C a) after mixing. b) at 41 h demonstrating the line broadening peak of liberated diethylaniline.

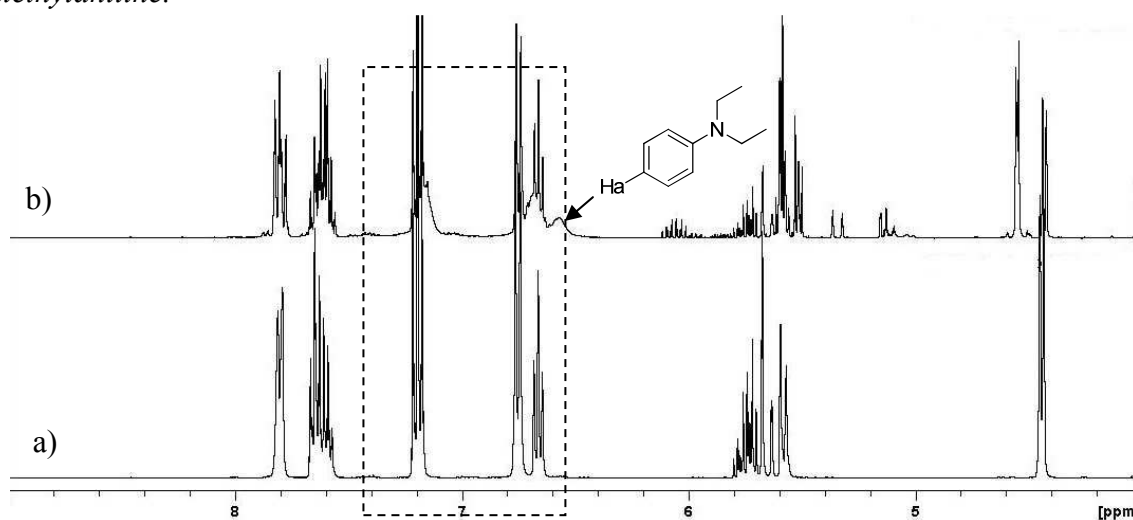


Figure 4.6. $^1\text{H-NMR}$ spectra for the exchange reaction between **1e-Br** and **4a** in CD_3CN at 60°C a) after mixing b) at 50 h demonstrating the line broadened peaks of liberated diethylaniline.

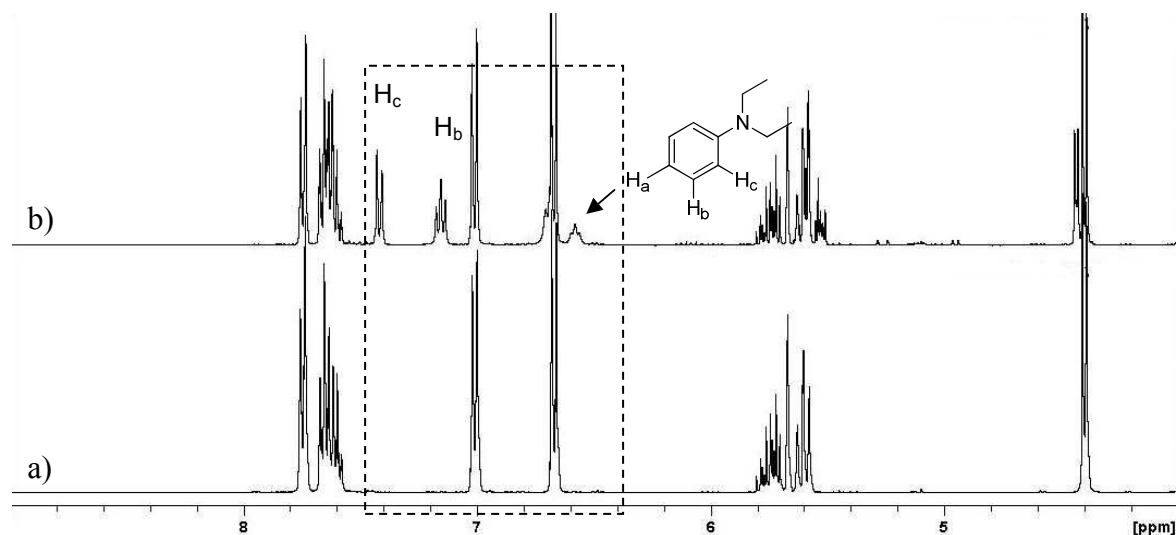


Figure 4.7 ¹H-NMR spectra for the exchange reaction between **1e-I** and **4b** in CD₃CN at 60°C a) after mixing. b) at 8 h demonstrating the sharp peak of liberated diethylaniline.

In addition, the dissociation of **1a-Br** was studied by dissolving **1a-Br** in CD₃CN at 60°C (Figure 4.8). Again the broadening of the aromatic proton signals of liberated dimethyl aniline was observed and assumed to be due to the formation of its radical. The electronic absorption spectrum of this reaction mixture (Figure 4.9) also provided evidence that the radical of dimethyl aniline^[80] was generated under these conditions. Next, the dissociation of **1a-Br** was examined in the presence of iodide ion (Figure 4.10). The line broadening of the free dimethylaniline signals appeared after 2 h and disappeared after 43 h. Taken together, these results support the conclusion that the radical cation of dimethyl aniline was generated in these experiments and that it was reduced by iodide.

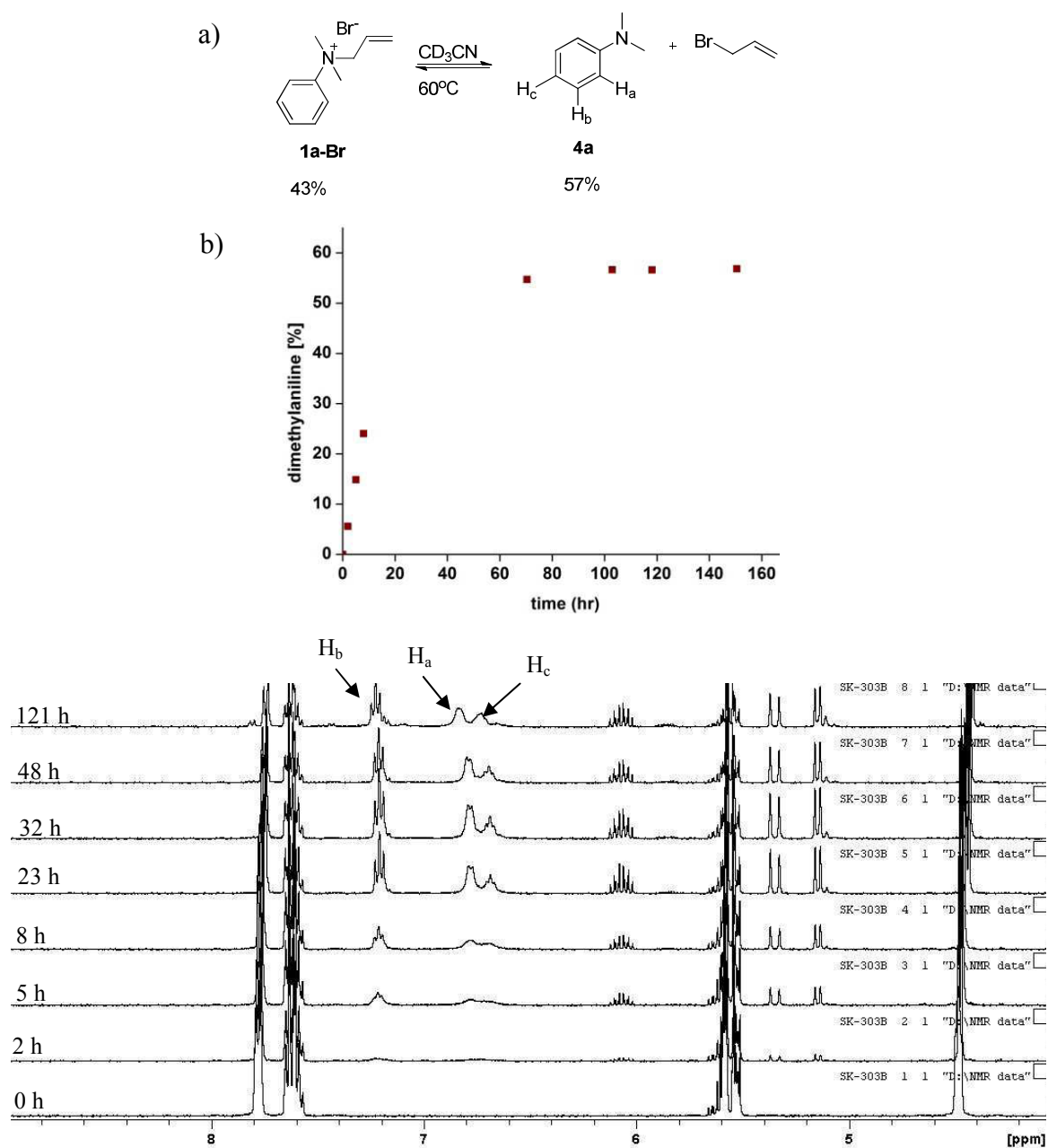


Figure 4.8. a) The dissociation of **1a-Br** and %-compound at equilibrium. b) Kinetic trace of the dissociation of **1a-Br**. c) $^1\text{H-NMR}$ spectrum of the dissociation of **1a-Br** as a function of time showing the line broadening of the peaks of liberated dimethyl aniline due to the exchange with the paramagnetic radical of dimethyl aniline.

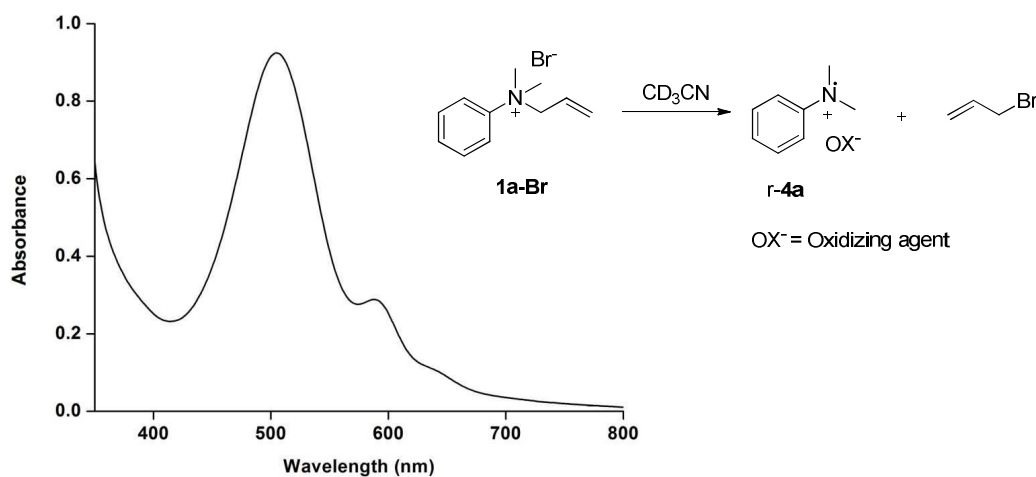


Figure 4.9 The electronic absorption spectrum of the mixture produced by deallylation of **1a-Br** ($\lambda_{\text{max}} 505 \text{ nm}$) in CH_3CN (5 mM), showing evidence of absorption due to the radical cation of dimethyl aniline (**r-4a**) in the visible region.^[80,81] (The electronic spectrum was measured after reacting **1a-Br** (20 mM) in CD_3CN at 60°C overnight. The solution for this spectrum was prepared from this reaction mixture after the purple color was observed by dilution from 20 mM to 5 mM)

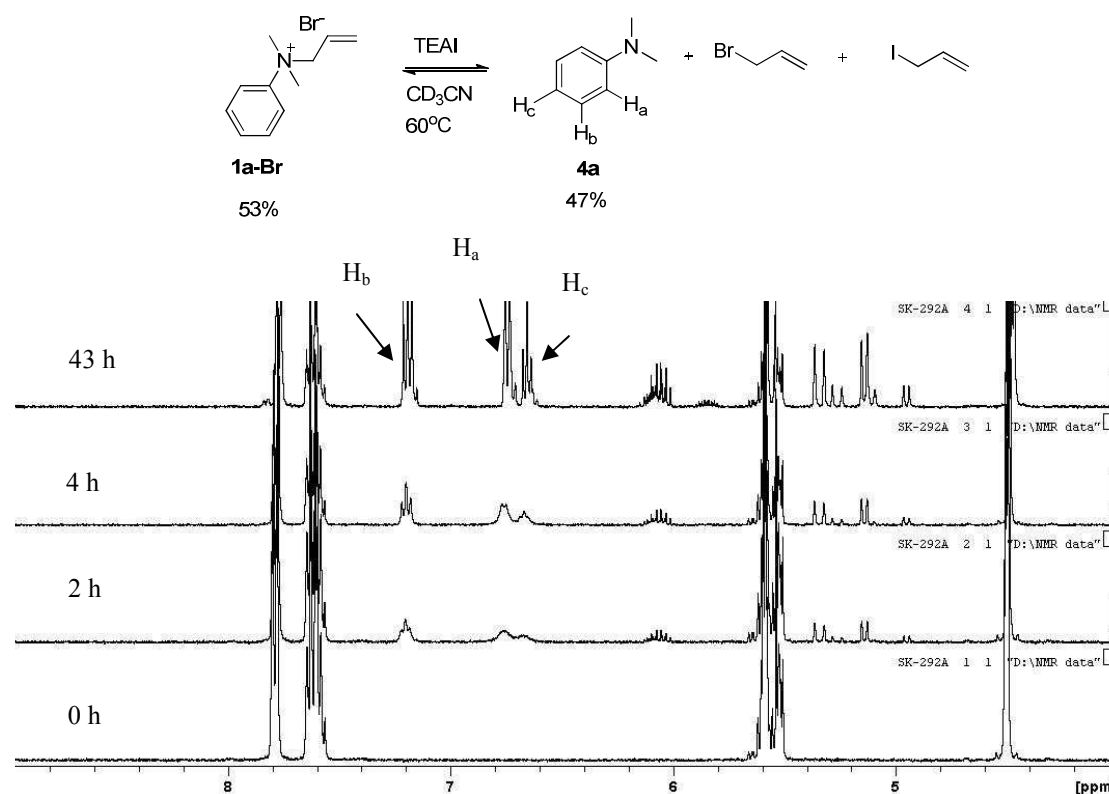
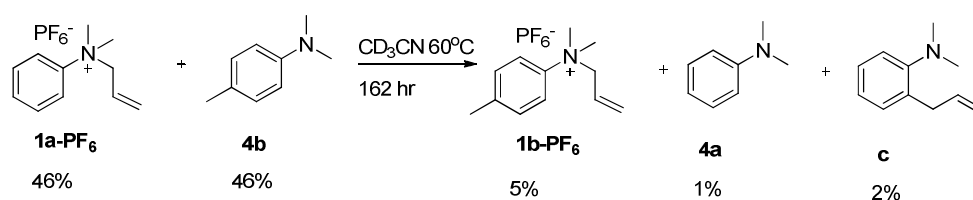


Figure 4.10 a) The product distribution at equilibrium, attained after 43 h, in the dissociation of **1a-Br** in the presence of iodide ion. b) $^1\text{H-NMR}$ spectra showing the progress of the deallylation of **1a-Br** in the presence of iodide ion in CD_3CN at 60°C as a function of time.

To evaluate the influence of the counter-anion nucleophilicity on the exchange kinetics and the possibility of “direct” exchange by attack of the amine on the allyl group of the quaternary reactant, the ammonium salt **1a-PF₆** with the very weakly nucleophilic hexafluoro-phosphate (PF₆⁻) anion was prepared and tested for its reaction with the aromatic amine **4b** (Scheme 4.2). The reaction was very slow, giving only 5% **1b-PF₆** after 162 h, about 40 times slower than for the bromide salt. This result confirmed that the reaction in the presence of halide ions (e.g. bromide or iodide) must proceed predominantly through the intermediacy of the allyl halides. Nonetheless, the formation of the small amount of **1b-PF₆** indicates that the direct reaction pathway can make a small contribution.



Scheme 4.2 Exchange reaction of **1a-PF₆** and **4b**. % ($\pm 4\%$) of compounds after 162h reaction time. **c** = Amino-Claisen rearrangement products.

In the reactions of **1a-Br** with the aliphatic amines **2a** or **2b**, small amounts of allyl bromide were detected. In contrast, for the exchange between **1a** and **2c** or **2d** no allyl bromide was observed. This could mean that the substrates **2c** and **2d** compete more effectively than **2a** and **2b** with bromide for an attack on the terminal allyl carbon atom of **1a-Br** (Scheme 4.3b). We have tested this hypothesis by reacting **2c** or **2d** with the salt **1a-PF₆** containing hexafluorophosphate anion, which is far less nucleophilic than any of the halides (Figures 7.65 and 7.67, Chapter 7). The results show that **3c-PF₆** and **3d-PF₆** do form under these conditions at similar rates to those with the bromide salts ($0.172 \times 10^{-3} \text{ M}^{-1}\text{s}^{-1}$ for **1a-PF₆⁻** and **2c**; $0.325 \times 10^{-3} \text{ M}^{-1}\text{s}^{-1}$ for **1a-PF₆⁻** and **2d**) in the absence of iodide as catalyst. In contrast, the reaction of **1a-PF₆⁻** with **2a** was about 20 times slower than that of **1a-Br** with **2a**. This difference in reactivity might be due to steric bulk which would hinder the reaction of the more bulky amine **2a** at the γ -carbon of the allyl group of **1a-Br**, compared to the amines **2c** and **2d** (see also chapter 7).

From the results mentioned above, lead to a proposed plausible mechanism of the tertiary amine exchange processes between quaternary allyl-ammonium salts and tertiary amines as will be described here. The exchange of the amine moiety between quaternary *N*-allyl-*N,N*-dimethylanilinium salts and a tertiary amine may be considered to take place following two mechanistic pathways both of S_N2' type as outlined in *Scheme 4.3*: The exchange of the amine moiety between quaternary *N*-allyl-*N,N*-dimethylanilinium salts and a tertiary amine may occur via S_N2 or S_N2' mechanisms. The latter S_N2' may itself follow either a direct or an indirect pathway, as outlined in *Scheme 4.3*.

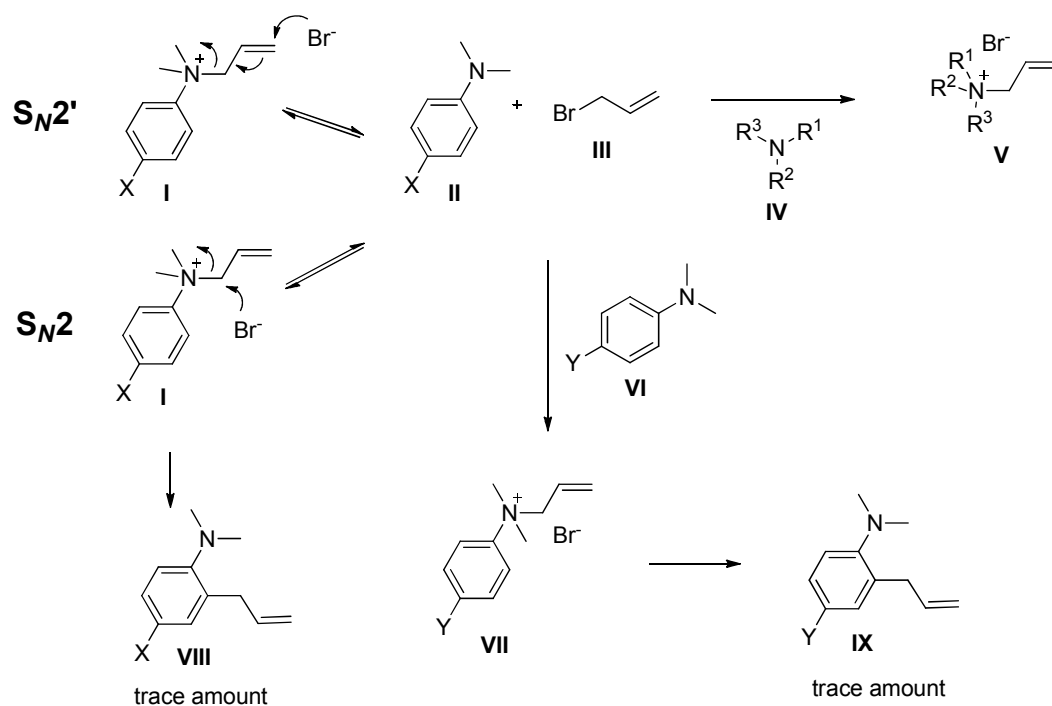
i) an indirect pathway (*Scheme 4.3a*) involving a) the nucleophilic attack of bromide anion at the γ -carbon of the allyl group of the *N*-allyl-*N,N*-dimethylanilinium salt (**I**) to liberate *N,N*-dimethylaniline (**II**) and allyl bromide (**III**), b) subsequent reaction of **III** with the introduced tertiary amine **IV** or **VI** to furnish the exchange product **V** or **VII** in an irreversible or a reversible process respectively with an aliphatic **IV** or an aromatic **VI** tertiary amine.

ii) a direct pathway (*Scheme 4.3b*) whereby the tertiary amine introduced reacts directly at the γ -carbon of the allyl group to provide the exchange product **V** or **VII**.

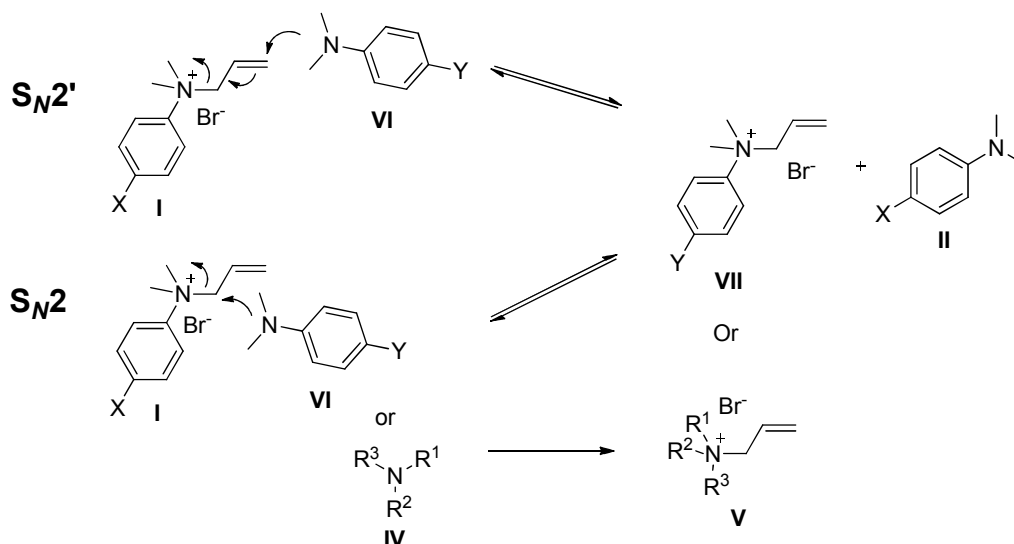
In addition, trace amounts of the amino-Claisen rearrangement product of the *N*-allyl-*N,N*-dimethylanilinium cation were also observed as a side reaction during the exchange process. The Claisen rearrangement reaction is an indication of the electrophilicity of the allyl group (presumably enhanced by the fact that the reaction is intramolecular)

Taken together, the results obtained indicate that the exchange reactions studied here may occur by the indirect pathway, via the intermediate formation of allyl bromide/halide as well as by the direct pathway, by attack on the free amine at the γ carbon of the allyl group. The presence of catalytic iodide anions may be expected to favour the indirect pathway via the formation of allyl iodide. Some comments can be made on the basis of the results obtained: 1) much faster exchange rates for bromide than for PF_6^- salts are observed for the aromatic aniline compounds together with the formation of allyl bromide, favouring an indirect S_N2' mechanism (*Entries 1 and 3 in Table 4.5*); 2) with the more nucleophilic aliphatic benzylamines there is a comparatively small rate difference between bromide and PF_6^- salts and no allyl bromide is observed, indicating that the direct mechanism is favored (*Entries 3, and 4, Table 4.4*); 3) steric bulk also affects the exchange process, slowing down the rate and shifting it towards the indirect mechanism, as is particularly notable in the case of *N*(diethyl) on both partners (*Entry 6, Table 4.4*). Of course, the different mechanisms probably coexist and may be favored depending on these various factors (nucleophilicity of the amine, steric bulk, nature of the counteranion....).

a) Indirect exchange pathway via allyl bromide



b) Direct exchange pathway



Scheme 4.3 Possible pathways for exchange of the amine moiety between *N*-allyl-*N,N*-dimethylanilinium bromide and an aliphatic or aromatic tertiary amine via an S_{N2}' mechanism

4.2.2 Study of exchange processes between quaternary benzyl-ammonium salts and tertiary amines via S_N2 type nucleophilic substitution.

DCC involving exchange of the tertiary amine may also take place with quaternary benzyl ammonium salts. Thus, we extended the generation of DCLs of quaternary ammonium cations by exploring amine exchange reactions between the *N*-benzyl-*N,N*-dimethylanilinium salts (**5a-c-Br**) and the tertiary amines (**4a-c**). An evaluation of the effect of iodide anion as a catalyst by addition tetrabutylammonium iodide (TBAI) on the exchange reaction of **5a-Br** and **4b** (Figure 4.11) indicated similar reaction rates using 1 or 2 equiv. Therefore, the addition of 1 equiv. of iodide was chosen for the exchange study.

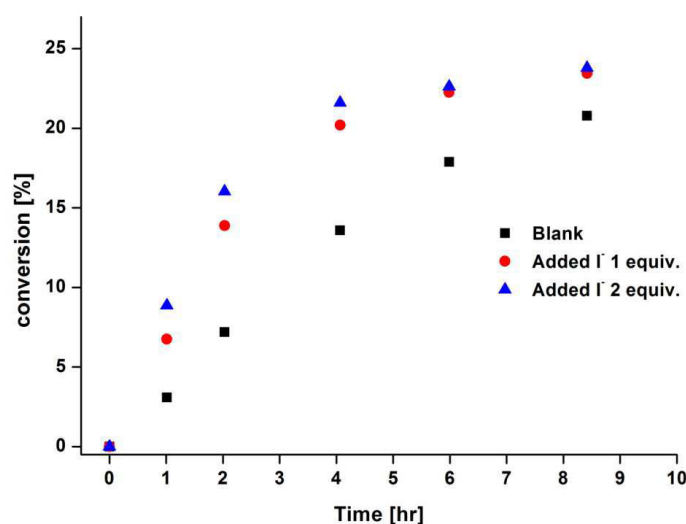
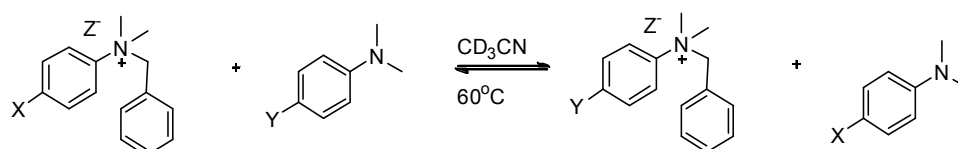


Figure 4.11 Effect of the addition of iodide anion on the nucleophilic substitution exchange reaction between **5a-Br** and **4b** in CD_3CN at $60^\circ C$. Tetrabutylammonium iodide (TBAI) was used as iodide source (1 and 2 equiv.)

The exchange reactions between the salts **5a-c-Br** and the tertiary dimethyl-aniline amines **4a-c** were studied in CD_3CN at $60^\circ C$ (Table 4.6). The rate constants and half-lives were calculated using the same method as for the exchange reaction of allyl ammonium salt with tertiary amines (Chapter 7). The reactions in the forward and reverse directions gave identical product distributions within experimental error, showing that the reactions reached a true equilibrium. The rates were about 2-fold faster in both directions on addition of 1 equiv. of iodide. To investigate the role of the bromide ion in assisting the exchange reaction, the salt **5a-OTf** was prepared by substitution of the bromide ion of **5a** with trifluoromethanesulfonate (OTf) as counterion. The exchange of **5a-OTf** and **4b**

(Figure 7.68) was slower than **5a-Br** and **4b** by a factor of about 76, confirming that the presence of the nucleophile bromide strongly increased the rate of reaction. Similarly, the reaction of **5a-PF₆** (PF₆⁻ as a counter anion) with **4b** (Figure 7.69, Chapter 7), gave the exchange products **5b-PF₆** (13%) and **4a** (13%) after 137 h being slower than the reaction of **5a-Br** and **4b** by a factor of 215. In comparison, the exchange reaction of quaternary benzyl ammonium salts with aromatic tertiary amine (**5a-Br** + **4b**, Table 4.6, Entry 1; rate constant $6.66 \times 10^{-3} \text{ M}^{-1}\text{s}^{-1}$) was faster than the exchange of quaternary allyl ammonium salt (**1a-Br** + **4b**; rate constant $0.663 \times 10^{-3} \text{ M}^{-1}\text{s}^{-1}$, with a final solution 20 mM) by about 10-fold.

Table 4.6 Kinetic and Thermodynamic Parameters for the exchange reaction between the *N*-benzyl-*N,N*-anilinium salts **5a-c-Br** and the *N,N*-dimethylaniline derivatives **4a-4c** in 1/1 ratio at 20 mM concentration in CD₃CN at 60°C. Half-life $t_{1/2}$. Proportion (%) of the different compounds. **a** = benzyl bromide, **b** = benzyl iodide. In this table only the organic cation is indicated, all anions are bromide.



5a-Br; X=H, Z=Br **4a**; Y=H
5a-OTf; X=H, Z=OTf **4b**; Y=Me
5a-PF₆; X=H, Z=OMe **4c**; Y=OMe
5b-Br; X=Me, Z=Br
5b-OTf; X=Me, Z=OTf
5b-PF₆; X=Me, Z=OMe
5c-Br; X=OMe, Z=Br

Entry	Starting compound	a)	Compound distribution [%] ^{b)}						$k [\times 10^{-3} \text{ M}^{-1} \text{ s}^{-1}]$	$t_{1/2} [\text{h}]$	$K_b^c)$	$K_c^d)$
			5a	4b	5b	4a	a	b				
1	5a + 4b	f_b	6	32	23	30	9	n.a. ^{e)}	6.66	1.5	4.6	4.3
		f_c	6	34	23	29	6	2	12.3	0.9		
	5b + 4a	r_b	7	20	25	35	13	n.a. ^{e)}	2.72	1.8		
		r_c	7	20	21	39	10	3	5.83	1.2		
2	5a + 4c	f_b	6	10	33	41	10	n.a. ^{e)}	5.40	2.0	22.0	23.7
		f_c	6	8	34	42	7	2	10.7	1.1		
	5c + 4a	r_b	4	14	29	44	8	n.a. ^{e)}	2.31	1.5		
		r_c	5	13	29	45	6	2	2.90	1.1		

^{a)} f_b , forward reaction in the absence of catalyst; f_c , forward reaction in the presence of TBAI (20 mM) as catalyst; r_b , Reverse reaction in the absence of catalyst; r_c , Reverse reaction in the presence of TBAI (20 mM) as catalyst. ^{b)} Error in ¹H-NMR signal integration: $\pm 4\%$. ^{c)} K_b , Equilibrium constant of the uncatalyzed reaction. ^{d)} K_c , Equilibrium constant of the catalyzed reaction. ^{e)} n.a., not applicable.

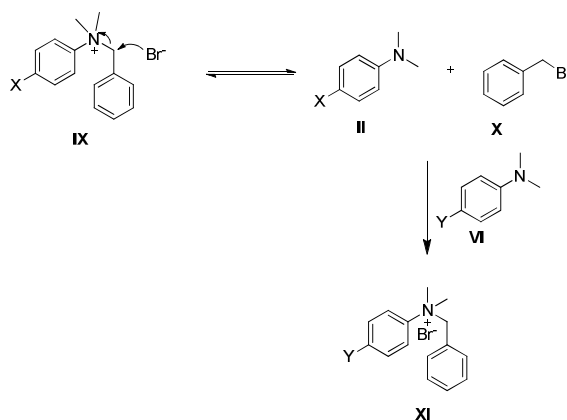
As in the case of quaternary allyl ammonium salts discussed above and the results mentioned in this part, the mechanism of the exchange of the tertiary amine moiety between quaternary *N*-benzyl-*N,N*-dimethylanilinium salts and a tertiary amine can be described as following two mechanistic pathways both of S_N2 type as outlined in *Scheme 4.4*:

i) an indirect pathway (*Scheme 4.4a*) involving a) the nucleophilic attack of bromide anion at CH_2 carbon of the benzyl group of the *N*-benzyl-*N,N*-dimethylanilinium salt (**IX**) to liberate the *N,N*-dimethylaniline (**II**) and benzyl bromide (**X**), b) subsequent reaction of **X** with the introduced tertiary amine **VI** giving the exchange product **XI** in a reversible process.

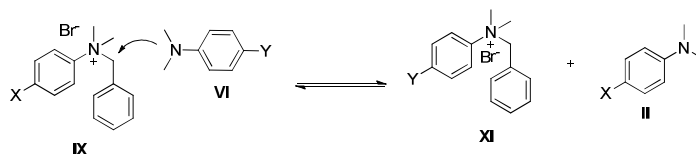
ii) a direct pathway (*Scheme 4.4b*) whereby the tertiary amine **VI** introduced reacts directly at the CH_2 carbon of the benzyl group of **IX** to provide the exchange product **XI**.

As in the previous case, for the allyl anilinium quaternary cations above, the much slower reaction observed above when PF_6^- or OTf^- were used as counteranions as compared to bromide indicates that the exchange processes studied here occur mainly through the indirect pathway 4.4a) via the intermediate formation of benzyl bromide/halide, with negligible if any participation of the direct pathway 4.4b). Thus, the exchange rate is much slower for (benzyl) **5a-PF₆** + **4b** than for **5a-Br** + **4b**, and the change from bromide to PF_6^- slows down the rate much more for the benzylic cations than for the comparable allyl cations (compare (benzyl) **5a-PF₆** + **4b** 215 times slower than **5a-Br** + **4b**; (allyl) **1a-PF₆** + **4b** 40 times slower than **1a-Br** + **4b**).

a) Indirect S_N2 pathway exchange via benzyl bromide



b) Direct S_N2 pathway exchange



Scheme 4.4 Pathways for exchange of the tertiary amine moiety between *N*-benzyl-*N,N*-dimethylanilinium bromide and an aromatic tertiary amine via an S_N2 mechanism

4.2.3 Study of exchange processes between *N*-allyl- and *N*-benzyl-pyridinium salts and pyridine components via S_N2 and S_N2' nucleophilic substitution processes.

To further extend the range of DCLs generated via nucleophilic substitution processes of S_N2 and S_N2' types, we investigated the exchange reactions between the *N*-benzyl- and *N*-allyl-pyridinium salts **6a-6f** and the pyridine derivatives **7a-7d** (Table 4.8). Initial exploration of solvents and temperatures (Table 4.7) led to the use of microwave irradiation at 150°C (300 W) for 60 minutes in acetonitrile- d_3 which provided the best reaction conditions. The composition of the final solutions and the corresponding equilibrium constants (K_{eq}) are listed in Table 4.8.

Table 4.7 Optimization of solvent in the S_N2 exchange reaction of **6a** and **7b**.^a

Entry	Solvent	T/°C	MW ^b	Time (min)	%-product 6b
1	CD ₃ CN	60	no	1440	- ^c)
2	CDCl ₃	rt	no	1440	- ^c)
3	DMSO- d_6	90	no	1440	4
4	CD ₃ CN	130	yes	10	6
5	CD ₃ CN	150	yes	15	27
6	CD ₃ CN	150	yes	30	31
7	CD ₃ CN	150	yes	45	34
8	CD ₃ CN	150	yes	60	35
9	CD ₃ CN	150	yes	90	35
10	CD ₃ CN	150	yes	120	35

^a) Reaction condition: The final solution is 20 mM.

^b) MW, microwave irradiation at 300 W. ^c) Product did not form.

In terms of exchange mechanisms and on the basis of the discussions above concerning both the quaternary allyl- and benzyl-anilinium compounds, the reactions of Table 4.8 involving the *N*-benzyl-pyridinium bromides may be considered to occur via an S_N2 pathway with direct attack of bromide anion on the benzylic CH₂ center and formation of benzyl bromide, which then reacts further with the added pyridine, in analogy with the discussion above (Scheme 4.4a). On the other hand, the processes involving the *N*-allyl-pyridinium salts appear to follow an S_N2' pathway via the intermediate generation of allyl bromide, which then reacts further (see also Scheme 4.3a).

The ability of pyridinium salts and pyridine derivatives to undergo interconversion was studied by considering the effect of *ortho* and *para*-substitution on pyridine derivatives. The component exchange between **6a** and 2-methylpyridine resulted in the starting compounds **6a** (26%), 2-methylpyridine (38%) and exchange products 1-benzyl-2-methylpyridinium bromide (12%), pyridine (17%), and benzyl bromide (7%). Due to steric

hindrance at the *ortho*-position in 2-methylpyridine, only a small amount of the exchange product was obtained, together with a significant amount of liberated benzyl bromide. Therefore, for the following investigations, only *para*-substituted pyridine derivatives (**7a-d**) were used, giving the results shown in *Table 4.8*. The interconversion between **6a** and **7b** (*Figure 4.12* and *Table 4.8, Entry 1*) and the reverse reaction under the conditions mentioned above, gave the exchange products as **6b** (35%) and **7a** (33%) with a trace amount of benzyl bromide (2%).

Next, the reaction of the pyridinium salt **6a** and pyridine **7c** (bearing the electron donating dimethylamino group in *para*-position) under the same conditions, was found to afford **6c** (50%) and **7a** (50%) (*Table 4.8, Entry 2*). The full conversion indicated that this reaction would not be reversible. Indeed, similar treatment of (**6c** + **7a**) did not provide the exchange products, confirming that this process was irreversible. On the other hand, exchange between **6a** and **7d** afforded **6d** and **7a** and was reversible (*Table 4.8, Entry 3*), reaching thermodynamic equilibrium.

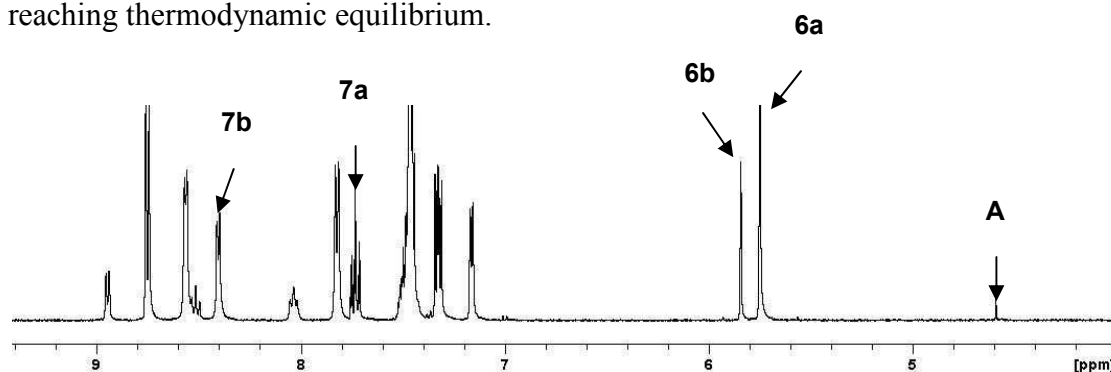
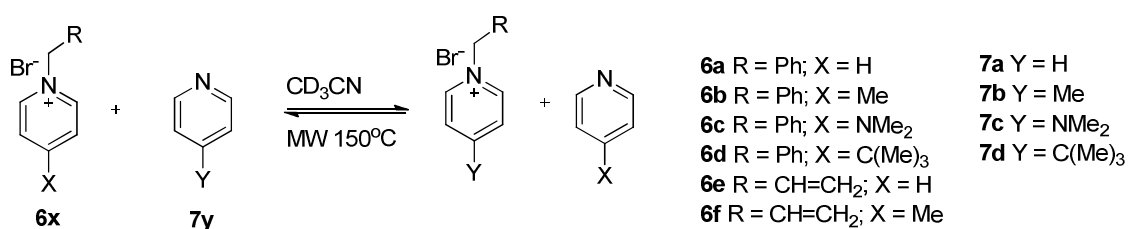


Figure 4.12 $^1\text{H-NMR}$ spectrum of the distribution of constituents obtained by component exchange between **6a** (14%) and **7b** (16%) to give the product **6b** (35%) and **7a** (33%) at equilibrium. The characteristic $-\text{CH}_2\text{-Ph}$ signals are indicated for **6a**, **6b** and benzyl bromide (**A**), 4-methylpyridine (**7b**), pyridine (**7a**).

The exchange of the pyridine component of allylpyridinium salts was investigated by combining the *N*-allylpyridinium bromide **6e** and pyridine **7b**. The reaction yielded **6f** and **7a** in 30% and 29% proportions together with 3% free allyl bromide (*Table 4.8, Entry 4*). The reversibility was studied by starting with **6f** and **7a** to give products **6e** and **7b** in similar amounts to those obtained in the forward process, thus indicating thermodynamic equilibrium was attained. In line with the discussion above, the mechanism of this exchange is expected to follow a $\text{S}_{\text{N}}2'$ nucleophilic substitution pathway (*Scheme 4.3a*) starting with attack of bromide ion at the γ -carbon of the allyl group of the pyridinium cation.

Table 4.8 Component exchange between the *N*-benzylpyridinium salts (**6a-f**) and the pyridines (**7a-d**) in CD₃CN under microwave irradiation 300 W at 150°C for 60 min. Proportion (%) of the different compounds. **a** = benzyl bromide and **b** = allyl bromide.



Entry	Reaction	a)	Compound distribution [%] ^{b)}					<i>K</i> _{eq}
			6a	7b	6b	7a	a	
1	6a + 7b	f	14	16	35	33	2	5.16
	6b + 7a	r	14	16	35	33	2	
2	6a + 7c	f	- ^{c)}	- ^{c)}	50	50	- ^{c)}	n.d. ^{d)}
	6c + 7a	r	- ^{c)}	- ^{c)}	50	50	- ^{c)}	
3	6a + 7d	f	13	15	36	33	3	6.23
	6d + 7a	r	12	16	35	35	2	
4	6e + 7b	f	16	22	30	29	3	3.99
	6f + 7a	r	11	16	34	35	4	

^{a)} f, Forward reaction; r, reverse reaction. ^{b)} Error in ¹H-NMR signal integration: ±4%. ^{c)} Compound not observed. ^{d)} n.d., not determined.

Finally, cross-exchange between *N*-benzyl and *N*-allyl-pyridinium salts involving nucleophilic substitution interconversion by both S_N2' and S_N2 pathways, was investigated by combining **6b** and **6e**. The desired products **6f** (16%) and **6a** (9%) were observed together with significant amounts of other released components as shown in Table 4.9. This reaction was shown to be reversible by mixing **6f** and **6a** which gave the products **6e** (6%) and **6b** (14%). The forward reaction was also conducted for 90 min and afforded a similar distribution as for 30 min, indicating that equilibrium was reached after 30 min. The reverse reaction was slower and equilibrium was not reached after 90 min.

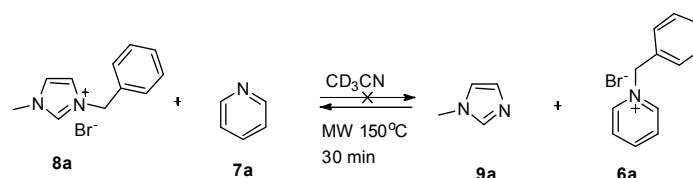
Table 4.9 Reversible component cross-exchange between *N*-benzyl- (**6a**, **6b**) and *N*-allyl- (**6e**, **6f**) pyridinium bromides in CD₃CN using microwave irradiation 300 W at 150°C. Proportion (%) of the different compounds. **7a** = pyridine, **7b** = 4-methylpyridine, **a** = benzyl bromide and **b** = allyl bromide.

Reaction	Time [min]	a)	Compound distribution [%] ^{b)}				
			6e	6b	6f	6a	7a/7b/a/b
6b + 6e	30	f	16	27	12	9	13/5/6/11
	90	f	16	25	15	12	13/4/5/10
6f + 6a	30	r	6	14	25	17	16/3/10/9
	90	r	9	17	25	18	14/3/7/8

^{a)} f, Forward reaction; r, Reverse reaction. ^{b)} Error in ¹H-NMR signal integration: ±4%.

In addition, the nucleophilic substitution exchange of an ionic liquid compound derived from imidazole derivatives was investigated in a molecular solvent under the same conditions as used for the pyridinium salt. 3-Benzyl-1-methyl-1H-imidazol-3-ium bromide (**8a**) was synthesized then used to exchange with pyridine (**7a**) under the same conditions as the exchange of pyridinium salts were performed. The result showed that this exchange reaction did not occur because of the stability of **8a**. In contrast, the inverse of this reaction was studied by combining **9a** and **6a**, giving the desired exchange products **8a** (38% after 30 min) and **7a** (34% after 30 min) as shown in Table 4.10.

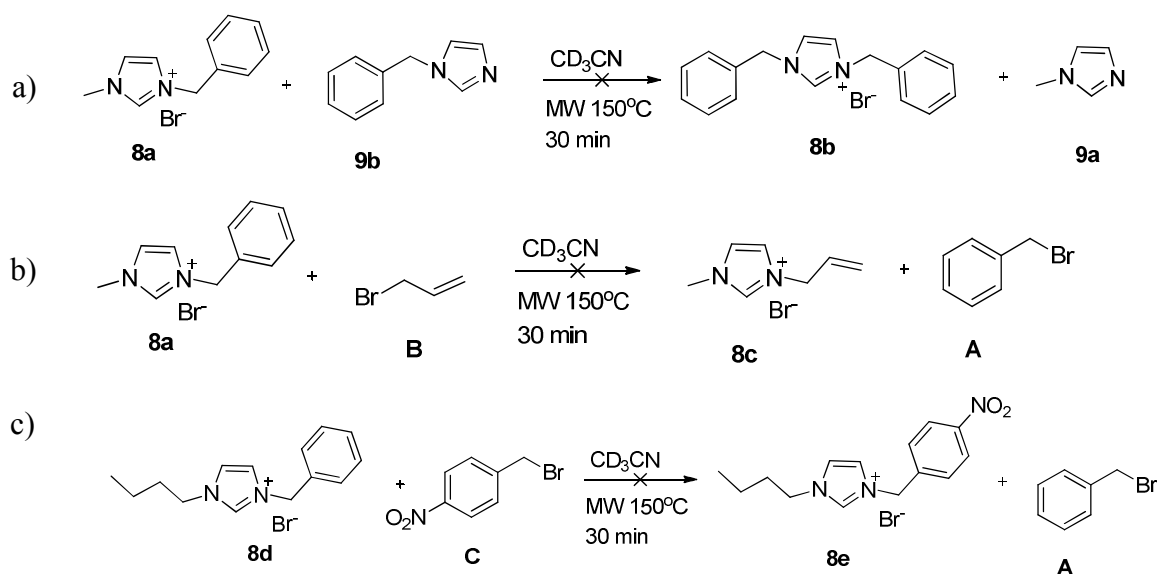
Table 4.10 The S_N2 exchange reaction between **8a** and **7a** in CD₃CN and its converse.



Reaction	Compound distribution [%] ^{a)}				
	8a	7a	9a	6a	Benzyl bromide
8a + 7a	50	50	- ^{b)}	- ^{b)}	- ^{b)}
9a + 6a	38	34	8	20	- ^{b)}

^{b)} Error in ¹H-NMR signal integration: ±4%. ^{b)} Compound not observed.

Next, the exchange reactions between **8a** and either **9b** or allyl bromide (**B**) were examined (Schemes 4.5a and 4.5b, respectively). In addition, another derivative of imidazolium salt **8d** was used to exchange with 4-nitrobenzyl bromide (**C**) as shown in Scheme 4.5c. None of these reactions was detectable and we can conclude that all of the imidazolium salts were highly stable and resistant to exchange with other compounds.

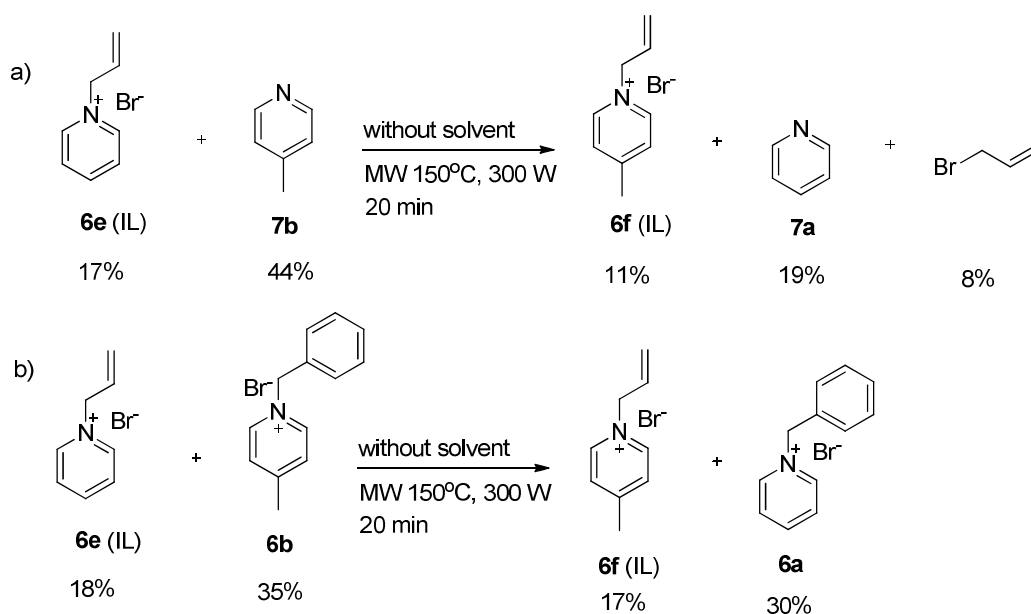


Scheme 4.5 The nucleophilic reaction of a) **8a** and **9b**, b) **8a** and allyl bromide (**B**), c) **8d** and 4-nitrobenzyl bromide (**C**) in CD_3CN under microwave irradiation $150^\circ C$ (300 W) for 30 min.

4.2.4 Generation of libraries of Dynamic Ionic Liquids (DILs)

Ionic liquids have attracted great interest and acquired much importance in many areas of chemistry.^[82–87] They usually involve organic quaternary cations, in particular, imidazolium and pyridinium derivatives.^[76] We thus were interested in the possibility of generating dynamic libraries of ionic liquids, which might present specific properties not presented by the usual ones based on “static” constituents. Considering the results obtained for the pyridinium salts, in particular, **6e** and **6f**, we performed some experiments aimed at the generation of dynamic libraries of ionic liquids.

To this end, we have investigated the exchange reaction of pyridinium salts with derivative of pyridines in the absence of added molecular solvent taking into account that **6e** and **6f** are known to be ionic liquids.^[76] Combining **6e** and in a ratio of 1:2 afforded **6f** (11%) and **7a** (19%) as the exchange products (*Scheme 4.6a*) together with some free allyl bromide (8%). However, the reaction medium became coloured, indicating that some decomposition had taken place.



Scheme 4.6 Exchange reaction between a) **6e** and **7b** and b) **6e** and **6b** in the absence of molecular solvent under microwave irradiation at 150°C for 20 minutes.

Of special interest is the generation of a dynamic ionic liquid library by component exchange in the solid state, i.e. from solid constituents. Thus, starting from a mixture of the two solid precursors **6e** and **6b**, in the absence of solvent, and heating by microwave irradiation, an ionic liquid mixture was obtained having the composition **6e** (18%), **6b** (35%), **6f** (17%), and **6a** (30%) (Scheme 4.6b). These results, although limited at this stage, demonstrate that dynamic ionic liquid libraries may in principle be generated from solid materials. One may point out that such a passage from solid to liquid phase also raises the question whether it may be accompanied by a component selection, i.e. whether component exchange and selection would lead to those constituents that provide the ionic liquid presenting the lowest solidification temperature. As it seems that no ionic liquids based on anilinium salts have been reported, the exchange reaction between **5b-Br** and **1c-Br** was tried in the absence of solvent. Only decomposition of the components was observed after heating.

4.3 Conclusions

The results described here extend dynamic covalent chemistry to both a new class of constituents, quaternary ammonium salts, and a new class of dynamic reactions, nucleophilic substitutions. They are thus of interest whenever processes implementing such compounds and transformations are pursued. They also suggest further exploration, for instance towards exchanges and DCLs based on other nucleophilic substitution reactions (e.g. R-X / R'-Y) or towards other classes of compounds such as quaternary phosphonium salts,^[88] or also towards other types of applications such as the generation of dynamic ionic liquid phases, thus pushing further the realm of dynamic structural diversity and functional complexity.

4.4 References

- [1] J.-M. Lehn, *Chem. Soc. Rev.* **2007**, *36*, 151–160.
- [2] P. T. Corbett, J. Leclaire, L. Vial, K. R. West, J.-L. Wietor, J. K. M. Sanders, S. Otto, *Chem. Rev.* **2006**, *106*, 3652–3711.
- [3] Y. Jin, C. Yu, R. J. Denman, W. Zhang, *Chem. Soc. Rev.* **2013**, *42*, 6634–6654.
- [4] S. Ladame, *Org. Biomol. Chem.* **2008**, *6*, 219–226.
- [5] S. J. Rowan, S. J. Cantrill, G. R. L. Cousins, J. K. M. Sanders, J. F. Stoddart, *Angew. Chem. Int. Ed.* **2002**, *41*, 898–952.
- [6] J.-M. Lehn, *Chem. – Eur. J.* **1999**, *5*, 2455–2463.
- [7] C. Saiz, P. Wipf, E. Manta, G. Mahler, *Org. Lett.* **2009**, *11*, 3170–3173.
- [8] I. Huc, J.-M. Lehn, *Proc. Natl. Acad. Sci.* **1997**, *94*, 2106–2110.
- [9] J. R. Nitschke, J.-M. Lehn, *Proc. Natl. Acad. Sci.* **2003**, *100*, 11970–11974.
- [10] R. Nguyen. and I. Huc, *Chem. Commun.* **2003**, 942–943.
- [11] P. Wipf, S. G. Mahler, K. Okumura, *Org. Lett.* **2005**, *7*, 4483–4486.
- [12] O. Ramström, J.-M. Lehn, *ChemBioChem* **2000**, *1*, 41–48.
- [13] S. Otto, R. L. E. Furlan, J. K. M. Sanders, *J. Am. Chem. Soc.* **2000**, *122*, 12063–12064.
- [14] H. Hioki, W. C. Still, *J. Org. Chem.* **1998**, *63*, 904–905.
- [15] C. Brändli, T. R. Ward, *Helv. Chim. Acta* **1998**, *81*, 1616–1621.
- [16] K. C. Nicolaou, R. Hughes, S. Y. Cho, N. Winssinger, C. Smethurst, H. Labischinski, R. Endermann, *Angew. Chem. Int. Ed.* **2000**, *39*, 3823–3828.
- [17] N. Wilhelms, S. Kulchat, J.-M. Lehn, *Helv. Chim. Acta* **2012**, *95*, 2635–2651.
- [18] M. Ciaccia, R. Cacciapaglia, P. Mencarelli, L. Mandolini, S. D. Stefano, *Chem. Sci.* **2013**, *4*, 2253–2261.
- [19] M. Ciaccia, S. Pilati, R. Cacciapaglia, L. Mandolini, S. D. Stefano, *Org. Biomol. Chem.* **2014**, *12*, 3282–3287.
- [20] S. Kulchat, K. Meguellati, J.-M. Lehn, *Helv. Chim. Acta* **2014**, *97*, 1219–1236.
- [21] I. Nakazawa, S. Suda, M. Masuda, M. Asai, T. Shimizu, *Chem. Commun.* **2000**, 881–882.
- [22] L. M. Greig, A. M. Z. Slawin, M. H. Smith, D. Philp, *Tetrahedron* **2007**, *63*, 2391–2403.
- [23] P. G. Swann, R. A. Casanova, A. Desai, M. M. Frauenhoff, M. Urbancic, U. Slomczynska, A. J. Hopfinger, G. C. Le Breton, D. L. Venton, *Pept. Sci.* **1996**, *40*, 617–625.
- [24] P. J. Boul, P. Reutenauer, J.-M. Lehn, *Org. Lett.* **2005**, *7*, 15–18.
- [25] P. Reutenauer, E. Buhler, P. J. Boul, S. J. Candau, J.-M. Lehn, *Chem. – Eur. J.* **2009**, *15*, 1893–1900.
- [26] P. Reutenauer, P. J. Boul, J.-M. Lehn, *Eur. J. Org. Chem.* **2009**, *2009*, 1691–1697.
- [27] N. Roy, J.-M. Lehn, *Chem. – Asian J.* **2011**, *6*, 2419–2425.
- [28] J.-M. Lehn, *Prog. Polym. Sci.* **2005**, *30*, 814–831.

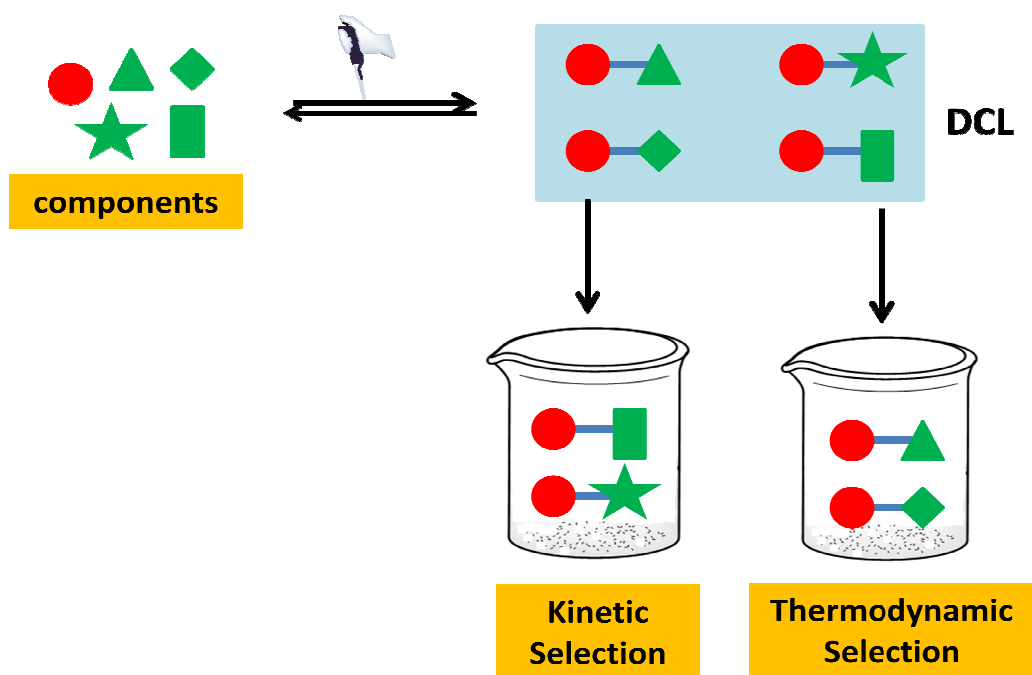
- [29] J. Lehn, *Aust. J. Chem.* **2010**, *63*, 611–623.
- [30] D. Zhao, J. S. Moore, *J. Am. Chem. Soc.* **2002**, *124*, 9996–9997.
- [31] R. J. Williams, A. M. Smith, R. Collins, N. Hodson, A. K. Das, R. V. Ulijn, *Nat. Nanotechnol.* **2009**, *4*, 19–24.
- [32] S. Otto, *Nat. Nanotechnol.* **2009**, *4*, 13–14.
- [33] R. Nguyen, E. Buhler, N. Giuseppone, *Macromolecules* **2009**, *42*, 5913–5915.
- [34] N. Roy, E. Buhler, J.-M. Lehn, *Polym. Int.* **2014**, *63*, 1400–1405.
- [35] J. Li, P. Nowak, S. Otto, *J. Am. Chem. Soc.* **2013**, *135*, 9222–9239.
- [36] N. Giuseppone, *Acc. Chem. Res.* **2012**, *45*, 2178–2188.
- [37] H. Otsuka, *Polym. J.* **2013**, *45*, 879–891.
- [38] C. Wang, Z. Wang, X. Zhang, *Acc. Chem. Res.* **2012**, *45*, 608–618.
- [39] A.-J. Avestro, M. E. Belowich, J. F. Stoddart, *Chem. Soc. Rev.* **2012**, *41*, 5881–5895.
- [40] A. Ciesielski, P. Samori, *Nanoscale* **2011**, *3*, 1397–1410.
- [41] T. Maeda, H. Otsuka, A. Takahara, *Prog. Polym. Sci.* **2009**, *34*, 581–604.
- [42] A. L. Korich, P. M. Iovine, *Dalton Trans.* **2010**, *39*, 1423–1431.
- [43] O. Ramström, J.-M. Lehn, *Nat. Rev. Drug Discov.* **2002**, *1*, 26–36.
- [44] O. Ramström, S. Lohmann, T. Bunyapaiboonsri, J.-M. Lehn, *Chem. – Eur. J.* **2004**, *10*, 1711–1715.
- [45] T. Hotchkiss, H. B. Kramer, K. J. Doores, D. P. Gamblin, N. J. Oldham, B. G. Davis, *Chem. Commun.* **2005**, 4264–4266.
- [46] G. Nasr, E. Petit, C. T. Supuran, J.-Y. Winum, M. Barboiu, *Bioorg. Med. Chem. Lett.* **2009**, *19*, 6014–6017.
- [47] D. E. Scott, G. J. Dawes, M. Ando, C. Abell, A. Ciulli, *ChemBioChem* **2009**, *10*, 2772–2779.
- [48] R. Caraballo, H. Dong, J. P. Ribeiro, J. Jiménez-Barbero, O. Ramström, *Angew. Chem. Int. Ed.* **2010**, *49*, 589–593.
- [49] M. Hochgürtel, J.-M. Lehn, in *Fragm.-Based Approaches Drug Discov.* (Eds.: W. Jahnke, D.A. Erlanson), Wiley-VCH Verlag GmbH & Co. KGaA, **2006**, pp. 341–364.
- [50] O. Ramstromöm, J.-M. Lehn, in *Compr. Med. Chem. II* (Ed.: J.B.T.J. Triggler), Elsevier, Oxford, **2007**, pp. 959–976.
- [51] E. Wedekind, E. Fröhlich, *Zur Stereochemie des Funfwertigen Stickstoffes*, Verlag Von Veit & Comp., Leipzig, **1907**, pp. 72–83.
- [52] E. Havinga, *Biochim. Biophys. Acta* **1954**, *13*, 171–174.
- [53] R. G. Kostyanovsky, V. R. Kostyanovsky, G. K. Kadorkina, K. A. Lyssenko, *Mendeleev Commun.* **2001**, *11*, 1–5.

- [54] R. G. Kostyanovsky, K. A. Lyssenko, O. N. Krutius, V. R. Kostyanovsky, *Mendeleev Commun.* **2009**, *19*, 19–20.
- [55] O. Marianacci, G. Micheletti, L. Bernardi, F. Fini, M. Fochi, D. Pettersen, V. Sgarzani, A. Ricci, *Chem. – Eur. J.* **2007**, *13*, 8338–8351.
- [56] T. Ooi, K. Maruoka, *Angew. Chem. Int. Ed.* **2007**, *46*, 4222–4266.
- [57] M. J. O'Donnell, W. D. Bennett, S. Wu, *J. Am. Chem. Soc.* **1989**, *111*, 2353–2355.
- [58] J. Ding, D. W. Armstrong, *Chirality* **2005**, *17*, 281–292.
- [59] J. Pernak, J. Feder-Kubis, *Chem. – Eur. J.* **2005**, *11*, 4441–4449.
- [60] S. Zhang, Y. Huang, H. Jing, W. Yao, P. Yan, *Green Chem.* **2009**, *11*, 935–938.
- [61] D. A. Lenev, K. A. Lyssenko, R. G. Kostyanovsky, *Mendeleev Commun.* **2004**, *14*, 312–314.
- [62] F. G. Bordwell, D. L. Hughes, *J. Am. Chem. Soc.* **1986**, *108*, 7300–7309.
- [63] I. Lee, Y. K. Park, C. Huh, H. W. Lee, *J. Phys. Org. Chem.* **1994**, *7*, 555–560.
- [64] Y. Kondo, H. Kambe, S. Kusabayashi, *J. Chem. Soc. Perkin Trans. 2* **1990**, 915–919.
- [65] M. Sawada, Y. Takai, C. Chong, T. Hanafusa, S. Misumi, Y. Tsuno, *Tetrahedron Lett.* **1985**, *26*, 5065–5068.
- [66] H. Castejon, K. B. Wiberg, *J. Am. Chem. Soc.* **1999**, *121*, 2139–2146.
- [67] H. M. Yau, A. K. Croft, J. B. Harper, *Chem. Commun.* **2012**, *48*, 8937–8939.
- [68] E. E. L. Tanner, H. M. Yau, R. R. Hawker, A. K. Croft, J. B. Harper, *Org. Biomol. Chem.* **2013**, *11*, 6170–6175.
- [69] H. M. Yau, A. G. Howe, J. M. Hook, A. K. Croft, J. B. Harper, *Org. Biomol. Chem.* **2009**, *7*, 3572–3575.
- [70] M.-L. Bennasar, J.-M. Jiménez, B. Vidal, B. A. Sufi, J. Bosch, *J. Org. Chem.* **1999**, *64*, 9605–9612.
- [71] S. Yamada, C. Morita, *J. Am. Chem. Soc.* **2002**, *124*, 8184–8185.
- [72] D. L. Comins, S. P. Joseph, R. R. Goehring, *J. Am. Chem. Soc.* **1994**, *116*, 4719–4728.
- [73] J. T. Kuethe, D. L. Comins, *J. Org. Chem.* **2004**, *69*, 5219–5231.
- [74] A. B. Charette, M. Grenon, A. Lemire, M. Pourashraf, J. Martel, *J. Am. Chem. Soc.* **2001**, *123*, 11829–11830.
- [75] K. Patel, O. Š. Miljanić, J. F. Stoddart, *Chem. Commun.* **2008**, 1853–1855.
- [76] N. Jiang, Y. Pu, R. Samuel, A. J. Ragauskas, *Green Chem.* **2009**, *11*, 1762–1766.
- [77] P.Y. Bruice, *Organic Chemistry*, Pearson Prentice Hall, *4th ed.* **2004**, p. 1222.
- [78] H. Katayama, *Chem. Pharm. Bull. (Tokyo)* **1978**, *26*, 2027–2035.
- [79] H. Katayama, N. Takatsu, *Chem. Pharm. Bull. (Tokyo)* **1981**, *29*, 2465–2477.
- [80] M. Jonsson, J. Lind, T. E. Eriksen, G. Merenyi, *J. Am. Chem. Soc.* **1994**, *116*, 1423–1427.

- [81] G. W. Dombrowski, J. P. Dinnocenzo, P. A. Zielinski, S. Farid, Z. M. Wosinska, I. R. Gould, *J. Org. Chem.* **2005**, *70*, 3791–3800.
- [82] M. Freemantle, *An Introduction to Ionic Liquids*, The Royal Society Of Chemistry, Cambridge, **2010**, p. 281.
- [83] A. M. Scurto, W. Leitner, *Chem. Commun.* **2006**, 3681–3683.
- [84] K. J. Fraser, E. I. Izgorodina, M. Forsyth, J. L. Scott, D. R. MacFarlane, *Chem. Commun.* **2007**, 3817–3819.
- [85] S. Yazaki, M. Funahashi, J. Kagimoto, H. Ohno, T. Kato, *J. Am. Chem. Soc.* **2010**, *132*, 7702–7708.
- [86] K. C. Lethesh, K. Van Hecke, L. Van Meervelt, P. Nockemann, B. Kirchner, S. Zahn, T. N. Parac-Vogt, W. Dehaen, K. Binnemans, *J. Phys. Chem. B* **2011**, *115*, 8424–8438.
- [87] M. K. Muthayala, A. Kumar, *ACS Comb. Sci.* **2012**, *14*, 5–9.
- [88] A. A. Bredikhin, R. M. Eliseenkova, Z. A. Bredikhina, A. B. Dobrynin, R. G. Kostyanovsky, *Chirality* **2009**, *21*, 637–641.

CHAPTER 5

Kinetic and Thermodynamic selectivity of Imine formation in Dynamic Covalent Chemistry



5.1 Introduction

One of the fundamental aspects for the generation of dynamic combinatorial chemistry (DCC) is the operation of one or several reversible inter- or intramolecular exchanges involving covalent or non-covalent interactions. Of these reversible reactions, imine formation by condensation of carbonyl groups with amines is of considerable interest, in view of its role in both chemical synthesis and in biology. Imines have been used recently in dynamic covalent chemistry, adaptive chemistry, and also in supramolecular chemistry because they allow facile formation/breaking of covalent bonds to exchange with other molecules. Thus, many DCC processes are based on imine formation, selection, exchange, and/or hydrolysis.^[1-5]

The nature of amine condensation with aldehydes has been evaluated widely. Primary amines, hydroxylamine, and hydrazine derivatives have all been investigated to develop useful strategies in imine formation as conjugates in chemistry and biology.^[6-17] Nucleophiles such as hydrazine and hydroxylamine where the amino group has an alpha-substituent bearing a lone pair have long been known to act as stronger nucleophiles than normal primary amines^[18] and their low basicity allows the formation of more stable imine products.^[19] In recent times, imine formation from these alpha nucleophiles has received much attention in chemical biology,^[6-8] polymer chemistry,^[9-11] dynamic combinatorial chemistry,^[12-16] and reaction development^[20].

This chapter describes studies of the efficiency of imine formation from different aldehydes and various amino derivatives (including primary amine, hydrazine, hydrazide and aminoxy compounds) in aqueous solution (under pD control) and in organic solvents (CD₃OD or CD₃CN). Moreover, competitive reactions (to generate Dynamic Covalent Libraries, DCLs) between different amino derivatives to form different imines in a single system have been studied in order to understand the relative reactivity and stability of these imines in aqueous solutions and organic solvents. These experiments were designed to provide a basis for predicting the stability of imines and their formation efficiency in various systems. They were also directed to the exploration of the regioselective transformation of one molecule possessing different functional groups in order to select different products based on kinetic or thermodynamic selectivity as shown in *Figure 5.1*.

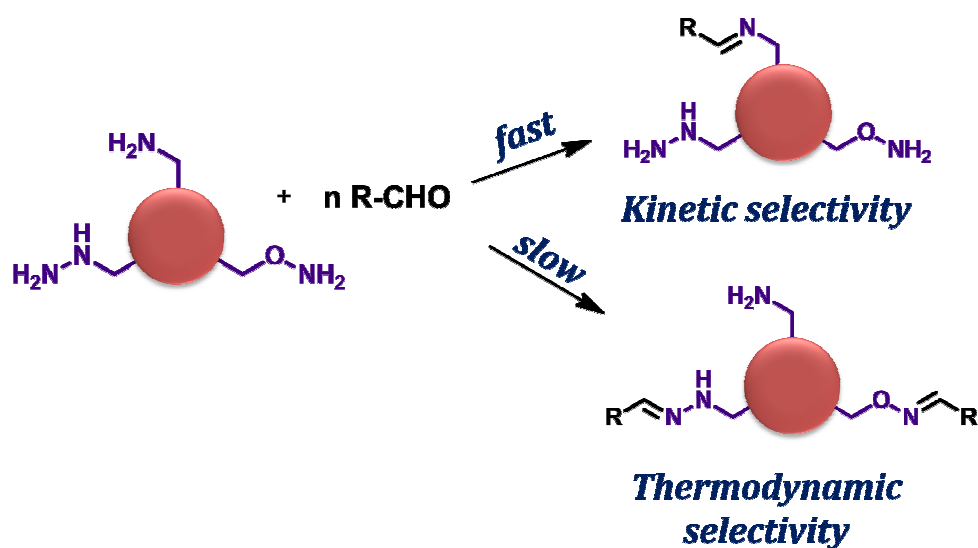
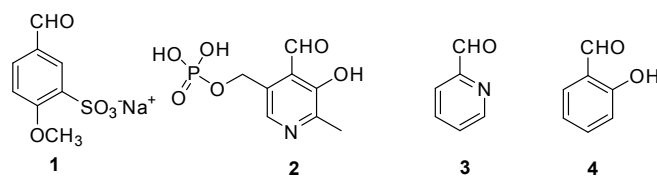


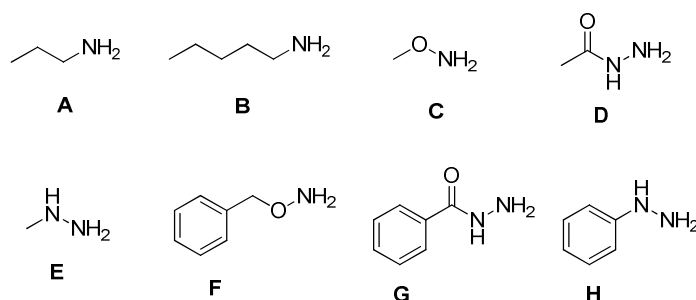
Figure 5.1 Model for the regioselective of one molecule involving different functional groups in order to select different products based on kinetic or thermodynamic selectivity.

5.2 Results and Discussion

In this investigation, the selected aldehydes fall into two groups (*Scheme 5.1*). The first group is that of the water-soluble aldehydes sodium 5-formyl-2-methoxybenzene sulfonate (**1**) and pyridoxal phosphate (**2**) used in aqueous solution studies. The second is composed of 2-pyridyl aldehyde (**3**) and salicylaldehyde (**4**) used for experimentation in organic solvents. The different amino-compounds chosen are shown in *Scheme 5.2* and comprise aliphatic amines (propylamine (**A**), pentylamine (**B**)), *O*-methoxyamine (**C**), acethydrazide (**D**), methylhydrazine (**E**), *O*-benzylhydroxylamine (**F**), benzhydrazide (**G**), and phenylhydrazine (**H**).



Scheme 5.1 Structures of aldehydes (**1-4**) used in this study.



Scheme 5.2 Structures of the different amino derivatives (A-H) used in this study

Two criteria defining the reactivity and stability are the rate of conversion (kinetic products: *kinetic selectivity*) and the degree of conversion (thermodynamic products: *thermodynamic selectivity*). Both the rates and equilibrium positions of processes investigated were monitored by $^1\text{H-NMR}$ spectroscopy, with the fractions of different compounds being determined by signal integration with respect to the peak of 1,4-dioxane as an internal standard. Over the initial stages of the reaction (*i.e.* when reverse reaction of the products could be ignored), the time dependence of the concentrations provided a good fit to simple second-order kinetics (for details, *Chapter 7*), thus providing the rate constants given herein.

5.2.1 Study of imine formation in aqueous solution from reaction of sodium 5-formyl-2-methoxybenzene sulfonate (“sulfonate aldehyde”) (1) and pyridoxal phosphate (2) with different amino derivatives (A, B, C, D, and E)

Imine formation reactions are generally well understood, but studies of imine formation in water are limited and insufficient to establish the stability of imines with low equilibrium constants.^[21–25] This is because the hydration of the aldehyde or the imine will always compete with imine formation to a greater or lesser extent depending on the electronic properties of the amine or aldehyde.^[26] Thus, imine formation reactions were performed in organic solvents not only to avoid hydration of aldehyde but also to shift the equilibrium toward the condensation products by favoring elimination of water from carbinolamine intermediates. DCC of imine compounds has been investigated in organic solvents,^[27] aqueous-organic mixtures,^[28] and aqueous solutions.^[13,29–33] The objective here was to extend these works to assess the reactivity of several different amino derivatives towards a single aldehyde in a competition reaction to generate a DCL.

5.2.1.1 The study of imine formation from sulfonate aldehyde (I)

In preliminary studies, imine formation was assessed under different conditions using sulfonate aldehyde **1** with several amino derivatives separately (propylamine (**A**), pentylamine (**B**), *O*-methoxyamine (**C**), acethydrazide (**D**), and methylhydrazine (**E**). DMSO-*d*₆ and D₂O were employed as solvents (Table 5.1) for equimolar (20 mM) mixtures of the aldehyde and a single amino compound at 25°C.

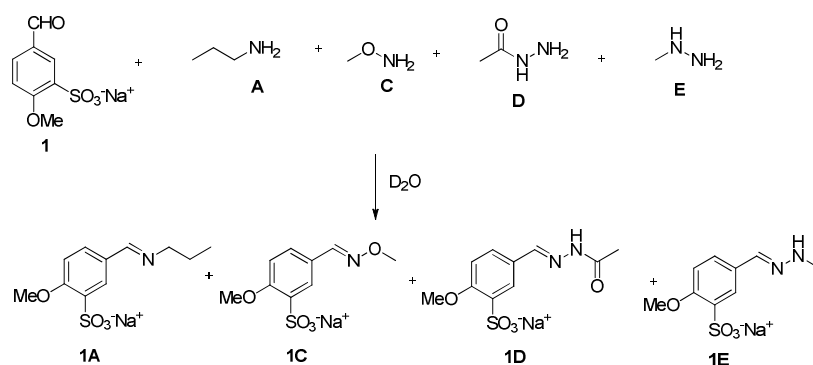
In most cases, imine formation was much slower in DMSO-*d*₆ than in D₂O (the formation of hydrazone **1E**, was the only exception). Imines **1A** and **1B** derived from aliphatic amines formed about 4000-fold slower in DMSO-*d*₆ than in D₂O. That imines derived from these aliphatic amines form faster in D₂O may in part be due to the different solvation in DMSO-*d*₆ and D₂O. The oxime **1C** also formed faster in D₂O than DMSO-*d*₆ but gave a lower %-product at equilibrium. Compound **1D** derived from acethydrazide did not form in DMSO-*d*₆ and was obtained only in a very low %-yield in D₂O (6% after 120 h). Lastly, **1E** was formed slower in D₂O but was more stable than in DMSO-*d*₆, attaining a higher %-product (92% yield after 140 h). Given these preliminary results indicating that imine formation from sulfonate aldehyde **1** and various amino compounds is mostly faster and proceeds further in D₂O than in DMSO-*d*₆, D₂O was chosen as a solvent for all other studies.

Table 5.1 Reaction time and %-product of imines formed in separate reactions between sulfonate aldehyde **1** and each of several amino derivatives in DMSO-*d*₆ and D₂O. Equimolar, 20 mM solutions of reactants were employed at 25°C.

Entry	Product	Time [h] ^{c)}	Product [%] ^{d)}
1 ^{a)}	1A	120	18
1 ^{b)}		0.03 ^{f)}	11
2 ^{a)}	1B	119	31
2 ^{b)}		0.05 ^{f)}	32
3 ^{a)}	1C	15	31
3 ^{b)}		2	15
4 ^{a)}	1D	23	- ^{e)}
4 ^{b)}		120	6
5 ^{a)}	1E	17	41
5 ^{b)}		17	5
		140 ^{f)}	92

^{a)} DMSO-*d*₆ was employed as a solvent. ^{b)} D₂O was employed as a solvent. ^{c)} Reaction time indicates the time when further changes in the reactant concentrations were below the limit of detection. ^{d)} Error in ¹H-NMR signal integration: ±5%. ^{e)} Compound not formed. ^{f)} Reaction reached equilibrium.

In the next screening experiment (without any pH control, this experiment could only be expected to give very rough indications of rates and equilibria), a DCL was generated by combining all the amino derivatives **A**, **C**, **D**, **E**, together with sulfonate aldehyde **1** in D₂O (Scheme 5.3) in a mixture of 20 mM of each compound at 25°C. The ¹H-NMR spectra were recorded immediately after mixing, and the reaction was followed until sulfonate aldehyde **1** could no longer be detected. This took 5 h (Figure 5.2). After mixing, all imines (**1A**, **1C**, **1D**, **1E**) were formed initially but **1A** rapidly disappeared as the reaction continued. The thermodynamically most preferred (high conversion) products in this system were **1C** and **1E**. At equilibrium, the %-formation of imines was in the order **1C** > **1E** > **1D** indicating that **1C** was the most stable compound. The pD value measured after equilibration was 6.0. The second screening experiment was performed in the same conditions as the previous one but pentylamine **B** was employed instead of propylamine **A**. The results shown in Figure 5.2 indicate that only the oxime (**1C**) and hydrazone (**1E**) were formed while compounds **1B** and **1D** did not form in appreciable concentrations at anytime during the reaction. The pD value of this reaction mixture was 8.4 as measured after equilibration. That changing the primary amine from propylamine (pK_a 10.71) to pentylamine (pK_a 10.63) led to very different pD of the final solution was a surprising result given that both amines appeared to be free in the final solutions, which thus would have been expected to have a pD close to 11 in both cases. Assuming that both the lower pD values and the fact that **1D** was formed in quite different amounts in the two tests might have been consequences of acid-bases reactions between the amines and the weakly acidic acetylhydrazone, further experiments were conducted using buffered solutions.



Scheme 5.3 DCL of the 5 components **1**, **A**, **C**, **D**, **E** and the four possible imine products **1A**, **1C**, **1D**, **1E**. The study was performed at 25°C using a solution where each component was initially present at a concentration of 20 mM.

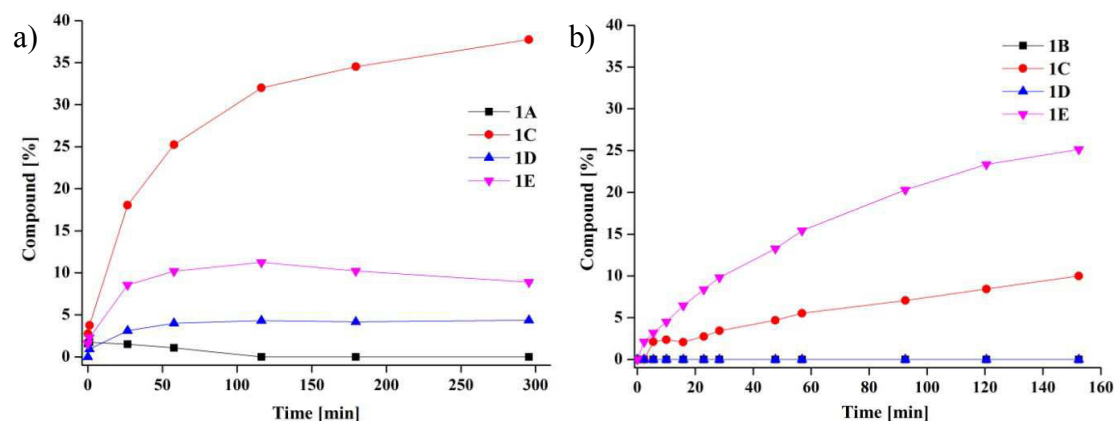


Figure 5.2 a) Kinetics of imine formation (**1A**, **1C**, **1D**, **1E**) in D_2O (pD = 6.0 after equilibration). b) Kinetic trace of the imine formation (**1B**, **1C**, **1D**, **1E**) in D_2O (pD = 8.4 after equilibration). Each data point was obtained by integration of the 1H -NMR signal corresponding to the $-CH=N-$ proton with respect to an internal standard, 1,4-dioxane. Error in 1H -NMR integration: ~ 4 -5%.

In addition, it is of course well known for imine formation in general that both the rates and equilibria are pH-dependent.^[34–38] Thus, further experiments were performed under controlled pD conditions (pD = 5.0, 8.5, and 11.4; the pD value was calculated employing $pD = pH + 0.4$ where “pH” is the apparent pH value indicated by the conventional glass electrode^[26,39]) using phosphate buffers (160 mM NaH_2PO_4/Na_2HPO_4) mixtures.

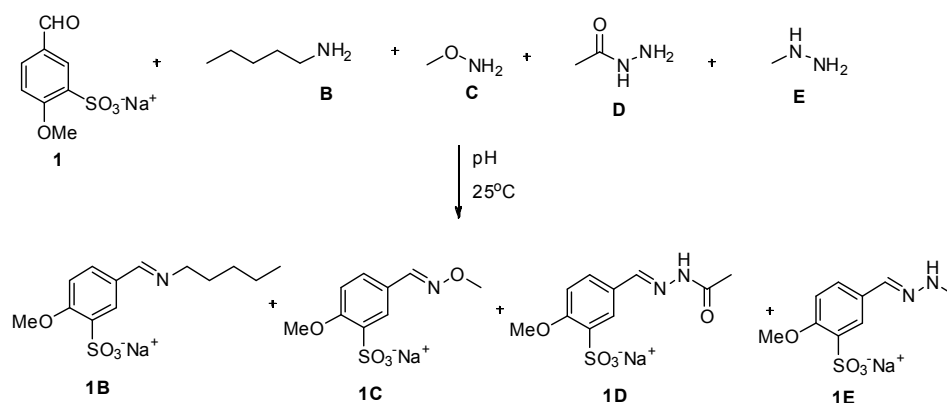
Firstly, the formation of **1B**, **1C**, **1D** and **1E** was studied in order to determine the kinetic and thermodynamic parameters of each individual reaction using initial reactant concentrations of 20 mM in all three buffers at 25°C (Table 5.2). The results showed that **1B** did not form at pD 5.0. At pD 8.5 and 11.4, **1B** formed rapidly after mixing but the %-product at equilibrium was very low. The oxime **1C** formed faster at pD 5.0 than at higher pD values, showing that acidic media are preferable for oxime formation, although it is presumed that if the solution were acidic enough to protonate completely the amine **C**, nucleophilic addition to the aldehyde would be inhibited. The pK_a of *O*-methoxyamine is 4.6, and thus at pD 5.0 (pH = 4.6), approximately half of the reactant should still be present as neutral methoxyamine to attach the aldehyde.

1D also formed faster at pD 5.0 than at pD 11.4 but did not form at all at pD 8.5. The pD values of all three buffers exceed the pK_a of acetylhydrazide ($pK_a = 3.25$) meaning that acetylhydrazide would have been at least predominantly in its neutral form in all three buffers. Finally, the hydrazone **1E** formation was nearly insensitive to solution pD but formed slightly slower at pD 11.4, despite the fact that, given the pK_a of the conjugate acid of **E** (methylhydrazine) is 7.87, the reactant would have been present very largely in its protonated form at pD 5.0 but largely in its neutral form at pD 8.5 and 11.4. These results provide a good illustration of the possible complexity of the pH dependence of imine formation.^[26]

Table 5.2 Reaction time, %product formation, and second order rate constants for imine formation from sulfonate aldehyde (**1**) and several amino derivatives (**B**, **C**, **D**, **E**) separately. Reactions were performed in D_2O in phosphate buffer at pD 5.0, 8.5, and 11.4. Solutions were equimolar (20 mM) in each reactant.

Entry	pD	Product	Product [%] ^{a)}	Time [h] ^{b)}	$k^c)$ [$\times 10^{-3} \text{ M}^{-1} \text{ s}^{-1}$]
1	5.0	1B	- ^{d)}	- ^{d)}	n.d. ^{e)}
		1C	89	1.0	203.5
		1D	37	0.5	20.32
		1E	31	1.2	4.25
2	8.5	1B	4	0.03 ^{f)}	n.d. ^{e)}
		1C	36	3.7	3.05
		1D	- ^{d)}	- ^{d)}	n.d. ^{e)}
		1E	44	3.4	5.12
3	11.4	1B	41	0.03 ^{f)}	n.d. ^{e)}
		1C	39	17	0.537
		1D	28	142	0.172
		1E	44	24	2.575

^{a)} Error in $^1\text{H-NMR}$ determination: $\pm 5\%$. ^{b)} Reaction time indicates the time when the reactions were terminated. ^{c)} Rate constant is calculated from a fit to a second-order reaction over the first 10% of the reaction. ^{d)} Compound not formed. ^{e)} n.d., not determined. ^{f)} Reaction reached equilibrium within the time of mixing.



Scheme 5.4 DCL of the 5 components **1**, **B**, **C**, **D**, **E** and the four possible imines **1B**, **1C**, **1D**, **1E** to be analyzed in different buffers ($pD = 5.0$, 8.5 , and 11.4). The study was performed at 25°C using an initial solution concentration of 20 mM for each reactant.

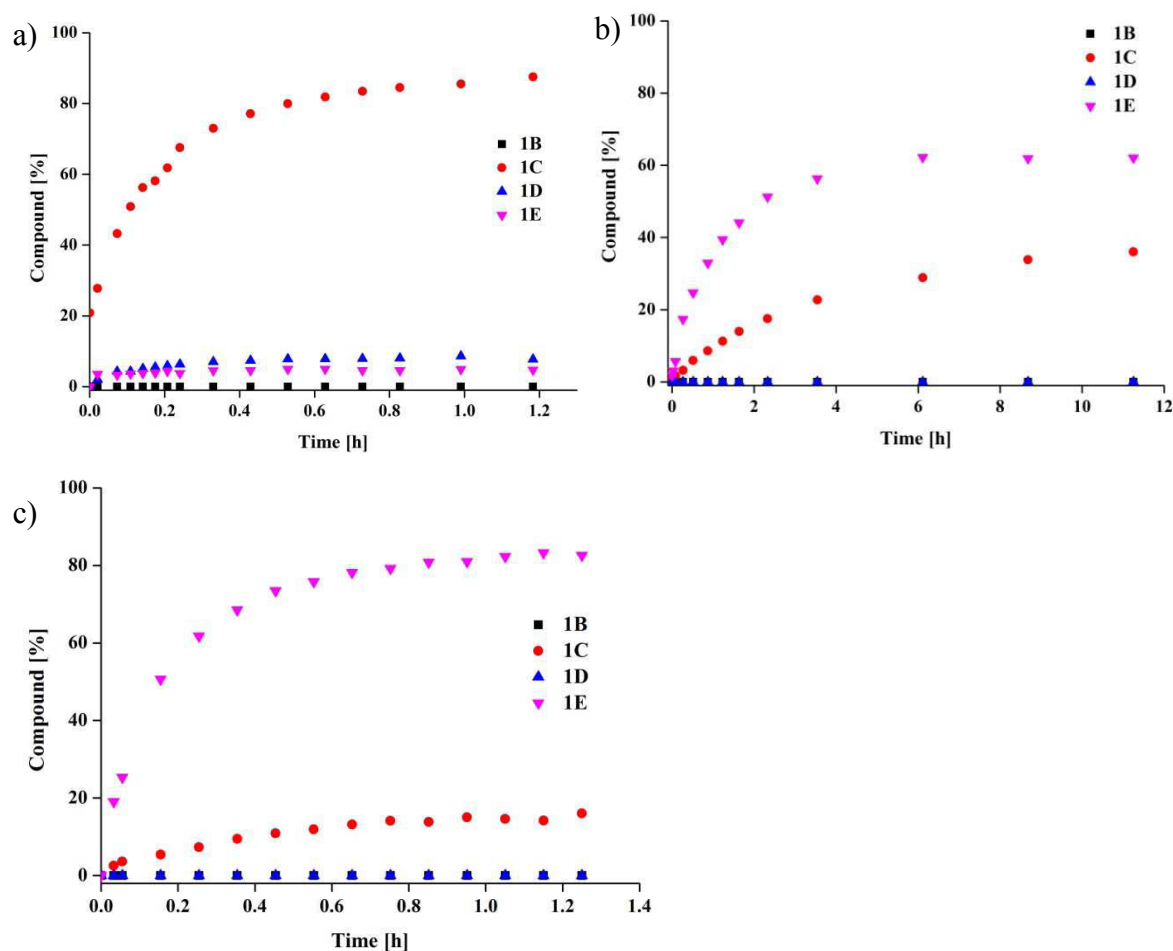


Figure 5.3 Kinetic trace for imine formation from the 5 components **1**, **B**, **C**, **D**, **E** in D_2O in phosphate buffers a) $pD = 5.0$ b) $pD = 8.5$ c) $pD = 11.4$. The concentrations of reactants were 20 mM in all cases. Error in $^1\text{H-NMR}$ integration: $\sim 4\text{-}5\%$.

DCLs from sulfonate aldehyde **1**, and the amino derivatives **B**, **C**, **D**, and **E** were generated similarly in the three buffers (Scheme 5.4) at 25°C. The results show that the reactions reached equilibrium after 1 h at pD 5.0 (Figure 5.3a and Table 5.3, Entry 1), giving the compound distribution **1C** (86%), **1D** (9%), **1E** (5%) with no **1B** (indicating, as expected from its pK_a , that pentylamine was protonated and could not react with sulfonate aldehyde **1**). **1C** was both a kinetically and thermodynamically stable product. This is in agreement with the first set of results of the individual rates of formation of imines **1B**, **1C**, **1D**, and **1E** (Table 5.2, Entry 1) which showed that **1C** was formed fastest and **1E** slowest.

Table 5.3 Equilibrium distribution of imines **1B**, **1C**, **1D**, and **1E** in dynamic mixtures generated from a mixture of the sulfonate aldehyde **1** and different amino derivatives **B**, **C**, **D**, **E** (in phosphate buffers of pD 5.0, 8.5 and 11.4). The study was performed using an initial concentration of 20 mM for all reactants at 25°C.

Entry	pD	Time [h] ^a	Compound Distribution [%] ^b			
			1B	1C	1D	1E
1	5.0	1.0	- ^c	86	9	5
2	8.5	11.2	- ^c	37	- ^c	63
3	11.4	1.2	- ^c	15	- ^c	85

^a) Reaction times indicate when no further change (<2%) was detectable in the concentrations. ^b) Error in ¹H-NMR determination: ±5%. ^c) Compound not formed.

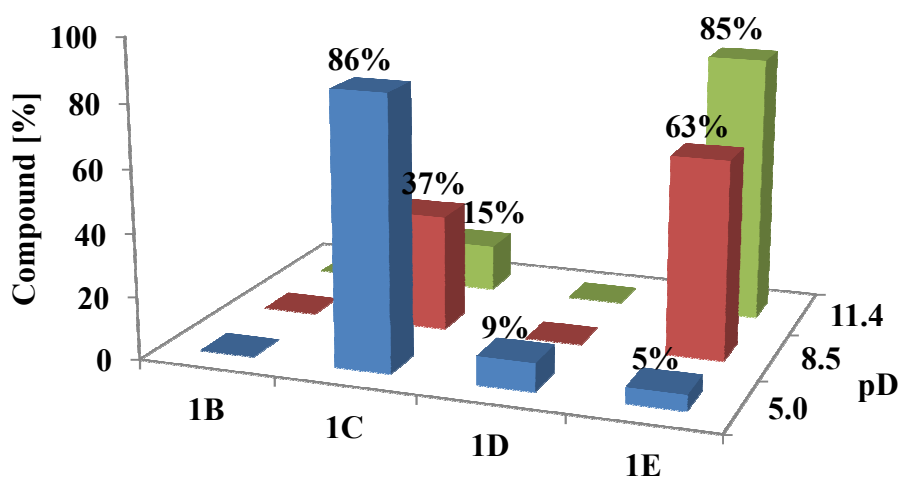


Figure 5.4 Equilibrium distribution of different imines **1B-1E** in the DCL generated from a mixture of the sulfonate aldehyde **1** and various amino derivatives **B**, **C**, **D**, **E** at pD values of 5.0, 8.5 and 11.4.

The DCL of an equimolar mixture of **1**, **B**, **C**, **D**, and **E** was next examined at pD 8.5, the results showing that the reaction was slower than at pD 5.0, reaching equilibrium after 11 h (*Figure 5.3b* and *Table 5.3, Entry 2*), and that only two imine compounds **1C** (37%) and **1E** (63%) were formed while **1B** and **1D** were not detected. At equilibrium, **1E** was more abundant than **1C**. Finally, the DCL of the same mixture was established at pD 11.4 (*Figure 5.3c* and *Table 5.3, Entry 3*). The rate of the reaction was similar to that at pD 5.0, with equilibrium reached after 1.2 h. The equilibrium compound distribution was **1C** (15%) and **1E** (85%), with again no evidence that **1B** and **1D** were present.

In summary, DCLs of the mixture of **1**, **B**, **C**, **D**, and **E** in acidic conditions were dominated by the oxime **1C** whereas, in basic solution, the hydrazone **1E** was more stable. The times to reach equilibrium for both acidic and basic media were about 1 h. Meanwhile, in slightly basic solutions (pD 8.5), the reaction progressed relatively slowly. At all pD values, imine **1B** was not detectable, meaning that it was less stable than oxime **1C** or hydrazone **1E**. These results show that the acidity of the medium is an effective tool for controlling the relative concentration of imines in a DCL in aqueous solution.

5.2.1.2 The study of imine formation from pyridoxal phosphate (**2**)

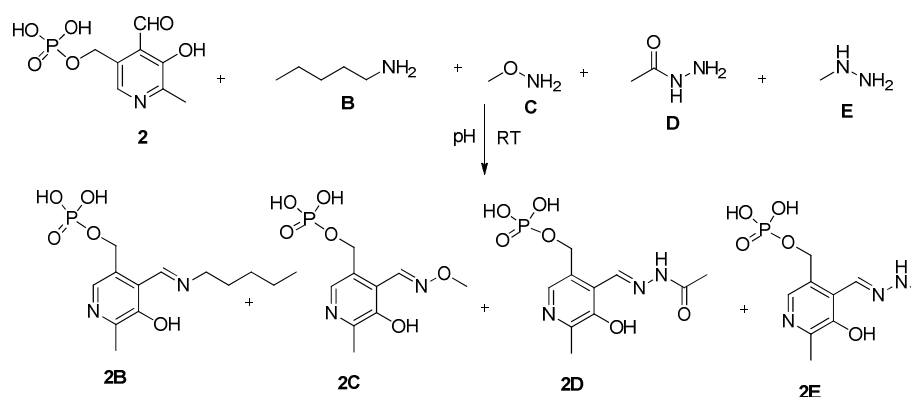
Pyridoxal phosphate (**2**) was chosen as an aldehyde reactant because it is known to exist in nature as the coenzyme for a wide range of different reactions,^[40–43] and to play a significant role in the metabolism of amino acids and other biological processes,^[44,45] as well as in dynamic covalent systems.^[46]

Firstly, imine formation between pyridoxal phosphate **2** and the different amino derivatives (**B**, **C**, **D**, **E**) was monitored separately at different pD values (pD = 5.0, 8.5, and 11.4) under the same conditions as used with the sulfonated aldehyde **1** (*Table 5.4*). Imine formation from pyridoxal phosphate **2** and pentylamine **B** did not occur at any pD because of the dominance of the hydrated form of pyridoxal phosphate (as detected by ¹H-NMR). The formation of **2C** occurred quickly at all pD values, reaching equilibrium after 5 min without any residual hydrated form of **2** being detectable. In contrast, very little of imine **2D** was formed at any of the three pD values (3% yield). The hydrazone **2E** was formed in 100% yield at both pD 5.0 and 8.5 while at pD 11.4 the reaction was faster (reaching equilibrium after 5 min) but with only 70% conversion at equilibrium.

Table 5.4 Separate studies of imine formation between pyridoxal phosphate (**2**) and several amino derivatives (**B**, **C**, **D**, **E**) in D₂O/phosphate buffers at pD values of 5.0, 8.5, and 11.4 at 25°C. The initial concentration of each reactant was 20 mM.

Entry	pD	Product	Time [min] ^{a)}	Compound [%] ^{b)}
1	5.0	2B	120	- ^{c)}
2		2C	5	99
3		2D	120	2
4		2E	120	99
5	8.5	2B	120	- ^{c)}
6		2C	5	99
7		2D	120	3
8		2E	120	99
9	11.4	2B	120	- ^{c)}
10		2C	5	99
11		2D	5	4
12		2E	5	70

^{a)} Reaction time indicates the time when no further change in the composition could be detected. ^{b)} Error in ¹H-NMR integration: ~4-5%. ^{c)} Product not formed.



Scheme 5.5 Potential DCL of the 5 components **2**, **B**, **C**, **D**, **E** and the four possible imine products **2B**, **2C**, **2D**, **2E** studied in phosphate buffers at different pD values (5.0, 8.5, and 11.4) at 25°C.

A DCL from pyridoxal phosphate **2** and the amino derivatives **B**, **C**, **D**, and **E** (Scheme 5.5) was generated and analyzed in exactly the same way as with aldehyde **1**. All of the competitive reactions (DCLs) at the three pD values reached equilibrium after approximately 2-3 min (Table 5.5). In all cases, only oxime **2C** and hydrazone **2E** were detected in significant concentrations. At pD 5.0 and 8.5, **2C** was more stable than **2E**, as shown by the compound distributions of **2C** (85%) and **2E** (15%) at pD 5.0 and **2C** (60%) and **2E** (40%) at pD 8.5. At pD 11.4, **2E** dominated. LC-MS confirmed imine formation at pD 8.5 and 11.4 by the observed peaks at m/z 298.87 ($[\mathbf{2C} + \text{K}^+]$) and at m/z 277.16 ($[\mathbf{2E} + \text{H}_3\text{O}^+]$).

These results show that in the DCL generated from an equimolar mixture of **2**, **B**, **C**, **D**, and **E** at different pD values, the oxime **2C** and the hydrazone **2E** are the dominant species. At low pD, **2C** had the highest %-product while, at high pD, **2E** dominated.

Table 5.5 Equilibrium distribution of imines **2B**, **2C**, **2D**, and **2E** in DCLs generated from a mixture of pyridoxal phosphate **2** and different amino derivatives **B**, **C**, **D**, **E** at pD values of 5.0, 8.5 and 11.4 at 25°C. All reactions reached equilibrium within < 3 min.

Entry	pD	Compound Distribution [%] ^{a)}			
		2B	2C	2D	2E
1	5.0	- ^{b)}	85	- ^{b)}	15
2	8.5	- ^{b)}	60	- ^{b)}	40
3	11.4	- ^{b)}	45	- ^{b)}	55

^{a)} Error in ¹H-NMR integration: ~4-5%. ^{b)} Product did not form.

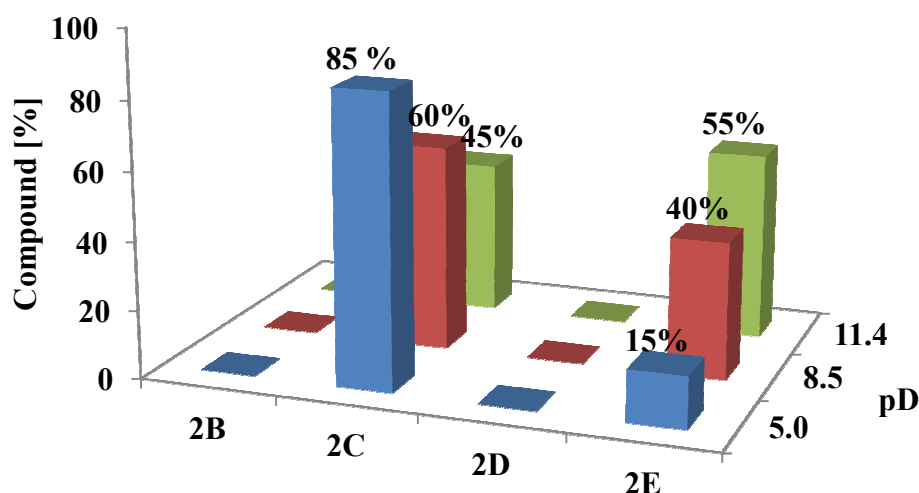


Figure 5.5 Equilibrium distributions of different imines **2B-2E** in the DCL generated from a mixture of pyridoxal phosphate **2** and various amino derivatives **B**, **C**, **D**, **E** at pD values of 5.0, 8.5 and 11.4.

5.2.2 Imine formation from 2-pyridyl aldehyde (**3**) and salicylaldehyde (**4**) and various amino derivatives (**B**, **F**, **G**, and **H**) in organic solvents

5.2.2.1 Imine formation from 2-pyridyl aldehyde (**3**)

2-pyridyl aldehyde (**3**) is known to react efficiently with amino compounds. It contains a sp² nitrogen atom that can be used as a binding site for metal-ion, thus offering other means of modifying its properties.^[47] Furthermore, the pyridine-N can serve as a site for intramolecular H-bonding of inappropriately functionalized imines, thus serving, for example, to stabilize the *Z* isomer of hydrazones susceptible to photochemical interconversion between *E* and *Z* forms.^[47,48] In 2013, Stadler studied competitive imine formation in the reactions of a mixture of a primary amine and hydrazine with 2-pyridyl aldehyde and its derivatives in CD₃CN, showing that the kinetic product was the imine derived from the primary amine while the thermodynamic product was the hydrazone.^[49] DCC of the imines derived from aldehyde **3** has been widely investigated.^[47,48,50,51] Here we extend these studies to determine the kinetic and thermodynamic selectivity for imine formation resulting from the reaction of aldehyde **3** with different amino compounds both separately and within DCLs.

Firstly, imine formation between **3** and four different amino derivatives (pentylamine (**B**), *O*-benzylhydroxylamine (**F**), benzhydrazide (**G**), and phenyl hydrazine (**H**)) was evaluated in pure CD₃OD. The results shown in *Table 5.6* indicate that imine **3B** was formed very quickly with the reactions reaching equilibrium after 2 h with 86% conversion. **3F**, **3G**, and **3H** were formed more slowly than **3B** and reached equilibrium after ca. 18 h, with about 92% conversion each. In the process of imine formation, the hemiaminal intermediate was observed in all the reactions.^[52] The measurements of imine formation here were just meant to provide a rough guide as to the differences given that, because there was no pH control and various intermediates were detectable, a proper kinetic analysis would be impossibly complicated.

Table 5.6 Equilibrated times and final imine percentages for the reaction between 2-pyridyl aldehyde **3** and amino derivatives **B**, **F**, **G**, and **H** separately in CD₃OD. The study was performed at 25°C using reactant concentrations of 20 mM.

Entry	Product	Product [%] ^{a)}	Time [h] ^{b)}
1	3B	86	2
2	3F	92	18
3	3G	93	18
4	3H	92	18

^{a)} Error in ¹H-NMR integration: ±5%. ^{b)} Reaction time indicates the time when no further change (<2%) could be detected.

Competitive reactions of two amino compounds with 2-pyridyl aldehyde (**3**)

The reaction between aldehyde **3** and equimolar amounts of pentylamine **B** and *O*-benzylhydroxylamine **F** was followed in pure CD₃OD at 25°C (Figure 5.6a, Table 5.7, Entry 1). In this case, only imine **3B** (34%) was detected immediately after mixing, being present along with the hemiaminal intermediate. Subsequently, the concentrations of **3B** and **3F** increased with time but at different rates such that after about 50 min, the concentration of **3B** began to decrease and **3F** became the predominant species. The reaction was followed up to 27 h, at which point the product conversions were **3B** (15%) and **3F** (85%).

Next, an equimolar mixture of the two amino derivatives **B** and **G** with aldehyde **3** was studied at 25°C (Figure 5.6b and Table 5.7, Entry 2). Initially, aldehyde **3** reacted rapidly with both amino compounds, giving imine **3B** (23%) and acylhydrazone **3G** (6%), with the presence of the hemi-aminals again being detectable. Later, **3B** was lost, to be replaced by more **3G**, that was then the major final product at 3.5 h, when the amounts were **3B** (13%) and **3G** (87%). Then, an equimolar mixture of the two amino compounds, **B** and **H**, with aldehyde **3** was analyzed under the same conditions as in the preceding cases (Figure 5.6c and Table 5.7, Entry 3). For this mixture, only **3B** (28%) was observed immediately after mixing all the components together. Subsequently, the concentration of **3B** increased rapidly until about 18 min, reaching 57% composition, before slowly beginning to decrease. **3H** started to appear after 5 min and slowly increased in concentration with time. The reaction was followed up to 5 h, giving **3H** (73%) as a major product and **3B** (27%) as a minor product.

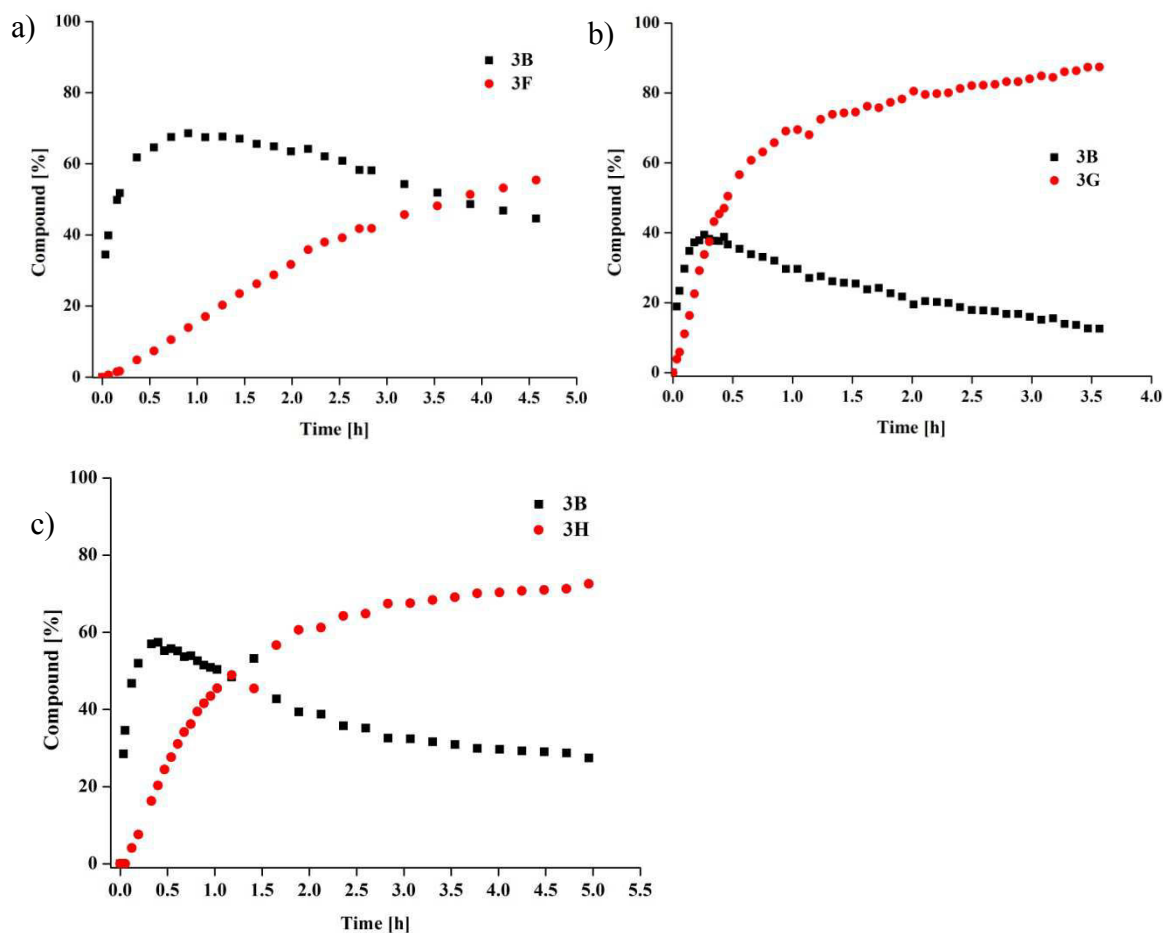


Figure 5.6 Kinetic traces for imine formation from the reactions between a) **3** + **B** + **F**, b) **3** + **B** + **G**, and c) **3** + **B** + **H** in CD₃OD in at 25°C. Initial reactant concentration were all 20 mM. Error in ¹H-NMR integration: ~5%.

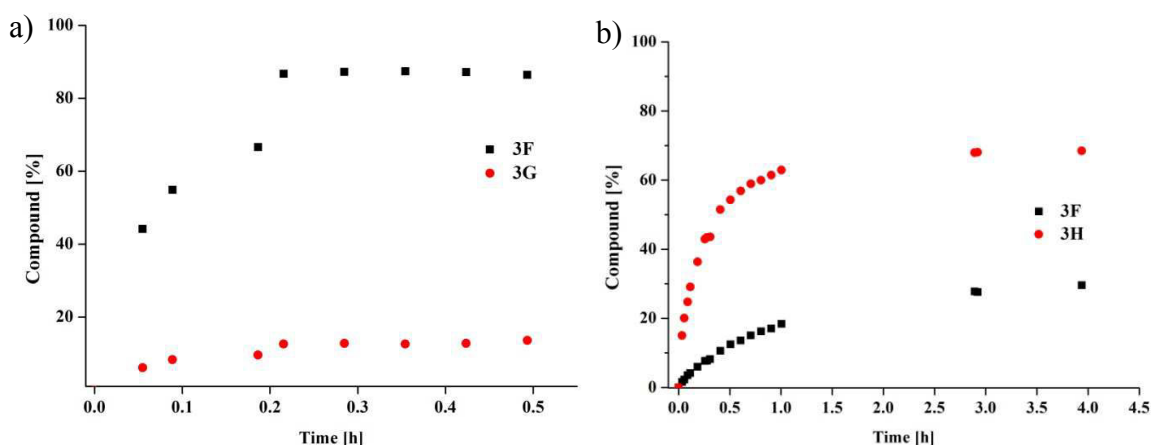
These results show that oxime **3F**, acylhydrazone **3G**, and hydrazone **3H** are more stable than imine **3B**. Pentylamine **B** has a higher basicity than the other amino compounds (for comparison, the pK_a of pentylamine is 10.63,^[53] while the pK_a of benzhydrazide is 3.0,^[54] *O*-benzyl hydroxylamine is 4.23,^[55] and phenylhydrazine is 5.21).^[56] Imine **3B** formed faster than **3F**, **3G** and **3H** at the beginning of the reaction and was, therefore, the kinetic product, whereas **3F**, **3G**, and **3H** were the thermodynamic products. The thermodynamic preference is due to the oxime, acylhydrazone, and hydrazone having electron pairs on a heteroatom near the nitrogen of the imine bond (–CH=N-X; X = O or N) which can delocalize over the molecule thus stabilizing it.^[19,57]

Table 5.7 Time-dependence of component distributions for competitive reactions of pairs of amino derivatives with a 2-pyridyl aldehyde (**3**).

Entry	Reaction	Time [h] ^{a)}	Compound distribution [%] ^{b)}			
			3B	3F	3G	3H
1	3 + B + F	0.03	34	- ^{c)}	n.d. ^{d)}	n.d. ^{d)}
		4.5	45	55	n.d. ^{d)}	n.d. ^{d)}
		27.2	15	85	n.d. ^{d)}	n.d. ^{d)}
2	3 + B + G	0.03	23	n.d. ^{d)}	6	n.d. ^{d)}
		3.5	13	n.d. ^{d)}	87	n.d. ^{d)}
3	3 + B + H	0.03	28	n.d. ^{d)}	n.d. ^{d)}	- ^{c)}
		0.3	57	n.d. ^{d)}	n.d. ^{d)}	18
		4.9	27	n.d. ^{d)}	n.d. ^{d)}	73
4	3 + F + G	0.03	n.d. ^{d)}	67	9	n.d. ^{d)}
		0.18	n.d. ^{d)}	87	13	n.d. ^{d)}
5	3 + F + H	0.03	n.d. ^{d)}	2	n.d. ^{d)}	15
		3.9	n.d. ^{d)}	30	n.d. ^{d)}	68

^{a)} Reaction times indicate the certain time of the reaction. ^{b)} Error in ¹H-NMR integration: ±4-5%. ^{c)} Compound not formed. ^{d)} n.d.; not determined.

The reaction of **3**, **F**, and **G** (Figure 5.7a and Table 5.7, Entry 4) showed **3F** and **3G** to be formed very rapidly upon mixing, with %-compositions of 67% and 9%, respectively. At equilibrium, attained in about 0.18 h, the composition was 87% **3F** and 13% **3G**. The reaction of **3**, **F**, and **H** was studied (Figure 5.7b and Table 5.7, Entry 5) under the same conditions, giving **3F** (2%) and **3H** (15%) after mixing and reaching equilibrium in about 4 h, with **3F** (30%) and **3H** (68%), respectively. These results show that the stability of the condensation products lies in the order **3H** > **3F** > **3G**.

**Figure 5.7** Kinetic traces for imine formation in CD₃OD in the reaction mixtures of a) **3 + F + G**, b) **3 + F + H**. Error in ¹H-NMR integration: ~5%.

Reactions of three and four amino compounds with 2-pyridyl aldehyde (3)

For the reaction of an equimolar mixture of **3**, **B**, **G** and **H** in pure CD₃OD and at 25°C (Figure 5.8a and Table 5.8, Entry 1), only imine **3B** (23%) and acylhydrazone **3G** (7%) were detectable immediately after mixing. After about 15 min, **3B** started to decrease in concentration and completely disappeared after 2 h as **3G** (79%) and **3H** (21%) rose in concentration. Interestingly, for this system, **3G** was formed more efficiently than **3H** suggesting that intramolecular hydrogen bonding in **3G** made it more stable than **3H**. Next, the equimolar mixture of **3**, **F**, **G**, and **H** was run, with only **3F** (1%) and **3H** (11%) being detectable immediately after mixing (Figure 5.8b and Table 5.8, Entry 2). The reaction reached equilibrium after 1.6 h, giving **3F** (20%), **3G** (3%), **3H** (71%). In the reactions without pentylamine **B**, **3G** is strongly diminished compared to when pentylamine is present, meaning that pentylamine could well be a catalyst for the formation of **3G**.^[58]

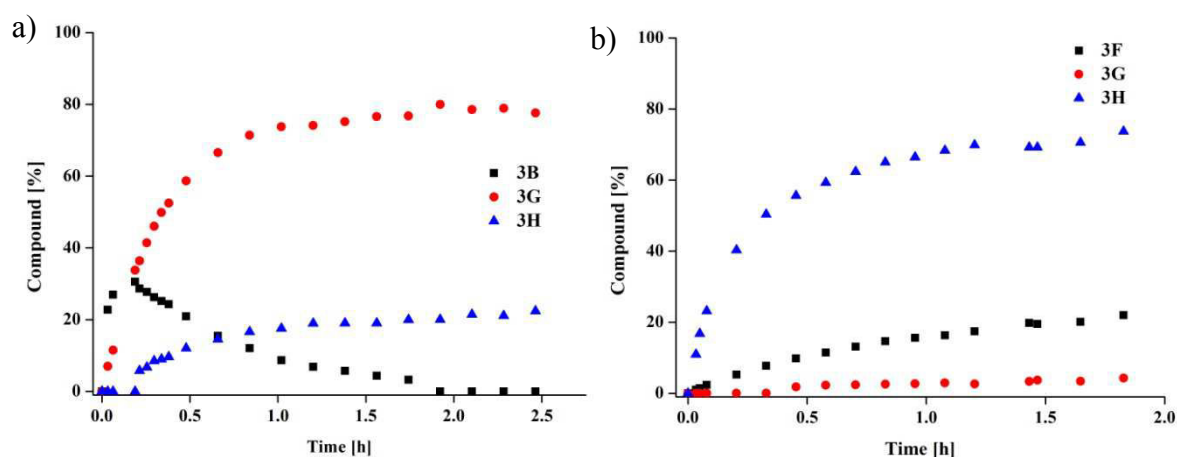


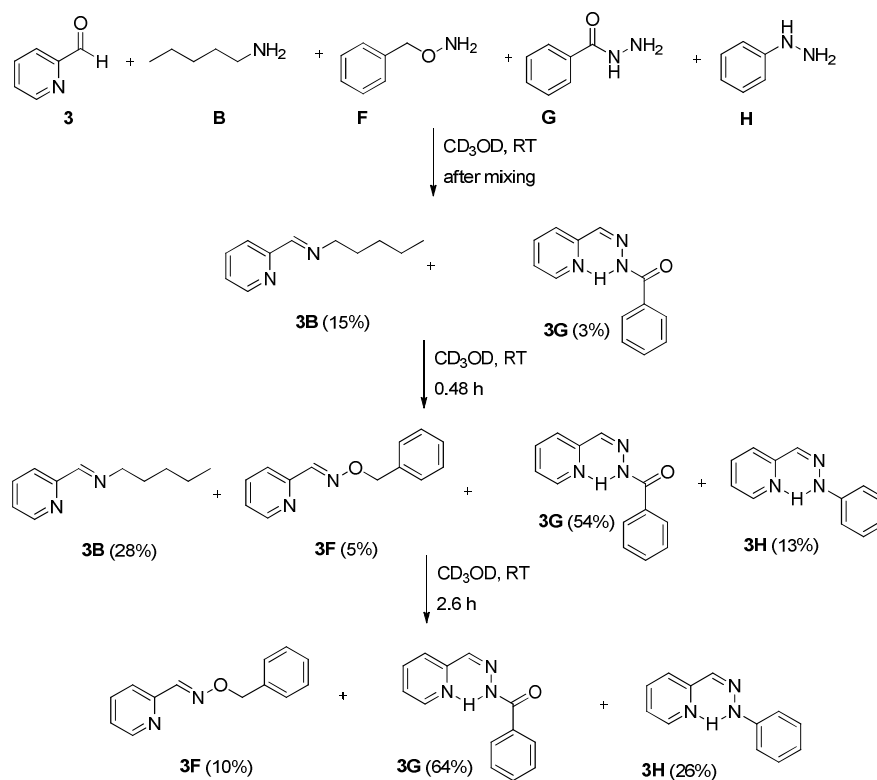
Figure 5.8 Kinetic traces for imine formation in CD₃OD in the reaction mixtures of a) **3** + **B** + **G** + **H**, and b) **3** + **G** + **F** + **H**. Error in ¹H-NMR integration: ~5%.

Table 5.8 Time-dependence of a DCL distribution in the competitive reactions between mixed amino derivatives and 2-pyridyl aldehyde (**3**) in CD₃OD. The study was performed at 25°C using initial reactant concentration of 20 mM each.

Entry	Reaction	Time [h] ^{a)}	Compound distribution [%] ^{b)}			
			3B	3F	3G	3H
1	3 + B + G + H	0.03	23	n.d. ^{d)}	7	- ^{c)}
		0.99	9	n.d. ^{d)}	74	18
		2.00	- ^{c)}	n.d. ^{d)}	79	21
2	3 + F + G + H	0.03	n.d. ^{d)}	1	- ^{b)}	11
		0.42	n.d. ^{d)}	10	2	56
		1.6	n.d. ^{d)}	20	3	71
3	3 + B + F + G + H	0.05	15	- ^{c)}	3	- ^{c)}
		0.48	28	5	54	13
		2.63	<1	10	64	26
		21.8	- ^{c)}	16	53	32

^{a)} Reaction times indicate the certain time of the reaction. ^{b)} Error in ¹H-NMR integration: ±5%. ^{c)} Compound not formed. ^{d)} n.d.; not determined.

Finally, the DCL of the mixture of aldehyde **3** and four different amino derivatives (**B**, **F**, **G**, **H**) was studied under the same conditions (Scheme 5.6, Figure 5.9, and Table 5.8, Entry 3). Only **3B** (15%) and **3G** (3%) were detectable immediately after mixing while the hemiaminal species were also observed. At about 0.5 h, the compound distribution changed to **3B** (28%), **3F** (5%), **3G** (54%), and **3H** (13%). After this, **3B** started decreasing in concentration and completely disappeared after 2.6 h while the concentrations of the other imines increased with time, giving **3F** (10%), **3G** (64%), and **3H** (26%). Interestingly, the concentration of **3G** decreased slightly after 2.6 h whereas those of **3F** and **3H** slightly increased, indicating that the components in the mixture were still able to exchange with each other, giving **3F** (16%), **3G** (53%), and **3H** (32%) at 22 h. After about 238 h, the concentration of **3G** had decreased to 29% while those of **3F** and **3H** had increased to 32% and 39%.



Scheme 5.6 The DCL formed from the 5 components **3**, **B**, **F**, **G**, **H** and its transformations with time.

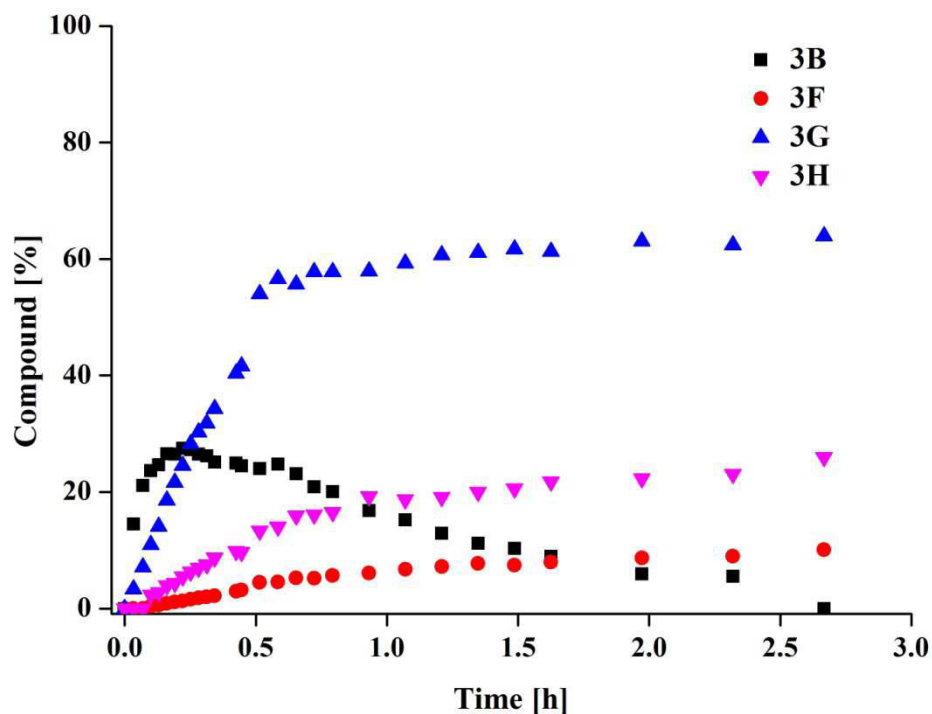


Figure 5.9 Kinetic traces of imines formation in CD_3OD in the mixture **3** + **B** + **F** + **G** + **H**. Error in $^1\text{H-NMR}$ integration: $\sim 5\%$.

In summary, for the study of imine formation for 2-pyridyl aldehyde **3** and different amino derivatives (**B**, **F**, **G**, and **H**) in pure CD₃OD at 25°C, the most reactive amino compound was pentylamine **B**, and **3B** was the kinetic product (*kinetic selectivity*). In contrast, the imines ultimately present in the DCL were **3F**, **3G**, and **3H**, so all three could be classified as thermodynamic products (*thermodynamic selectivity*). **3G**, in particular, was formed in higher %-composition than **3F** and **3H** at the beginning of the reaction (after 2 or 3 h) showing some kinetic selectivity to apply to its formation also. However, equilibrium had not been attained even after 10 days of reaction and further work is required to define the true equilibrium for this DCL.

5.2.2.2 Study of imine formation from salicylaldehyde (**4**)

Salicylaldehyde **4** has displayed remarkable imine formation and exchange properties in DCC studies.^[5,59–63] It can provide internal hydrogen bonding between the amine nitrogen and the hydroxyl group of the aldehyde that gives the resulting imine the ability to display dynamic covalent motion in DCC.^[5] In the following the kinetic and thermodynamic selectivity of aldehyde **4** toward different amino derivatives (pentylamine **B**, *O*-benzylhydroxylamine **F**, benzhydrazide **G**, and phenylhydrazine **H**) is examined.

Initially, the individual reactions forming imines **4B**, **4F**, **4G**, and **4H** were monitored in pure CD₃OD at 25°C (*Table 5.9*). The rate constants for imine formation were estimated from the initial changes in the system and were in the order **4B** > **4H** > **4F** > **4G**, indicating that pentylamine **B** was more reactive than the alpha-substituted nucleophiles towards **4**. Amongst the alpha nucleophiles, phenylhydrazine **H**, was the most reactive.

Table 5.9 The reaction time, %-composition and second order reaction rate constant for imine formation between salicylaldehyde **4** and several amino derivatives in CD₃OD at 25°C. The initial solution was equimolar (20 mM) in all the reactants.

Entry	Product	Product [%] ^{a)}	Time [h] ^{b)}	<i>k</i> [x 10 ⁻³ M ⁻¹ s ⁻¹] ^{c)}
1	4B	90	1.5	40.37
2	4F	76	4.8	8.17
3	4G	10	4.6	0.423
4	4H	75	4.6	17.5

^{a)} Error in ¹H-NMR integration: ±5%. ^{b)} Reaction time indicates the time when reactions were terminated. ^{c)} Rate constants were calculated from a fit to a unidirectional second-order reaction.

The competitive reaction between aldehyde **4** and the amines, **B**, **G**, **H** was followed at 25°C in a mixture where the initial concentration of each reactant was 20 mM (Figure 5.10a and Table 5.10, Entry 1). Three imines were detected immediately after mixing, being **3B** (44%), **3G** (6%), and **3H** (32%). The concentration of **3B** then decreased as a function of time to reach 2% at equilibrium. In contrast, the concentrations of both **3G** and **3H** increased, being **3G** (18%), **3H** (81%) at equilibrium after 3 h. Thus, **3B** was a kinetic product and **3G** and **3H** the thermodynamic products. The reaction of aldehyde **4** with amines **F**, **G**, **H** was followed similarly (Figure 5.10b and Table 5.10, Entry 2). **4F** and **4H** were detectable immediately after mixing at concentrations of 2% and 14%, respectively. Their concentrations at equilibrium (after 4 h) were **4F** (18%) and **4H** (81%). In contrast, **4G** barely formed, representing only 1% of the reaction mixture. Thus, the hydrazone **4H** was clearly the dominant component of this DCL.

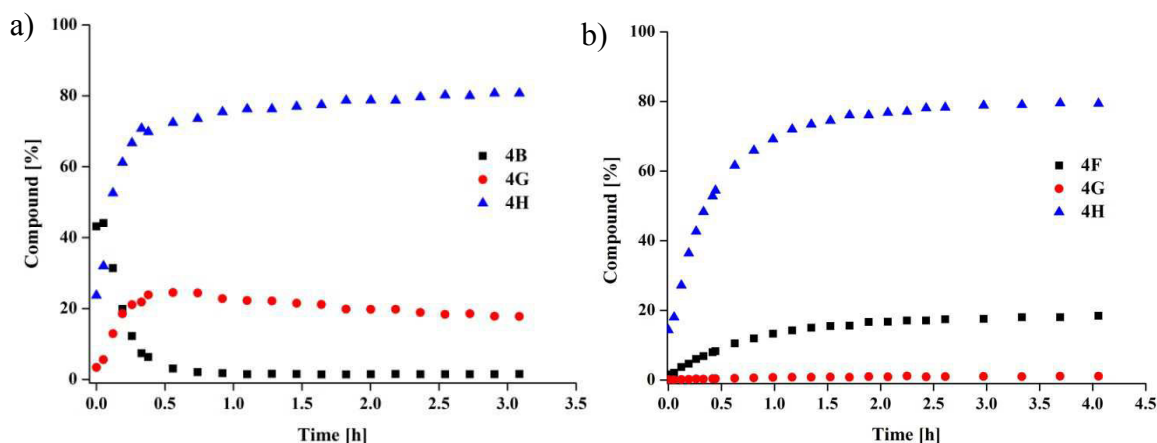


Figure 5.10 Kinetic traces of imine formation in CD_3OD in the reaction mixture of a) **4** + **B** + **G** + **H**, b) **4** + **F** + **G** + **H**. Error in 1H -NMR integration: ~5%.

The reaction of aldehyde **4** with four different amino derivatives (**B**, **F**, **G**, and **H**) was also examined under the same conditions (Figure 5.11a and Scheme 5.7). All of the imine compounds were found to be present immediately after mixing with relative %-compositions of **4B** (42%), **4F** (6%), **4G** (4%), and **4H** (23%). As the reaction progressed, **4B** was gradually lost and replaced by the other imines in the mixture, being undetectable after 0.6 h. Compounds **4F**, **4G**, and **4H** rose in concentration over time, attaining **4F** (27%), **4G** (16%), and **4H** (58%), at 1.4 h respectively. After 3.5 h, **4G** started to be lost, the concentrations then being **4F** (29%), **4G** (9%), and **4H** (63%), and after 21h only **4H** (65%) and **4F** (35%) were detectable as products. Thus, the most favored compound for

kinetic selection is the imine **4B** whereas for thermodynamic selection it is the hydrazone **4H**. The same DCL was then monitored in pure CD₃CN rather than CD₃OD (Figure 5.11b), again at 25°C. Only the imine **4B** was detectable immediately upon mixing and after 1 h, it began to be slowly consumed at the expense of growth of the other three imines **4F**, **4G**, and **4H**. Thus, similar DCL characteristics are observed in CD₃CN as in CD₃OD except that overall the reactions are slowed down dramatically.

Table 5.10 Time-dependence of the distribution of DCL components in the competitive reaction of mixed amino derivatives with salicylaldehyde **4**.

Entry	Reaction	Time [h] ^{a)}	Compound distribution [%] ^{b)}			
			3B	3F	3G	3H
1	4 + B + G + H	0.05	44	n.d. ^{c)}	6	32
		0.74	2	n.d. ^{c)}	24	74
		2.54	2	n.d. ^{c)}	18	81
2	4 + F + G + H	0.05	n.d. ^{c)}	2	- ^{d)}	14
		0.8	n.d. ^{c)}	12	1	66
		4.0	n.d. ^{c)}	18	1	81
3	4 + B + F + G + H	0.03	42	6	4	23
		1.4	- ^{d)}	27	16	58
		3.5	- ^{d)}	29	9	63
		21	- ^{d)}	35	- ^{d)}	65

^{a)} Reaction times indicate the certain time of the reaction. ^{b)} Error on ¹H-NMR integration: ±5%. ^{c)} n.d.; not determined. ^{d)} Compound not formed.

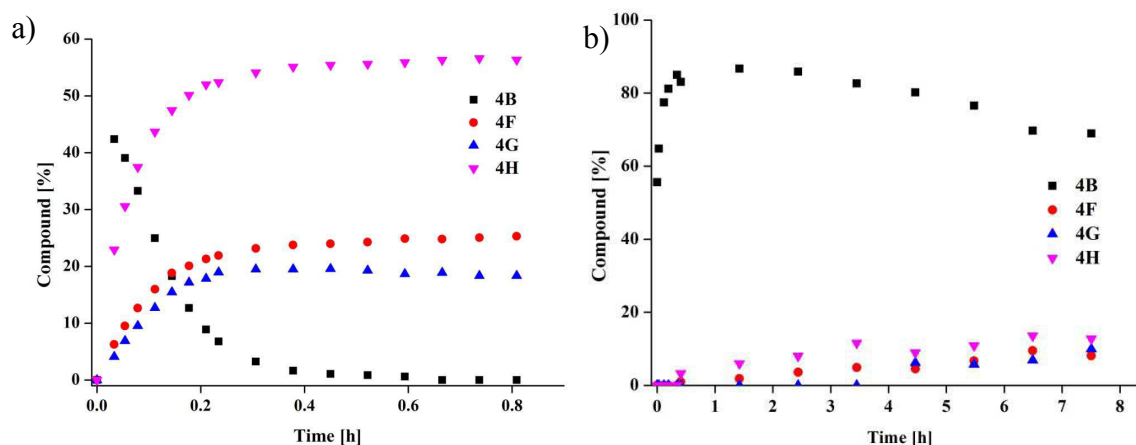
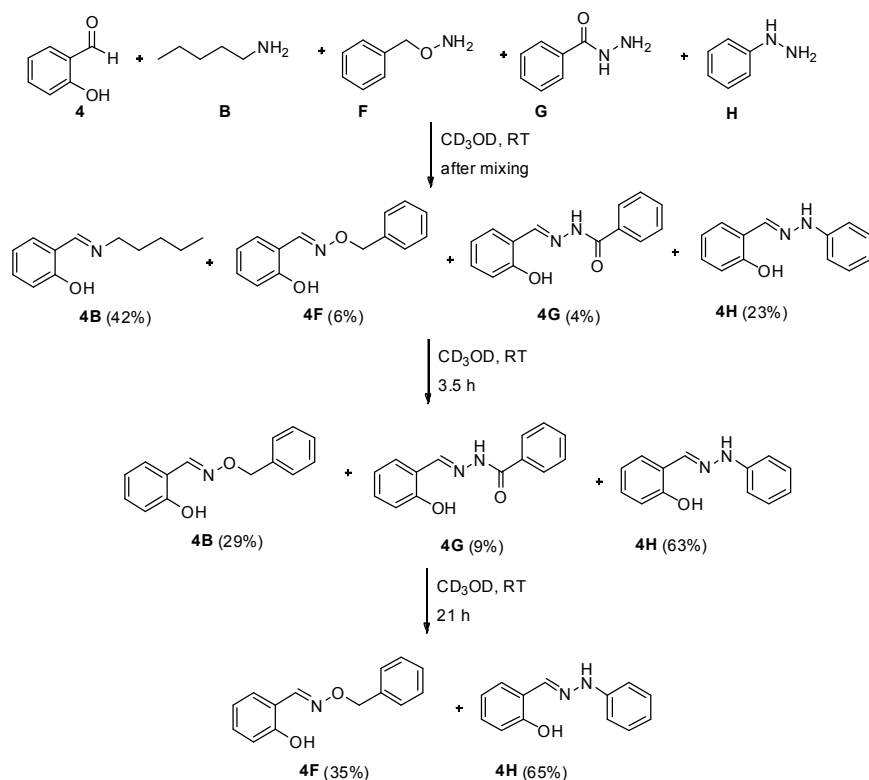


Figure 5.11 Kinetic traces for imine formation in a) CD₃OD, b) CD₃CN in a mixture of **4 + B + F + G + H** at 25°C. Error in ¹H-NMR integration: ~5%.



Scheme 5.7 Time-dependence of the composition of a DCL of the 5 components **4**, **B**, **F**, **G**, **H** and their four possible imine products **4B**, **4F**, **4G**, **4H** in CD_3OD at room temperature.

To summarize, imine formation from aldehyde **4** with different amino derivatives (**B**, **G**, **H**, and **G**) in CD_3OD at 25°C , was dominated by imine **4B** at early times indicating that this imine is the kinetic product. The most stable imines were **4F** and **4H** (the thermodynamic products). In contrast to the case of aldehyde **3**, compound **4G** did not form competitively in the presence of the four amino compounds (**B**, **F**, **G**, and **H**). This may mean that the intramolecular hydrogen bonding in **3G** is stronger than in **4G**.

5.2.3 The kinetic/thermodynamic selectivity of imine formation on aminoglycoside

An aminoglycoside is a molecule containing amino-modified sugars. These compounds are composed of an inositol moiety substituted with two amino or guanidino groups as well as with either sugars or amino sugars on the molecule, for instance, amikacin, arbekacin, gentamicin, kanamycin, neomycin, and streptomycin. They are used to treat infections caused by gram-negative bacteria and are also classified as bactericidal because of their interference with bacterial replication. All of the aminoglycoside antibiotics are highly toxic, requiring monitoring of blood serum levels at frequent

intervals and careful observation of the patient for signs of toxicity, particularly ototoxicity and nephrotoxicity.

Imine formation of the amino group of aminoglycosides has been reported in aqueous alcoholic media.^[64] In 2012, Dikiy *et al.* reported imine formation from kanamycin A and pyridoxal 5'-phosphate as well as with other aldehydes in aqueous solution.^[65] They found that imines were formed with an equimolar ratio of aldehydes with close to 100% yield at pH 7. They also defined the specific amino group at which imine formation occurred using ¹H-NMR spectroscopy. The DFT-GIAO B3LYP/6-31G (d) level was used to calculate the possible structure. They concluded that kanamycin A had the ability to form imine derivatives in high percent yields in an equimolar mixture with aldehydes.

In this investigation, the aminoglycoside neomycin was chosen as the substrate to study imine formation including its kinetic and thermodynamic selectivity. According to the structure of neomycin shown in *Figure 5.12*, there are six amino groups in one molecule indicating that there are six possible sites for imine formation. The aim of this work is to examine the possibility of forming imine bonds in aqueous solution with positional selectivity for neomycin in the presence of an aldehyde.

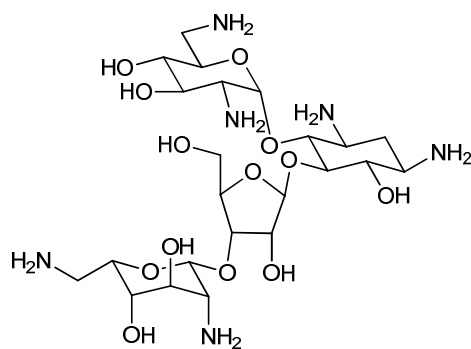
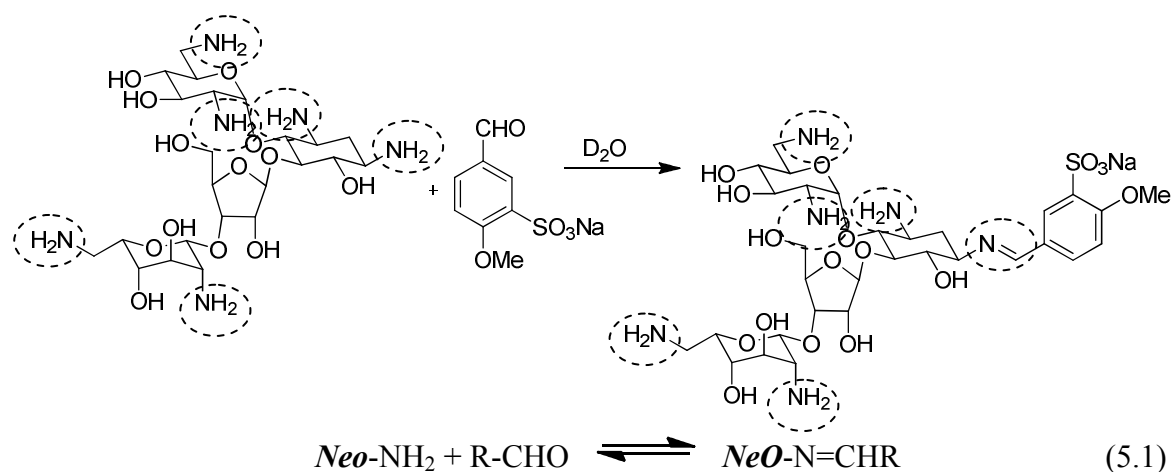


Figure 5.12 *The molecular structure of neomycin*

Imine formation from sulfonate aldehyde (1) and neomycin was followed at 25°C in D₂O where the initial concentrations of each reactant were equimolar (20 mM) as shown in *Scheme 5.8*. The ¹H-NMR spectrum (*Figure 5.13*), showed that the integration of each peak at 8.35, 8.12, 7.75, 7.21 ppm equaled 1.00. This preliminary result suggested that only one imine formed on this molecule.



Scheme 5.8 The reaction of neomycin and sulfonate aldehyde (**1**). The final concentration of neomycin was 20 mM and aldehyde, 20 mM.

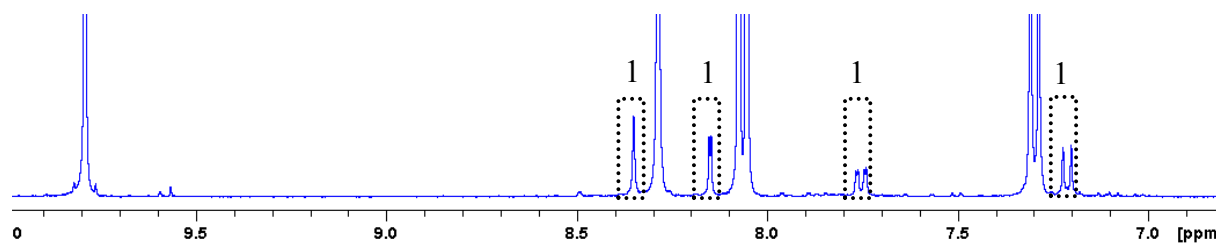


Figure 5.13 $^1\text{H-NMR}$ spectrum for the imine formation reaction of neomycin (20 mM) and sulfonate aldehyde **1** (20 mM) in D_2O .

Next, the mole ratios of neomycin to sulfonate aldehyde (**1**) in the reaction solution were varied from 1:0.25, 1:0.5, 1:0.75, 1:2, 1:3, 1:6, and 1:10. All of these experiments showed similar results as the previous experiment (1:1 ratio). This further confirms that imine formation occurs at only one amine site on the neomycin. The fact that imine formation between neomycin and sulfonate aldehyde (**1**) was selective for only one position suggests that it is an example of kinetic and thermodynamic selectivity of imine formation for the biological compound. Further exploration is required to confirm the exact position of imine formation of neomycin in this case.

5.3 Conclusions

The results described constitute a wide-ranging investigation of the kinetic and thermodynamic selectivity of imine formation arising from the reaction of an aldehyde with an amine.

1) Formation in aqueous phosphate buffer solutions having pD values of 5.0, 8.5 and 11.4 of imines derived from sulfonate aldehyde **1** and amino derivatives **B**, **C**, **D** and **E** occurs such that the conversion efficiency is in the order **1C**>**1D**>**1E** (**1B** was not formed) at pD 5.0, **1B**>**1E**>**1C** (**1D** was not formed) at pD 8.5, and **1B**>**1E**>**1C**>**1D** at pD 11.4. Imine formation from pyridoxal phosphate **2** and the same amino derivatives separately was not sensitive to pD and the conversion efficiency was in the order **2C**>**2E**>**2D**, **2B** not being a significant component of any equilibrium mixture.

2) The DCLs formed by sulfonate aldehyde **1** and the four amino derivatives **B**, **C**, **D**, and **E** in buffers at three different pD values reflected the fact that the kinetic and thermodynamic products under all conditions were **1C** and **1E**, respectively. The DCLs for pyridoxal phosphate **2** and the same amino derivatives under the same conditions showed similar trends, with **2C** and **2E** the kinetic and thermodynamic products. The preferred compounds in an acidic medium were oximes **1C** and **2C** whereas in a basic solution they were hydrazones **1E** and **2E**.

3) Imine formation from 2-pyridyl aldehyde **3** and salicylaldehyde **4** with each of the amino derivatives **B**, **F**, **G**, and **H** in organic solvents showed that the product stability was in the order **B** > **H** > **F** > **G**.

4) The DCL for equimolar mixtures of 2-pyridyl aldehyde **3** or salicylaldehyde **4** with different amino derivatives (**B**, **F**, **G**, and **H**), showed that the kinetic product was always imine **3B** or **4B** while the thermodynamic products were **3F** and **3H** or **4F**, and **4H**.

The knowledge gained here could be applied in future synthetic work, for instance, regioselective synthesis. It could also be applied to more complicated DCC systems involving amino derivatives, aldehydes, and imines.

5.4 References

- [1] S. J. Rowan, S. J. Cantrill, G. R. L. Cousins, J. K. M. Sanders, J. F. Stoddart, *Angew. Chem. Int. Ed.* **2002**, *41*, 898–952.
- [2] T. Maeda, H. Otsuka, A. Takahara, *Prog. Polym. Sci.* **2009**, *34*, 581–604.
- [3] M. N. Chaur, D. Collado, J.-M. Lehn, *Chem. – Eur. J.* **2011**, *17*, 248–258.
- [4] J.-M. Lehn, *Chem. Soc. Rev.* **2007**, *36*, 151–160.
- [5] P. Kovaříček, J.-M. Lehn, *J. Am. Chem. Soc.* **2012**, *134*, 9446–9455.
- [6] V. W. Cornish, K. M. Hahn, P. G. Schultz, *J. Am. Chem. Soc.* **1996**, *118*, 8150–8151.
- [7] Y. Zeng, T. N. C. Ramya, A. Dirksen, P. E. Dawson, J. C. Paulson, *Nat. Methods* **2009**, *6*, 207–209.
- [8] A. Dirksen, S. Dirksen, T. M. Hackeng, P. E. Dawson, *J. Am. Chem. Soc.* **2006**, *128*, 15602–15603.
- [9] M. A. Gauthier, H.-A. Klok, *Chem. Commun.* **2008**, 2591–2611.
- [10] S. Bandyopadhyay, X. Xia, A. Maiseiyeu, G. Mihai, S. Rajagopalan, D. Bong, *Macromolecules* **2012**, *45*, 6766–6773.
- [11] S. N. S. Alconcel, S. H. Kim, L. Tao, H. D. Maynard, *Macromol. Rapid Commun.* **2013**, *34*, 983–989.
- [12] S. Otto, R. L. Furlan, J. K. Sanders, *Curr. Opin. Chem. Biol.* **2002**, *6*, 321–327.
- [13] R. Nguyen, I. Huc, *Chem. Commun.* **2003**, 942–943.
- [14] M. G. Simpson, M. Pittelkow, S. P. Watson, J. K. M. Sanders, *Org. Biomol. Chem.* **2010**, *8*, 1181–1187.
- [15] W. R. Algar, D. E. Prasuhn, M. H. Stewart, T. L. Jennings, J. B. Blanco-Canosa, P. E. Dawson, I. L. Medintz, *Bioconjug. Chem.* **2011**, *22*, 825–858.
- [16] Z. Rodriguez-Docampo, S. Otto, *Chem. Commun.* **2008**, 5301–5303.
- [17] E. T. Kool, P. Crisalli, K. M. Chan, *Org. Lett.* **2014**, *16*, 1454–1457.
- [18] N. J. Fina, J. O. Edwards, *Int. J. Chem. Kinet.* **1973**, *5*, 1–26.
- [19] J. Kalia, R. T. Raines, *Angew. Chem. Int. Ed.* **2008**, *47*, 7523–7526.
- [20] S. A. Loskot, J. Zhang, J. M. Langenhan, *J. Org. Chem.* **2013**, *78*, 12189–12193.
- [21] W.P. Jencks, *Catalysis in Chemistry and Enzymology*, Dover, New York, **1987**, 133 - 146.
- [22] S. Patai, *The Chemistry of the Amino Group*, Wiley, London, **1968**, 350 - 364.

- [23] S. Patai, *The Chemistry of the Carbon-Nitrogen Double Bond.*, Wiley, London, **1970**, 64 - 83.
- [24] S. Patai, *The Chemistry of the Carbonyl Group.*, Wiley, London, **1966**, 600 - 619.
- [25] R. W. Layer, *Chem. Rev.* **1963**, *63*, 489–510.
- [26] C. Godoy-Alcántar, A. K. Yatsimirsky, J.-M. Lehn, *J. Phys. Org. Chem.* **2005**, *18*, 979–985.
- [27] D. M. Epstein, S. Choudhary, M. R. Churchill, K. M. Keil, A. V. Eliseev, J. R. Morrow, *Inorg. Chem.* **2001**, *40*, 1591–1596.
- [28] V. Goral, M. I. Nelen, A. V. Eliseev, J.-M. Lehn, *Proc. Natl. Acad. Sci.* **2001**, *98*, 1347–1352.
- [29] I. Huc, J.-M. Lehn, *Proc. Natl. Acad. Sci.* **1997**, *94*, 2106–2110.
- [30] O. Ramström, S. Lohmann, T. Bunyapaiboonsri, J.-M. Lehn, *Chem. – Eur. J.* **2004**, *10*, 1711–1715.
- [31] V. A. Polyakov, M. I. Nelen, N. Nazarpak-Kandlousy, A. D. Ryabov, A. V. Eliseev, *J. Phys. Org. Chem.* **1999**, *12*, 357–363.
- [32] J. R. Nitschke, J.-M. Lehn, *Proc. Natl. Acad. Sci.* **2003**, *100*, 11970–11974.
- [33] A. González-Álvarez, I. Alfonso, F. López-Ortiz, Á. Aguirre, S. García-Granda, V. Gotor, *Eur. J. Org. Chem.* **2004**, *2004*, 1117–1127.
- [34] J. B. Conant, P. D. Bartlett, *J. Am. Chem. Soc.* **1932**, *54*, 2881–2899.
- [35] W. P. Jencks, *J. Am. Chem. Soc.* **1959**, *81*, 475–481.
- [36] J. M. Sayer, W. P. Jencks, *J. Am. Chem. Soc.* **1973**, *95*, 5637–5649.
- [37] A. Williams, M. L. Bender, *J. Am. Chem. Soc.* **1966**, *88*, 2508–2513.
- [38] A. S. Stachissini, L. Do Amaral, *J. Org. Chem.* **1991**, *56*, 1419–1424.
- [39] A. K. Covington, M. Paabo, R. A. Robinson, R. G. Bates, *Anal. Chem.* **1968**, *40*, 700–706.
- [40] R. N. F. Thorneley, H. Diebler, *J. Am. Chem. Soc.* **1974**, *96*, 1072–1076.
- [41] J. L. Palmer, W. P. Jencks, *J. Am. Chem. Soc.* **1980**, *102*, 6466–6472.
- [42] V. M. Shanbhag, A. E. Martell, *Inorg. Chem.* **1990**, *29*, 1023–1031.
- [43] P. M. Robitaille, R. D. Scott, J. Wang, D. E. Metzler, *J. Am. Chem. Soc.* **1989**, *111*, 3034–3040.
- [44] J. M. Sánchez-Ruiz, J. M. Rodríguez-Pulido, J. Llor, M. Cortijo, *J. Chem. Soc. Perkin Trans. 2* **1982**, 1425–1428.
- [45] D. E. Metzler, E. E. Snell, *J. Am. Chem. Soc.* **1952**, *74*, 979–983.

- [46] N. Hafezi, J.-M. Lehn, *J. Am. Chem. Soc.* **2012**, *134*, 12861–12868.
- [47] S. Ulrich, E. Buhler, J.-M. Lehn, *New J. Chem.* **2009**, *33*, 271–292.
- [48] G. Vantomme, S. Jiang, J.-M. Lehn, *J. Am. Chem. Soc.* **2014**, *136*, 9509–9518.
- [49] A.-M. Stadler, *Isr. J. Chem.* **2013**, *53*, 113–121.
- [50] G. Vantomme, N. Hafezi, J.-M. Lehn, *Chem. Sci.* **2014**, *5*, 1475–1483.
- [51] G. Vantomme, J.-M. Lehn, *Angew. Chem. Int. Ed.* **2013**, *52*, 3940–3943.
- [52] J. K. Clegg, J. Harrowfield, Y. Kim, Y. H. Lee, J.-M. Lehn, W. T. Lim, P. Thuéry, *Dalton Trans.* **2012**, *41*, 4335–4357.
- [53] Jones, F. M., Arnett, E. M. in *Progress in Physical Organic Chemistry*, Vol 11 (Eds.: Streitwieser, JR, Taft, R.W.), John Wiley & Son, Canada, **1974**, pp. 263–323.
- [54] P. R. Campodónico, M. E. Aliaga, J. G. Santos, E. A. Castro, R. Contreras, *Chem. Phys. Lett.* **2010**, *488*, 86–89.
- [55] J. Mollin, F. Kasperek, J. Lasovsky, **1975**, *29*, 39–43.
- [56] Korpela, P.C., *Biochemistry of Vitamin B6: Proceedings of the 7th International Congress on Chemical and Biological Aspects of Vitamin B6 Catalysis*, Springer, **2003**, p. 461.
- [57] K. B. Wiberg, R. Glaser, *J. Am. Chem. Soc.* **1992**, *114*, 841–850.
- [58] M. Ciaccia, R. Cacciapaglia, P. Mencarelli, L. Mandolini, S. D. Stefano, *Chem. Sci.* **2013**, *4*, 2253–2261.
- [59] D. L. Leussing, B. E. Leach, *J. Am. Chem. Soc.* **1971**, *93*, 3377–3384.
- [60] C. M. Metzler, A. Cahill, D. E. Metzler, *J. Am. Chem. Soc.* **1980**, *102*, 6075–6082.
- [61] R. S. McQuate, D. L. Leussing, *J. Am. Chem. Soc.* **1975**, *97*, 5117–5125.
- [62] B. Klekota, M. H. Hammond, B. L. Miller, *Tetrahedron Lett.* **1997**, *38*, 8639–8642.
- [63] A. Star, I. Goldberg, B. Fuchs, *J. Organomet. Chem.* **2001**, *630*, 67–77.
- [64] B. N. Strunin, *Russ. Chem. Rev.* **1977**, *46*, 749.
- [65] Y. Fuentes-Martínez, C. Godoy-Alcántar, F. Medrano, A. Dikiy, *J. Phys. Org. Chem.* **2012**, *25*, 1395–1403.

CHAPTER 6
Conclusions and Perspective

Conclusions and Perspectives

This thesis has treated in detail dynamic covalent/combinatorial chemistry (DCC) focusing on the generation of dynamic covalent libraries (DCLs) via reversible exchange reactions of several types of compounds such as imines, *Knoevenagel* compounds, and ammonium salts. It began in the first chapter with a general introduction of the concept of dynamic chemistry as well as the important features of imine and *Knoevenagel* chemistry.

The main focus of the second chapter was the using of organocatalysts in the generation of DCLs via imine/imine (C=N/C=N), *Knoevenagel*/imine (C=C/C=N), and *Knoevenagel*/*Knoevenagel* (C=C/C=C) exchange reactions. The results showed that 10% mol L-proline as an organocatalyst facilitated DCL generation and most of the reactions reached a true equilibrium. The best conditions for imine exchange were 10 mol% L-proline in DMSO-*d*₆/D₂O 99/1 with 10 equiv. BIS-TRIS at room temperature, for which the imine exchange reaction was enhanced up to 22-fold compared to in the absence of catalyst. Imines derived from aliphatic/nucleophilic amines and highly electrophilic aldehydes were found to be the most suitable starting components, giving only the exchange products with no hydrolysis observed. For C=C/C=N exchange, the best conditions were 10 mol% L-proline in pure DMSO-*d*₆ at 60°C. L-proline accelerated the C=C/C=N exchange up to 22-fold and starting materials bearing electron-donating groups gave the least hydrolysis products during the cross-exchange. Finally, the C=C/C=C exchange benefitted from the same conditions as optimized for the C=C/C=N exchange, giving a 89-fold catalytic enhancement. In the latter case however, Michael-type adducts were formed during the exchange process. Once again, the efficiency of C=C/C=C exchange depended on the electron affinity of the starting materials.

In the third chapter, the DCC of *Knoevenagel*/imine (C=C/C=N) exchange involving *N,N*-dimethyl barbituric acid was evaluated. The exchange reactions were fast at room temperature in the absence of catalyst. The exchange mechanism is possibly a metathesis-like process via an azetidine intermediate. Furthermore, some of the *Knoevenagel* compounds formed gels in EtOH or MeOH and a preliminary gel selection study was undertaken based on C=C/C=N exchange.

In Chapter 4, novel DCC generation was reported based on nucleophilic substitution (S_N2/S_N2') component exchange of quaternary ammonium cations with tertiary amines. The exchange reactions between either *N*-allyl-*N,N*-anilinium salt or *N*-benzyl-*N,N*-anilinium salt and tertiary amines were conducted at 60°C to generate DCLs under thermodynamic and kinetic control and were accelerated using iodide as a nucleophilic catalyst. Moreover, microwave irradiation was used to assist the exchange reaction between pyridinium salts and pyridine derivatives. The generation of dynamic ionic liquids was also initiated.

Finally in the fifth chapter, the kinetic and thermodynamic selectivity of imine formation in DCC was described. In this investigation, two systems were chosen, sulfonate aldehyde and pyridoxal phosphate in aqueous solution at different pD (5.0, 8.5, 11.4), and 2-pyridyl aldehyde and salicylaldehyde in organic solvents. The results showed that oxime and hydrazone were the kinetic and thermodynamic products in aqueous solution. However, in organic solvent, the kinetic product was an imine derived from an aliphatic amine and the thermodynamic products were oxime and hydrazone.

Taken together the results of this thesis extend the fundamental knowledge of dynamic covalent chemistry, but they also clearly show its power to quickly generate molecular diversity. Furthermore, turning external parameters such as pH and catalyst completely modified the final composition of the molecular libraries, pointing the way to future adaptive and evolutive chemistry with great potential application in materials and biological sciences.

CHAPTER 7
Experimental Part

7.1 General Methods and Materials

7.1.1 Reagents

Entry	Reagents	Purity (%)	Supplier
1	n-Heptylamine	99	Sigma-Aldrich
2	2-Thiophenecarboxaldehyde	98	Sigma-Aldrich
3	Benzaldehydes	98	Sigma-Aldrich
4	Propylamine	98	Sigma-Aldrich
5	4-Pyridinecarboxaldehyde	97	Sigma-Aldrich
6	2-Pyridinecarboxaldehyde	99	Sigma-Aldrich
7	Cyclohexylamine	99	Sigma-Aldrich
8	4-(dimethylamino)benzaldehydes	99	Sigma-Aldrich
9	4-Nitrobenzaldehyde	98	Sigma-Aldrich
10	Malononitrile	99	Sigma-Aldrich
11	Barbituric acid	99	Sigma-Aldrich
12	1,3-Dimethyl barbituric acid	99	Sigma-Aldrich
13	Benzylamine	99	Sigma-Aldrich
14	Isopentylamine	99	Sigma-Aldrich
15	2-Bis(2-hydroxyethyl)amino-2-(hydroxymethyl)-1,3-propanediol (BIS-TRIS)	99	Sigma-Aldrich
16	Diethylaniline	99.5	Sigma-Aldrich
17	<i>p</i> -Anisidine	99	Sigma-Aldrich
18	4-Bromo- <i>N,N</i> -dimethylaniline	97	Sigma-Aldrich
19	<i>N,N</i> ,4-Trimethylaniline	99	Sigma-Aldrich
20	<i>N</i> -Ethylmethylamine	98	Sigma-Aldrich
21	<i>N,N</i> -Dimethylbenzylamine	99	Sigma-Aldrich
22	<i>N,N</i> -Dimethyl ethanolamine	99.5	Sigma-Aldrich
23	Allyl bromide	99	Sigma-Aldrich
24	Allyl iodide	98	Sigma-Aldrich
25	Potassium hexafluorophosphate	98	Sigma-Aldrich
26	Potassium trifluoromethanesulfonate	98	Sigma-Aldrich
27	4-Picoline	99	Sigma-Aldrich
28	Julolidene	97	Sigma-Aldrich
29	Ethyl cyanoacetate	98	Sigma-Aldrich
30	Malonic acid	99	Sigma-Aldrich
31	4-Ethoxybenzaldehyde	97	Sigma-Aldrich
32	1-Bromobutane	99	Sigma-Aldrich
33	1-Bromohexadecane	97	Sigma-Aldrich
34	<i>O</i> -Methoxylamine	98	Sigma-Aldrich
35	<i>O</i> -Benzylhydroxylamine	99	Sigma-Aldrich
36	Methylhydrazine	98	Sigma-Aldrich

Entry	Reagents	Purity (%)	Supplier
37	4-Dimethylaminopyridine	99	Sigma-Aldrich
38	Tetraethylammonium iodide	98	Sigma-Aldrich
39	Tetraethylammonium iodide	98	Sigma-Aldrich
40	Tetraethylammonium fluoride	98	Sigma-Aldrich
41	Phenylhydrazine	97	Sigma-Aldrich
42	Benzhydrazide	98	Sigma-Aldrich
43	<i>N,N</i> -Dimethylaniline	99	Alfa Aesar
44	Salicylaldehyde	99	Alfa Aesar
45	4-Methoxybenzaldehyde	98	Alfa Aesar
46	1-Heptylisocyanate	98	Alfa Aesar
47	Triethylamine	99	Riedel-de Haën
48	Benzyl bromide	99.5	Acros-organic
49	Pyridine	99	Acros-organic
50	Sodium-5-formyl-2-methoxybenzene sulfonate	96	Acros-organic
51	4-(tert-butylamino)pyridine	99	Janssen Chimica
52	L-proline	99	Avocado
53	Acetichydrazide	98	Avocado
54	4-Chlorobenzaldehyde	98	Lancaster

Deuterated solvents were purchased from *Euriso-TOP* and used without further purification except CDCl_3 , which was passed through a column of activated alumina (aluminium oxide 90 active basic). Anhydrous CH_2Cl_2 was obtained by passage through columns of activated molecular sieves. Deionized water was obtained from a *Millipore Elix 10* water purifier.

7.1.2 Instruments

● Nuclear Magnetic Resonance (NMR)

^1H -NMR spectra were recorded with a *Bruker Avance 400* MHz spectrometer and were referenced to the solvent. Chemical shifts are given in ppm. Residual solvent peaks were taken as reference (CHCl_3 : 7.24 ppm, DMSO: 2.50 ppm, CH_3CN 1.94 ppm and CH_3OH : 4.78 ppm). The coupling constants J are given in hertz. Peaks are described as singlet (s), doublet (d), triplet (t), quartet (q), quintet (quin), doublet of doublet (dd), and multiplet (m). The assigned proton is written in italics. Unless otherwise noted, spectra were recorded at 25°C.

^{13}C -NMR spectra were recorded with a *Bruker Avance 400* MHz spectrometer at 100 MHz. Chemical shifts are given in ppm. Residual solvent peaks were taken as reference (CHCl_3 : 77.0 ppm, DMSO: 39.43 ppm, CH_3CN 1.24 ppm and CH_3OH : 49.05)

2D NMR (COSY, NOESY) were recorded with a *Bruker Avance 400* MHz spectrometer.

● Mass Spectrometry

High-resolution Electrospray Ionization Mass spectrometry (HR-ESI-MS) was carried out using a *Bruker Micro TOF* mass spectrometer at the Service de Spectrometrie de Masse, Université de Strasbourg. The observed pattern was always confirmed to match the theoretical pattern. LC/MS was performed using reverse phase on a MSQ Plus mass spectrometer with Accela LC system from *Thermo Fisher Scientific* with a hypersil gold C8, 2 μm column.

● Elemental Analysis

Elemental analysis was performed at the Service de Microanalyse, Université de Strasbourg on a *Flash 2000* from *Thermo Fisher Scientific*. Data are given in percentage and were measured with a “Vario EL III” from Elementar to analyze simultaneously the elements C, H and N.

● pH Measurement

All pH and pD measurements were recorded directly after calibration of the pH-meter in aqueous pH 4, pH 7, and pH 10 buffer (Fluka) on a *Metler-Toledo Multi-Seven pHmeter* using a *Hamilton Spintrodemini*-probe.

● Melting points Measurement

Melting points were measured on a *Büchi B-540* apparatus.

● Microwave oven

The reactions were performed on a CEM Discovery microwave, with power up to 300 W, in a pressure vessel.

● UV/Vis spectra

UV-Vis spectra were recorded on a JASCO dual beam spectrophotometer.

● Column Chromatography

Column chromatography (CC) was performed using silica gel (Gedurun silica gel 60 (230 – 400 mesh, 40-63 μm , Merck) on a classic glass column.

7.2 Chapter 2, Organocatalysis of Exchange Processes between Knoevenagel and Imine Compounds in Dynamic Covalent Chemistry

7.2.1 Synthesis Procedure and Characterization

Standard Procedure for the synthesis of imines and Knoevenagel compounds

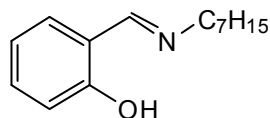
● *General procedure for the synthesis of imines.* Equimolar amounts of amine and aldehyde were dissolved in dry CH_2Cl_2 and MgSO_4 was added. The mixture was stirred at r.t. for 24 h – 5 days and the solid was filtered off. After drying or distillation in vacuum the products were isolated as colored oils or needles.

● *General procedure for the synthesis of Knoevenagel condensation products.* To 30 mL anhydrous ethanol was added barbituric acid (3.0 mmol), the corresponding substituted benzaldehyde (3.0 mmol), and L-proline in a catalytic amount (10%). The solution was then refluxed for 3-4 hr. The *Knoevenagel* condensation products that precipitated out of the cooled solution were filtered and washed with diethyl ether.

Characterization Part

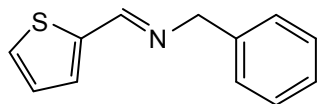
Imines compounds

1. (E)-2-((heptylimino)methyl)phenol (**1a**)^[1]

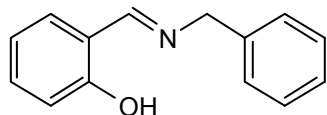


Yield: 2.08 g, 99%; yellow oil. $^1\text{H-NMR}$ (400 MHz, CDCl_3 , 25°C ; δ/ppm): 0.89 (t, $J = 6.72$ Hz, 3 H), 1.46–1.20 (m, 8 H), 1.75–1.65 (m, 2 H), 3.58 (t, $J = 6.82$ Hz, 2 H), 6.86 (t, $J = 7.44$ Hz, 1 H), 6.96 (d, $J = 8.25$ Hz, 1 H), 7.24 (d, $J = 6.32$ Hz, 1 H), 7.32–7.26 (m, 1 H), 8.33 (s, 1 H). $^{13}\text{C-NMR}$ (100 MHz, CDCl_3 , 25°C ; δ/ppm): 14.0, 22.6, 27.1, 29.0, 30.9, 31.7, 59.5, 117.0, 118.3, 118.8, 131.0, 132.0, 161.4, 164.4. ESI-MS: m/z: 220.2 (100%). HRMS (ESI, m/z): calcd. for $\text{C}_{14}\text{H}_{22}\text{NO}$ 220.170; found 220.170.

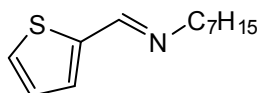
2. (E)-1-phenyl-N-(thiophen-2-ylmethylene)methanamine (**1b**)^[2]



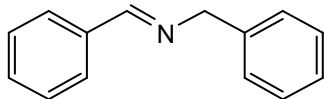
Yield: 1.93 g, 90%; yellow oil. $^1\text{H-NMR}$ (400 MHz, CDCl_3 , 25°C ; δ/ppm): 4.80 (s, 2 H), 7.15–6.96 (m, 1 H), 7.39–7.23 (m, 6 H), 7.41 (d, $J = 5.0$ Hz, 1 H), 8.46 (s, 1 H). $^{13}\text{C-NMR}$ (100 MHz, CDCl_3 , 25°C ; δ/ppm): 64.4, 127.0, 127.3, 128.0, 128.5, 129.0, 130.6, 139.0, 142.4, 155.2. ESI-MS: m/z: 202.1 (100%). HRMS (ESI, m/z): calcd. for $\text{C}_{12}\text{H}_{12}\text{NS}$ 202.068; found 202.070.

3. (*E*)-2-((benzylimino)methyl)phenol (**1c**)^[3]

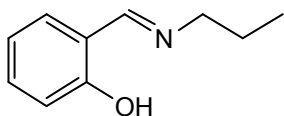
Yield: 0.143 g, 68%; yellow needles. ¹H-NMR (400 MHz, CDCl₃, 25°C; δ/ppm): 4.82 (s, 2 H), 6.89 (t, *J* = 7.5 Hz, 1 H), 6.97 (d, *J* = 8.3 Hz, 1 H), 7.40–7.25 (m, 7 H), 8.45 (s, 1 H), 13.41 (s, 1 H). ¹³C-NMR (100 MHz, CDCl₃, 25°C; δ/ppm): 63.2, 117.1, 118.6, 127.4, 127.8, 127.9, 128.7, 131.4, 132.4, 138.2, 161.2, 165.6. ESI-MS: *m/z*: 212.1 (100%). HRMS (ESI, *m/z*): calcd. for C₁₄H₁₄NO 212.107; found 212.107.

4. (*E*)-*N*-(thiophen-2-ylmethylene)heptan-1-amine (**1d**)^[4]

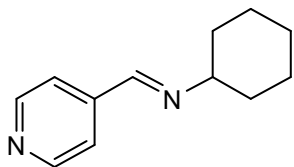
Yield: 1.68 g, 75%; yellow oil. ¹H-NMR (400 MHz, CDCl₃, 25°C; δ/ppm): 0.88 (t, *J* = 6.5 Hz, 3 H), 1.21–1.39 (m, 9 H), 1.64–1.72 (m, 2 H), 3.56 (t, *J* = 7.1 Hz, 2 H), 7.06 (t, *J* = 4.2 Hz, 1 H), 7.28 (d, *J* = 3.5 Hz, 2 H), 7.38 (d, *J* = 4.8 Hz, 2 H), 8.35 (s, 1 H). ESI-MS: *m/z*: 210.131 (100%). HRMS (ESI, *m/z*): calcd. for C₁₂H₂₀NS 210.131; found 210.131.

5. (*E*)-*N*-benzylidene-1-phenylmethanamine (**1f**)^[5]

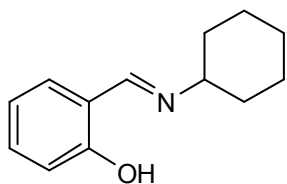
Yield: 0.463 g, 79 %; yellow oil. ¹H-NMR (400 MHz, DMSO-*d*₆, 25°C; δ/ppm): 4.78 (s, 2 H), 7.25–7.30 (m, 1 H), 7.33–7.38 (m, 4 H), 7.45–7.49 (m, 3 H), 7.78–7.81 (m, 2 H), 8.52 (s, 1 H).

6. (*E*)-2-((propylimino)methyl)phenol (**1h**)^[6]

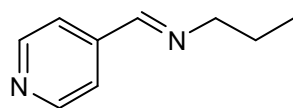
Yield: 3.39 g, 75 %; yellow oil. ¹H-NMR (400 MHz, DMSO-*d*₆, 25°C; δ/ppm): 0.92 (t, *J* = 7.34 Hz, 3 H), 1.64 (sext., *J* = 7.0 Hz, 2 H), 3.54 (t, *J* = 6.7 Hz, 2H), 6.94–6.78 (m, 2 H), 7.31 (t, *J* = 7.8 Hz, 1 H), 7.42 (d, *J* = 7.5 Hz, 1 H), 8.53 (s, 1 H). ESI-MS: *m/z*: 164.1 (100%). HRMS (ESI, *m/z*): calcd. for C₁₀H₁₄NO 164.107; found 164.107.

7. (*E*)-*N*-(pyridin-4-ylmethylene)cyclohexanamine (**1i**)^[7]

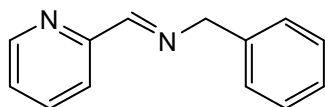
Yield: 1.99 g, quant.; yellow oil. ¹H-NMR (400 MHz, CDCl₃, 25°C; δ/ppm): 1.20–1.42 (m, 3 H), 1.57 (ddd, *J* = 15.0, 12.7, 3.2 Hz, 2 H), 1.76–1.63 (m, 3 H), 1.90–1.77 (m, 2 H), 3.47–2.92 (m, 1 H), 7.57 (d, *J* = 5.9 Hz, 2 H), 8.27 (s, 1 H), 8.65 (d, *J* = 5.9 Hz, 2 H). ¹³C-NMR (100 MHz, CDCl₃, 25°C; δ/ppm): 24.5, 25.5, 34.1, 70.0, 121.9, 143.3, 150.3, 156.5. ESI-MS: *m/z*: 189.1 (100%). HRMS (ESI, *m/z*): calcd. for C₁₂H₁₇N₂ 189.139; found 189.138.

8. (*E*)-2-((cyclohexylimino)methyl)phenol (**1j**)^[8]

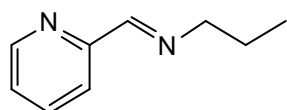
Yield: 1.80 g, 93%; yellow oil. ¹H-NMR (400 MHz, CDCl₃, 25°C; δ/ppm): 1.46–1.23 (m, 3 H), 1.61–1.49 (m, 2 H), 1.65 (d, *J* = 11.4 Hz, 1 H), 1.88–1.77 (m, 4 H), 3.24 (t, *J* = 9.8 Hz, 1 H), 6.86 (t, *J* = 7.4 Hz, 1 H), 6.95 (d, *J* = 8.3 Hz, 1 H), 7.24 (d, *J* = 7.6 Hz, 1 H), 7.32–7.26 (m, 1 H), 8.36 (s, 1 H), 13.83 (s, 1 H). ¹³C-NMR (100 MHz, CDCl₃, 25°C; δ/ppm): 24.3, 25.5, 34.3, 67.4, 117.0, 118.3, 118.9, 131.0, 131.9, 161.5. ESI-MS: *m/z*: 204.1 (100%). HRMS (ESI, *m/z*): calcd. for C₁₃H₁₈NO 204.138; found 204.137.

9. (*E*)-*N*-(pyridin-4-ylmethylene)propan-1-amine (**1k**)^[9]

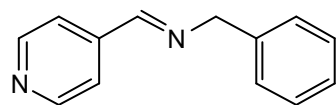
Yield: 1.49 g, 95%; yellow oil. ¹H-NMR (400 MHz, CDCl₃, 25°C; δ/ppm): 0.95 (t, *J* = 7.4 Hz, 3 H), 1.74 (sext., *J* = 7.20 Hz, 2 H), 3.62 (t, *J* = 6.80 Hz, 2 H), 7.58 (d, *J* = 5.3 Hz, 2 H), 8.25 (s, 1 H), 8.67 (d, *J* = 5.2 Hz, 2 H). ¹³C-NMR (100 MHz, CDCl₃, 25°C; δ/ppm): 60.6, 63.6, 73.6, 88.3, 93.6, 95.4, 97.6. ESI-MS: *m/z*: 149.1 (100%). HRMS (ESI, *m/z*): calcd. for C₉H₁₃N₂ 149.107; found 149.107.

10. (*E*)-1-phenyl-*N*-(pyridin-2-ylmethylene)methanamine (**1l**)^[10]

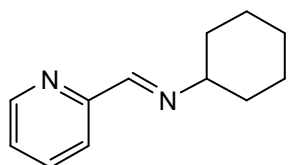
Yield: 0.947 g, 92%; yellow oil. ¹H-NMR (400 MHz, CDCl₃, 25°C; δ/ppm): 4.88 (s, 2 H), 7.30 (ddd, *J* = 4.9, 7.5, 15.8 Hz, 2 H), 7.35 (d, *J* = 4.2 Hz, 4 H), 7.74 (t, *J* = 7.7 Hz, 1 H), 8.07 (d, *J* = 7.9 Hz), 8.49 (s, 1 H), 8.65 (d, *J* = 4.6 Hz, 1 H). ¹³C-NMR (100 MHz, CDCl₃, 25°C; δ/ppm): 64.9, 121.3, 124.8, 127.1, 128.1, 128.5, 136.5, 138.6, 149.4, 154.5, 162.8. ESI-MS: *m/z*: 197.1 (100%). HRMS (ESI, *m/z*): calcd. for C₁₃H₁₃N₂ 197.107; found 197.108.

11. (*E*)-*N*-(pyridin-2-ylmethylene)propan-1-amine (**1m**)^[11]

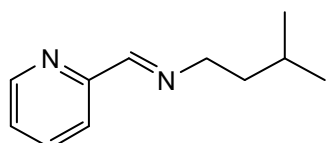
Yield: 0.357 g, 80%; orange oil. ¹H-NMR (400 MHz, DMSO-*d*₆, 25°C; δ/ppm): 0.95 (t, *J* = 7.4 Hz, 3 H), 1.74 (m, *J* = 7.2 Hz, 2 H), 3.63 (t, *J* = 6.9 Hz, 2 H), 7.28 (m, *J* = 1.1, 4.9, 7.4 Hz, 1 H), 7.72 (dt, *J* = 1.6, 7.7 Hz, 1 H), 7.97 (d, *J* = 7.9 Hz, 1 H), 8.36 (s, 1 H), 8.63 (d, *J* = 4.80 Hz, 1 H). ESI-MS: *m/z*: 149.1 (100%). HRMS (ESI, *m/z*): calcd. for C₉H₁₃N₂ 149.107; found 149.107.

12. (*E*)-1-phenyl-*N*-(pyridin-4-ylmethylene)methanamine (**1n**)^[12]

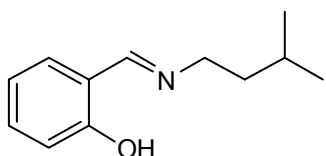
Yield: 1.87 g, 90%; yellow oil. ¹H-NMR (400 MHz, CDCl₃, 25°C; δ/ppm): 4.87 (s, 2 H), 7.39–7.24 (m, 5 H), 7.63 (d, *J* = 4.8 Hz, 2 H), 8.36 (s, 1 H), 8.69 (d, *J* = 4.9 Hz, 2 H). ¹³C-NMR (100 MHz, CDCl₃, 25°C; δ/ppm): 65.0, 122.0, 127.2, 128.0, 138.4, 142.8, 150.4, 159.8. ESI-MS: *m/z*: 197.1 (100%). HRMS (ESI, *m/z*): calcd. for C₁₃H₁₃N₂ 197.107; found 197.107.

13. (*E*)-*N*-(pyridin-2-ylmethylene)cyclohexanamine (**1o**)^[7]

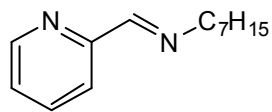
Yield: 1.80 g, 91%; orange oil. ¹H-NMR (400 MHz, CDCl₃, 25°C; δ/ppm): 1.31–1.17 (m, 1 H), 1.37 (dd, *J* = 25.0, 12.3 Hz, 2 H), 1.64–1.52 (m, 2 H), 1.68 (d, *J* = 12.5 Hz, 1 H), 1.79 (dd, *J* = 28.1, 12.2 Hz, 4 H), 3.38–3.19 (m, 1 H), 7.29 (d, *J* = 6.0 Hz, 1 H), 7.71 (t, *J* = 7.6 Hz, 1 H), 7.98 (d, *J* = 7.8 Hz, 1 H), 8.39 (s, 1 H), 8.63 (d, *J* = 4.3 Hz, 1 H). ¹³C-NMR (100 MHz, CDCl₃, 25°C; δ/ppm): 24.7, 25.6, 34.1, 68.6, 121.3, 124.5, 136.5, 149.3, 154.9, 159.5. ESI-MS: *m/z*: 189.1 (100%). HRMS (ESI, *m/z*): calcd. for C₁₂H₁₇N₂ 189.139; found 189.141.

14. (*E*)-3-methyl-*N*-(pyridin-2-ylmethylene)butan-1-amine (**1p**)

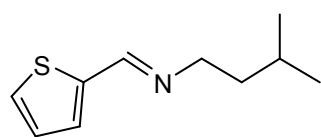
Yield: 0.492 g, 93%; orange oil. ¹H-NMR (400 MHz, DMSO-*d*₆, 25°C; δ/ppm): 0.97 (d, *J* = 6.5 Hz, 6 H), 1.63 (q, *J* = 7.2 Hz, 2 H), 1.71 (m, *J* = 6.7 Hz, 1 H), 3.71 (t, *J* = 7.3 Hz, 2 H), 7.32 (m, 1H), 7.75 (dt, *J* = 1.5, 7.7 Hz, 1 H), 8.00 (d, *J* = 7.9 Hz, 1 H), 8.40 (s, 1 H), 8.66 (d, *J* = 4.6 Hz, 1 H). ¹³C-NMR (100 MHz, CDCl₃, 25°C; δ/ppm): 22.4, 25.4, 39.3, 58.5, 120.3, 125.0, 136.8, 149.3, 154.2, 161.5. Anal. calc. for C₁₁H₁₆N₂ (176.258): C 74.96, H 9.15, N 15.89 ; found: C 74.87, H 9.16, N 15.69 ESI-MS: *m/z*: 177.1 (100%). HRMS (ESI, *m/z*): calcd. for C₁₁H₁₇N₂ 177.139; found 177.138.

15. (*E*)-2-((isopentylimino)methyl)phenol (**1q**)^[13]

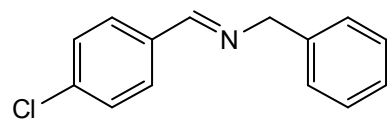
Yield: 0.489 g, 85%; orange oil. ¹H-NMR (400 MHz, DMSO-*d*₆, 25°C; δ/ppm): 0.99 (d, *J* = 6.6 Hz, 6 H), 1.62 (q, *J* = 7.1 Hz, 2 H), 1.76 (m, 1 H), 3.64 (t, *J* = 7.1 Hz, 2 H), 6.90 (t, *J* = 7.5 Hz, 1 H), 6.99 (d, *J* = 8.3 Hz, 1 H), 7.27 (d, *J* = 7.6 Hz, 1 H), 7.33 (t, *J* = 7.5 Hz, 1 H), 8.37 (s, 1 H), 13.73 (br s, 1 H). ESI-MS: *m/z*: 192.1 (100%). HRMS (ESI, *m/z*): calcd. for C₁₂H₁₈NO 192.138; found 192.139.

16. (*E*)-*N*-(pyridin-2-ylmethylene)heptan-1-amine (**1r**)^[14]

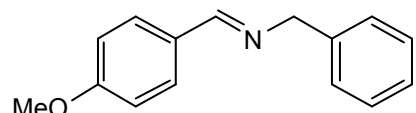
Yield: 0.368 g, 86%; brown oil. ¹H-NMR (400 MHz, DMSO-*d*₆, 25°C; δ/ppm): 0.84 (t, *J* = 6.8 Hz, 3 H), 1.36–1.13 (m, 8 H), 1.68–1.52 (m, 2 H), 3.61 (t, *J* = 6.4 Hz, 2 H), 7.55–7.31 (m, 1 H), 7.85 (dt, *J* = 7.7, 1.6 Hz, 1 H), 7.94 (d, *J* = 7.8 Hz, 1 H), 8.32 (s, 1 H), 8.62 (d, *J* = 4.8 Hz, 1 H). ESI-MS: *m/z*: 205.2 (100%). HRMS (ESI, *m/z*): calcd. for C₁₃H₂₁N₂ 205.170; found 205.170.

17. (*E*)-3-methyl-*N*-(thiophen-2-ylmethylene)butan-1-amine (**1s**)^[4]

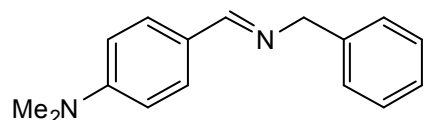
Yield: 0.314 g, 81%; yellow oil. ¹H-NMR (400 MHz, DMSO-*d*₆, 25°C; δ/ppm): 0.90 (dd, *J* = 6.5, 3.3 Hz, 6 H), 1.46 (dd, *J* = 14.0, 7.0 Hz, 2 H), 1.60 (dt, *J* = 13.3, 6.7 Hz, 1 H), 3.51 (t, *J* = 7.02 Hz, 2 H), 7.27–6.99 (m, 1 H), 7.43 (d, *J* = 2.9 Hz, 1 H), 7.63 (d, *J* = 4.8 Hz, 1 H), 8.46 (s, 1 H). ESI-MS: *m/z*: 182.1 (100%). HRMS (ESI, *m/z*): calcd. for C₁₀H₁₆NS 182.100; found 182.101.

18. (*E*)-*N*-(4-chlorobenzylidene)-1-phenylmethanamine (**1t**)^[15]

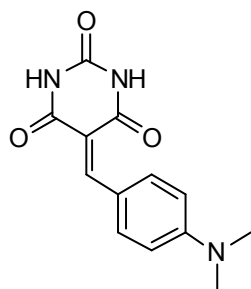
Yield: 0.592 mg, 86%; white oil. ¹H-NMR (400 MHz, CDCl₃, 25°C; δ/ppm) 4.80 (s, 2 H), 7.38–7.25 (m, 7 H), 7.70 (d, *J* = 8.4 Hz, 2H), 8.34 (s, 1 H, N=CH). ¹³C NMR (100 MHz, CDCl₃, 25°C; δ/ppm): 65.2, 127.3, 128.2, 128.7, 129.1, 129.7, 134.9, 136.9, 139.3, 160.7.

19. (*E*)-*N*-(4-methoxybenzylidene)-1-phenylmethanamine (**1u**)^[16]

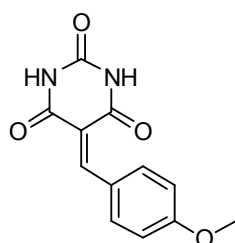
Yield: 2.308 g, 93%; pale yellow solid. ¹H-NMR (400 MHz, CDCl₃, 25°C; δ/ppm) 3.88 (s, 3 H), 4.83 (s, 2 H), 6.96 (d, *J* = 9.1 Hz, 2 H), 7.31–7.26 (m, 1 H), 7.39–7.34 (m, 4 H), 7.76 (d, *J* = 8.4 Hz, 2 H), 8.36 (s, 1 H, N=CH). ¹³C NMR (100 MHz, CDCl₃, 25°C; δ/ppm): 55.6, 65.2, 114.2, 127.1, 128.2, 128.7, 129.4, 130.0, 139.8, 161.5, 161.9.

20. (*E*)-4-((benzylimino)methyl)-*N,N*-dimethylaniline (**1v**)^[17]

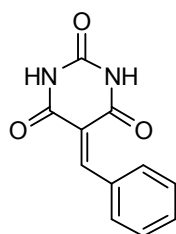
Yield: 0.698 g, 98%; pale yellow solid. ¹H-NMR (400 MHz, CDCl₃, 25°C; δ/ppm): 2.99 (s, NMe₂, 6 H), 4.74 (s, 2 H), 6.68 (d, *J* = 8.8 Hz, 2 H), 7.21 (m, 1 H), 7.31 (d, *J* = 4.4 Hz, 4 H), 7.64 (d, *J* = 8.7 Hz, 2 H), 8.25 (s, 1 H, N=CH). ¹³C NMR (100 MHz, CDCl₃, 25°C; δ/ppm): 40.4, 65.2, 111.8, 124.6, 126.9, 128.1, 128.6, 129.9, 140.3, 152.3, 162.2.

Knoevenagel Compounds1. 5-(4-(dimethylamino)benzylidene)pyrimidine-2,4,6(1H,3H,5H)-trione (**2a**)^[18]

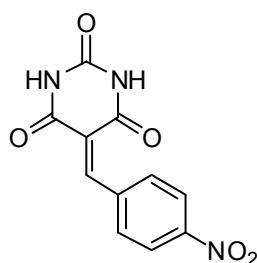
Yield: 0.620 g, 80%; orange solids. M.p.: 259-260 °C, lit m.p. 262-263 °C. ¹H-NMR (400 MHz, DMSO-*d*₆, 25°C; δ/ppm): 3.12 (s, 6 H), 6.80 (d, *J* = 9.3 Hz, 2 H), 8.15 (s, 1 H), 8.43 (d, *J* = 9.3 Hz, 2 H), 10.92 (s, 1 H), 11.05 (s, 1 H). ¹³C-NMR (100 MHz, DMSO-*d*₆, 25°C; δ/ppm): 109.5, 111.2, 119.9, 138.9, 150.3, 154.1, 155.4, 162.7, 164.6.

2. 5-(4-methoxybenzylidene)pyrimidine-2,4,6(1H,3H,5H)-trione (**2b**)^[19]

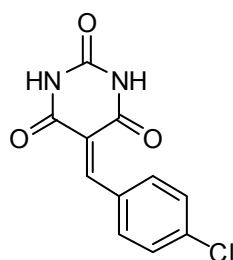
Yield: 0.622 g, 90%; yellow solids. M.p.: 278 °C, lit m.p. 276 °C. ¹H-NMR (400 MHz, DMSO-*d*₆, 25°C; δ/ppm): 3.88 (s, 3 H), 7.07 (d, *J* = 9.1 Hz, 2 H), 8.25 (s, 1 H), 8.37 (d, *J* = 8.9 Hz, 2 H), 11.17 (s, 1 H), 11.29 (s, 1 H). ¹³C-NMR (100 MHz, DMSO-*d*₆, 25°C; δ/ppm): 55.7, 113.9, 115.5, 125.1, 137.4, 150.2, 154.9, 162.1, 163.4, 163.9.

3. 5-benzylidenepyrimidine-2,4,6(1H,3H,5H)-trione (**2c**)^[20]

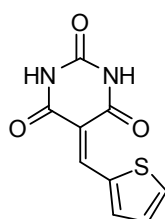
Yield: 0.261 g, 40%. White solids. ¹H-NMR (400 MHz, DMSO-*d*₆, 25°C; δ/ppm): 7.45 – 7.56 (*m*, 3H); 8.08 (*d*, *J* = 7.6, 2 H); 8.28 (*s*, 1H), 11.23 (*s*, 1H); 11.39 (*s*, 1H). ¹³C-NMR (100 MHz, DMSO-*d*₆, 25°C; δ/ppm): 119.1, 128.0, 132.2, 132.6, 133.0, 150.2, 154.6, 161.5, 163.3.

4. 5-(4-nitrobenzylidene)pyrimidine-2,4,6(1H,3H,5H)-trione (**2d**)^[20]

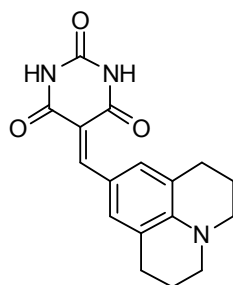
Yield: 0.72 g, 92%. Pale yellow solids. ¹H-NMR (400 MHz, DMSO-*d*₆, 25°C; δ/ppm): 8.02 (*d*, *J* = 8.8, 2 H); 8.25 (*d*, *J* = 9.0, 2 H); 8.33 (*s*, 1H); 11.32 (*s*, 1H); 11.49 (*s*, 1H). ¹³C-NMR (100 MHz, DMSO-*d*₆, 25°C; δ/ppm): 122.3, 122.6, 132.2, 140.0, 148.0, 150.2, 151.1, 161.1.

5. 5-(4-chlorobenzylidene)pyrimidine-2,4,6(1H,3H,5H)-trione (**2e**)^[19]

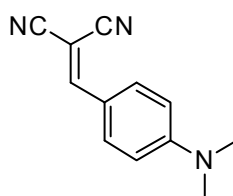
Yield: 0.505 g, 67%; yellow solids. M.p.: 282°C, lit m.p. 280°C. ¹H-NMR (400 MHz, DMSO-*d*₆, 25°C; δ/ppm): 7.54 (d, *J* = 8.8 Hz, 2 H), 8.08 (d, *J* = 8.6 Hz, 2 H), 8.25 (s, 1 H), 11.27 (s, 1 H), 11.41 (s, 1 H). ¹³C-NMR (100 MHz, DMSO-*d*₆, 25°C; δ/ppm): 119.7, 131.6, 134.6, 136.7, 150.1, 152.9, 161.5, 163.2.

6. 5-(thiophen-2-ylmethylene)pyrimidine-2,4,6(1H,3H,5H)-trione (**2f**)^[19]

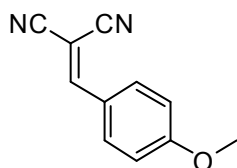
Yield: 0.580 g, 87%; brown yellow solids. M.p.: 275°C, lit m.p. 273°C. ¹H-NMR (400 MHz, DMSO-*d*₆, 25°C; δ/ppm): 7.36 (dd, *J* = 5.0 Hz, 1 H), 8.18 (d, *J* = 3.9 Hz, 1 H), 8.28 (d, *J* = 4.6 Hz, 1 H), 8.57 (s, 1 H), 11.26 (s, 1 H), 11.30 (s, 1 H). ¹³C-NMR (100 MHz, DMSO-*d*₆, 25°C; δ/ppm): 111.6, 128.3, 136.3, 142.1, 145.7, 145.8, 150.2, 162.9, 163.5.

7. 5-((1,2,3,5,6,7-hexahydropyrido[3,2,1-*ij*]quinolin-9-yl)methylene)pyrimidine-2,4,6(1H,3H,5H)-trione (**2g**)

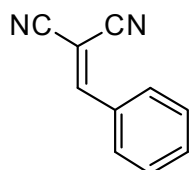
Yield: 0.82 g, 88%. red solids. ¹H-NMR (400 MHz, DMSO-*d*₆, 25°C; δ/ppm): 1.89 (*t*, *J* = 5.5, 4 H); 2.68 (*t*, *J* = 5.7, 4H); 3.38 (*t*, *J* = 6.2, 4H); 7.99 (*s*, 1H); 8.06 (*s*, 2H); 10.77 (*s*, 1H); 10.92 (*s*, 1H). ¹³C-NMR (100 MHz, DMSO-*d*₆, 25°C; δ/ppm): 20.5, 26.9, 49.7, 107.3, 119.2, 120.0, 136.6, 148.8, 150.4, 154.9, 162.7, 164.9.

8. 2-(4-(dimethylamino)benzylidene)malononitrile (**3a**)^[21]

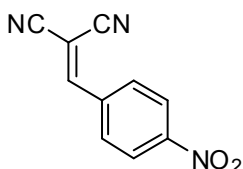
Yield: 0.410 g, 70%. Orange solids. M.p. 177 – 181°C, lit m.p. 180 – 182°C). ¹H-NMR (400 MHz, DMSO-*d*₆, 25°C; δ/ppm): 3.10 (*s*, 6 H); 6.86 (*d*, *J* = 9.3, 2 H); 7.84 (*d*, *J* = 9.4, 1 H); 8.05 (*s*, 1H). ¹³C-NMR (100 MHz, DMSO-*d*₆, 25°C; δ/ppm): 39.6, 68.6, 111.8, 115.5, 116.2, 118.7, 133.6, 154.3, 158.9.

9. 2-(4-methoxybenzylidene)malononitrile (**3b**)^[22]

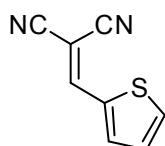
Yield: 0.45 g, 80%. Pale yellow solids. ¹H-NMR (400 MHz, DMSO-*d*₆, 25°C; δ/ppm): 3.89 (s, 3 H); 7.20 (d, *J* = 8.8, 2 H); 7.98 (d, *J* = 9.1, 2 H); 8.41 (s, 1 H). ¹³C-NMR (100 MHz, DMSO-*d*₆, 25°C; δ/ppm): 55.9, 76.9, 113.9, 114.8, 115.2, 124.1, 133.3, 160.4, 164.3.

10. 2-benzylidenemalononitrile (**3c**)^[23,24]

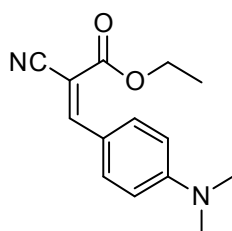
Yield: 0.128 g, 83%. White solids. M.p. 84 – 85° ([23]: 83.5 – 84°). ¹H-NMR (400 MHz, DMSO-*d*₆, 25°C; δ/ppm): 7.61 – 7.72 (m, 3H); 7.96 (d, *J* = 7.8, 2H); 8.56 (s, 1H). ¹³C-NMR (100 MHz, DMSO-*d*₆, 25°C; δ/ppm): 81.6, 113.2, 114.2, 129.5, 130.5, 131.3, 134.3, 161.6.

11. 2-(4-nitrobenzylidene)malononitrile (**3d**)^[24]

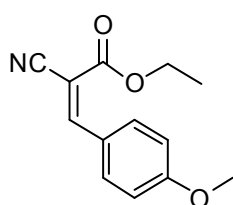
Yield: 0.49 g; 82%. Yellow solids. M.p. 157 – 158° ([24]: 159 – 160°). ¹H-NMR (400 MHz, DMSO-*d*₆, 25°C; δ/ppm): 8.13 (d, *J* = 9.1, 2 H); 8.44 (d, *J* = 8.6, 2 H); 8.73 (s, 1 H). ¹³C NMR (100 MHz, DMSO-*d*₆, 25°C; δ/ppm): 85.9, 112.5, 113.6, 124.4, 131.4, 136.7, 149.7, 159.3.

12. 2-(thiophen-2-ylmethylene)malononitrile (**3e**)^[25]

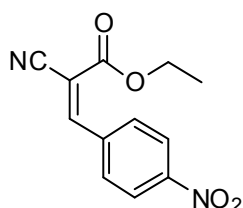
Yield: 0.191 g, 40%. Brown yellow solids. ¹H-NMR (400 MHz, DMSO-*d*₆, 25°C; δ/ppm): 7.40 (d, *J* = 4.1 Hz, 1 H); 7.95 (d, *J* = 3.6 Hz, 1 H); 8.30 (d, *J* = 4.3 Hz, 1 H); 8.74 (s, 1 H). ¹³C-NMR (100 MHz, DMSO-*d*₆, 25°C; δ/ppm): 75.9, 113.6, 114.3, 129.2, 135.3, 138.6, 140.4, 153.4.

13. Ethyl 2-cyano-3-(4-(dimethylamino)phenyl)acrylate (**3f**)^[26]

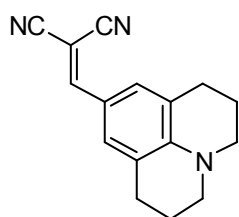
Yield: 0.289 g, 39%. Orange solid. ¹H-NMR (400 MHz, DMSO-*d*₆, 25°C; δ/ppm): 1.28 (t, *J* = 7.0 Hz, 3H); 3.09 (s, 6H), 4.26 (q, *J* = 7.2 Hz, 2H); 6.84 (d, *J* = 9.3 Hz, 2H); 7.96 (d, *J* = 9.1 Hz, 2H); 8.12 (s, 1H). ¹³C-NMR (100 MHz, DMSO-*d*₆, 25°C; δ/ppm): 14.1, 61.4, 92.0, 111.7, 117.5, 118.3, 133.8, 153.7, 154.1, 163.4.

14. Ethyl 2-cyano-3-(4-methoxyphenyl)acrylate (**3g**)^[27]

Yield: 0.464 g, 67%. Yellow solid. ¹H-NMR (400 MHz, DMSO-*d*₆, 25°C; δ/ppm): 1.30 (t, *J* = 7.1 Hz, 3H); 3.87 (s, 3H); 4.30 (q, *J* = 7.0 Hz, 2H); 7.16 (d, *J* = 9.0 Hz, 2H); 8.09 (d, *J* = 9.0 Hz, 2H); 8.32 (s, 1H). ¹³C-NMR (100 MHz, DMSO-*d*₆, 25°C; δ/ppm): 13.9, 55.7, 62.0, 98.5, 114.9, 116.2, 123.9, 133.5, 154.4, 162.3, 163.5.

15. Ethyl-2-cyano-3-(4-nitrophenyl)acrylate (**3h**)^[27]

Yield: 0.633 g, 85%. Yellow solid. ¹H-NMR (400 MHz, DMSO-*d*₆, 25°C; δ/ppm): 1.32 (t, *J* = 7.2 Hz, 3H); 4.35 (q, *J* = 7.0 Hz, 2H); 8.23 (d, *J* = 8.9 Hz, 2H), 8.41 (d, *J* = 8.9 Hz, 2H), 8.57 (s, 1H). ¹³C-NMR (100 MHz, DMSO-*d*₆, 25°C; δ/ppm): 13.9, 62.7, 106.7, 114.9, 124.1, 131.6, 137.2, 149.2, 152.6, 161.1.

16. 2-((1,2,3,5,6,7-hexahydropyrido[3,2-*l*-*ij*]quinolin-9-yl)methylene)malononitrile (**3i**)^[28]

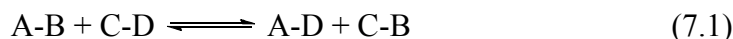
Yield: 0.49 g, 86%. Orange solid. ¹H-NMR (400 MHz, DMSO-*d*₆, 25°C; δ/ppm): 1.71 (q, *J* = 5.6 Hz, 4H); 2.35 (m, 4H); 3.21 (t, *J* = 5.5 Hz, 4H), 7.26 (s, 2H), 7.61 (s, 1H). ¹³C-NMR (100 MHz, DMSO-*d*₆, 25°C; δ/ppm): 20.3, 26.9, 49.6, 65.7, 116.1, 116.9, 117.8, 120.7, 130.8, 148.6, 157.6.

7.2.2 Study of Imine/Imine (C=N/C=N) exchange

- *General procedure for C=N/C=N exchange.* All reactions with 2 imines were carried out at r.t. with a final concentration of 19.35 mM and a total volume of 620 μL with 10 equiv. of BIS-TRIS to maintain a constant pH. For mixtures of 3 imines the final concentration was about 14.63 mM and the total volume 615 μL. All stock solutions of reactants and catalyst were 60 mM and had a total volume of 1 mL. The BIS-TRIS stock solution was 600 mM.

- *General procedure for C=N/C=N exchange of 2 imines.* A NMR tube was first charged with 200 μL of BIS-TRIS stock solution (600 mM in DMSO-*d*₆/D₂O, 99/1). For the catalyzed reaction, 20 μL of a L-proline stock solution (60 mM in DMSO-*d*₆/D₂O, 99/1) was added. For the uncatalyzed reaction, 20 μL DMSO-*d*₆/D₂O, 99/1 was mixed with 200 μL of BIS-TRIS stock solution (600 mM in DMSO-*d*₆/D₂O, 99/1) in another NMR tube. To these prepared solutions, 200 μL of each imine solution (60 mM in DMSO-*d*₆/D₂O, 99/1) were added and the NMR spectra were measured immediately after mixing.

● *Kinetics of imine exchange (C=N/C=N) exchange.* The imine exchange reaction as following (Eq. (7.1)) could, in principle, occur as a single, concerted process passing through a four-membered-ring transition state^[29] and thus be considered as a reversible, second-order reaction.



This would be a thermally forbidden process by Woodward-Hoffmann rules and in fact there is no evidence that the reaction will occur at a significant rate in the absence of an acid or a nucleophilic catalyst (including water). Attempts to fit the present data to the equation for a reversible second-order reaction were unsuccessful (the Rorabacher equation^[30] plot being far from linear) and, as seen in a study of a simpler catalyzed imine exchange reaction,^[31] the data actually provided a good fit to a reversible first-order reaction. Given that the imine exchange reaction is at least formally bimolecular, the reason for the observation of reversible first-order behavior deserves a closer explanation.

For a true reversible first-order reaction:



The equilibrium constant for the reaction (K_{eq}) is:

$$K_{\text{eq}} = [\text{B}]_{\text{eq}}/[\text{A}]_{\text{eq}} = k_f/k_r \quad (7.3)$$

And rate law can be written as

$$R = -d[\text{A}]/dt = k_f[\text{A}]_t - k_b[\text{B}]_t \quad (7.4)$$

Where $[\text{A}]_{\text{eq}}$ and $[\text{B}]_{\text{eq}}$ are the concentration of $[\text{A}]$ and $[\text{B}]$ respectively at equilibrium, and $[\text{A}]_t$ and $[\text{B}]_t$ are the concentration of $[\text{A}]$ and $[\text{B}]$, respectively, at any given time t . If the initial conditions are $[\text{A}] = [\text{A}]_0$ and $[\text{B}] = [\text{B}]_0 = 0$, so that, by stoichiometry, $B_t = [\text{A}]_0 - [\text{A}]_t$, then

$$R = d[\text{A}]/dt = k_b([\text{A}]_0 - [\text{A}]_t) - k_f[\text{A}]_t = k_b[\text{A}]_0 - (k_f + k_b)[\text{A}]_t \quad (7.5)$$

Thus, this equation connects two variables ($[A]_t$ and t) and their measurement followed by fitting to this equation enables determination of the rate constants. The direct relationship between $[A]_t$ and t is obtained by integration of the rate equation, which takes the form after separation of the variables of

$$\int_{A_0}^{A_t} d[A]/(k_b[A]_0 - (k_f + k_b)[A]_t) = \int_0^t dt, \quad (7.6)$$

which becomes

$$\ln\{(k_f + k_b)[A]_t - k_b[A]_0\}/k_f[A]_0 = -(k_f + k_b)t, \text{ or} \quad (7.7)$$

$$\{(k_f + k_b)[A]_t - k_b[A]_0\}/k_f[A]_0 = e^{-(k_f + k_b)t}$$

when $t = \infty$, $[A]_t = [A]_{eq}$ and $e^{-\infty} = 0$, thus, this equation give

$$(k_f + k_b)[A]_{eq} = k_b[A]_0 \quad (7.8)$$

This is also clear directly from the equilibrium condition that the rates of the forward and backward reactions are equal, i.e. $k_f[A]_{eq} = k_b[B]_{eq} = k_b([A]_0 - [A]_{eq})$, leading to:

$$(k_f + k_b)[A]_t - k_b[A]_0 = \{(k_f + k_b)[A]_t - (k_f + k_b)[A]_{eq} = ([A]_t - [A]_{eq})(k_f + k_b)\} \quad (7.9)$$

And that $k_f[A]_0 = ([A]_0 - [A]_{eq})(k_f + k_b)$ so that, finally,

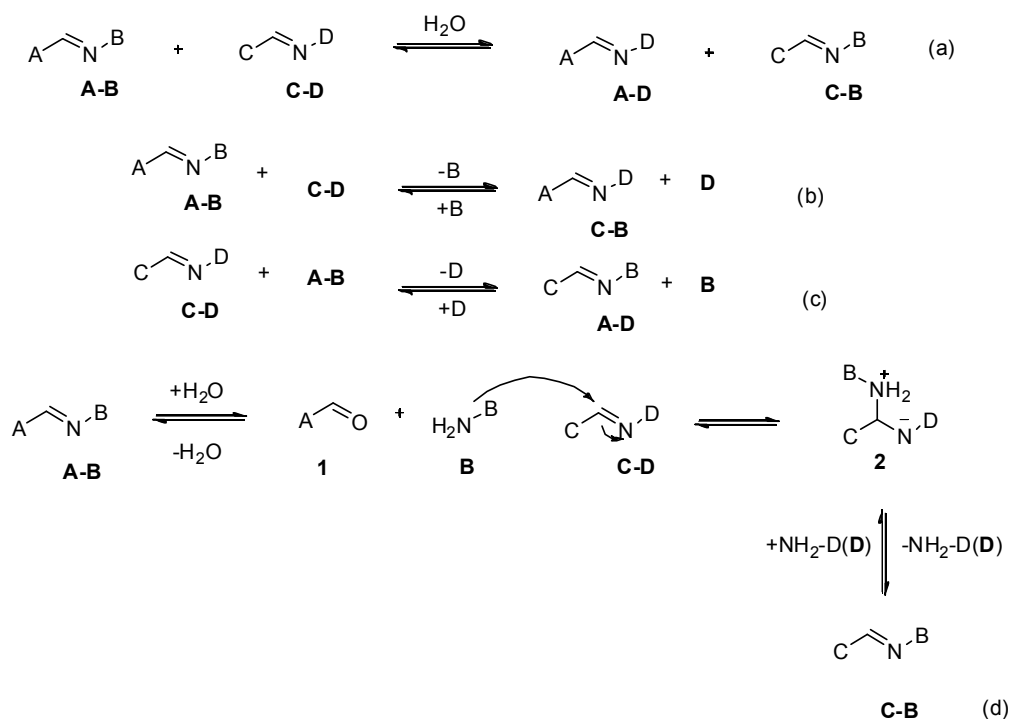
$$([A]_t - [A]_{eq})/([A]_0 - [A]_{eq}) = e^{-(k_f + k_b)t} \quad (7.10)$$

$$\text{Or equivalently } \ln \frac{([A]_t - [A]_{eq})}{([A]_0 - [A]_{eq})} = -(k_f + k_b)t \quad (7.11)$$

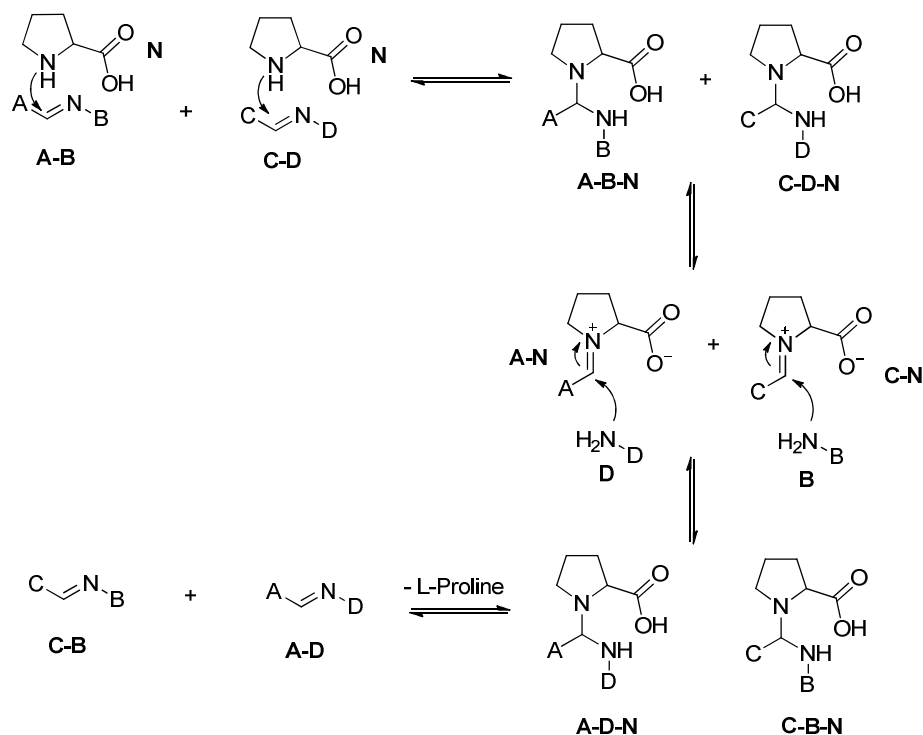
Thus the quantity $\ln([A]_t - [A]_{eq})$ should be linear as a function of time and indeed that for any parameter X (such as the integral of an NMR peak) proportional to the concentration of A, that $\ln([X]_t - [X]_e)$ should be a linear function of time (since the proportionality constant just adds another constant to the equation).

In earlier studies of the imine exchange,^[32,33] it was shown that the reaction is subject to catalysis by water, although not simply through hydrolysis of both reactant imines followed by reformation in the mixture of both reactant and product imines. Instead, it has been shown that amine attack on imines is much faster than that on carbonyl compounds, so that exchange occurs principally through the attack of some initially released amine upon residual imine(s), as shown in *Scheme 7.1*. The rate determining step in these reactions was proposed to be proton transfer within the aminal intermediates.

According to the imine exchange reaction in *Scheme 7.1*, a common feature of the two reversible reactions ((b) and (c)) is that the imine reactant in (b) is also a reactant in (c), and vice versa. Therefore, if a small amount of H₂O is present in a mixture of **A-B** and **C-D**, **A-B** will be hydrolyzed to liberate amine (**B**), then, it will react with imine **C-D** through the aminal-intermediate mechanism to provide an imine **C-B** as an exchange product. Similarly, **C-D** will be hydrolyzed to liberate amine (**D**), and **D** will then react with **A-B** to give **A-D** as the exchange product. The net result is that **A-D** and **C-B** gradually increase in the reaction mixture at the expense of **A-B** and **C-D**, respectively, until the two equilibria ((b) and (c)) are simultaneously established.

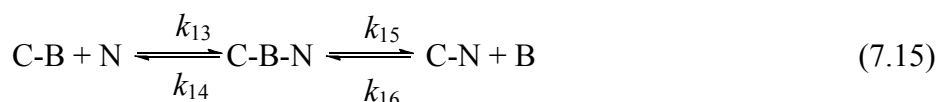
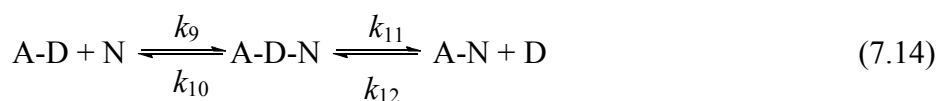
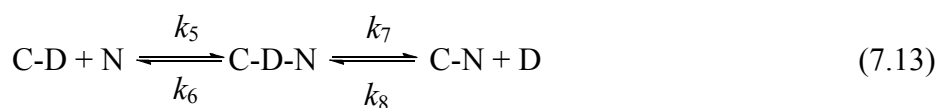
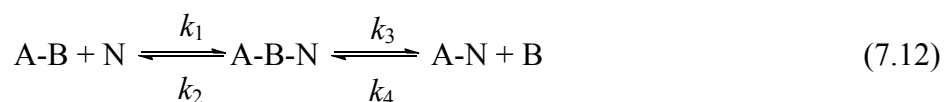


Scheme 7.1 The imine exchange mechanism in the absence of organocatalyst via hydrolysis and recondensation reaction (the water acts as a nucleophilic catalyst).

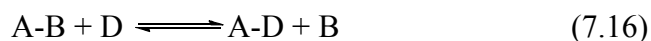


Scheme 7.2 The imine exchange mechanism in the presence of *L*-proline as a catalyst.

Next, if the imine exchange reaction above (*Scheme 7.2*) is considered to occur through catalysis by a nucleophile N where the nucleophile can undergo addition (followed by elimination) to all four reagents, a simplified reaction can be written as:



This is simplified in that proton transfers involved in the addition and elimination steps are not separated from the actual addition and elimination processes (following Mandolini,^[31] it would be assumed that the values of the overall rate constants would in fact be determined by the proton transfer rate constants) and also in that the direct reactions as following below are not included.



This doesn't affect greatly the conclusions that can be drawn from analysis of the above scheme. A standard treatment of complex reaction schemes such as that of equation (1) – (4) involves the use of the steady state approximation (SSA). This is based on the assumption that where reactive intermediates are involved, after a short initial period where their concentration rises, their concentration then stays effectively constant over the major period of the reaction. If the concentration of X as a function of time is constant, then of course $dX/dt = 0$. Note that this does not mean that the concentration must be very small, even though this appears to be true for all species other than A-B, C-D, A-D, and C-B in the imine exchange reaction.

Thus, applying the SSA to the reactive intermediate of equation (7.12) – (7.15) leads to

$$d[\text{A-B-N}]/dt = k_1[\text{A-B}][\text{N}] + k_4[\text{A-N}][\text{B}] - (k_2 + k_3)[\text{A-B-N}] = 0 \quad (7.18)$$

$$d[\text{C-D-N}]/dt = k_5[\text{C-B}][\text{N}] + k_8[\text{C-N}][\text{D}] - (k_6 + k_7)[\text{C-D-N}] = 0 \quad (7.19)$$

$$d[\text{A-D-N}]/dt = k_9[\text{A-D}][\text{N}] + k_{12}[\text{A-N}][\text{D}] - (k_{10} + k_{11})[\text{A-D-N}] = 0 \quad (7.20)$$

$$d[\text{C-B-N}]/dt = k_{13}[\text{C-B}][\text{N}] + k_{16}[\text{C-N}][\text{B}] - (k_{14} + k_{15})[\text{C-B-N}] = 0 \quad (7.21)$$

$$d[\text{B}]/dt = k_3[\text{A-B-N}] + k_{15}[\text{C-B-N}] - (k_4[\text{A-N}][\text{B}] + k_{16}[\text{C-N}][\text{B}]) = 0 \quad (7.22)$$

$$d[\text{D}]/dt = k_7[\text{C-D-N}] + k_{11}[\text{A-D-N}] - (k_8[\text{C-N}][\text{D}] + k_{12}[\text{A-N}][\text{D}]) = 0 \quad (7.23)$$

$$d[\text{A-N}]/dt = k_3[\text{A-B-N}] + k_{11}[\text{A-D-N}] - (k_4[\text{A-N}][\text{B}] + k_{12}[\text{A-N}][\text{D}]) = 0 \quad (7.24)$$

$$d[\text{C-N}]/dt = k_7[\text{C-D-N}] + k_{15}[\text{C-B-N}] - (k_8[\text{C-N}][\text{D}] + k_{16}[\text{C-N}][\text{B}]) = 0 \quad (7.25)$$

$$d[\text{N}]/dt = k_2[\text{A-B-N}] + k_6[\text{C-D-N}] + k_{10}[\text{A-D-N}] + k_{14}[\text{C-B-N}] - (k_1[\text{A-B}] + k_5[\text{C-D}] + k_9[\text{A-D}] + k_{13}[\text{C-B}])[\text{N}] = 0 \quad (7.26)$$

These equations are based upon the rate law for a single reaction step being proportional to the product of the concentration of each of the reactants raised to the power that it appears in the given reaction equation, being one in all the present cases.

In principle, the simultaneous equation (7.18) – (7.26) can be solved so as to allow the rates of interest, i.e., $d[A-B]/dt$, $d[C-D]/dt$, $d[A-D]/dt$ and $d[C-B]/dt$ to be expressed in terms of just the measurable concentrations $[A-B]$, $[C-D]$, $[A-D]$, and $[C-B]$ and the 16 rate constants. However, it isn't essential to go this far to understand the behavior of the present system. Taking the species A-B, for example, the rate of reaction with respect to it is given by

$$R_{A-B} = d[A-B]/dt = k_2[A-B-N] - k_1[A-B][N] \quad (7.27)$$

From application of the SSA to the rate of reaction of A-B-N (equation (7.18))

$$[A-B-N] = (k_1[A-B][N] + k_4[A-N][B]) / (k_2 + k_3) \quad (7.28)$$

So that

$$R_{A-B} = [A-N][B]k_2k_4 / (k_2 + k_3) - [A-B][N]k_1k_3 / (k_2 + k_3) \quad (7.29)$$

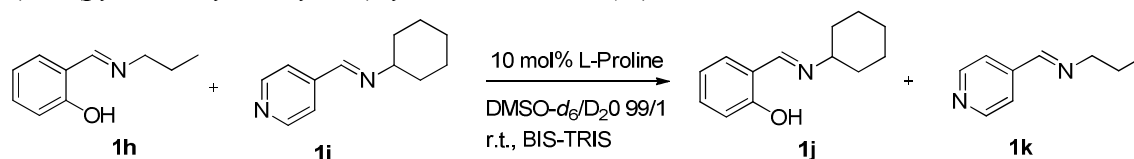
Since the application of the SSA is based upon the condition that $[A-N]$, $[B]$ and $[N]$ are constant so that this equation is mathematically equivalent to

$$R_{A-B} = -d[A-B]/dt = (\text{constant})[A-B] - \text{another constant} \quad (7.30)$$

i.e. the differential equation for a reversible first-order reaction. Note, however, that the k_{obs} obtained by fitting the time dependence of $[A-B]$ is not then the sum of the forward and back rate constants for a single step.

Results of kinetic study of imine/imine derivatives exchange

1. The imine/imine exchange reaction between (*E*)-2-((propylimino)methyl)phenol (**1h**) (*E*)-*N*-(pyridin-4-ylmethylene)cyclohexanamine (**1i**).



In an NMR tube, compound **1h** and **1i** were mixed with a final concentration 19.35 mM and a total volume of 0.62 mL with 10 equiv. of BIS-TRIS in the presence of 10 mol% L-proline as catalyst. The ¹H-NMR of –CH=N- protons of the starting materials (8.53 ppm for **1h** and 8.39 ppm for **1i**) and the exchange products (8.56 ppm for **1j** and 8.37 ppm for **1k**) were followed until the reaction reached equilibrium. The kinetic data were fit assuming a reversible first-order reaction as shown in *Figure 7.1*.

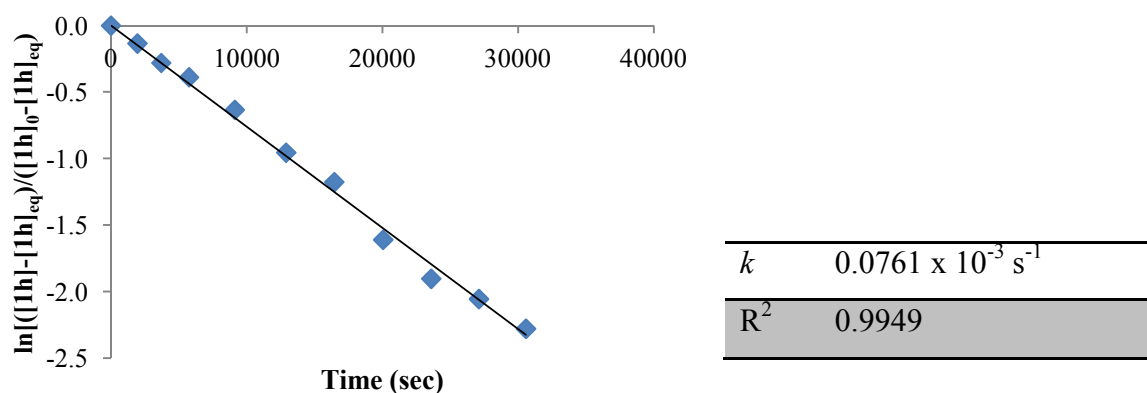
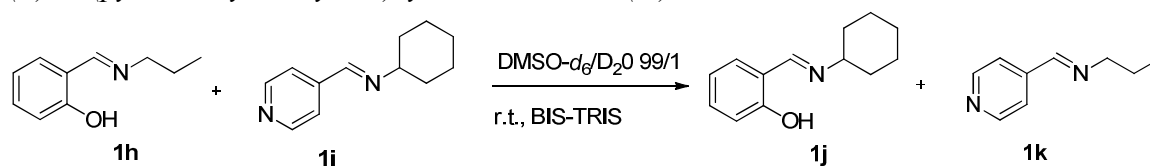


Figure 7.1 The plot of the kinetic study of the imine exchange between **1h** and **1i** in DMSO-*d*₆/D₂O 99/1 in the presence of 10 mol% L-proline and 10 equiv. BIS-TRIS at room temperature. Data were fit assuming a reversible first-order reaction.

2. The imine/imine exchange reaction between (*E*)-2-((propylimino)methyl)phenol (**1h**) (*E*)-*N*-(pyridin-4-ylmethylene)cyclohexanamine (**1i**).



In an NMR tube, compound **1h** and **1i** were mixed with a final concentration 19.35 mM and a total volume of 0.62 mL with 10 equiv. of BIS-TRIS. The ¹H-NMR of –CH=N- protons of the starting materials (8.53 ppm for **1h** and 8.39 ppm for **1i**) and the exchange products (8.56 ppm for **1j** and 8.37 ppm for **1k**) were followed until the reaction reached equilibrium. The kinetic data were fit assuming a reversible first-order reaction as shown in *Figure 7.2*.

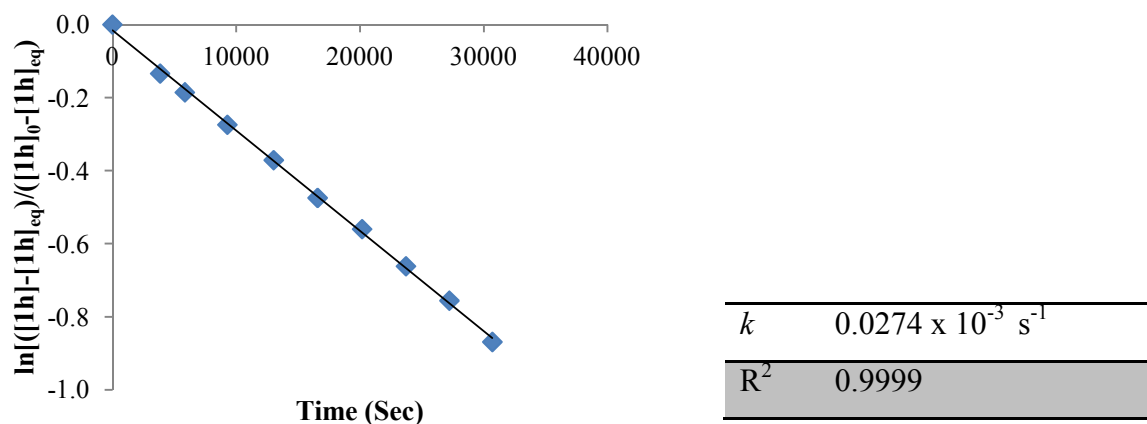
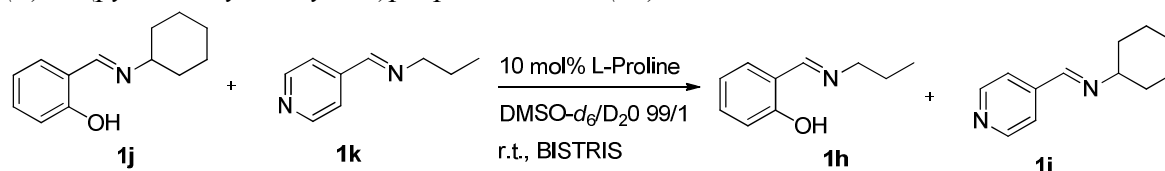


Figure 7.2 The plot of the kinetic study of the imine exchange between **1h** and **1i** in DMSO- d_6 /D $_2$ O 99/1 and 10 equiv. BIS-TRIS at room temperature. Data were fit assuming a reversible first-order reaction.

3. The imine/imine exchange reaction between (*E*)-2-(cyclohexylimino)methylphenol (**1j**) (*E*)-*N*-(pyridin-4-ylmethylene)propan-1-amine (**1k**).



In an NMR tube, compound **1j** and **1k** were mixed with a final concentration 19.35 mM and a total volume of 0.62 mL with 10 equiv. BIS-TRIS in the presence of 10 mol% L-proline as catalyst. The $^1\text{H-NMR}$ of $-\text{CH}=\text{N}-$ protons of the starting materials (8.56 ppm for **1j** and 8.37 ppm for **1k**) and the exchange products (8.53 ppm for **1h** and 8.39 ppm for **1i**) were followed until the reaction reached equilibrium. The kinetic data were fit assuming a reversible first-order reaction as shown in *Figure 7.3*.

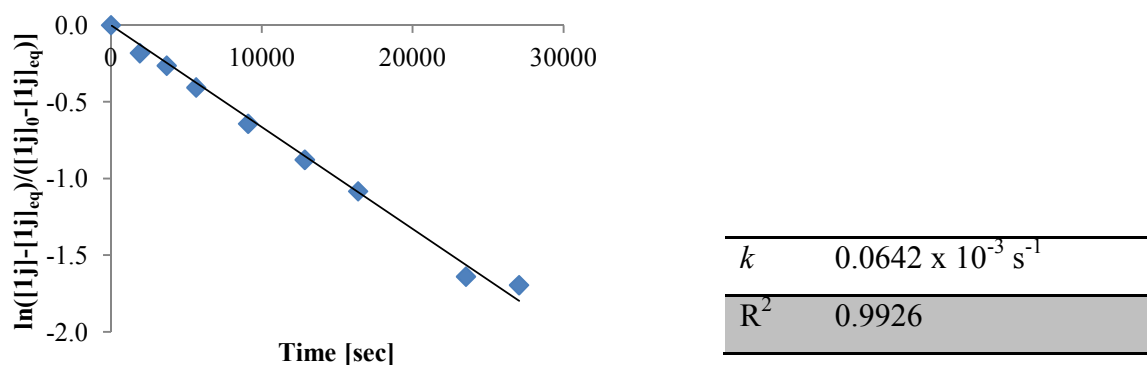
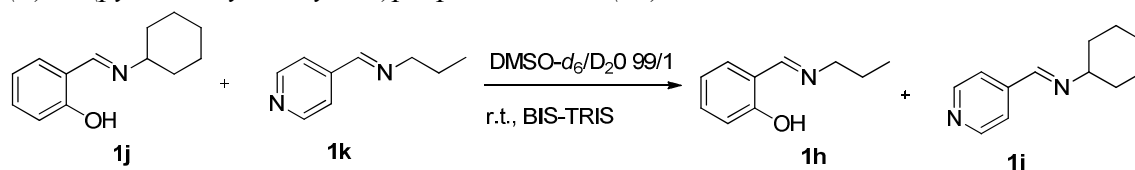


Figure 7.3 The plot of the kinetic study of the imine exchange between **1j** and **1k** in DMSO- d_6 /D $_2$ O 99/1 in the presence of 10 mol% L-proline and 10 equiv. of BIS-TRIS at room temperature. Data were fit assuming a reversible first-order reaction.

4. The imine/imine exchange reaction between (*E*)-2-(cyclohexylimino)methylphenol (**1j**) and (*E*)-*N*-(pyridin-4-ylmethylene)propan-1-amine (**1k**).



In an NMR tube, compound **1j** and **1k** were mixed with a final concentration 19.35 mM and a total volume of 0.62 mL with 10 equiv. BIS-TRIS. The $^1\text{H-NMR}$ of $-\text{CH}=\text{N}$ -protons of the starting materials (8.56 ppm for **1j** and 8.37 ppm for **1k**) and the exchange products (8.53 ppm for **1h** and 8.39 ppm for **1i**) were followed until the reaction reached equilibrium. The kinetic data were fit assuming a reversible first-order reaction as shown in Figure 7.4.

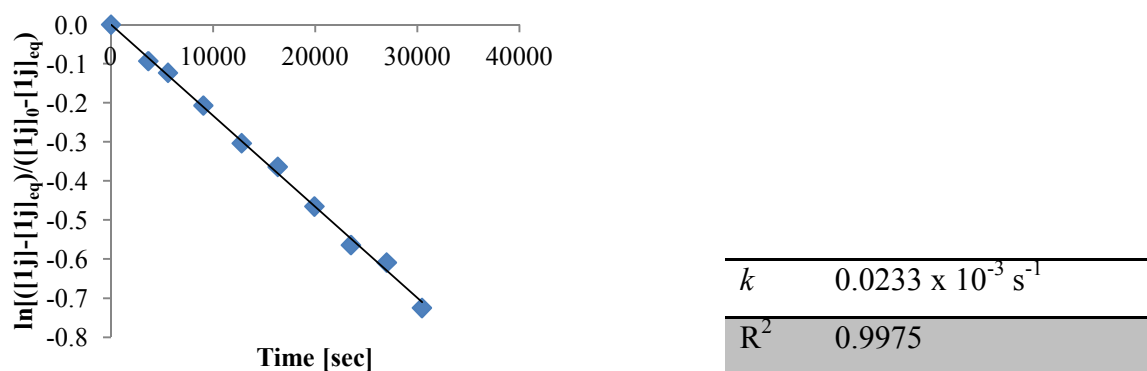
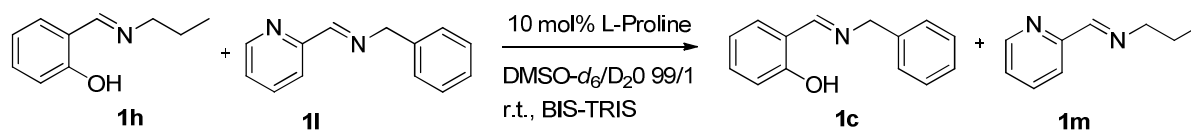


Figure 7.4 The plot of the kinetic study of the imine exchange between **1j** and **1k** in $\text{DMSO-}d_6/\text{D}_2\text{O}$ 99/1 and 10 equiv. BIS-TRIS at room temperature. Data were fit assuming a reversible first-order reaction.

5. The imine/imine exchange reaction between (*E*)-2-((propylimino)methyl)phenol (**1h**) and (*E*)-1-phenyl-*N*-(pyridin-2-ylmethylene)methanamine (**1l**).



In an NMR tube, compound **1h** and **1l** were mixed with a final concentration 19.35 mM and a total volume of 0.62 mL with 10 equiv. BIS-TRIS in the presence of 10 mol% L-proline as catalyst. The $^1\text{H-NMR}$ of $-\text{CH}=\text{N}$ -protons of the starting materials (8.53 ppm for **1h** and 8.48 ppm for **1l**) and the exchange products (8.70 ppm for **1c** and 8.33 ppm for **1m**) were followed until the reaction reached equilibrium. The kinetic data were fit assuming a reversible first-order reaction as shown in Figure 7.5.

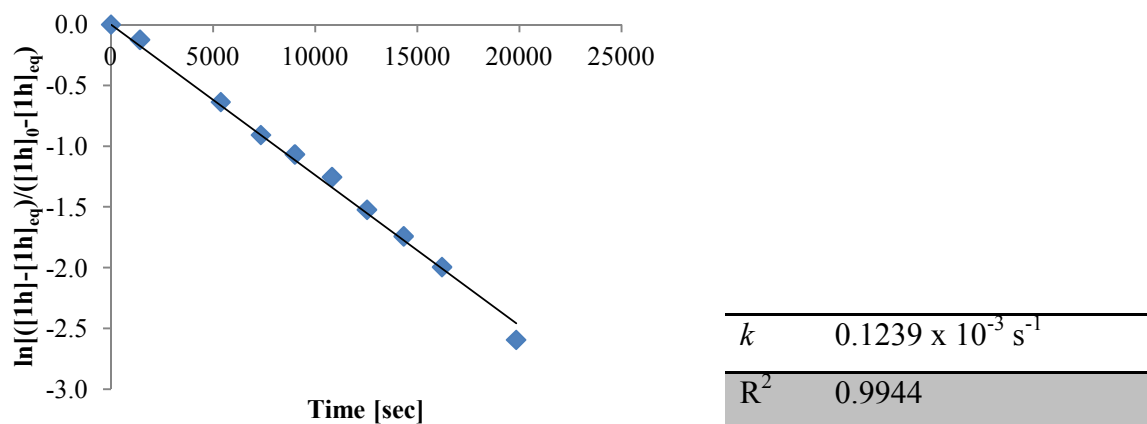
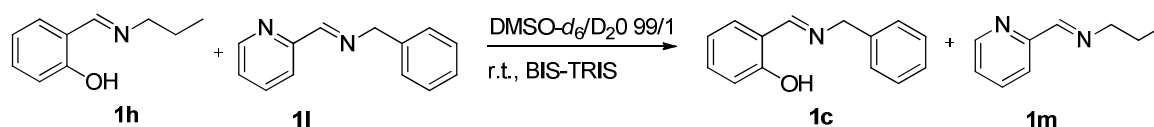


Figure 7.5 The plot of the kinetic study of the imine exchange between **1h** and **1l** in $\text{DMSO-}d_6/\text{D}_2\text{O}$ 99/1 in the presence of 10 mol% *L*-proline and 10 equiv. of BIS-TRIS at room temperature. Data were fit assuming a reversible first-order reaction.

6. The imine/imine exchange reaction between (*E*)-2-((propylimino)methyl)phenol (**1h**) and (*E*)-1-phenyl-*N*-(pyridin-2-ylmethylene)methanamine (**1l**).



In an NMR tube, compound **1h** and **1l** were mixed with a final concentration 19.35 mM and a total volume of 0.62 mL with 10 equiv. of BIS-TRIS. The $^1\text{H-NMR}$ of $-\text{CH}=\text{N}$ -protons of the starting materials (8.53 ppm for **1h** and 8.48 ppm for **1l**) and the exchange products (8.70 ppm for **1c** and 8.33 ppm for **1m**) were followed until the reaction reached equilibrium. The kinetic data were fit assuming a reversible first-order reaction as shown in Figure 7.6.

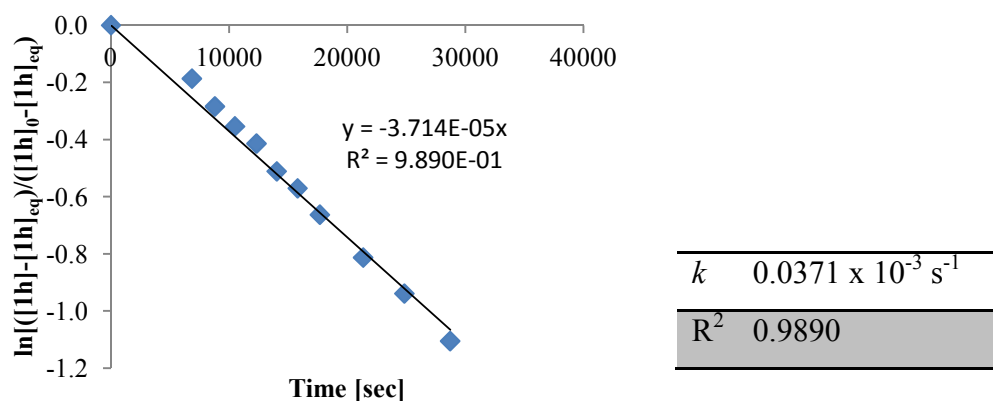
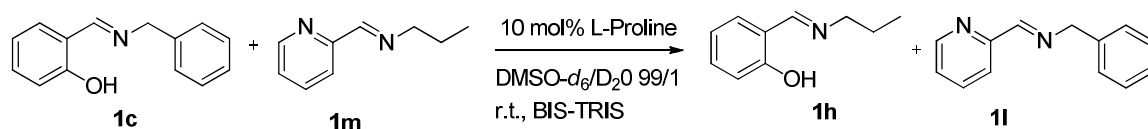


Figure 7.6 The plot of the kinetic study of the imine exchange between **1h** and **1l** in $\text{DMSO-}d_6/\text{D}_2\text{O}$ 99/1 and 10 equiv. BIS-TRIS at room temperature. Data were fit assuming a reversible first-order reaction.

7. The imine/imine exchange reaction between (*E*)-2-((benzylimino)methyl)phenol (**1c**) (*E*)-*N*-(pyridin-2-ylmethylene)propan-1-amine (**1m**).



In an NMR tube, compound **1c** and **1m** were mixed with a final concentration 19.35 mM and a total volume of 0.62 mL with 10 equiv. of BIS-TRIS in the presence of 10 mol% L-proline as catalyst. The ¹H-NMR of –CH=N- protons of the starting materials (8.70 ppm for **1c** and 8.33 ppm for **1m**) and the exchange products (8.53 ppm for **1h** and 8.48 ppm for **1l**) were followed until the reaction reached equilibrium. The kinetic data were fit assuming a reversible first-order reaction as shown in *Figure 7.7*.

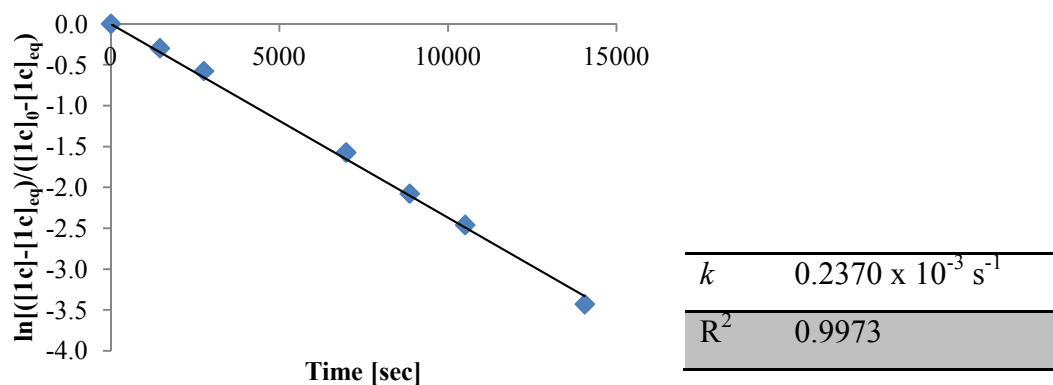
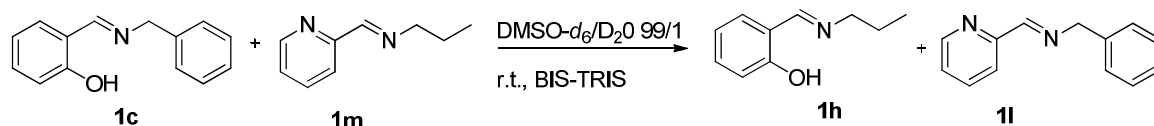


Figure 7.7 The plot of the kinetic study of the imine exchange between **1c** and **1m** in DMSO-*d*₆/D₂O 99/1 in the presence of 10 mol% L-proline and 10 equiv. of BIS-TRIS at room temperature. Data were fit assuming a reversible first-order reaction.

8. The imine/imine exchange reaction between (*E*)-2-((benzylimino)methyl)phenol (**1c**) (*E*)-*N*-(pyridin-2-ylmethylene)propan-1-amine (**1m**).



In an NMR tube, compound **1c** and **1m** were mixed with a final concentration 19.35 mM and a total volume of 0.62 mL with 10 equiv. of BIS-TRIS. The ¹H-NMR of –CH=N- protons of the starting materials (8.70 ppm for **1c** and 8.33 ppm for **1m**) and the exchange products (8.53 ppm for **1h** and 8.48 ppm for **1l**) were followed until the reaction reached equilibrium. The kinetic data were fit assuming a reversible first-order reaction as shown in *Figure 7.8*.

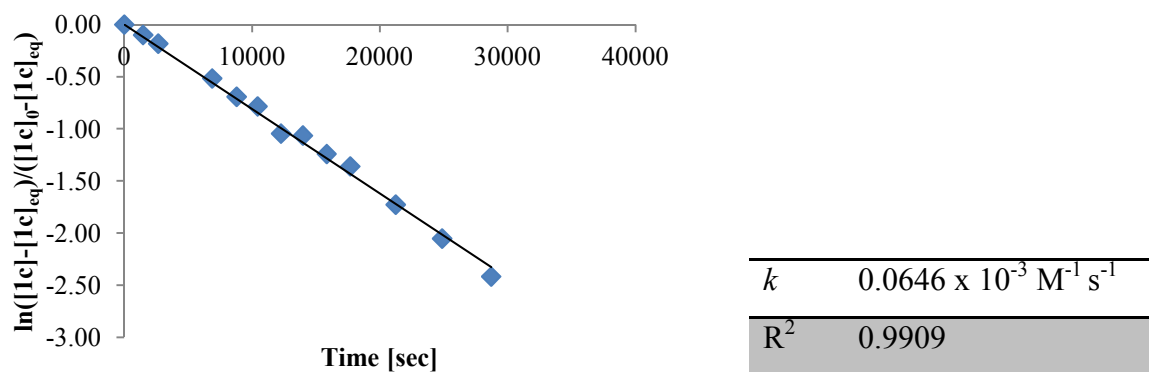
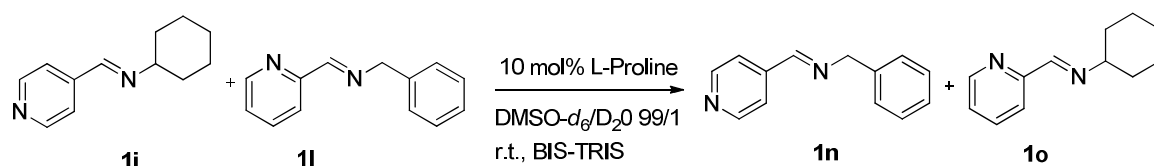


Figure 7.8 The plot of the kinetic study of the imine exchange between **1c** and **1m** in DMSO- d_6 /D $_2$ O 99/1 and 10 equiv. BIS-TRIS at room temperature. Data were fit assuming a reversible first-order reaction.

9. The imine/imine exchange reaction between (*E*)-4-((cyclohexylimino) methyl) pyridin-3-ol (**1i**) (*E*)-1-phenyl-*N*-(pyridin-2-ylmethylene)methanamine (**1l**).



In an NMR tube, compound **1i** and **1l** were mixed with a final concentration 19.35 mM and a total volume of 0.62 mL with 10 equiv. BIS-TRIS in the presence of 10 mol% L-proline as catalyst. The $^1\text{H-NMR}$ of $-\text{CH}=\text{N}-$ protons of the starting materials (8.39 ppm for **1i** and 8.50 ppm for **1l**) and the exchange products (8.34 ppm for **1n** and 8.54 ppm for **1o**) were followed until the reaction reached equilibrium. The kinetic data were fit assuming a reversible first-order reaction as shown in *Figure 7.9*.

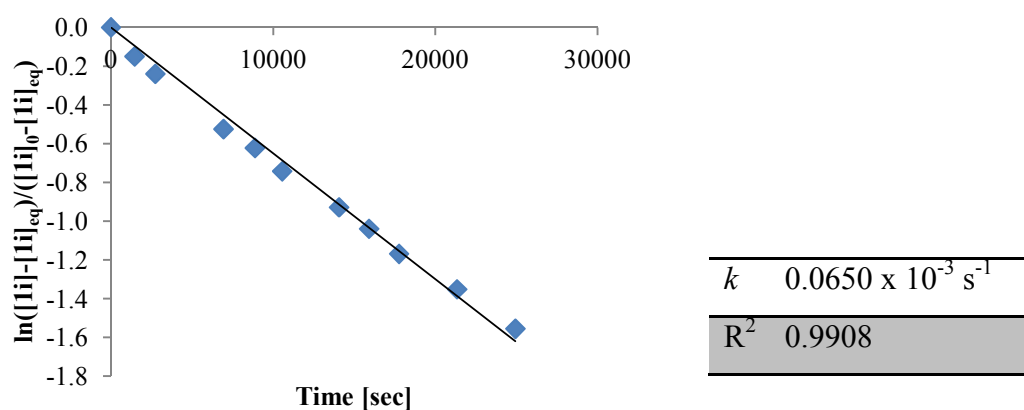
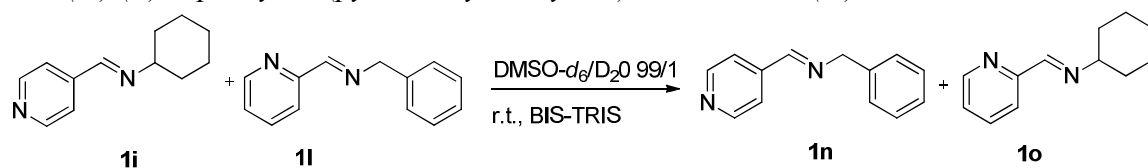


Figure 7.9 The plot of the kinetic study of the imine exchange between **1i** and **1l** in DMSO- d_6 /D $_2$ O 99/1 in the presence of 10 mol% L-proline and 10 equiv. of BIS-TRIS at room temperature. Data were fit assuming a reversible first-order reaction.

10. The imine/imine exchange reaction between (*E*)-4-((cyclohexylimino) methyl) pyridin-3-ol (**1i**) (*E*)-1-phenyl-*N*-(pyridin-2-ylmethylene)methanamine (**1l**).



In an NMR tube, compound **1i** and **1l** were mixed with a final concentration 19.35 mM and a total volume of 0.62 mL with 10 equiv. of BIS-TRIS. The $^1\text{H-NMR}$ of $-\text{CH}=\text{N}$ -protons of the starting materials (8.39 ppm for **1i** and 8.50 ppm for **1l**) and the exchange products (8.34 ppm for **1n** and 8.54 ppm for **1o**) were followed until the reaction reached equilibrium. The kinetic data were fit assuming a reversible first-order reaction as shown in Figure 7.10.

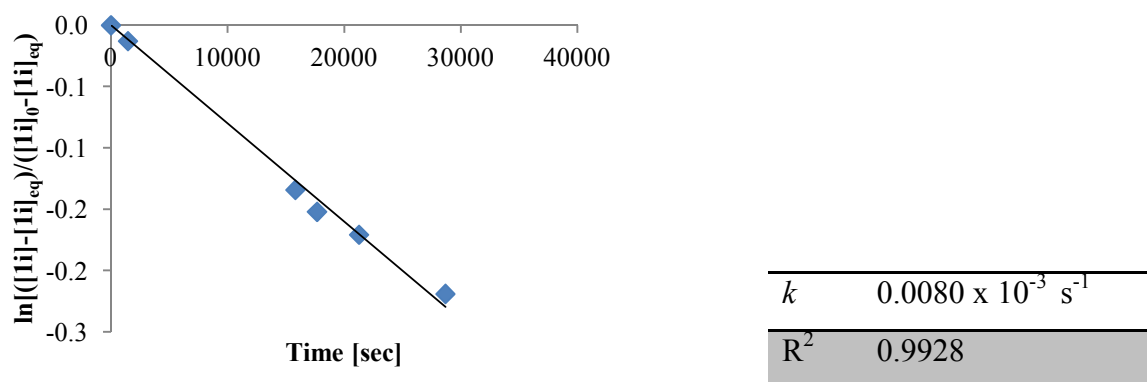
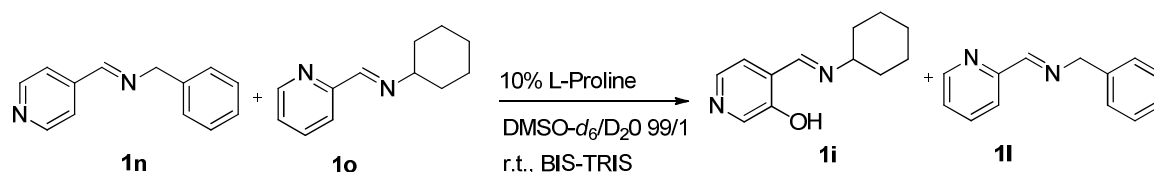


Figure 7.10 The plot of the kinetic study of the imine exchange between **1i** and **1l** in $\text{DMSO-}d_6/\text{D}_2\text{O}$ 99/1 and 10 equiv. BIS-TRIS at room temperature. Data were fit assuming a reversible first-order reaction.

11. The imine/imine exchange reaction between (*E*)-1-phenyl-*N*-(pyridin-4-ylmethylene)methanamine (**1n**) (*E*)-*N*-(pyridin-2-ylmethylene)cyclohexanamine (**1o**).



In an NMR tube, compound **1n** and **1o** were mixed with a final concentration 19.35 mM and a total volume of 0.62 mL with 10 equiv. of BIS-TRIS in the presence of 10 mol% L-proline as catalyst. The $^1\text{H-NMR}$ of $-\text{CH}=\text{N}$ - protons of the starting materials (8.34 ppm for **1n** and 8.54 ppm for **1o**) and the exchange products (8.39 ppm for **1i** and 8.50 ppm for **1l**) were followed until the reaction reached equilibrium. The kinetic data were fit assuming a reversible first-order reaction as shown in Figure 7.11.

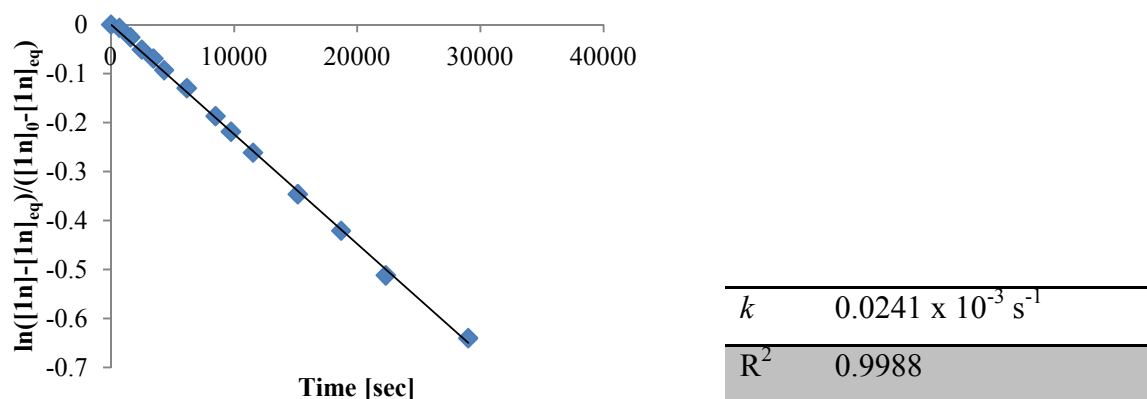
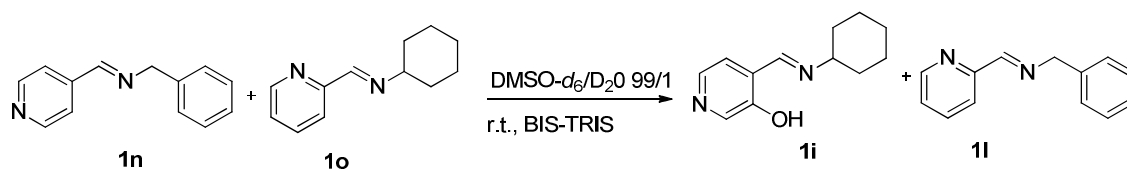


Figure 7.11 The plot of the kinetic study of the imine exchange between **1n** and **1o** in DMSO- d_6 /D $_2$ O 99/1 in the presence of 10 mol% L-proline and 10 equiv. of BIS-TRIS at room temperature. Data were fit assuming a reversible first-order reaction.

12. The imine/imine exchange reaction between (*E*)-1-phenyl-*N*-(pyridin-4-ylmethylene)methanamine (**1n**) (*E*)-*N*-(pyridin-2-ylmethylene)cyclohexanamine (**1o**).



In an NMR tube, compound **1n** and **1o** were mixed with a final concentration 19.35 mM and a total volume of 0.62 mL with 10 equiv. of BIS-TRIS. The $^1\text{H-NMR}$ of $-\text{CH}=\text{N}$ -protons of the starting materials (8.34 ppm for **1n** and 8.54 ppm for **1o**) and the exchange products (8.39 ppm for **1i** and 8.50 ppm for **1l**) were followed. This reaction was not reached equilibrium; thus, the kinetic data were fit assuming an irreversible first-order reaction as shown in Figure 7.12.

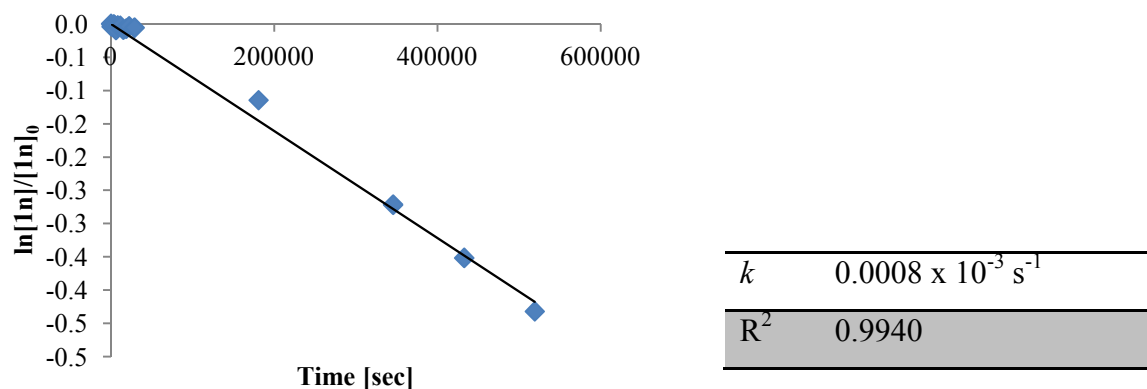
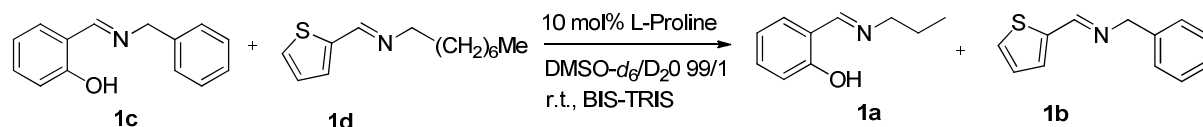


Figure 7.12 The plot of the kinetic study of the imine exchange between **1n** and **1o** in DMSO- d_6 /D $_2$ O 99/1 and 10 equiv. BIS-TRIS at room temperature. Data were fit assuming an irreversible first-order reaction.

13. The imine/imine exchange reaction between (*E*)-2-((benzylimino)methyl)phenol (**1c**) and (*E*)-*N*-(thiophen-2-ylmethylene)octan-1-amine (**1d**).



In an NMR tube, compound **1c** and **1d** were mixed with a final concentration 19.35 mM and a total volume of 0.62 mL with 10 equiv. of BIS-TRIS in the presence of 10 mol% L-proline as catalyst. The ¹H-NMR of –CH=N- protons of the starting materials (8.70 ppm for **1c** and 8.42 ppm for **1d**) and the exchange products (8.60 ppm for **1a** and 8.53 ppm for **1b**) were followed until the reaction reached equilibrium. The kinetic data were fit assuming a reversible first-order reaction as shown in *Figure 7.13*.

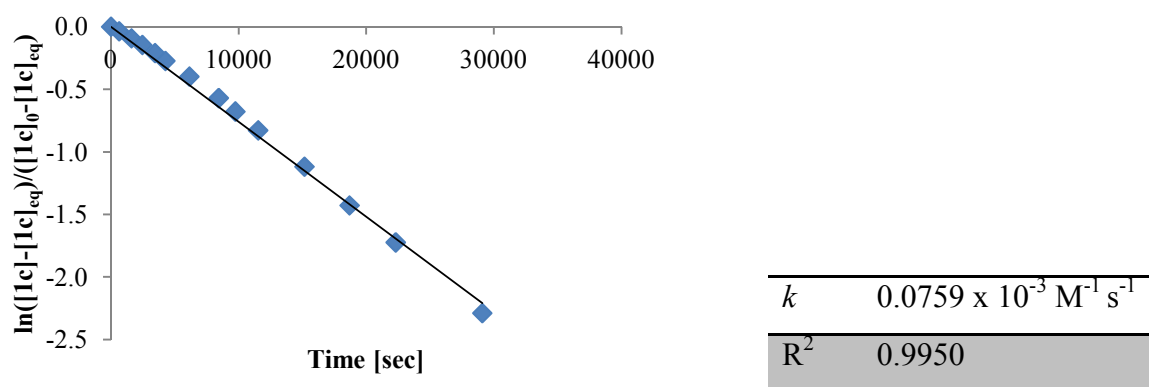
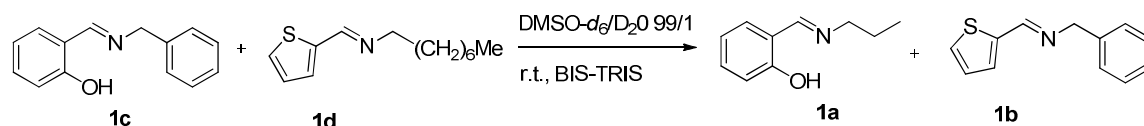


Figure 7.13 The plot of the kinetic study of the imine exchange between **1c** and **1d** in DMSO-*d*₆/D₂O 99/1 in the presence of 10 mol% L-proline and 10 equiv. of BIS-TRIS at room temperature. Data were fit assuming a reversible first-order reaction.

14. The imine/imine exchange reaction between (*E*)-2-((benzylimino)methyl)phenol (**1c**) and (*E*)-*N*-(thiophen-2-ylmethylene)octan-1-amine (**1d**).



In an NMR tube, compound **1c** and **1d** were mixed with a final concentration 19.35 mM and a total volume of 0.62 mL with 10 equiv. of BIS-TRIS. The ¹H-NMR of –CH=N- protons of the starting materials (8.70 ppm for **1c** and 8.42 ppm for **1d**) and the exchange products (8.60 ppm for **1a** and 8.53 ppm for **1b**) were followed until the reaction reached equilibrium. The kinetic data were fit assuming a reversible first-order reaction as shown in *Figure 7.14*.

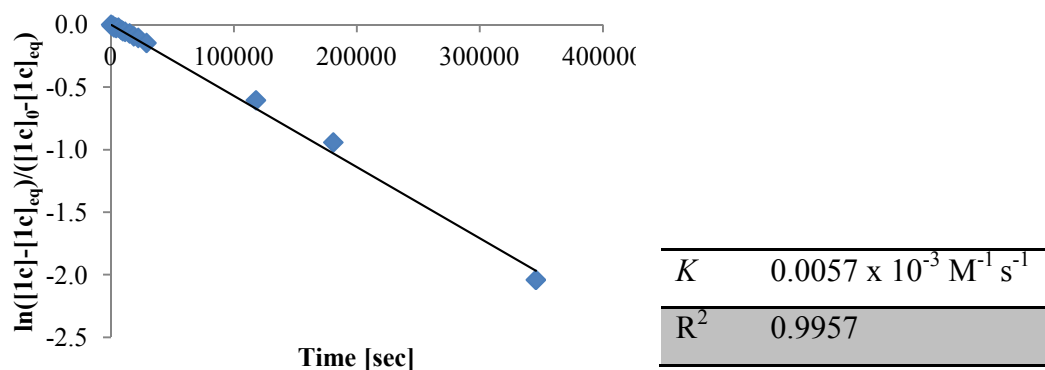
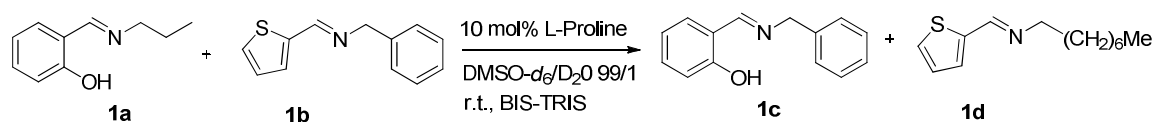


Figure 7.14 The plot of the kinetic study of the imine exchange between **1c** and **1d** in $\text{DMSO-}d_6/\text{D}_2\text{O}$ 99/1 and 10 equiv. BIS-TRIS at room temperature. Data were fit assuming a reversible first-order reaction.

15. The imine/imine exchange reaction between (*E*)-2-((benzylimino)methyl)phenol (**1a**) and (*E*)-*N*-(thiophen-2-ylmethylene)octan-1-amine (**1b**).



In an NMR tube, compound **1a** and **1b** were mixed with a final concentration 19.35 mM and a total volume of 0.62 mL with 10 equiv. of BIS-TRIS in the presence of 10mol% L-proline as catalyst. The $^1\text{H-NMR}$ of $-\text{CH}=\text{N}-$ protons of the starting materials (8.60 ppm for **1a** and 8.53 ppm for **1b**) and the exchange products (8.70 ppm for **1c** and 8.42 ppm for **1d**) were followed until the reaction reached equilibrium. The kinetic data were fit assuming a reversible first-order reaction as shown in *Figure 7.15*.

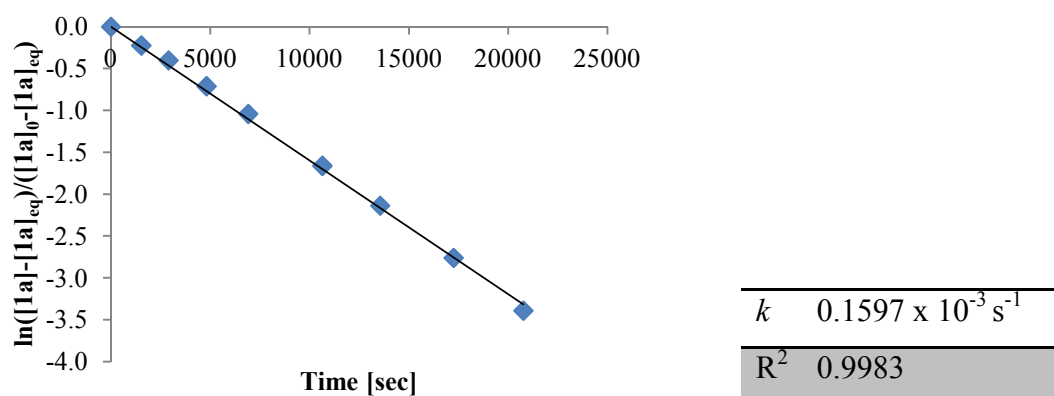
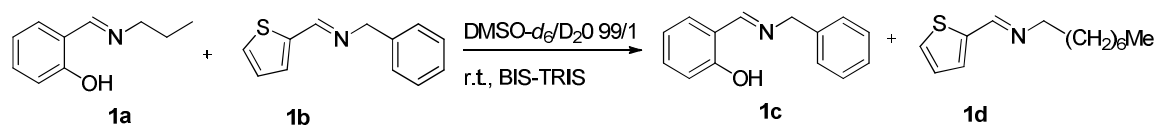


Figure 7.15 The plot of the kinetic study of the imine exchange between **1a** and **1b** in $\text{DMSO-}d_6/\text{D}_2\text{O}$ 99/1 in the presence of 10 mol% L-proline and 10 equiv. of BIS-TRIS at room temperature. Data were fit assuming a reversible first-order reaction.

16. The imine/imine exchange reaction between (*E*)-2-((benzylimino)methyl)phenol (**1a**) and (*E*)-*N*-(thiophen-2-ylmethylene)octan-1-amine (**1b**).



In an NMR tube, compound **1a** and **1b** were mixed with a final concentration 19.35 mM and a total volume of 0.62 mL with 10% of BIS-TRIS as a buffer solution. The ¹H-NMR of –CH=N– protons of the starting materials (8.60 ppm for **1a** and 8.53 ppm for **1b**) and the exchange products (8.70 ppm for **1c** and 8.42 ppm for **1d**) were followed and the reaction did not reach equilibrium. The kinetic data were fit assuming an irreversible first-order reaction as shown in *Figure 7.16*.

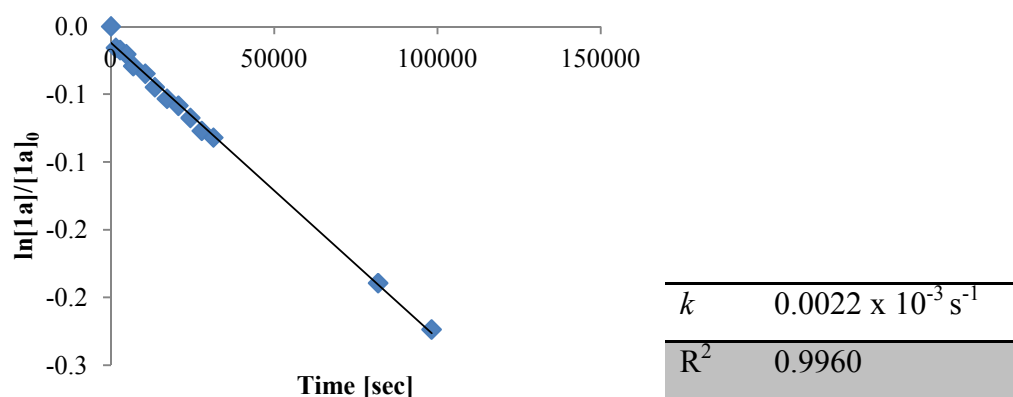
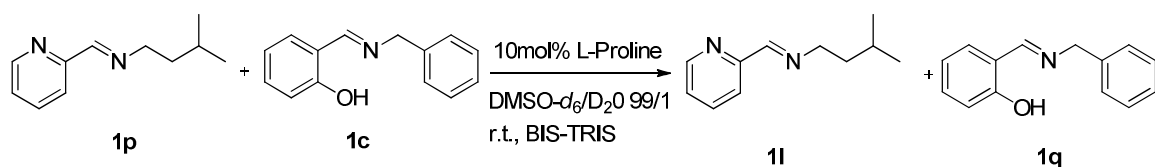


Figure 7.16 The plot of the kinetic study of the imine exchange between **1a** and **1b** in DMSO-*d*₆/D₂O 99/1 and 10 equiv. BIS-TRIS at room temperature. Data were fit assuming a reversible first-order reaction.

17. The imine/imine exchange reaction between (*E*)-3-methyl-*N*-(pyridin-2-ylmethylene)butan-1-amine (**1p**) and (*E*)-2-((benzylimino)methyl)phenol (**1c**).



In an NMR tube, compound **1p** and **1c** were mixed with a final concentration 19.35 mM and a total volume of 0.62 mL with 10 equiv. of BIS-TRIS in the presence of 10mol% L-proline as catalyst. The ¹H-NMR of –CH=N– protons of the starting materials (8.34 ppm for **1p** and 8.70 ppm for **1c**) and the exchange products (8.48 ppm for **1l** and 8.55 ppm for **1q**) were followed until the reaction reached equilibrium. The kinetic data were fit assuming a reversible first-order reaction as shown in *Figure 7.17*.

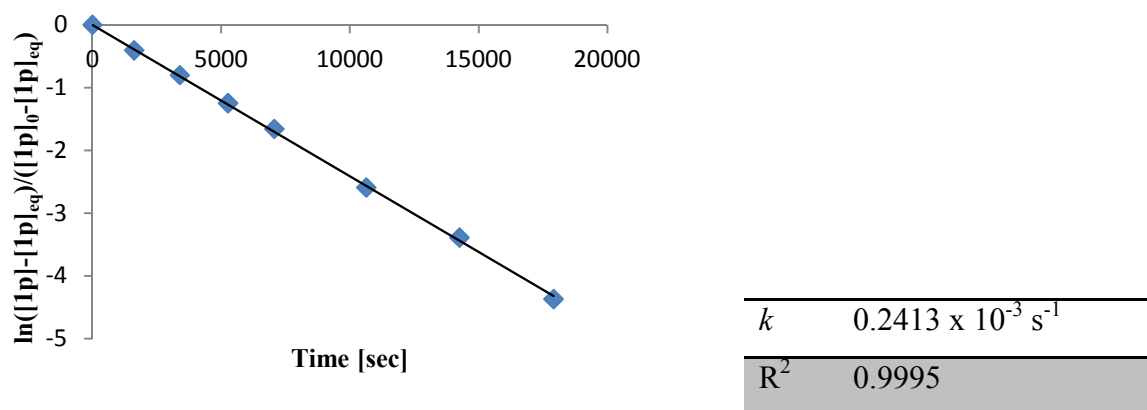
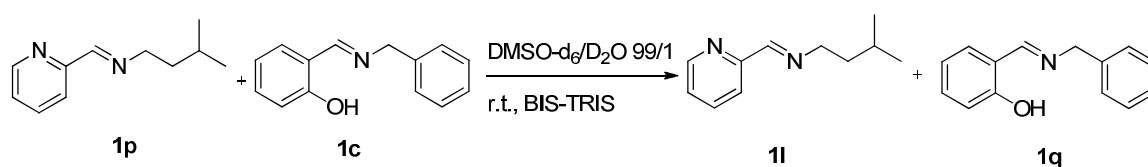


Figure 7.17 The plot of the kinetic study of the imine exchange between **1p** and **1c** in $\text{DMSO-}d_6/\text{D}_2\text{O}$ 99/1 in the presence of 10% *L*-proline and 10 equiv. of BIS-TRIS at room temperature. Data were fit assuming a reversible first-order reaction.

18. The imine/imine exchange reaction between (*E*)-3-methyl-*N*-(pyridin-2-ylmethylene)butan-1-amine (**1p**) and (*E*)-2-((benzylimino)methyl)phenol (**1c**).



In an NMR tube, compound **1p** and **1c** were mixed with a final concentration 19.35 mM and a total volume of 0.62 mL with 10 equiv. of BIS-TRIS. The $^1\text{H-NMR}$ of $-\text{CH}=\text{N}$ -protons of the starting materials (8.34 ppm for **1p** and 8.70 ppm for **1c**) and the exchange products (8.48 ppm for **1l** and 8.55 ppm for **1q**) were followed until the reaction reached equilibrium. The kinetic data were fit assuming a reversible first-order reaction as shown in Figure 7.18.

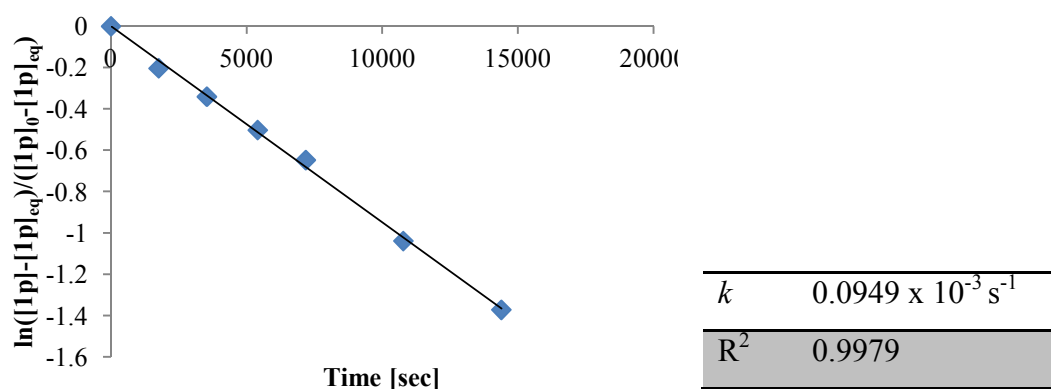
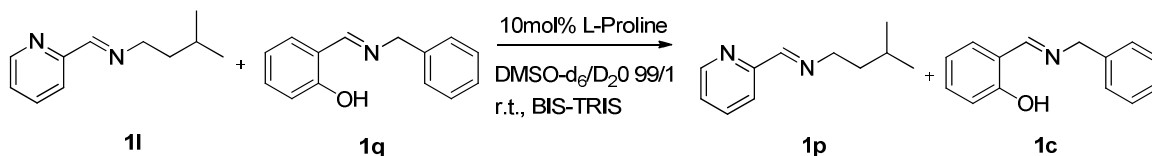


Figure 7.18 The plot of the kinetic study of the imine exchange between **1p** and **1c** in $\text{DMSO-}d_6/\text{D}_2\text{O}$ 99/1 and 10 equiv. of BIS-TRIS as buffer solution at room temperature. Data were fit assuming a reversible first-order reaction.

19. The imine/imine exchange reaction between (*E*)-3-methyl-*N*-(pyridin-2-ylmethylene)butan-1-amine (**1l**) and (*E*)-2-((benzylimino)methyl)phenol (**1q**).



In an NMR tube, compound **1l** and **1q** were mixed with a final concentration 19.35 mM and a total volume of 0.62 mL with 10 equiv. of BIS-TRIS in the presence of 10 mol% L-proline as catalyst. The $^1\text{H-NMR}$ of $-\text{CH}=\text{N}-$ protons of the starting materials (8.48 ppm for **1l** and 8.55 ppm for **1c**) and the exchange products (8.34 ppm for **1p** and 8.70 ppm for **1c**) were followed until the reaction reached equilibrium. The kinetic data were fit assuming a reversible first-order reaction as shown in Figure 7.19.

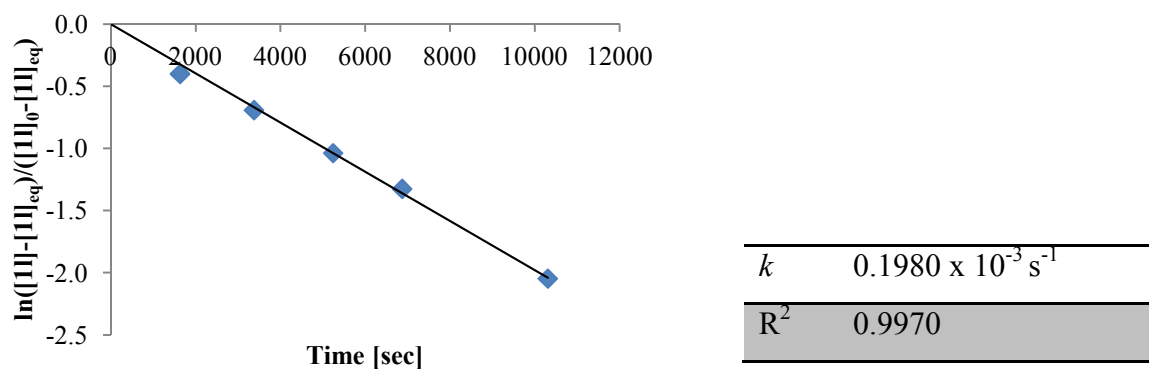
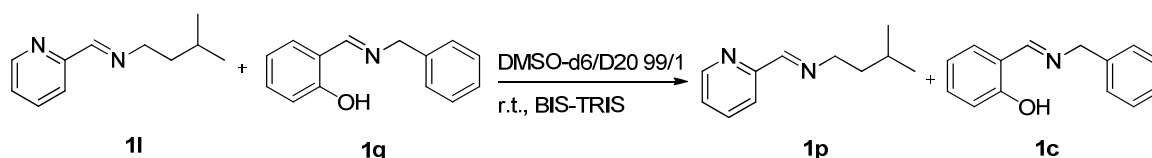


Figure 7.19 The plot of the kinetic study of the imine exchange between **1l** and **1q** in $\text{DMSO-}d_6/\text{D}_2\text{O}$ 99/1 in the presence of 10% L-proline and 10 equiv. of BIS-TRIS at room temperature. Data were fit assuming a reversible first-order reaction.

20. The imine/imine exchange reaction between (*E*)-3-methyl-*N*-(pyridin-2-ylmethylene)butan-1-amine (**1l**) and (*E*)-2-((benzylimino)methyl)phenol (**1q**).



In an NMR tube, compound **1l** and **1q** were mixed with a final concentration 19.35 mM and a total volume of 0.62 mL with 10 equiv. of BIS-TRIS. The $^1\text{H-NMR}$ of $-\text{CH}=\text{N}-$ protons of the starting materials (8.48 ppm for **1l** and 8.55 ppm for **1c**) and the exchange products (8.34 ppm for **1p** and 8.70 ppm for **1c**) were followed until the reaction reached equilibrium. The kinetic data were fit assuming a reversible first-order reaction as shown in Figure 7.20

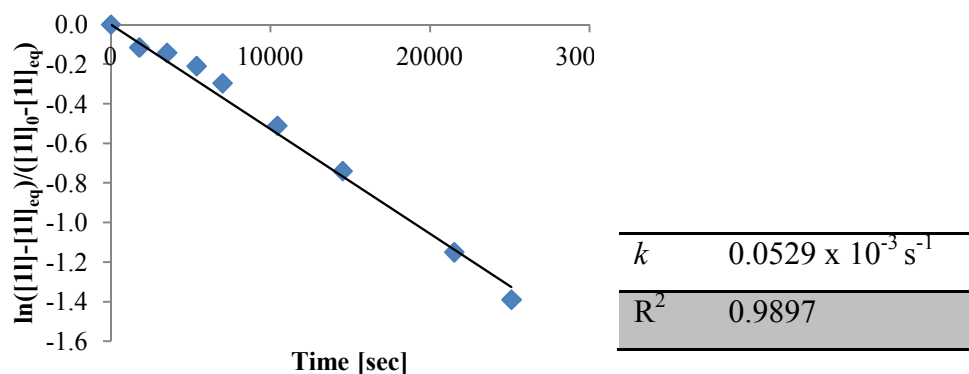
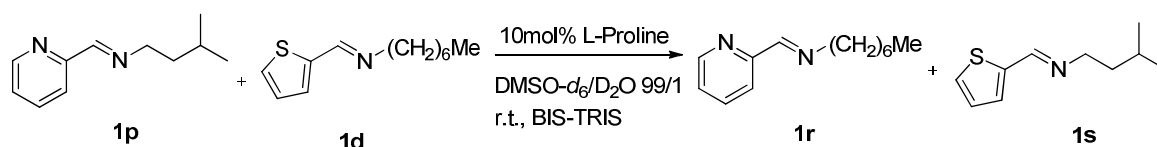


Figure 7.20 The plot of the kinetic study of the imine exchange between **1l** and **1q** in $\text{DMSO-}d_6/\text{D}_2\text{O}$ 99/1 in 10 equiv. of BIS-TRIS at room temperature. Data were fit assuming a reversible first-order reaction.

21. The imine/imine exchange reaction between (*E*)-3-methyl-*N*-(pyridin-2-ylmethylene)butan-1-amine (**1p**) and (*E*)-*N*-(thiophen-2-ylmethylene)heptan-1-amine (**1d**).



In an NMR tube, compound **1p** and **1d** were mixed with a final concentration 19.35 mM and a total volume of 0.62 mL with 10 equiv. of BIS-TRIS in the presence of 10mol% L-proline as catalyst. The $^1\text{H-NMR}$ of $-\text{CH}=\text{N}-$ protons of the starting materials (8.34 ppm for **1p** and 8.43 ppm for **1d**) and the exchange products (8.32 ppm for **1r** and 8.45 ppm for **1s**) were followed until the reaction reached equilibrium. The kinetic data were fit assuming a reversible first-order reaction as shown in *Figure 7.21*.

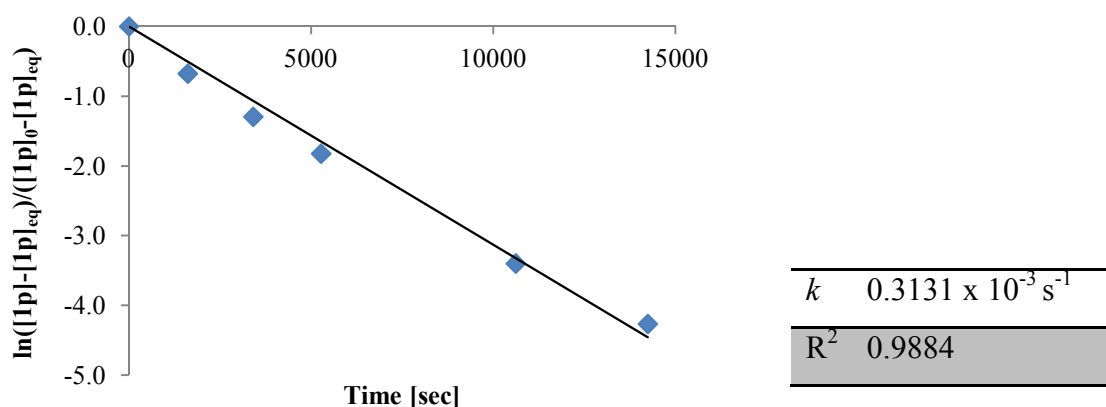
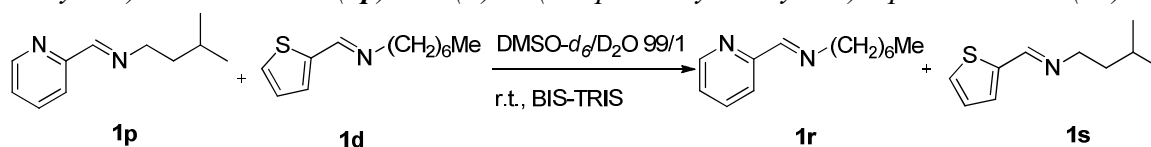


Figure 7.21 The plot of the kinetic study of the imine exchange between **1p** and **1d** in $\text{DMSO-}d_6/\text{D}_2\text{O}$ 99/1 in the presence of 10% L-proline and 10 equiv. of BIS-TRIS at room temperature. Data were fit assuming a reversible first-order reaction.

22. The imine/imine exchange reaction between (*E*)-3-methyl-*N*-(pyridin-2-ylmethylene)butan-1-amine (**1p**) and (*E*)-*N*-(thiophen-2-ylmethylene)heptan-1-amine (**1d**).



In an NMR tube, compound **1p** and **1d** were mixed with a final concentration 19.35 mM and a total volume of 0.62 mL with 10 equiv. of BIS-TRIS. The $^1\text{H-NMR}$ of $-\text{CH}=\text{N}$ -protons of the starting materials (8.34 ppm for **1p** and 8.43 ppm for **1d**) and the exchange products (8.32 ppm for **1r** and 8.45 ppm for **1s**) were followed until the reaction reached equilibrium. The kinetic data were fit assuming a reversible first-order reaction as shown in Figure 7.22.

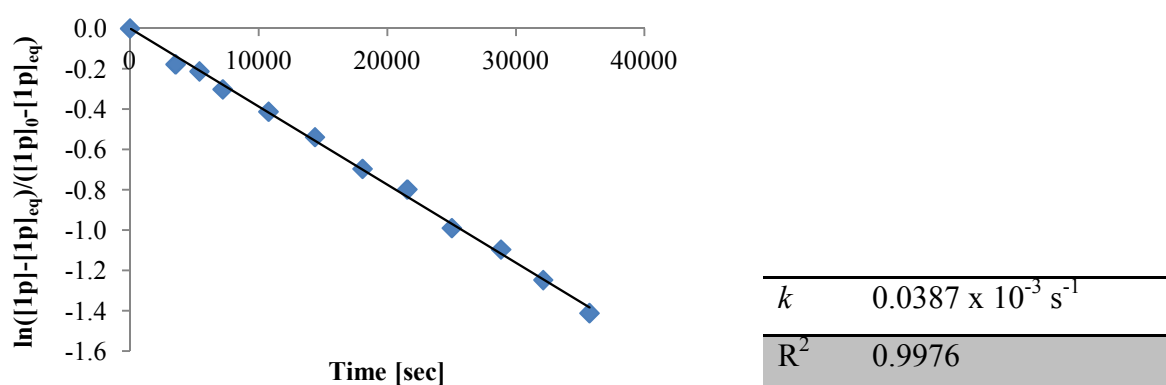
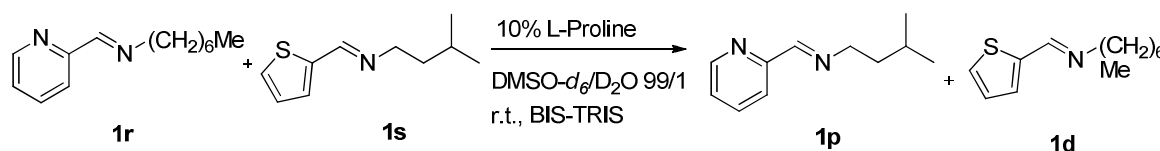


Figure 7.22 The plot of the kinetic study of the imine exchange between **1p** and **1d** in $\text{DMSO-}d_6/\text{D}_2\text{O}$ 99/1 and 10 equiv. of BIS-TRIS at room temperature. Data were fit assuming a reversible first-order reaction.

23. The imine/imine exchange reaction between (*E*)-*N*-(pyridin-2-ylmethylene)heptan-1-amine (**1r**) and (*E*)-3-methyl-*N*-(thiophen-2-ylmethylene)butan-1-amine (**1s**).



In an NMR tube, compound **1r** and **1s** were mixed with a final concentration 19.35 mM and a total volume of 0.62 mL with 10 equiv. of BIS-TRIS in the presence of 10mol% L-proline as catalyst. The $^1\text{H-NMR}$ of $-\text{CH}=\text{N}$ - protons of the starting materials (8.32 ppm for **1r** and 8.45 ppm for **1s**) and the exchange products (8.34 ppm for **1p** and 8.43 ppm for **1d**) were followed until the reaction reached equilibrium. The kinetic data were fit assuming a reversible first-order reaction as shown in Figure 7.23.

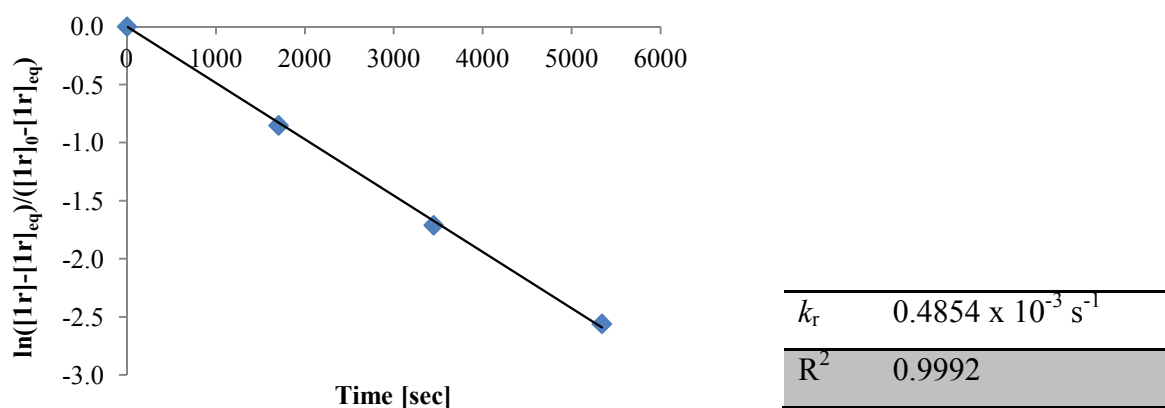
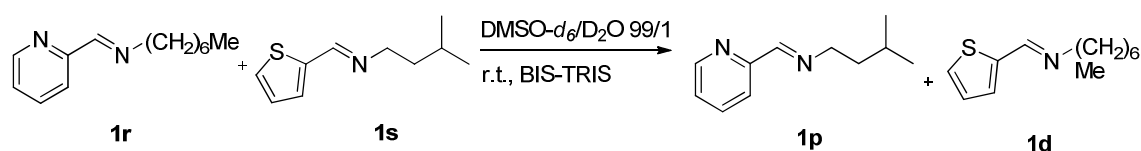


Figure 7.23 The plot of the kinetic study of the imine exchange between **1r** and **1r** in $\text{DMSO-}d_6/\text{D}_2\text{O}$ 99/1 in the presence of 10% *L*-proline and 10 equiv. of BIS-TRIS at room temperature. Data were fit assuming a reversible first-order reaction.

24. The imine/imine exchange reaction between (*E*)-*N*-(pyridin-2-yl methylene)heptan-1-amine (**1r**) and (*E*)-3-methyl-*N*-(thiophen-2-ylmethylene)butan-1-amine (**1s**).



In an NMR tube, compound **1r** and **1s** were mixed with a final concentration 19.35 mM and a total volume of 0.62 mL with 10 equiv. of BIS-TRIS. The $^1\text{H-NMR}$ of $-\text{CH}=\text{N}$ -protons of the starting materials (8.32 ppm for **1r** and 8.45 ppm for **1s**) and the exchange products (8.34 ppm for **1r** and 8.43 ppm for **1s**) were followed until the reaction reached equilibrium. The kinetic data were fit assuming a reversible first-order reaction as shown in *Figure 7.24*.

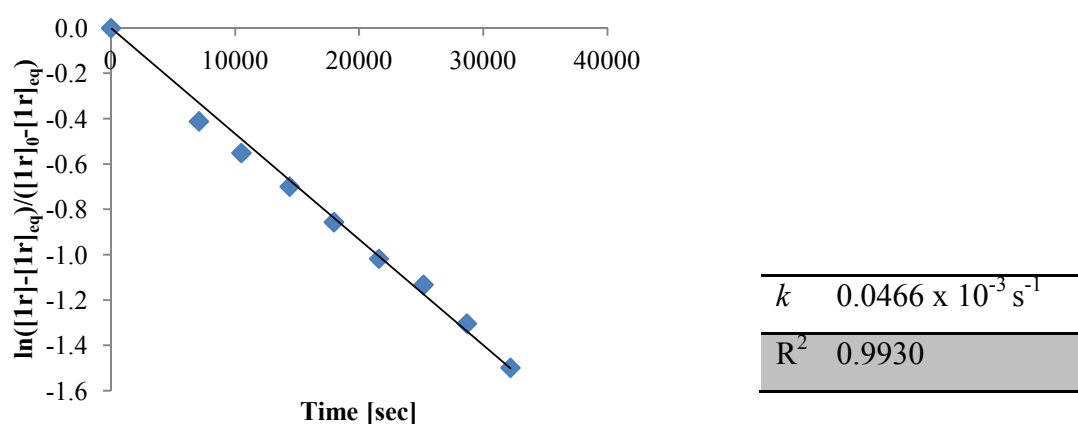
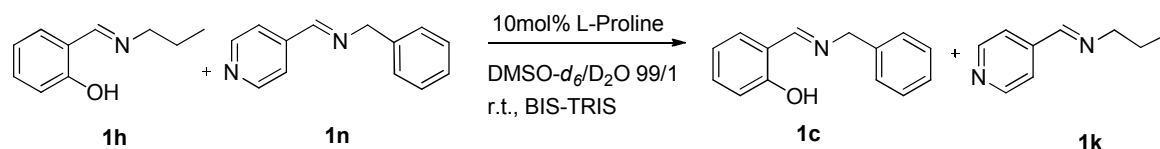


Figure 7.24 The plot of the kinetic study of the imine exchange between **1r** and **1r** in $\text{DMSO-}d_6/\text{D}_2\text{O}$ 99/1 and 10 equiv. BIS-TRIS at room temperature. Data were fit assuming a reversible first-order reaction.

25. The imine/imine exchange reaction between (*E*)-2-((propylimino)methyl)phenol (**1h**) and (*E*)-1-phenyl-*N*-(pyridin-4-ylmethylene)methanamine (**1n**).



In an NMR tube, compound **1h** and **1n** were mixed with a final concentration 19.35 mM and a total volume of 0.62 mL with 10 equiv. of BIS-TRIS in the presence of 10 mol% L-proline as catalyst. The ¹H-NMR of –CH=N- protons of the starting materials (8.53 ppm for **1h** and 8.51 ppm for **1n**) and the exchange products (8.70 ppm for **1c** and 8.37 ppm for **1k**) were followed until the reaction reached equilibrium. The kinetic data were fit assuming a reversible first-order reaction as shown in Figure 7.25.

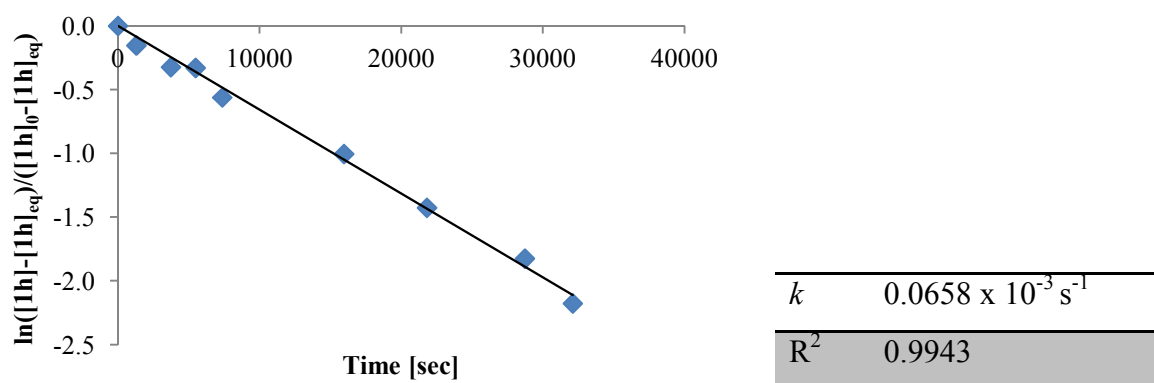
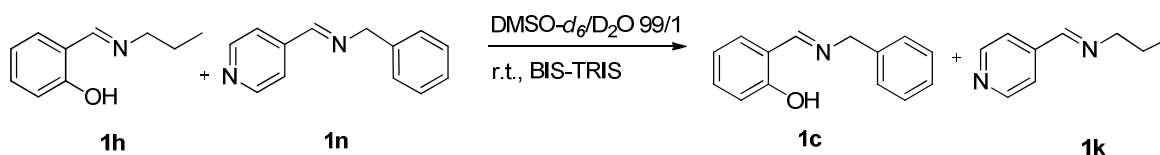


Figure 7.25 The plot of the kinetic study of the imine exchange between **1h** and **1n** in DMSO-*d*₆/D₂O 99/1 in the presence of 10 mol% L-proline and 10 equiv. of BIS-TRIS at room temperature. Data were fit assuming a reversible first-order reaction.

26. The imine/imine exchange reaction between (*E*)-2-((propylimino)methyl)phenol (**1h**) and (*E*)-1-phenyl-*N*-(pyridin-4-ylmethylene)methanamine (**1n**).



In an NMR tube, compound **1h** and **1n** were mixed with a final concentration 19.35 mM and a total volume of 0.62 mL with 10 equiv. of BIS-TRIS. The ¹H-NMR of –CH=N- protons of the starting materials (8.53 ppm for **1h** and 8.51 ppm for **1n**) and the exchange products (8.70 ppm for **1c** and 8.37 ppm for **1k**) were followed until the reaction reached equilibrium. The kinetic data were fit assuming a reversible first-order reaction as shown in Figure 7.26.

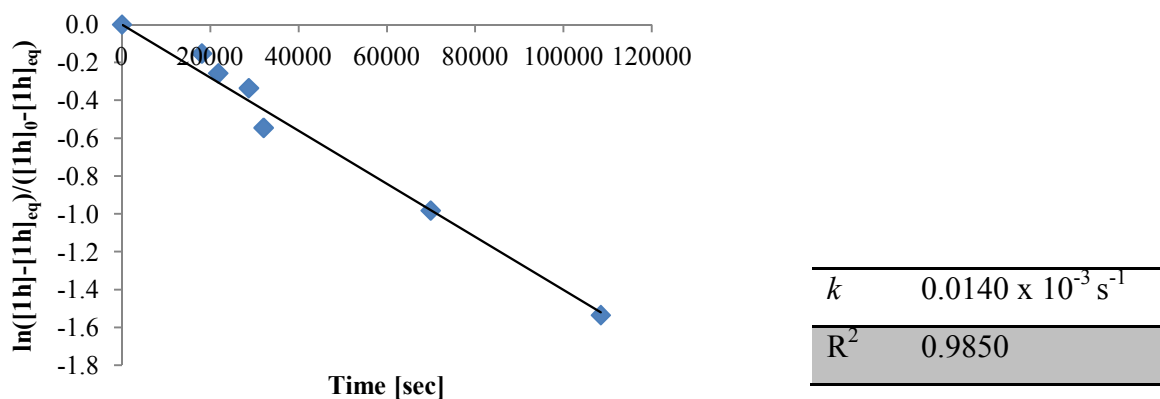
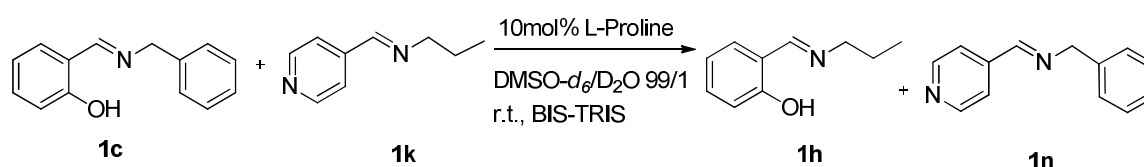


Figure 7.26 The plot of the kinetic study of the imine exchange between **1h** and **1n** in DMSO- d_6 /D $_2$ O 99/1 and 10 equiv. BIS-TRIS at room temperature. Data were fit assuming a reversible first-order reaction.

27. The imine/imine exchange reaction between (*E*)-2-((benzylimino)methyl)phenol (**1c**) and (*E*)-*N*-(pyridin-4-ylmethylene)propan-1-amine (**1k**).



In an NMR tube, compound **1c** and **1k** were mixed with a final concentration 19.35 mM and a total volume of 0.62 mL with 10 equiv. of BIS-TRIS in the presence of 10 mol% L-proline as catalyst. The $^1\text{H-NMR}$ of $-\text{CH}=\text{N}-$ protons of the starting materials (8.70 ppm for **1c** and 8.37 ppm for **1k**) and the exchange products (8.53 ppm for **1h** and 8.51 ppm for **1n**) were followed until the reaction reached equilibrium. The kinetic data were fit assuming a reversible first-order reaction as shown in Figure 7.27.

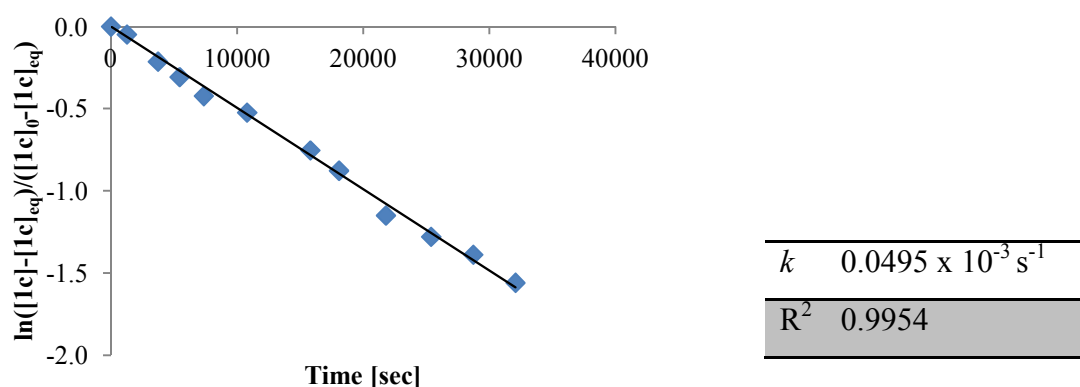
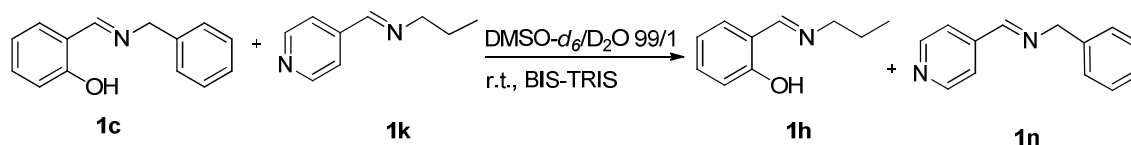


Figure 7.27 The plot of the kinetic study of the imine exchange between **1c** and **1k** in DMSO- d_6 /D $_2$ O 99/1 in the presence of 10 mol% L-proline and 10 equiv. of BIS-TRIS. Data were fit assuming a reversible first-order reaction.

28. The imine/imine exchange reaction between (*E*)-2-((benzylimino)methyl)phenol (**1c**) and (*E*)-*N*-(pyridin-4-ylmethylene)propan-1-amine (**1k**).



In an NMR tube, compound **1c** and **1k** were mixed with a final concentration 19.35 mM and a total volume of 0.62 mL with 10 equiv. of BIS-TRIS. The ¹H-NMR of –CH=N- protons of the starting materials (8.70 ppm for **1c** and 8.37 ppm for **1k**) and the exchange products (8.53 ppm for **1h** and 8.51 ppm for **1n**) were followed until the reaction reached equilibrium. The kinetic data were fit assuming a reversible first-order reaction as shown in Figure 7.28.

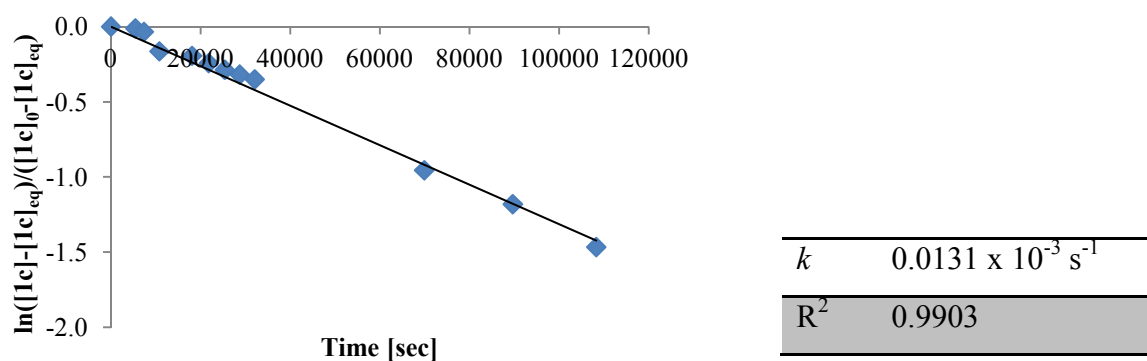
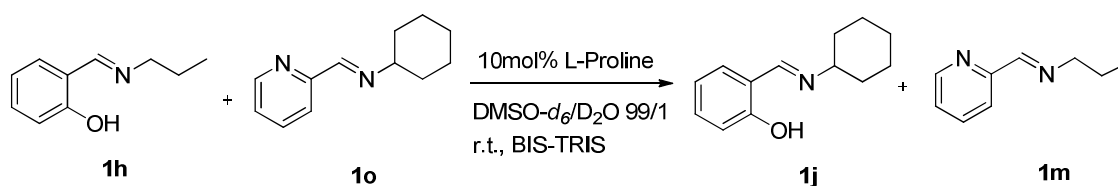


Figure 7.28 The plot of the kinetic study of the imine exchange between **1c** and **1k** in DMSO-*d*₆/D₂O 99/1 and 10 equiv. of BIS-TRIS at room temperature. Data were fit assuming a reversible first-order reaction.

29. The imine/imine exchange reaction between (*E*)-2-((propylimino)methyl)phenol (**1h**) and (*E*)-*N*-(pyridin-2-ylmethylene)cyclohexanamine (**1o**).



In an NMR tube, compound **1h** and **1o** were mixed with a final concentration 19.35 mM and a total volume of 0.62 mL with 10 equiv. of BIS-TRIS in the presence of 10mol% L-proline as catalyst. The ¹H-NMR of –CH=N- protons of the starting materials (8.53 ppm for **1h** and 8.35 ppm for **1o**) and the exchange products (8.55 ppm for **1j** and 8.33 ppm for **1m**) were followed until the reaction reached equilibrium. The kinetic data were fit assuming a reversible first-order reaction as shown in Figure 7.29.

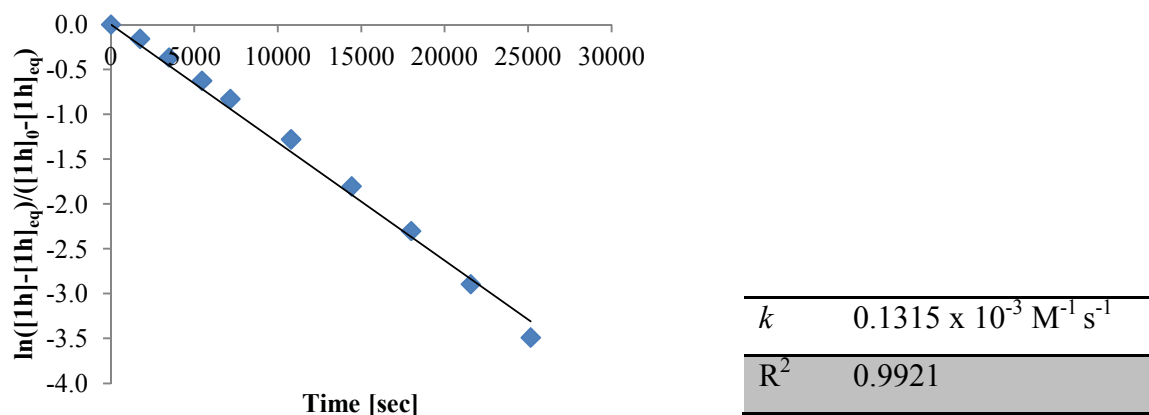
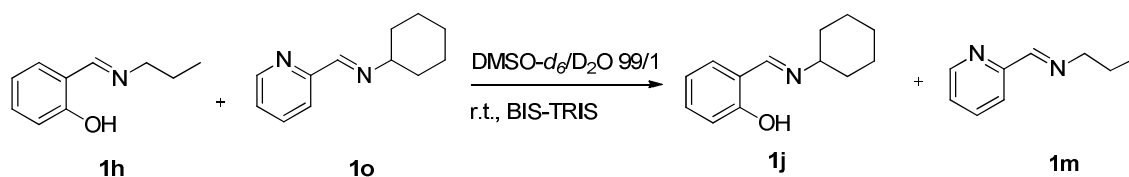


Figure 7.29 The plot of the kinetic study of the imine exchange between **1h** and **1o** in $\text{DMSO-}d_6/\text{D}_2\text{O}$ 99/1 in the presence of 10 mol% *L*-proline and 10 equiv. of BIS-TRIS at room temperature. Data were fit assuming a reversible first-order reaction.

30. The imine/imine exchange reaction between (*E*)-2-((propylimino)methyl)phenol (**1h**) and (*E*)-*N*-(pyridin-2-ylmethylene)cyclohexanamine (**1o**).



In an NMR tube, compound **1h** and **1o** were mixed with a final concentration 19.35 mM and a total volume of 0.62 mL with 10 equiv. of BIS-TRIS. The $^1\text{H-NMR}$ of $-\text{CH}=\text{N}$ -protons of starting materials (8.53 ppm for **1h** and 8.35 ppm for **1o**) and exchange products (8.55 ppm for **1j** and 8.33 ppm for **1m**) were followed until the reaction reached equilibrium. The kinetic data were fit assuming a reversible first-order reaction as shown in Figure 7.30.

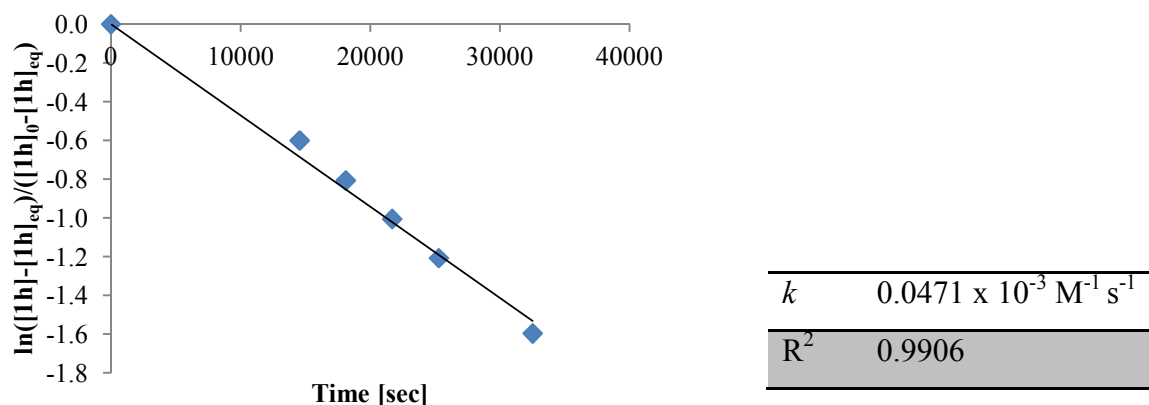
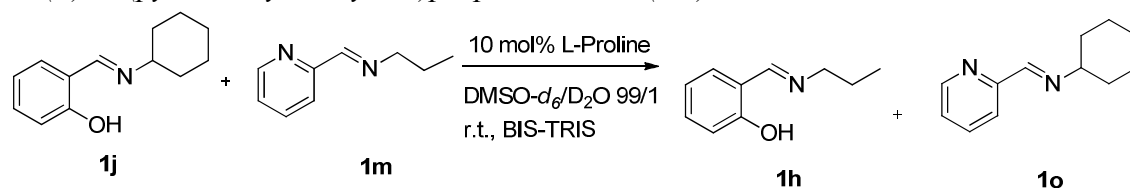


Figure 7.30 The plot of the kinetic study of the imine exchange between **1h** and **1o** in $\text{DMSO-}d_6/\text{D}_2\text{O}$ 99/1 and 10 equiv. BIS-TRIS at room temperature. Data were fit assuming a reversible first-order reaction.

31. The imine/imine exchange reaction between 2-((cyclohexylimino)methyl)phenol (**1j**) and (E)-N-(pyridin-2-ylmethylene)propan-1-amine (**1m**).



In an NMR tube, compound **1j** and **1m** were mixed with a final concentration 19.35 mM and a total volume of 0.62 mL with 10 equiv. of BIS-TRIS in the presence of 10mol% L-proline as catalyst. The $^1\text{H-NMR}$ of $-\text{CH}=\text{N}-$ protons of starting materials (8.55 ppm for **1j** and 8.33 ppm for **1m**) and exchange products (8.53 ppm for **1h** and 8.35 ppm for **1o**) were followed until the reaction reached equilibrium. The kinetic data were fit assuming a reversible first-order reaction as shown in Figure 7.31.

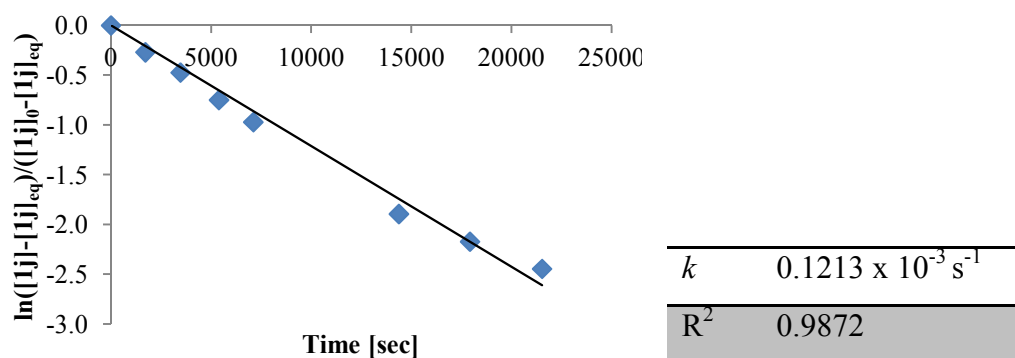
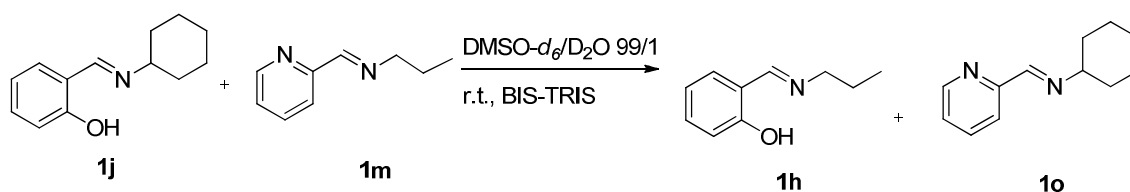


Figure 7.31 The plot of the kinetic study of the imine exchange between **1j** and **1m** in $\text{DMSO-}d_6/\text{D}_2\text{O}$ 99/1 in the presence of 10 mol% L-proline and 10 equiv. of BIS-TRIS at room temperature. Data were fit assuming a reversible first-order reaction.

32. The imine/imine exchange reaction between 2-((cyclohexylimino)methyl)phenol (**1j**) and (E)-N-(pyridin-2-ylmethylene)propan-1-amine (**1m**).



In an NMR tube, compound **1j** and **1m** were mixed with a final concentration 19.35 mM and a total volume of 0.62 mL with 10 equiv. of BIS-TRIS. The $^1\text{H-NMR}$ of $-\text{CH}=\text{N}-$ protons of the starting materials (8.55 ppm for **1j** and 8.33 ppm for **1m**) and the exchange products (8.53 ppm for **1h** and 8.35 ppm for **1o**) were followed until the reaction reached equilibrium. The kinetic data were fit assuming a reversible first-order reaction as shown in Figure 7.32.

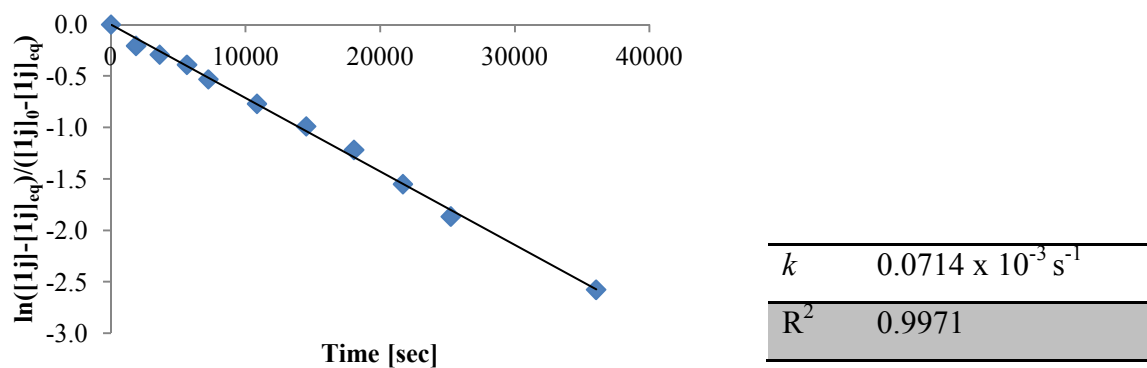


Figure 7.32 The plot of the kinetic study of the imine exchange between **1j** and **1m** in DMSO- d_6 /D₂O 99/1 and 10 equiv. BIS-TRIS as buffer solution at room temperature. Data were fit assuming a reversible first-order reaction.

7.2.3 Studying of Knoevenagel/Imine (C=C/C=N) derivatives exchange

- *General procedure for C=C/C=N exchange.* Stock solutions (0.50 mL) of Knoevenagel and imine products (60 mM) in DMSO- d_6 /D₂O 99/1 were freshly prepared. For the uncatalyzed reaction, 200 μL of each solution was added to a NMR tube then followed by 220 μL of DMSO- d_6 /D₂O 99/1 to adjust to a final volume of 620 μL . For the catalyzed reaction, 20 μL of L-proline stock solution (60 mM in DMSO- d_6 /D₂O 99/1) was added to a NMR tube, followed by the addition of 200 μL of each solution and 200 μL of DMSO- d_6 /D₂O 99/1. The procedure for C=C/C=N exchange in DMSO- d_6 is similar to that described for DMSO- d_6 /D₂O 99/1.

Results of the study Knoevenagel/Imine (C=C/C=N) derivatives exchange

1. The cross-exchange C=C/C=N reaction between 5-(4-(dimethylamino) benzylidene) pyrimidine-2,4,6(1H,3H,5H)-trione (**2a**) and (*E*)-*N*-(4-chlorobenzylidene)-1-phenylmethanamine (**1t**)

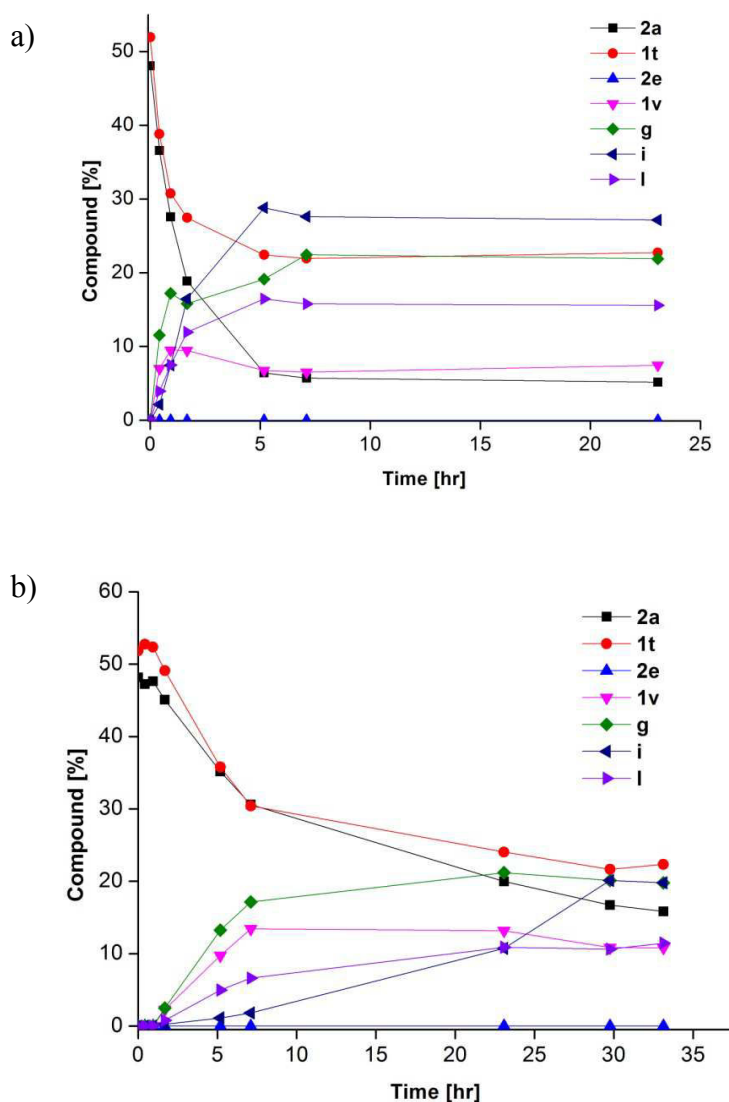
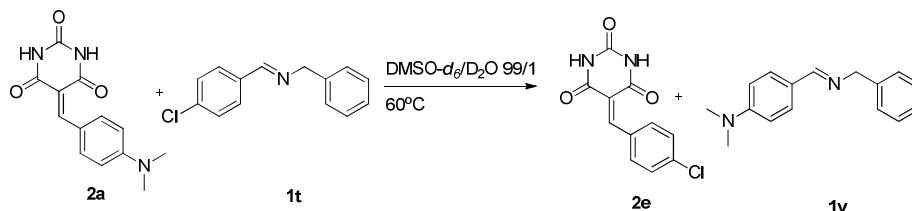


Figure 7.33 The exchange reaction between **2a** and **1t** as a function of time a) in the presence of 10 mol% L-proline and b) in the absence of catalyst. **g** = 4-chlorobenzaldehyde, **i** = 4-(dimethylamino)benzaldehyde, **l** = 4-chlorobenzaldehyde hydrate. Error in ¹H-NMR integration: ~4-5%.

2. The cross-exchange C=C/C=N reaction between 5-(4-chlorobenzylidene) pyrimidine-2,4,6(1H,3H,5H)-trione (**2e**) and (*E*)-4-((benzylimino)methyl)-*N,N*-dimethylaniline (**1v**)

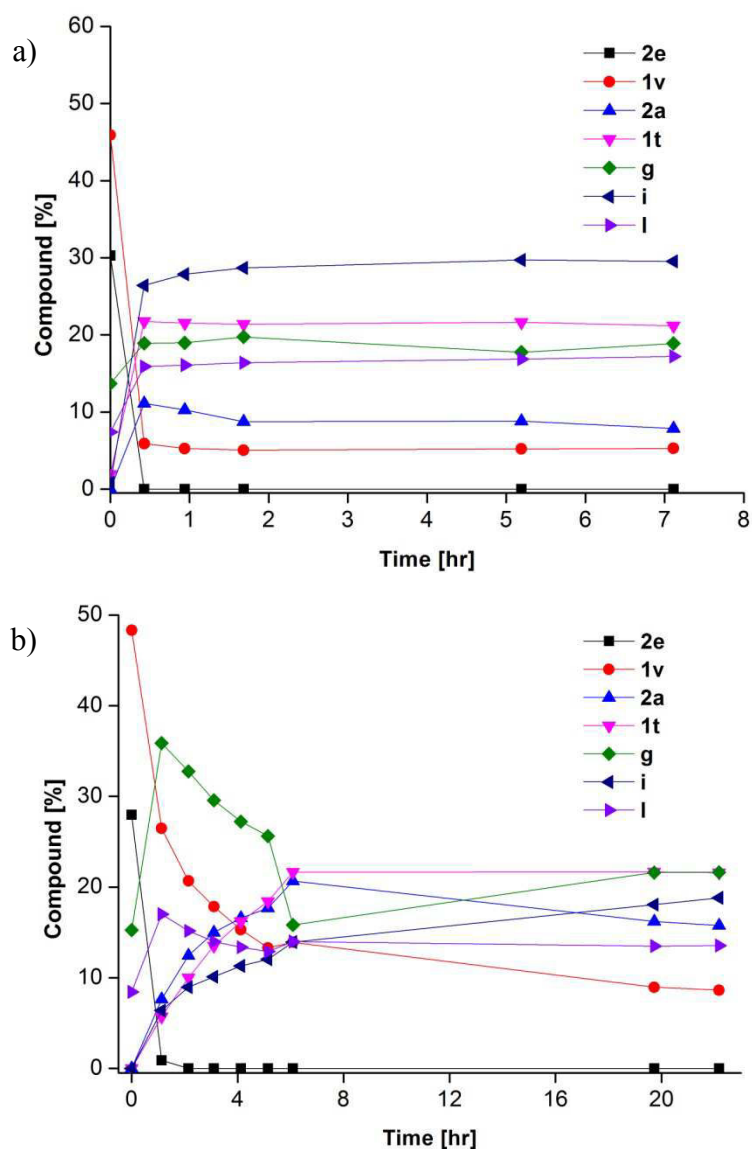
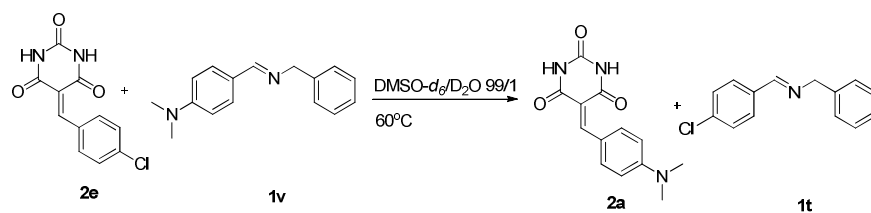


Figure 7.34 The exchange reaction between **2e** and **1v** as a function of time a) in the presence of 10 mol% *L*-proline and b) in the absence of catalyst. **g** = 4-chlorobenzaldehyde, **i** = 4-(dimethylamino)benzaldehyde, **l** = 4-chlorobenzaldehyde hydrate. Error in ¹H-NMR integration: ~4-5%.

3. The cross-exchange $C=C/C=N$ reaction between 5-(4-(dimethylamino) benzylidene) pyrimidine-2,4,6(1H,3H,5H)-trione (**2a**) and (*E*)-1-phenyl-*N*-(thiophen-2-ylmethylene) methanamine (**1b**)

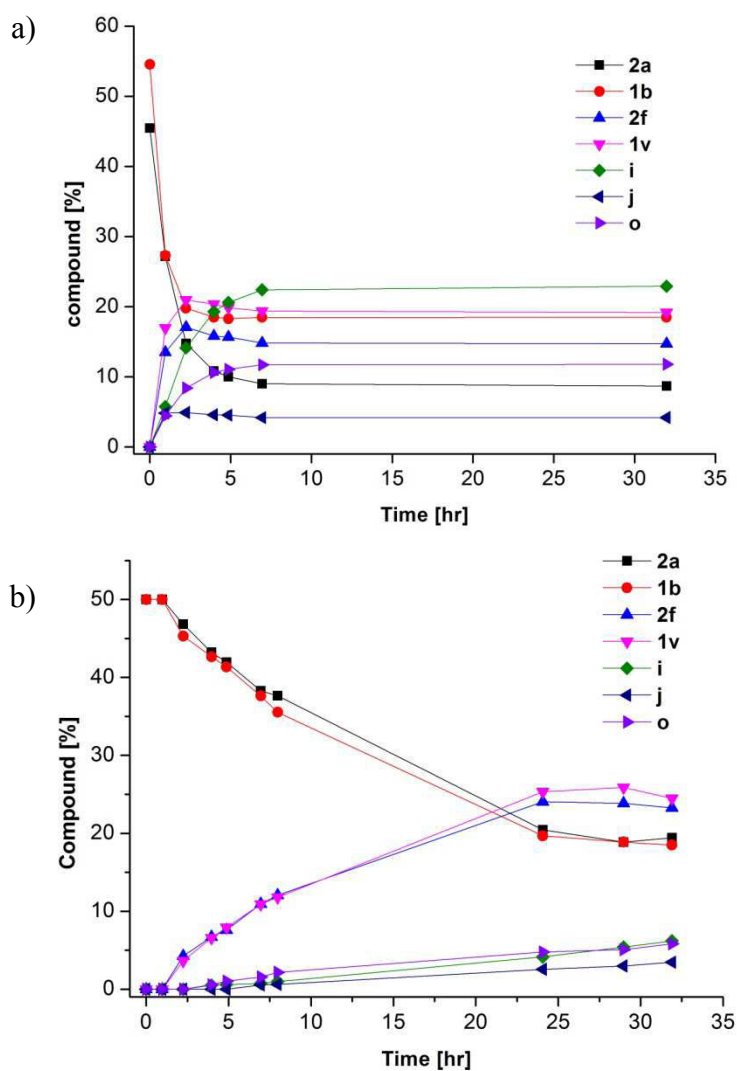
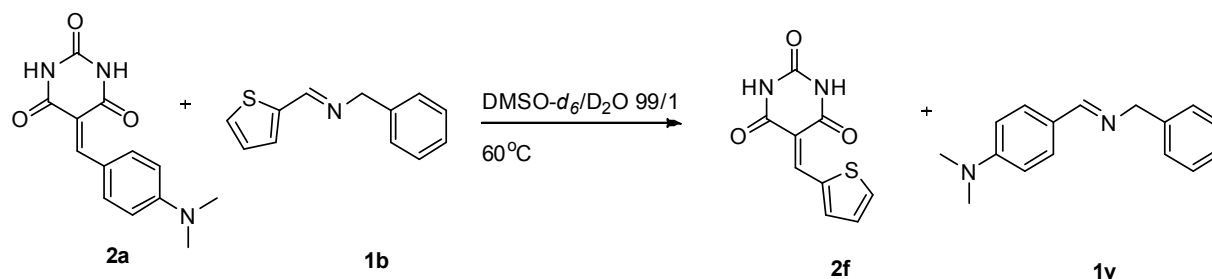


Figure 7.35 The exchange reaction between **2a** and **1b** as a function of time a) in the presence of 10 mol% L-proline and b) in the absence of catalyst. **i** = 4-(dimethylamino)benzaldehyde, **l** = 4-chlorobenzaldehyde hydrate, and **o** = 2-thiophene carboxaldehyde hydrate. Error in 1H -NMR integration: ~ 4 -5%.

4. The cross-exchange $C=C/C=N$ reaction between 5-(thiophen-2-ylmethylene) pyrimidine-2,4,6(1H,3H,5H)-trione (**2f**) and (*E*)-4-((benzylimino)methyl)-*N,N*-dimethyl aniline (**1v**)

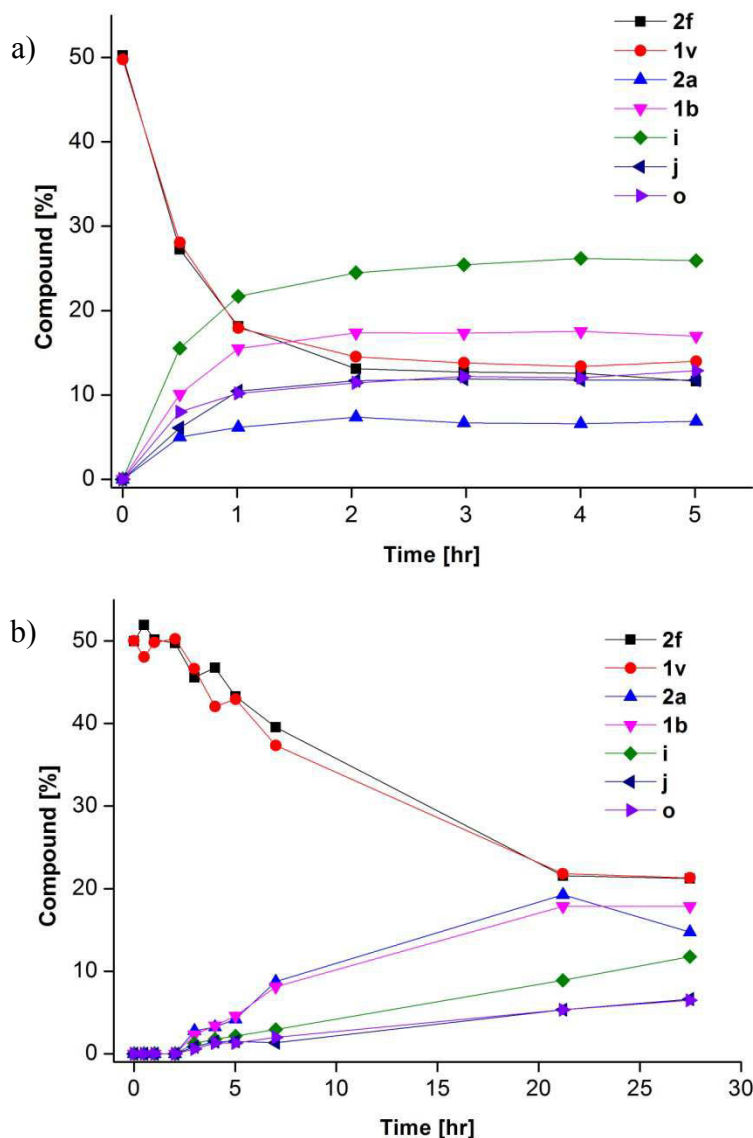
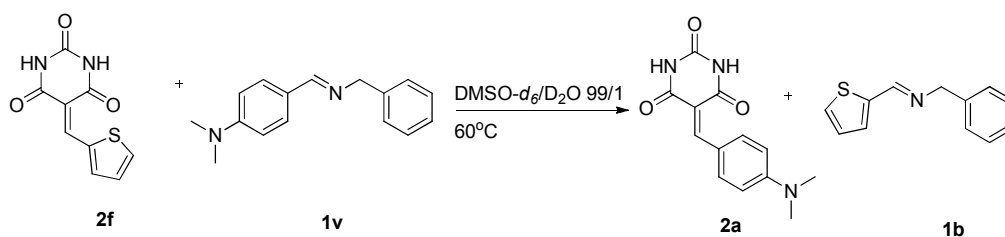


Figure 7.36 The exchange reaction between **2f** and **1v** as a function of time a) in the presence of 10 mol% *L*-proline and b) in the absence of catalyst. **i** = 4-(dimethylamino)benzaldehyde, **l** = 4-chlorobenzaldehyde hydrate, and **o** = 2-thiophene carboxaldehyde hydrate, Error in $^1\text{H-NMR}$ integration: $\sim 4\text{-}5\%$.

5. The cross-exchange $C=C/C=N$ reaction between 5-(4-methoxybenzylidene) pyrimidine-2,4,6(1H,3H,5H)-trione (**2b**) and (*E*)-4-((benzylimino)methyl)-*N,N*-dimethylaniline (**1v**)

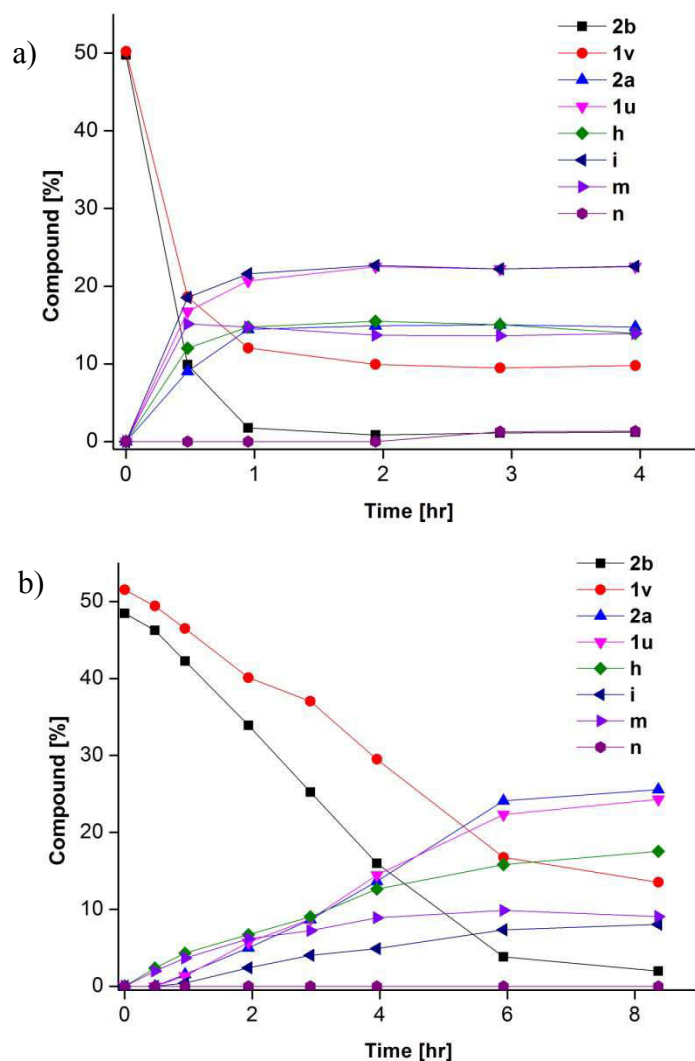
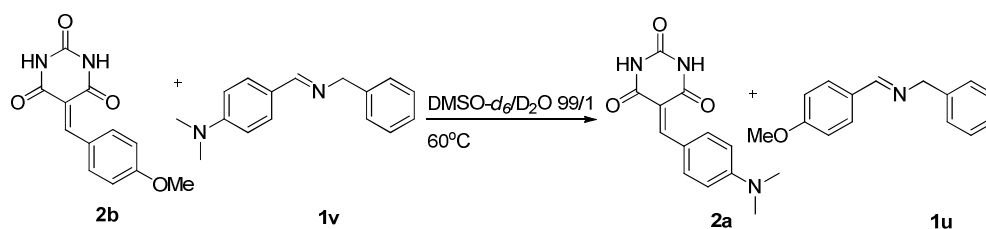


Figure 7.37 The exchange reaction between **2b** and **1v** as a function of time a) in the presence of 10 mol% *L*-proline and b) in the absence of catalyst. **h** = 4-methoxybenzaldehyde, **i** = 4-(dimethylamino)benzaldehyde, **m** = 4-methoxybenzaldehyde hydrate, **n** = 4-(dimethylamino)benzaldehyde hydrate. Error in 1H -NMR integration: ~ 4 -5%.

6. The cross-exchange $C=C/C=N$ reaction between 5-(4-(dimethylamino)benzylidene)pyrimidine-2,4,6(1H,3H,5H)-trione (**2a**) and (*E*)-*N*-(4-methoxybenzylidene)-1-phenylmethanamine (**1u**)

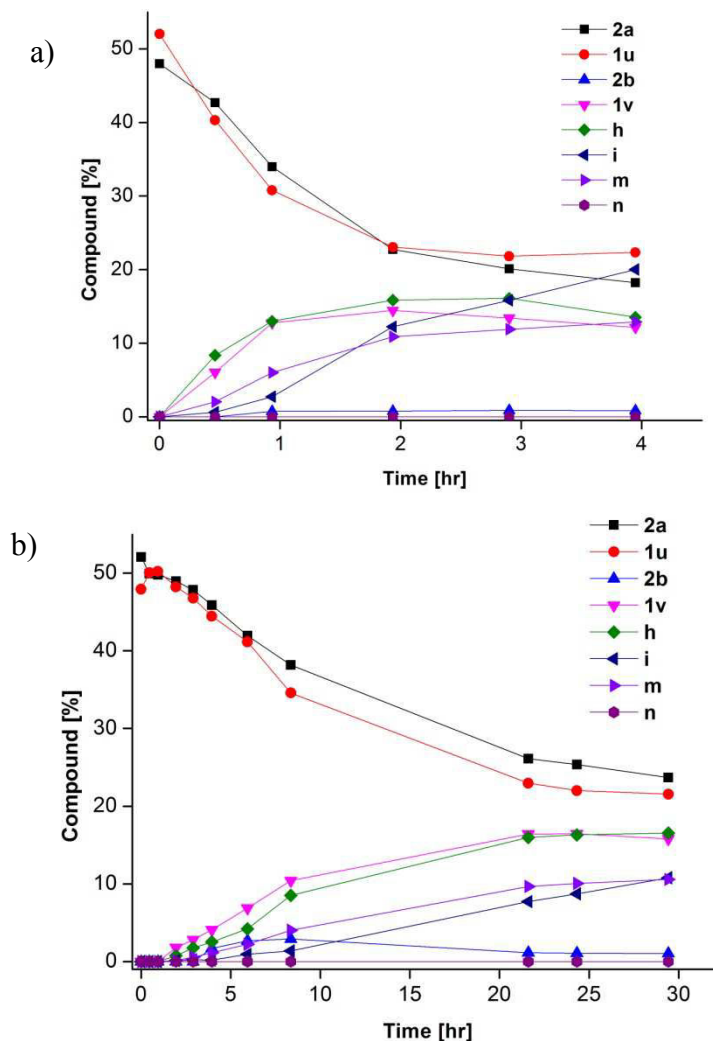
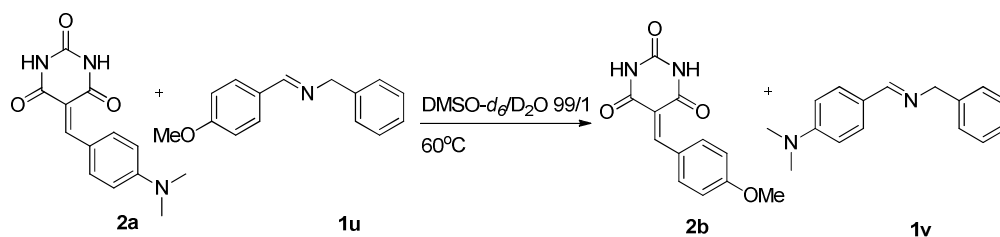


Figure 7.38 The exchange reaction between **2a** and **1u** as a function of time a) in the presence of 10 mol% *L*-proline and b) in the absence of catalyst. **h** = 4-methoxybenzaldehyde, **i** = 4-(dimethylamino)benzaldehyde, **m** = 4-methoxybenzaldehyde hydrate, **n** = 4-(dimethylamino)benzaldehyde hydrate. Error in $^1\text{H-NMR}$ integration: ~4-5%.

7. The cross-exchange $C=C/C=N$ reaction between 5-(4-methoxybenzylidene) pyrimidine-2,4,6(1H,3H,5H)-trione (**2b**) and (E)-4-((benzylimino)methyl)-N,N-dimethylaniline (**1v**)

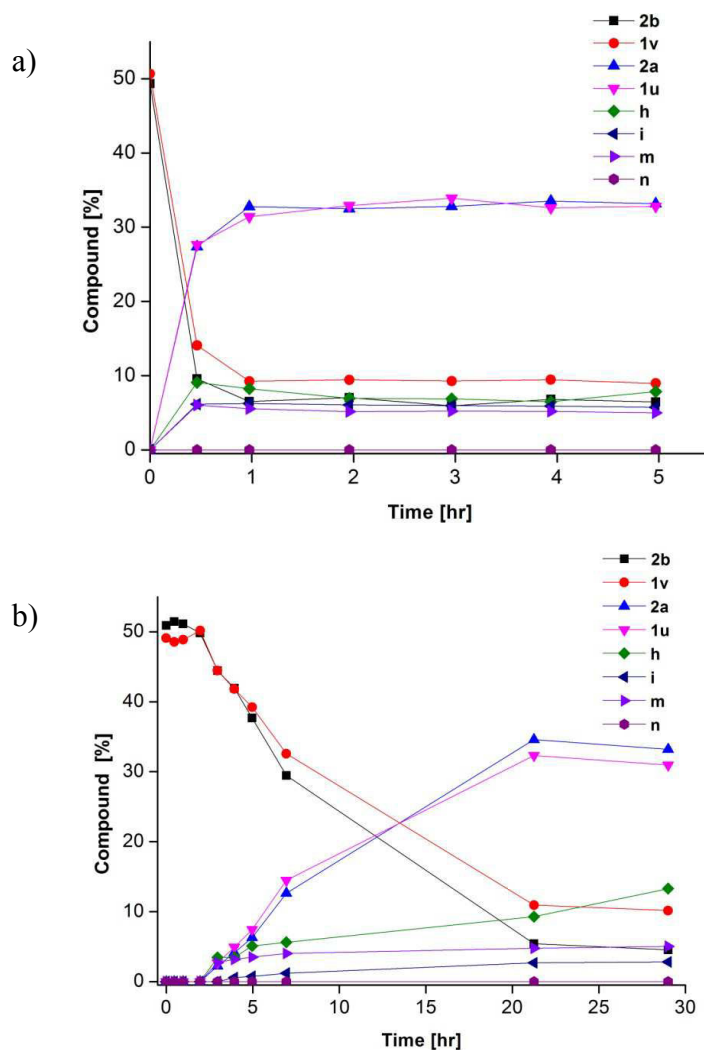
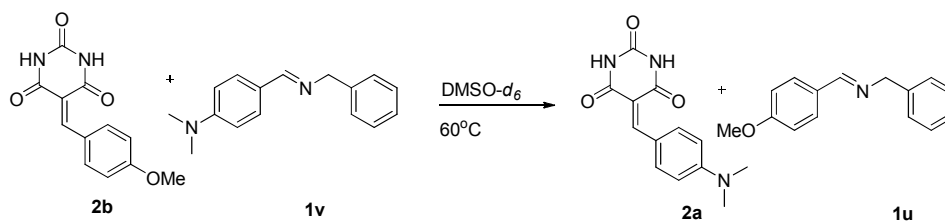


Figure 7.39 The exchange reaction between **2b** and **1v** as a function of time a) in the presence of 10 mol% L-proline and b) in the absence of catalyst. **h** = 4-methoxybenzaldehyde, **i** = 4-(dimethylamino)benzaldehyde, **m** = 4-methoxybenzaldehyde hydrate, **n** = 4-(dimethylamino)benzaldehyde hydrate. Error in $^1\text{H-NMR}$ integration: ~4-5%.

8. The cross-exchange $C=C/C=N$ reaction between 5-[4-(Dimethylamino)benzylidene]pyrimidine-2,4,6(1H,3H,5H)-trione (**2a**) and *N*-[(1*E*)-(4-methoxyphenyl)methylidene]benzenemethanamine (**1u**)

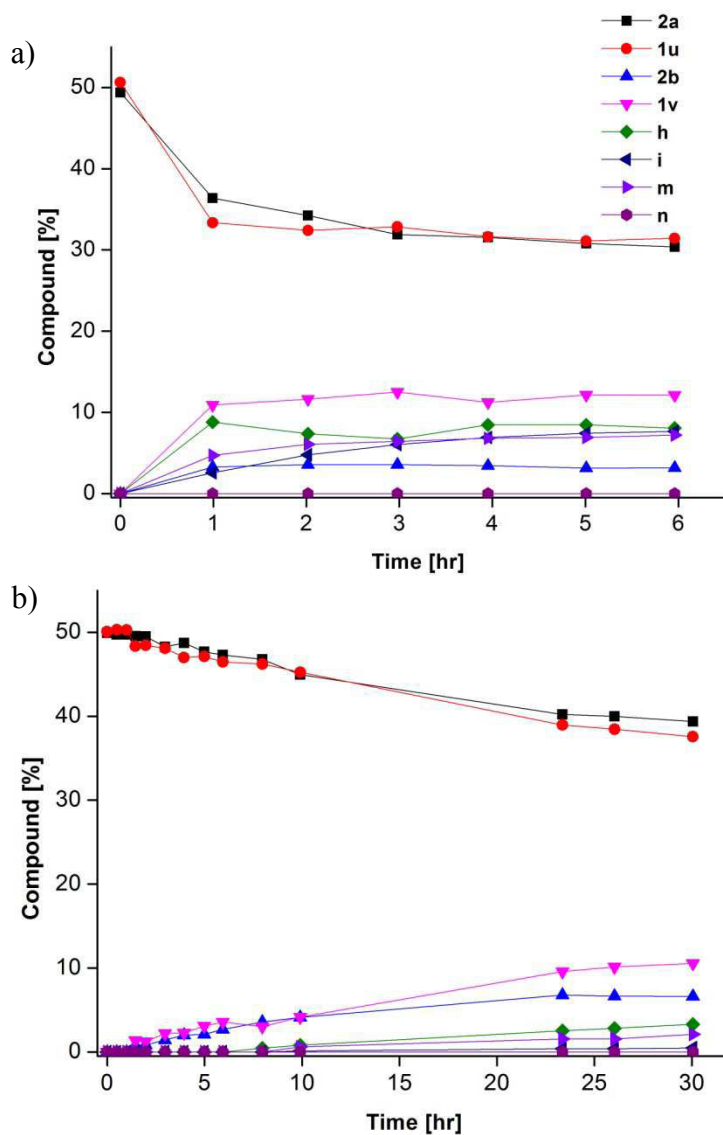
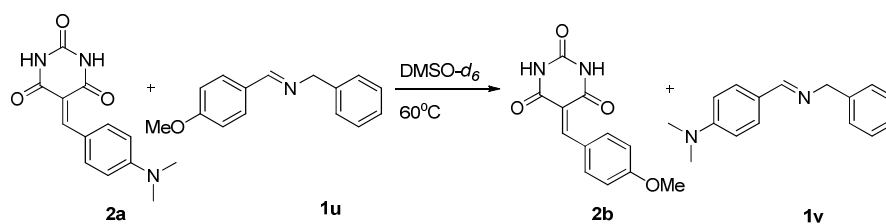


Figure 7.40 The exchange reaction between **2a** and **1u** as a function of time a) in the presence of 10 mol% *L*-proline and b) in the absence of catalyst. **h** = 4-methoxybenzaldehyde, **i** = 4-(dimethylamino)benzaldehyde, **m** = 4-methoxybenzaldehyde hydrate, **n** = 4-(dimethylamino)benzaldehyde hydrate. Error in $^1\text{H-NMR}$ integration: ~4-5%.

9. The cross-exchange $C=C/C=N$ reaction between 5-(thiophen-2-ylmethylene) pyrimidine-2,4,6(1*H*,3*H*,5*H*)-trione (**2f**) and (*E*)-4-((benzylimino)methyl)-*N,N*-dimethyl aniline (**1v**)

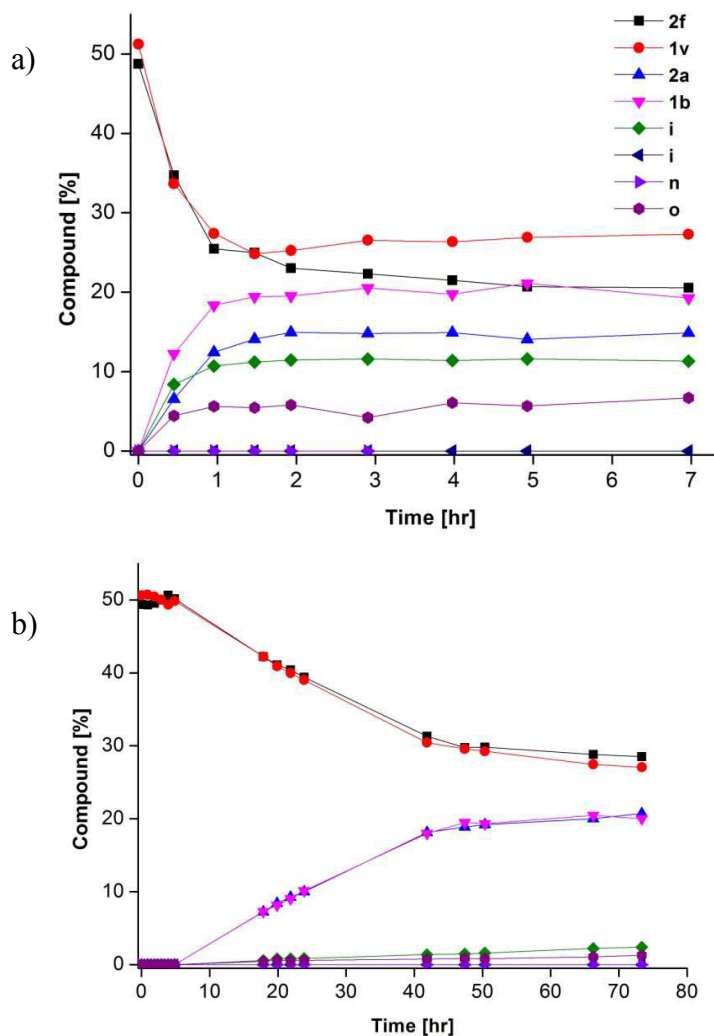
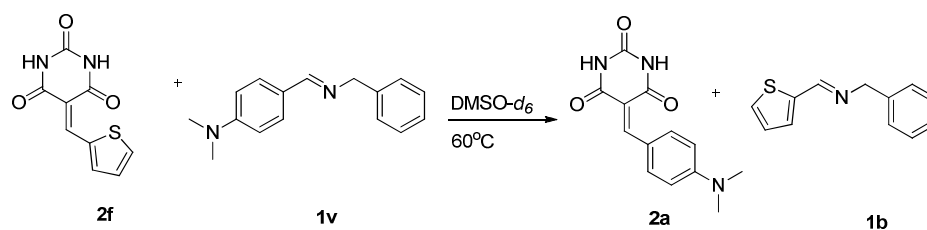


Figure 7.41 The exchange reaction between **2f** and **1v** as a function of time a) in the presence of 10 mol% *L*-proline and b) in the absence of catalyst. *i* = 4-(dimethylamino)benzaldehyde, *j* = 2-thiophene carboxaldehyde, *n* = 4-(dimethylamino)benzaldehyde hydrate, and *o* = 2-thiophene carboxaldehyde hydrate. Error in $^1\text{H-NMR}$ integration: $\sim 4\text{-}5\%$.

10. The cross-exchange $C=C/C=N$ reaction between 5-(4-(dimethylamino)benzylidene)pyrimidine-2,4,6(1H,3H,5H)-trione (**2a**) and (*E*)-1-phenyl-*N*-(thiophen-2-ylmethylene)methanamine (**1b**)

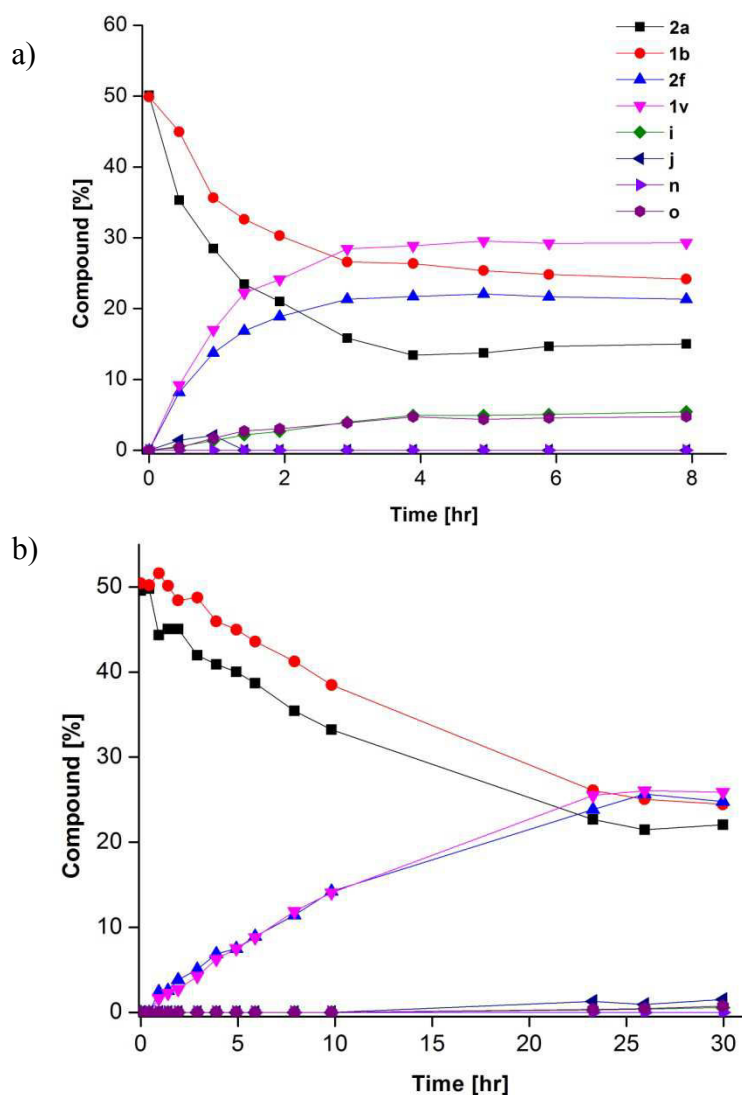
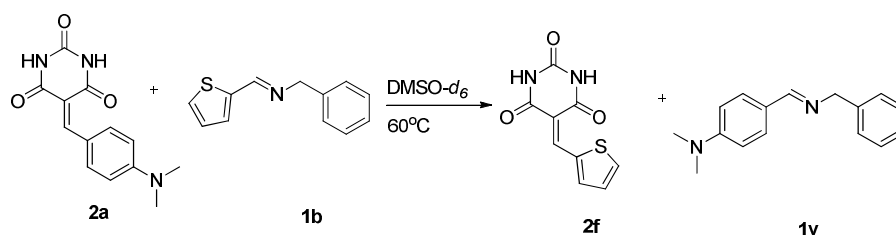


Figure 7.42 The exchange reaction between **2a** and **1b** as a function of time a) in the presence of 10 mol% *L*-proline and b) in the absence of catalyst. **i** = 4-(dimethylamino)benzaldehyde, **j** = 2-thiophene carboxaldehyde, **n** = 4-(dimethylamino)benzaldehyde hydrate, and **o** = 2-thiophene carboxaldehyde hydrate. Error in $^1\text{H-NMR}$ integration: $\sim 4\text{-}5\%$.

11. The cross-exchange $C=C/C=N$ reaction between 5-(4-(dimethylamino)benzylidene)pyrimidine-2,4,6(1H,3H,5H)-trione (**2a**) and (*E*)-*N*-(4-chlorobenzylidene)-1-phenylmethanamine (**1t**)

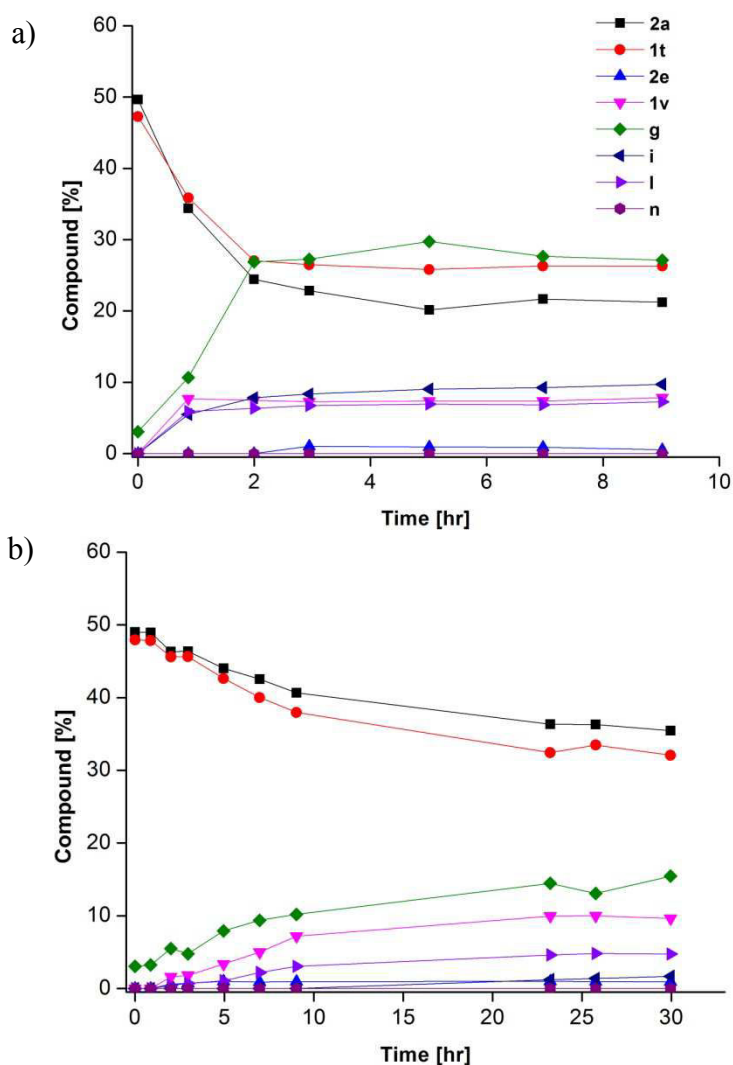
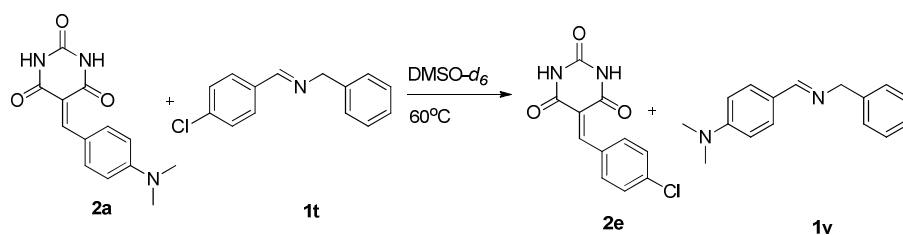


Figure 7.43 The exchange reaction between **2a** and **1t** as a function of time a) in the presence of 10 mol% L-proline and b) in the absence of catalyst. **g** = 4-Chlorobenzaldehyde, **i** = 4-(dimethylamino)benzaldehyde, **l** = 4-chlorobenzaldehyde hydrate, **n** = 4-(dimethylamino)benzaldehyde hydrate. Error in $^1\text{H-NMR}$ integration: $\sim 4\text{-}5\%$.

12. The cross-exchange C=C/C=N reaction between 5-(4-chlorobenzylidene) pyrimidine-2,4,6(1H,3H,5H)-trione (**2e**) and (E)-4-((benzylimino)methyl)-N,N-dimethylaniline (**1v**)

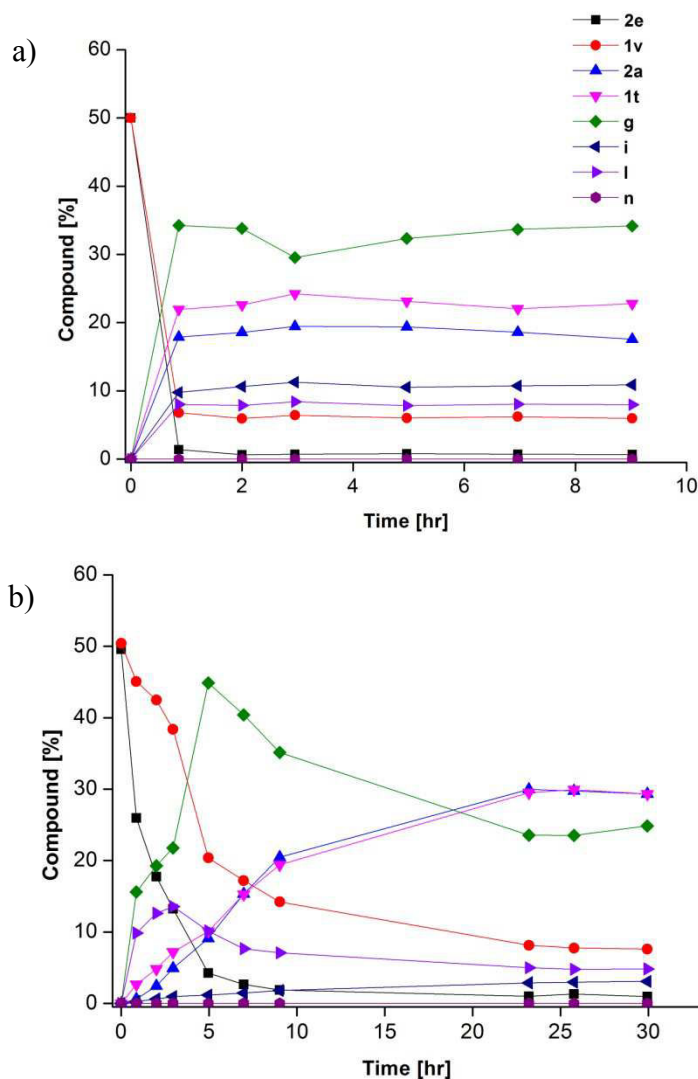
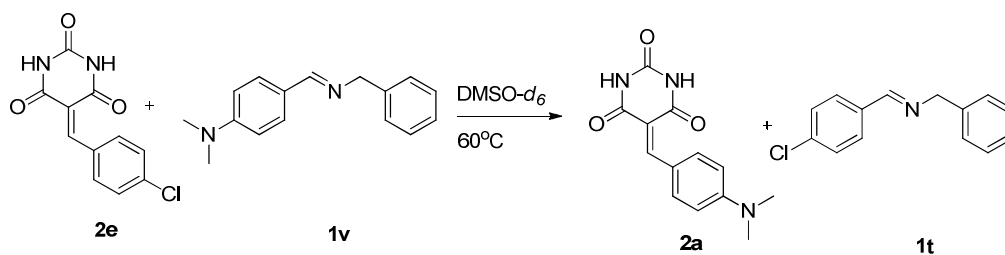


Figure 7.44 The exchange reaction between **2e** and **1v** as a function of time a) in the presence of 10 mol% L-proline and b) in the absence of catalyst. **g** = 4-Chlorobenzaldehyde, **i** = 4-(dimethylamino)benzaldehyde, **l** = 4-chlorobenzaldehyde hydrate, **n** = 4-(dimethylamino)benzaldehyde hydrate. Error in ¹H-NMR integration: ~4-5%.

7.2.4 Study of Knoevenagel/Knoevenagel (C=C/C=C) derivatives exchange

● *General Procedure for Knoevenagel Cross Exchange Reaction (C=C/C=C Exchange).* All reactions with two Knoevenagel compounds were carried out at 60°C with a final concentration 12.8 mM and total volume of 600 μl . Stock solns. of Knoevenagel compounds in DMSO- d_6 were prepared. The stock solns. of reactants were 60 mM and had a total volume of 0.5 ml. The stock soln. of L-proline was 12.8 mM and had a total volume of 0.5 ml. For the uncatalyzed reaction, 128 μl of the soln. of each Knoevenagel compound was added to a NMR tube, followed by 344 μl of DMSO- d_6 to adjust to a final volume of 600 μl . For the catalyzed reaction, 38 μl of a L-proline stock soln. (12.8 mM in DMSO- d_6) was added to a NMR tube, followed by the addition of 128 μl of soln. of each Knoevenagel compound and 306 μl of DMSO- d_6 .

Results of the study of Knoevenagel/Knoevenagel (C=C/C=N) derivatives exchange

1. The cross-exchange C=C/C=C reaction between 5-(4-(dimethylamino)benzylidene)pyrimidine-2,4,6(1H,3H,5H)-trione (**2a**) and 2-(4-nitrobenzylidene)malononitrile (**3d**)

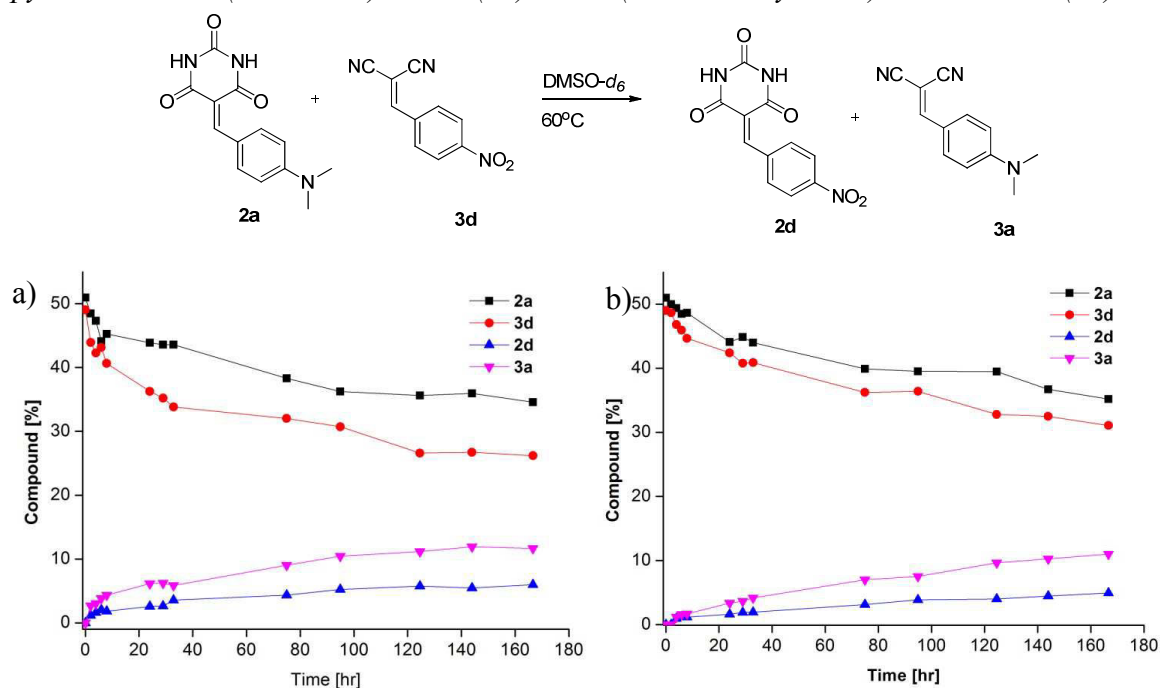


Figure 7.45 The exchange reaction between **2a** and **3d** as a function of time a) in the presence of 10 mol% L-proline and b) in the absence of catalyst.

2. The cross-exchange $C=C/C=C$ reaction between 5-benzylidenepyrimidine-2,4,6(1H,3H,5H)-trione (**2c**) and 2-(4-nitrobenzylidene)malononitrile (**3d**)

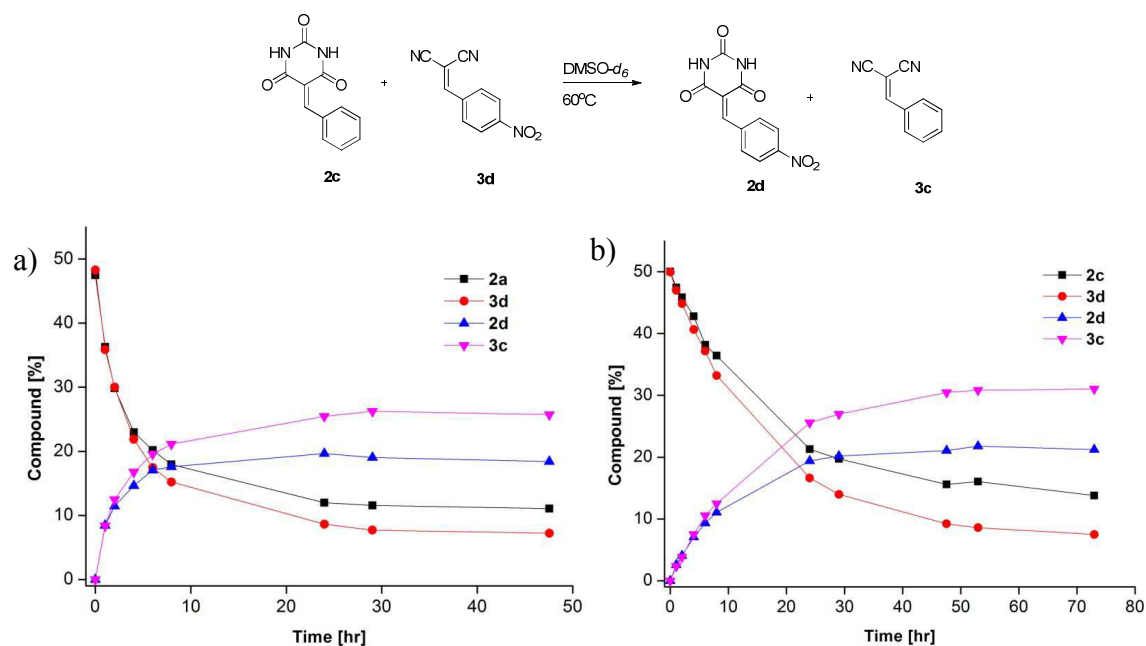


Figure 7.46 The exchange reaction between **2c** and **3d** as a function of time a) in the presence of 10 mol% L-proline and b) in the absence of catalyst.

3. The cross-exchange $C=C/C=C$ reaction between 5-benzylidenepyrimidine-2,4,6(1H,3H,5H)-trione (**2d**) and 2-(4-nitrobenzylidene)malononitrile (**3c**)

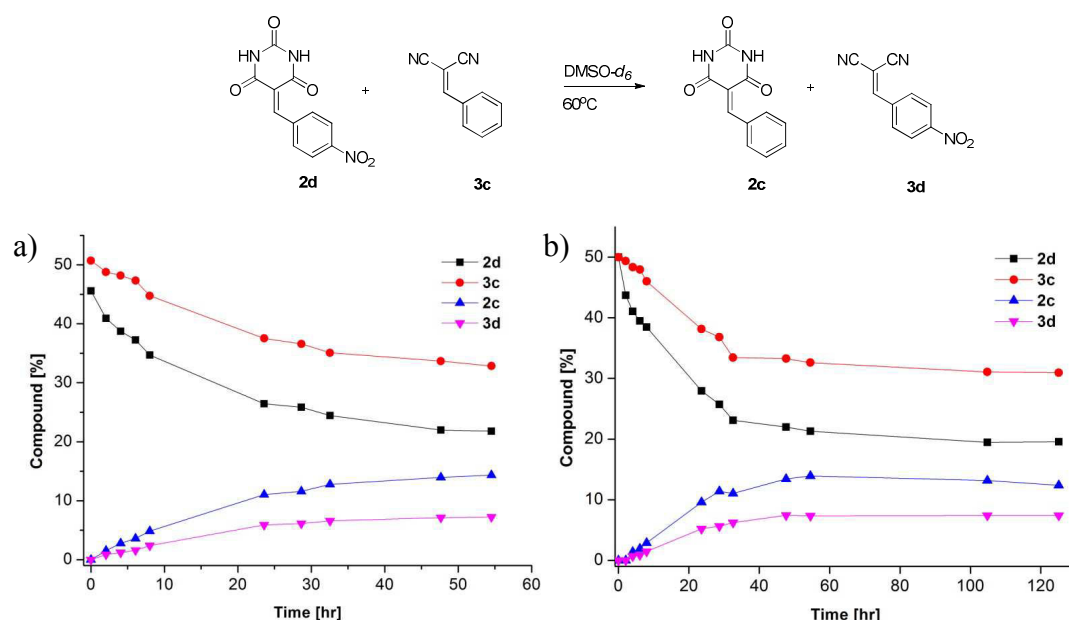


Figure 7.47 The exchange reaction between **2d** and **3c** as a function of time a) in the presence of 10 mol% L-proline and b) in the absence of catalyst.

4. The cross-exchange C=C/C=C reaction between 5-(4-(dimethylamino)benzylidene)pyrimidine-2,4,6(1H,3H,5H)-trione (**2a**) and 2-(4-methoxybenzylidene)malononitrile (**3b**)

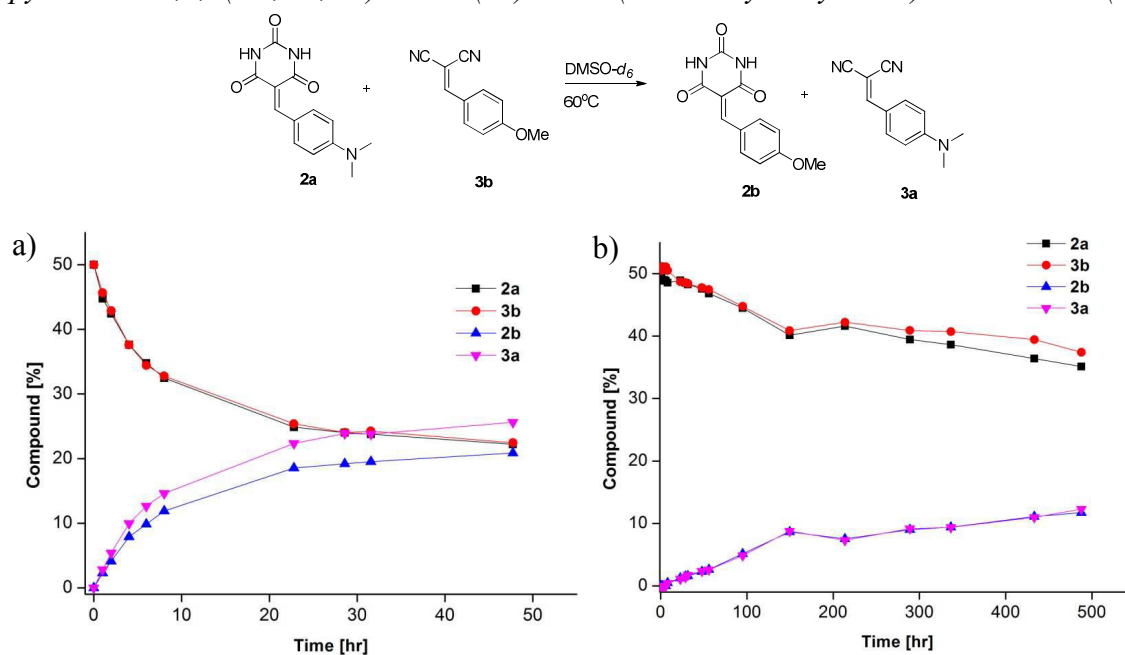


Figure 7.48 The exchange reaction between **2a** and **3b** as a function of time a) in the presence of 10 mol% L-proline and b) in the absence of catalyst.

5. The cross-exchange C=C/C=C reaction between 5-(4-methoxybenzylidene)pyrimidine-2,4,6(1H,3H,5H)-trione (**2b**) and 2-(4-(dimethylamino)benzylidene)malononitrile (**3a**)

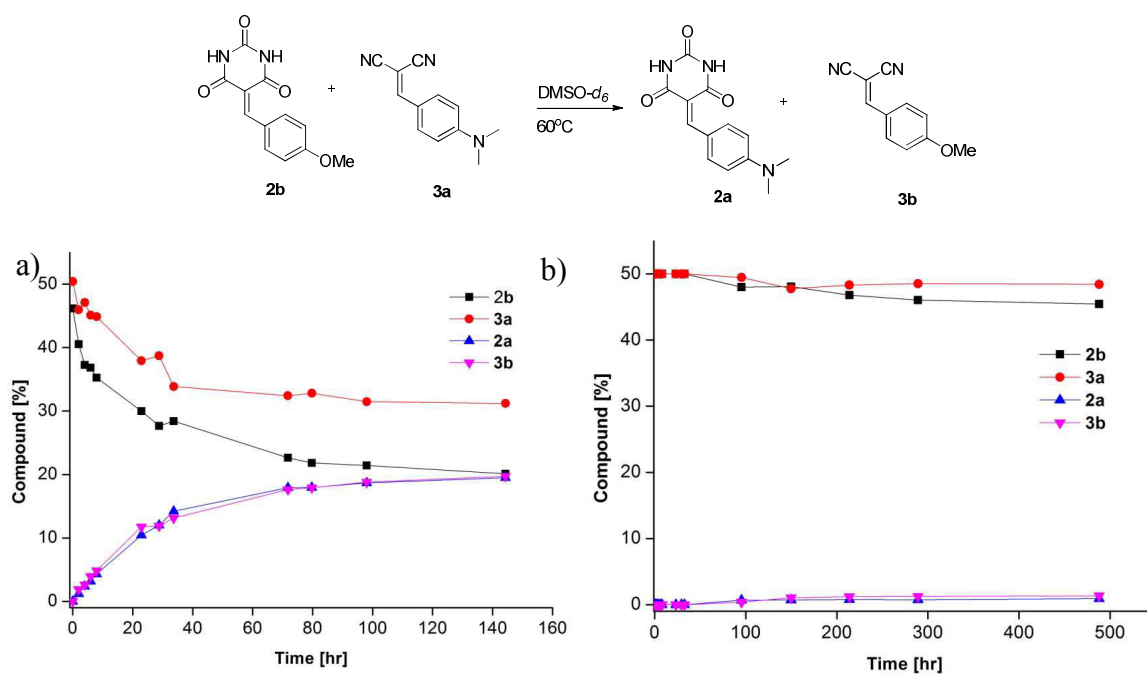


Figure 7.49 The exchange reaction between **2b** and **3a** as a function of time a) in the presence of 10 mol% L-proline and b) in the absence of catalyst.

6. The cross-exchange $C=C/C=C$ reaction between 5-(thiophen-2-ylmethylene)pyrimidine-2,4,6(1H,3H,5H)-trione (**2f**) and 2-(4-(methoxy)benzylidene)malononitrile (**3b**)

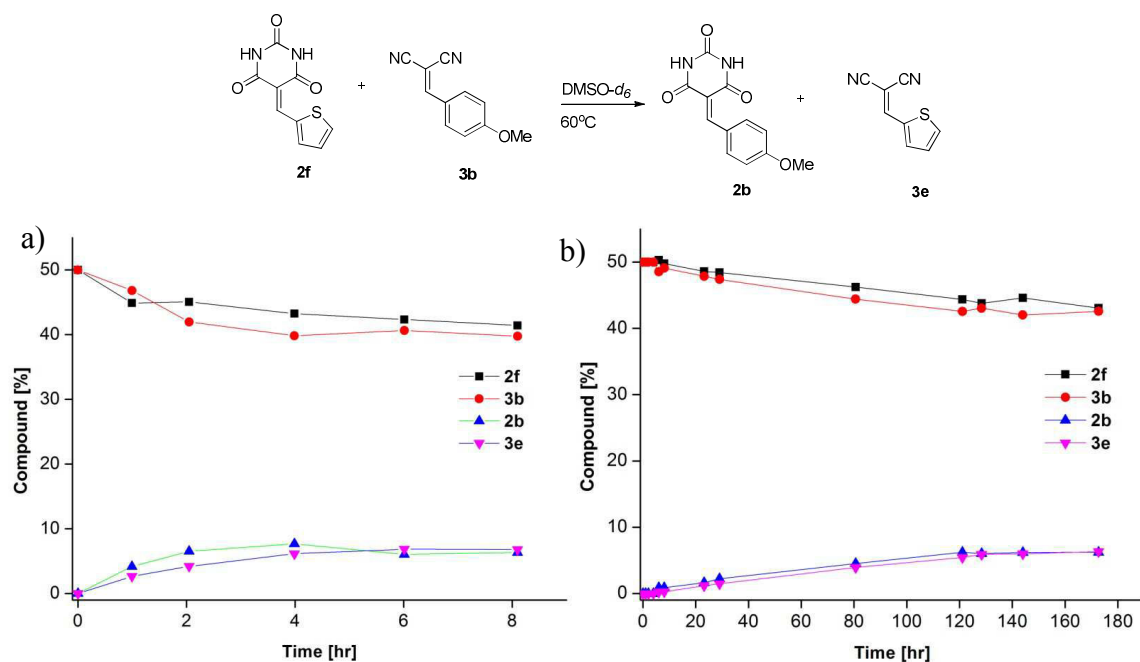


Figure 7.50 The exchange reaction between **2f** and **3b** as a function of time a) in the presence of 10 mol% L-proline and b) in the absence of catalyst.

7. The cross-exchange $C=C/C=C$ reaction between 5-(4-methoxybenzylidene)pyrimidine-2,4,6(1H,3H,5H)-trione (**2b**) and 2-(thiophen-2-ylmethylene)malononitrile (**3b**)

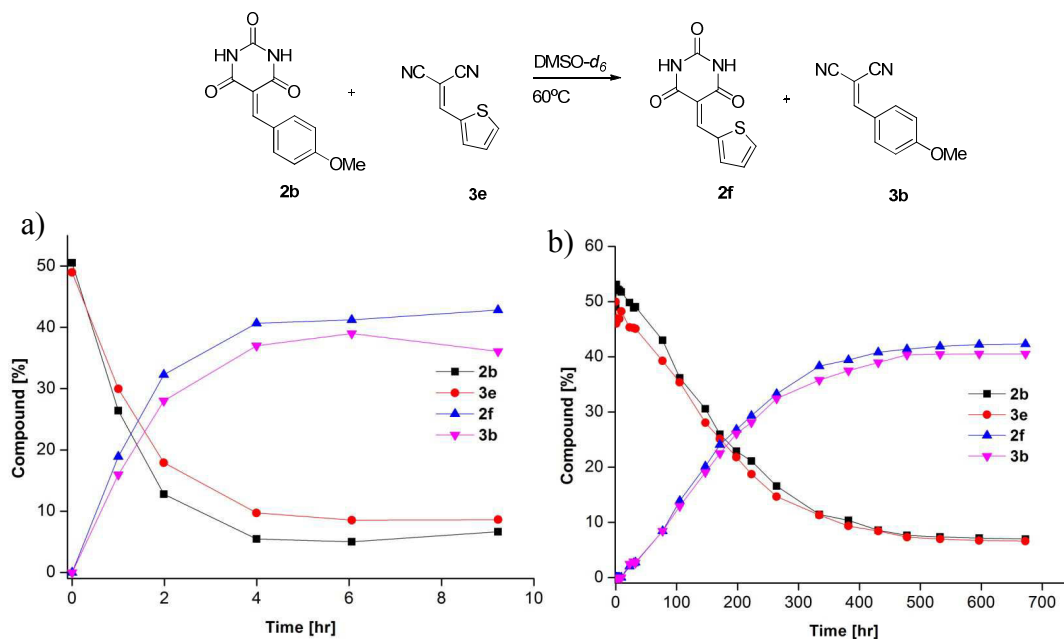


Figure 7.51 The exchange reaction between **2b** and **3e** as a function of time a) in the presence of 10 mol% L-proline and b) in the absence of catalyst.

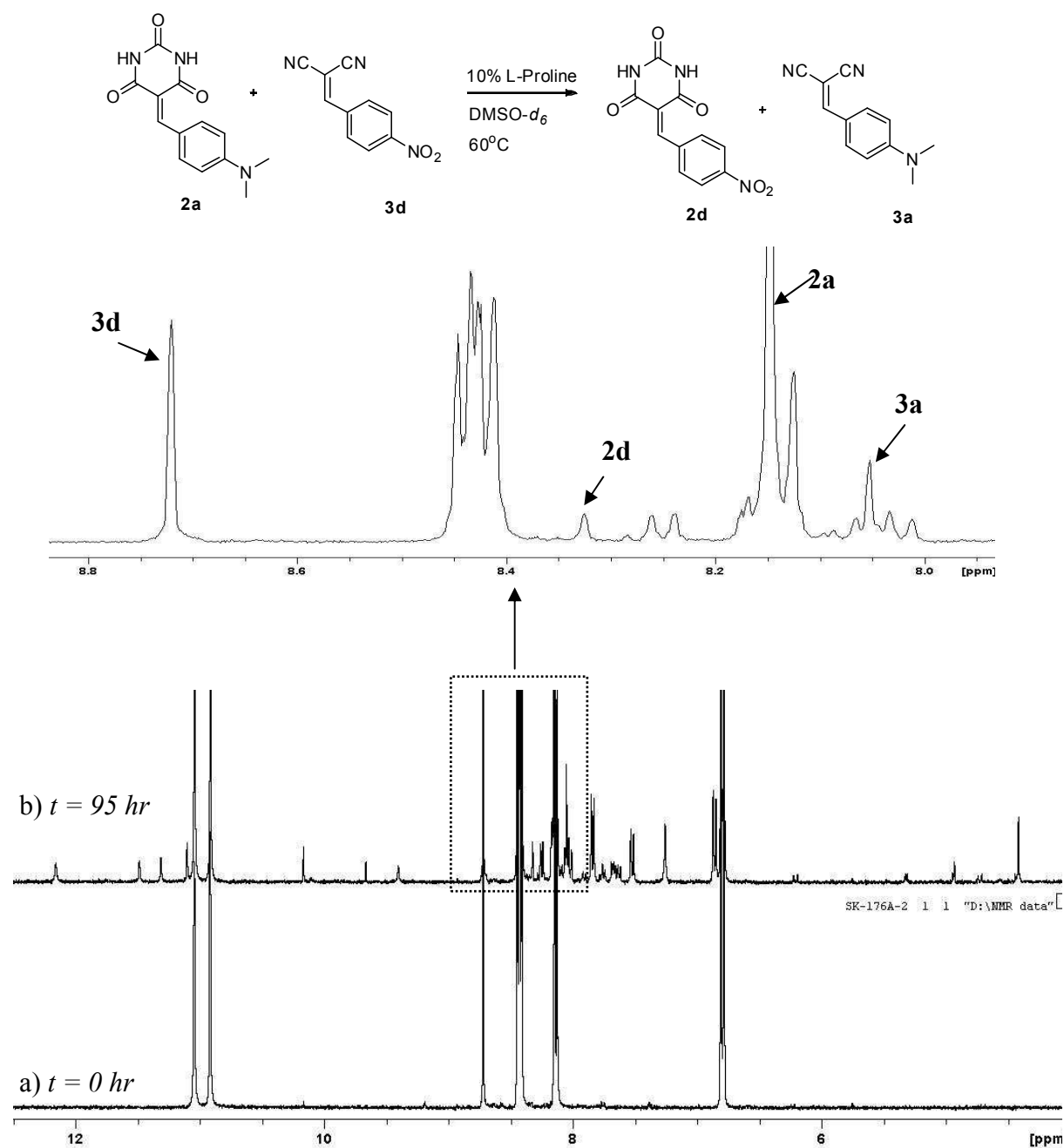


Figure 7.52 The $^1\text{H-NMR}$ spectrum of the exchange reaction between **2a** and **3d** in $\text{DMSO-}d_6$ in the presence of 10 mol% L-proline. a) after mixing, b) at 95 hr showing the exchange products **2d** and **3a** involving the hydrolysis products and Michael-type adducts **XI** and **XII**.

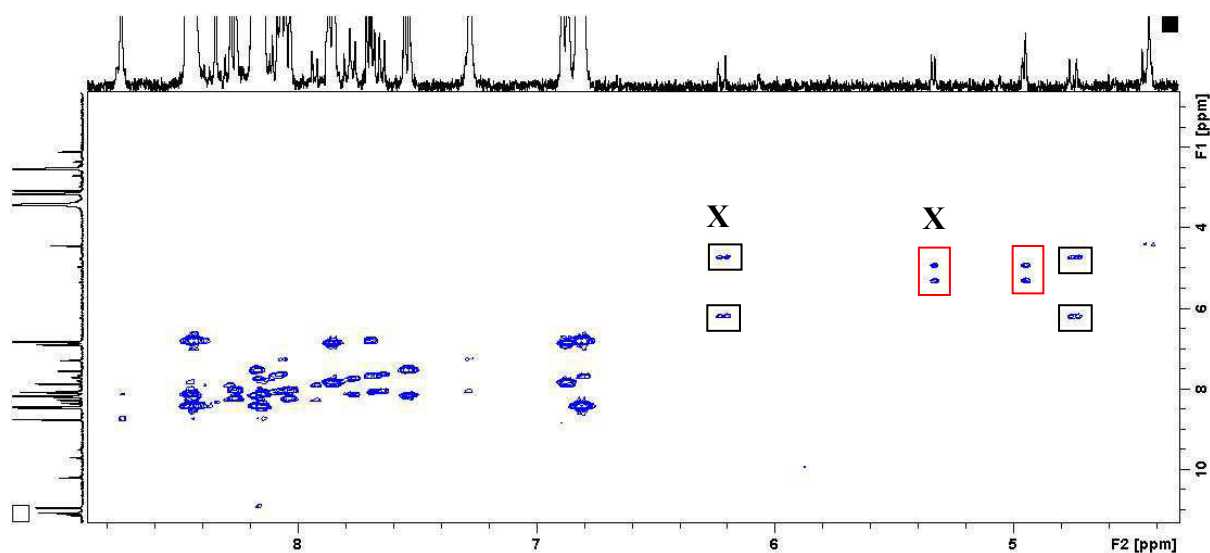
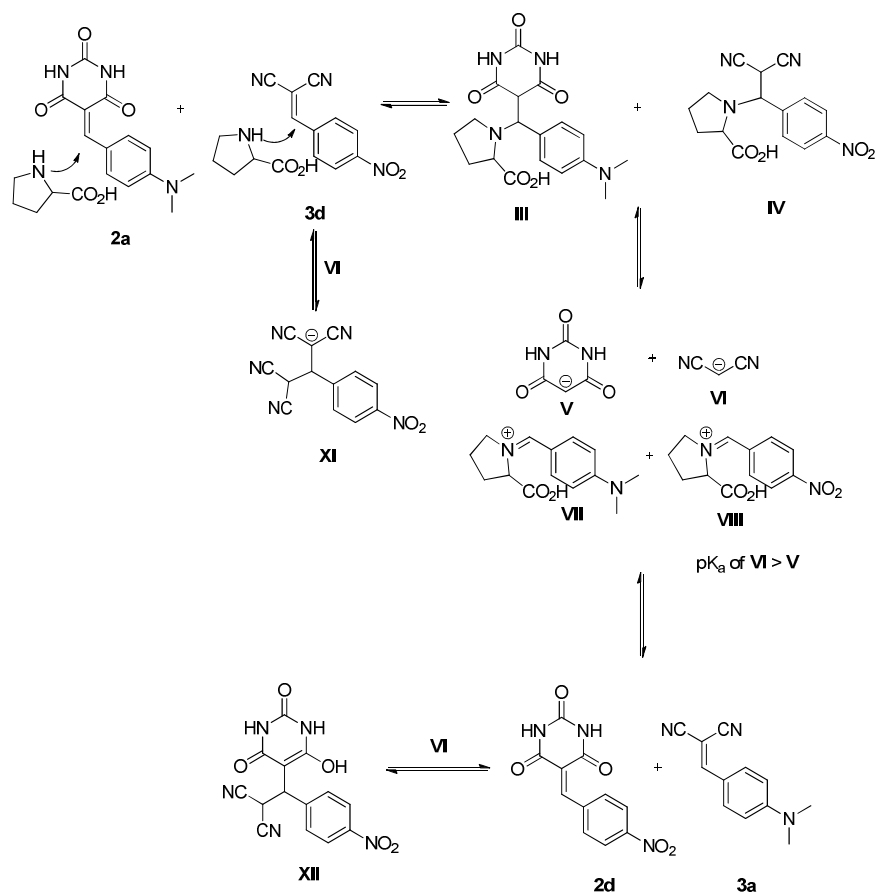


Figure 7.53 An example of a 2D ^1H -COSY spectrum of the exchange reaction between **2a** and **3d** in $\text{DMSO-}d_6$ in the presence of 10 mol% *L*-proline. The signal from 4.73 – 6.21 ppm showed the formation of the Michael-type adducts **XI** and **XII**.

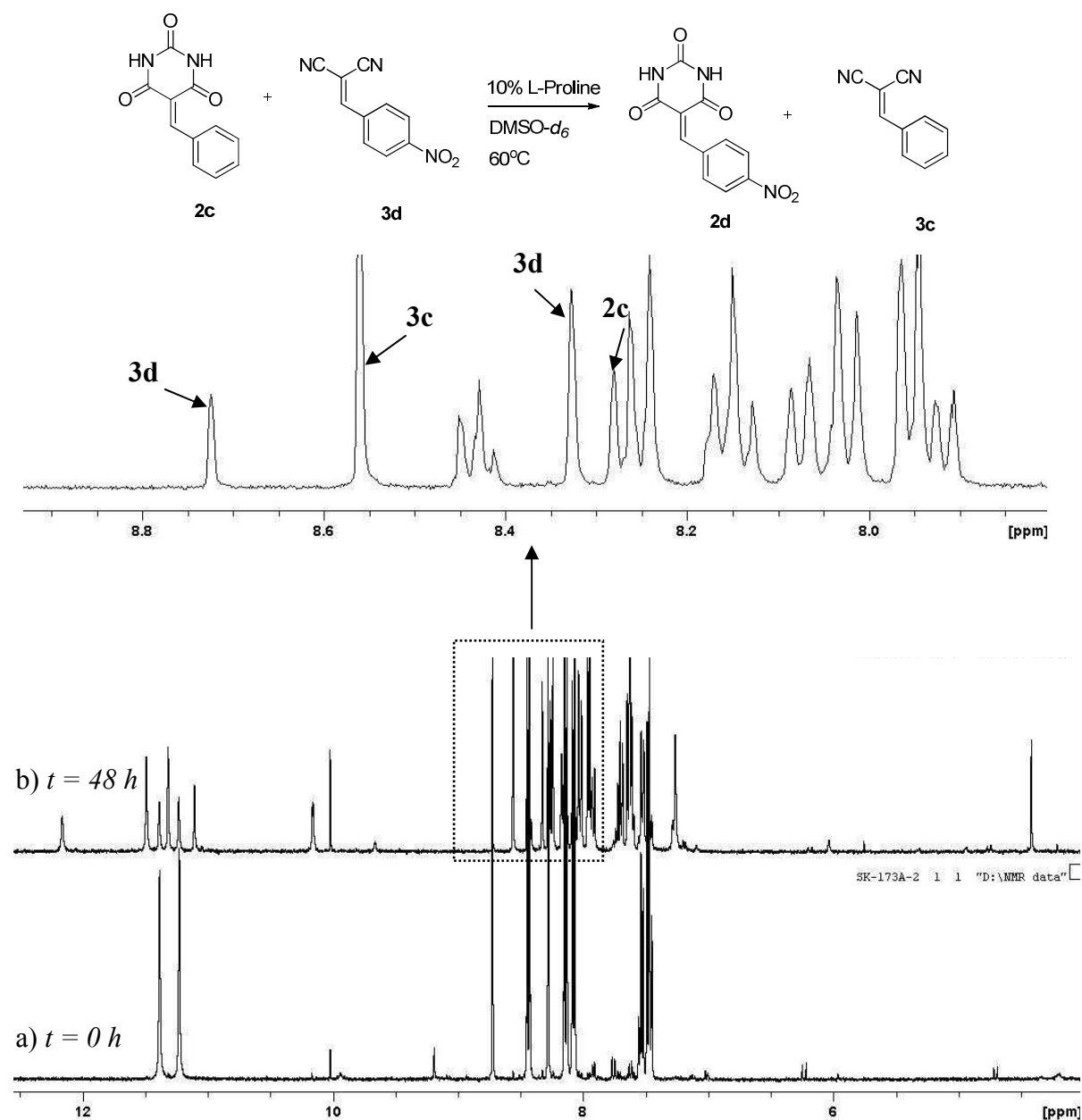


Figure 7.54 The $^1\text{H-NMR}$ spectrum of the exchange reaction between **2c** and **3d** in $\text{DMSO-}d_6$ in the presence of 10 mol% L-proline. a) after mixing, b) at 48 hr showing the exchange products **2d** and **3c** involving the hydrolysis products and Michael-type adducts **XI** and **XII**.

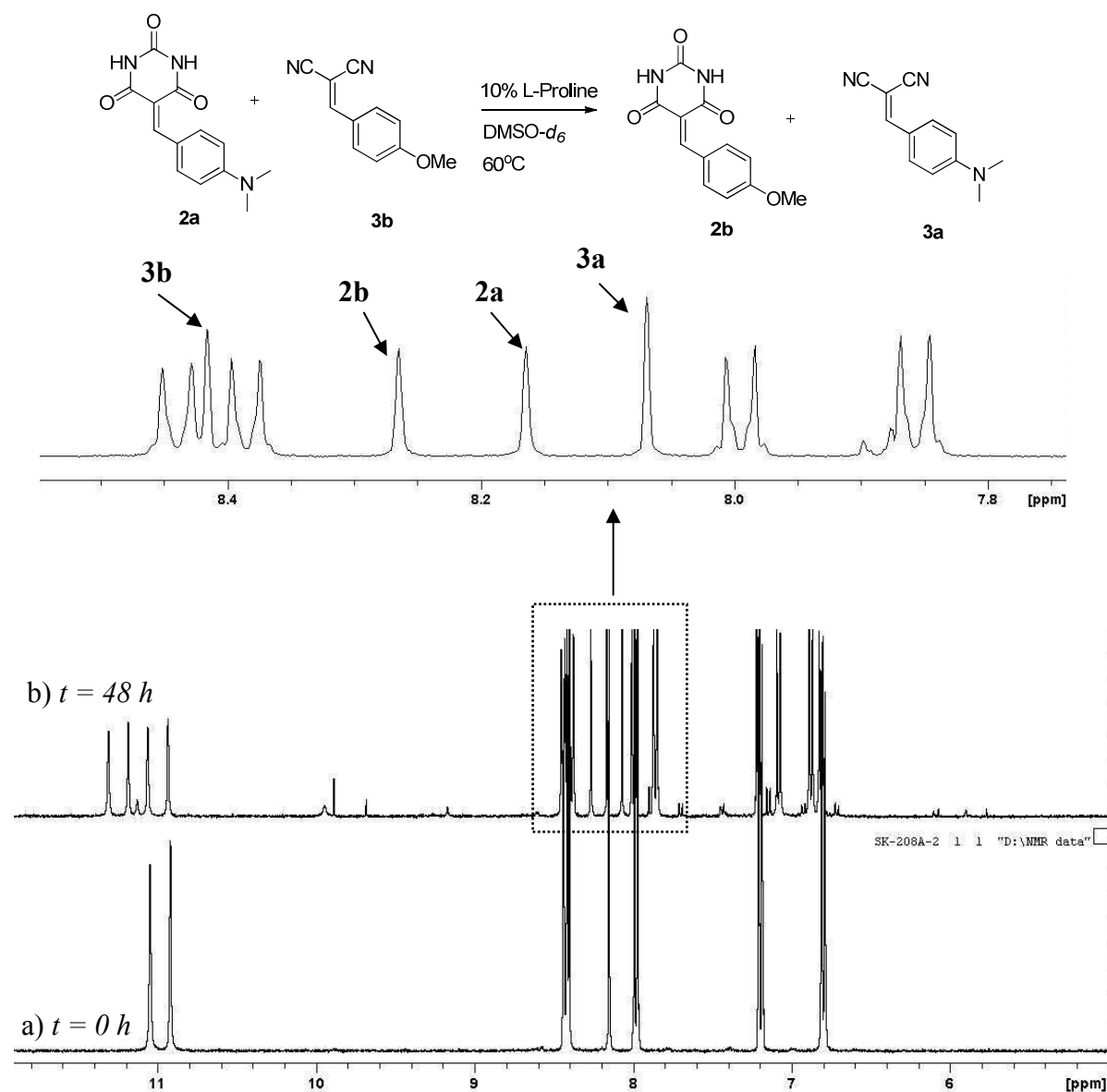


Figure 7.55 The $^1\text{H-NMR}$ spectrum of the exchange reaction between **2a** and **3b** in $\text{DMSO-}d_6$ in the presence of 10 mol% L-proline. a) after mixing, b) at 48 hr showing the exchange products **2b** and **3a** involving the hydrolysis products and Michael-type adducts **XI** and **XII**.

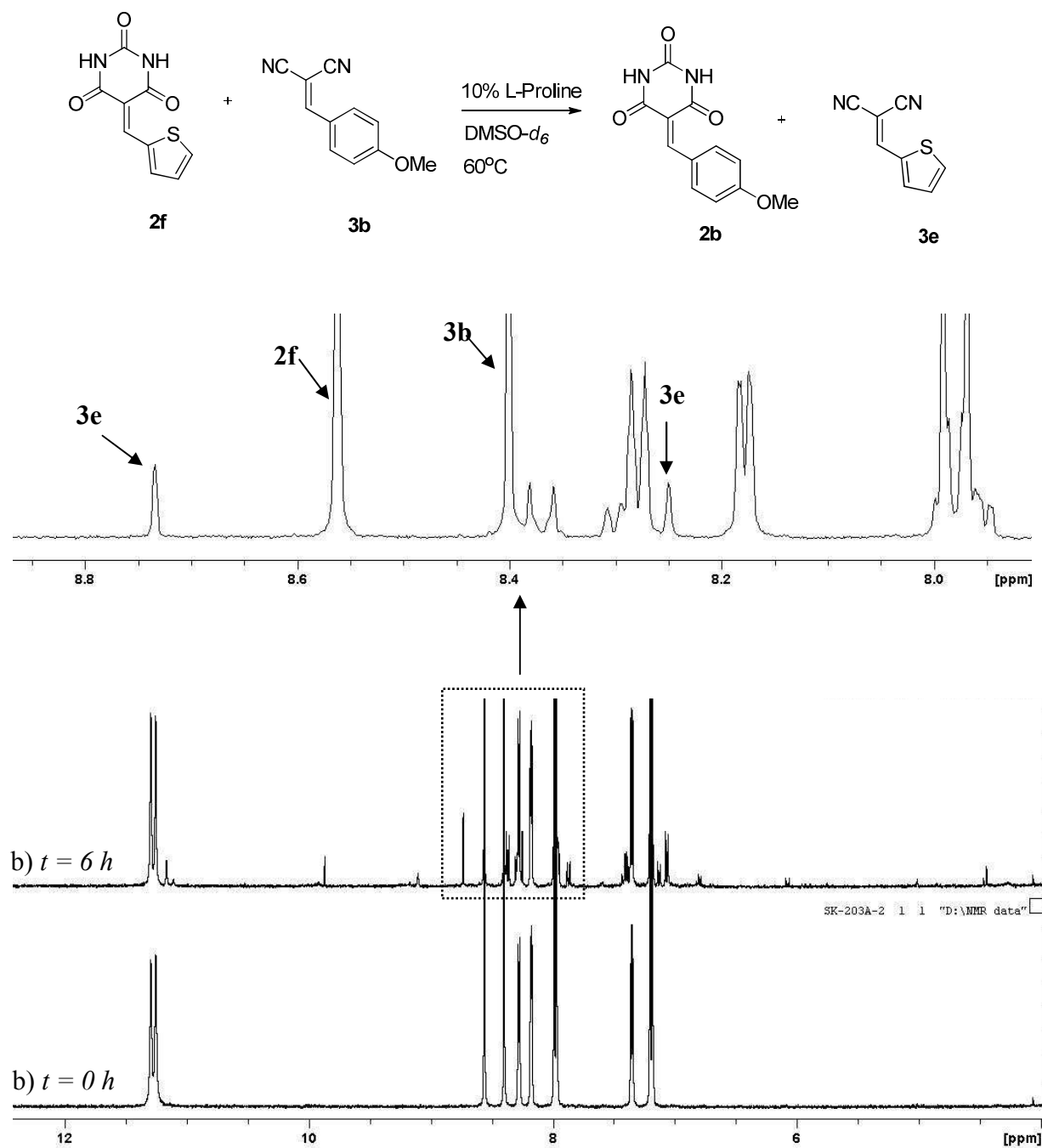


Figure 7.56 The $^1\text{H-NMR}$ spectrum of the exchange reaction between **2f** and **3b** in $\text{DMSO-}d_6$ in the presence of 10 mol% L-proline. a) after mixing, b) at 48 hr showing the exchange products **2b** and **3e** involving the hydrolysis products and Michael-type adducts **XI** and **XII**.

7.3 Chapter 3, Uncatalyzed C=C/C=N exchange Processes between Knoevenagel and Imine Compounds in Dynamic Covalent Chemistry

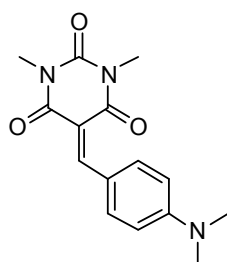
7.3.1 Synthesis and Characterization

Synthesis of Knoevenagel compounds

● *General procedure for the synthesis of Knoevenagel condensation products.* To 30 mL anhydrous ethanol was added barbituric acid (3.0 mmol), the corresponding substituted benzaldehyde (3.0 mmol), and L-proline in a catalytic amount (10%). The solution was then refluxed for 3-4 hr. The *Knoevenagel* condensation products that precipitated out of the cooled solution were filtered and washed with diethyl ether and dried under vacuum for 2-3 h.

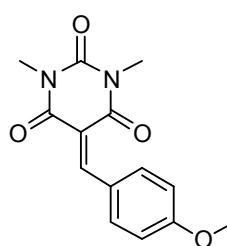
Characterization of Knoevenagel compounds

1.5-(4-(dimethylamino)benzylidene)-1,3-dimethylpyrimidine-2,4,6(1H,3H,5H)-trione (4a)^[34,35]



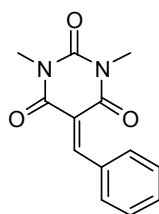
Yield: 0.78 g, 90%. Orange solids. ¹H-NMR (400 MHz, CDCl₃): 3.14 (s, 6 H); 3.38 (s, 3 H); 3.39 (s, 3 H); 6.69 (d, *J* = 9.5, 2 H); 8.39 (d, *J* = 9.3, 2 H); 8.42 (s, 1 H). ¹³C-NMR (100 MHz, CDCl₃; δ/ppm): 28.4, 29.1, 40.3, 109.0, 111.3, 121.3, 139.7, 152.1, 154.6, 159.0, 161.9, 164.2. LC-MS (m/z) calcd. for [C₁₅H₁₇N₃O₃+MeOH+K]⁺ 358.118; found 358.83.

2. 5-(4-methoxybenzylidene)-1,3-dimethylpyrimidine-2,4,6(1H,3H,5H)-trione (4b)^[35]

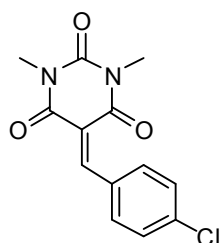


Yield: 0.73 g, 88%. Yellow solids. ¹H-NMR (400 MHz, CDCl₃): 3.38 (s, 3 H); 3.39 (s, 3 H), 3.89 (s, 3 H); 6.96 (d, *J* = 9.0, 2 H); 8.30 (d, *J* = 8.6, 2H); 8.50 (s, 1 H). ¹³C-NMR (100 MHz, CDCl₃; δ/ppm): 28.6, 29.3, 55.8, 114.21, 114.6, 125.8, 138.2, 151.7, 159.1, 161.2, 163.4, 164.5. LC-MS (m/z) calcd. for [C₁₄H₁₄N₂O₄+H]⁺ 275.103; found 275.87.

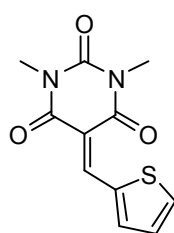
3. 5-benzylidene-1,3-dimethylpyrimidine-2,4,6(1H,3H,5H)-trione (4c)^[35]



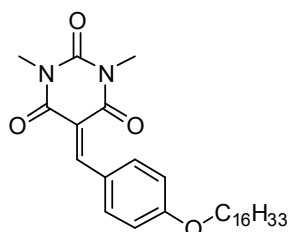
Yield: 0.398 g, 54%. Yellow solids. ¹H-NMR (400 MHz, CDCl₃): 3.36 (s, 3 H); 3.41 (s, 3 H); 7.43 – 7.53 (m, 3 H); 8.04 (d, *J* = 7.7, 2 H); 8.57 (s, 1 H). ¹³C-NMR (100 MHz, CDCl₃; δ/ppm): 28.6, 29.3, 117.8, 128.5, 132.9, 133.1, 133.6, 151.5, 159.5, 160.6, 162.7. LC-MS (m/z) calcd. for [C₁₃H₁₃N₂O₃+H]⁺ 245.09; found 245.79.

4. 5-(4-chlorobenzylidene)-1,3-dimethylpyrimidine-2,4,6(1H,3H,5H)-trione (**4d**)^[36]

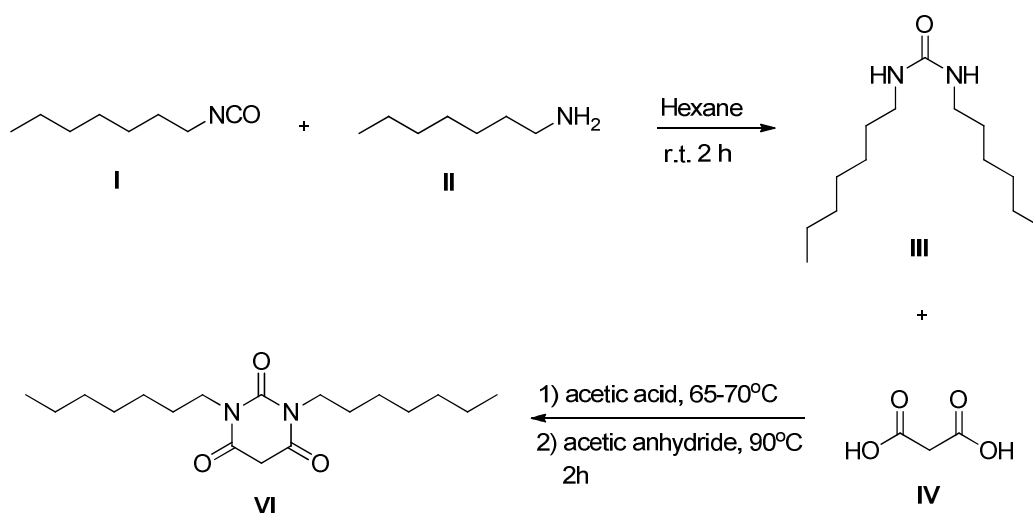
Yield: 0.373 g, 45%. Yellow solid. ¹H-NMR (400 MHz, CDCl₃): 3.36 (s, 3 H); 3.41 (s, 3 H); 7.42 (d, *J* = 8.6, 2 H); 8.01 (d, *J* = 8.9, 2 H); 8.48 (s, 1H). ¹³C-NMR (100 MHz, CDCl₃; δ/ppm): 28.7, 29.4, 118.0, 128.8, 131.2, 135.1, 139.5, 151.4, 157.7, 160.6, 162.5. LC-MS (m/z) calcd. for [C₁₃H₁₁ClN₂O₃+K]⁺ 317.010; found 317.82.

5. 1,3-dimethyl-5-(thiophen-2-ylmethylene)pyrimidine-2,4,6(1H,3H,5H)-trione (**4e**)^[37]

Yield: 0.65 g, 87%. Brown yellow solid. ¹H-NMR (400 MHz, CDCl₃): 3.40 (s, 3 H); 3.41 (s, 3 H); 7.28 (dd, *J* = 4.0, 1 H); 7.89 (d, *J* = 5.1, 1 H); 7.96 (d, *J* = 5.6, 1 H). ¹³C-NMR (100 MHz, CDCl₃; δ/ppm): 28.4, 29.2, 110.8, 128.4, 137.2, 142.1, 145.6, 149.2, 151.6, 161.9, 162.9. LC-MS (m/z) calcd. for [C₁₁H₁₀N₂O₃S] 250.04; found 250.63.

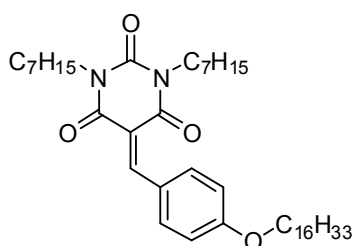
6. 5-(4-(hexadecyloxy)benzylidene)-1,3-dimethylpyrimidine-2,4,6(1H,3H,5H)-trione (**4f**)^[37]

Yield: 0.722 g, 74%. Yellow solid. ¹H-NMR (400 MHz, CDCl₃): 0.86 (t, *J* = 6.5, 3 H), 1.15 – 1.47 (m, 26H), 1.78 (quint, *J* = 7.1, 2 H), 3.37 (s, 3H), 3.39 (s, 3H), 4.04 (t, *J* = 6.5, 2H), 6.94 (d, *J* = 9.4, 2H), 8.30 (d, *J* = 9.4, 2H), 8.5 (s, 1H).

7. 1,3-diheptyl barbituric acid (**VI**)^[38]

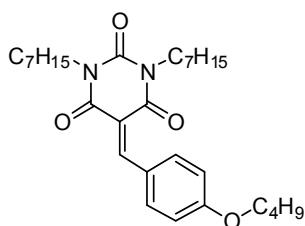
Heptyl isocyanate (**I**) (3.22 mL, 20.00 mmol) was dissolved in hexane (100 mL) and then the mixture was cooled to 0°C. A solution of n-heptylamine (**II**) (3.26 mL, 22.00 mmol) in hexane (20 mL) was carefully added. A white solid precipitated from the solution after which the solution was kept stirring for another 2 h. The product was collected by filtration and washed with cooled n-hexane to obtain a white solid (**III**) (3.93 g, 77%). Next, diheptylurea (**III**) (3.0 g, 11.7 mmol) and malonic acid (**IV**) (1.118 g, 10.74 mmol) were dissolved in acetic acid (20 mL). The mixture was stirred at 65 – 70°C then acetic acid (30 mL) was added dropwise. Then, the mixture was kept stirring at 90°C for 2 hr. The solution was evaporated under pressure to obtain a yellow liquid (3.00 g, 79% yield). ¹H-NMR (400 MHz, CDCl₃): 0.85 (t, *J* = 6.8, 6H), 1.21 – 1.34 (m, 19H), 1.51 – 1.61 (m, 4H), 3.62 (s, 2H), 3.83 (t, *J* = 7.8, 4H).

8. 1,3-diheptyl-5-(4-(hexadecyloxy)benzylidene)pyrimidine-2,4,6(1H,3H,5H)-trione (**4g**)



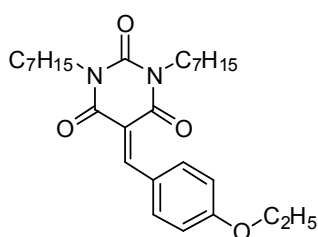
Yield: 0.32 g, 33%. Yellow solid. ¹H-NMR (400 MHz, CDCl₃): 0.86 (br, 9H), 1.21 – 1.34 (m, 40), 1.44 (br, 2H), 1.62 (br, 4H), 1.79 (quint, *J* = 6.9, 2H), 3.94 (br, 4H), 4.04 (t, *J* = 6.8, 2H), 6.93 (d, *J* = 8.8, 2H), 8.27 (d, *J* = 9.2, 2H), 8.5 (s, 1H)

9. 5-(4-butoxybenzylidene)-1,3-diheptylpyrimidine-2,4,6(1H,3H,5H)-trione (**4h**)

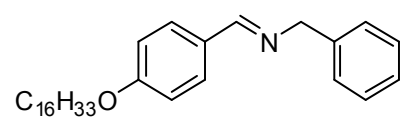


Yield: 0.332 g, 34%. Yellow solid. ¹H-NMR (400 MHz, CDCl₃): 0.86 (t, *J* = 6.5, 6H), 0.97 (t, *J* = 7.4, 3H), 1.20 – 1.35 (m, 16), 1.48 (t, *J* = 7.2, 2H), 1.62 (br, 4H), 1.78 (quint, *J* = 6.9, 2H), 3.93 (br, 4H), 4.05 (t, *J* = 6.6, 2H), 6.9 (d, *J* = 9.0, 2H), 8.27 (d, *J* = 9.0, 2H), 8.47 (s, 1H).

10. 5-(4-ethoxybenzylidene)-1,3-diheptylpyrimidine-2,4,6(1H,3H,5H)-trione (**4i**)



Yield: 0.465 g, 51%. Yellow solid. ¹H-NMR (400 MHz, CDCl₃): 0.86 (t, *J* = 6.1, 6H), 1.21 – 1.36 (m, 16H), 1.44 (t, *J* = 7.4, 3H), 1.57 – 1.68 (m, 4H), 3.89 – 3.98 (m, 4H), 4.11 (q, *J* = 6.9, 2H), 6.93 (d, *J* = 9.3, 2H), 8.28 (d, *J* = 9.3, 2H), 8.47 (s, 1H)

11. (*E*)-*N*-(4-(hexadecyloxy)benzylidene)-1-phenylmethanamine (**1w**)

Yield: 0.52 g, 60%. White solid. ¹H-NMR (400 MHz, CDCl₃): 0.85 (t, *J* = 6.1, 3H), 1.21 – 1.48 (m, 26H), 1.77 (t, *J* = 8.1, 2H), 3.97 (t, *J* = 6.8, 2H), 4.77 (s, 2H), 6.89 (d, *J* = 8.7, 2H), 7.30-7.33 (m, 5H), 7.69 (d, *J* = 8.4, 2H), 8.29 (s, 1H)

7.3.2 Study of Knoevenagel/Imine (C=C/C=N) derivatives exchange

● *General Procedure for C=C/C=N Exchange.* Stock solns. (40 mM, 0.4 ml) of *Knoevenagel* compounds were prepared in CDCl₃. For each reaction, 350 μl of each soln. was added to a NMR tube to obtain a final volume of 700 μl. The final solution was 20 mM in each component. The % composition of the reactions at equilibrium were determined by integration of the *Knoevenagel* compound C=CH and the imine N=CH ¹H-NMR signals and the corresponding equilibrium constants *K* were calculated.

7.3.3 $^1\text{H-NMR}$ spectra for Knoevenagel and imine ($\text{C}=\text{C}/\text{C}=\text{N}$) exchange process

7.3.3.1 The exchange reaction between **4a** and **1b** (forward reaction) and between **4e** and **1v** (reverse reaction) in CDCl_3 at room temperature.

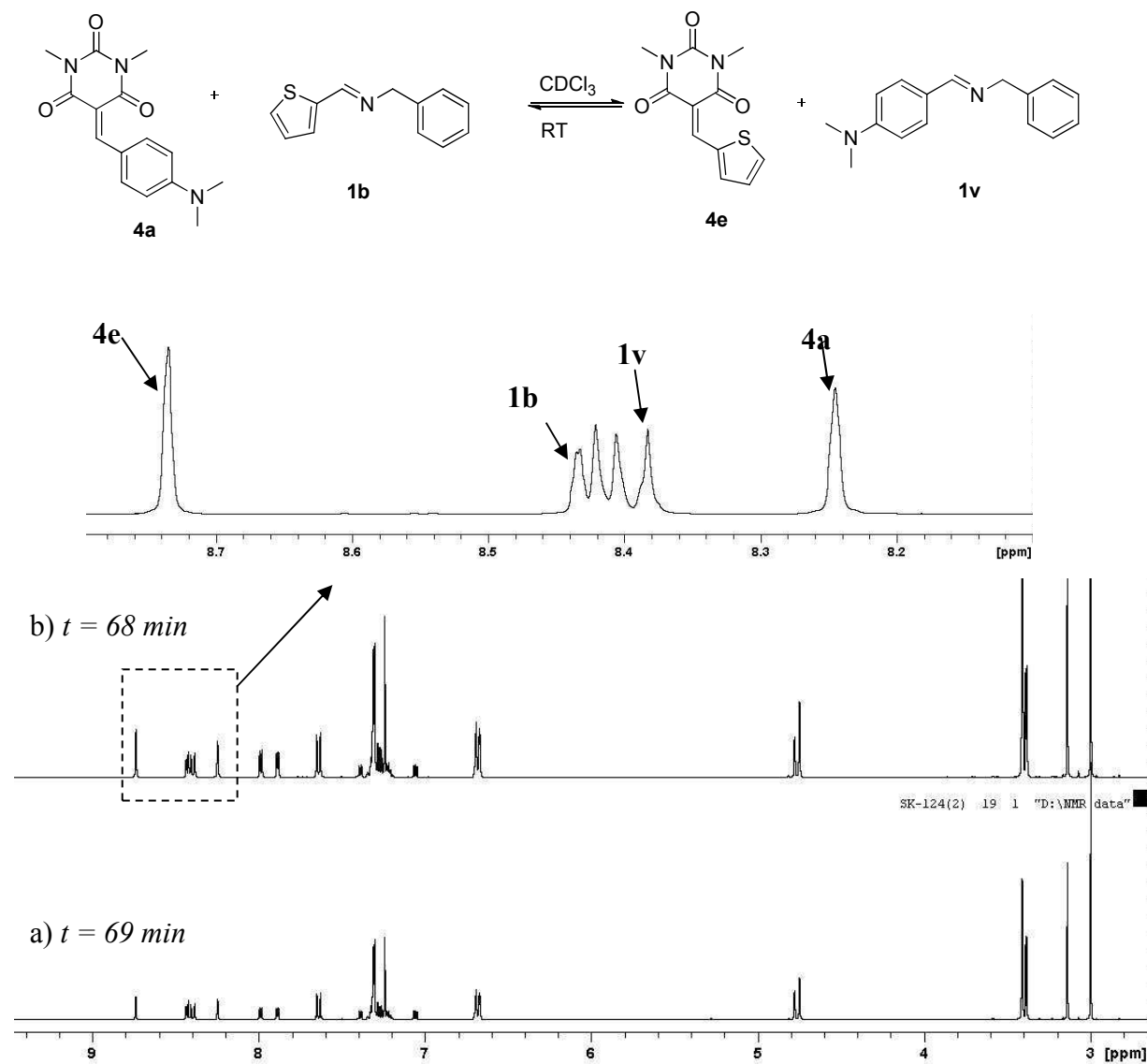


Figure 7.57 The $^1\text{H-NMR}$ spectrum of the exchange reaction at equilibrium between a) **4a** and **1b**, b) **4e** and **1v** in CDCl_3 at room temperature.

7.3.3.2 The exchange reaction between **4b** and **1f** (forward reaction) and between **4c** and **1u** (reverse reaction) in CDCl_3 at room temperature.

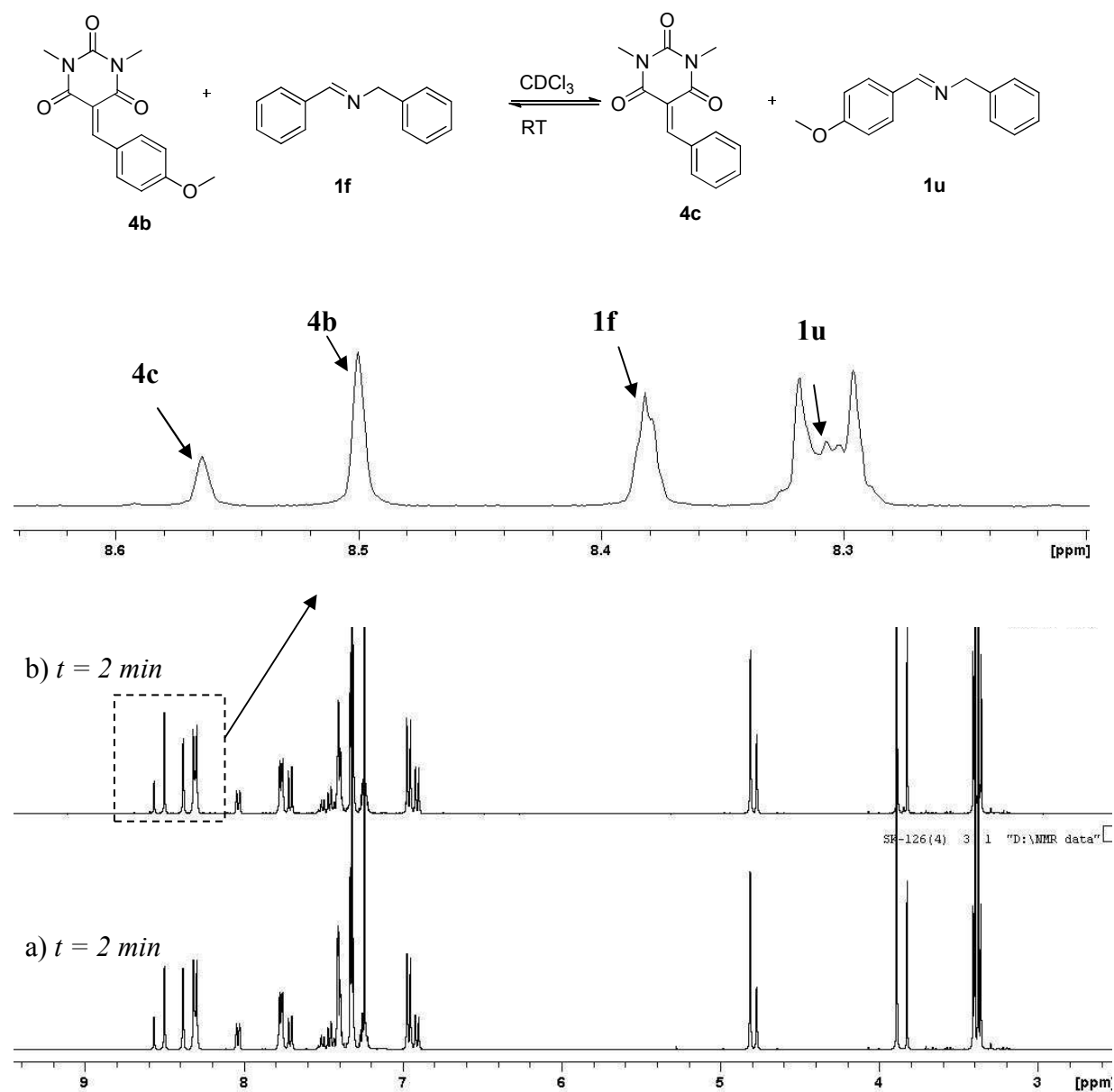


Figure 7.58 The $^1\text{H-NMR}$ spectrum of the exchange reaction at equilibrium between a) **4b** and **1f**, b) **4c** and **1u** in CDCl_3 at room temperature.

7.3.3.3 The exchange reaction between **4b** and **1b** (forward reaction) and between **4e** and **1u** (reverse reaction) in CDCl_3 at room temperature.

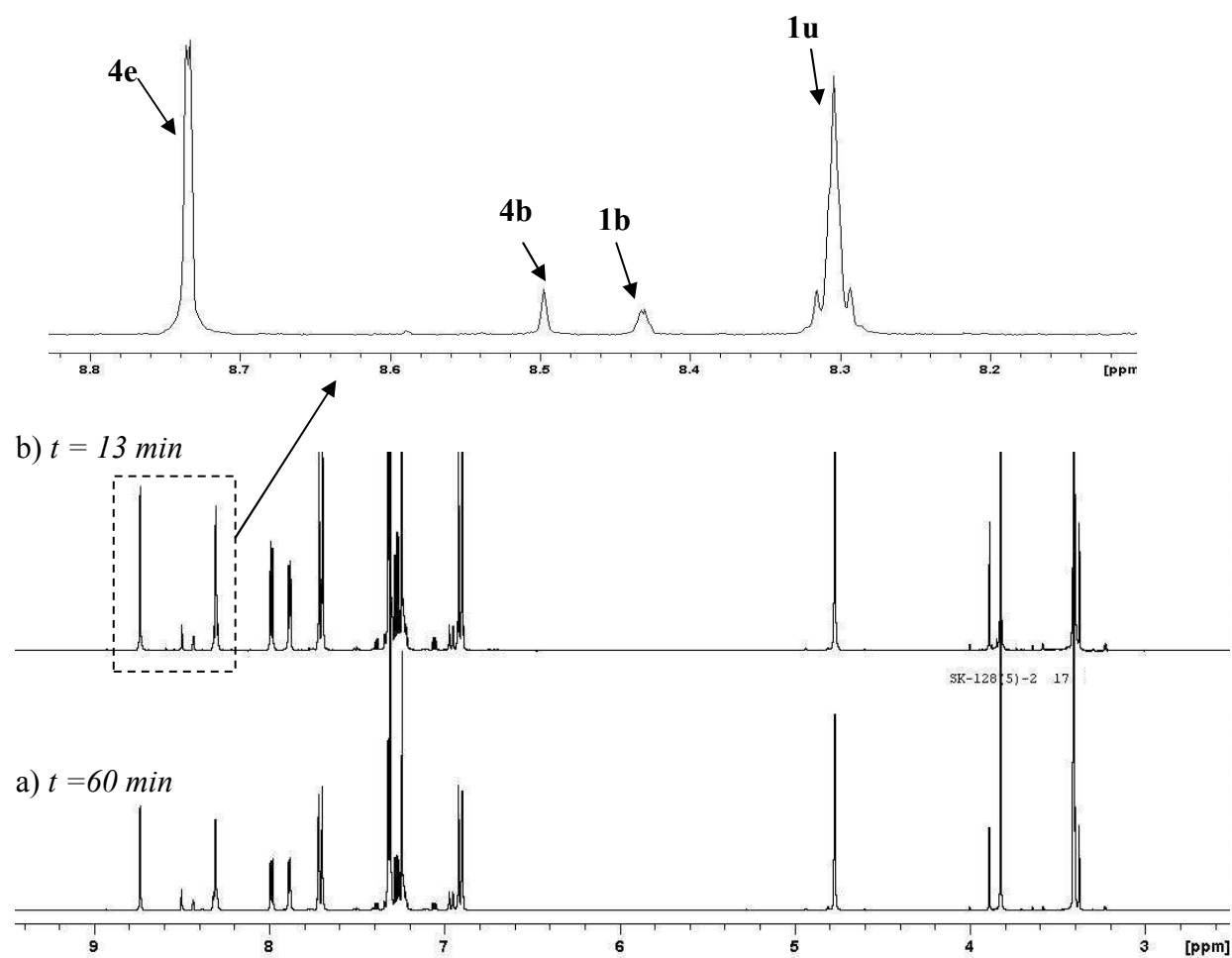
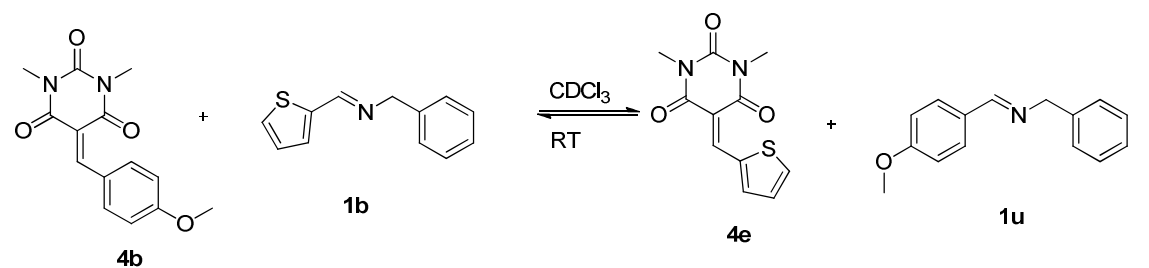


Figure 7.59 The $^1\text{H-NMR}$ spectrum of the exchange reaction at equilibrium between a) **4b** and **1b**, b) **4e** and **1u** in CDCl_3 at room temperature.

7.3.3.4 The exchange reaction between **4d** and **1v** (forward reaction) and between **4a** and **1t** (reverse reaction) in CDCl_3 at room temperature.

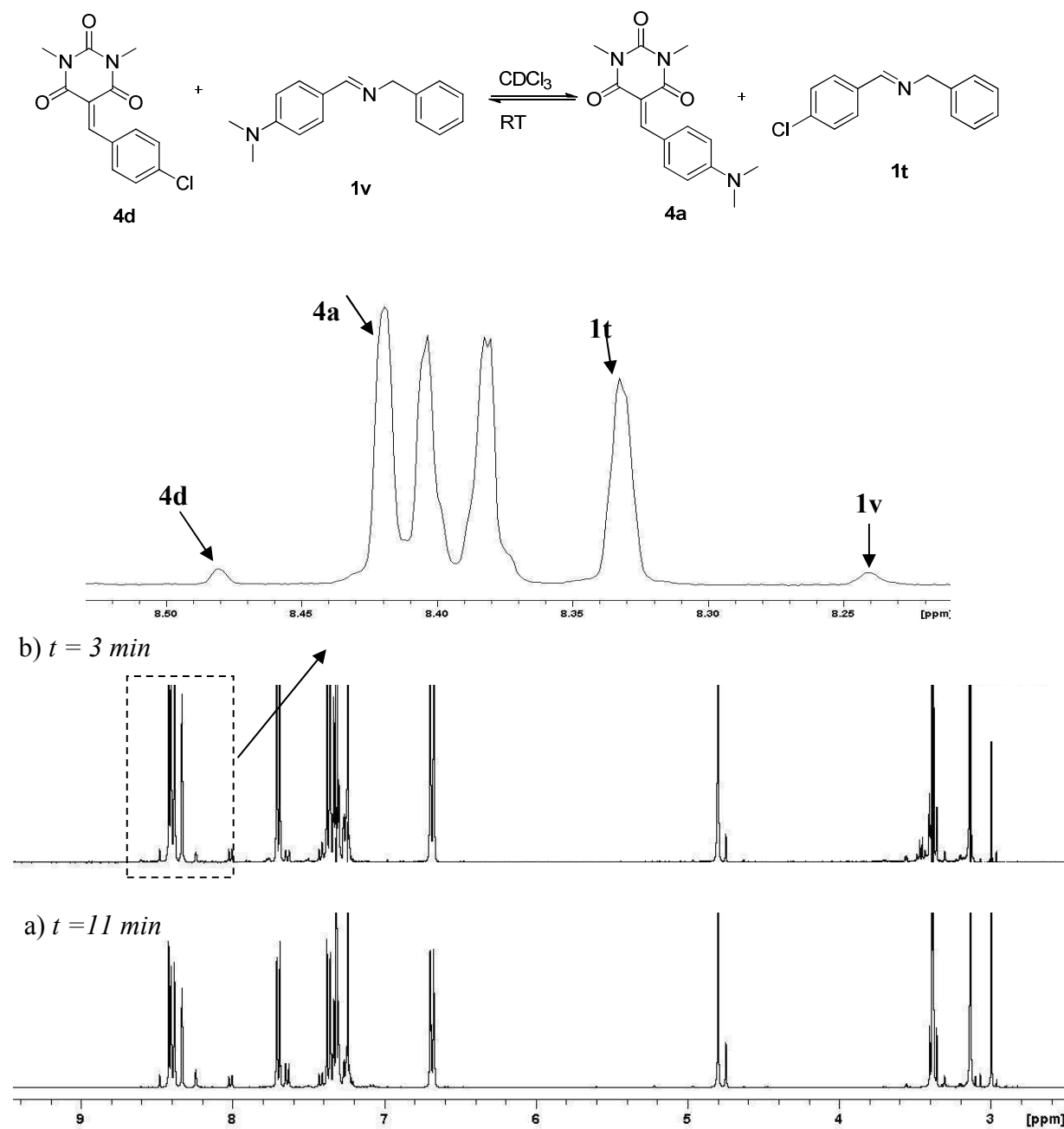


Figure 7.60 The $^1\text{H-NMR}$ spectrum of the exchange reaction at equilibrium between a) **4d** and **1v**, b) **4a** and **1t** in CDCl_3 at room temperature.

7.3.3.4 The exchange reaction between **4d** and **1u** (forward reaction) and between **4b** and **1t** (reverse reaction) in CDCl_3 at room temperature.

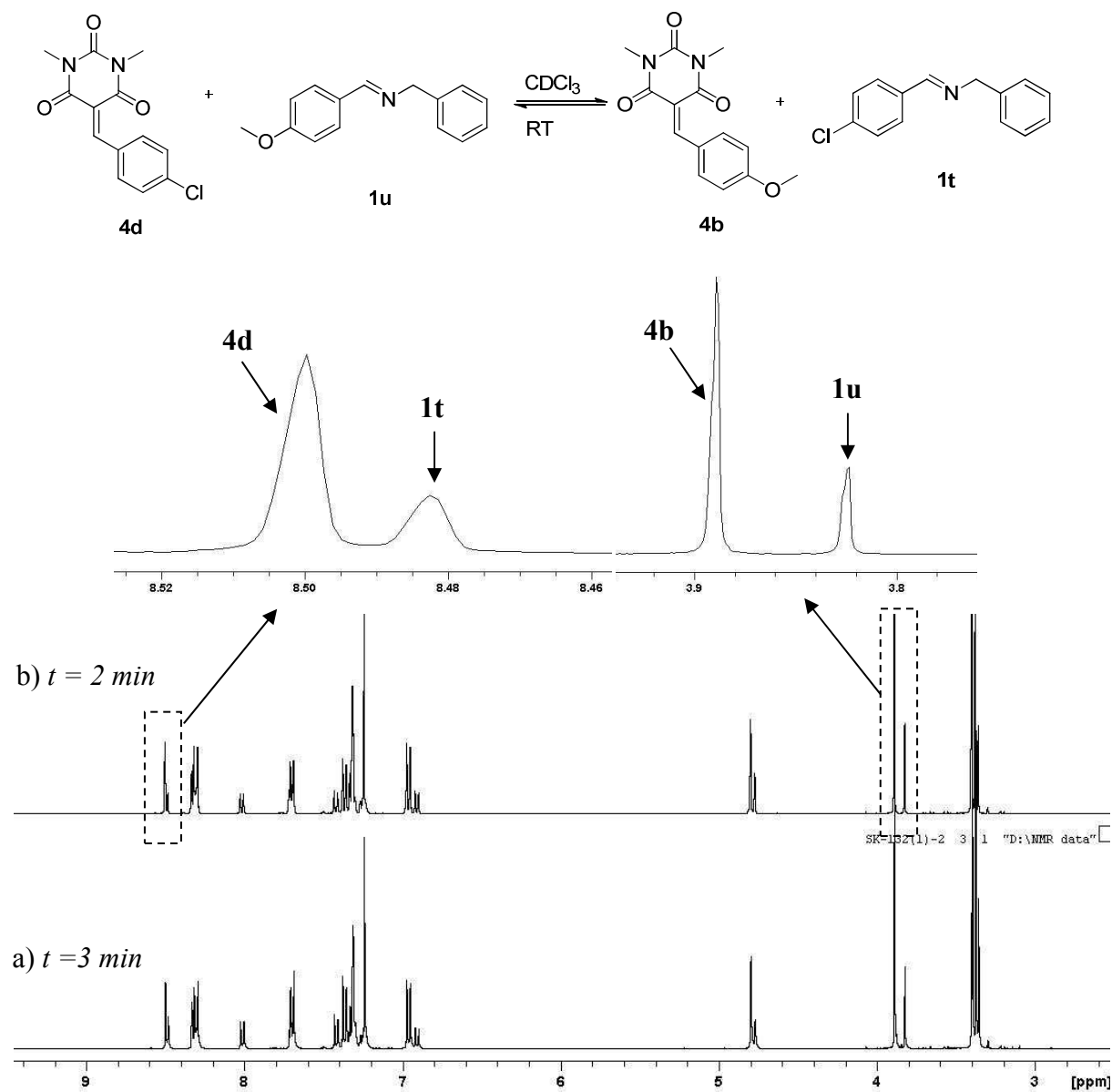


Figure 7.61 The $^1\text{H-NMR}$ spectrum of the exchange reaction at equilibrium between a) **4d** and **1u**, b) **4b** and **1t** in CDCl_3 at room temperature.

7.4 Chapter 4, Dynamic Covalent Chemistry of Nucleophilic Substitution Component Exchange of Ammonium Salts

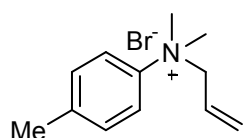
7.4.1 Synthesis and Characterization

1. *N*-allyl-*N,N*-dimethylbenzenaminium bromide (**1a-Br**)^[39]



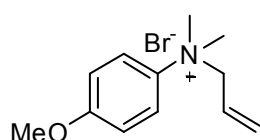
The oil bath was preheated to 100°C. Then dimethylaniline (0.38 mL, 3.0 mmol) was mixed with allylbromide (1.56 mL, 18.0 mmol) and refluxed for 2 hours. The white precipitate appeared as the reaction progressed changing to be a pink colored solid later. The reaction mixture was allowed to cool to room temperature. Then, the mixture was washed by diethyl ether and dried under vacuum for 4 hr to afford **1a** as a white solid, 0.55 g, 76% yield). m.p. not determined, hygroscopic white solid. ¹H-NMR (CD₃CN) δ ppm: 7.82 (d, *J* = 8.1 Hz, 2H), 7.60 (m, 3H), 5.59 (m, 2H), 5.52 (m, 1H), 4.55 (dd, *J* = 1.8 Hz, 2H), 3.58 (s, 6H).

2. *N*-allyl-*N,N*,4-trimethylbenzenaminium (**1b-Br**)^[40]

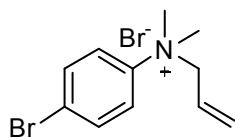


4,*N,N*-trimethylaniline (0.87 mL, 6.0 mmol) and allyl bromide (1.0 mL, 12.0 mmol) were combined in acetone. The solution was refluxed for 4 hours and then the solvent was evaporated. The product was dried under vacuum to afford **1b** as a yellow liquid (1.235 g, 81% yield). M.p. not determined, liquid at room temperature. ¹H-NMR (CD₃CN) δ ppm: 7.68 (d, *J* = 8.7 Hz, 2H), 7.41 (d, *J* = 8.7 Hz, 2H), 5.59 (m, 2H), 5.51 (m, 1H), 4.52 (br, 2H), 3.55 (s, 6H), 2.39 (s, 3H).

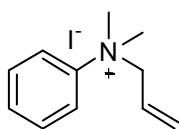
3. *N*-allyl-4-methoxy-*N,N*-dimethylbenzenaminium bromide (**1c-Br**)^[41]



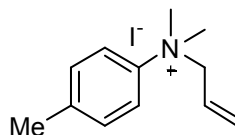
4-methoxy-*N,N*-dimethylaniline (**4c**) (0.4533 g, 3.0 mmol) was combined with allylbromide (0.78 mL, 9.0 mmol). The reaction was stirred at 40°C for 10 minutes and a white solid precipitated as the reaction went on. The product was washed with diethyl ether and dried under vacuum for 4 hours to afford **1c** as a white solid (0.6052, 74% yield). M.p. 139°C, lit m.p. 141-142°C. ¹H-NMR (CDCl₃) δ ppm: 7.82 (d, *J* = 8 Hz, 2H), 7.04 (d, *J* = 9.3 Hz, 2H), 5.79 (d, *J* = 16.9 Hz, 1H), 5.44 (m, 2H), 5.08 (d, *J* = 6.8 Hz, 2H), 3.90 (s, 6H), 3.83 (s, 3H).

4. *N*-allyl-4-bromo-*N,N*-dimethylbenzenaminium bromide (**1d-Br**)^[42]

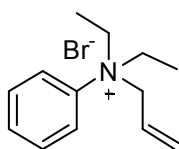
Prepared in 25% yield as a white solid analogous to the route described for **1c**. M.p. 148°C, lit m.p. 151-152°C. ¹H-NMR (CD₃CN) δ ppm: 7.79 (d, *J* = 9.4 Hz, 2H), 7.68 (d, *J* = 9.2 Hz, 2H), 5.61 (m, 3H), 4.42 (d, *J* = 6.3 Hz, 2H), 3.52 (s, 6H).

5. *N*-allyl-*N,N*-dimethylbenzenaminium iodide (**1a-I**)^[42]

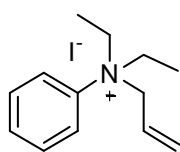
To a stirred solution of dimethylaniline (0.38 mL, 3.0 mmol) was added allyl iodide (0.82 mL, 9.0 mmol), then the solution was stirred at 30°C overnight. The color of the solution became yellow as the reaction went on. The solvent was evaporated and dried under vacuum for 3 hours to give a dark-brown solid (0.860 g, 99% yield). M.p. 87–88°C, lit m.p. 87-88°C. ¹H-NMR (CD₃CN) δ ppm: 7.75 (d, *J* = 8.2 Hz, 2H), 7.61 (m, 3H), 5.59 (m, 3H), 4.44 (d, *J* = 5.6, 2H), 3.53 (s, 6H).

6. *N*-allyl-*N,N*,4-trimethylbenzenaminium iodide (**1b-I**)

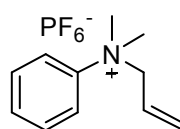
Prepared in 90% yield as an orange liquid by a route analogous to that described for **1e**. M.p. not determined, liquid at room temperature. ¹H-NMR (CDCl₃) δ ppm: 7.76 (d, *J* = 7.4, 2H), 7.42 (d, *J* = 8.8 Hz, 2H), 5.87 (d, *J* = 16 Hz, 1H), 5.58 (d, *J* = 10 Hz, 1H), 5.49 (m, 1H), 5.07 (d, *J* = 7.4 Hz, 2H), 3.93 (s, 6H), 2.44 (s, 3H). ¹³C-NMR (100 MHz, CDCl₃): 21.0, 54.6, 71.1, 120.8, 124.8, 129.9, 131.4, 141.3. ESI-MS: 176.142 (100) (C₁₂H₁₈N⁺; calc. 176.143). HR-ESI-MS: 302.0369 (100) (C₁₂H₁₇IN⁺; calc. 302.0400).

7. *N*-allyl-*N,N*-diethylbenzenaminium bromide (**1e-Br**)^[43]

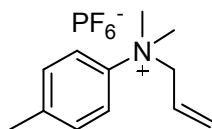
Diethylaniline (0.48 mL, 3.0 mmol) and allyl bromide (0.78 mL, 9.0 mmol) were combined and kept stirring at 50°C for 48 hours. The white solid was precipitated then washed with diethyl ether. The product was dried under vacuum to obtain a white solid (0.702, 87% yield). M.p. 144 – 146°C. ¹H-NMR (CD₃CN) δ ppm: 7.72 (br, 2H), 7.63 (m, 3H), 5.69 (m, 3H), 4.38 (d, *J* = 7.1 Hz, 2H), 3.81 (m, 4H), 1.10 (t, *J* = 7.1 Hz, 6H).

8. *N*-allyl-*N,N*-diethylbenzenaminium iodide (**1e-I**)

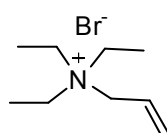
Prepared in 98% yield as a white solid by a route analogous to that described for **1g**. M.p. 105 – 106°C ¹H-NMR (CDCl₃) δ ppm: 7.96 (d, *J* = 8.5, 2H), 7.65 (t, *J* = 7.8 Hz, 2H), 7.54 (t, *J* = 7.4 Hz, 1H), 5.62 – 5.79 (m, 3H), 4.65 (d, *J* = 5.9 Hz, 2H), 4.20 (dt, *J* = 7.3, 2H), 4.07 (dt, *J* = 7.2 Hz, 2H), 1.22 (t, *J* = 7.0 Hz, 6H). ¹³C-NMR (100 MHz, CDCl₃): 8.8, 58.0, 63.3, 122.7, 124.2, 129.4, 130.8, 131.3, 141.4. ESI-MS: 190.158 (100) (C₁₃H₂₀N⁺; calc. 190.159). HR-ESI-MS: 316.0529 (100) (C₁₃H₁₉IN⁺; calc. 316.064).

9. *N*-allyl-*N,N*-dimethylbenzenaminium hexafluorophosphate (**1a-PF₆**)

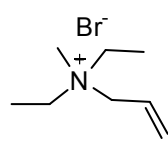
N-allyl-*N,N*-dimethylbenzenaminium bromide (**1a**) (0.072 g, 0.3 mmol) was dissolved in water (1 mL) and combined with a saturated solution of potassium hexafluorophosphate in water. A white solid immediately precipitated. The compound was extracted with dichloromethane and dried with magnesium sulfate. The solvent was evaporated to afford a pink solid then recrystallized by dichloromethane/diethyl ether to afford **1i** (0.08 g, 87 % yield). m.p. 88 - 90°. The compound was tested with silver nitrate (AgNO₃) demonstrating the absence of bromide ion. ¹H-NMR (CD₃CN) δ ppm: 7.57 – 7.70 (m, 5H), 5.49 – 5.65 (m, 3H), 4.32 (d, *J* = 6.1, 2H), 3.48 (s, 6H).

10. *N*-allyl-*N,N*,4-trimethylbenzenaminium (**1b-PF₆**)

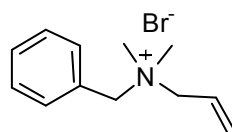
Prepared in 80% yield as a white solid by a route analogous to that described for **1i**. ¹H-NMR (CD₃CN) δ ppm: 7.55 (d, *J* = 8.6 Hz, 2H), 7.43 (d, *J* = 8.4 Hz, 2H), 5.49 – 5.65 (m, 3H), 4.29 (d, *J* = 6.5 Hz, 2H), 3.45 (s, 6H), 2.40 (s, 3H).

11. *N,N,N*-triethylprop-2-en-1-aminium bromide (**3a-Br**)^[44,45]

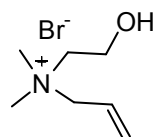
Prepared in 92% yield as a white hygroscopic solid by a route analogous to that described for **1a**. ¹H-NMR (CD₃CN) δ ppm: 5.93 (m, 1H), 5.68 (d, *J* = 12.1 Hz, 1H), 5.65 (d, *J* = 5.4 Hz, 1H), 3.76 (d, *J* = 7.0 Hz, 2H), 3.19 (q, *J* = 7.2 Hz, 6H), 1.25 (tt, *J* = 1.2 Hz, 9H).

12. *N,N*-diethyl-*N*-methylprop-2-en-1-aminium bromide (**3b-Br**)

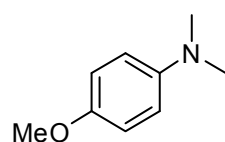
Prepared in 73% yield as a yellow solid by a route analogous to that described for **1a**. ¹H-NMR (CD₃CN) δ ppm: 5.97 (m, 1H), 5.69 (d, *J* = 11.6 Hz, 1H), 5.66 (d, *J* = 4.6 Hz, 1H), 3.85 (d, *J* = 7.5 Hz, 2H), 3.27 (q, *J* = 7.24 Hz, 4H), 2.89 (s, 3H), 1.28 (tt, *J* = 1.5 Hz, 6H). ¹³C-NMR (100 MHz, CD₃CN): 8.2, 47.7, 57.1, 63.7, 125.9, 129.0. ESI-MS: 128.145 (100) (C₈H₁₈N⁺; calc. 128.143). HR-ESI-MS: 335.2053 (100) (C₁₆H₃₆BrN₂⁺; calc. 335.2056).

13. *N*-benzyl-*N,N*-dimethylprop-2-en-1-aminium bromide (**3c-Br**)^[43]

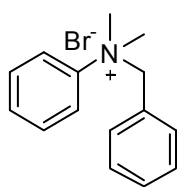
Prepared in 30% yield as a white hygroscopic solid by a route analogous to that described for **1a**. ¹H-NMR (CD₃CN) δ ppm: 7.54 (m, 5H), 6.08 (m, 1H), 5.72 (d, *J* = 9.8 Hz, 1H), 5.70 (d, *J* = 16.9 Hz, 1H), 4.51 (s, 2H), 3.97 (d, *J* = 7.4 Hz, 2H), 2.94 (s, 6H).

14. *N,N*-diethyl-*N*-(2-hydroxyethyl)prop-2-en-1-aminium bromide (**3d-Br**)^[46]

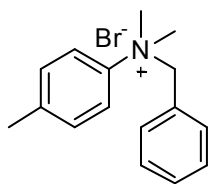
Prepared in 72% yield as a white solid by a route analogous to that described for **1a**. ¹H-NMR (CD₃CN) δ ppm: 6.04 (m, 1H), 5.7 (d, *J* = 6.2 Hz, 1H), 5.67 (br, 1H), 4.03 (d, *J* = 7.7 Hz, 2H), 3.97 (m, 2H), 3.41 (t, *J* = 4.9 Hz, 2H), 3.08 (s, 6H).

15. 4-methoxy-*N,N*-dimethylaniline (**4c**)^[47]

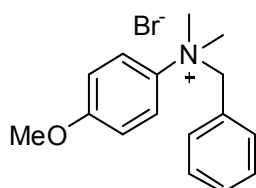
A 50 mL round bottom flask equipped with a reflux condenser was charged with 4-methoxyaniline (1.51 g, 12.26 mmol), tetra-*N*-butylammonium iodide (0.316 g, 0.856 mmol), potassium hydroxide (1.644 g, 29.2 mmol), benzene 14 mL, and water 2 mL. After 10 min, iodomethane (0.78 mL, 12.58 mmol) was added dropwise over 2 min and stirred at room temperature for 7 hours. Then, additional tetra-*n*-butylammonium iodide (0.156 g, 0.42 mmol), potassium hydroxide (0.726 g, 12.92 mmol) and iodomethane (0.14 mL) were added and stirred at room temperature for 11 hours. The organic layer was separated and washed with a 10 mL portion of water, saturated sodium carbonate and brine, and dried over anhydrous sodium sulfate. Filtration and solvent removal under vacuum gave a dark yellow oil. The crude product was purified by chromatography (silica gel) using 5% ethylacetate/pentane as an eluent to afford a yellow solid (0.953 g, 51% yield). ¹H-NMR (CDCl₃) δ ppm: 6.92 (d, *J* = 8.9 Hz, 2H), 6.82 (d, *J* = 9.2 Hz, 2H), 3.82 (s, 3H), 2.92 (s, 6H).

16. *N*-benzyl-*N,N*-dimethylbenzenaminium bromide (**5a-Br**)^[48]

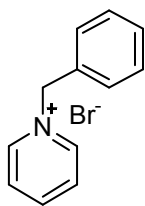
Dimethylaniline (0.70 mL, 5.5 mmol) and benzylbromide (0.59 mL, 5.0 mmol) were combined in dry benzene and stirred at room temperature for 24 hr. A white solid precipitated in the solution. The compound was washed with diethylether and dried under vacuum for 4 hr to afford white solids (0.288 g, 20%). M.p. 148 – 149° ([18]: 149-151°). ¹H-NMR (CD₃CN) δ ppm: 7.57 – 7.67 (m, 5H), 7.46 (t, *J* = 8 Hz, 1H), 7.32 (t, *J* = 8 Hz, 2H), 7.07 (d, *J* = 7.7 Hz, 2H), 4.93 (s, 2H), 3.55 (s, 6H).

17. *N*-benzyl-*N,N*,4-trimethylbenzenaminium bromide (**5b-Br**)^[48]

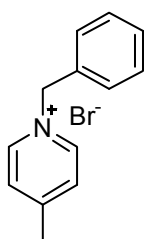
Prepared in 40% yield as a white solid by a route analogous to that described for **5a**. M.p. 183 - 184°. ¹H-NMR (CD₃CN) δ ppm: 7.52 (d, *J* = 8.9 Hz, 2H), 7.46 (t, *J* = 7.6 Hz, 1H), 7.38 (d, *J* = 8.7 Hz, 2H), 7.32 (t, *J* = 8.3 Hz, 2H), 7.08 (d, *J* = 7.6 Hz, 2H), 4.92 (s, 2H), 3.52 (s, 6H), 2.40 (s, 3H).

18. *N*-benzyl-4-methoxy-*N,N*-dimethylbenzenaminium bromide (**5c-Br**)^[48]

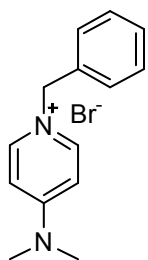
Prepared in 25% yield as a white solid by a route analogous to that described for **5a**. M.p. 148 - 149° ¹H-NMR (CD₃CN) δ ppm: 7.44 – 7.56 (m, 3H), 7.34 (t, *J* = 8.4 Hz, 2H), 7.05 – 7.08 (m, 4H), 4.87 (s, 2H), 3.85 (s, 3H), 3.50 (s, 6H).

19. 1-benzylpyridin-1-ium bromide (**6a**)^[49]

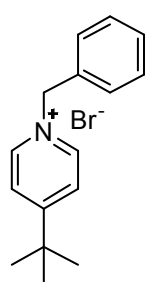
A solution of pyridine (0.4 mL, 5 mmol) and benzylbromide (0.59 mL, 5 mmol) in dry toluene (20 mL) was stirred at room temperature for 24 hr. After filtration, the solid was washed with diethyl ether to give **6a** as a white solid (1.052, 84% yield). M.p. 66 - 70° ¹H-NMR (CD₃CN) δ ppm: 8.91 (t, *J* = 5.5 Hz, 2H), 8.51 (t, *J* = 8.0 Hz, 1H), 8.03 (t, *J* = 6.8 Hz, 2H), 7.46 – 7.51 (m, 5H), 5.82 (d, *J* = 3.0 Hz, 2H).

20. 1-benzyl-4-methylpyridin-1-ium bromide (**6b**)^[50]

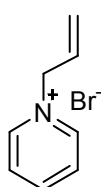
A solution of 4-picoline (0.68 mL, 7 mmol) and benzylbromide (0.83, 7 mmol) in acetonitrile (1 mL) was stirred at 45°C for 3 hr. The precipitate formed was washed with diethyl ether and dried under vacuum to give **6b** as a white crystal (1.665 g, 80%). M.p. 159 - 160° ¹H-NMR (CD₃CN) δ ppm: 8.70 (br, 2H), 7.82 (d, *J* = 6.3 Hz, 2H), 7.46 (s, 5H), 5.72 (s, 2H), 2.61 (s, 3H).

21. 1-benzyl-4-(dimethylamino)pyridin-1-ium bromide (**6c**)^[51]

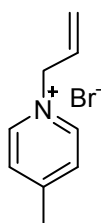
Prepared in 92% yield as a white solid by a route analogous to that described in the literature. M.p. 216 - 217° ¹H-NMR (CD₃CN) δ ppm: 8.06 (d, *J* = 7.9 Hz, 2H), 7.40 – 7.46 (m, 3H), 7.34 – 7.37 (m, 2H), 6.85 (d, *J* = 8.0 Hz, 2H), 5.30 (s, 2H), 3.16 (s, 6H).

22. 1-benzyl-4-(tert-butyl)pyridin-1-ium bromide (**6d**)^[51]

Prepared in 73% yield as a white solid by a route analogous to that described for **6c**. M.p. 163° ¹H-NMR (CD₃CN) δ ppm: 8.87 (d, *J* = 6.5 Hz, 2H), 8.01 (d, *J* = 6.7 Hz, 2H), 7.43 – 7.53 (m, 5H), 5.78 (s, 2H), 1.37 (s, 9H).

23. 1-allylpyridin-1-ium bromide (**6e**)^[52]

A solution of pyridine (0.81, 10 mmol) and allylbromide (1.1 mL, 10 mmol) in acetonitrile (10 mL) was stirred at 50°C overnight. The crude product was concentrated and dried under vacuum to obtain a light brown solid (1.8902 g, 95% yield). M.p. 92 - 94° ¹H-NMR (CD₃CN) δ ppm: 8.89 (d, *J* = 6.3 Hz, 2H), 8.54 (t, *J* = 8.1 Hz, 1H), 8.06 (t, *J* = 6.8 Hz, 2H), 6.09 – 6.20 (m, 1H), 5.52 (d, *J* = 14 Hz, 2H), 5.28 (d, *J* = 6.6 Hz, 2H).

24. 1-allyl-4-methylpyridin-1-ium bromide (**6f**)^[53]

Prepared in 96% yield as a brown solid by a route analogous to that described for **6e**. M.p. 76 - 78° ¹H-NMR (CD₃CN) δ ppm: 8.78 (d, *J* = 6.5 Hz, 2H), 7.86 (d, *J* = 6.2 Hz, 2H), 6.08 – 6.18 (m, 1H), 5.48 (d, *J* = 13.8 Hz, 2H), 5.24 (d, *J* = 6.5 Hz, 2H), 2.63 (s, 3H).

7.4.2 Kinetic Study for Ammonium salt exchange with tertiary amines

General Procedure for ammonium salt and tertiary amine exchange. Stock solutions (0.5 ml) of ammonium salt (60 mM or 180 mM), tertiary amine (60 mM or 180 mM), tetraethylammonium iodide (TEAI) 60 mM, and tetrabutylammonium iodide (TBAI) stock solution (180 mM) were prepared in the desired solvent. For the uncatalyzed reaction, 200 μL of each solution was added to a NMR tube followed by 200 μL of solvent to adjust to a final volume of 600 μL . For the catalyzed reaction, 200 μL of iodide stock solution was added to a NMR tube, followed by the addition of 200 μL of each solution. The stock solution of 60 mM was used to make the final solution of 20 mM. The stock solution of 180 mM was used to make the final solution of 60 mM.

General Procedure for *N*-benzyl-*N,N*-dimethylanilinium salts and tertiary amine exchange. Stock solutions (0.5 ml) of *N*-benzyl-*N,N*-dimethylanilinium salts (60 mM), tertiary amine (60 mM) and tetrabutylammonium iodide (60 mM) in CD_3CN were prepared. Then, 200 μL of each stock solution was added to a NMR tube to a final volume 600 μL . The final solution was 20 mM in each component.

General procedure for pyridinium salt and derivative of pyridine exchange using microwave irradiation. Stock solutions (500 μL) of pyridinium salt (40 mM) and tertiary amine or the derivative of pyridine (40 mM) in CD_3CN were prepared. Then, 400 μL of each stock solution was added to a microwave tube to a final volume of 800 μL .

General Procedure for kinetic measurement of exchange reaction between ammonium salts and tertiary amine.

The concentrations of each component were determined by integration of the *N*-allyl-*N,N*-dimethylanilinium salts $\text{CH}_2=\text{CH}_2\text{-Ph}$, *N*-benzyl-*N,N*-dimethylanilinium salts $\text{-CH}_2\text{-Ph}$, tertiary amine $\text{-N(CH}_3)_2$, allyl bromide $\text{CH}_2=\text{CH}_2\text{-Br}$, and benzyl bromide $\text{Br-CH}_2\text{-Ph}$ $^1\text{H-NMR}$ signals respectively as a function of time. The reaction rate constants were calculated from plots of reactant concentration versus time during the first 10% of the reaction, where $[A]_0 = [B]_0$.^[54] It was found that [A] and [B] reacted with 1:1 stoichiometry over this time scale. The plot of $1/[A]$ (or $1/[B]$) vs t was linear. This is consistent with an overall second order reaction at early time, first order in [A] and [B], respectively. The half-lives ($t_{1/2}$) of the reactions were determined by integration of the decreasing $^1\text{H-NMR}$ signals of the starting material as a function of time and taken to be the time at which the starting material was reduced to 50% with respect to the equilibrium value. The equilibrium constants are obtained from the amounts of reactants and products according to equation (7.20).

$$K = [C][D]/[A][B] \quad (7.20)$$

Results of kinetic experiments for the ammonium salt exchange with tertiary amine

Figure 7.62. Representative linear least-squares fit ($1/[A]$ vs. t) during the first 10% of the exchange reaction between *N*-allyl-*N,N*-anilinium salt (**1a-Br**) and different aliphatic tertiary amines (**2a-e**) in CD_3CN at $60^\circ C$. Slopes correspond to the overall second order rate constant at early time; R^2 values shown.

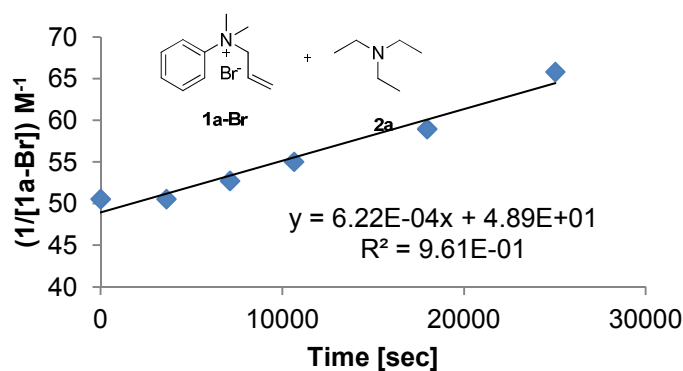


Figure 7.62-1 The exchange reaction between **1a-Br** and **2a** (in the absence of catalyst)

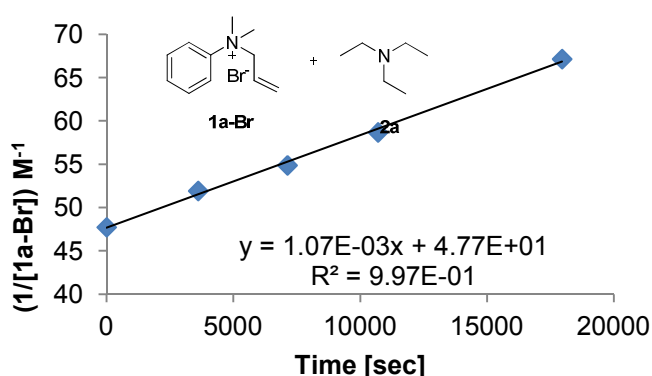


Figure 7.62-2 The exchange reaction between **1a-Br** and **2a** (in the presence of iodide as catalyst)

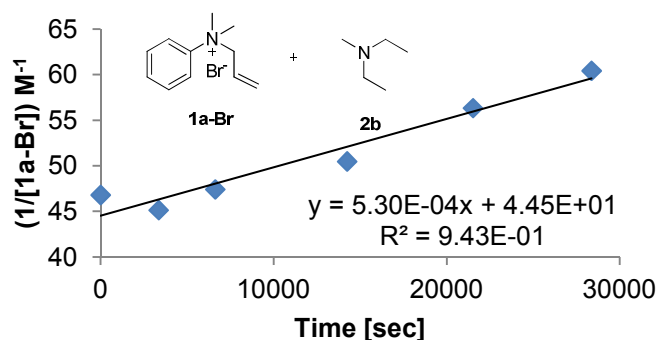


Figure 7.62-3 The exchange reaction between **1a-Br** and **2b** (in the absence of catalyst)

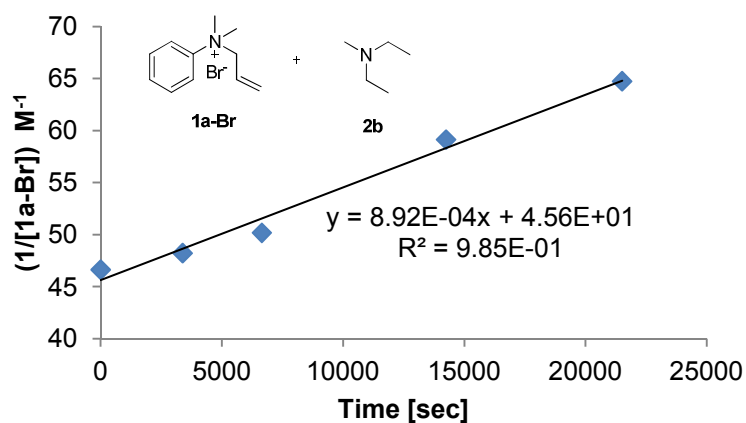


Figure 7.62-4 The exchange reaction between **1a-Br** and **2b** (in the presence of iodide as catalyst)

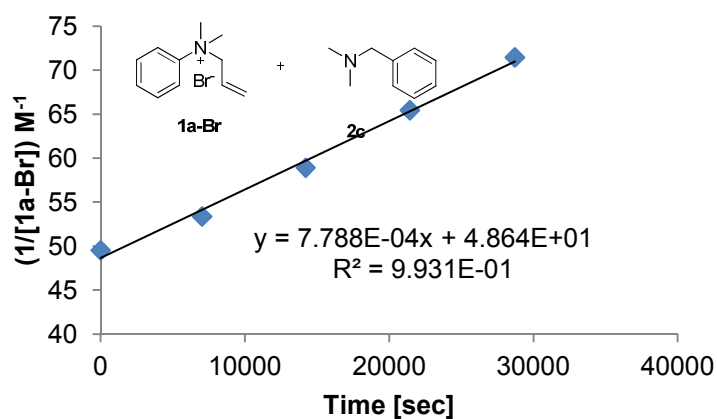


Figure 7.62-5 The exchange reaction between **1a-Br** and **2c** (in the absence of catalyst)

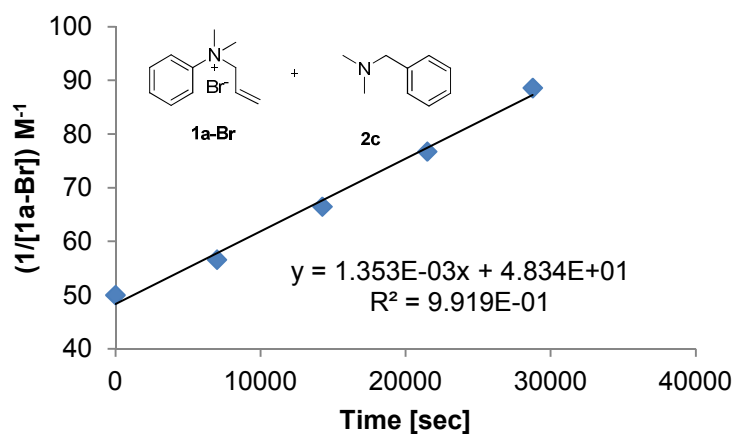


Figure 7.62-6 The exchange reaction between **1a-Br** and **2c** (in the presence of iodide as catalyst)

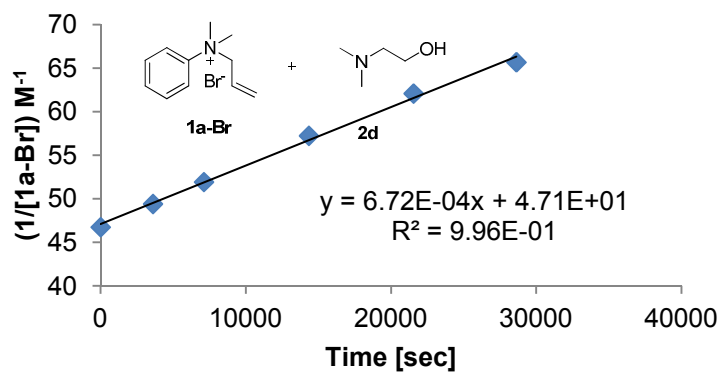


Figure 7.62-7 The exchange reaction between **1a-Br** and **2d** (in the absence of catalyst)

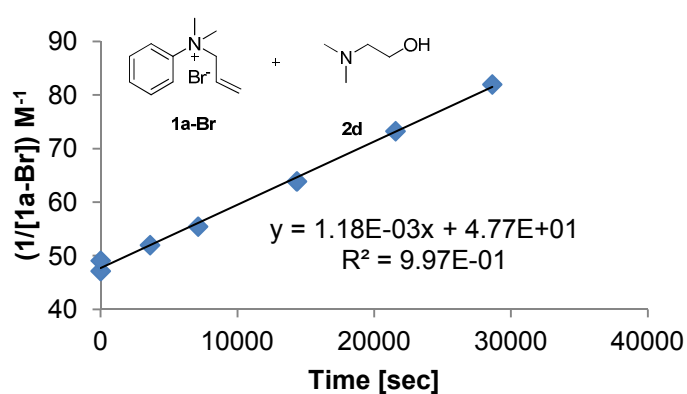


Figure 7.62-8 The exchange reaction between **1a-Br** and **2d** (in the presence of iodide as catalyst)

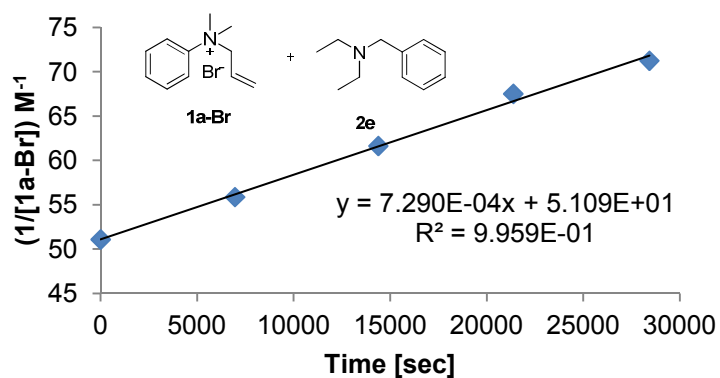


Figure 7.62-9 The exchange reaction between **1a-Br** and **2e** (in the absence of catalyst)

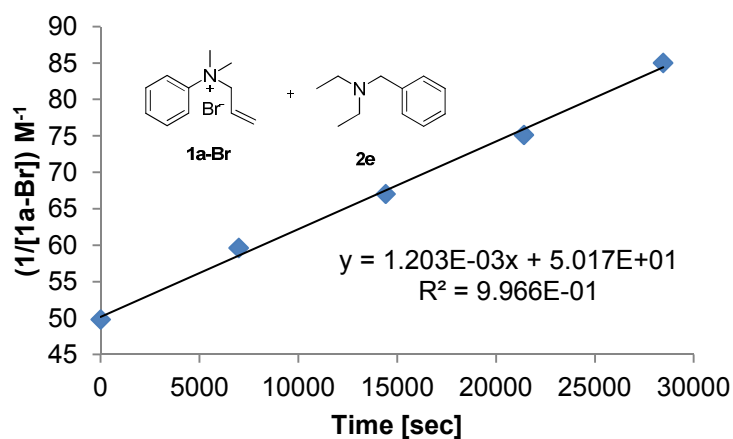


Figure 7.62-10 The exchange reaction between **1a-Br** and **2e** (in the presence of iodide as catalyst)

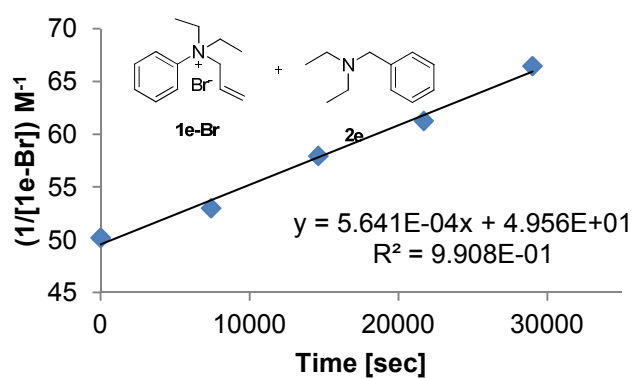


Figure 7.62-11 The exchange reaction between **1e-Br** and **2e** (in the absence of catalyst)

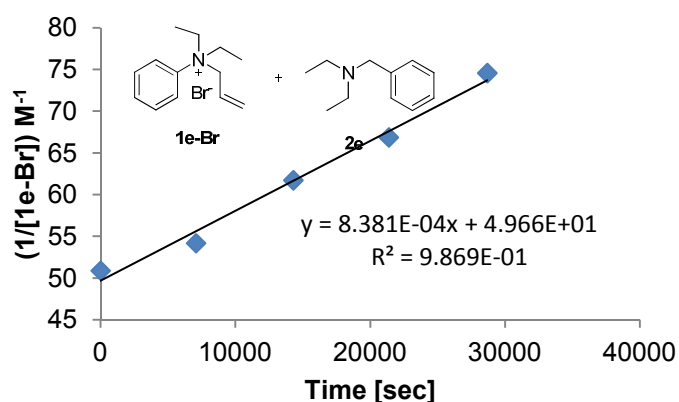


Figure 7.62-12 The exchange reaction between **1e-Br** and **2e** (in the presence of iodide as catalyst)

Figure 7.63. Representative linear least-squares fit ($1/[A]$ vs. t) during the first 10% of the exchange reaction between *N*-allyl-*N,N*-anilinium salt and aromatic tertiary amine in CD_3CN at $60^\circ C$. Slopes correspond to the overall second order rate constant at early time; R^2 values shown.

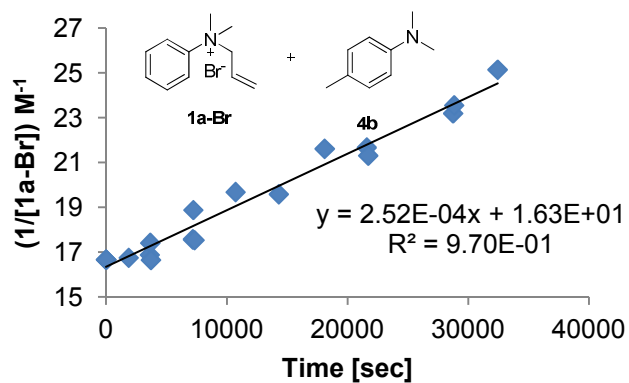


Figure 7.63-1 The exchange reaction between **1a-Br** and **4b** (in the absence of catalyst)

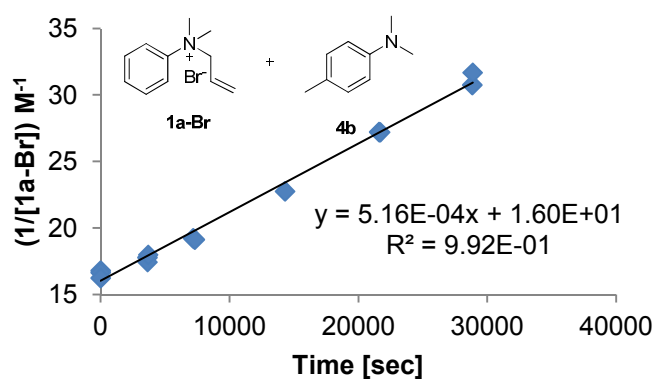


Figure 7.63-2 The exchange reaction between **1a-Br** and **4b** (in the presence of iodide as catalyst)

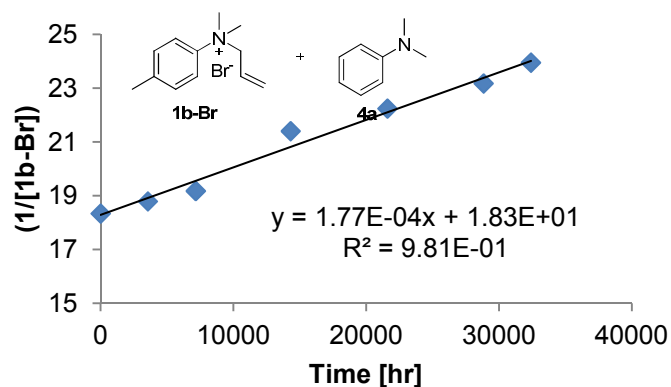


Figure 7.63-3 The exchange reaction between **1b-Br** and **4a** (in the absence of catalyst)

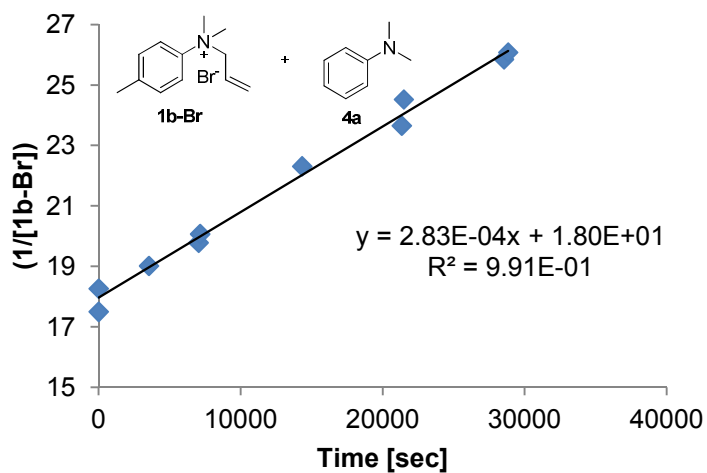


Figure 7.63-4 The exchange reaction between **1b-Br** and **4a** (in the presence of iodide as catalyst)

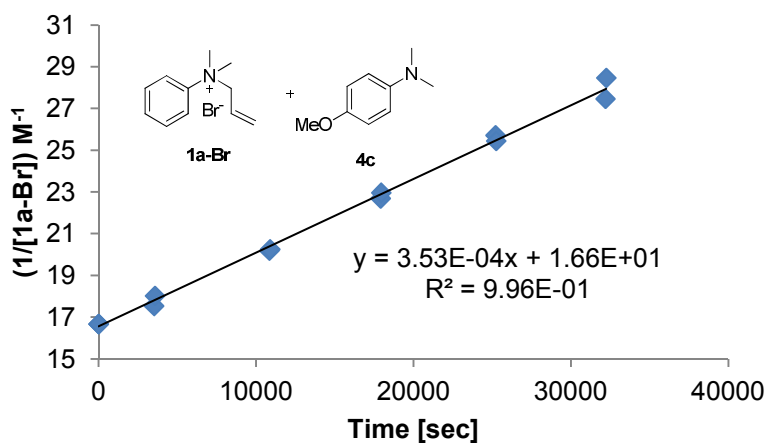


Figure 7.63-5 The exchange reaction between **1a-Br** and **4c** (in the absence of catalyst)

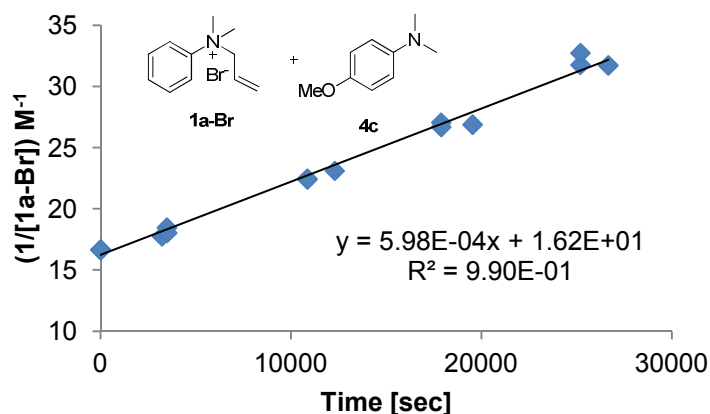


Figure 7.63-6 The exchange reaction between **1a-Br** and **4c** (in the presence of iodide as catalyst)

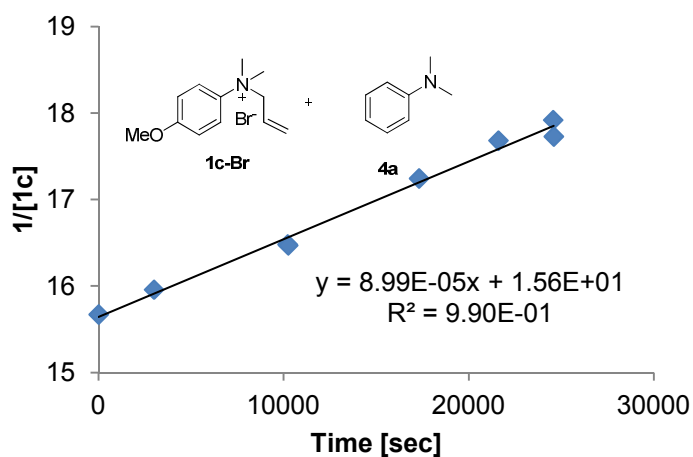


Figure 7.63-7 The exchange reaction between **1c-Br** and **4a** (in the absence of catalyst)

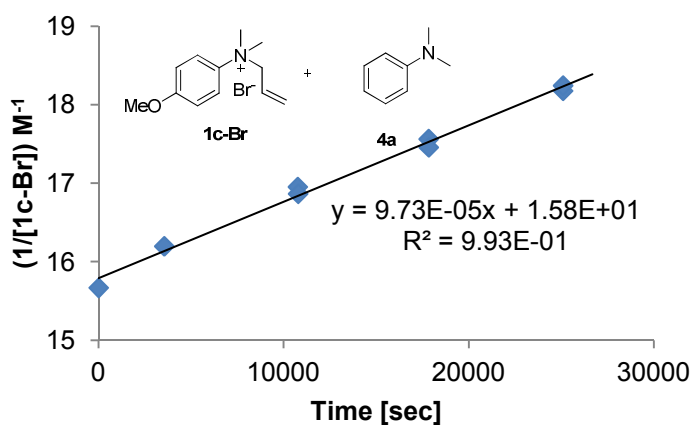


Figure 7.63-8 The exchange reaction between **1c-Br** and **4a** (in the presence of iodide as catalyst)

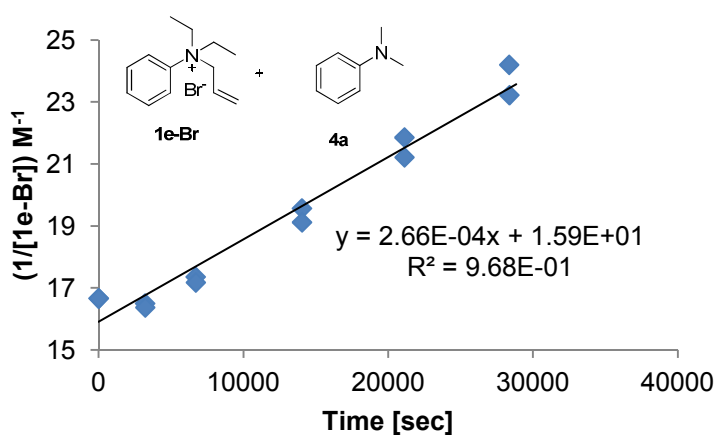


Figure 7.63-9 The exchange reaction between **1e-Br** and **4a** (in the absence of catalyst)

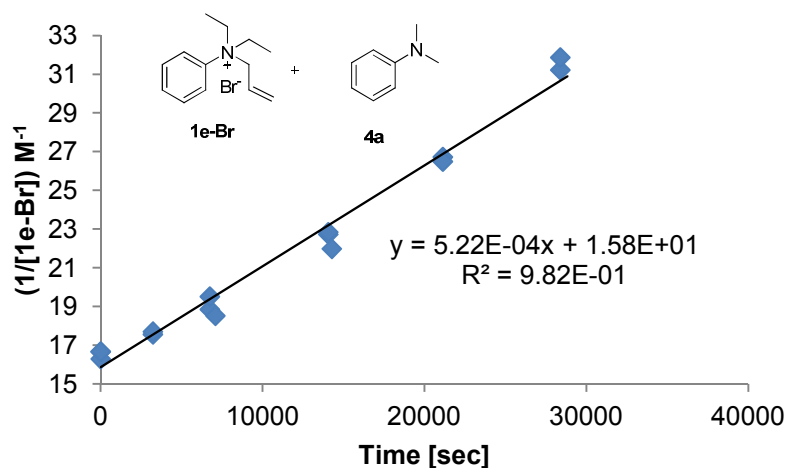


Figure 7.63-10 The exchange reaction between **1e-Br** and **4a** (in the presence of iodide as catalyst)

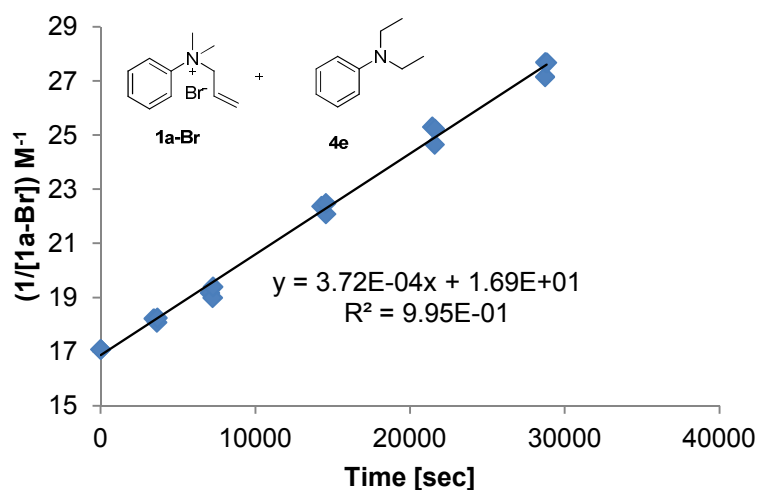


Figure 7.63-11 The exchange reaction between **1a-Br** and **4e** (in the absence of catalyst)

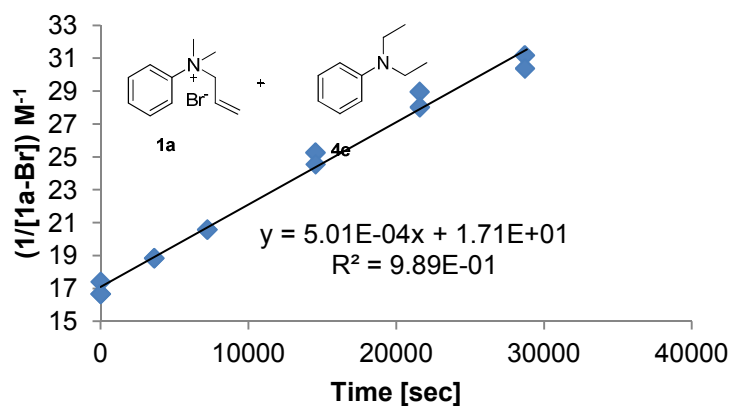


Figure 7.63-12 The exchange reaction between **1a-Br** and **4e** (in the presence of iodide as catalyst)

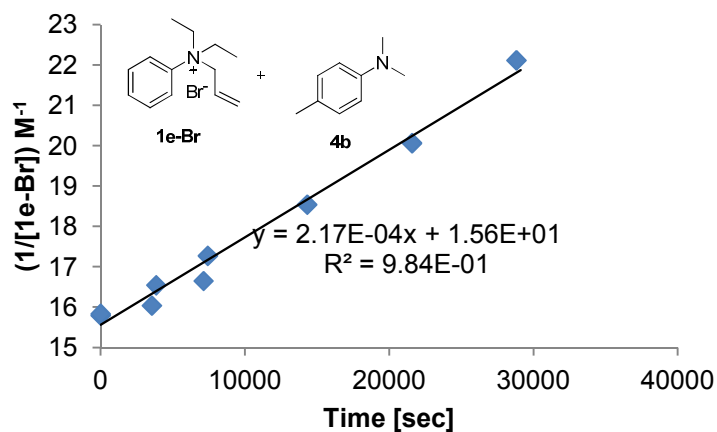


Figure 7.63-13 The exchange reaction between **1e-Br** and **4b** (in the absence of catalyst)

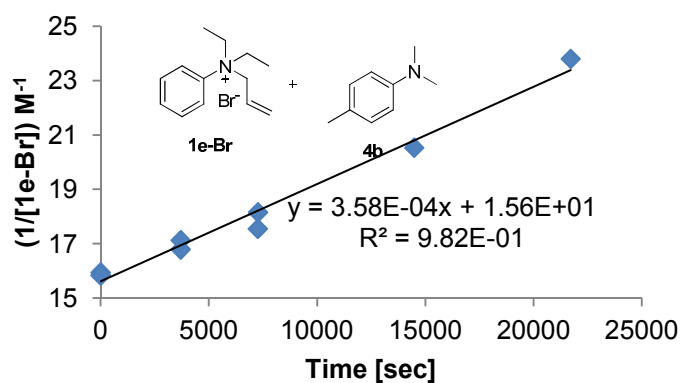


Figure 7.63-14 The exchange reaction between **1e-Br** and **4b** (in the presence of iodide as catalyst)

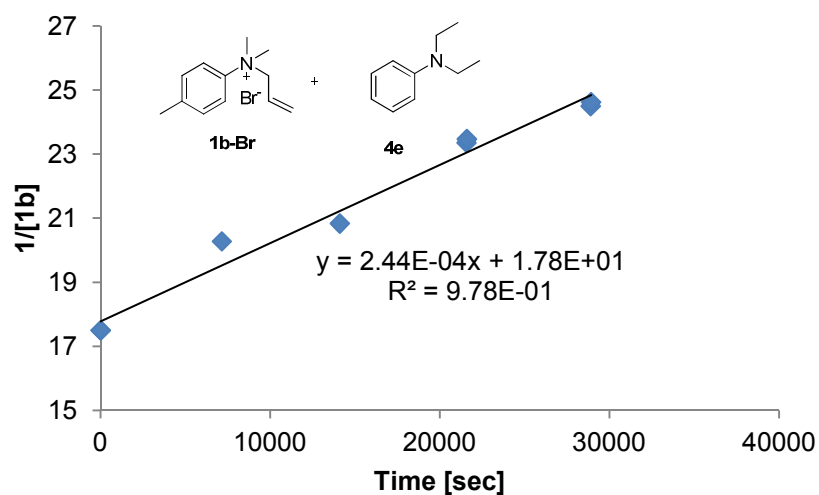


Figure 7.63-15 The exchange reaction between **1b-Br** and **4e** (in the absence of catalyst)

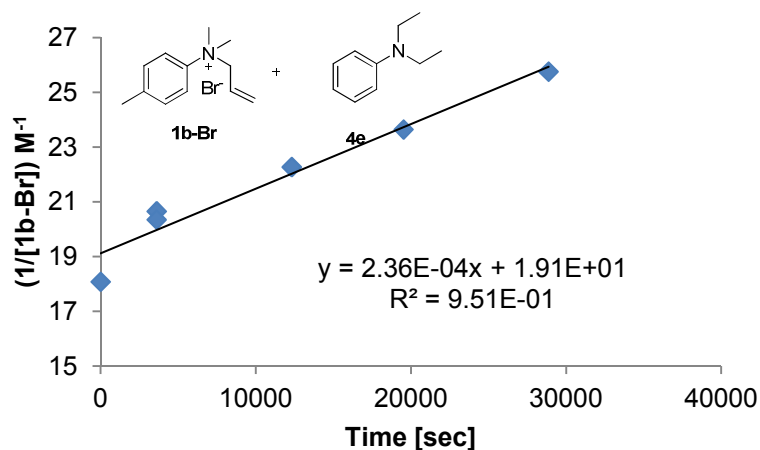


Figure 7.63-16 The exchange reaction between **1b-Br** and **4e** (in the presence of iodide as catalyst)

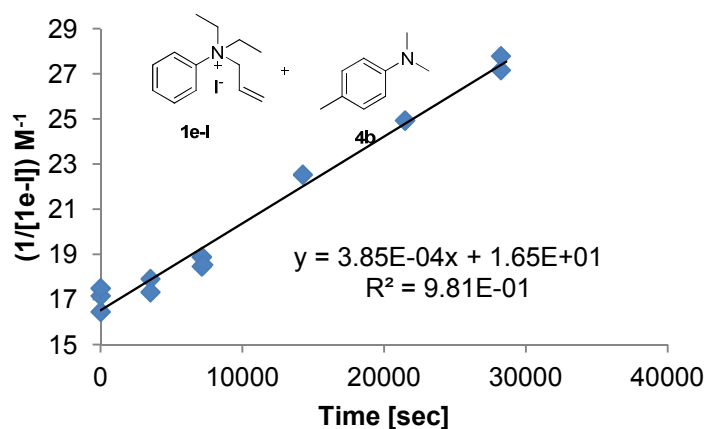


Figure 7.63-17 The exchange reaction between **1e-I** and **4b** (in the absence of catalyst)

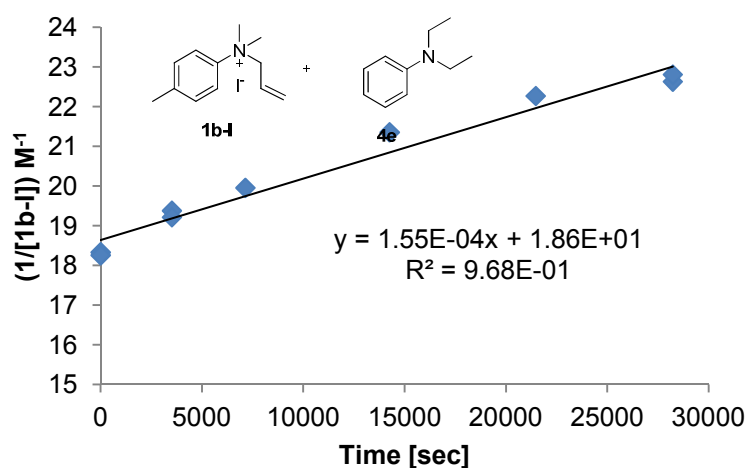


Figure 7.63-18 The exchange reaction between **1b-I** and **4e** (in the absence of catalyst)

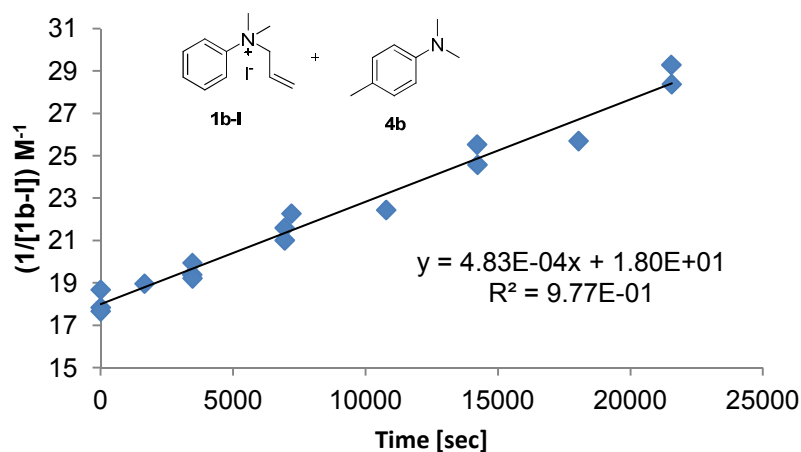


Figure 7.63-19 The exchange reaction between **1b-I** and **4b** (in the absence of catalyst)

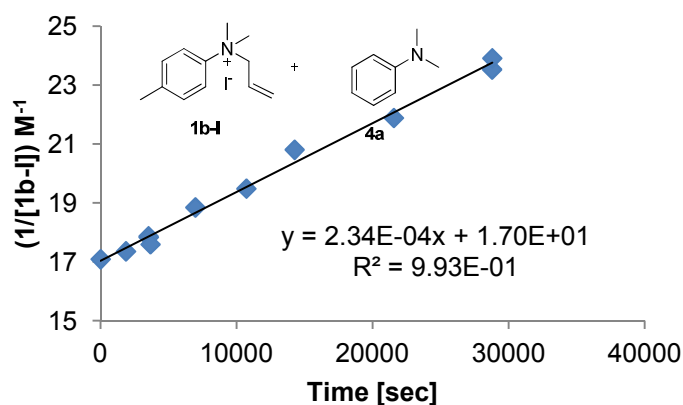


Figure 7.63-20 The exchange reaction between **1b-I** and **4a** (in the absence of catalyst)

Figure 7.64 Representative linear least-squares fit ($1/[A]$ vs. t) during the first 10% of the exchange reaction between *N*-benzyl-*N,N*-dimethylanilinium salt (**5a-c-Br**) and different aromatic tertiary amines (**4a-4c**) in CD_3CN at $60^\circ C$. Slopes correspond to the overall second order rate constant at early time; R^2 values shown.

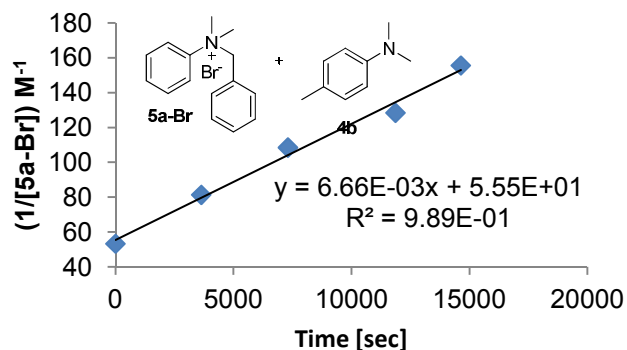


Figure 7.64-1 The exchange reaction between **5a-Br** and **4b** (in the absence of catalyst)

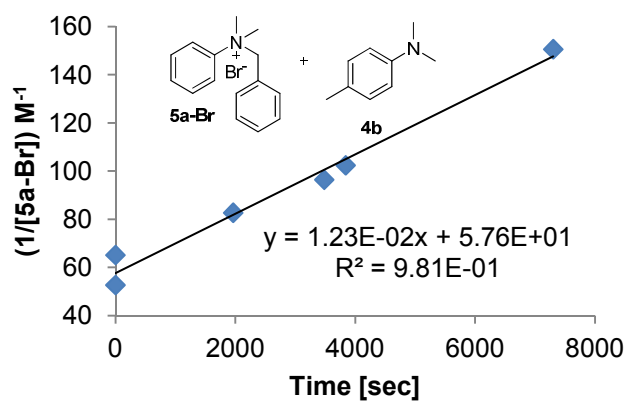


Figure 7.64-2 The exchange reaction between **5a-Br** and **4b** (in the presence of iodide as catalyst)

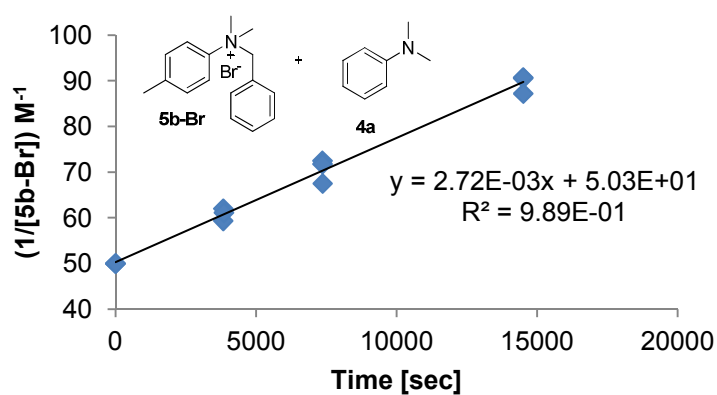


Figure 7.64-3 The exchange reaction between **5b-Br** and **4a** (in the absence of catalyst)

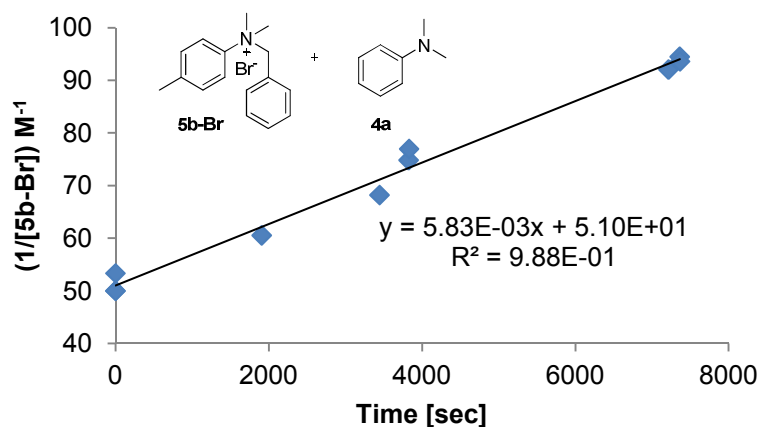


Figure 7.64-4 The exchange reaction between **5b-Br** and **4a** (in the presence of iodide as catalyst)

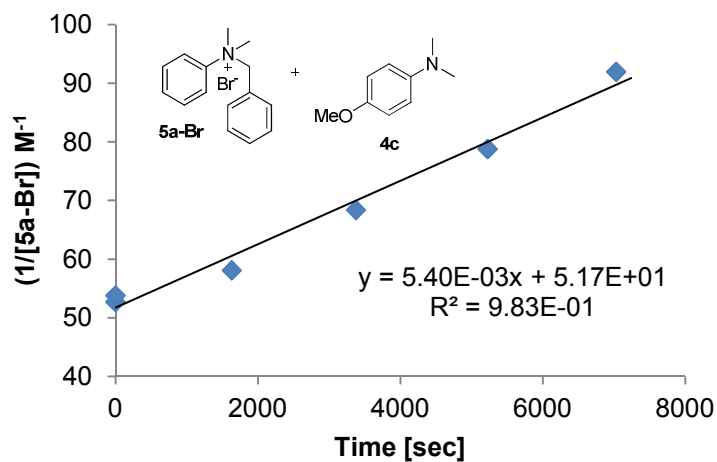


Figure 7.64-5 The exchange reaction between **5a-Br** and **4c** (in the absence of catalyst)

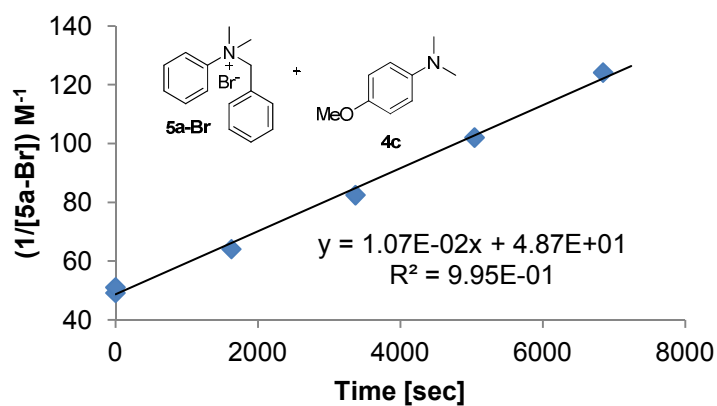


Figure 7.64-6 The exchange reaction between **5a-Br** and **4c** (in the presence of iodide as catalyst)

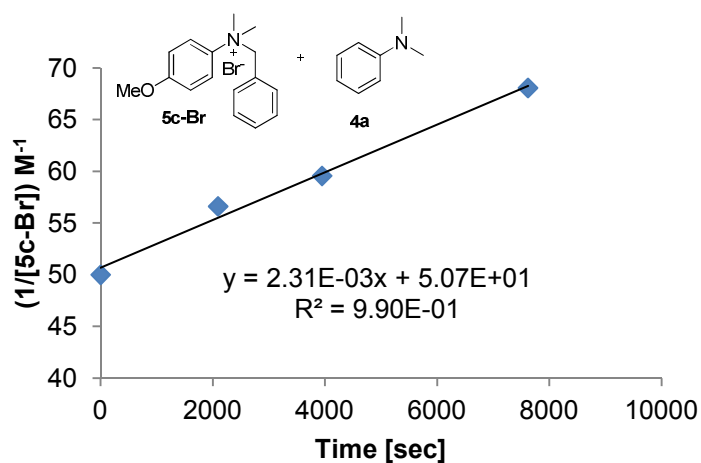


Figure 7.64-7 The exchange reaction between **5c-Br** and **4a** (in the absence of catalyst)

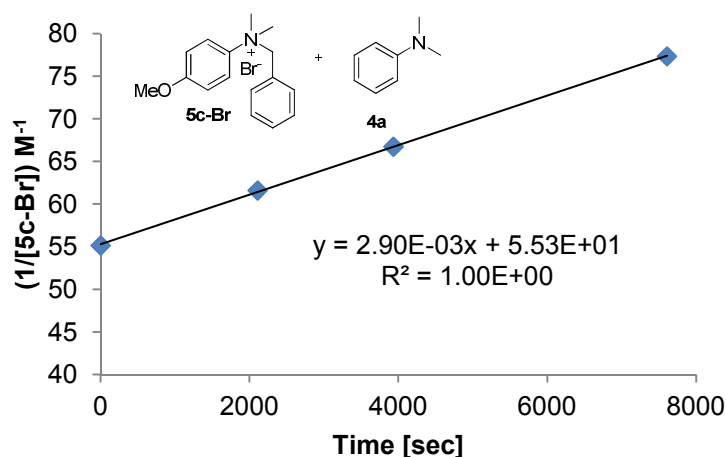


Figure 7.64-8 The exchange reaction between **5c-Br** and **4a** (in the presence of iodide as catalyst)

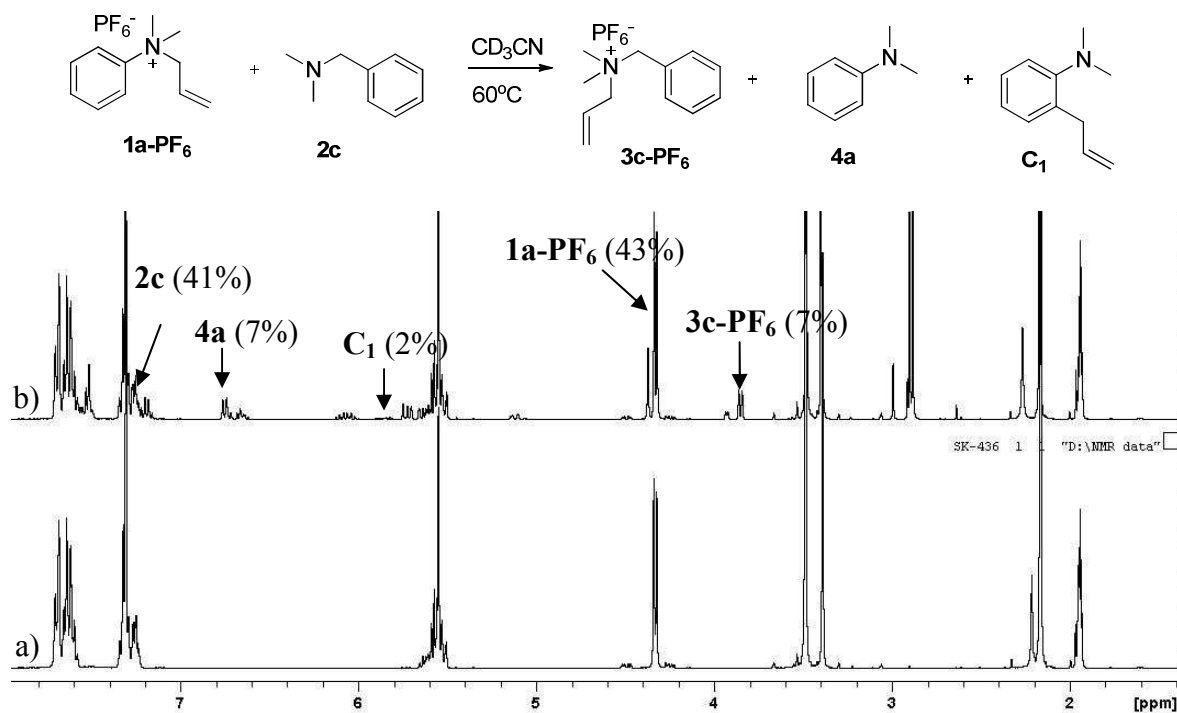


Figure 7.65 ^1H NMR spectra of the exchange reaction between **1a-PF₆** and **2c** in CD_3CN at 60°C to afford the exchange products **3c-PF₆** and **4a**. a) after mixing b) at 16 hr.

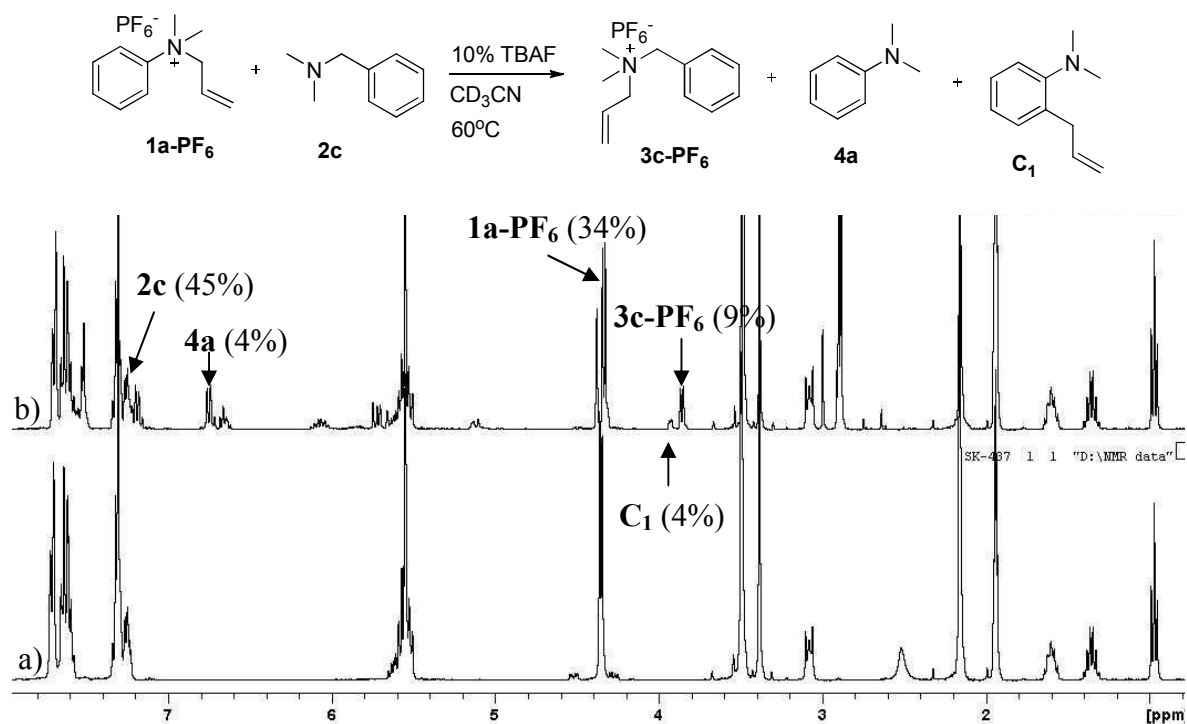


Figure 7.66 ¹H-NMR spectra of the exchange reaction between **1a-PF₆** and **2c** in CD₃CN at 60°C to afford the exchange products **3c-PF₆** and **4a**. a) after mixing b) at 18 hr.

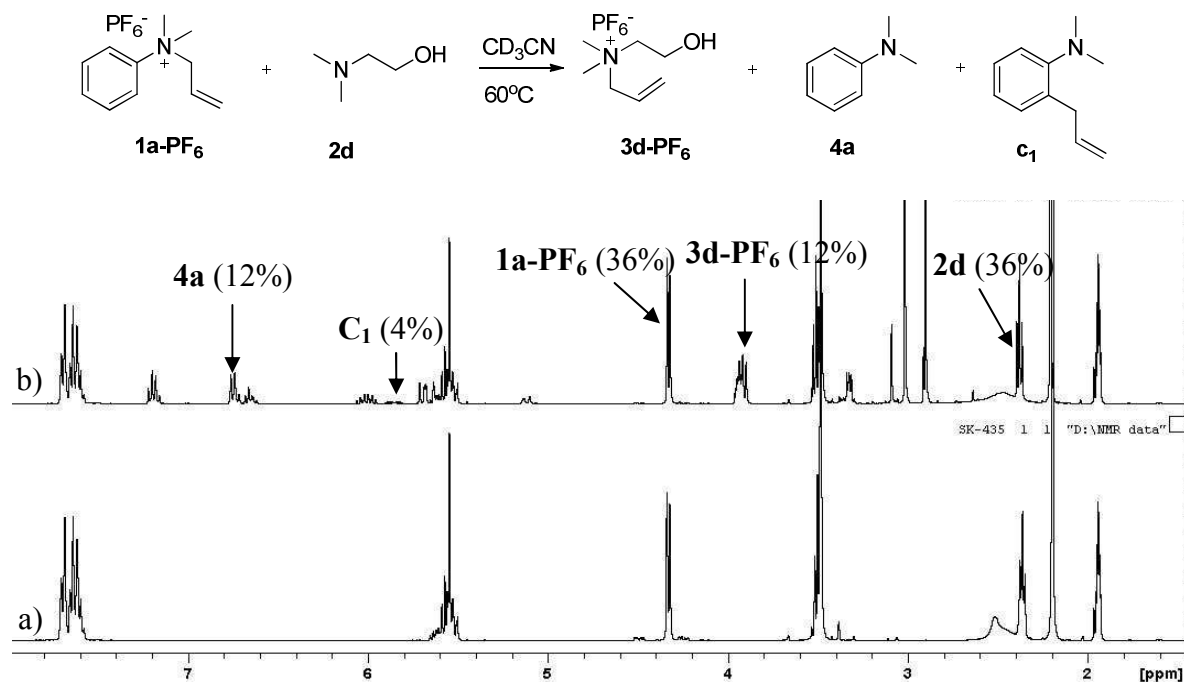


Figure 7.67 ¹H-NMR spectra of the exchange reaction between **1i** and **2d** in CD₃CN at 60°C to afford the exchange products **3d-PF₆** and **4a**. a) after mixing b) at 16 hr.

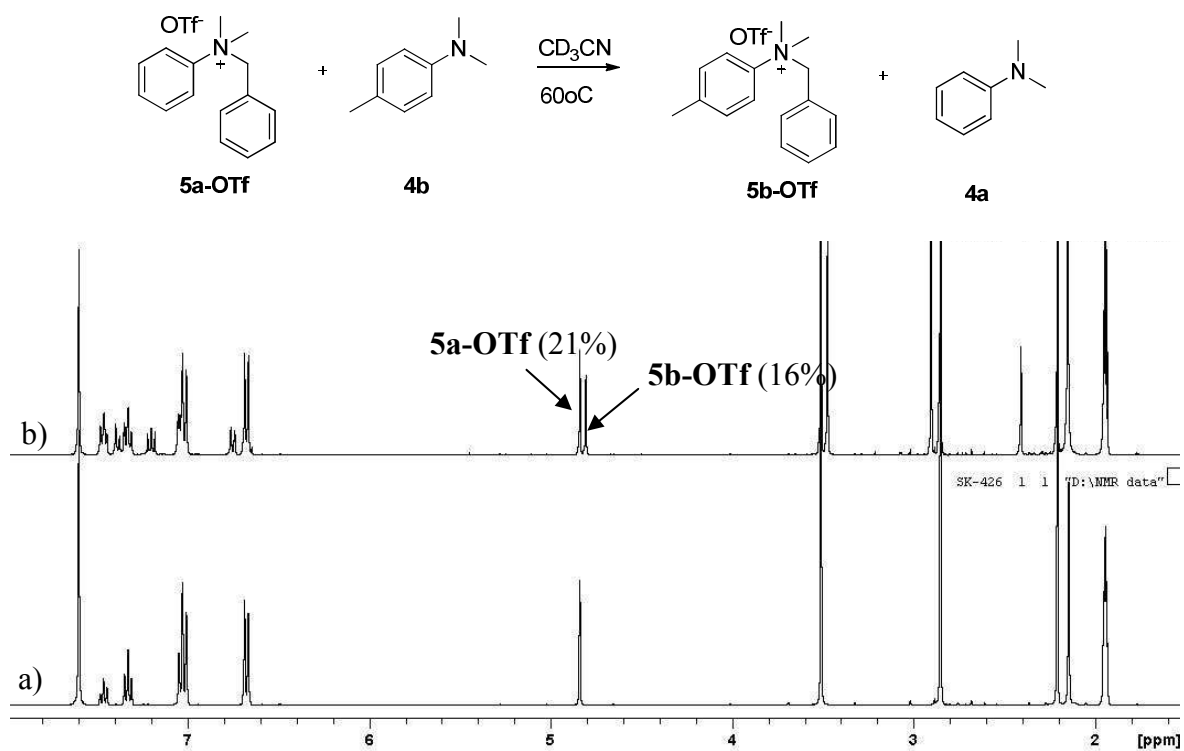


Figure 7.68 ¹H-NMR spectra of the exchange reaction between **5a-OTf** and **4b** in CD₃CN at 60°C a) after mixing b) at 161 hr.

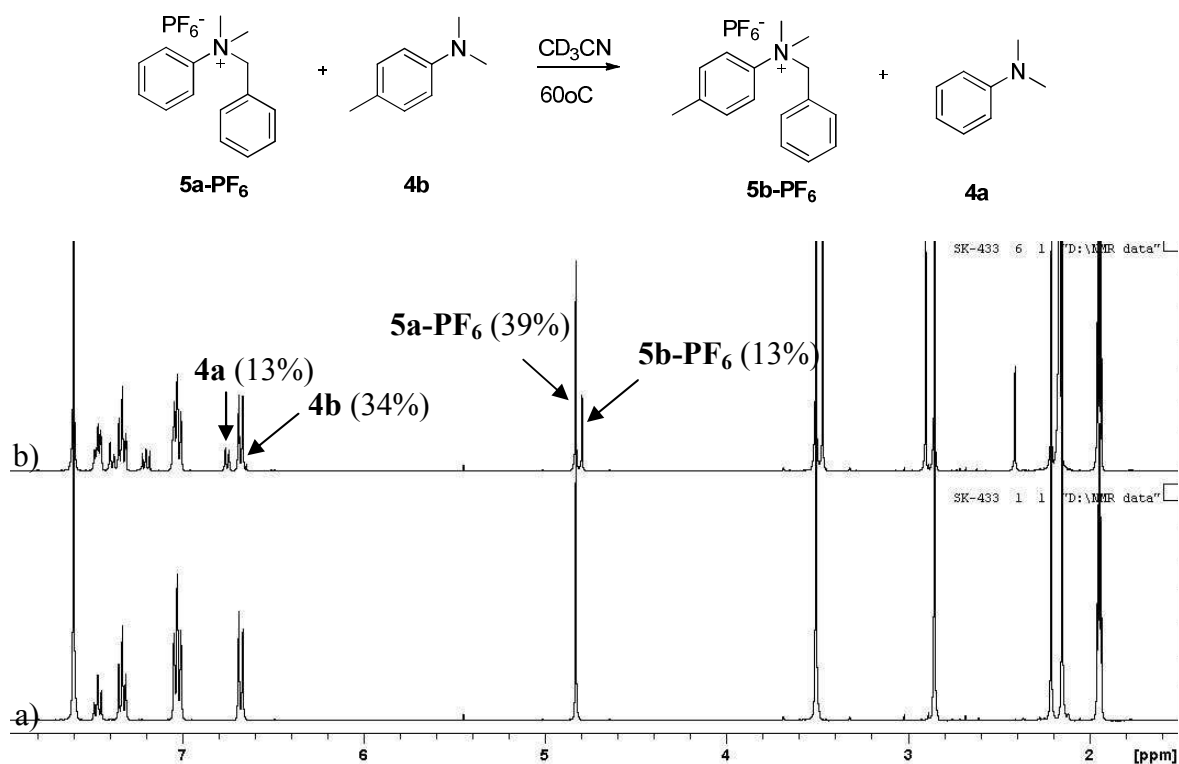
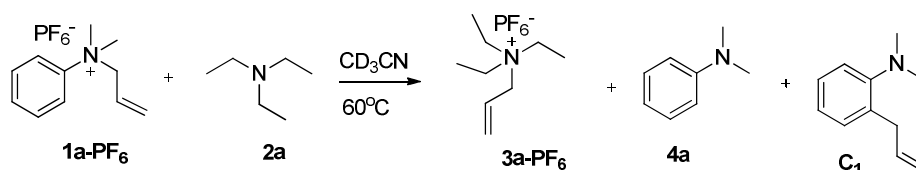


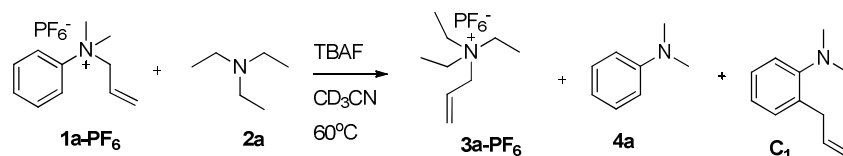
Figure 7.69 ¹H-NMR spectra of the exchange reaction between **5a-PF₆** and **4b** in CD₃CN at 60°C to afford exchange products **5b-PF₆** and **4a**. a) after mixing b) at 137 hr.

The reaction of **1a-PF₆** and **2a** (Scheme 7.1), giving **1a-PF₆** (48%), **2a** (44%), **3a-PF₆** (3%), **4a** (3%), **c₁** (2%) after 23 hr with a rate constant = $3.26 \times 10^{-5} \text{ M}^{-1} \text{ s}^{-1}$ (about 20 times slower than **1a-PF₆** + **2a**).



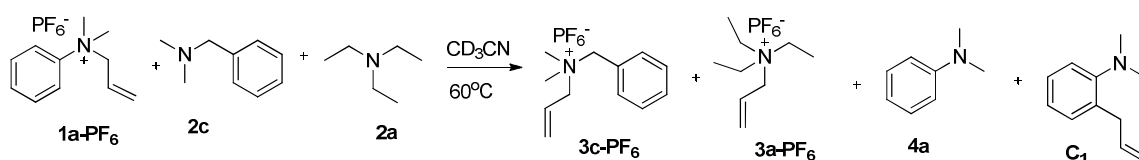
Scheme 7.1 The exchange reaction between **1a-PF₆** and **2a** in CD_3CN at 60°C .

Next, the reaction of **1a-PF₆** and **2a** (Scheme 7.2) was examined in the presence of 10mol% TBAF, giving **1a-PF₆** (48%), **2a** (45%), **3a-PF₆** (2%), **4a** (3%), **c₁** (2%) at 21 hr. The reaction between **1a-PF₆** and **2c** was also performed in presence of 10mol% TBAF (Figure 7.66), the same results were obtained, indicating that no allyl fluoride was formed.



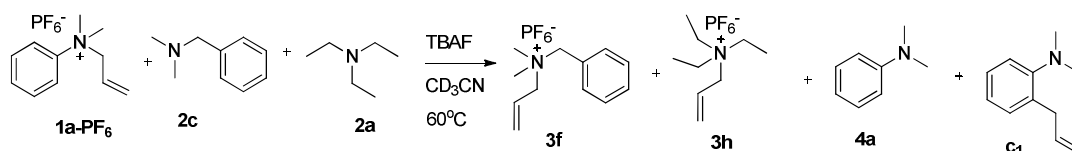
Scheme 7.2 The exchange reaction between **1a-PF₆** and **2a** in CD_3CN at 60°C in the presence of 10mol% TBAF.

The reaction of **1a-PF₆** + **2c** + **2a** (Scheme 7.3) was performed, giving **1a-PF₆** (25%), **2c** (30%), **2a** (27%), **3c-PF₆** (7%), **3a-PF₆** (2%), **4a** (7%), **c** (3%) at 23 hr.



Scheme 7.3 The exchange reaction between **1a-PF₆**, **2a**, and **2c** in CD_3CN at 60°C .

The reaction of **1a-PF₆** + **2c** + **2a** (Scheme 7.4) was performed in the presence of 10mol% TBAF, giving **1a-PF₆** (26%), **2c** (32%), **2a** (25%), **3c-PF₆** (5%), **3a-PF₆** (1%), **4a** (9%), **c₁** (2%) at 21 hr.

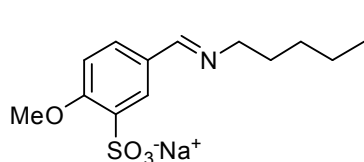


Scheme 7.4 The exchange reaction between **1a-PF₆**, **2a**, and **2c** in CD_3CN at 60°C in the presence of 10mol% TBAF.

7.5 Chapter 5, Thermodynamic and Kinetic Selection of Imine formation in Dynamic Covalent chemistry

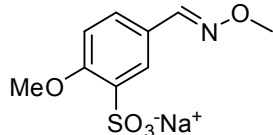
7.5.1 Synthesis and Characterization

1. Sodium (*E*)-2-methoxy-5-((pentylimino)methyl)benzenesulfonate (**1B**)



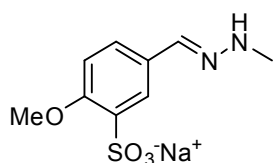
A sodium 5-formyl-2-methoxybenzenesulfonate (0.280 g, 1.18 mmol) was dissolved in methanol (20 mL) and followed by adding pentylamine (0.15 mL, 1.30 mmol). The solution was stirred at 50°C for 48 hr. Then, the solvent was removed by evaporator and the product washed with diethyl ether to afford **1A** as a white solid (0.30 g, 81% yield). ¹H-NMR (D₂O) δ ppm: 8.20 (s, 1H), 8.14 (d, *J* = 2.6 Hz, 1H), 7.78 (dd, *J* = 2.2 Hz, 1H), 7.09 (d, *J* = 8.8 Hz, 1H), 3.89 (s, 3H), 3.50 (t, *J* = 7.3 Hz, 2H), 1.61 (q, *J* = 7.3 Hz, 2H), 1.29 (m, 4H), 0.85 (t, *J* = 6.8 Hz, 3H).

2. Sodium (*E*)-2-methoxy-5-((methoxyimino)methyl)benzenesulfonate (**1C**)

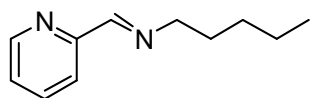


A sodium 5-formyl-2-methoxybenzenesulfonate (0.217 g, 1.00 mmol) and *O*-methoxylamine (0.092, 1.10 mmol) were dissolved in methanol (20 mL) then phosphate buffer pH 11 (2 mL) was added. The solution was stirred at 50°C for 24 hr. Then, the solvent was removed by evaporator. The product was extracted with ethanol and the solvent removed again. The compound was washed with diethyl ether to obtain **1C** as a white solid (0.23 g, 86% yield). ¹H-NMR (D₂O) δ ppm: 8.63 (s, 1H), 8.48 (d, *J* = 8.8 Hz, 1H), 7.91 (s, 1H), 7.33 (d, *J* = 8.8 Hz, 1H), 4.04 (s, 3H), 3.87 (s, 3H).

3. Sodium (*E*)-2-methoxy-5-((2-methylhydrazono)methyl)benzenesulfonate (**1E**)

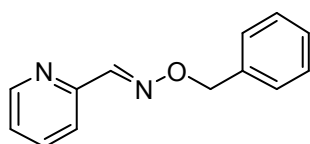


A sodium 5-formyl-2-methoxybenzenesulfonate (1.191 g, 5.00 mmol) was dissolved in phosphate buffer pH 8.0 (20 mL). Then, methylhydrazine (0.29 mL, 5.50 mmol) was slowly dropped into the solution followed by stirring at 50°C overnight. The solvent was removed by evaporator and the product extracted with methanol. The methanol was removed then the compound was washed with diethyl ether to give a white solid (0.9182, 69% yield). ¹H-NMR (D₂O) δ ppm: 7.97 (d, *J* = 2.2 Hz, 1H), 7.88 (s, 1H), 7.77 (d, *J* = 9.3 Hz, 1H), 7.22 (d, *J* = 8.8 Hz, 1H), 3.97 (s, 3H), 2.87 (s, 3H). ¹³C-NMR (100 MHz, D₂O; δ/ppm): 34.4, 55.9, 112.9, 126.4, 126.9, 130.1, 130.9, 141.8, 156.8.

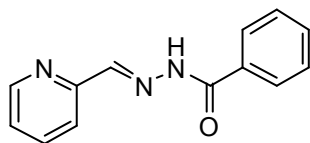
4. *Pentyl-pyridin-2-ylmethylene-amine (3B)*^[55]

Prepared in 95% yield as a pale yellow liquid by a route analogous to that described for imine synthesis in *Chapter 2*.

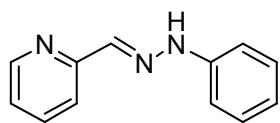
¹H-NMR (CD₃OD) δ ppm: 0.87 (t, *J* = 7.31 Hz, 1H), 1.29 – 1.36 (m, 4H), 1.67 (quint, *J* = 7.2 Hz, 2H), 3.62 (t, *J* = 7.15 Hz, 2H), 7.39 – 7.43 (m, 1H), 7.84 (t, *J* = 7.8 Hz, 1H), 7.93 (d, *J* = 8.0 Hz, 1H), 8.30 (s, 1H), 8.55 (d, *J* = 4.29 Hz, 1H). ¹³C-NMR (100 MHz, CD₃OD; δ/ppm): 14.5, 23.6, 30.7, 31.5, 62.4, 122.8, 126.7, 138.8, 150.4, 155.3, 163.2.

5. *(E)-picolinaldehyde O-benzyl oxime (3F)*^[56]

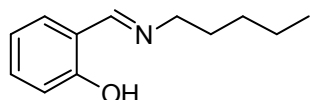
Pyridine (0.89 mL, 11.00 mmol, 1.1 equiv.) was added dropwise to a stirred solution of *O*-benzylhydroxylamine hydrochloride (1.996 g, 13.00 mmol, 1.3 equiv.) and 2-pyridine carboxaldehyde (1.07, 10.00 mmol, 1.0 equiv.) in methanol 40 mL and the mixture was heated at reflux for 4 h. The solvent was removed under reduced pressure, and the remaining solid residue was dissolved in dichloromethane (200 mL) and washed with water (200 mL). The aqueous layer was extracted with dichloromethane (200 mL x 3) and the combined organic layers were dried over MgSO₄. The solvent was removed under reduced pressure and the crude product was purified by flash column chromatography to obtain a yellow liquid (1.50 g, 71% yield). ¹H-NMR (CD₃OD) δ ppm: 8.48 (d, *J* = 5 Hz, 1H), 8.11 (s, 1H), 7.79 (t, *J* = 6.8 Hz, 2H), 7.21 – 7.37 (m, 6H), 5.18 (s, 2H).

6. *(E)-N'-(pyridin-2-ylmethylene)benzohydrazide (3G)*^[57]

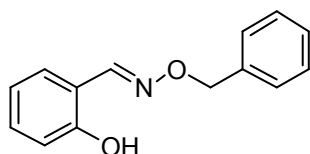
Benzhydrazide (0.408 g, 3 mmol) was dissolved in methanol (10 mL) then a solution of 2-pyridine carboxaldehyde (0.29 mL, 3.00) in methanol (10 mL) was added drop wise to the solution. The mixture was refluxed for 2 h. Then, the solution was evaporated on a steam bath and cooled to room temperature to obtain a white solid (0.33 g, 49% yield). ¹H-NMR (CD₃OD) δ ppm: 8.53 (d, *J* = 5.5 Hz, 1H), 8.35 (s, 1H), 8.27 (d, *J* = 8.2 Hz, 1H), 7.91 (d, *J* = 8.0 Hz, 2H), 7.86 (t, *J* = 8.4 Hz, 1H), 7.57 (t, *J* = 6.5 Hz, 1H), 7.49 (t, *J* = 7.6 Hz, 2H), 7.39 (t, *J* = 5.4 Hz, 1H), 4.5 (s, 1H).

7. (*E*)-2-((2-phenylhydrazono)methyl)pyridine (**3H**)^[58]

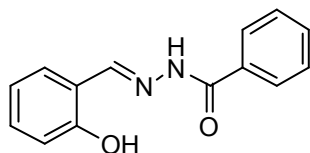
Phenylhydrazine (1.08 mL, 11.00 mmol) was dissolved in methanol (10 mL) and then a solution of 2-pyridyl aldehyde (0.95 mL, 10.00 mmol) in methanol (10 mL) was added dropwise. The product precipitated after a short time and was left standing for 2 h. Then, the product was washed with methanol and dried under vacuum to afford a white solid (0.753, 37% yield). ¹H-NMR (CD₃OD) δ ppm: 8.37 (d, *J* = 5.2 Hz, 1H), 7.95 (d, *J* = 8.0 Hz, 1H), 7.75 (d, *J* = 5.5 Hz, 2H), 7.08 – 7.21 (m, 5H), 6.76 (t, *J* = 7.4 Hz, 1H). ¹³C-NMR (100 MHz, CD₃OD; δ/ppm): 113.9, 120.9, 121.3, 123.8, 130.3, 136.6, 138.5, 146.4, 149.6, 156.6.

8. (*E*)-*N*-(pyridin-2-ylmethylene)pentan-1-amine (**4B**)^[59]

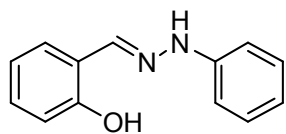
Prepared in 90% yield as a yellow liquid by a route analogous to that described for imine synthesis in *Chapter 2*. ¹H-NMR (CD₃OD) δ ppm: 0.85 (t, *J* = 7.4 Hz, 1H), 1.29 – 1.34 (m, 4H), 1.63 (quint, *J* = 7.2 Hz, 2H), 3.53 (t, *J* = 6.98, 2H), 6.68 – 6.74 (m, 2.17), 7.18 – 7.23 (m, 2H), 8.33 (s, 1H). ¹³C-NMR (100 MHz, CD₃OD; δ/ppm): 14.5, 23.6, 30.5, 31.7, 58.8, 118.8, 118.9, 119.7, 133.1, 134.3, 165.7, 166.9.

9. (*E*)-picolinaldehyde *O*-benzyl oxime (**4F**)^[60]

O-benzylhydroxylamine hydrochloride (0.479 g, 3.00 mmol) was dissolved in methanol then salicylaldehyde (0.32 mL, 3.00 mmol) was added dropwise to the solution. The mixture was refluxed overnight and then the solvent was removed to obtain a white solid (0.45 g, 66% yield). ¹H-NMR (CD₃OD) δ ppm: 8.27 (s, 1H), 7.23 – 7.35 (m, 6H), 7.17 (t, *J* = 8.1 Hz, 1H), 6.79 (t, *J* = 6.5 Hz, 2H), 5.09 (s, 2H). ¹³C-NMR (100 MHz, CD₃OD; δ/ppm): 77.7, 117.4, 118.3, 120.8, 129.3, 129.6, 129.7, 131.3, 132.4, 138.7, 152.2, 158.5.

10. (*E*)-*N'*-(pyridin-2-ylmethylene)benzohydrazide (**4G**)^[61]

Benzhydrazide (0.408 g, 3.00 mmol) was dissolved in methanol then salicylaldehyde (0.32 mL, 3.00 mmol) was added dropwise to the solution. The mixture was refluxed overnight and then the solvent was removed and the product washed with hexane to obtain a white solid (0.67 g, 73% yield). ¹H-NMR (CD₃OD) δ ppm: 8.44 (s, 1H), 7.86 (d, *J* = 7.7 Hz, 2H), 7.54 (t, *J* = 7.2 Hz, 1H), 7.46 (t, *J* = 7.6 Hz, 2H), 7.35 (d, *J* = 7.9 Hz, 1H), 7.23 (t, *J* = 7.2 Hz, 1H), 6.85 (t, *J* = 8.4 Hz, 2H). ¹³C-NMR (100 MHz, CD₃OD; δ/ppm): 117.8, 119.6, 120.7, 128.9, 129.9, 131.9, 133.0, 133.6, 134.1, 152.0, 159.6, 166.5.

11. (*E*)-2-((2-phenylhydrazono)methyl)pyridine (**4H**)^[62]

Phenylhydrazine (0.295, 3.00 mmol) was dissolved in methanol then salicylaldehyde (0.32 mL, 3.00 mmol) was added dropwise to the solution. The mixture was refluxed for 4 h then solvent was evaporated to an oily residue that crystallized upon cooling. The residue was dissolved in hot hexane to get a white solid (0.563 g, 88% yield). ¹H-NMR (DMSO-*d*₆) δ ppm: 10.52 (s, 1H), 10.39 (s, 1H), 8.14 (s, 1H), 7.54 (d, *J* = 7.3 Hz, 1H), 7.24 (d, *J* = 7.7 Hz, 2H), 7.16 (t, *J* = 7.7 Hz, 1H), 6.97 (d, *J* = 7.5 Hz, 2H), 6.87 (t, *J* = 9.0 Hz, 2H), 6.77 (t, *J* = 7.5 Hz, 1H). ¹³C-NMR (100 MHz, CD₃OD; δ/ppm): 113.2, 117.2, 120.6, 120.9, 120.94, 130.2, 130.5, 141.6, 146.1 158.2.

7.5.2 General procedures for the study of kinetic and thermodynamic experiments

A typical protocol was realized by the preparation in a NMR tube of a fresh solution of the compounds in D₂O, DMSO-*d*₆, CD₃OD, CD₃CN, and sodium phosphate buffer solution. All reactions with aldehyde and amine were carried out at room temperature with a final concentration of 20 mM and a total volume of 600 μL.

The buffer concentration was 160 mM in all cases and buffer solution at different pDs were made to pD 5.0 (NaH₂PO₄/Na₂HPO₄ + NaOD), pD 8.5 (NaH₂PO₄/ Na₂HPO₄ + NaOD), and pD 11.4 (NaH₂PO₄/Na₂HPO₄ + NaOD). The pD was calculated using pD = pH + 0.4.^[63]

1) For the imine formation study: A NMR tube was first charged with solvent. Then, the prepared solutions 200 μL of aldehyde and amine (60 mM in both) were added to the NMR tube to obtain a final volume of 600 μL. The NMR tubes were topped with Teflon caps to keep a constant volume (concentration). ¹H-NMR spectra were measured immediately after mixing.

2) For the competition reactions: The stock solutions (120 mM) were prepared using the desired solvents. A NMR tube was first charged with 1,4-dioxane (100 μL) followed by the addition of 100 μL of each solution. Finally, aldehyde was added and ¹H-NMR spectra were measured immediately after mixing and at least 8 acquisitions of the ¹H-NMR spectra were obtained for each time point.

The course of imine formation was followed by the appearance of a signal due to the -CH=N- of the imine products in the ¹H-NMR spectra. The %-formation of imine was determined by integration of the imine products signal referenced to the signal of an internal standard (1,4-dioxane). The time required for equilibration depended on the starting compound and varied with different conditions. The error in ¹H-NMR integration is about 4-5%.

7.5.3 Results of kinetic experiments for the imine formation study

7.5.3.1 Sodium (E)-2-methoxy-5-(2-methoxyvinyl)benzenesulfonate formation

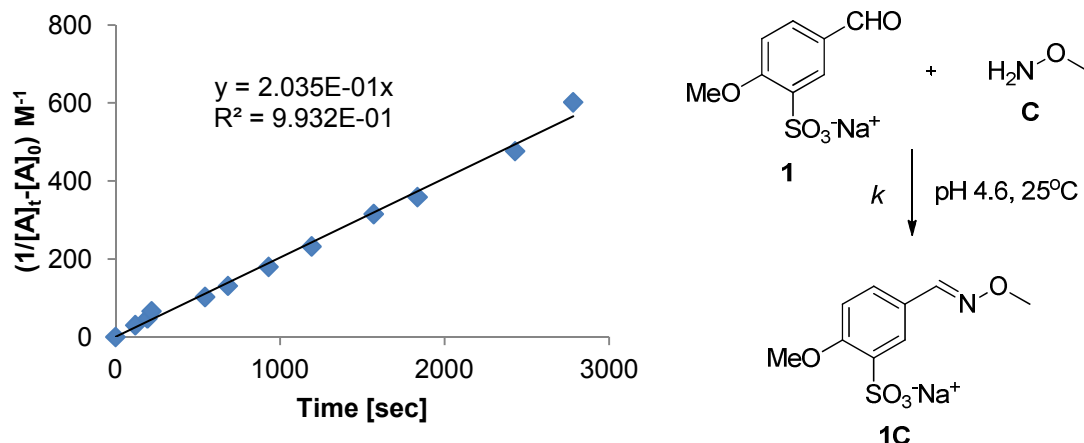


Figure 7.70 Representative linear least-squares fit ($\frac{1}{[A]_t} - \frac{1}{[A]_0}$ vs. t) of the imine formation between sulfonate aldehyde **1** and methoxylamine **C** in phosphate buffer (160 mM NaH_2PO_4 / Na_2HPO_4 + NaOD) pH 4.6 at 25°C. The final solution is 20 mM. The slope of the fit corresponds to the second order rate constant; R^2 values shown.

7.5.3.2 Sodium (E)-5-((2-acetylhydrazono)methyl)-2-methoxybenzenesulfonate formation

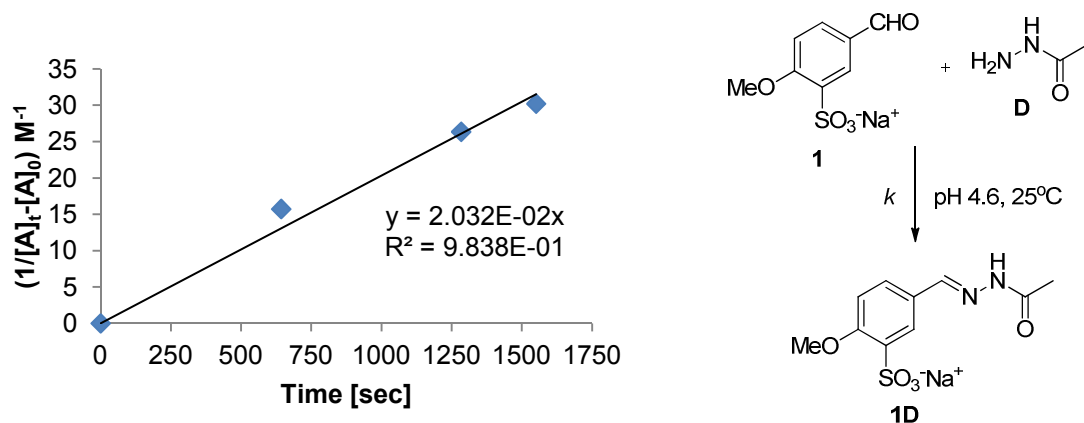


Figure 7.71 Representative linear least-squares fit ($\frac{1}{[A]_t} - \frac{1}{[A]_0}$ vs. t) of the imine formation between sulfonate aldehyde **1** and acetylhydrazide **D** in phosphate buffer (160 mM NaH_2PO_4 / Na_2HPO_4 + NaOD) pH 4.6 at 25°C. The final solution is 20 mM. The slope of the fit corresponds to the second order rate constant; R^2 values shown.

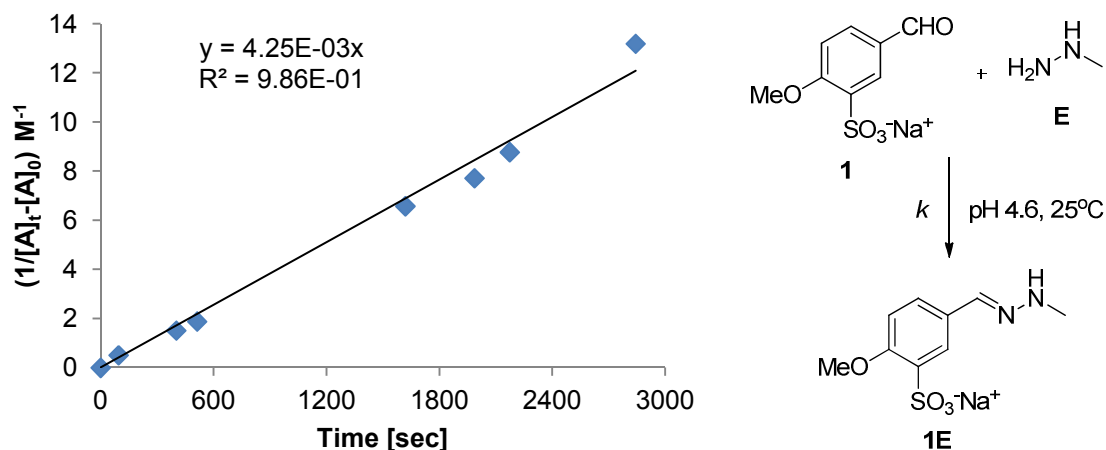
7.5.3.3 Sodium (*E*)-2-methoxy-5-((2-methylhydrazono)methyl)benzenesulfonate formation

Figure 7.72 Representative linear least-squares fit ($\frac{1}{[A]_t} - \frac{1}{[A]_0}$ vs. t) of the imine formation between sulfonate aldehyde **1** and methylhydrazine **E** in phosphate buffer (160 mM $\text{NaH}_2\text{PO}_4/\text{Na}_2\text{HPO}_4 + \text{NaOD}$) pH 4.6 at 25°C. The final solution is 20 mM. The slope of the fit corresponds to the second order rate constant; R^2 values shown.

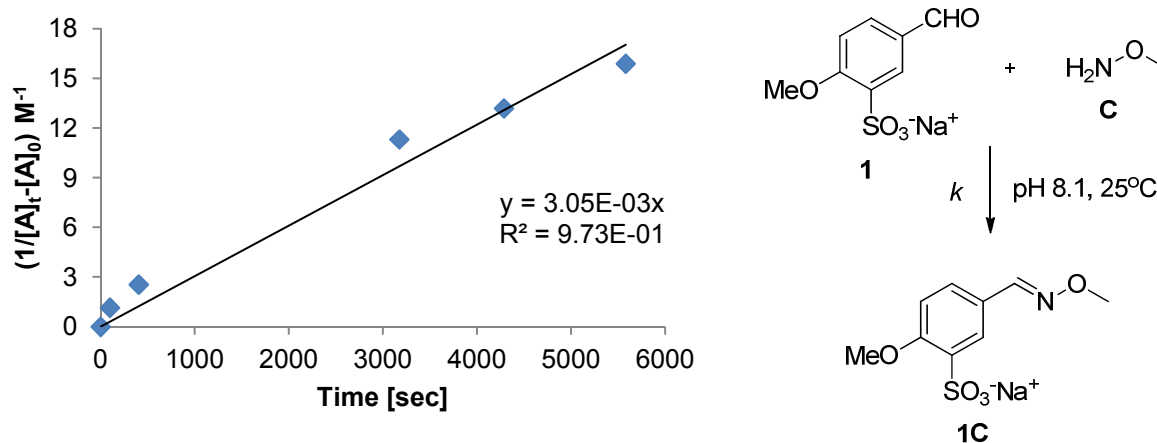
7.5.3.4 Sodium (*E*)-2-methoxy-5-(2-methoxyvinyl)benzenesulfonate formation

Figure 7.73 Representative linear least-squares fit ($\frac{1}{[A]_t} - \frac{1}{[A]_0}$ vs. t) of the imine formation between sulfonate aldehyde **1** and methylhydrazine **C** in phosphate buffer (160 mM $\text{NaH}_2\text{PO}_4/\text{Na}_2\text{HPO}_4 + \text{NaOD}$) pH 8.1 at 25°C. The final solution is 20 mM. The slope of the fit corresponds to the second order rate constant; R^2 values shown.

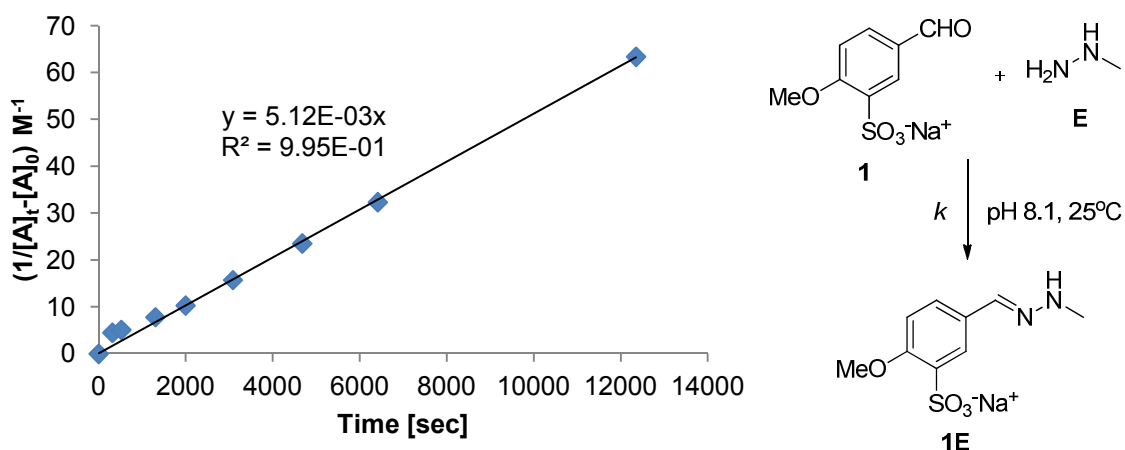
7.5.3.5 Sodium (*E*)-2-methoxy-5-((2-methylhydrazono)methyl)benzenesulfonate formation

Figure 7.74 Representative linear least-squares fit ($\frac{1}{[A]_t} - \frac{1}{[A]_0}$ vs. t) of the imine formation between sulfonate aldehyde **1** and methylhydrazine **E** in phosphate buffer (160 mM $NaH_2PO_4/Na_2HPO_4 + NaOD$) pH 8.1 at 25°C. The final solution is 20 mM. The slope of the fit corresponds to the second order rate constant; R^2 values shown.

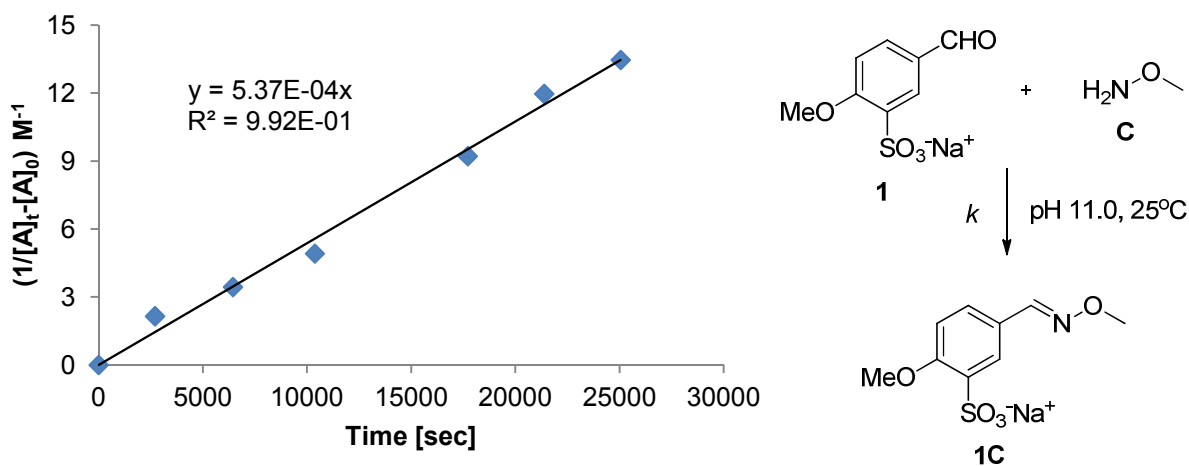
7.5.3.6 Sodium (*E*)-2-methoxy-5-(2-methoxyvinyl)benzenesulfonate formation

Figure 7.75 Representative linear least-squares fit ($\frac{1}{[A]_t} - \frac{1}{[A]_0}$ vs. t) of the imine formation between sulfonate aldehyde **1** and methylhydrazine **C** in phosphate buffer (160 mM $NaH_2PO_4/Na_2HPO_4 + NaOD$) pH 11.0 at 25°C. The final solution is 20 mM. The slope of the fit corresponds to the second order rate constant; R^2 values shown.

7.5.3.7 Sodium (E)-5-((2-acetylhydrazono)methyl)-2-methoxybenzenesulfonate formation

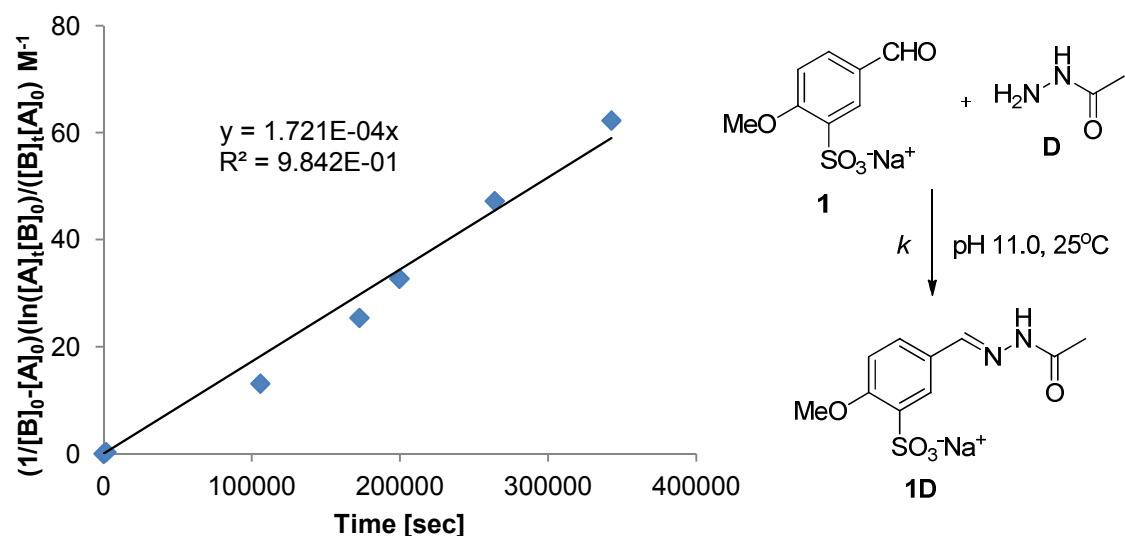


Figure 7.76 Representative linear least-squares fit ($\frac{1}{[B]_0 - [A]_0} \ln \frac{[A]_t[B]_0}{[B]_t[A]_0}$ vs. t) of the imine formation between sulfonate aldehyde **1** and acetylhydrazide **D** in phosphate buffer (160 mM $\text{NaH}_2\text{PO}_4/\text{Na}_2\text{HPO}_4 + \text{NaOD}$) pH 11.0 at 25°C. The final solution is 20 mM. Slope correspond to the second order rate constant; R^2 values shown. (Data were processed according to second-order reaction kinetics with correction for non-stoichiometric reagent mixing ratio)

7.5.3.8 Sodium (E)-2-methoxy-5-((2-methylhydrazono)methyl)benzenesulfonate formation

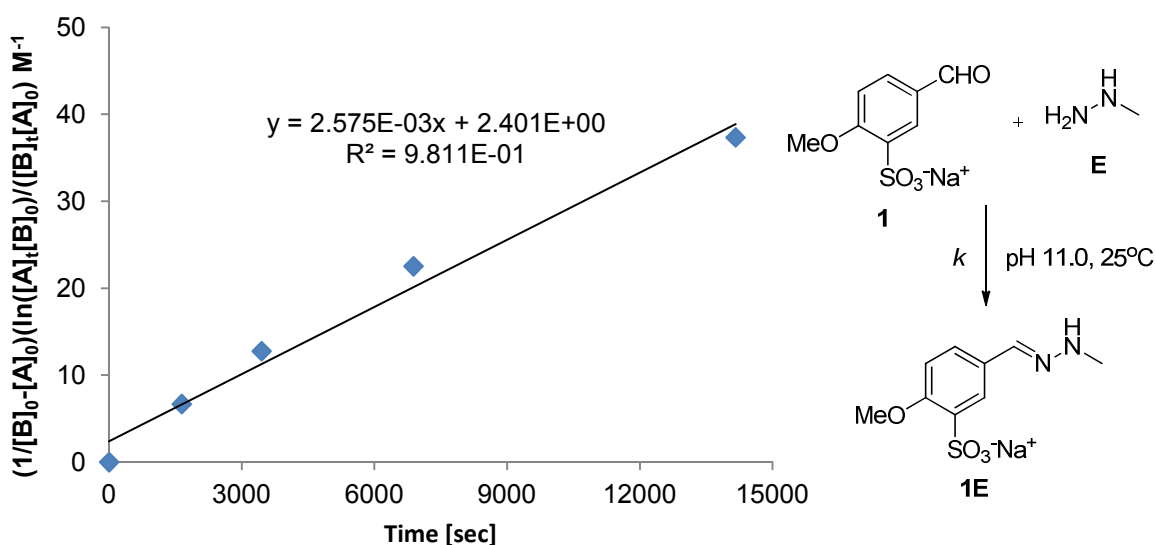


Figure 7.78 Representative linear least-squares fit ($\frac{1}{[B]_0 - [A]_0} \ln \frac{[A]_t[B]_0}{[B]_t[A]_0}$ vs. t) of the imine formation between sulfonate aldehyde **1** and methylhydrazine **H** in phosphate buffer (160 mM $\text{NaH}_2\text{PO}_4/\text{Na}_2\text{HPO}_4 + \text{NaOD}$) pH 11.0 at 25°C. The final solution is 20 mM. Slope correspond to the second order rate constant; R^2 values shown. (Data were processed according to second-order reaction kinetics with correction for non-stoichiometric reagent mixing ratio)

7.5.3.9 (E)-2-((pentylimino)methyl)phenol formation

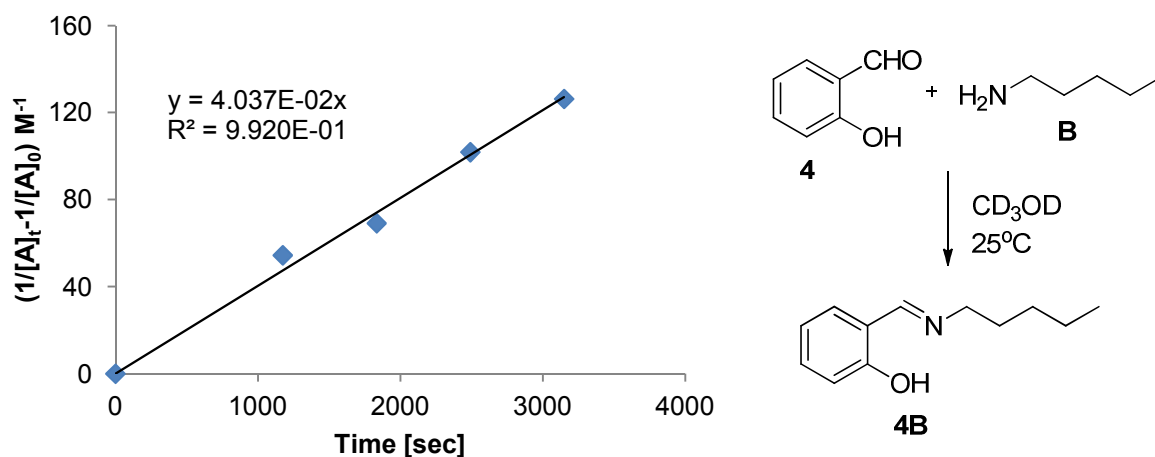


Figure 7.79 Representative linear least-squares fit ($\frac{1}{[A]_t} - \frac{1}{[A]_0}$ vs. t) of the imine formation between Salicylaldehyde **4** and pentylamine **B** in CD_3OD at 25°C . The final solution is 20 mM. Slope correspond to the second order rate constant; R^2 vaues shown.

7.5.3.10 (E)-2-hydroxybenzaldehyde O-benzyl oxime formation

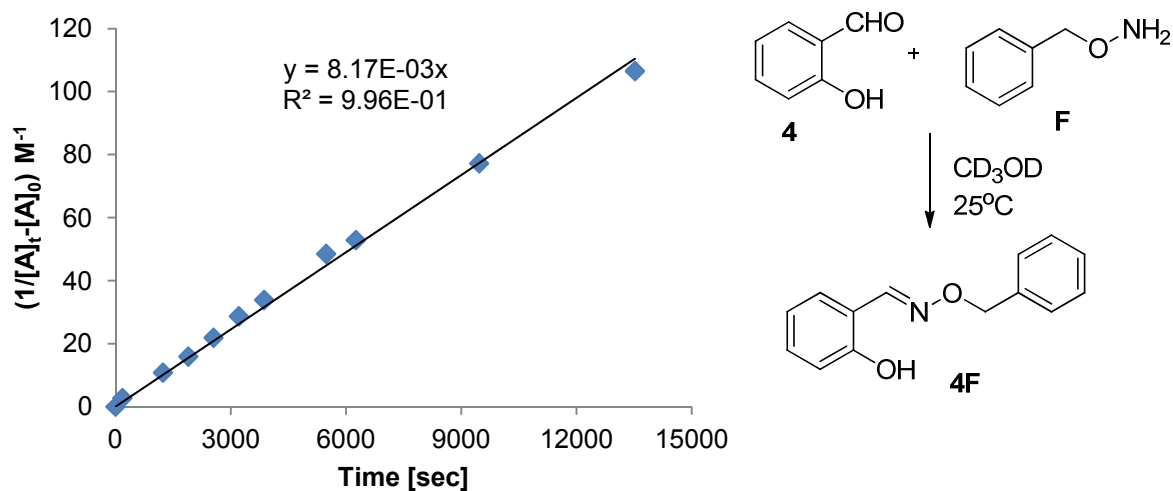


Figure 7.80 Representative linear least-squares fit ($\frac{1}{[A]_t} - \frac{1}{[A]_0}$ vs. t) of the imine formation between Salicylaldehyde **4** and O-benzylhydroxylamine **F** in CD_3OD at 25°C . The final solution is 20 mM. The slope of the fit corresponds to the second order rate constant; R^2 vaues shown.

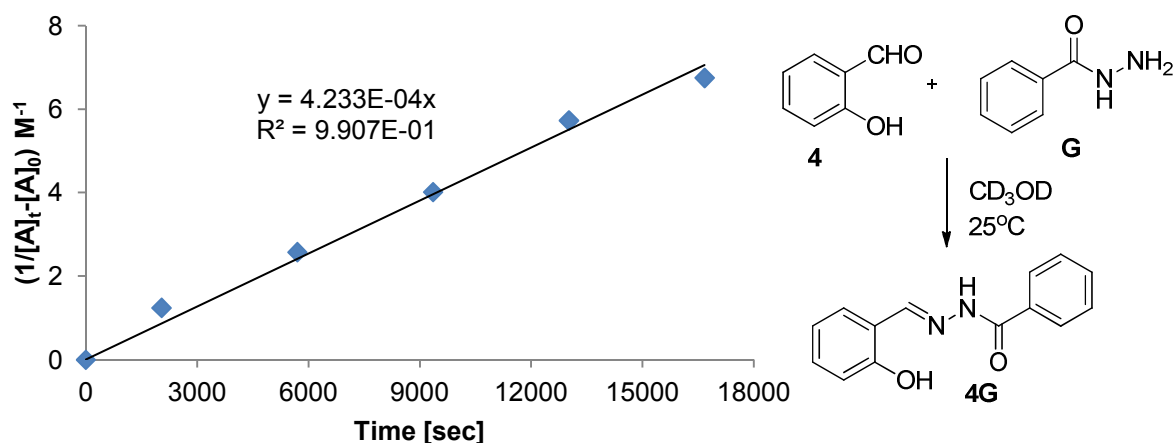
7.5.3.11 (*E*)-*N'*-(2-hydroxybenzylidene)benzohydrazide formation

Figure 7.81 Representative linear least-squares fit ($\frac{1}{[A]_t} - \frac{1}{[A]_0}$ vs. t) of the imine formation between Salicylaldehyde **4** and Benzhydrazide **G** in CD_3OD at $25^\circ C$. The final solution is 20 mM. The slope of the fit corresponds to the second order rate constant; R^2 values shown.

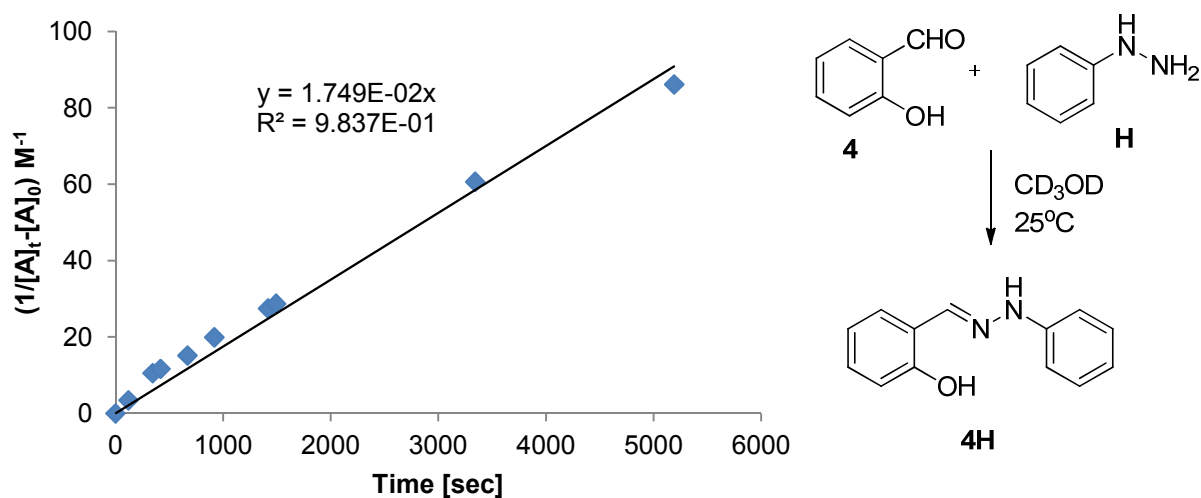
7.5.3.12 (*E*)-2-((2-phenylhydrazono)methyl)phenol formation

Figure 7.82 Representative linear least-squares fit ($\frac{1}{[A]_t} - \frac{1}{[A]_0}$ vs. t) of the imine formation between Salicylaldehyde **4** and Phenylhydrazine **H** in CD_3OD at $25^\circ C$. The final solution is 20 mM. The slope of the fit corresponds to the second order rate constant; R^2 values shown.

7.5.4 $^1\text{H-NMR}$ spectra of dynamic covalent libraries in the mixture of one aldehyde with various amines

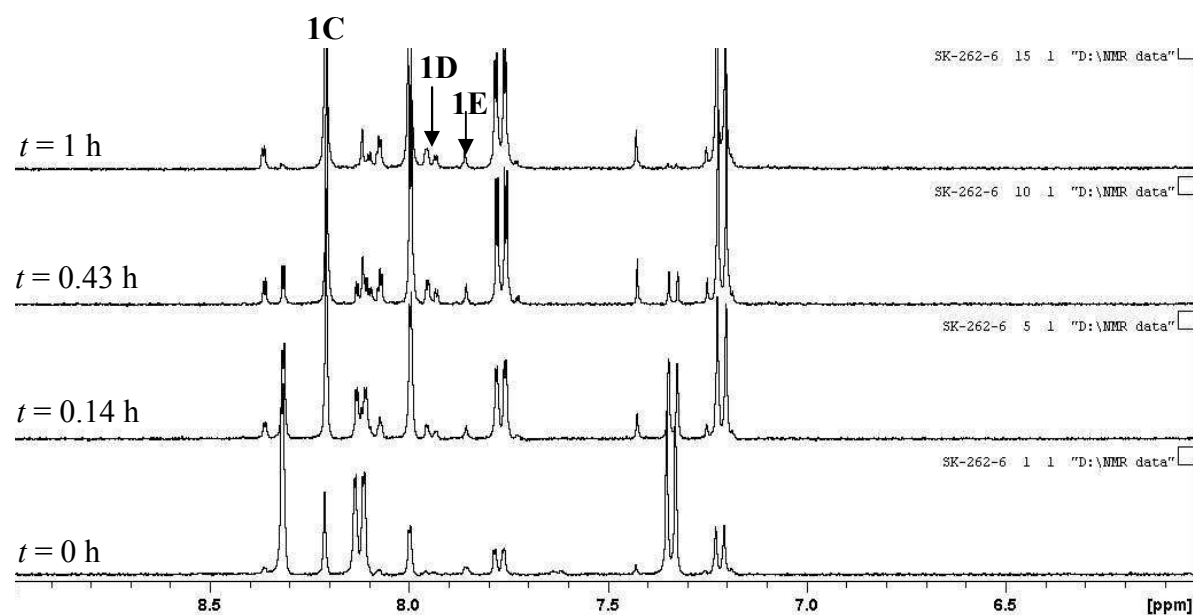


Figure 7.83 $^1\text{H-NMR}$ spectra of imine formation in CD_3OD in the mixture of **1** + **B** + **C** + **D** + **E** at $\text{pD } 5.0$ as a function of time.

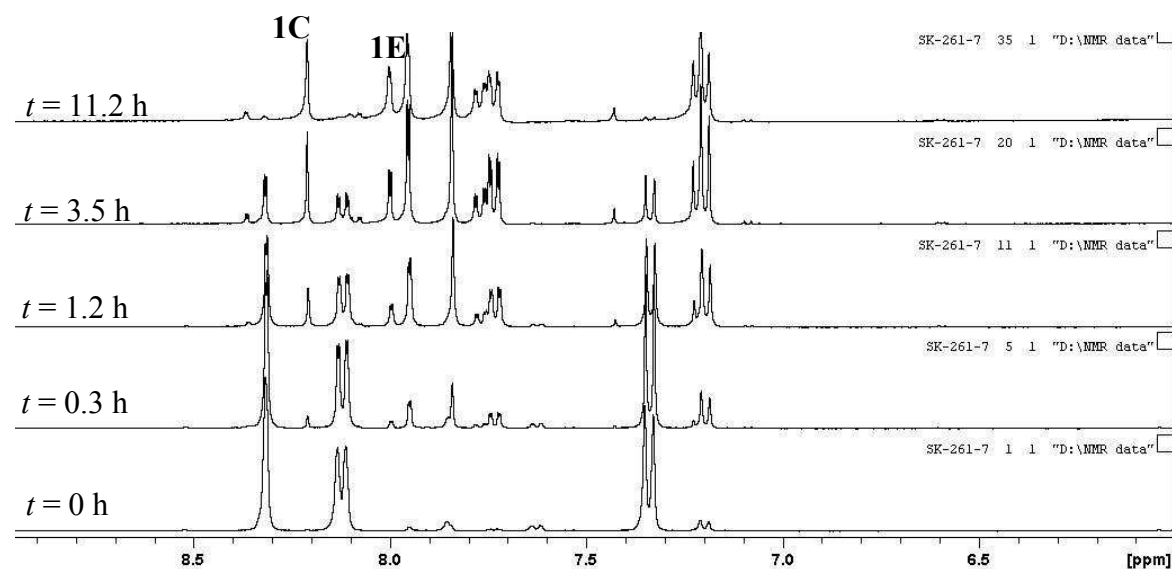


Figure 7.84 $^1\text{H-NMR}$ spectra of imine formation in CD_3OD in the mixture of **1** + **B** + **C** + **D** + **E** at $\text{pD } 8.5$ as a function of time.

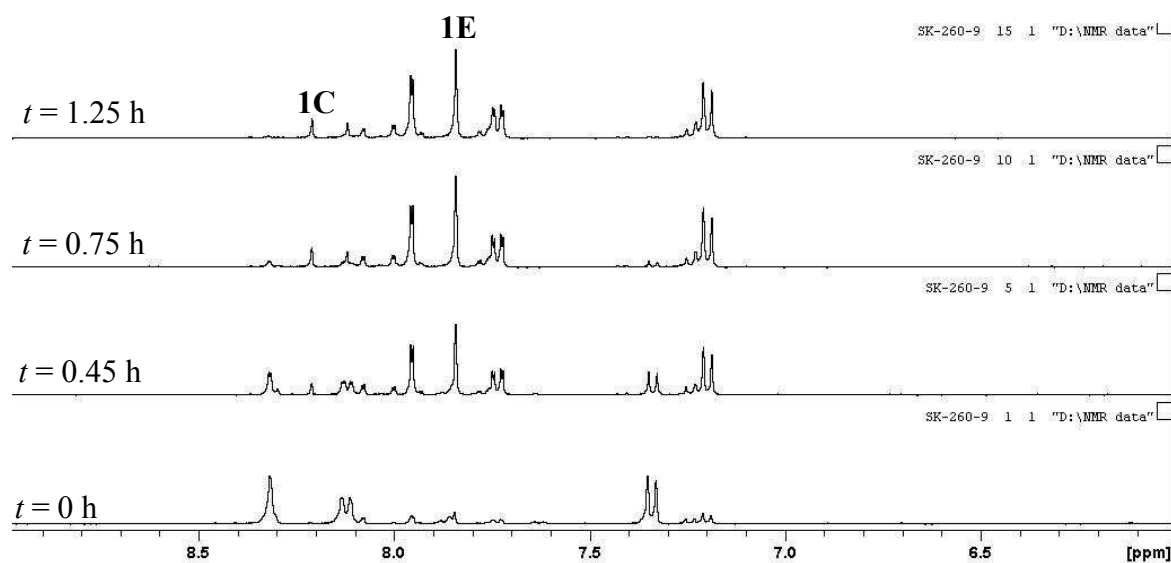


Figure 7.85 ^1H -NMR spectra of imine formation in CD_3OD in the mixture of **1** + **B** + **C** + **D** + **E** at pD 11.4 as a function of time.

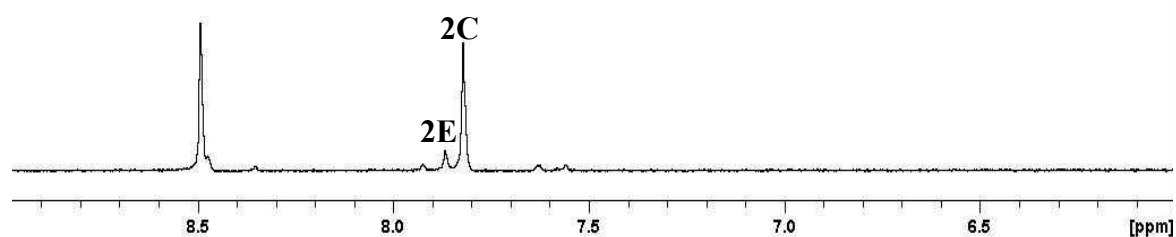


Figure 7.86 ^1H -NMR spectra of imine formation in CD_3OD in the mixture of **2** + **B** + **C** + **D** + **E** at pD 5.0 at equilibrium.

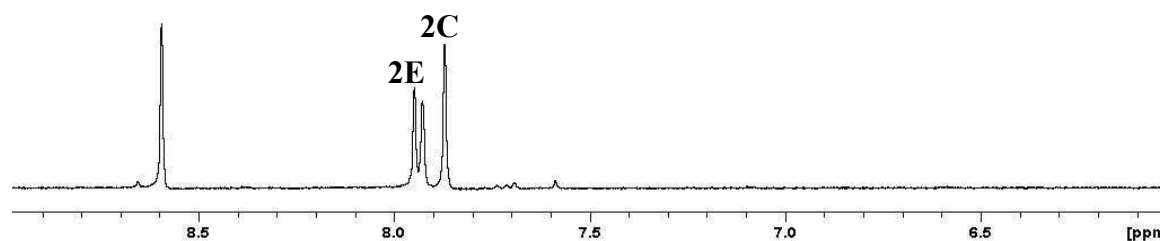


Figure 7.87 ^1H -NMR spectra of imine formation in CD_3OD in the mixture of **2** + **B** + **C** + **D** + **E** at pD 8.5 at equilibrium.

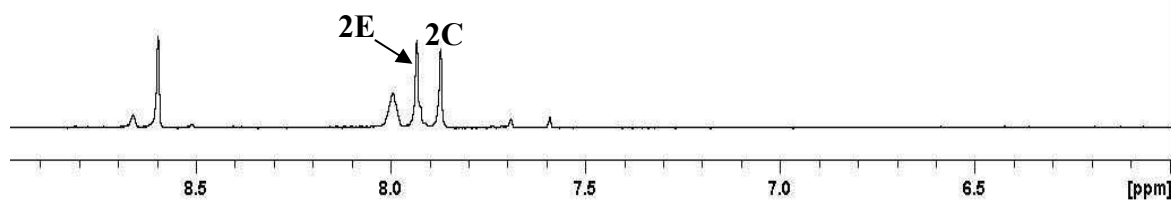


Figure 7.88 $^1\text{H-NMR}$ spectra of imine formation in CD_3OD in the mixture of **2** + **B** + **C** + **D** + **E** at $p\text{D } 11.4$ at equilibrium.

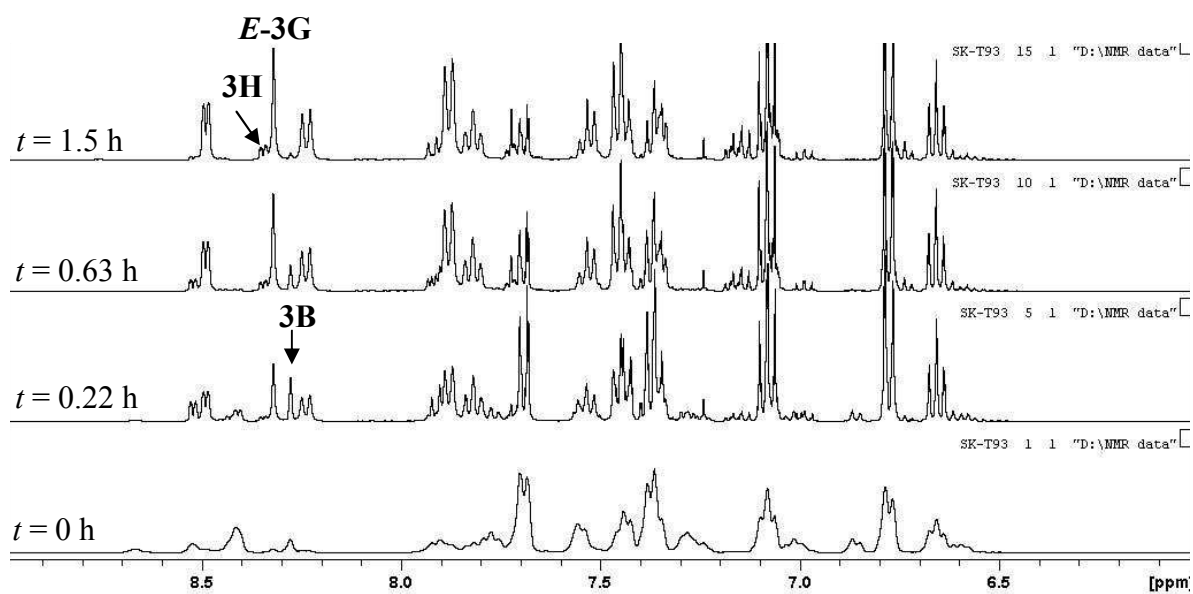


Figure 7.89 $^1\text{H-NMR}$ spectra of imine formation in CD_3OD in the mixture of **3** + **B** + **G** + **H** as a function of time.

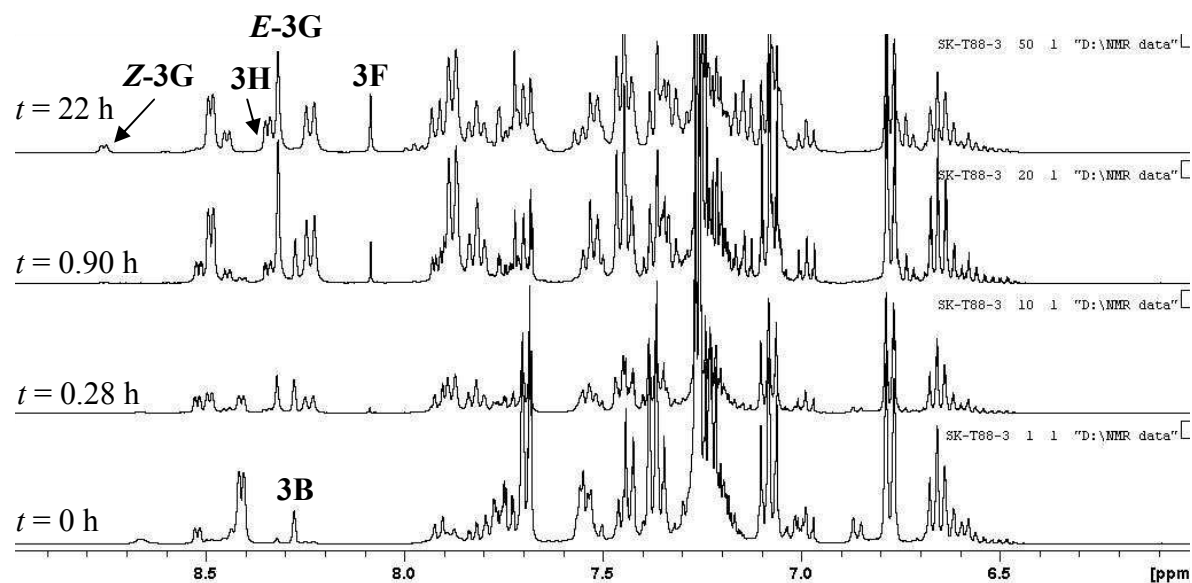


Figure 7.90 $^1\text{H-NMR}$ spectra of imine formation in CD_3OD in the mixture of **3** + **B** + **F** + **G** + **H** as a function of time.

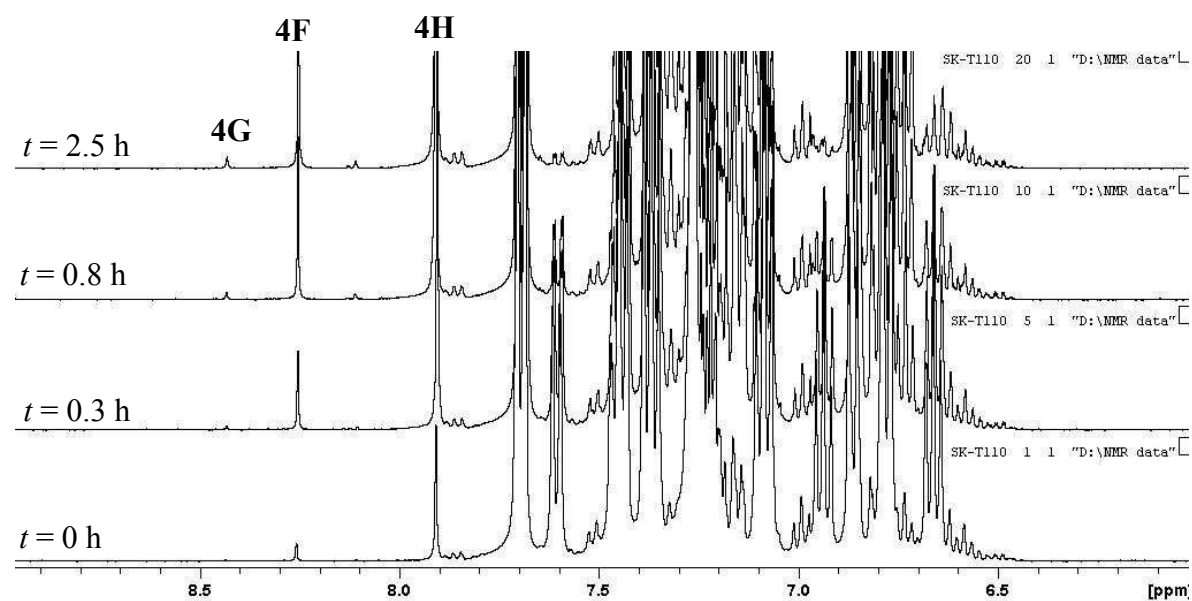


Figure 7.91 $^1\text{H-NMR}$ spectra of imine formation in CD_3OD in the mixture of **4** + **F** + **G** + **H** as a function of time.

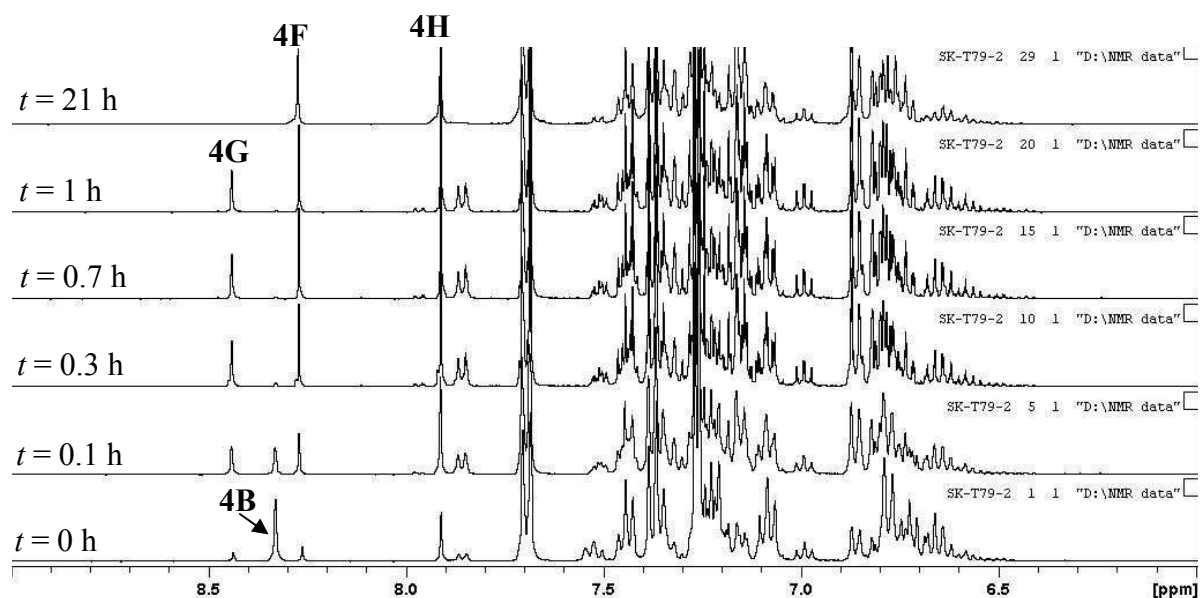


Figure 7.92 ^1H -NMR spectra of imine formation in CD_3OD in the mixture of **4** + **B** + **F** + **G** + **H** as a function of time.

7.6 References

- [1] L. Sacconi, R. Cini, M. Ciampolini, F. Maggio, *J. Am. Chem. Soc.* **1960**, *82*, 3487–3491.
- [2] L. Cuesta, I. Maluenda, T. Soler, R. Navarro, E. P. Urriolabeitia, *Inorg. Chem.* **2011**, *50*, 37–45.
- [3] A. Simion, C. Simion, T. Kanda, S. Nagashima, Y. Mitoma, T. Yamada, K. Mimura, M. Tashiro, *J. Chem. Soc. [Perkin 1]* **2001**, 2071–2078.
- [4] Y. Hoshika, *J. Chromatogr. A* **1977**, *136*, 253–258.
- [5] J. Chandrasekharan, P. V. Ramachandran, H. C. Brown, *J. Org. Chem.* **1985**, *50*, 5446–5448.
- [6] P. Kovaříček, J.-M. Lehn, *J. Am. Chem. Soc.* **2012**, *134*, 9446–9455.
- [7] M. Ortega, M. A. Rodríguez, P. J. Campos, *Tetrahedron* **2005**, *61*, 11686–11691.
- [8] J. M. Fernández-G, F. del Rio-Portilla, B. Quiroz-García, R. A. Toscano, R. Salcedo, *J. Mol. Struct.* **2001**, *561*, 197–207.
- [9] N. C. Antonels, J. R. Moss, G. S. Smith, *J. Organomet. Chem.* **2011**, *696*, 2003–2007.

- [10] R. M. Ceder, G. Muller, M. Ordinas, J. I. Ordinas, *Dalton Trans.* **2006**, 83–90.
- [11] P. K. Srivastava, V. Choudhary, *J. Appl. Polym. Sci.* **2012**, *125*, 31–37.
- [12] G. H. Hakimelahi, S.-C. Tsay, J. R. Hwu, *Helv. Chim. Acta* **1995**, *78*, 411–420.
- [13] A. Brink, H. G. Visser, A. Roodt, *J. Coord. Chem.* **2011**, *64*, 122–133.
- [14] D. M. Haddleton, M. C. Crossman, B. H. Dana, D. J. Duncalf, A. M. Heming, D. Kukulj, A. J. Shooter, *Macromolecules* **1999**, *32*, 2110–2119.
- [15] J. Albert, J. M. Cadena, J. Granell, X. Solans, M. Font-Bardia, *J. Organomet. Chem.* **2004**, *689*, 4889–4896.
- [16] O.-Y. Lee, K.-L. Law, D. Yang, *Org. Lett.* **2009**, *11*, 3302–3305.
- [17] O. Cifuentes, R. Contreras, A. Laguna, O. Crespo, *Inorganica Chim. Acta* **2011**, *379*, 81–89.
- [18] C. Saravanan, S. Easwaramoorthi, L. Wang, *Dalton Trans.* **2014**, *43*, 5151–5157.
- [19] S. Shinde, G. Rashinkar, A. Kumbhar, S. Kamble, R. Salunkhe, *Helv. Chim. Acta* **2011**, *94*, 1943–1951.
- [20] C.S. Reddy, A. Nagaraj, P. Jalapathi, *Indian J. Chem., Sect. B n.d.*, *2007*, 660–663.
- [21] X.-C. Yang, H. Jiang, W. Ye, *Synth. Commun.* **2011**, *42*, 309–312.
- [22] Y. Lv, X. Yan, L. Yan, Z. Wang, J. Chen, H. Deng, M. Shao, H. Zhang, W. Cao, *Tetrahedron* **2013**, *69*, 4205–4210.
- [23] B. B. Corson, R. W. Stoughton, *J. Am. Chem. Soc.* **1928**, *50*, 2825–2837.
- [24] S. Wang, Z. Ren, W. Cao, W. Tong, *Synth. Commun.* **2001**, *31*, 673–677.
- [25] Y. Bouazizi, K. Beydoun, A. Romdhane, H. Ben Jannet, H. Doucet, *Tetrahedron Lett.* **2012**, *53*, 6801–6805.
- [26] S. J. Mountford, A. L. Albiston, W. N. Charman, L. Ng, J. K. Holien, M. W. Parker, J. A. Nicolazzo, P. E. Thompson, S. Y. Chai, *J. Med. Chem.* **2014**, *57*, 1368–1377.
- [27] P. P. Kumar, Y. D. Reddy, C. V. R. Reddy, B. R. Devi, P. K. Dubey, *Tetrahedron Lett.* **2014**, *55*, 2177–2182.
- [28] F. Zhou, J. Shao, Y. Yang, J. Zhao, H. Guo, X. Li, S. Ji, Z. Zhang, *Eur. J. Org. Chem.* **2011**, *2011*, 4773–4787.
- [29] M. C. Burland, T. Y. Meyer, M.-H. Baik, *J. Org. Chem.* **2004**, *69*, 6173–6184.
- [30] N. E. Meagher, D. B. Rorabacher, *J. Phys. Chem.* **1994**, *98*, 12590–12593.
- [31] M. Ciaccia, R. Cacciapaglia, P. Mencarelli, L. Mandolini, S. D. Stefano, *Chem. Sci.* **2013**, *4*, 2253–2261.
- [32] E. H. Cordes, W. P. Jencks, *J. Am. Chem. Soc.* **1962**, *84*, 832–837.

- [33] H. Fischer, F. X. DeCandis, S. D. Ogden, W. P. Jencks, *J. Am. Chem. Soc.* **1980**, *102*, 1340–1347.
- [34] M. K. Haldar, M. D. Scott, N. Sule, D. K. Srivastava, S. Mallik, *Bioorg. Med. Chem. Lett.* **2008**, *18*, 2373–2376.
- [35] M. C. Rezende, I. Almodovar, *Magn. Reson. Chem.* **2012**, *50*, 266–270.
- [36] M. L. Deb, P. J. Bhuyan, *Tetrahedron Lett.* **2005**, *46*, 6453–6456.
- [37] A. Pałasz, *Monatshefte Für Chem. - Chem. Mon.* **2012**, *143*, 1175–1185.
- [38] A. Głębowska, K. Kamińska-Trela, A. Krówczyński, D. Pocięcha, J. Szydłowska, J. Szczytko, A. Twardowski, J. Wójcik, E. Górecka, *J. Mater. Chem.* **2008**, *18*, 3419–3421.
- [39] H. Katayama, *Chem. Pharm. Bull. (Tokyo)* **1978**, *26*, 2027–2035.
- [40] H. Katayama, N. Takatsu, *Chem. Pharm. Bull. (Tokyo)* **1981**, *29*, 2465–2477.
- [41] S. J. A. Grove, J. Kaur, A. W. Muir, E. Pow, G. J. Tarver, M.-Q. Zhang, *Bioorg. Med. Chem. Lett.* **2002**, *12*, 193–196.
- [42] M. Finkelstein, R. C. Petersen, S. D. Ross, *J. Am. Chem. Soc.* **1959**, *81*, 2361–2364.
- [43] S. D. Venkataramu, G. D. Macdonell, W. R. Purdum, G. A. Dilbeck, K. D. Berlin, *J. Org. Chem.* **1977**, *42*, 2195–2200.
- [44] R. S. Underhill, G. Liu, *Chem. Mater.* **2000**, *12*, 3633–3641.
- [45] F. M. Menger, U. V. Venkataram, *J. Am. Chem. Soc.* **1986**, *108*, 2980–2984.
- [46] R. R. Ravu, Y.-L. Chen, M. R. Jacob, X. Pan, A. K. Agarwal, S. I. Khan, J. Heitman, A. M. Clark, X.-C. Li, *Bioorg. Med. Chem. Lett.* **2013**, *23*, 4828–4831.
- [47] J. P. Dinnocenzo, S. B. Karki, J. P. Jones, *J. Am. Chem. Soc.* **1993**, *115*, 7111–7116.
- [48] F. G. Bordwell, D. L. Hughes, *J. Am. Chem. Soc.* **1986**, *108*, 7300–7309.
- [49] D. Passarella, R. Favia, A. Giardini, G. Lesma, M. Martinelli, A. Silvani, B. Danieli, S. M. N. Efange, D. C. Mash, *Bioorg. Med. Chem.* **2003**, *11*, 1007–1014.
- [50] I. Y. Chernyshov, V. V. Levin, A. D. Dilman, P. A. Belyakov, M. I. Struchkova, V. A. Tartakovsky, *Russ. Chem. Bull.* **2010**, *59*, 2102–2107.
- [51] T. Chang, H. Jing, L. Jin, W. Qiu, *J. Mol. Catal. Chem.* **2007**, *264*, 241–247.
- [52] N. Jiang, Y. Pu, R. Samuel, A. J. Ragauskas, *Green Chem.* **2009**, *11*, 1762–1766.
- [53] W. Zhao, W. Liu, W. Zhang, L. Zeng, Z. Fan, J. Wu, P. Wang, *Analyst* **2012**, *137*, 1853–1859.
- [54] K. J. Hall, T. I. Quickenden, D. W. Watts, *J. Chem. Educ.* **1976**, *53*, 493.
- [55] R. Chen, J. Bacsá, S. F. Mapolie, *Polyhedron* **2003**, *22*, 2855–2861.

- [56] T. J. Donohoe, L. P. Fishlock, P. A. Procopiou, *Org. Lett.* **2008**, *10*, 285–288.
- [57] O. Pouralimardan, A.-C. Chamayou, C. Janiak, H. Hosseini-Monfared, *Inorganica Chim. Acta* **2007**, *360*, 1599–1608.
- [58] G. L. Perlovich, V. P. Kazachenko, N. N. Strakhova, K.-J. Schaper, O. A. Raevsky, *J. Chem. Eng. Data* **2013**, *58*, 2659–2667.
- [59] A. D. Garnovskii, A. S. Burlov, K. A. Lysenko, D. A. Garnovskii, I. G. Borodkina, A. G. Ponomarenko, G. G. Chigarenko, S. A. Nikolaevskii, V. I. Minkin, *Russ. J. Coord. Chem.* **2009**, *35*, 120–127.
- [60] T.-T. Zhao, X. Lu, X.-H. Yang, L.-M. Wang, X. Li, Z.-C. Wang, H.-B. Gong, H.-L. Zhu, *Bioorg. Med. Chem.* **2012**, *20*, 3233–3241.
- [61] M. Alagesan, N. S. P. Bhuvanesh, N. Dharmaraj, *Eur. J. Med. Chem.* **2014**, *78*, 281–293.
- [62] G. L. Backes, D. M. Neumann, B. S. Jursic, *Bioorg. Med. Chem.* **2014**, *22*, 4629–4636.
- [63] A. K. Covington, M. Paabo, R. A. Robinson, R. G. Bates, *Anal. Chem.* **1968**, *40*, 700–706.

Publications and Conferences (October 2011 – July 2015)***Publications***

Nadine Wilhelms, Sirinan Kulchat, and Jean-Marie Lehn: Organocatalysis of C=N/C=N and C=C/C=N Exchange in Dynamic Covalent Chemistry, *Helv. Chim. Acta*, **2012**, *95*, 2635-2651.

Sirinan Kulchat, Kamel Meguellati, and Jean-Marie Lehn: Organocatalyzed and Uncatalyzed C=C/C=C and C=C/C=N Exchange Processes between *Knoevenagel* and Imine Compounds in Dynamic Covalent Chemistry, *Helv. Chim. Acta*, **2014**, *97*, 1219-1236.

Sirinan Kulchat and Jean-Marie Lehn: Dynamic Covalent Chemistry of Nucleophilic Substitution Component Exchange of Quaternary Ammonium Salts, *Chem. Asian J.*, **2015**, *Accepted*.

Sirinan Kulchat, Manuel N. Chaur, and Jean-Marie Lehn: Kinetic and Thermodynamic selectivity of Imine formation in Dynamic Covalent Chemistry, *Manuscript in Preparation*.

Conferences

- 11/2014 Poster Presentation, JSPS Bilateral Joint Research Seminar Interdisciplinary Seminar (France ,Strasbourg)for Innovative Organic Chemistry
- 08/2014 Poster Presentation, The 7th International Conference on Molecular Electronic (Strasbourg, France)
- 06/2014 Poster presentation, Workweek 2014, Universities of Strasbourg – Groningen (Strasbourg, France)
- 09/2012 Poster presentation, Suprachem 2012 (Strasbourg, France)

DYNAMIC COVALENT CHEMISTRY OF C=N, C=C AND QUATERNARY AMMONIUM CONSTITUENTS

Résumé

Cette thèse décrit la Chimie Covalente Dynamique (CCD) des échanges imine/imine, *Knoevenagel*/imine et *Knoevenagel*/*Knoevenagel*. La L-proline est un excellent organocatalyseur pour la formation de Bibliothèques Covalentes Dynamiques (BCDs). Cependant, l'interconversion entre des dérivées *Knoevenagel* de l'acide diméthylbarbiturique et des imines se déroule rapidement sans catalyseur. Une nouvelle classe de CCD basée sur des échanges par substitutions nucléophiles (S_N2/S_N2') entre des sels d'ammonium quaternaires et des amines tertiaires est développée, impliquant la catalyse par l'iodure. Les réactions d'échange entre des sels de pyridinium et un dérivé de pyridine génèrent des liquides ioniques dynamiques. Enfin, la sélection cinétique et thermodynamique de la formation d'imines dans la CCD est réalisée en solution aqueuse et en solvant organique.

Mots clés : bibliothèque covalente dynamique, organocatalyse, imine, composé de *Knoevenagel*, substitution nucléophile, sel d'ammonium, réaction réversible, catalyse par l'iodure.

Résumé en anglais

This thesis describes the dynamic covalent chemistry (DCC) of imine/imine, *Knoevenagel*/imine, and *Knoevenagel*/*Knoevenagel* exchange. L-proline is shown to be an excellent organocatalyst to accelerate the formation of dynamic covalent libraries (DCLs). The interconversion between *Knoevenagel* derivatives of dimethylbarbituric acid and imines is found to occur rapidly in the absence of catalyst. A new class of DCC based on nucleophilic substitution (S_N2/S_N2') component exchange between quaternary ammonium salts and tertiary amines is developed, by the use of iodide as a catalyst. The exchange reactions between pyridinium salts and a pyridine derivative generate dynamic ionic liquids. Finally, kinetic and thermodynamic selection of imine formation in a DCC is performed in aqueous solution and organic solvent.

Keywords : dynamic covalent library, organocatalysis, imine, *Knoevenagel* compound, nucleophilic substitution, ammonium salt, reversible reaction, iodide catalysis